Contribution of waterborne nitrogen emissions to hypoxia-driven marine eutrophication: modelling of damage to ecosystems in life cycle impact assessment (LCIA)

Cosme, Nuno Miguel Dias

Publication date:
2016

Document Version
Publisher's PDF, also known as Version of record

Contribution of waterborne nitrogen emissions to hypoxia-driven marine eutrophication: modelling of damage to ecosystems in life cycle impact assessment (LCIA)

Nuno Miguel Dias Cosme

PhD Thesis

May 2016

Division for Quantitative Sustainability Assessment
Department of Management Engineering
Technical University of Denmark

Preface

This PhD thesis presents the work conducted and the results obtained during the PhD project "Impacts of waterborne nitrogen emissions to hypoxia-driven marine eutrophication: modelling of damage to ecosystems in life cycle impact assessment (LCIA)". The research work was completed at the Division for Quantitative Sustainability Assessment of the Department of Management Engineering at the Technical University of Denmark from December 2012 to May 2016. The project was internally funded and supervised by Professor Michael Zwicky Hauschild, as principal supervisor, Associate Professor Morten Birkved, and by former Associate Professor Ralph Klaus Rosenbaum, now Director at Irstea – France.

The thesis is a synopsis of six scientific articles of original research published or submitted for publication in international scientific journals. The articles' manuscripts, of which two have been published and four submitted at the time of the thesis completion, are included as appendices. The articles are referred herein by adding roman numerals from I to VI to the citation – e.g. **Article II**: Cosme et al. (2015), and listed below:

Article I: Cosme, N., Mayorga, E. & Hauschild, M.Z. Spatially explicit fate factors for waterborne nitrogen emissions at the global scale. *International Journal of Life Cycle Assessment*, submitted in 2016 – manuscript in pre-print version.

Article II: Cosme, N., Koski, M. & Hauschild, M.Z. (2015). Exposure factors for marine eutrophication impacts assessment based on a mechanistic biological model. *Ecological Modelling* 317:50–63. DOI: 10.1016/j.ecolmodel.2015.09.005 – published, manuscript in post-print version.

Article III: Cosme, N. & Hauschild, M.Z. (2016). Effect factors for marine eutrophication in LCIA based on species sensitivity to hypoxia. *Ecological Indicators* 69:453-462, DOI: 10.1016/j.ecolind. 2016.04.006 – published, manuscript in post-print version.

Article IV: Cosme, N., Jones, M.C., Cheung, W.W.L. & Larsen, H.F. Spatial differentiation of marine eutrophication damage indicators based on species density. *Ecological Indicators*, submitted in 2016 – manuscript in pre-print version.

Article V: Cosme, N. & Hauschild M.Z. Characterization of waterborne nitrogen emissions for marine eutrophication modelling in life cycle impact assessment at the damage level and global scale. *International Journal of Life Cycle Assessment*, submitted in 2016 – manuscript in pre-print version.

Article VI: Cosme, N. & Niero, M. Modelling the influence of changing climate in present and future marine eutrophication impacts from spring barley production. *Journal of Cleaner Production*, submitted in 2016 – reviewed, manuscript in pre-print version R1.

Acknowledgments

When I embarked in this PhD voyage I was erroneously confident on the simplicity of the task ahead – 'read and investigate, write and publish'! I could not have been more mistaken. Not only the task was formidably more complex but, more importantly, I had underestimated the necessary time to live and contribute – live a healthy day-to-day office and social life with colleagues and friends, enjoy family time, enjoy time off, and contribute back to DTU, to the department and the division that so generously had received me. I see now that the joy of being part of something bigger has made me, at times, forget about the main objective. I had the valuable support of many to bring me back on the right track.

I am grateful to my principal supervisor Michael Zwicky Hauschild for his mighty pen, all the challenging and fruitful discussions, and for sharing his patience, time and knowledge with me. Wise to make me add the necessary structure and logic to my research, wise to let me pursue my own approaches. I think we balanced it well. I would like to extend my appreciation to my co-supervisors Morten Birkved for his friendship and guidance all-round, and Ralph K. Rosenbaum, a skilful educator, for his confidence on me and generous, although brief, collaboration.

I also wish to thank the my co-authors for keeping up with my ideas, both the good and the bad, for engaging in constructive sessions, and reading my long paragraphs: Marja Koski, Monia Niero, Emilio Mayorga, Henrik F. Larsen, William W. L. Cheung, Miranda Jones, Michael Z. Hauschild. Also, to all of those I contacted to help me making ideas into numbers or numbers into meaningful ideas: Alexis Laurent, Morten Ryberg, Stig. I. Olsen, Peter Fantke, Colin Stedmon, Andre Visser, Jane Behrens, Torkel G. Nielsen, Ligia B. Azevedo, Jørgen L.S. Hansen, Guy Claireaux, and to anyone else I might have inadvertently forgotten.

I am in debt to all my past and current colleagues and friends at the Division for Quantitative Sustainability Assessment (QSA) for the enthusiastic, informal and informed work environment. Fellow PhD students, faculty and administrative staff, postdocs and researchers, MSc and BSc students – only diversity makes us better. I will not name them all for the risk of forgetting someone.

My thanks also to the LC-IMPACT team with whom I have learned about new developments in impact assessment indicators. It has truly opened a door into the LCIA network for me.

A word of appreciation to my fellow members of the KPBT PhD Committee in 2014 and 2015, for the interesting discussions and views into DTU's functioning. Although labelled as 'mandatory work', my participation in the committee's tasks and duties was undeniably rewarding.

Finally, and above all, I want to express my profound gratitude to my wife Cristina, unconditional and tireless partner in crime, for her continuous encouragement and support, and to my devoted children Rodrigo mini-me and princess Maria for their unfailing enthusiasm and patience – my three best friends. Thank you for being there for me even when I was not available for you – I will be eternally in your debt. Words are immensely vague to fully express your contribution, and for that, this is also your achievement.

A todos, muito obrigado!

Nuno Cosme

Who wants an easy challenge anyway?

"(…) eutrophication is an intellectually rich problem that weaves together plant, animal, and microbial physiology, physics, climatology, hydrology, biogeochemistry, soil science, agriculture, forestry, urban infrastructure, demography, and nutrition. It involves every level of the ecosystem from abiotic factors to top carnivores. It draws on our skills of observation across wide scales of time and space. The eutrophication literature is full of the results of studies using microscopes, satellite images, sediment cores, stable and radioactive isotopes, analyses of shells and scales and bones, field surveys, buoy sensor data records, mesocosm experiments, long time-series analyses, historical documents, field manipulations, physiological rate measurements, plant and animal tissue analyses, growth studies, and complex numerical models of atmospheric chemistry, oceanic circulation, and ecosystems."

Scott W. Nixon, Eutrophication and the macroscope, *Hydrobiologia* 2009, **629**, 5–19.

Summary

Purpose

Marine eutrophication refers to the ecosystem response to the loading of a growth limiting nutrient, typically nitrogen (N), to coastal waters, where it may cause several impacts. One of the possible impact pathways to these impacts involves the excessive depletion of dissolved oxygen (hypoxia) in bottom waters. Hypoxia is identified as an important and widespread cause of disturbance to marine ecosystems and has been linked to the increasing anthropogenic pressure. This is driven by environmental emissions of reactive nitrogen, mainly from N-containing fertilizers used in agriculture and atmospheric deposition as a consequence of fossil fuels combustion.

The hypoxia-driven eutrophication impacts vary significantly with the type and location of the emissions. Understanding and modelling (i) the environmental fate of waterborne forms of nitrogen, (ii) the biological processes responsible for nitrogen and organic matter cycling in coastal waters that leads to bottom oxygen consumption, and (iii) the effects of that oxygen depletion on exposed animal communities, are therefore essential contributions to the quantification of those impacts on coastal marine ecosystems.

The scientific research work composing this thesis introduces a method to calculate spatially explicit endpoint characterisation factors (CF). These factors are applied to waterborne nitrogen emissions to quantify hypoxia-driven marine eutrophication impacts.

Methods

Life cycle impact assessment (LCIA) is a tool to estimate environmental impacts from the emissions originated by human activities. However, current LCIA methods lack a consistent and globally applicable characterisation model relating

nitrogen enrichment of coastal waters to the marine eutrophication impacts at the endpoint level of the impact pathway.

The method proposed here combines environmental fate factors (FF, [yr]) with marine ecosystem exposure factors (XF, [$kgO_2 \cdot kgN^{-1}$]) and effect factors (EF, [$(PAF) \cdot m^3 \cdot kgO_2^{-1}$] expressed as a potentially affected fractions (PAF) of species). The CF [$(PAF) \cdot m^3 \cdot yr \cdot kgN^{-1}$] is derived from the product of those three factors.

The FF integrates N-removal processes in (i) soils and rivers, based on the Global NEWS 2-DIN model, and (ii) in coastal waters, based on water residence time, modelled for five emissions routes (from natural and agricultural soils, in sewage, to river, and to marine water) in 5,772 river basin of the world.

The XF is based on biological cycling processes described by N-limited primary production, metazoan consumption, and bacterial degradation, in four distinct organic carbon sedimentation routes, and modelled for 66 large marine ecosystems (LME).

The EF is based on sensitivity of species to hypoxia integrated with a species sensitivity distribution (SSD) method to derive the average effect on exposed demersal communities, modelled at a five climate zone scale.

Damage factors (DF, [$(PDF \cdot PAF^{-1}) \cdot species \cdot m^{-3}$]) are further modelled for the metrics conversion and harmonisation with other LCIA indicators that also contribute to damage to ecosystems. DFs are based on LME-dependent demersal species density and are multiplied by CFs to quantify the indicator for the damage to ecosystems dimension ([species·yr]).

Results and discussion

Endpoint CFs show 6 orders of magnitude (o.m.) spatial differentiation for the soil-related emission routes, 4 for the river-related, and 3 for emissions to coastal waters. After applying the DFs the variation shows 8, 6 and 4 o.m. for the same routes. Emission-weighted regionally aggregated CFs are consistently found in

Europe and South Asia, but the aggregation reduces spatial differentiation to around 1 o.m. for each route. Overall, CFs decrease from direct emissions to coastal waters over freshwater-related emissions and to soil-related emissions.

The FFs, especially those for soil-related emissions, are responsible for most of the spatial differentiation of the results. Further analyses show that coastal water residence time is the most influential parameter to the characterisation model. Uncertainty is also higher for this parameter, mainly due to scarcity and inconsistency of data sources.

Conclusions

Major contributions to the current state-of-the-art of marine eutrophication characterisation and damage modelling are (i) the full pathway coverage, thus reaching endpoint level, (ii) the significant increase in geographic coverage, (iii) the mechanistic modelling of exposure and effect factors, and (iv) the development of spatially explicit damage to ecosystem factors based on species density. Application of CFs in LCIA is recommended at a river basin scale, provided that emission location is known.

Future work should include the environmental fate of airborne nitrogen emissions, in order to achieve full completeness of the relevant environmental mechanisms involved in the marine eutrophication phenomenon.

The information the present model work provides, and its application as an LCIA method for marine eutrophication, may be critical to various levels of decision making and management of human activities.

Dansk sammenfatning

Vandbårne kvælstofemissioners påvirkning til hypoxia-dreven marin eutrofiering: Modellering af skader på økosystemet i miljøpåvirkningsvurdering i livscyklus (LCIA)

Formål

Marin eutrofiering refererer til økosystemets reaktion på belastning af kystvande med et vækst-begrænsende næringsstof, typisk kvælstof (N), hvilket kan forårsage flere påvirkninger. Et stærkt forøget forbrug af opløst ilt i bundvandet er en af de mulige påvirkningsveje. Hypoxia er identificeret som en vigtig og udbredt årsag til forstyrrelser af de marine økosystemer og er knyttet til den stigende menneskelige belastning. Disse belastninger er emissioner af reaktivt kvælstof, hovedsagelig fra N-holdige gødninger anvendt i landbruget og via atmosfærisk deposition som en konsekvens af fossile brændstoffer forbrænding.

Hypoxia-drevne eutrofieringspåvirkninger varierer betydeligt med type og placering af emissionerne. Forståelse og modellering af (i) den miljømæssige skæbne af vandbårne former for kvælstof, (ii) de biologiske processer, der er ansvarlige for cirkulering af kvælstof og organisk stof og som fører til iltforbrug på bunden, og (iii) dette iltsvinds effekter på de udsatte dyresamfund, bidrager således væsentligt til en kvantificering af disse påvirkninger på kystnære marine økosystemrecipienter.

Den videnskabelige forskning i denne afhandling introducerer en metode til at beregne stedspecifikke karakteriseringsfaktorer (CF) til slutpunktsvurdering. Disse faktorer anvendes til at kvantificere hypoxia-drevne marine eutrofieringspåvirkninger af vandbårne kvælstofudledninger.

Metoder

Livscyklusvurdering af miljøpåvirkninger (LCIA) er et værktøj til at estimere miljøpåvirkninger af antropogene emissioner. Eksisterende LCIA metoder

mangler en sammenhængende og globalt gældende karakteriseringsmodel til slutpunktsvurdering af marine eutrofieringspåvirkninger fra berigelse af kystvande med kvælstof.

Den foreslåede metode kombinerer miljømæssige skæbne faktorer (FF, [år]) med faktorer for eksponering af marine økosystemer (XF, [kgO2 · kgN-1]) og effektfaktorer (EF, [(PAF) · m3 · kgO2-1] udtrykt som den potentielt berørte fraktion af arter (PAF)). Karakteriseringsfaktoren CF [(PAF) · m3 · yr · kgN-1] er produktet af disse tre faktorer.

Skæbnefaktoren FF integrerer processer til fjernelse af N i jord og floder, baseret på Global NEWS 2-DIN model, med N-fjernelse i kystnære farvande baseret på opholdstiden i vand. Den er modelleret for fem emissionsveje (fra naturlige jorde og landbrugsjorde, i spildevand, til floder, og til havvand) i 5772 vandløbsopland i verden. Eksponeringsfaktoren XF er baseret på cykliske biologiske processer modelleret på baggrund af N-begrænset primærproduktion, metazoan-forbrug, og bakteriel nedbrydning, for fire forskellige sedimentationsveje for organiske kulstof, og 66 store marine økosystemer (LME). Effektfaktoren EF udleder den gennemsnitlige effekt på udsatte demersale samfund, modelleret på en skala over fem klimazoner. Den er baseret på arters følsomheds overfor hypoxia integreret med en metode til artsfølsomhedfordeling (SSD). Karakteriseringfaktorer for slutpunktsvurdering, skadesfaktorer (DF, [$(PDF \cdot PAF^{-1}) \cdot arter \cdot m^{-3}$]) modelleres yderligere for at kunne harmonisere med andre LCIA indikatorer, som også bidrager til skader på økosystemer, samt i forhold til konvertering af målinger. DF baseres på den LME-afhængige artstæthed af demersale arter og multipliceres med CF for at kvantificere indikatoren i forhold til skader på økosystemniveau ([arter·yr]).

Resultater og diskussion

Der er stor differentiering af karakteriseringsfaktorerne, CF, for slutpunktsvurdering i forhold til den rumlige dimension, henholdsvis 6 størrelsesordener for jordbundsrelaterede emissionsveje, 4 for flod-relaterede, og

3 for emissioner til kystvande. Efter anvendelse af DF variationen er det henholdsvis 8, 6 og 4 størrelsesordener for de samme emissionsveje. En konsekvent beregning af regionalt aggregerede CFer vægtede i forhold til emissioner i Europa og Sydasien, reducerer den rumlige differentiering til omkring 1 størrelsesorden for hver emissionsvej. Overordnet ses et fald i CF fra direkte emissioner til kystvande over emissioner til ferskvand og til jord-emissioner.

FFer, især dem for jord-relaterede emissioner, er ansvarlige for størstedelen af den rumlige differentiering. Yderligere analyser viser, at opholdstiden af kystnært vand er den parameter som har størst indflydelse på karakteriseringsmodellen. Usikkerheden er også højere for denne parameter, primært på grund af knaphed og manglende sammenhæng af datakilder.

Konklusioner

I forhold til state-of-the-art for karakterisering af marin eutrofiering og modellering af skader bidrager denne forskning primært til (i) dækning af den fulde årsags-effekt sammenhæng og dermed slutpunktsvurdering, (ii) en betydelig højere geografisk dækning, (iii) mekanistisk modellering af eksponerings- og effektfaktorer, samt (iv) udvikling af stedspecifikke faktorer for skader på økosystemer baseret på artstæthed. Anvendelse af CFer i LCIA anbefales på niveauet for vandløbsopland, forudsat at placering af udledningen er kendt.

Det fremtidige arbejde bør omfatte skæbnen af luftbårne kvælstofemissioner, for at således fuldstændig at inkludere de relevante miljømæssige mekanismer involveret i marin eutrofiering.

Det nuværende arbejde med modellen, og dens anvendelse som en LCIA metode til marine eutrofiering, kan bidrage med kritiske informationer på forskellige niveauer af beslutningsprocesser og i forhold til forvaltning af menneskelige aktiviteter.

Table of contents

1 Introduction

1.1 Marine eutrophication

Marine eutrophication is the term applied to describe the syndrome of ecosystem responses to the load of a growth-limiting plant nutrient to coastal waters (Smith et al. 1999; Rabalais et al. 2002; Cloern et al. 2016). Nitrogen (N) is assumed to be this growth-limiting nutrient in marine waters (Vitousek et al. 2002; Howarth and Marino 2006). Acknowledging possible spatial and temporal exceptions, due to limitations by phosphorus or silica (Turner et al. 1998; Elser et al. 2007) and cases of co-limitation (Arrigo 2005), that assumption is a necessary and justified simplification for modelling purposes.

The N-enrichment of the euphotic zone (well-lit upper layers) in coastal waters promotes planktonic growth (Chavez et al. 2011). While beneficial to fish populations to a certain extent (Rabalais 2002; Rabalais et al. 2009), the enhanced primary production may lead to excessive accumulation of phytoplankton biomass, which increases water turbidity and reduces light penetration, and in the eventual increase of vertical export of organic matter to bottom waters. In other cases, an imbalance of nutrients ratio may alter phytoplankton species composition and lead to nuisance and toxic algae to growth (harmful algal blooms or HABs, e.g. red tides, blue-green algae or cyanobacteria). The shading effect may lead to the decline and elimination of submerged aquatic vegetation (SAV) and loss of habitat for feeding, predator avoidance, and nursery, among other services (Kelly 2008; Rabalais et al. 2009). HABs may kill living marine resources and be responsible for shellfish poisoning in humans (Diaz et al. 2012). The increased sedimentation of organic matter on the seabed leads to dissolved oxygen depletion in bottom waters due to aerobic respiration by heterotrophic bacteria. If oxygen replenishment is insufficient, due to e.g. low mixing or high density stratification, hypoxic or anoxic conditions

(low or no oxygen, respectively) may onset (Pihl et al. 1992; Conley et al. 2009). With the decreasing oxygen levels, hypoxic stress on exposed demersal animals may reduce their abundance and diversity. The most sensitive and least mobile are affected first; physiological and behavioural responses play a critical role in buffering damage and determining survival (Gamperl and Driedzic 2009; Perry et al. 2009), but as oxygen depletion intensifies death or escape follows (Breitburg 1992; Diaz and Rosenberg 1995). In anoxia, anaerobic bacteria use other compounds than oxygen as electron acceptors (including nitrate NO_3^-, sulphate SO_4^{2-}, and carbon dioxide CO_2) and may lead to the release of e.g. hydrogen sulphide (H_2S) and methane (CH_4) from the sediments (Middelburg and Levin 2009; Reed et al. 2011; Steckbauer et al. 2011) – and these are greenhouse gases and toxic to any metazoan life remaining (Diaz et al. 2012). The pathways of the various marine eutrophication impacts mentioned are compiled in Figure 1. The research work developed in this thesis focuses on the highlighted hypoxia-related pathway – one of the most severe and widespread causes of disturbance to marine ecosystems (GESAMP 2001; Diaz and Rosenberg 2008).

On the whole, eutrophication impacts affect the provision of ecosystem services, namely (i) the supporting service by interfering with e.g. nutrient recycling and primary production, (ii) the provisioning service by potentially reducing the production of e.g. biotic and genetic resources, water and energy, (iii) the regulating service by reducing the capacity for climate and water flow regulation, water filtration and coastal erosion prevention, and (iv) the cultural service from hindered leisure and recreational use, aesthetic and cultural experiences – see more in Böhnke-Henrichs et al. (2013) and Hattam et al. (2015). In addition, other social and economic impacts may stem from the ecological impacts, mainly due to the impairment of the normal use of the services otherwise available. Practical examples may include direct health impacts from water quality degradation and HABs, or indirectly as potential job

and income losses from tourism and leisure activities or from deprived/depressed economic value of commercial resources from affected fishing, aquaculture, boating, and other productive activities – see also UNEP (2006) and UNEP-WCMC (2009).

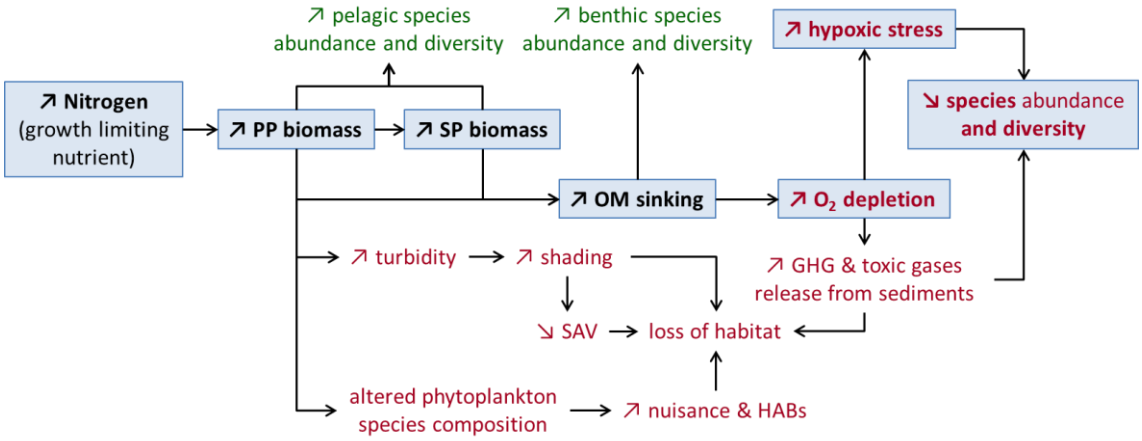

Figure 1 Schematic representation of the causality chain of cascading effects of nitrogen enrichment of coastal waters. Blue shaded boxes represent the pathway for hypoxia-driven marine eutrophication impacts; bold text refers to the processes covered by the research work in this thesis; green text refers to positive effects and red text to harmful effects to the marine ecosystem. Legend: primary producers (PP), secondary producers (SP), organic matter (OM), oxygen (O_2), submerged aquatic vegetation (SAV), greenhouse gases (GHG), harmful algal blooms (HABs).

1.2 Nitrogen sources and emissions

The growing demand for fertilizers use in agriculture and the increase in fossil fuels combustion for energy production have led to an increase of more than 10 fold of reactive nitrogen creation in the last 150 years (Galloway et al. 2008). Human activities are currently mobilizing more than twice the amount of N as natural processes do (Vitousek et al. 1997; Galloway et al. 2004). River basins are exporting 4 to 6 fold more dissolved inorganic nitrogen (DIN) than in the pre-industrial period (Galloway and Cowling 2002; Green et al. 2004). These are clear signs of the anthropogenic alteration of the natural N cycle, extensively reviewed by e.g. Howarth et al. (1996), Vitousek et al. (1997), Van Drecht et al. (2003), Galloway et al. (2008), Lee et al. (2016).

Nitrogen-containing fertilizers are used in agriculture because nitrogen is often a limiting growth factor for crops and forage species (Laegreid et al. 1999; Keeney and Hatfield 2001). Fertilizers in both organic (manure) and inorganic (synthetic) forms are applied worldwide to supplement N to crops and secure agriculture yields (Keeney and Hatfield 2001; Brady and Weil 2007). Other anthropogenic inputs to the N soil budget include biological fixation of atmospheric N_2 to (mainly) NH_4^+ by means of leguminous crops cultivation, and also atmospheric deposition of nitrogen oxides (NO_x) and of volatilised ammonia (NH_3) (Galloway et al. 2004). Crop removal by harvesting and grazing, ammonia volatilization, and denitrification in the soil comprise the processes responsible for the reduction of the N input (Bouwman et al. 2005). The remainder N amount constitutes a surplus. Such N-surplus from agricultural and natural soils constitutes a non-point environmental emission of DIN. Point sources, like sewage water discharges, direct emissions to rivers or to coastal waters, complete the five emission routes to the aquatic system (**Article I**: Cosme et al., 2016b; Van Drecht et al., 2003). The waterborne nitrogen emissions covered by this work refer to DIN forms, i.e. nitrate (NO_3^-), nitrite (NO_2^-), and ammonium (NH_4^+). In the text, the generic term DIN refers to any of these forms. Although airborne N emission, dispersion, and deposition are not modelled here, any quantified amount of nitrogen oxides (NO_x) or ammonia (NH_3) deposited on soil, river or coastal water can be characterised as these.

1.3 Characterisation modelling in life cycle impact assessment

Considering the environmental emissions and consumptions throughout the entire life cycle of products and services, e.g. agri-food products, packaging solutions, or energy production, life cycle assessment (LCA) can be used as an environmental assessment tool. The information provided by such tool may be useful to various levels of decision making and management. LCA is designed to

systematically evaluate the potential impacts of those anthropogenic interventions on the environment (Hauschild 2005). In its life cycle impact assessment (LCIA) phase, impact categories are identified and assigned (selection and classification) to the inventoried quantities of emissions and consumptions (i.e. elementary flows). The flows are then multiplied (characterised) by substance-specific characterisation factors (CFs), which represent the ability of the elementary flows to impact on representative indicators for the impact category (Hauschild and Huijbregts 2015). Marine eutrophication can be one of such indicators.

The development of CFs in LCIA is typically based on characterisation models (Pennington et al. 2004b). A generic model framework for emission-related impact categories proposes that CFs are estimated as the product of a fate factor (FF), an ecosystem exposure factor (XF), an effect factor (EF) on exposed species, and a damage factor (DF) for the severity of the impact on the ecosystem (Udo de Haes et al. 2002). The endpoint impacts are typically attributable to main areas of recognisable value for society and determined worth of protection, i.e. Areas of Protection (AoP) (Udo de Haes et al. 1999; van Zelm 2010), namely 'human health', 'ecosystems' and 'resources depletion' (and approximated variations of these). The unit of the 'Ecosystems' AoP-related indicators (e.g. acidification, ecotoxicity, eutrophication) is expressed as a time and space (or volume) integrated fraction of species potentially disappeared (PDF). If a potentially affected fraction (PAF) of species is derived, a relationship between PAF and PDF must be given for the purpose of harmonisation with indicators of other impact categories.

1.3.1 Current methods for marine eutrophication impacts assessment

Various LCIA methods generically address aquatic eutrophication at a midpoint between emission and damage to the ecosystem (the endpoint) in the impact pathway (Hauschild 2005), e.g. ReCiPe (Goedkoop et al. 2013), EDIP 2003 (Hauschild and Potting 2005), IMPACT 2002+ (Jolliet et al. 2003), and

CML 2002 (Guinée et al. 2002) methods. Only the ReCiPe method and LIME (Itsubo and Inaba 2012) model midpoint impacts specifically for marine eutrophication, however with an European and Japanese scope, respectively. Other methods, like EDIP2003 (Hauschild and Potting 2005), EPS (Steen 1999), LUCAS (Toffoletto et al. 2007), TRACI (Norris 2003), CML 2002 (Guinée et al. 2002) (also used in IMPACT 2002+ (Jolliet et al. 2003) and MEEuP (Kemna et al. 2005)), showing a combined aquatic eutrophication indicator, are based on Redfield ratio's stoichiometric equivalencies to distinguish N and phosphorus (P) flows and model, more or less completely, the environmental fate of emitted substances (including N forms) based on e.g. air and water transport models, except in CML 2002 method. At the endpoint level, however, ReCiPe lacks model work (EC-JRC-IES 2010a; Goedkoop et al. 2013; Hauschild et al. 2013) and LIME has limited extrapolation beyond local Japanese application (Henderson 2015). Also, spatial differentiation for this indicator is insufficiently covered in current methods and a consistent application at global scale is lacking, as only regional or continental coverage is found in most methods for e.g. Europe, Japan, Canada, U.S. (Hauschild et al. 2013; Henderson 2015) – see **Article V**: Cosme and Hauschild (2016a) for details on current LCIA methods for marine eutrophication impacts.

1.3.2 Research needs

Considering the importance of marine eutrophication in many regions of the world, (i) a consistent link between midpoint and damage level, (ii) spatial differentiation at an adequate and relevant resolution, and (iii) a global scale coverage, would be useful improvements to current marine eutrophication impact assessment methods in LCA (Hauschild et al. 2013; Henderson 2015). Extending the impact pathway coverage by adding ecosystem exposure and effects on biota to available midpoint characterisation models, could deliver endpoint-based indicators.

Spatial differentiation has been shown to increase the environmental relevance and discriminatory power of the underlying models (Udo de Haes et al. 2002). This is especially relevant for impact pathways extending at the local to regional scale, i.e. in which the level of impact depends on the location of the emission (Potting and Hauschild 2006), such as marine eutrophication. An adequate spatial resolution, in view of the spatial variability of the impacts, and a wide geographic coverage (ideally global) of the model components (i.e. factors) may increase the environmental relevance of the CFs estimation. This could work towards the increase in compatibility of model results and harmonisation with other LCIA indicators and better applicability of LCA studies.

2 Research goals

Considering (i) the causality chain of the processes leading to marine eutrophication impacts, (ii) the importance of the environmental mechanisms determining the magnitude of those impacts, (iii) the relevance of including spatial differentiation in the modelling of those mechanisms, (iv) that an impact assessment method is lacking in LCIA to consistently link waterborne nitrogen emissions and impacts on marine ecosystems, this thesis grounds its research aims on the development of a model-based method for the quantification of spatially explicit marine eutrophication impacts potentials driven by benthic hypoxia and caused by waterborne nitrogen emissions from anthropogenic sources.

With the above considerations and supported by state-of-the-art science consistent with the accepted LCIA modelling framework, the goals of this thesis are:

- To build a spatially explicit and science-based fate model to describe and quantify the environmental fate processes affecting waterborne nitrogen emissions that contribute to marine eutrophication impacts;
- To describe the processes involved in the exposure of marine ecosystem to nitrogen and quantify its contribution to benthic hypoxia and marine eutrophication impacts by means of a spatially explicit and science-based exposure model;
- To understand the effect of exposure to oxygen-depleted waters on demersal animal species and quantify such effect on exposed ecological communities by means of a spatially explicit effect model;
- To derive spatially explicit damage factors to express the severity of the impacts to the ecosystem;
- To describe a method that combines the fate, exposure, effect and damage models in an overall spatially explicit characterisation model at a global

scale that is able to link the waterborne nitrogen emissions to the loss of marine demersal species as an indicator for the damage to ecosystems dimension;

– To discuss the applicability of such method and characterisation model in the context of LCIA.

The thesis is structured as follows. First, the fate, exposure, and effect factors based on model work published in **Article I**: Cosme et al. (2016b), **Article II**: Cosme et al. (2015), and **Article III**: Cosme and Hauschild (2016b), are described, then the estimation of damage to ecosystems based on species density is presented in **Article IV**: Cosme et al. (2016a), and the CFs for waterborne nitrogen emission composed from those models is given in **Article V**: Cosme and Hauschild (2016a). Finally, an application of the characterisation model and its adaptation to the influence of climate change in the CF parameterisation, is described in **Article VI**: Cosme and Niero (2016).

3 Model development

The research work introduced here, and described in the accompanying articles, addresses the development of a LCIA characterisation model for the estimation of CFs for waterborne nitrogen emissions with impacts on marine eutrophication induced by benthic hypoxia. The proposed model is consistent with the generic framework proposed by Udo de Haes et al. (2002). In this line, factors for environmental fate, ecosystem exposure and its effects on target species, and damage to ecosystems, were developed. The method defined for that, is briefly described in the sections ahead, and fully documented in the accompanying articles provided in the appendices. The illustration in Figure 2 summarises and structures the work done, identifying the impact pathway (i.e. cause-effect chain) and the model components.

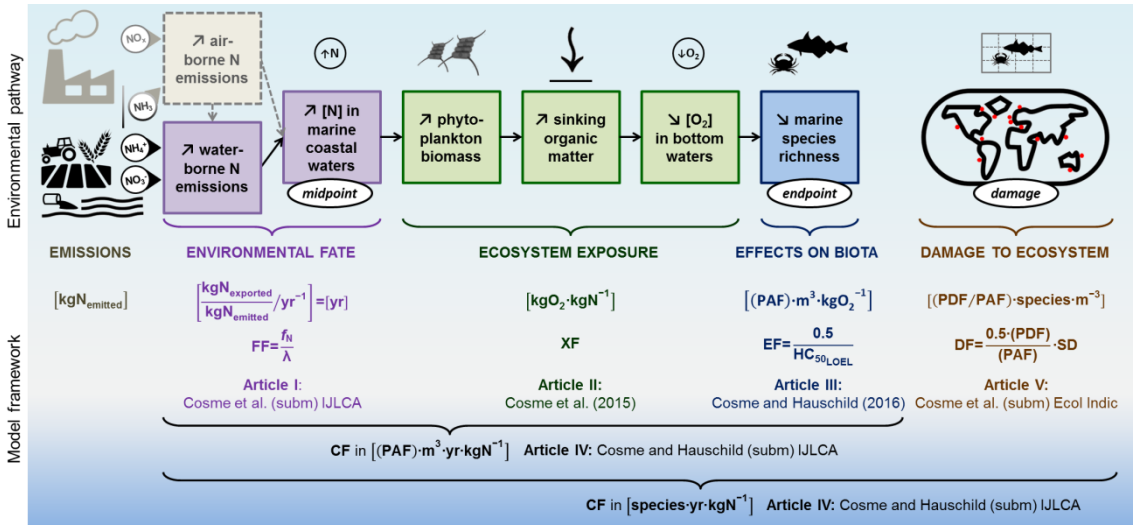

Figure 2 Characterisation model for the marine eutrophication indicator in life cycle impact assessment (LCIA). Representation of the hypoxia-related impact pathway for waterborne nitrogen (N) emissions and model framework used for the development of fate (FF), exposure (XF), effects (EF), and damage factors (DF), with indication of the respective reference documentation. Atmospheric fate modelling of airborne N emissions are excluded (shaded and dashed objects). Adapted from **Article V**: Cosme and Hauschild (2016a).

The model work behind the method is based on the linearity of the causality that forms the impact pathway – emissions trigger responses that cause

impacts, which are proportional to the substance flows emitted. To that aim, the fate model work in **Article I**: Cosme et al. (2016b) describes the environmental fate processes of N in soil and riverine systems, aggregated at a river basin scale (Vörösmarty et al. 2000), and in the coastal marine compartment, at Large Marine Ecosystem (LME) scale (Sherman and Alexander 1986). The ecosystem exposure to N and the oxygen depletion that results from the organic matter degradation are modelled at a LME scale in **Article II**: Cosme et al. (2015). Effect factors, based on the sensitivity of marine species to hypoxia, are modelled for five climate zones, later disaggregated to 66 LMEs, in **Article III**: Cosme and Hauschild (2016b). Demersal species richness per LME are used to estimated species densities and damage factors at that resolution in **Article IV**: Cosme et al. (2016a). Factors are applied together in **Article V**: Cosme and Hauschild (2016a) to estimate endpoint CFs in [(PAF) $\cdot m^3 \cdot yr \cdot kgN^{-1}$], or damage CFs in [species$\cdot$yr$\cdot kgN^{-1}$] as summarised in Eq. (1) for waterborne nitrogen emissions with hypoxia-related eutrophying impacts:

$$CF_{i,jl} = FF_{i,jl} \times XF_l \times EF_l \times DF_l \qquad \text{Eq. (1)}$$

where $FF_{i,jl}$ [yr] is the fate factor for emission route *i* in river basin *j* to receiving ecosystem *l*, XF_l [$kgO_2 \cdot kgN^{-1}$] the exposure factor, EF_l [(PAF)$\cdot m^3 \cdot kgO_2^{-1}$] the effect factor, and DF_l [(PDF/PAF)$\cdot$species$\cdot m^{-3}$] the damage factor in ecosystem *l*. As each river basin exports to a single LME, *jl* are coupled in the subscript of CF and FF notations.

The LME biogeographical classification system (Sherman and Alexander 1986) divides the coastal waters of the planet into 66 spatial units, from river basins and estuaries to the seaward boundaries of continental shelves and the outer margins of the major ocean current systems (Sherman et al. 2009)

3.1 Environmental fate of waterborne nitrogen emissions

In the LCIA framework, FFs quantify the persistence of a substance in the environment (**Article I**: Cosme et al., 2016b; Henderson et al. 2011). This thesis proposes a method based on the quantification of (i) the fraction of the original DIN emission that reaches coastal waters, by modelling soil-to-river and in-river removal processes (i.e. the inland component, modelled at a river basin scale), and (ii) the removal processes in the receiving marine compartment (i.e. the marine component, modelled at a LME scale). These components, combined in Eq. (2), were applied to derive spatially explicit FFs for 5,772 river basin of the world (**Article I**: Cosme et al., 2016b).

$$FF_{i,jl} = \frac{f_{N_{i,j}}}{\lambda_l} = \frac{f_{N_{i,j}}}{\lambda_{adv,l}+\lambda_{denitr,l}} = \frac{f_{N_{i,j}}}{\frac{1}{\tau_l}+\lambda_{denitr,l}} \quad \text{Eq. (2)}$$

where the fate factor (FF, [yr]) is calculated for each emission route *i* in river basin *j* to receiving ecosystem *l*, as the product of the fraction exported to coastal waters (f_N, [dimensionless]) and the inverse of the sum of the removal rates (λ, [yr^{-1}]) by denitrification (λ_{denitr}, [yr^{-1}]) and advection ($\lambda_{adv,l}$, [yr^{-1}]). The latter corresponds to the inverse of the surface water residence time (τ_l, [yr]). The emission routes *i* are defined as 'N from natural soil' (N_{ns}), 'N from agricultural soil' (N_{as}), 'N in sewage to river' (N_{sew}), 'N to river' (N_{riv}), and 'N to marine water' (N_{marw}).

The estimation of the inland component is described in detail in **Article I**: Cosme et al. (2016b) and is based on the DIN-removal processes coefficients extracted from the second generation of the Global Nutrient Export from WaterSheds model (NEWS 2-DIN) (Dumont et al. 2005; Seitzinger et al. 2005; Seitzinger et al. 2010; Mayorga et al. 2010). These coefficients correspond to (i) calibrated runoff functions from natural and agricultural soils, (ii) empirical DIN

fractions in discharged sewage water, and (iii) riverine DIN losses by denitrification, retention, and water consumption. In the marine fate component, the surface water residence time is used to derive the advective transport removal and empirically relate to the removal by denitrification (see details in **Article I**: Cosme et al., 2016b).

Estimated FFs at a river basin scale (Table 1) show a decrease from a maximum for direct emissions to marine water (N_{marw}), intermediate values for emissions to river and sewage water (N_{riv} and N_{sew}, respectively), and minimum for agricultural and natural soils (N_{as} and N_{ns}, respectively). Spatial variability shows 6 orders of magnitude for soil-related emissions (N_{ns}, N_{as}), 4 for river-related emissions (N_{riv}, N_{sew}), and 2 for marine water emissions (N_{marw}). The global distribution of FFs for the five emission routes are given in **Article I**: Cosme et al. (2016b). The results for the emission route 'N from agricultural soil' are shown in Figure 3.

Table 1 Statistics of the distribution of fate factors (FF_{N_i}) results per emission route at a river basin scale. Adapted from **Article I**: Cosme et al. (2016b).

Statistics	FF [yr] per emission route				
	N_{ns}	N_{as}	N_{sew}	N_{riv}	N_{marw}
Minimum	1.7E-06	1.7E-06	1.1E-04	2.2E-04	0.024
Mean	0.17	0.28	0.58	1.0	1.9
Maximum	4.6	4.6	5.2	7.7	13
Spatial variability	*3E+06*	*3E+06*	*5E+04*	*3E+04*	*5E+02*

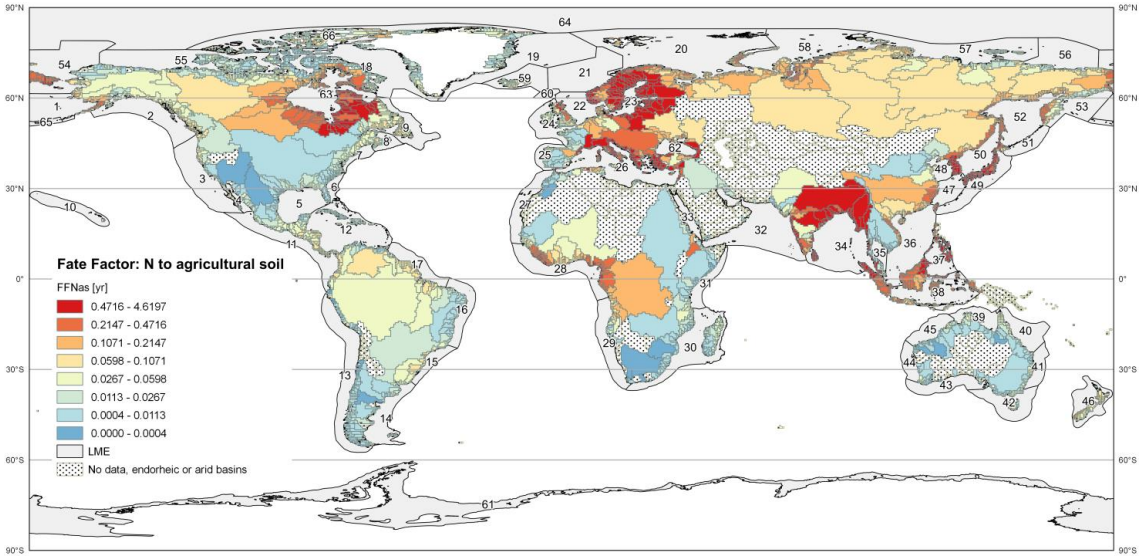

Figure 3 Distribution of the fate factors (FF_{Nas}, [yr]) for marine eutrophication due to nitrogen (N) emissions from agricultural soils (watershed runoff) to river at a basin resolution. Dotted areas correspond to basins that are arid (mainly Arabian Peninsula, Northern Africa and Southwest Australia), endorheic, or for other reason have no available FF. Note the non-linear scale. Retrieved from **Article I**: Cosme et al. (2016b).

Spatial differentiation in fate model work for nutrients emissions has been adopted in various LCIA methods – EDIP2003 (Hauschild and Potting 2005), ReCiPe (Goedkoop et al. 2013), LUCAS (Toffoletto et al. 2007), and TRACI (Norris 2003), however at a coarse spatial resolution and limited scope (see **Article I**: Cosme et al., 2016b). The fate model developed in this thesis work, consistently applied to waterborne N emissions at the global scale, and the spatially explicit results at a river basin resolution, represent a significant increase in geographic coverage for application in LCIA.

3.2 Exposure of marine coastal waters to DIN

Coastal marine ecosystems respond to the increase of DIN inputs by increasing primary production (PP), i.e. the photosynthetic reduction of inorganic carbon into energy-rich organic carbon involving the assimilation of inorganic dissolved plant nutrients and the utilization of light energy by primary producers, mainly phytoplankton, in the well-lit upper layers of the ocean (euphotic zone)

(Falkowski and Raven 2007; Chavez et al. 2011). The synthesised phytoplankton biomass fuels the organic carbon cycles that eventually contribute to the vertical carbon export to bottom layers of the water column, where it is degraded. These biologically mediated processes were modelled in **Article II**: Cosme et al. (2015) as N-limited PP, metazoan consumption, and bacterial degradation, in four distinct carbon sinking routes to derive 'conversion' potentials of N-uptake into organic carbon and into oxygen consumption. These 'conversion' potentials were defined as ecosystem exposure factors (XF, [$kgO_2 \cdot kgN^{-1}$]).

Model details and results are available in **Article II**: Cosme et al. (2015) as spatially-explicit XFs for 66 LMEs worldwide (see distribution in Figure 4), varying from 0.45 $kgO_2 \cdot kgN^{-1}$ in the central Arctic Ocean to 15.9 $kgO_2 \cdot kgN^{-1}$ in the Baltic Sea.

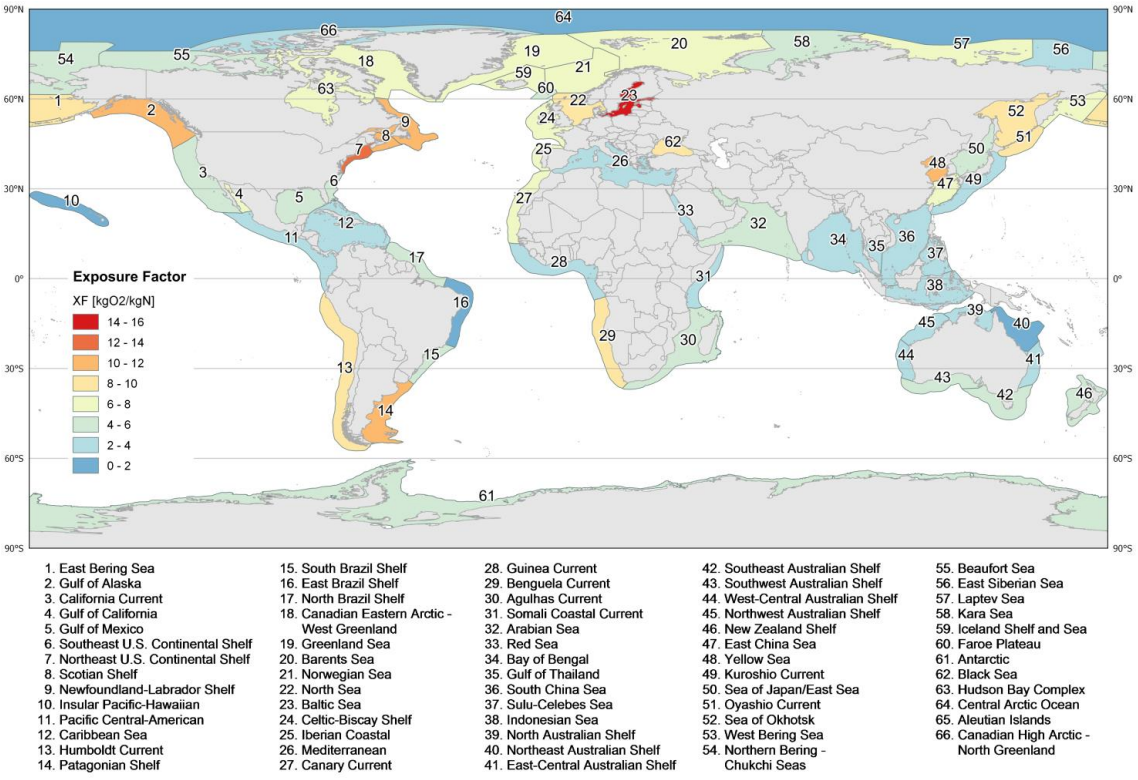

Figure 4 Distribution of ecosystem exposure factors (XF) estimated per large marine ecosystem (LME). Retrieved from **Article IV**: Cosme et al. (2016a), adapted from **Article II**: Cosme et al. (2015).

3.3 Effects of hypoxia on exposed species

Low concentrations of dissolved oxygen (DO) in bottom layers of the water column may be due to oxygen consumption (from the aerobic respiration of organic matter) in excess of the system's ability to replenish its levels. Strong vertical density stratification may hinder mixing and gas transfer into bottom layers, and lead to the onset of hypoxic or even anoxic conditions (Rosenberg et al. 1991; Pihl et al. 1992; Conley et al. 2009). Excessive oxygen depletion have effects on exposed species that range from physiological to behavioural (Davis 1975; Diaz and Rosenberg 1995; Gray et al. 2002; Miller et al. 2002; Vaquer-Sunyer and Duarte 2008; Levin et al. 2009; Ekau et al. 2010); Impacts listed in Table S1 (Supporting Information) of **Article III**: Cosme and Hauschild (2016b).

Demersal species, including benthic and benthopelagic, are those that depend, to some extent, on the bottom habitat to feed, hide, and reproduce. Each species have its own threshold sensitivity to hypoxia, i.e. the lowest stressor intensity (highest DO concentration) at which an alteration of the biological endpoint tested is triggered. The sensitivity thresholds to hypoxia of 91 species were converted to temperature-dependent DO concentrations corresponding to sea bottom water temperature at 100 m depth (a necessary model simplification) in a method described and discussed in **Article III**: Cosme and Hauschild (2016b). The resulting 582 sensitivity data points were then integrated with a species sensitivity distribution (SSD) probabilistic function (Posthuma et al. 2002) to derive a hazard concentration HC_{50} value per climate zone (CZ), i.e. the concentration of DO affecting 50% of the species above their threshold. The effect factors (EF, $[(PAF)\cdot m^3\cdot kgO_2^{-1}]$), expressed in a potentially affected fraction (PAF) of species metric, were then calculated as the variation of the effect on the exposed community (ΔPAF, dimensionless) due to a variation of the stressor intensity (ΔDO, $[kgO_2\cdot m^{-3}]$) in receiving ecosystem *l*, Eq. (3), following the current scientific consensus and the average gradient approach (Pennington et al. 2004a; Larsen and Hauschild 2007).

$$EF_l = \frac{\Delta PAF_l}{\Delta DO_l} = \frac{0.5}{HC_{50l}} \qquad \text{Eq. (3)}$$

The estimated EFs are available at a five climate zone scale (Table 2) and can be disaggregated into the respective LMEs (Figure 5) by applying a correspondence key based on sea bottom water temperature (see **Article III**: Cosme and Hauschild (2016b)).

Table 2 HC_{50} values and effect factors (EF) estimated per climate zone and a global average. For method details see **Article III**: Cosme and Hauschild (2016b).

Climate zone	HC_{50} [$mgO_2 \cdot L^{-1}$]	EF [$(PAF) \cdot m^3 \cdot kgO_2^{-1}$]
Polar	2.3	220
Subpolar	2.1	240
Temperate	1.8	280
Subtropical	1.8	270
Tropical	1.6	310
Global	1.9	260

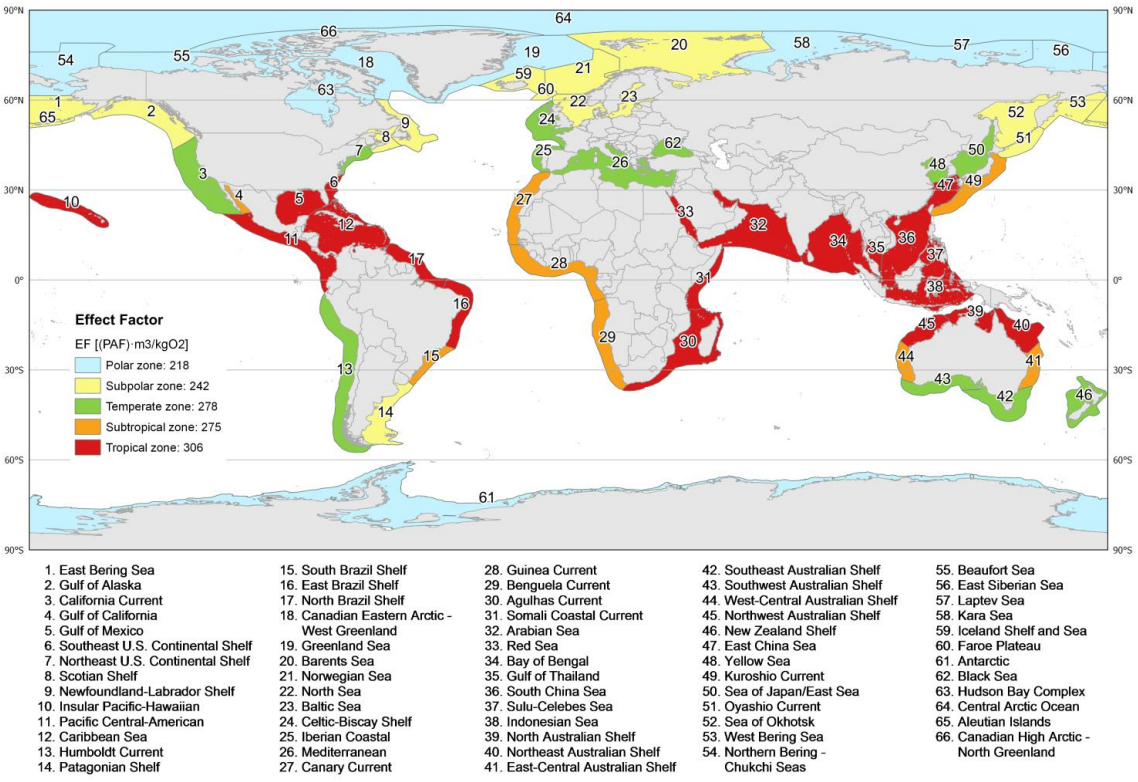

Figure 5 Distribution of effects factors (EF, $(PAF) \cdot m^3 \cdot kgO_2^{-1}$) disaggregated from climate zones to large marine ecosystem (LME). Retrieved from **Article IV**: Cosme et al. (2016a), produced with data from **Article III**: Cosme and Hauschild (2016b).

3.4 Damage to ecosystems

Loss of biodiversity is the dimension that the damage indicators are trying to express. The loss of species richness is currently the practice in LCIA, due to the limitations of the methodological framework itself (Curran et al. 2011), although alternative approaches are being explored – e.g. Lindeijer (2000); Souza et al. (2013); Verones et al. (2015). The loss of species accounted in the potentially disappeared fraction (PDF) of species metric is intended to cross-represent the indicators of the impacts categories contributing to the 'Ecosystems' AoP. Methodologically, these impact scores can be aggregated to express the joint damage to ecosystems (Udo de Haes et al. 1999). However, diverse metrics are found in LCIA methods: (PDF)·$m^{2\ or\ 3}$·yr (respectively for area or volume and time integrated PDF) and similarly for PAF-based indicators (like in ecotoxicity impacts estimation based on the USEtox model (Rosenbaum et al. 2008)), increase in number of extinct species (EINES) (Itsubo and Inaba 2012), or normalized extinction of species (NEX, dimensionless) (Steen 1999) – see discussion in **Article IV**: Cosme et al. (2016a).

Harmonisation of the present marine eutrophication indicator (a PAF-based metric), requires conversion to a PDF-based metric. **Article IV**: Cosme et al. (2016a) discusses the adoption of a site-generic 0.5 factor from PAF to PDF (i.e. the assumption that half the species affected above their sensitivity to hypoxia threshold disappear). Potential developments towards spatial explicit adjustment of such conversion factor are also discussed there, by adding e.g. vulnerability or recoverability indices.

Both PAF- and PDF-based units are relative metrics – they simply represent a fraction of species, useful for certain comparative assessments but unable to fully quantify the damage to ecosystems it tries to represent. This is tied in with the limitation that these units do not necessarily refer to a comparable biotic component of the ecosystem – see discussion in **Article IV**: Cosme et al. (2016a).

Terrestrial, freshwater, and marine species may all be quantified differently in the PDF-based metric of different indicators (e.g. ecotoxicity, eutrophication, acidification, land use) and the use of a fraction may misrepresent the actual magnitude of the impact. As such, the spatial distribution of species and the different composition of ecological communities may be useful to beat the limitation given by a relative metric.

Species occurrence is typically heterogeneous in time and space (Levin 1994). The variability of this occurrence may be critical to consistently quantify the damage in impact pathways occurring at local to regional scales (like marine eutrophication). To overcome this limitation, LME-dependent species density values were developed (**Article IV**: Cosme et al. 2016a) (Figure 6) and applied as a damage factor (DF) (see also Figure 2) to estimate spatially explicit damage to marine eutrophication as an absolute, and LME-dependent, metric for loss of species richness. This approach was adopted earlier in the ReCiPe impact method (Goedkoop et al. 2013) but with a (too) coarse differentiation into site-generic terrestrial, freshwater, and marine species density.

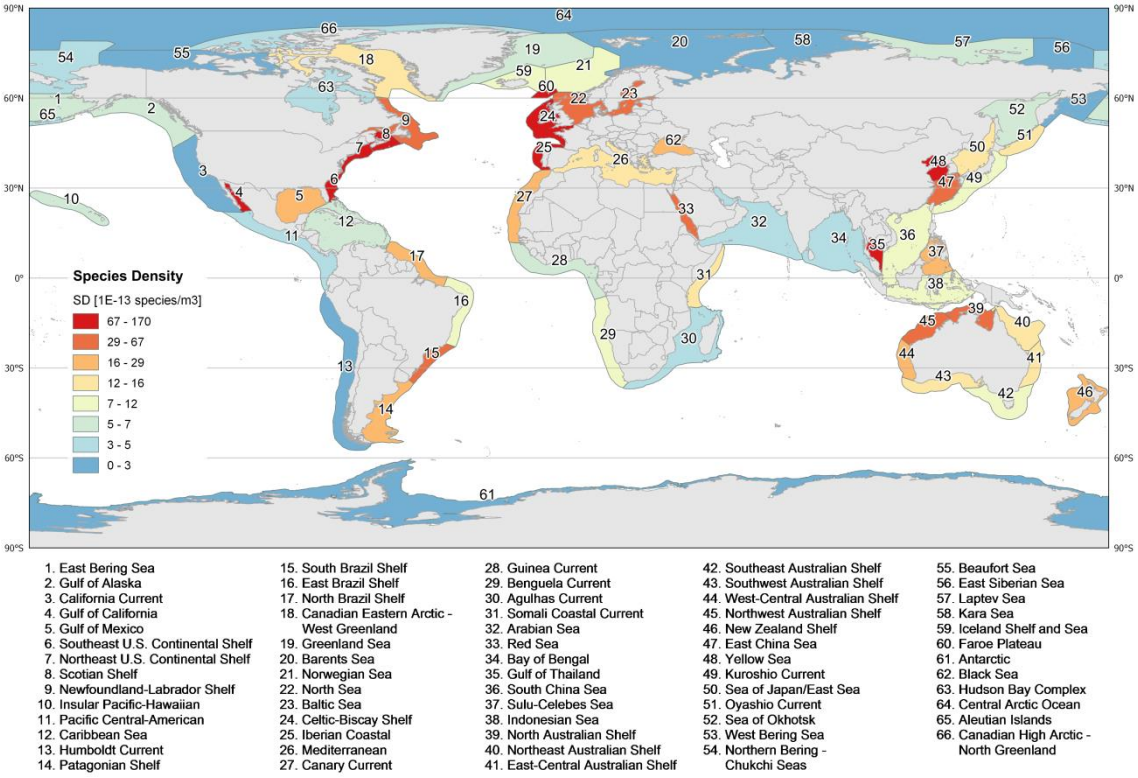

Figure 6 Distribution of demersal marine species density (SD, species·m^{-3}) per Large Marine Ecosystem (LME) species. Note the non-linear scale. Retrieved from **Article IV**: Cosme et al. (2016a).

3.5 Characterisation factors

As seen from Eq. (1) and Figure 2 the endpoint CFs integrate the fate, exposure and effect terms, and additionally the damage factor for the calculation of LME-dependent damage CFs. The factors, which the terms refer to, were adopted from the underlying models described in the previous sections and presented in the supporting articles. The CFs were therefore calculated at a river basin (5,772) scale for the five identified emission routes – 'N from natural soil' (N_{ns}), 'N from agricultural soil' (N_{as}), 'N in sewage water to river' (N_{sew}), 'N to river' (N_{riv}), and 'N to marine water' (N_{marw}), thus totalling 28,860 CFs. A list of these can be found in Electronic Supplementary Material 2 of **Article V**: Cosme and Hauschild (2016a), along with distribution maps of the resulting CFs per river basin of the world for each of the emission routes (in Electronic

Supplementary Material 1), exemplified here for 'N from agricultural soil' (Figure 7).

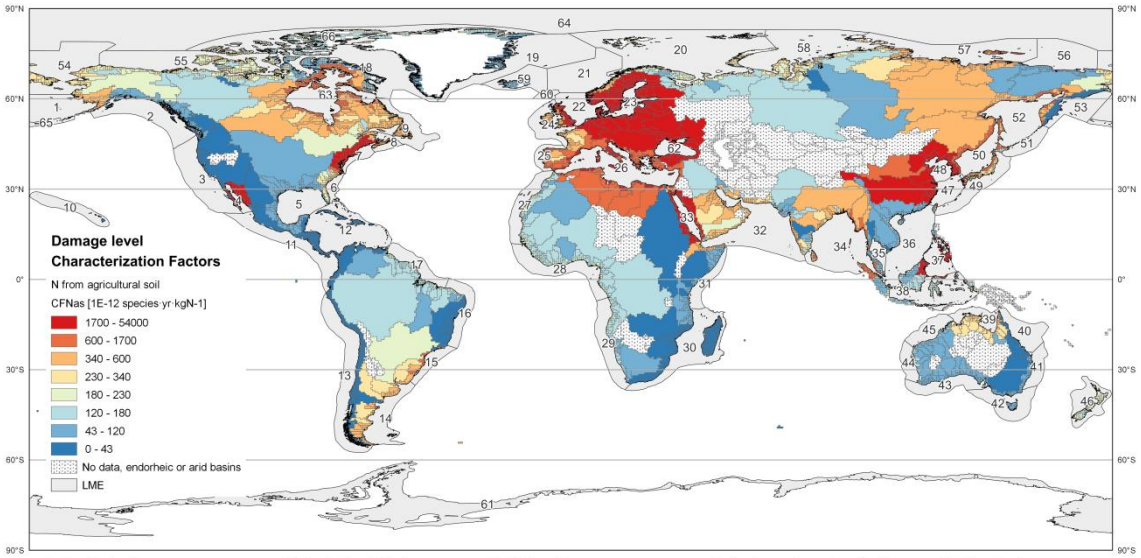

1. East Bering Sea
2. Gulf of Alaska
3. California Current
4. Gulf of California
5. Gulf of Mexico
6. Southeast U.S. Continental Shelf
7. Northeast U.S. Continental Shelf
8. Scotian Shelf
9. Newfoundland-Labrador Shelf
10. Insular Pacific-Hawaiian
11. Pacific Central-American
12. Caribbean Sea
13. Humboldt Current
14. Patagonian Shelf
15. South Brazil Shelf
16. East Brazil Shelf
17. North Brazil Shelf
18. Canadian Eastern Arctic - West Greenland
19. Greenland Sea
20. Barents Sea
21. Norwegian Sea
22. North Sea
23. Baltic Sea
24. Celtic-Biscay Shelf
25. Iberian Coastal
26. Mediterranean
27. Canary Current
28. Guinea Current
29. Benguela Current
30. Agulhas Current
31. Somali Coastal Current
32. Arabian Sea
33. Red Sea
34. Bay of Bengal
35. Gulf of Thailand
36. South China Sea
37. Sulu-Celebes Sea
38. Indonesian Sea
39. North Australian Shelf
40. Northeast Australian Shelf
41. East-Central Australian Shelf
42. Southeast Australian Shelf
43. Southwest Australian Shelf
44. West-Central Australian Shelf
45. Northwest Australian Shelf
46. New Zealand Shelf
47. East China Sea
48. Yellow Sea
49. Kuroshio Current
50. Sea of Japan/East Sea
51. Oyashio Current
52. Sea of Okhotsk
53. West Bering Sea
54. Northern Bering - Chukchi Seas
55. Beaufort Sea
56. East Siberian Sea
57. Laptev Sea
58. Kara Sea
59. Iceland Shelf and Sea
60. Faroe Plateau
61. Antarctic
62. Black Sea
63. Hudson Bay Complex
64. Central Arctic Ocean
65. Aleutian Islands
66. Canadian High Arctic - North Greenland

Figure 7 Global distribution of the marine eutrophication characterisation factors (CF_{Nas}, [species·yr·kgN-1]) at the damage to ecosystem level for emissions from agricultural soil at a river basin scale. Note the non-linear scale.

3.5.1 Spatial differentiation

The analysis of the damage CFs estimated (Table 3) shows spatial differentiation of almost 8 orders of magnitude for the soil-related emissions, 6 for the river-related, and 4 for direct emissions to marine waters. The CF values increase from the coastal waters over to river-related discharges and to soil-related emissions, i.e. reflecting a pattern of reduction of the marine eutrophication potential as the emission point moves further away from the sea in the hydrological cycle (**Article V**: Cosme and Hauschild 2016a). Finally, higher factors tend to verify in river basins discharging to LMEs with (i) longer residence times, such as the Baltic Sea (LME #23), Bay of Bengal (#34), Sulu-

Celebs Sea (#37), Mediterranean Sea (#26), Black Sea (#62) and Hudson Bay Complex (#63), and (ii) denser species occurrence, namely in the Northeast and Southeast U.S. Continental Shelves (LME #7 and #6, respectively), Gulf of California (#4), Gulf of Thailand (#35), Iberian Coastal (#25), Scotian Shelf (#8), and Yellow Sea (#48) (**Article V**: Cosme and Hauschild 2016a).

Table 3 Statistics of the distribution of characterisation factors (CF_{N_i}) at damage level per emission route at a river basin scale. Adapted from **Article V**: Cosme and Hauschild (2016a).

Statistics	CF [species·yr·kgN^{-1}] per emission route				
	N_{ns}	N_{as}	N_{sew}	N_{riv}	N_{marw}
Minimum	3.9E-16	3.9E-16	2.5E-14	5.1E-14	5.0E-12
Mean	3.9E-10	4.5E-10	1.0E-09	1.7E-09	3.4E-09
Maximum	3.2E-08	3.2E-08	3.6E-08	5.4E-08	8.8E-08
Spatial variability	*8E+07*	*8E+07*	*1E+06*	*1E+06*	*2E+04*

Similar results per emission route and spatial differentiation are found in the analysis of the endpoint CF results expressed in (PAF)·m^3·yr·kgN^{-1} (see **Article V**: Cosme and Hauschild (2016a)). Differentiation is however lower by ca. 1.5 orders of magnitude revealing the effect of the species density applied in the damage factor that varies by 3 orders of magnitude among LMEs (**Article IV**: Cosme et al. 2016a).

3.5.2 Regional aggregation

Regionally aggregated and global site-generic CFs may be useful when spatial information is only available at a coarse resolution or not available (or relevant) at all, respectively. Spatially aggregated CFs over regions/continents were calculated by emission-weighted averages – see data and calculation details in **Article V**: Cosme and Hauschild (2016a). Aggregated CFs score consistently higher for Europe across all five emission routes, spatial differentiation is modest (varying between 1.4 and 2.1 orders of magnitude) with no relevant differences between emission routes. North and South America consistently show higher variability in all emission routes, except for marine emissions, for which no dominance is noticeable (**Article V**: Cosme and Hauschild 2016a).

3.5.3 Contribution analysis

A regression analysis of the contribution of the different factors to the differentiation found in the CFs showed a dominant contribution by FF, followed by SD in any of the emission routes (**Article V**: Cosme and Hauschild 2016a). The EF variation had no significant contribution mainly due to the low spatial differentiation and, more importantly, the different (and coarser) spatial resolution at climate zones. In fact, the justification for these results may lie on the scale at which the factors are modelled – EF results are differentiated at a five climate zone scale, whereas SD and XF are at a 66 LME scale and FF at a 5,772 river basin scale.

3.5.4 Model sensitivity, uncertainty and key issues

The sensitivity of the CF model to the various parameters applied in the estimation of the composing factors was tested by means of calculation of sensitivity ratios (SRs) for all the relevant parameters. SR results show highest, and the most relevant, model sensitivity to variations in surface water residence time (applied in the FF estimation); this value is followed by PP rate (applied in XF estimation) (**Article V**: Cosme and Hauschild 2016a). Inconsistency and scarcity of LME-dependent data for surface water residence time were identified as major reasons for the uncertainty (**Article I**: Cosme et al. 2016b). Residence time is applied to estimate N-removal by advection and denitrification in the marine fate modelling component of the FF. Given the high model sensitivity and the uncertainty indications, the surface water residence time is assigned as the key issue in the CFs modelling.

4 Discussion on the applicability in LCIA

4.1 Characterisation of future emissions

As seen earlier, the conversion of inventoried flows of emissions and consumptions into potential impacts on indicators for specific categories is done in the characterisation step in LCIA by applying characterisation factors (Hauschild and Huijbregts 2015). These are based on characterisation models that quantitatively represent the environmental mechanism(s) responsible for the causality from emission or consumption into impact. The model work developed to estimate CFs for marine eutrophication, described in this thesis, shows relevant spatial differentiation by assigning documented variability to most of the parameters of the various composing factors. However, temporal variability is not accounted for, so the impacts typically represent the annual integration given by the inventoried flows (Hauschild 2005). Short term variability (intrannual) might be relevant for this impact category given the seasonality of primary production and plankton species succession, determined by both nutrients and light availability, as also noted in **Article II**: Cosme et al. (2015) as a potential model improvement.

An attempt to introduce the influence of long term variation of environmental conditions in the characterisation model work was done in **Article VI**: Cosme and Niero (2016). In that exploratory research, future environmental conditions altered by the effect of a changing climate, were considered in the parameterisation of some governing terms in the factors' modelling. The analysis of the time variation compares the marine eutrophication impacts of contemporary and future nitrogen emissions from spring barley production in Denmark, based on the inventory data of a case study by Niero et al. (2015). There, N emissions were found to increase in the future scenario mainly due to reduced production yield. The influence of climate change (mainly temperature

increase) was introduced in the FF, XF, and EF modelling – see Table 2 in **Article VI**: Cosme and Niero (2016). However, the fate modelling used there does not refer to the one developed in **Article I**: Cosme et al. (2016b), rather it is based on the one developed for the LC-IMPACT project (Azevedo et al. (2013); http://www.lc-impact.eu) – the models are similar in essence, but the latter, although at a coarser resolution, includes fate modelling of atmospheric deposition of nitrogen oxides (NO_x) and ammonia (NH_3) modelled at a country-scale.

The comparison of the impacts on two distinct spatial units receiving emissions from the production in Denmark (the North Sea and the Baltic Sea), quantifies the spatial differentiation in either the contemporary production system and in the future scenario, whereas the comparison between time scenarios quantifies the influence of the modified model parameterisation (i.e. CFs). Damage factors, adopted from **Article IV**: Cosme et al. (2016a) were further applied to estimate damage in the two receiving coastal areas. The assessment shows an increase of impacts from the present to the future scenario (Figure 8) in both the North Sea and Baltic Sea (factors 1.34 and 1.28, respectively), and 2.5 and 2.3 times higher in the Baltic Sea for the present and future scenario, respectively.

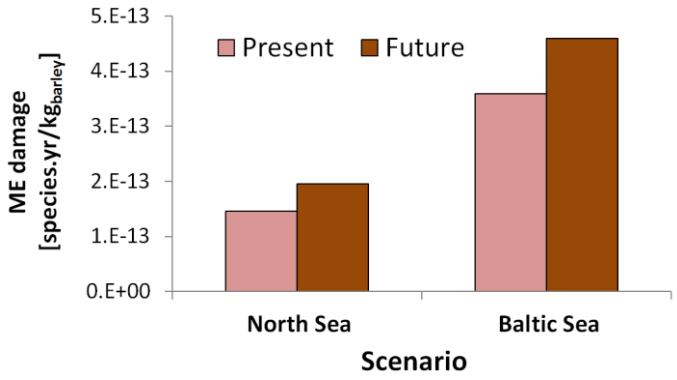

Figure 8 Marine eutrophication (ME) damage scores for nitrogen emissions to the North Sea and Baltic Sea from spring barley production in Denmark in present and future scenarios. Retrieved from **Article VI**: Cosme and Niero (2016).

Regardless of the inconsistency between the fate model used in Azevedo et al. (2013) and recent waterborne N fate modelling (**Article I**: Cosme et al. 2016b) applied in the development of CFs, this exploratory research is useful as a proof of concept for forecast modelling of marine eutrophication impacts and its relevance to LCA in the assessment of environmental performance and sustainability of human activities. Further work is required to improve the influence of future environmental pressures in the marine eutrophication impact pathway both qualitatively and quantitatively.

4.2 Major assumptions

In the fate modelling of the inland component, the approach adopted uses watershed-aggregated export fractions from the NEWS 2-DIN model. As no finer scale is possible, an assumption is forced, i.e. emissions located upstream or downstream in the watershed are equivalent as they result in the same export fraction coefficient – see discussion in **Article I**: Cosme et al. (2016b) for subtleties of the assumption.

In the XF estimation model work, the match-mismatch hypothesis (Cushing 1975) is an important assumption in the quantification of the algal biomass fraction that sinks off the euphotic zone and the fraction that is consumed by zooplankton and modelled further on. Under ‘match’ events biomass is grazed, whereas under ‘mismatch’ a larger fraction is left ungrazed and sinks. The coefficients used to quantify those fractions are assumed representative of that phenomenon in the five climate zones differently. Not surprisingly, as a conceptual description of a complex natural phenomenon (Cushing 1990; Durant et al. 2007), any estimation of the actual variability of the parameters under this hypothesis is of questionable relevance, however the concept has wide scientific acceptance. Details of this discussion are found in **Article II**: Cosme et al. (2015).

The effects of hypoxia on demersal species are estimated based on water temperatures at 100 m depth. This particular depth corresponds to a model simplification based on the assumption that all those species occur at half the depth of the continental shelf to represent average conditions of the benthic habitat (Tait and Dipper 1998; UNESCO 2009). In natural conditions, species occur in habitats at different depths within the continental shelf, in which water temperature varies differently than that modelled, and thus sensitivity threshold concentrations (LOECs) may vary significantly from those used to estimate $HC50_{LOEC}$ and EFs. See also the discussion on modelling average conditions in **Article III**: Cosme and Hauschild (2016b) for its relevance in the assumed representativeness of data and results. Only under such approach, species that may typically occur at shallower depths (probably above the oxycline) and are exposed to advective mixing (from winds, waves, and currents) that reduces the chance of hypoxic conditions, can still be modelled towards the estimation of EFs.

The biological endpoints tested in the experimental work to determine species sensitivity to oxygen are assumed to be equivalent, when in fact they represent responses that are not consistent, e.g. avoidance behaviour and physiological rates change. A loose definition of oxygen sensitivity threshold as the ambient DO concentration at which a response is measured or observed, may therefore best apply. See the sensitivity estimation method in **Article III**: Cosme and Hauschild (2016b) to complement on this discussion.

The EF estimation is based on the GM_{taxon} to derive $HC50_{LOEC}$ values (i.e. geometric mean at taxon level of the geometric mean of LOECs at species level) (**Article III**: Cosme and Hauschild 2016b). This calculation method assumes that very tolerant or very sensitive species data are due to the uncertainty of their estimation (not to the true value of their sensitivity threshold) and then minimises the influence of this variability.

The temporal and spatial aggregation of impacts, expressed in the indicator units, assumes that (i) there are no peaks of oxygen depletion throughout the year and within the benthic area of the LME, (ii) species occur equally dispersed, i.e. no patchiness, contrary to real situations (Levin 1994), (iii) species do overlap in time and space thus composing the modelled community and justifying its joint estimated sensitivity, and (iv) no trophic relationships or any other biotic interactions, that could distort the joint sensitivity values, verify.

The species richness values, used to estimate species density (SD) per LME, are based on data from commercial species. Predicted SDs may be biased by the sampled species and taxonomic resolution of catch statistics. See discussion on the species estimation method and assumptions associated with species distribution models (SDMs) in **Article IV**: Cosme et al. (2016a) and references therein. Nevertheless, those species and SDs are assumed to be representative of the ecological communities in the respective spatial units.

The assumption that one half of the species affected (expressed in the PAF-based metric) would tend to not occur (and be included in the PDF-based metric), i.e. a factor of 0.5, was chosen to define the metrics conversion (**Article IV**: Cosme et al. 2016a). Some considerations are drawn on the seasonality of the planktonic production, water temperature, and N emission flows, to justify this assumption under an annual integration of impacts, but objectively the value is still arbitrary. Finally, all species are valued equally for the damage quantification as their e.g. vulnerability, recoverability, rareness, or endemism, is not considered. A 'media recovery' is also assumed i.e. species reappear when the stressor intensity is reduced below their sensitivity threshold (Larsen and Hauschild 2007). See discussion in **Article IV**: Cosme et al. (2016a) addressing the shortcomings of the damage factor estimation and potential ways of improving metrics harmonisation.

4.3 Sources of uncertainty

The N-removal coefficients extracted from the NEWS 2-DIN model, applied in the inland fate component of the FF, are based on regression models that lump processes into watershed-aggregated export constants. These use watershed-dependent empirical runoff coefficients, which regard emission points as the whole watershed, thus lacking the spatial differentiation and predictive ability given by finer grid cell based models. The calibration of the NEWS 2-DIN, i.e. predicted against observed DIN yields at river mouths in 66 river basins across the world (size ranging from 28 to $5{,}847\times10^3$ km^2), shows reasonable robustness (explained variance R^2=0.54) with an absolute model error of 6% (Mayorga et al. 2010). The uncertainty associated with those coefficients alone is not quantified but is likely to be lower than the model's, as river sources (i.e. emissions), to which the coefficients are applied, are not used in the present fate model work (**Article I**: Cosme et al. 2016b). Given the significant spatial differentiation in the CFs developed, and under a modelling parsimony principle, it seems the watershed-dependent coefficients extracted from NEWS 2-DIN adequately fit the research purpose and LCIA currents needs. Other models were assessed and found less suitable – see **Article I**: Cosme et al. (2016b)

The marine fate component of the FF uses surface water residence time to estimate N removal by denitrification and advective transport. The empirical relationship applied to link the residence time and losses by denitrification holds an reasonable explained variance of 0.56 (R^2) (Seitzinger et al. 2006). The residence time data sources were found inconsistent and scarce (**Article I**: Cosme et al. 2016b). Considering both aspects, the uncertainty of the residence dataset appears to be more relevant. As seen before, the high model sensitivity to this parameter (**Article V**: Cosme and Hauschild 2016a) makes it a key issue for the characterisation model.

The variation of the primary production (PP) rates data explain 56% of the variance of the XFs modelled with the method described in **Article II**: Cosme et

al. (2015). The variability of the PP dataset is deemed modest and data uncertainty set to low given the estimation method, i.e. average monthly records from ca. 12-year period of state-of-the-art satellite data (seaWIFS) and interannual variation below 5% for the majority of the PP dataset (Watson et al. 2014). The unexplained variation is then assigned to the effect of spatially differentiated (CZ-dependent) parameterisation included in the XF model work. The PP parameter contributes the most to the XF model sensitivity but is not considered a key issue given the low assigned uncertainty.

The major sources of uncertainty in the EF model are related to the sensitivity thresholds (LOEC) estimation methods (i.e. the inconsistent biological endpoints tested), and to the representativeness of the dataset (i.e. low number of species and coarse spatial differentiation in five CZs). To minimise the variability of LOEC data, the GM_{taxon} estimation method was preferred, as seen before (Section 4.2 and **Article III**: Cosme and Hauschild (2016b)). The species representativeness per CZ is a critical aspect but found adequate and the best estimate available, given the extensive literature review, the large number of taxonomic groups covered, and the global coverage of temperature-dependent LOEC data. An overall good completeness of the effect model is therefore achieved. The methodological choices and necessary simplifications when modelling average conditions, are also seen as not contributing significantly to the variability of the EF estimation (**Article III**: Cosme and Hauschild 2016b).

The adoption of an arbitrary PAF-PDF conversion factor adds an unquantified amount of uncertainty. However, it is likely to have low impact on the quality of the final results compared to other sources of uncertainty. Its introduction in the damage estimation contributes equally to every emission route and emission location thus not adding any bias to the model results.

LME-dependent species density values were estimated from fisheries catch statistics for commercial species. Although a possible bias towards sampling data from the Northeast and Northwest Atlantic may verify, due to

higher taxonomic resolution of sampled species and catch data, the use of an ensemble of three species distribution models (SDMs) – Maxent, AquaMaps and the *Sea Around Us Project* method (**Article IV**: Cosme et al. 2016a), increases the robustness of and the confidence on the species occurrence estimation. Considering that the SD term has a significant contribution to the spatial differentiation of the CFs estimated (**Article V**: Cosme and Hauschild 2016a), and given its relevance to the harmonisation of endpoint units (**Article IV**: Cosme et al. 2016a), their estimation and application, as the best estimate available, is seen as an essential addition to the state-of-the-art of the marine eutrophication indicator in LCIA.

Regionally aggregated CFs are estimated by emission-weighted averages of all non-zero CFs belonging to that region for the respective route. Emission data refer to year 2000 and were extracted from the NEWS 2-DIN model (Mayorga et al. 2010). The uncertainty of that data was not assessed, but assumed as a best estimate available given the published sources used and the accepted methods followed in those. In any case, when averaging up to the level of regions or continents, it is likely that the emissions data uncertainty is of minor importance (**Article V**: Cosme and Hauschild 2016a).

4.4 Limitations

As mentioned in the two previous sections, the use of watershed-dependent empirical runoff coefficients to quantify the export fractions from soil to river, reduces the discriminatory power of the fate model. This approach limits the spatial resolution of the emission location which, as discussed in **Article I**: Cosme et al. (2016b), may have little practical effect in the representation of the impacts but rather be relevant to the uncertainty in the watershed export estimation.

The adoption of export coefficients extractable from alternative sources, such as the IMAGE-GNM model (Beusen et al. 2015), as suggested in **Article I**:

Cosme et al. (2016b) may have predictive advantages by adding detailed modelling of land fate processes at a 0.5°×0.5° grid cell spatial resolution, and including explicit groundwater denitrification in the soil/aquifer matrix and riparian zones (**Article I**: Cosme et al. 2016b). Assuming those coefficients can be applied to properly represent the export fractions for the soil-related emissions, they can overcome the NEWS-2 DIN model's limitation of missing the non-linearity of biogeochemical processes, as noted by Beusen et al. (2015) – see also **Article I**: Cosme et al. (2016b).

The exposure model has limited application to characterise local carbon vertical fluxes at spatial resolutions finer than LME and, currently, only considers temporal resolution of one year. The estimated carbon export and oxygen depletion in bottom waters does not consider external forcing that might distort the results, e.g. variable coastal hydrodynamics intensifying either mixing or stratification, and factors determining nutrient limitation and variable N:P ratios of the anthropogenic loadings. Seasonal variability of species succession or dominance may be used to improve the method robustness.

Airborne N emissions from anthropogenic sources are not modelled in this research work and currently constitute a significant limitation in scope and applicability for a fully operational LCIA method. Future research should aim at including environmental flows for those emissions in the fate model component by adding deposition fractions, as developed by e.g. Dentener et al. (2006) or Roy et al. (2012).

The EFs are modelled for a five climate zone scale, mainly due to the relatively small number of species sensitivity data, thus limiting the spatial differentiation of the results and the significance of the disaggregation into the 66 LMEs.

4.4.1 Water column stratification

Surface water residence time is highly relevant to the planktonic production in the euphotic layer – the longer N is available the greater its uptake can be. However, it does not add any information on the persistence of hypoxia in bottom water masses. Similarly, data on the water column stratification was neither used nor found available to quantify such hypoxia persistence. In practice, hypoxia onset is expected to follow a seasonal pattern and not extend to the whole year. Correspondingly, severe and persistent hypoxia conditions (or even anoxia) are not likely to verify for the entirety of the LME bottom area, as some habitats would be lying above the oxycline or exposed to sufficient advective mixing to ensure ventilation. Therefore, the time and space integration of impacts levels temporal and spatial peaks of intensity to an overall representative average. A possible method improvement may anticipate the inclusion of temporal variation and spatial extension of stratification occurrence to refine the impact assessment.

4.4.2 Misleading time and space aggregation?

The CF model results for LME #5 Gulf of Mexico, for instance, show a practical example of the space and time integration. These coastal waters are known to be among the most severely affected by hypoxia – see studies on Gulf of Mexico's 'dead zone' by e.g. Rabalais et al. (2002) or Diaz and Rosenberg (2008). The area of concern for hypoxic events is located in the northern part of the Gulf, on the Louisiana/Texas continental shelf. The severity of a short mid-summer long (ca. a month duration) and localized (ca. 1% of the LME area) hypoxic event is incommensurable larger than for the remainder time of the year and area of the LME, whereas the shelf area of the LME is quantified as 567,620 km^2 and the total LME area is 1,487,243 km^2 (www.seaaroundus.org). The 'dead zone' there extended for 16,760 km^2 (ca. 1% of LME area) in mid-summer 2015, with the last 30-year average around 13,752 km^2, and the highest peak at 20,700 km^2 in mid-summer 2001 (Rabalais et al. 2002; LUMCON 2015). The integrated

impact potential, for each kg N emitted to the environment as expressed in the CF, ranks the Gulf of Mexico's at ca. 12th percentile of the CFs distribution (**Article V**: Cosme and Hauschild 2016a) and the ecosystem response potential in a modest 27th place out of 66 LMEs (**Article IV**: Cosme et al. 2016a), while biotic and ecological effects are extensively described (Diaz and Rosenberg 1995; Wu 2002; Levin et al. 2009; Middelburg and Levin 2009; Zhang et al. 2010). A similar analysis, although with smaller discrepancies between modelled and observed impacts, can be made to other LMEs of eutrophication-wise interest, such as the Baltic Sea, Yellow Sea, Mediterranean Sea, Northeast U.S. coast, and others (Diaz and Rosenberg 2008; Rabalais et al. 2010).

The average approach given by the time and space integration is an important aspect to the effects modelling exercise too. The cumulating effect of the environmental pressure is not represented in the EF model (and generally in ecosystem-related LCIA indicators), due to possible non-linearity of persistent pressures and recurrence of these, i.e. persistence of chronical and recurrence of acute stress, both at a 1-year period scale and, most importantly, over consecutive years. The 'media recovery' assumption, the reversibility of impacts, and the species equal weighting are (current) necessary model simplifications to represent the impact on the biotic structural component of the ecosystem (see also **Article IV**: Cosme et al. (2016a). Possible future improvements to its quantification may consider e.g. the inclusion of vulnerability indices to richness assessments (Curran et al. 2011; Verones et al. 2013; Verones et al. 2015), or to move into modelling of the functional component (Tilman 2001; Souza et al. 2013).

4.5 Method assessment

The suitability of the introduced model to integrate a LCIA method for marine eutrophication impact category indicator was assessed in an exercise similar to that by Hauschild et al. (2013). The five scientific criteria:

completeness of scope; environmental relevance; scientific robustness and certainty; documentation, transparency, and reproducibility; and applicability, were used as proposed by EC-JRC-IES (2010b).

4.5.1 Completeness of scope

The scope of the model for the evaluation of eutrophying substances is applicable for marine eutrophication where it addresses all relevant issues. However, it lacks and atmospheric fate model. No temporal differentiation is modelled. Results have global validity.

Fate model is based on export coefficients from the NEWS-2 DIN model (Mayorga et al. 2010) and residence time dependent marine fate modelling. Spatial differentiation for 5,772 river basins of the world. Research not published (submitted to the International Journal of Life Cycle Assessment, under review, as per May 2016).

Exposure model is based on biological coastal processes explaining the conversion of uptaken nitrogen (in the euphotic zone) to oxygen consumption (in the bottom layer). Spatial differentiation for 66 large marine ecosystems (LME), with global coverage. Research published (Ecological Modelling 2015; 317, 50-53).

Effect model based on species sensitivity to hypoxia and HC_{50} estimation based on the SSD method. 91 marine demersal species included, converted to 582 bottom-water temperature dependent thresholds. Spatial differentiation for five climate zones and global coverage. Research published (Ecological Indicators 2016; 69, 453-462).

Damage factor based on a 0.5 conversion factor from PAF-based to PDF-based metrics and spatially explicit species density to convert to species·yr. Spatial differentiation for 66 LMEs. Research not published (submitted to Ecological Indicators, under review, as per May 2016).

Characterisation model combines the fate, exposure, effect, and damage factors above. Waterborne nitrogen emission included (DIN). No deposition of airborne emission modelled. Spatial differentiation for 5,772 river basins of the world. No temporal differentiation. Research not published (submitted to the International Journal of Life Cycle Assessment, under review, as per May 2016).

4.5.2 Environmental relevance

Environmental relevance of the hypoxia-related pathway is high, although deposition of airborne nitrogen emissions is missing. Important N removal processes are included as inland (soil to river, in-river) and marine (coastal waters) fate.

Impact pathway is fully covered for waterborne N emissions in five routes (N in runoff from natural and agricultural soils, N in sewage water to river, N to river, and N to marine water), and then from N in coastal waters to organic matter from biomass synthesis, and to oxygen consumption in bottom waters, and the effect on exposed species in spatially differentiated demersal animal communities.

4.5.3 Scientific robustness and certainty

Exposure and effect model components have been peer reviewed. The fate model is under review, but the inland component is based on the NEWS 2-DIN model, reviewed and widely accepted, and the marine component is based on peer reviewed work in the LC-IMPACT project. The damage factor component is based on species occurrence data from reviewed and widely used species distribution models.

Only qualitative uncertainty assessment is done.

4.5.4 Documentation, transparency, and reproducibility

The method is documented and accessible for use in a reproducible way. Input data obtained from literature review and available online and widely

accepted sources. Datasets and calculations are available or described in supplementary information appendices easily accessible.

4.5.5 Applicability

Characterisation factors for all the waterborne inorganic nitrogen compounds are available but stoichiometric conversions are needed, widely available or easily obtainable, for DIN forms: convert flows as ammonium (NH_4^+) by multiplying by 0.776, N in nitrate (NO_3^-) by 0.226, and N in nitrite (NO_2^-) by 0.304 – then apply CF.

Relevant airborne nitrogen compounds, such as nitrogen oxides (NO_x) and volatilised ammonia (NH_3) are not included.

4.5.6 Science based criteria overall evaluation

Based on a model for global conditions, it addresses all aspects of marine eutrophication for waterborne emissions. Spatial differentiation found of high relevance and significant magnitude, but only available for river basins of the world and not at a country scale. Method and CFs are documented and accessible, most are reviewed. No quantitative treatment of uncertainty in resulting CFs.

CFs are available for five relevant emission routes (‘N from natural soil’, ‘N from agricultural soil’, ‘N in sewage discharge to river’, ‘N to river’, and ‘N to marine water’) and covering all DIN compounds (NH_4^+, NO_3^-, NO_2^-). Airborne NO_x and NH_3 are not included.

5 Conclusions and outlook

Characterisation factors for marine eutrophication impacts at the endpoint level were developed in a LCIA framework. These factors represent the impact potential of dissolved inorganic nitrogen (DIN) forms to cause hypoxia-related eutrophication impacts on marine demersal ecological communities. Five emission routes, i.e. N in runoff from agricultural and natural soils, N in sewage waters discharge to river, and direct emissions to either riverine systems or coastal waters, were modelled.

The underlying model work is supported by recent scientific research on environmental fate of waterborne N emissions, ecosystem exposure to N loadings, effects of hypoxic stress on exposed animal species in exposed demersal habitats, and species density estimates based on those species' global occurrence. The combination of that research in a LCIA method quantifies the potential marine eutrophication-induced hypoxia impacts from waterborne nitrogen emissions from anthropogenic sources.

The characterisation factors were developed at a river basin scale with global geographic coverage, i.e. for 5,772 river basins of the world, and for the five N emission routes. The spatial differentiation of the resulting factors (up to 7 orders of magnitude) constitutes one of the outcomes of the research work in this thesis and a significant contribution to improve the state-of-the-art of this impact category in LCIA. Others, equally relevant and important, are the full pathway coverage, global spatial coverage, and mechanistic modelling of exposure and effect on ecosystems. Together, these outcomes successfully cover the research goals defined.

The information provided by the developed model work, and its application as a LCIA method for marine eutrophication, may be useful to various levels of decision making and management of human activities – examples may include planning, design, operation, and management of activities

as diverse as agri-food production, energy production, materials engineering, design, transportation, among others.

6 Main findings

A. A total of 28,860 fate factors (FF) were calculated, differentiated for 5,772 river basins in the world in five distinct emission routes. These represent the persistence of waterborne nitrogen (N) in the environment. Mean FF values decrease from a maximum for direct emissions to marine water, over to intermediate values for river-related emissions, and to a minimum for soil-related emissions.

B. Up to 6 orders of magnitude of spatial differentiation was observed in the FFs for N emissions from agricultural and natural soils, 4 for emissions in sewage water and to river, and 2 for direct emissions to marine water.

C. Airborne emissions of N forms, such as nitrogen oxides (NO_x) and ammonia (NH_3), outside the scope of the present research, constitute a relevant and significant flow from human activities to the environment. The inclusion of deposition factors for those substances seems an essential step forward for the applicability in fate modelling of anthropogenic-N emissions.

D. The input of anthropogenic N to coastal waters is an allochthonous source for organic carbon that results in higher downward carbon export from the euphotic zone, thus increasing the potential benthic oxygen depletion.

E. A mechanistic model based on coastal biological processes was developed to quantify the potential benthic oxygen consumption, as a function of N input, modelled as an exposure factor (XF) in $kgO_2 \cdot kgN^{-1}$. The XFs estimated for 66 large marine ecosystems (LMEs) show a factor 35 of spatial differentiation.

F. Effect factors (EFs) describe the increase in the fraction of species potentially affected by benthic oxygen depletion above their sensitivity threshold to hypoxia. The introduced method estimates HC_{50} values that express the joint sensitivity of the ecological community in each LME – the basis for the effects estimation in LCIA.

G. EF results based on the GM_{taxon} estimation method show lower spatial differentiation but are less sensitive to unintentional variability in species representation in the dataset and more reproducible, thus preferable.

H. The spatial differentiation of the EFs between the five climate zones is modest, but this scale is recommended over a site-generic global EF.

I. The combination of ecosystem exposure and effects on biota can be used to represent the ecosystem response potential to N uptake with a factor 39 of spatial differentiation among LMEs.

J. Damage factors based on a site-generic 0.5 conversion factor from PAF to PDF and LME-dependent species density were developed and applied to harmonise a relative endpoint metric [$(PAF)\cdot m^3\cdot yr\cdot kgN^{-1}$] to an absolute damage metric [$species\cdot yr\cdot kgN^{-1}$].

K. Up to 6 and 7 orders of magnitude of spatial differentiation were verified for, respectively, the relative and absolute metrics of the characterisation factors (CFs) at a river basin scale. In both cases, spatial differentiation is reduced to only 1 order of magnitude after aggregation to the level of continents.

L. A river basin spatial resolution is recommended for the adoption of the resulting CFs, provided that the emission location is known. Regionally aggregated CFs and a global site-generic CF, also available, may be used when that information is coarse or not available, respectively.

M. Major contributions to the current state-of-the-art of this impact category indicator in LCIA reside in (i) the full pathway coverage, thus reaching endpoint level, (ii) the significant increase in geographic coverage, (iii) the mechanistic modelling of XF and EF, and (iv) the derivation of spatially explicit damage factors based on species density.

N. The marine eutrophication CFs introduced, answer the identified research needs, by providing a consistent link between midpoint and damage levels, spatial differentiation at a river basin scale, and global coverage.

7 References

Arrigo KR (2005) Marine microorganisms and global nutrient cycles. Nature 437:349–356. doi: 10.1038/nature04159

Azevedo LB, Cosme N, Hauschild MZ, et al (2013) Recommended assessment framework, method and characterisation and normalisation factors for ecosystem impacts of eutrophying emissions: phase 3 (report, model and factors). FP7 (243827 FP7- ENV-2009-1) LC-IMPACT report. 154 pp.

Beusen AHW, Van Beek LPH, Bouwman AF, et al (2015) Coupling global models for hydrology and nutrient loading to simulate nitrogen and phosphorus retention in surface water – description of IMAGE–GNM and analysis of performance. Geosci Model Dev 8:4045–4067. doi: 10.5194/gmd-8-4045-2015

Böhnke-Henrichs A, Baulcomb C, Koss R, et al (2013) Typology and indicators of ecosystem services for marine spatial planning and management. J Environ Manage 130:135–145. doi: 10.1016/j.jenvman.2013.08.027

Bouwman AF, Van Drecht G, Knoop JM, et al (2005) Exploring changes in river nitrogen export to the world's oceans. Global Biogeochem Cycles 19:14. doi: 10.1029/2004GB002314

Brady NC, Weil RR (2007) The nature and properties of soils, 14th edn. Prentice Hall

Breitburg DL (1992) Episodic Hypoxia in Chesapeake Bay: Interacting Effects of Recruitment , Behavior, and Physical Disturbance. Ecol Monogr 62:525–546.

Chavez FP, Messié M, Pennington JT (2011) Marine Primary Production in Relation to Climate Variability and Change. Ann Rev Mar Sci 3:227–260. doi: 10.1146/annurev.marine.010908.163917

Cloern JE, Abreu PC, Carstensen J, et al (2016) Human activities and climate

variability drive fast-paced change across the world's estuarine-coastal ecosystems. Glob Chang Biol 513–529. doi: 10.1111/gcb.13059

Conley DJ, Carstensen J, Vaquer-Sunyer R, Duarte CM (2009) Ecosystem thresholds with hypoxia. Hydrobiologia 629:21–29. doi: 10.1007/s10750-009-9764-2

Cosme N, Hauschild MZ (2016a) Characterization of waterborne nitrogen emissions for marine eutrophication modelling in life cycle impact assessment at the damage level and global scale. Int J Life Cycle Assesment submitted.

Cosme N, Hauschild MZ (2016b) Effect factors for marine eutrophication in LCIA based on species sensitivity to hypoxia. Ecol Indic 69:453–462. doi: 10.1016/j.ecolind.2016.04.006

Cosme N, Jones MC, Cheung WWL, Larsen HF (2016a) Spatial differentiation of marine eutrophication damage indicators based on species density. Ecol Indic submitted.

Cosme N, Koski M, Hauschild MZ (2015) Exposure factors for marine eutrophication impacts assessment based on a mechanistic biological model. Ecol Modell 317:50–63. doi: 10.1016/j.ecolmodel.2015.09.005

Cosme N, Mayorga E, Hauschild MZ (2016b) Spatially explicit fate factors for waterbone nitrogen emissions at the global scale. Int J Life Cycle Assesment submitted.

Cosme N, Niero M (2016) Modelling the influence of changing climate in present and future marine eutrophication impacts from spring barley production. J Clean Prod submitted.

Curran M, de Baan L, De Schryver AM, et al (2011) Toward meaningful end points of biodiversity in life cycle assessment. Environ Sci Technol 45:70–9. doi: 10.1021/es101444k

Cushing DH (1975) Marine Ecology and Fisheries. Cambridge University Press, Cambridge

Cushing DH (1990) Plankton Production and Year-class Strength in Fish Populations: an Update of the Match/Mismatch Hypothesis. Adv Mar Biol 26:249–293.

Davis JC (1975) Minimal dissolved oxygen requirements of aquatic life with emphasis on Canadian species: a review. J Fish Res Board Canada 32:2295–2332.

Diaz RJ, Rabalais NN, Breitburg DL (2012) Agriculture's Impact on Aquaculture: Hypoxia and Eutrophication in Marine Waters.

Diaz RJ, Rosenberg R (1995) Marine Benthic Hypoxia: a Review of Its Ecological Effects and the Behavioural Responses of Benthic Macrofauna. Oceanogr Mar Biol Annu Rev 33:245–303.

Diaz RJ, Rosenberg R (2008) Spreading dead zones and consequences for marine ecosystems. Science (80-) 321:926–929. doi: 10.1126/science.1156401

Dumont E, Harrison JA, Kroeze C, et al (2005) Global distribution and sources of dissolved inorganic nitrogen export to the coastal zone: Results from a spatially explicit, global model. Global Biogeochem Cycles 19:GB4S02. doi: 10.1029/2005GB002488

Durant JM, Hjermann DØ, Ottersen G, Stenseth NC (2007) Climate and the match or mismatch between predator requirements and resource availability. Clim Res 33:271–283.

EC-JRC-IES (2010a) ILCD Handbook: Analysis of existing Environmental Impact Assessment methodologies for use in Life Cycle Assessment, 1st edit. Publications Office of the European Union, Luxembourg

EC-JRC-IES (2010b) ILCD Handbook: Framework and requirements for LCIA

models and indicators, 1st edit. Publications Office of the European Union, Luxembourg

Ekau W, Auel H, Pörtner H-O, Gilbert D (2010) Impacts of hypoxia on the structure and processes in pelagic communities (zooplankton, macro-invertebrates and fish). Biogeosciences 7:1669–1699. doi: 10.5194/bg-7-1669-2010

Elser JJ, Bracken MES, Cleland EE, et al (2007) Global analysis of nitrogen and phosphorus limitation of primary producers in freshwater, marine and terrestrial ecosystems. Ecol Lett 10:1135–42. doi: 10.1111/j.1461-0248.2007.01113.x

Falkowski PG, Raven JA (2007) Aquatic Photosynthesis, Second Edi. Princeton University Press, Oxford, UK

Galloway JN, Cowling EB (2002) Reactive nitrogen and the world: 200 years of change. Ambio 31:64–71. doi: 10.2307/4315217

Galloway JN, Dentener FJ, Capone DG, et al (2004) Nitrogen cycles: past, present, and future. Biogeochemistry 70:153–226.

Galloway JN, Townsend AR, Erisman JW, et al (2008) Transformation of the Nitrogen Cycle: Recent Trends, Questions, and Potential Solutions. Science (80-) 320:889–892. doi: 10.1126/science.1136674

Gamperl AK, Driedzic WR (2009) Cardiovascular function and cardiac metabolism. In: Richards JG, Farrel AP, Brauner CJ (eds) Fish Physiology, Vol. 27. Hypoxia. Academic Press, London, UK, pp 301–360

GESAMP (2001) A Sea of Troubles. Rep. Stud. GESAMP No. 70. Joint Group of Experts on the Scientific Aspects of Marine Environmental Protection and Advisory Committee on Protection of the Sea.

Goedkoop M, Heijungs R, Huijbregts MAJ, et al (2013) ReCiPe 2008 - A life cycle impact assessment method which comprises harmonised category

indicators at the midpoint and the endpoint level - First edition (version 1.08) - Report I: Characterisation. Den Haag, the Netherlands

Gray JS, Wu RS, Or YY (2002) Effects of hypoxia and organic enrichment on the coastal marine environment. Mar Ecol Prog Ser 238:249–279.

Green PA, Vörösmarty CJ, Meybeck M, et al (2004) Pre-industrial and contemporary fluxes of nitrogen through rivers: a global assessment based on typology. Biogeochemistry 68:71–105.

Guinée JB, Gorrée M, Heijungs R, et al (2002) Handbook on life cycle assessment. Operational guide to the ISO standards. I: LCA in perspective. IIa: Guide. IIb: Operational annex. III: Scientific background. Kluwer Academic Publishers, Dordrecht

Hattam C, Atkins JP, Beaumont N, et al (2015) Marine ecosystem services: Linking indicators to their classification. Ecol Indic 49:61–75. doi: 10.1016/j.ecolind.2014.09.026

Hauschild MZ (2005) Assessing Environmental Impacts in a Life-Cycle Perspective. Environ Sci Technol 39:81–88. doi: 10.1021/es053190s

Hauschild MZ, Goedkoop M, Guinée JB, et al (2013) Identifying best existing practice for characterization modeling in life cycle impact assessment. Int J Life Cycle Assess 18:683–697. doi: 10.1007/s11367-012-0489-5

Hauschild MZ, Huijbregts MAJ (2015) Introducing Life Cycle Impact Assessment. In: Hauschild MZ, Huijbregts MAJ (eds) Life Cycle Impact Assessment, LCA Compendium - The Complete World of Life Cycle Assessment. Springer Science+Business Media, Dordrecht, pp 1–16

Hauschild MZ, Potting J (2005) Spatial Differentiation in Life Cycle Impact Assessment - The EDIP2003 methodology.

Henderson AD (2015) Eutrophication. In: Hauschild MZ, Huijbregts MAJ (eds) Life Cycle Impact Assessment, LCA Compendium - The Complete World of

Life Cycle Assessment. Springer Science+Business Media Dordrecht, pp 177–196

Henderson AD, Hauschild MZ, van de Meent D, et al (2011) USEtox fate and ecotoxicity factors for comparative assessment of toxic emissions in life cycle analysis: sensitivity to key chemical properties. Int J Life Cycle Assess 16:701–709. doi: 10.1007/s11367-011-0294-6

Howarth RW, Billen G, Swaney D, et al (1996) Regional nitrogen budgets and riverine N & P fluxes for the drainages to the North Atlantic Ocean: Natural and human influences. Biogeochemistry 35:75–139. doi: 10.1007/ BF02179825

Howarth RW, Marino R (2006) Nitrogen as the limiting nutrient for eutrophication in coastal marine ecosystems: Evolving views over three decades. Limnol Oceanogr 51:364–376. doi: 10.4319/lo.2006.51.1 _part_2.0364

Itsubo N, Inaba A (2012) LIME2: Life-cycle Impact assessment Method based on Endpoint modeling. JLCA Newsl Life-Cycle Assess Soc Japan 12:16.

Jolliet O, Margni M, Charles R, et al (2003) Presenting a New Method IMPACT 2002 + : A New Life Cycle Impact Assessment Methodology. Int J LCA 8:324–330.

Keeney DR, Hatfield JL (2001) The Nitrogen cycle, historical perspectives, and current and potential future concerns. In: Follet RF, Hatfield JL (eds) Nitrogen in the Environment: Sources, Problems, and Management. Elsevier Science B.V., Amsterdam, The Netherlands, pp 3–16

Kelly JR (2008) Nitrogen Effects on Coastal Marine Ecosystems. In: Hatfield JL, Follet RF (eds) Nitrogen in the Environment: Sources, Problems, and Management. U.S. Environmental Protection Agency, (Amsterdam, Boston, et al.: Academic Press/Elsevier, pp 271–332

Kemna R, van Elburg M, Li W, van Holsteijn R (2005) Methodology Study Eco-

design of Energy-using Products: MEEuP methodology report. Delft

Laegreid M, Bockman OC, Kaarstad O (1999) Agriculture and Fertilizers. AB Int., New York

Larsen HF, Hauschild MZ (2007) LCA Methodology Evaluation of Ecotoxicity Effect Indicators for Use in LCIA. Int J 12:24–33.

Lee RY, Seitzinger SP, Mayorga E (2016) Land-based nutrient loading to LMEs: A global watershed perspective on magnitudes and sources. Environ Dev. doi: 10.1016/j.envdev.2015.09.006

Levin LA, Ekau W, Gooday AJ, et al (2009) Effects of natural and human-induced hypoxia on coastal benthos. Biogeosciences 6:2063–2098.

Levin SA (1994) Patchiness in marine and terrestrial systems: from individuals to populations. Philos Trans R Soc London, Ser B 343:99–103.

Lindeijer E (2000) Biodiversity and life support impacts of land use in LCA. J Clean Prod 8:313–319. doi: 10.1016/S0959-6526(00)00025-1

LUMCON (2015) Annual Shelfwide Cruise: July 28 - August 3, 2015. In: Press release - Louisiana Univ. Mar. Consort. http://www.gulfhypoxia.net. Accessed 27 May 2016

Mayorga E, Seitzinger SP, Harrison JA, et al (2010) Global Nutrient Export from WaterSheds 2 (NEWS 2): Model development and implementation. Environ Model Softw 25:837–853. doi: 10.1016/j.envsoft.2010.01.007

Middelburg JJ, Levin LA (2009) Coastal hypoxia and sediment biogeochemistry. Biogeosciences 6:1273–1293. doi: 10.5194/bg-6-1273-2009

Miller D, Poucher S, Coiro L (2002) Determination of lethal dissolved oxygen levels for selected marine and estuarine fishes, crustaceans, and a bivalve. Mar Biol 140:287–296. doi: 10.1007/s002270100702

Niero M, Ingvordsen CH, Peltonen-Sainio P, et al (2015) Eco-efficient production of spring barley in a changed climate: A Life Cycle Assessment

including primary data from future climate scenarios. Agric Syst 136:46–60. doi: 10.1016/j.agsy.2015.02.007

Norris GA (2003) Impact Characterization in the Tool for the Reduction and Assessment of Chemical and Other Environmental Impacts. J Ind Ecol 6:79–101. doi: 10.1162/108819802766269548

Pennington DW, Payet J, Hauschild MZ (2004a) Aquatic Ecotoxicological Indicators In Life-Cycle Assessment. Environ Toxicol Chem 23:1796–1807.

Pennington DW, Potting J, Finnveden G, et al (2004b) Life cycle assessment Part 2: Current impact assessment practice. Environ Int 30:721–39. doi: 10.1016/j.envint.2003.12.009

Perry SF, Jonz MG, Gilmour KM (2009) Oxygen sensing and the hypoxic ventilatory response. In: Richards JG, Farrel AP, Brauner CJ (eds) Fish Physiology, Vol. 27. Hypoxia. Academic Press, London, UK, pp 193–253

Pihl L, Baden SP, Diaz RJ, Schaffner LC (1992) Hypoxia-induced structural changes in the diet of bottom-feeding fish and Crustacea. Mar Biol 112:349–361.

Posthuma L, Suter II GW, Traas TP (eds) (2002) Species Sensitivity Distributions in Ecotoxicology.

Potting J, Hauschild MZ (2006) Spatial Differentiation in Life Cycle Impact Assessment: A decade of method development to increase the environmental realism of LCIA. Int J Life Cycle Assess 11:11–13.

Rabalais NN (2002) Nitrogen in Aquatic Ecosystems. Ambio 31:102–112.

Rabalais NN, Diaz RJ, Levin LA, et al (2010) Dynamics and distribution of natural and human-caused coastal hypoxia. Biogeosciences 7:585–619. doi: 10.5194/bgd-6-9359-2009

Rabalais NN, Turner RE, Diaz RJ, Justić D (2009) Global change and eutrophication of coastal waters. ICES J Mar Sci 66:1528–1537.

Rabalais NN, Turner RE, Wiseman WJ (2002) Gulf of Mexico Hypoxia, a.k.a. "the Dead Zone." Annu Rev Ecol Syst 33:235–263. doi: 10.1146/annurev.ecolsys.33.010802.150513

Reed DC, Slomp CP, Gustafsson BG (2011) Sedimentary phosphorus dynamics and the evolution of bottom-water hypoxia: A coupled benthic-pelagic model of a coastal system. Limnology 56:1075–1092. doi: 10.4319/lo.2011.56.3.1075

Rosenbaum RK, Bachmann TM, Gold LS, et al (2008) USEtox—the UNEP-SETAC toxicity model: recommended characterisation factors for human toxicity and freshwater ecotoxicity in life cycle impact assessment. Int J Life Cycle Assess 13:532–546. doi: 10.1007/s11367-008-0038-4

Rosenberg R, Hellman B, Johansson B (1991) Hypoxic tolerance of marine benthic fauna. Mar Ecol Prog Ser 79:127–131.

Seitzinger SP, Harrison JA, Böhlke JK, et al (2006) Denitrification across landscapes and waterscapes: A synthesis. Ecol Appl 16:2064–2090.

Seitzinger SP, Harrison JA, Dumont E, et al (2005) Sources and delivery of carbon, nitrogen, and phosphorus to the coastal zone: An overview of Global Nutrient Export from Watersheds (NEWS) models and their application. Global Biogeochem Cycles 19:1–11. doi: 10.1029/2005GB002606

Seitzinger SP, Mayorga E, Bouwman AF, et al (2010) Global river nutrient export: A scenario analysis of past and future trends. Global Biogeochem Cycles 24:GB0A08. doi: 10.1029/2009GB003587

Sherman K, Alexander LM (eds) (1986) Variability and Management of Large Marine Ecosystems. Westview Press Inc., Boulder, CO

Sherman K, Aquarone MC, Adams S (eds) (2009) Sustaining the World's Large Marine Ecosystems. IUCN, Gland, Switzerland

Smith VH, Tilman GD, Nekola JC (1999) Eutrophication: impacts of excess

nutrient inputs on freshwater, marine, and terrestrial ecosystems. Environ Pollut 100:179–196.

Souza DM de, Flynn DFB, Declerck F, et al (2013) Land use impacts on biodiversity in LCA: Proposal of characterization factors based on functional diversity. Int J Life Cycle Assess 18:1231–1242. doi: 10.1007/s11367-013-0578-0

Steckbauer A, Duarte CM, Carstensen J, et al (2011) Ecosystem impacts of hypoxia: thresholds of hypoxia and pathways to recovery. Environ Res Lett 6:12. doi: 10.1088/1748-9326/6/2/025003

Steen B (1999) A systematic approach to environmental priority strategies in product development (EPS). Version 2000 – General system characteristics. CPM report 1999:4. Gothenburg, Sweden

Tait RV, Dipper FA (1998) Elements of Marine Ecology, 4th edn. Butterworth Heinemann, Oxford

Tilman D (2001) Functional diversity. In: Levin SA (ed) Encyclopedia of Biodiversity. Academic Press, New Jersey, pp 109–120

Toffoletto L, Bulle C, Godin J, et al (2007) LCA Methodology LUCAS – A New LCIA Method Used for a CAnadian-Specific Context. Int J 12:93–102.

Turner RE, Qureshi N, Rabalais NN, et al (1998) Fluctuating silicate: nitrate ratios and coastal plankton food webs. Proc Natl Acad Sci U S A 95:13048–13051.

Udo de Haes HA, Finnveden G, Goedkoop M, et al (2002) Life-Cycle Impact Assessment: Striving Towards Best Practice. SETAC Press, Pensacola, FL, USA

Udo de Haes HA, Jolliet O, Finnveden G, et al (1999) Best Available Practice Regarding Impact Categories and Category Indicators in Life Cycle Impact Assessment. Int J LCA 4:66–74.

UNEP (2006) Marine and coastal ecosystems and human well-being: A synthesis report based on the findings of the Millennium Ecosystem Assessment.

UNEP-WCMC (2009) Marine and coastal ecosystem services: Valuation methods and their application.

UNESCO (2009) Global Open Oceans and Deep Seabed (GOODS) - Biogeographic Classification. IOC Technical Series N^{o} 84. Paris

Van Drecht G, Bouwman AF, Knoop JM, et al (2003) Global modeling of the fate of nitrogen from point and nonpoint sources in soils, groundwater, and surface water. Global Biogeochem Cycles 17:1–20. doi: 10.1029/2003GB002060

van Zelm R (2010) Damage modeling in life cycle impact assessment. Radboud University, Nijmegen

Vaquer-Sunyer R, Duarte CM (2008) Thresholds of hypoxia for marine biodiversity. Proc Natl Acad Sci U S A 105:15452–7. doi: 10.1073/pnas. 0803833105

Verones F, Huijbregts MAJ, Chaudhary A, et al (2015) Harmonizing the assessment of biodiversity effects from land and water use within LCA. Environ Sci Technol 49:3584–3592. doi: 10.1021/es504995r

Verones F, Saner D, Pfister S, et al (2013) Effects of consumptive water use on biodiversity in wetlands of international importance. Environ Sci Technol 47:12248–57. doi: 10.1021/es403635j

Vitousek PM, Aber JD, Howarth RW, et al (1997) Human alteration of the global nitrogen cycle: sources and consequences. Ecol Appl 7:737–750.

Vitousek PM, Hättenschwiler S, Olander L, Allison S (2002) Nitrogen and nature. Ambio 31:97–101.

Vörösmarty CJ, Fekete BM, Meybeck M, Lammers RB (2000) Global system of rivers: its role in organizing continental land mass and defining land-to-

ocean linkages. Global Biogeochem Cycles 14:599–621. doi: 10.1029/1999GB900092

Watson R, Zeller D, Pauly D (2014) Primary productivity demands of global fishing fleets. Fish Fish 15:231–241. doi: 10.1111/faf.12013

Wu RS (2002) Hypoxia: from molecular responses to ecosystem responses. Mar Pollut Bull 45:35–45.

Zhang J, Gilbert D, Gooday AJ, et al (2010) Natural and human-induced hypoxia and consequences for coastal areas: synthesis and future development. Biogeosciences 7:1443–1467. doi: 10.5194/bg-7-1443-2010

Appendices

Article I: Cosme, N., Mayorga, E. & Hauschild, M.Z. Spatially explicit fate factors for waterborne nitrogen emissions at the global scale. *International Journal of Life Cycle Assessment* submitted in 2016 – manuscript in pre-print version.

Article II: Cosme, N., Koski, M. & Hauschild, M.Z. (2015). Exposure factors for marine eutrophication impacts assessment based on a mechanistic biological model. *Ecological Modelling* 317:50–63. DOI: 10.1016/j.ecolmodel.2015.09.005 – published, manuscript in post-print version.

Article III: Cosme, N. & Hauschild, M.Z. (2016). Effect factors for marine eutrophication in LCIA based on species sensitivity to hypoxia. *Ecological Indicators* 69:453-462, DOI: 10.1016/j.ecolind.2016.04.006 – published, manuscript in post-print version.

Article IV: Cosme, N. & Hauschild M.Z. Characterization of waterborne nitrogen emissions for marine eutrophication modelling in life cycle impact assessment at the damage level and global scale. *International Journal of Life Cycle Assessment* submitted in 2016 – manuscript in pre-print version.

Article V: Cosme, N., Jones, M.C., Cheung, W.W.L. & Larsen, H.F. Spatial differentiation of marine eutrophication damage indicators based on species density. *Ecological Indicators* submitted in 2016 – manuscript in pre-print version.

Article VI: Cosme, N. & Niero, M. Modelling the influence of changing climate in present and future marine eutrophication impacts from spring barley production. *Journal of Cleaner Production* submitted in 2016 – reviewed, manuscript in pre-print version R1

Article I

Spatially explicit fate factors for waterborne nitrogen emissions at the global scale

Cosme, N., Mayorga, E. & Hauschild, M.Z.

submitted to *International Journal of Life Cycle Assessment* in 2016

(manuscript in pre-print version)

Spatially explicit fate factors of waterborne nitrogen emissions at the global scale

Nuno Cosme [a], Emilio Mayorga [b], Michael Z. Hauschild [a]

[a] Division for Quantitative Sustainability Assessment, Department of Management Engineering, Technical University of Denmark, Produktionstorvet 424, DK-2800 Kgs. Lyngby, Denmark

[b] Applied Physics Laboratory, University of Washington, 1013 NE 40th St., Seattle, WA 98105-6698, USA

Corresponding author: Nuno Cosme, nmdc@dtu.dk

Abstract

Purpose

Marine eutrophication impacts due to waterborne nitrogen (N) emissions may vary significantly with their type and location. The environmental fate of N-forms is essential to understand the impacts that they may trigger in receiving coastal waters. Current Life Cycle Impact Assessment (LCIA) methods apply fate factors (FFs) that do not adequately account for important specifics of the emission routes and the spatially determined variability of the relevant removal processes, and often lack global applicability. The paper describes a newly developed method to estimate spatially explicit FFs for marine eutrophication on a global scale at a river basin resolution.

Methods

The FFs modelling considers N-removal processes in both inland (soil and river) and marine compartments. Model input parameters are the removal coefficients extracted from the Global NEWS 2-DIN model and residence time of receiving coastal waters. The resulting FFs express the persistence of the riverine exported N-fraction in the receiving coastal Large Marine Ecosystems (LMEs). The method further discriminates five emission routes, i.e. N from either natural or agricultural soils, N in sewage water discharges, and direct N-emissions to fresh- or marine waters. Based on modelling of individual river basins, regionally aggregated FFs are calculated as emission-weighted averages.

Results and discussion

Among 5,772 river basins of the world, the calculated FFs show 6 orders of magnitude variation for the soil-related emission routes, 4 for the river-related, and 2 for emissions to marine water. Spatial aggregation of the FFs into eight regions decreases this variation to 1 order of magnitude for all routes. Coastal water residence time was found

to be the most influential model parameter, and the inconsistency and scarcity of literature sources for this parameter suggests the need for data quality improvement.

Conclusions

With the proposed method and factors, spatial information of N-emissions can be used to improve the environmental relevance and the discriminatory power of the assessment of marine eutrophication in geographically differentiated characterization modelling of marine eutrophication at a global scale.

Keywords Watershed · River basin · Coastal water · Large Marine Ecosystems · Denitrification · Removal processes · Residence time · Life cycle impact assessment

1. Introduction

Marine coastal eutrophication can be defined as the syndrome of ecosystem responses to the increase in supply of growth-limiting plant nutrients that boost planktonic growth and fuel organic carbon cycling processes (Nixon 1995; Cloern 2001). Nitrogen (N) is assumed to be the limiting nutrient is marine waters – a necessary and justified simplification in ecosystems modelling, considering average spatial and temporal representative conditions (see also Vitousek et al. (2002); Howarth and Marino (2006); Cosme et al. (2015)), although point limitations by phosphorus or silica (Turner et al. 1998; Elser et al. 2007) and cases of co-limitation (Arrigo 2005) may occur.

The cascading effects of N-enrichment in the marine ecosystem include increased plant biomass, algal blooms, shading, water quality degradation, loss of habitat, and oxygen deficiency (NRC 2000; Rabalais 2002; Kelly 2008). These can lead to important ecological impacts that range from altered ecological communities and species composition, and reduced abundance and diversity of biological resources, to mass mortality (Diaz and Rosenberg 1995; Wu 2002; Levin et al. 2009; Middelburg and Levin 2009; Zhang et al. 2010). The onset of hypoxic conditions and 'dead zones', due to excessive oxygen depletion by aerobic respiration of organic matter, has already been noted as one of the most severe and widespread causes of disturbance to marine ecosystems (GESAMP 2001; Diaz and Rosenberg 2008). Although hypoxia-driven eutrophication may occur naturally, it has been linked to the increasing anthropogenic pressure (Smith et al. 1999, 2006; Gray et al. 2002; Rabalais 2002; Doney 2010; Howarth et al. 2011). Marine eutrophication is of global concern and likely to increase due to the growing application of reactive nitrogen in agriculture and use of combustion-based energy sources. Galloway et al. (2004, 2008) estimated a >10-fold increase of reactive nitrogen creation in the last 150 years and current N mobilization more than doubles that of natural processes, while riverine export has increased 5-6 fold since the pre-industrial period (Galloway and Cowling 2002; Green et al. 2004).

Marine eutrophication is commonly accounted as an impact category in Life Cycle Assessment (LCA). In the Life Cycle Impact Assessment (LCIA) phase of LCA, inventoried emissions of substances are converted into potential impacts on the chosen indicator for the impact category by applying Characterization Factors (CFs). These, combine the environmental fate of the emitted substances, and the exposure and effects in relevant environmental compartments (Pennington et al. 2004). In this framework, Fate Factors (FFs) represent the persistence of a substance in the environment by quantifying its removal in the pathway from source to receiving ecosystem. In the present case, causes for N removal may include denitrification, advection, and abstraction by water consumption (Howarth et al. 1996; Seitzinger et al. 2005, 2006). The impact assessment further includes exposure (XF) and effect factors (EF) – in the example of hypoxia-driven eutrophication these may correspond to the conversion of N-uptake by primary producers into benthic oxygen consumption and the sensitivity of ecological communities to hypoxia, respectively, as modelled in Cosme et al. (2015) and Cosme and Hauschild (2016) for LCIA application.

Several LCIA methods have incorporated spatially explicit modelling of the FF for emissions of nutrients. The fate model CARMEN (Beusen 2005), with the EUTREND model (Van Jaarsveld 1995), is thus used at the European scale and country resolution in the EDIP2003 (Hauschild and Potting 2005) and ReCiPe (Goedkoop et al. 2012) impact methods, and also in a modified version for Canada in the LUCAS method (Toffoletto et al. 2007); model work by Vörösmarty et al. (2000a) and Fekete et al. (2000) at U.S. state scale is applied in TRACI method (Norris 2003). However, a spatially explicit method describing the fate of waterborne N-emissions consistently for application at the global scale is not available.

Spatial differentiation has been demonstrated to be an important feature in impact assessment. It increases both the environmental relevance and discriminatory power of the underlying models (Udo de Haes et al. 2002; Potting and Hauschild 2006), especially for impacts occurring at the local to regional scale, such as marine eutrophication. Coarse spatial resolution and incompatibility of model results for different regions may hinder harmonisation of LCIA methods and reduce the relevance and applicability of the studies. Ensuring both an adequate spatial resolution, in view of the spatial variability of the impacts, and a global coverage of the FF model, would contribute to improve the state-of-the-art of marine eutrophication impact assessment.

The goal of the present study is to develop a global method for spatial differentiation in fate modelling for waterborne nitrogen emissions and apply it to derive spatially explicit fate factors to be used in the assessment of marine eutrophication impacts at a global scale. For this purpose, the N removal processes used in the Global NEWS 2-DIN model (Seitzinger et al. 2005; Mayorga et al. 2010) were combined with those acting in the marine compartment. The driving environmental fate

processes were identified and analysed, and important assumptions and uncertainties discussed.

2. Methods

2.1. Framework

2.1.1. Nitrogen sources and emissions

Fertilizers (both inorganic and manure) applied in agriculture result in waterborne-N emissions to the environment, mainly in the form of dissolved NH_4^+ and NO_3^- to soil and water (Galloway et al., 2002; Socolow, 1999). Biological nitrogen fixation, i.e. the fixation of atmospheric N_2 to (mainly) NH_4^+, contributes with an additional input to the soil budget (Galloway et al. 2004). The N input is then reduced by crop removal (by harvesting and grazing), ammonia volatilization, and denitrification in the soil. The remainder constitutes the soil budget (N) surplus, which represents the environmental emission. Subsequently, it is leached from the root zone, and further reduced by denitrification in groundwater systems and retention in river systems (Bouwman et al. 2005). As such, emitted N-forms enter the aquatic system by surface runoff and leaching from either natural or agricultural soils to freshwater systems, by direct emissions to rivers or in sewage water discharges, by direct emissions to marine coastal waters, or by atmospheric deposition – the emission routes. Although the contributions from the latter (airborne) are not modelled here, the fate of any quantified deposition of nitrogen oxides (NO_x) or ammonia (NH_3) on soil, river or coastal water can be calculated with the FF for the respective emission route, independently of the source. Sources of waterborne N-inputs are typically categorized as point or non-point, mainly for management purposes, depending on the nature of the emission – if it occurs at specific emission locations (e.g. sewage water discharges) or is diffused in the landscape (e.g. runoff from agricultural soils).

2.1.2. Life cycle impact assessment

Characterization models in LCIA are the basis for the development of CFs. The method presented here supports the calculation of FFs for waterborne N-emissions from anthropogenic sources as part of the characterization of their ability to contribute to eutrophying effects in marine coastal waters. The underlying modelling work is consistent with the LCIA framework for emission-related impact indicators (Udo de Haes et al. 2002) by describing the modelling of environmental fate processes of N in soil and riverine systems, aggregated at river basin scale (Vörösmarty et al. 2000b), and in the coastal marine compartment, at Large Marine Ecosystem (LME) scale (Sherman and Alexander 1986). Additional modelling of (i) ecosystem responses to exposure to N and oxygen depletion resulting from organic carbon cycling processes, and (ii) effects

based on sensitivity of marine species to hypoxia, is needed to complete the characterization model for hypoxia-driven marine eutrophication impacts. The modelling of these elements, the exposure and the effects, are described in Cosme et al. (2015) and Cosme and Hauschild (2016) respectively. The combination of the fate, exposure, and effect models composes the characterization model for which the characterization factor (CF, [m^3·yr·kgN^{-1}]) is calculated as summarised in Eq. (1):

$$CF_{i,jl} = FF_{i,jl} \times XF_l \times EF_l \quad (1)$$

where $FF_{i,jl}$ [yr] is the fate factor for emission route *i* in river basin *j* to receiving ecosystem *l*, XF_l [kgO_2·kgN^{-1}] the exposure factor and EF_l [m^3·kgO_2^{-1}] the effect factor in ecosystem *l*. As each river basin exports to a single LME, *jl* are coupled in the subscript of CF and FF notations.

2.2. Model structure

The FF describes the persistence of the fraction of the original N emission that is exported to a receiving ecosystem, thus expressing its availability there. As such, the fate model is composed of an inland and a marine fate component. The inland component describes the removal processes that determine the fraction exported to coastal waters (f_N, [dimensionless]). The marine component describes the fate processes occurring in the marine compartment that ultimately determine the persistence of dissolved inorganic nitrogen (DIN) there, equivalent to the inverse of the sum of the removal rates (λ, [yr^{-1}]). The fate factor (FF, [yr]) is calculated by combining the inland fate and marine fate components, for each emission route *i* in river basin *j* to receiving ecosystem *l*, as presented in Eq. (2).

$$FF_{i,jl} = \frac{f_{N_{i,j}}}{\lambda_l} \quad (2)$$

The emission routes defined as 'N from natural soil' (N_{ns}), 'N from agricultural soil' (N_{as}), 'N in sewage to river' (N_{sew}), 'N to riv' (N_{riv}), and 'N to marine water' (N_{marw}). DIN-forms include nitrate (NO_3^-), nitrite (NO_3^-), and ammonium (NH_4^+). The term DIN is generically used throughout the text referring to any of these forms.

2.2.1. Inland fate component

The inland component estimation is based on the removal processes covered in the second generation of the Global Nutrient Export from WaterSheds suite of models (NEWS 2) (Dumont et al. 2005; Seitzinger et al. 2005, 2010; Mayorga et al. 2010). The NEWS 2 model estimates global and spatially explicit nutrient riverine exports covering N, P, C, and Si, their dissolved inorganic forms (DIN, DIP, DSi), dissolved organic

forms (DON, DOP, DOC), and particulate N, P and C forms (PN, PP, POC) (Mayorga et al. 2010). The model relates natural and anthropogenic nutrient emission sources and natural transformation processes in watersheds to their export to receiving coastal waters, basing its spatial differentiation on a geographical information system (GIS). Its sub-model describing the riverine DIN export (NEWS 2-DIN) contains parameterisation data essential to understand inland nutrient losses (in natural and agricultural soils and riverine systems) and derive fate-related coefficients.

The NEWS 2-DIN sub-model predicts the annual DIN-export at river mouth for 6,272 river basins by combining both point and diffused N-emissions with hydrologic, biogeochemical, climatic, and social variables (integrating various model work by Van Drecht et al. (2003, 2009), Green et al. (2004), Beusen et al. (2005), Bouwman et al. (2005, 2009), Dumont et al. (2005), Seitzinger et al. (2005), Dentener et al. (2006), Mayorga et al. (2010)), using modelled runoff (Fekete et al. 2000) applied on the STN-30p river system and basin delineation (Vörösmarty et al. 2000b), on a global spatially explicit 0.5° latitude × 0.5° longitude grid.

The DIN fractions exported (FE_{DIN}, dimensionless) are determined by:

- calibrated runoff functions from diffuse anthropogenic sources (agricultural soils) in the watersheds to rivers ($FE_{ws,ant,DIN}$) and from natural soils to rivers ($FE_{ws,nat,DIN}$);
- empirical DIN fractions in point source emissions ($FE_{pnt,DIN}$) (Dumont et al. 2005);
- riverine losses by denitrification (due to retention within reservoirs and along the river network) and consumptive water use (anthropogenic removal of river water containing DIN) ($FE_{riv,DIN}$).

In NEWS 2-DIN, each of these fractions apply to specific discrete N-flows distinguished into river and watershed sources (in $kgN \cdot km^{-2} \cdot yr^{-1}$), which are of either point (*pnt*) or diffuse (*dif*) type and of anthropogenic (*ant*) or natural (*nat*) origin, to estimate the total river basin DIN yield (in $kgN \cdot km^{-2} \cdot yr^{-1}$) (Mayorga et al. 2010). However, in the present model, the various FE fractions were identified and combined in order to determine the inland fate, per river basin and for each emission route (Table 1).

The DIN fractions exported from each exorheic river basin were linked to a receiving LME by means of the geographic location of the respective river mouth. This correspondence key was identified for 5,772 discharging systems, after excluding 164 endorheic basins and 145 systems discharging to coasts outside the 66 LMEs coverage. Basin discharge information was not available for receiving ecosystems #61 (Antarctic), #64 (Central Arctic Ocean), and #65 (Aleutian Islands).

When emissions are not reported as dissolved inorganic N (or e.g. total-N), a conversion based on molar mass may be needed to determine N mass in the DIN-form: for N in NH_4^+, multiply by 0.776, N in NO_3^-, by 0.226, N in NO_2^-, by 0.304. For emissions of dissolved organic N (DON) to river, the organic load may be assumed to fully mineralise to DIN and the respective FF_{Nriv} be applied, as a simplification. However, fate modelling of dissolved organic or particulate N-forms should adopt specific removal coefficients from the respective NEWS 2 sub-models, i.e. NEWS 2-DON or -PN.

Table 1 Inland fate equations derived to estimate export fractions (FE) per emission route.

Emission route	Inland fate coefficient	Derived equation for exported fraction
N from natural soil	fN_{ns} =	$FE_{riv,DIN} \times FE_{ws,nat,DIN}$
N from agricultural soil	fN_{as} =	$FE_{riv,DIN} \times FE_{ws,ant,DIN}$
N in sewage to river	fN_{sew} =	$FE_{riv,DIN} \times FE_{pnt,DIN}$
N to river	fN_{riv} =	$FE_{riv,DIN}$
N to marine water	fN_{marw} =	1 (no inland fate component)

2.2.2. Marine fate component

In the coastal zone, nitrogen is removed by advection and denitirification. Assuming that these removal processes are both first order, the resulting marine removal rate (λ, [yr^{-1}]) is estimated as the sum of the removal rates by advection (λ_{adv}) and denitrification (λ_{denitr}), in each receiving ecosystem *l* (i.e. LME), Eq. (3).

$$\lambda_l = \lambda_{adv,l} + \lambda_{denitr,l} \quad (3)$$

The advection removal coefficient ($\lambda_{adv,l}$, [yr^{-1}]), Eq. (4), corresponds to the inverse of the surface water residence time (τ_l, [yr]) in ecosystem *l*.

$$\lambda_{adv,l} = \frac{1}{\tau_l} \quad (4)$$

The advective transport is not modelled *per se* and τ_l is meant to represent all possible advective exchanges with the open ocean or deeper waters, assuming that net water exchange (and DIN) with adjacent LMEs is null. Acknowledging that such assumption may misestimate relevant DIN inputs, especially in LMEs where along-shore coastal currents may show an overall predominant direction, it was still found suitable for the modelling purpose, considering the intended global coverage and the adopted spatial resolution. The use of τ_l to represent an advective transport removal, is described elsewhere for similar modelling work in lakes, estuaries, and coastal waters (e.g. Vollenweider (1976), Andrews and Müller (1983), Nixon et al. (1996), Dettmann

(2001), Monsen et al. (2002), Seitzinger et al. (2006)). Literature review provided residence times for 39 out of 66 LMEs. Two coastal archetypes were defined based on decisive aspects like the coastal exposure to currents and regional ocean circulation, and continental shelf depth and profile. The remaining 27 LMEs were classified into one of these archetypes and their τ_l estimated based on this classification. The archetypes were also used to settle cases where literature sources were inconsistent (Table S.1 in Electronic Supplementary Material). Archetypes were described as type 1 (τ=0.25 yr) for short water persistence, with high dynamics and exposure to regional currents, mainly above narrow and deep shelves, and type 2 (τ=2 yr) with medium dynamics and exposure to local currents, mainly in broader and more shallow shelves. The τ_l values for the archetypes based on reported values for other LMEs with similar characteristics were compared.

Denitrification is the microbially-mediated reduction of oxidized N-forms (NO_3^-, NO_2^- and NO) into biologically unavailable forms (N_2 and N_2O) (Seitzinger 1988; Socolow 1999). The nitrification-denitrification balance that ultimately may regulate N limitation (in low N availability systems) or reduce N export (in enriched systems) varies with geography and over time (Seitzinger et al. 2006). Taking a modelling approach with integration over time (annual) and space (LME), the effect of time and space may be represented through an empirical relationship, Eq. (5), between N removal (Nrem, %) as a function of water residence time (in months) in estuaries, river reaches, lakes, and continental shelf, as described by Seitzinger et al. (2006) extending work by Nixon et al. (1996).

$$N_{rem,k} = 23.4 \cdot {\tau_k}^{0.204} \quad (5)$$

The LME(l)-dependent denitrification rate constant ($\lambda_{denitr,l}$), is determined from N_{rem} using a first-order removal equation in Eq. (6), with t set to 1 yr for the annual time integration represented in Eq. (5).

$$N_{rem,l} = e^{-\lambda_{denitr,l} \cdot t} \Leftrightarrow \lambda_{denitr,l} = -\frac{\ln N_{rem,l}}{t} \quad (6)$$

Although denitrification may be locally affected by temperature, supply of nitrate and organic matter, oxygen concentration, and also biotic parameters (Seitzinger 1988), it is a generic process independent of salinity (Fear et al. 2005; Magalhães et al. 2005). Therefore, the adoption of such empirical relationship is deemed representative of annual denitrification losses in marine coastal waters.

2.3. Regional aggregation

Combining the rate constants for denitrification and advection for an overall removal rate in the coastal ecosystems (Eq. (3)), and combining it with the fraction removed in the inland compartments (Table 1), yields fate factors for 5,772 discharging riverine systems. Considering the five emission routes, the number of possible FFs amounts to 28,860. If the exact emission location is known for a given emission, the corresponding FF can be applied in calculation of the characterization factor too be applied. Often such specific knowledge about emission locations is not at hand for many processes in the life cycle and in order to support application in LCA s are reported, the fate factors have also been aggregated at higher geographical scales. Regional aggregation of FFs over any desired region (*reg*, e.g. continent, world) for each N-emission route *i*, was calculated by emission(*Em*)-weighted averages, as shown in Eq. (7). Regional fate factors ($FF_{i,reg}$, [yr]) aggregate all river basins with non-zero $FF_{i,jl}$ belonging to region *reg*, with a corresponding emission *Em* in the respective route *i*. Emission data used refer to year 2000 and were extracted from the NEWS 2-DIN model.

$$FF_{i,reg} = \frac{\sum_{reg} FF_{i,reg} \cdot Em_{i,reg}}{\sum_{reg} Em_{i,reg}} \quad (7)$$

3. Results and discussion

3.1. Fate factors

The FFs for waterborne-N emissions are shown in Fig. 1 for the emission route 'N to river' (N_{riv}). Full results for the five emission routes in the 5,772 river basins are available in the Electronic Supplementary Material. All five emission routes are equally affected by the marine fate component (represented in the FF_{Nmarw}). This, can be seen as a baseline or *tier 1* (Fig. S1) and shows direct correlation with LME-dependent residence times (FF_{Nas} r=0.61; FF_{Nns} r=0.67; FF_{Nsew} r=0.94; FF_{Nriv} r=0.96; FF_{Nmarw} r=1.00). Removal processes in the river system (FF_{Nriv}, Fig. 1) and sewage treatment retention lie in a second tier. In a third tier, fate is further modulated by specific losses, either in natural or agricultural soil, to express the respective FFs.

The distribution of FF_{Nmarw} reflects the longer persistence in receiving marine systems like the Bay of Bengal, the Baltic, Mediterranean, and Black Seas, and the Hudson Bay Complex (Table S1). This pattern is altered by the influence of the riverine removal, represented by the FF_{Nriv}. Here, the river basin area andlength are determinant to estimate the riverine denitrification losses (Dumont et al. 2005), the removals by retention in reservoirs (Seitzinger et al. 2002), and anthropogenic consumption (Mayorga et al. 2010). In practice, smaller river basins discharge higher N-fractions, especially visible in the majority of small river basins in the Arabian Peninsula,

Philippines/Indonesia Sea, and subarctic river basins of Alaska, North of Canada, and Russia (Fig. 1). The distribution pattern of the FF_{Nsew} results shows no observable changes to FF_{Nriv} although the fate factors are slightly lower (Fig. S2). Fate factors for natural (FF_{Nns}) and agricultural soils (FF_{Nas}) (Fig. S3 and S4) show the influence of predominant soil use, based on modelling work by Bouwman et al. (2005, 2009) on explicit source and sink terms and agricultural surplus, respectively for natural and agricultural soils (Mayorga et al. 2010). These FFs for watershed diffuse emissions tend to show higher contributions from natural soil fixation in large subarctic basins (e.g. Alaska, Canada, and Russia), from agricultural use of soils (manure and agriculture fixation) in South America and Western Africa, and fertilizer use in South and Southeast Asia and Oceania, matching the contribution analysis in riverine discharges by Lee et al. (2016).

Fate factors are not available for endorheic basins (as no export to marine waters occurs), for emissions from agricultural and natural soils in arid areas (due to evaporation exceeding precipitation on an annual basis, runoff is null and so are $FE_{ws,nat,DIN}$ and $FE_{ws,nat,DIN}$ coefficients), and basins exporting to non-LME spatial units (mainly in East Indonesian Sea and New Guinea, for which no marine fate component is available).

3.2. Spatial differentiation

Spatial differentiation of the fate factors per emission route, at a river basin scale, is summarized in Table 2. The analysis across all calculated FFs shows 6 orders of magnitude variation for N emissions from agricultural and natural soils, 4 for emissions in sewage water and to river, and 2 for direct emissions to marine water. Mean FF values decrease from a maximum for direct emissions to marine water (N_{marw}) to lower values for river-related emissions even lower for soil-related emissions. These observations reflect the increased removal and additional spatial differentiation of the coefficients used in the model work, as the emission point moves further away from the sea in the hydrological cycle and processes like riverine removal (plus sewage treatment removal) (*tier 2*) and watershed/soil removal (*tier 3*) become active.

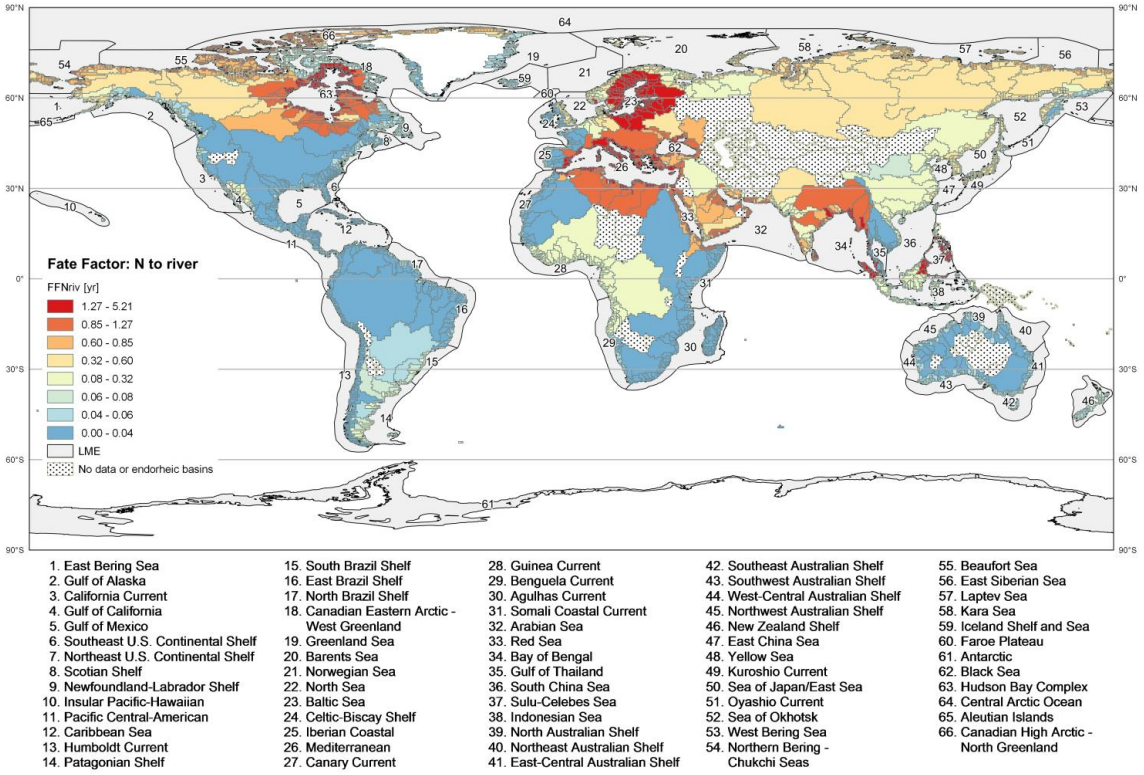

Figure 1 Global distribution of the fate factors (FF_{Nriv}, [yr]) for marine eutrophication due to N-emissions to river at a basin scale. Dotted areas correspond to basins that are endorheic, arid, or for other reason have no available FF. Note the non-linear scale. Identification of the receiving Large Marine Ecosystems (LMEs) included.

Table 2 Statistics of the distribution of FF results per emission route at a river basin scale.

Statistics	Fate Factor [yr] per emission route				
	N_{ns}	N_{as}	N_{sew}	N_{riv}	N_{marw}
Minimum	1.7E-06	1.7E-06	1.1E-04	2.2E-04	0.024
5th percentile	0.0014	0.0032	0.018	0.032	0.076
Mean	0.17	0.28	0.58	1.0	1.9
95th percentile	0.77	1.3	1.8	3.5	6.7
Maximum	4.6	4.6	5.2	7.7	13
Spatial variability	*3E+06*	*3E+06*	*5E+04*	*3E+04*	*5E+02*

Regionally aggregated fate factors at the level of continents (Table 3) show a maximum for South Asia followed by Europe for N_{ns}, South Asia and Oceania for N_{as}, Europe and South Asia for N_{sew}, Europe and South Asia for N_{riv}, South Asia and Europe for N_{marw}, reflecting predominant land uses, as noted by Lee et al. (2016). Regional FFs at the level of continents show modest variability among regions, i.e. 1 order of magnitude in the inter-regional comparison, with no relevant distinction between emission routes. The variability of the FFs in each region (intra-regional comparison)

shows maximum differentiation in North and South America, again higher for the soil-related emissions, with ca. 5 orders of magnitude in both cases. The global aggregation (World) of FFs shows about 10-fold increase from soil-related emissions to direct coastal emissions, in a pattern following the emission pathway (soil-river-coast). Overall, regional aggregation decreases the spatial differentiation from a maximum at the disaggregated FFs (river basin scale), by roughly 5 orders of magnitude for soil-related, 3 for river-related, and 1 for direct coastal emissions. This analysis suggests a recommended use of the river basin scale for application of the proposed FFs, whenever emission location information is available. Aggregated FFs can be applied if such information is coarse, and the global average FFs when the location is unknown or spatial information is not relevant.

Table 3 Regional fate factors (FF) by emission-weighted aggregation per emissions route at the level of continents. Intra-regional variability (*var*) and inter-regional variability (N_i) shown.

Aggregation scale	Fate Factor [yr] per emission route				
	N_{ns} *var*	N_{as} *var*	N_{sew} *var*	N_{riv} *var*	N_{marw} *var*
Africa	0.026 *4E+04*	0.082 *6E+03*	0.11 *6E+02*	0.22 *6E+02*	1.8 *8E+01*
Europe	0.42 *1E+03*	0.42 *1E+03*	0.86 *3E+02*	1.4 *3E+02*	3.8 *1E+02*
North America	0.050 *2E+05*	0.056 *2E+05*	0.11 *6E+03*	0.17 *6E+03*	0.48 *8E+01*
South America	0.014 *9E+04*	0.042 *9E+04*	0.037 *1E+03*	0.073 *1E+03*	0.23 *2E+01*
North Asia	0.11 *7E+01*	0.11 *7E+01*	0.35 *2E+01*	0.65 *2E+01*	1.9 *1E+01*
South Asia	0.53 *3E+04*	0.65 *5E+03*	0.56 *1E+03*	1.1 *9E+02*	4.2 *2E+02*
Oceania [a]	0.097 *3E+03*	0.62 *1E+03*	0.35 *5E+01*	0.72 *6E+01*	1.6 *4E+01*
Australia	0.021 *4E+02*	0.028 *4E+02*	0.047 *7E+00*	0.082 *7E+00*	0.19 *1E+00*
Spatial variability	*4E+01* --	*2E+01* --	*2E+01* --	*2E+01* --	*2E+01* --
World	0.29 --	0.38 --	0.39 --	0.72 --	2.6 --

[a] *(excluding Australia)*

3.3. Comparison with other models

The present work contributes with a method to estimate fate factors for waterborne N-emissions in a spatially explicit resolution that can consistently be applied at the global scale. The N-removal coefficients extracted from the NEWS 2-DIN model were applied in order to estimate the runoff to watersheds and riverine environmental fate at a river basin scale, and were then coupled with coastal fate processes to finally estimate FFs. These two components combined, i.e. inland and marine, to the knowledge of the authors, find no comparable model acting in these two distinct environmental compartments, at the same global coverage, and scoping at the removals alone, rather than a time-bound riverine export. However, for the inland fate modelling, a similar extraction of N-removal coefficients from the IMAGE-GNM model (Beusen et al. 2015) can be an option, although this would involve modelling additional spatial units and their aggregation – NEWS 2 is modelled at river basin scale, whereas IMAGE-GNM runs at a 0.5°×0.5° grid cell spatial resolution. River basins seem as appropriate working units, where the variability of the occurring processes does not compromise the manageability and relevance of the results, hence its application here.

However, IMAGE-GNM shows predictive advantages by adding detailed modelling of land fate processes, which includes explicit groundwater denitrification in the soil/aquifer matrix and riparian zones, instead of regression models that lump processes' behaviour within watersheds by means of export constants. As such, NEWS 2 addresses the spatial variability of sources and sinks to a limited extent, and thus misses the non-linearity of the biogeochemical processes (Beusen et al. 2015), especially for N sinks, as sources are based on the same model work by Bouwman et al. (2005, 2009) model. In practice, upstream emissions modelled in a watershed scale always result in the same export fraction as downstream emissions. Although this distinction could be environmentally relevant, some attenuation may occur due to the tendency of higher agricultural activity and population density in lower reaches of the watershed and lower emission rates in upstream draining areas. Nevertheless, the average approach adopted seems sufficient for the purpose, under a parsimony principle and considering the significant spatial differentiation that results for the FFs. Moreover, spatial information of life cycle inventories tends to show coarse hydrological resolution, so the simple identification of the receiving watershed would be adequate.

The SPARROW model (Smith et al. 1997; Alexander et al. 2008) adopts a hybrid statistical and process-based approach to estimate riverine N-yields in a U.S. river basin network (not compatible to the network used here) and does not include water consumption as a removal process. Similarly, TRACI (Norris 2003) is scoped to U.S. states, NH3 is not covered, and no explicit N-removal processes are modelled. CARMEN (Klepper et al. 1995) is restricted to European validity and removal processes do not cover riverine retention or water consumption. Other site-specific and mechanistic models are available (reviewed by Borah and Bera (2003)), but require extensive parameterisation and datasets, which are not consistent with a globally wide application. Comparison of the inland fate component to these models is therefore not possible.

The marine fate component is based on surface water residence time data to estimate removal rates by advection and denitrification to proxy the persistence of the newly added N-fraction in coastal waters. As such, no comparable approaches were found available, as most are steady-state box (often multidimensional) models aiming at rivers or estuaries residence time estimations (Lucas 2016). Specifically, for the removal rates by advective transport, the model approach by Laruelle et al. (2013) presents coastal water residence times with global coverage but for the entire water column, thus not consistent with the present purpose where focus is on water persistence in the euphotic zone for phytoplankton N-uptake. Literature review was therefore preferred, providing residence times for 39 of 66 LMEs and archetypical conditions defined for the remaining 27. Regarding the removal rates by denitrification, Seitzinger et al. (2006) extended work by Nixon et al. (1996) in the attempt to relate

denitrification losses and residence time. No further approaches at such wide coverage or specific to the desired scope of marine coastal waters were identified.

3.4. Sensitivity and uncertainties

The model sensitivity to the five input parameters, i.e. the inland fates $FE_{ws,nat,DIN}$, $FE_{ws,ant,DIN}$, $FE_{pnt,DIN}$, $FE_{riv,DIN}$ and the marine residence time (τ_{LME}), was assessed by means of sensitivity ratios (SR) calculated as the ratio between the relative change in the model output and the relative change in the input parameters. Neutral sensitivity (SR=1) to the four inland coefficients and SR=3.5 for τ_{LME}, were obtained, meaning that the data quality of the latter is an important aspect to consider in the FF estimation model.

It is beyond the present scope to discuss the uncertainty of the underlying models that compose the NEWS 2 model suite, namely soil budget, runoff, sewage water treatment efficiency, riverine retention and denitrification, river basin network, and others. However, as the NEWS 2-DIN was adopted, its validation is a relevant issue. NEWS 2 calibration against observed DIN yields at the mouths of 66 large river basins (28 – 5,847 x 10^3 km^2) across the world shows reasonable robustness (explained variance R^2=0.54) in predicted vs. observed DIN yields, with an absolute model error of 6% (Mayorga et al. 2010). As the present inland fate component does not include the watershed and river sources (quantified emissions), described by Mayorga et al. (2010), and their inherent uncertainty, the overall model error is likely to be lower for the removal coefficients alone.

The literature review of residence time data revealed high inconsistency of sources. Such variability lead to the adoption of best estimates, averaged source data, or checks for both consistency with adjacent areas and expected archetypical conditions. Therefore, the archetypes definition for 41% of the LMEs may hold a reasonable amount of (unquantified) uncertainty, although their FF_{Nmarw} values match those of adjacent LMEs. Expert judgement was applied to estimate probable shelf conditions based on bathymetric maps. Nevertheless, most of the archetype-based residence time values were positively checked against online sources. The inconsistency or scarcity of studies is therefore the major source of uncertainty in the residence time dataset. Considering the sensitivity of the FFs to this parameter, further research is suggested to improve its quality.

The adopted regression method to estimate N-removal by denitrification as a function of water residence time has R^2=0.56 while using several data points from freshwater systems and estuaries (Seitzinger et al. 2006). Although this fact seems to not influence the denitrification rates, a regression based on marine residence time data properly integrated for LME area and euphotic depth (as N uptake only occurs in this upper layer) would improve the confidence in the denitrification rates, and at the same time the quality and consistency of the advective DIN-transport term.

The emission-weighted averaging method applied to the regional aggregation of FFs is bound to the quality of the emissions data. The regional aggregation presented here is based on data for year 2000 and therefore may misrepresent any other given year of interest. An appropriate update of the regional FFs should be considered if relevant for their application, or the temporal inconsistency noted; interannual variability in DIN emissions and retention can be substantial at regional or basin scales (Beusen et al. 2016), while at continental to global scales long-term trends are also important (Seitzinger et al. 2010; Beusen et al. 2016); but the uncertainty of these numbers is likely to be of minor importance when averaging up to the level of continents.

4. Conclusions and outlook

Fate factors representing the persistence of riverine exports of waterborne nitrogen emissions in coastal marine waters were developed with global coverage at a river basin scale. These fate factors account for spatial differences pertaining to five emission sources, i.e. runoff from natural or agricultural soils, sewage water discharges, and direct emissions to either surface fresh- or marine waters. The Global NEWS 2-DIN model coefficients were applied to estimate the riverine fractions exported. Marine surface water residence time was used to estimate the persistence in this compartment, and found as the most influential model parameter. A total of 28,860 fate factors were calculated covering 5,772 river basins in the world. Up to six orders of magnitude of variation was observed for N-emissions to soil, dropping to just one order of magnitude variation when the fate factors were aggregated to the level of continents. Fate factors with spatial resolution at river basin scale are recommended over the regionally aggregated, provided that emission locations are available. The proposed method and its spatially explicit results enable a significant increase in geographic coverage for application in LCIA.

Airborne emissions of nitrogen forms such as NO_x and NH_3 undoubtedly constitute a relevant component of the environmental N-cycling and also a significant flow from human activities. Energy production and agricultural activity are the most significant sources of emission of these compounds via atmospheric dispersion and deposition (Socolow 1999; Galloway et al. 2002). The inclusion of these emissions seems an essential step forward in the fate modelling of anthropogenic-N emissions. Deposition fractions of any of these compounds, as done by e.g. Dentener et al. (2006) or Roy et al. (2012), can be coupled to the waterborne FFs described here to ensure that also airborne emissions can be covered in the modelling of marine eutrophication. This constitutes an area of future research.

References

Alexander RB, Smith RA, Schwarz GE, et al (2008) Differences in Phosphorus and Nitrogen Delivery to the Gulf of Mexico from the Mississippi River Basin. Environ Sci Technol 42:11–12.

Andrews JC, Müller H (1983) Space-time variability of nutrients in a lagoonal patch reef. Limnol Oceanogr 28:215–227. doi: 10.4319/lo.1983.28.2.0215

Arrigo KR (2005) Marine microorganisms and global nutrient cycles. Nature 437:349–356. doi: 10.1038/nature04159

Beusen AHW (2005) User manual of CARMEN1. (not published). Bilthoven, the Netherlands

Beusen AHW, Bouwman AF, Van Beek LPH, et al (2016) Global riverine N and P transport to ocean increased during the 20th century despite increased retention along the aquatic continuum. Biogeosciences 113:2441–2451. doi: 10.5194/bgd-12-20123-2015

Beusen AHW, Dekkers, Bouwman AF, et al (2005) Estimation of global river transport of sediments and associated particulate C, N, and P. Global Biogeochem Cycles 19:1–17. doi: 10.1029/2005GB002453

Beusen AHW, Van Beek LPH, Bouwman AF, et al (2015) Coupling global models for hydrology and nutrient loading to simulate nitrogen and phosphorus retention in surface water – description of IMAGE–GNM and analysis of performance. Geosci Model Dev 8:4045–4067. doi: 10.5194/gmd-8-4045-2015

Borah DK, Bera M (2003) Watershed-scale hydrologic and nonpoint-source pollution models: Review of mathematical bases. Trans Am Soc Agric Eng 46:1553–1566.

Bouwman AF, Beusen AHW, Billen G (2009) Human alteration of the global nitrogen and phosphorus soil balances for the period 1970–2050. Global Biogeochem Cycles. doi: 10.1029/2009GB003576

Bouwman AF, Van Drecht G, Knoop JM, et al (2005) Exploring changes in river nitrogen export to the world's oceans. Global Biogeochem Cycles 19:14. doi: 10.1029/2004GB002314

Cloern JE (2001) Our evolving conceptual model of the coastal eutrophication problem. Mar Ecol Prog Ser 210:223–253. doi: 10.3354/meps210223

Cosme N, Hauschild MZ (2016) Effect factors for marine eutrophication in LCIA based on species sensitivity to hypoxia. Ecol Indic 69:453-462. doi: 10.1016/j.ecolind.2016.04.006

Cosme N, Koski M, Hauschild MZ (2015) Exposure factors for marine eutrophication impacts assessment based on a mechanistic biological model. Ecol Modell 317:50–63. doi: 10.1016/j.ecolmodel.2015.09.005

Dentener F, Drevet J, Lamarque JF, et al (2006) Nitrogen and sulfur deposition on regional and global scales: A multimodel evaluation. Global Biogeochem Cycles. doi: 10.1029/2005GB002672

Dettmann EH (2001) Effect of Water Residence Time on Annual Export and Denitrification of Nitrogen in Estuaries: A Model Analysis. Estuaries 24:481–490.

Diaz RJ, Rosenberg R (1995) Marine Benthic Hypoxia: a Review of Its Ecological Effects and the Behavioural Responses of Benthic Macrofauna. Oceanogr Mar Biol Annu Rev 33:245–303.

Diaz RJ, Rosenberg R (2008) Spreading dead zones and consequences for marine ecosystems. Science (80-) 321:926–9. doi: 10.1126/science.1156401

Doney SC (2010) The Growing Human Footprint on Coastal and Open-Ocean Biogeochemistry. Science (80-) 328:1512–1516. doi: 10.1126/science.1185198

Dumont E, Harrison JA, Kroeze C, et al (2005) Global distribution and sources of dissolved inorganic nitrogen export to the coastal zone: Results from a spatially explicit, global model. Global Biogeochem Cycles 19:GB4S02. doi: 10.1029/2005GB002488

Elser JJ, Bracken MES, Cleland EE, et al (2007) Global analysis of nitrogen and phosphorus limitation of primary producers in freshwater, marine and terrestrial ecosystems. Ecol Lett 10:1135–42. doi: 10.1111/j.1461-0248.2007.01113.x

Fear J, Thompson S, Gallo T, Paerl H (2005) Denitrification rates measured along a salinity gradient in the eutrophic Neuse River estuary, North Carolina, USA. Estuaries and Coasts 28:608–619. doi: 10.1007/BF02696071

Fekete BM, Vörösmarty CJ, Grabs W (2000) Global Composite Runoff Fields on Observed River Discharge and Simulated Water Balances. GRDC Reports 115. doi: 10.1017/CBO9781107415324.004

Galloway JN, Cowling EB (2002) Reactive nitrogen and the world: 200 years of change. Ambio 31:64–71. doi: 10.2307/4315217

Galloway JN, Cowling EB, Seitzinger SP, Socolow RH (2002) Reactive nitrogen: too much of a good thing? Ambio 31:60–3.

Galloway JN, Dentener FJ, Capone DG, et al (2004) Nitrogen cycles: past, present, and future. Biogeochemistry 70:153–226.

Galloway JN, Townsend AR, Erisman JW, et al (2008) Transformation of the Nitrogen Cycle: Recent Trends, Questions, and Potential Solutions. Science (80-) 320:889–892. doi: 10.1126/science.1136674

GESAMP (2001) A Sea of Troubles. Rep. Stud. GESAMP No. 70. Joint Group of Experts on the Scientific Aspects of Marine Environmental Protection and Advisory Committee on Protection of the Sea.

Goedkoop M, Heijungs R, Huijbregts MAJ, et al (2012) ReCiPe 2008 - A life cycle impact assessment method which comprises harmonised category indicators at the midpoint and the endpoint level. First edition (revised) Report I: Characterisation; July 2012, http://www.lcia-recipe.net

Gray JS, Wu RS, Or YY (2002) Effects of hypoxia and organic enrichment on the coastal marine environment. Mar Ecol Prog Ser 238:249–279.

Green PA, Vörösmarty CJ, Meybeck M, et al (2004) Pre-industrial and contemporary fluxes of nitrogen through rivers: a global assessment based on typology. Biogeochemistry 68:71–105.

Hauschild MZ, Potting J (2005) Spatial Differentiation in Life Cycle Impact Assessment - The EDIP2003 methodology.

Howarth R, Chan F, Conley DJ, et al (2011) Coupled biogeochemical cycles: Eutrophication and hypoxia in temperate estuaries and coastal marine ecosystems. Front Ecol Environ 9:18–26. doi: 10.1890/100008

Howarth RW, Billen G, Swaney D, et al (1996) Regional nitrogen budgets and riverine N & P fluxes for the drainages to the North Atlantic Ocean: Natural and human influences. Biogeochemistry 35:75–139. doi: 10.1007/BF02179825

Howarth RW, Marino R (2006) Nitrogen as the limiting nutrient for eutrophication in coastal marine ecosystems: Evolving views over three decades. Limnol Oceanogr 51:364–376. doi: 10.4319/lo.2006.51.1_part_2.0364

Kelly JR (2008) Nitrogen Effects on Coastal Marine Ecosystems. In: Hatfield JL, Follet RF (eds) Nitrogen in the Environment: Sources, Problems, and Management. U.S. Environmental Protection Agency, (Amsterdam, Boston, et al.: Academic Press/Elsevier, pp 271–332

Klepper O, Beusen AHW, Meinardi CR (1995) Modelling the flow of nitrogen and phosphorus in Europe: From loads to coastal seas. Bilthoven, the Netherlands

Laruelle GG, Dürr HH, Lauerwald R, et al (2013) Global multi-scale segmentation of continental and coastal waters from the watersheds to the continental margins. Hydrol Earth Syst Sci 17:2029–2051. doi: 10.5194/hess-17-2029-2013

Lee RY, Seitzinger SP, Mayorga E (2016) Land-based nutrient loading to LMEs: A global watershed perspective on magnitudes and sources. Environ Dev. doi: 10.1016/j.envdev.2015.09.006

Levin LA, Ekau W, Gooday AJ, et al (2009) Effects of natural and human-induced hypoxia on coastal benthos. Biogeosciences 6:2063–2098.

Lucas L V (2016) Encyclopedia of Estuaries. In: Kennish MJ (ed). Springer Netherlands, Dordrecht, pp 502–503

Magalhães CM, Joye SB, Moreira RM, et al (2005) Effect of salinity and inorganic nitrogen concentrations on nitrification and denitrification rates in intertidal sediments and rocky biofilms of the Douro River estuary, Portugal. Water Res 39:1783–1794. doi: 10.1016/j.watres.2005.03.008

Mayorga E, Seitzinger SP, Harrison JA, et al (2010) Global Nutrient Export from WaterSheds 2 (NEWS 2): Model development and implementation. Environ Model Softw 25:837–853. doi: 10.1016/j.envsoft.2010.01.007

Middelburg JJ, Levin LA (2009) Coastal hypoxia and sediment biogeochemistry. Biogeosciences 6:1273–1293. doi: 10.5194/bg-6-1273-2009

Monsen NE, Cloern JE, Lucas L V., Monismith SG (2002) The use of flushing time, residence time, and age as transport time scales. Limnol Oceanogr 47:1545–1553. doi: 10.4319/lo.2002.47.5.1545

Nixon SW (1995) Coastal marine eutrophication: A definition, social causes, and future concerns. Ophelia 41:199–219.

Nixon SW, Ammerman JW, Atkinson LP, et al (1996) The fate of nitrogen and phosphorus at the land-sea margin of the North Atlantic Ocean. Biogeochemistry 35:141–180.

Norris GA (2003) Impact Characterization in the Tool for the Reduction and Assessment of Chemical and Other Environmental Impacts. J Ind Ecol 6:79–101. doi: 10.1162/108819802766269548

NRC (2000) Clean Coastal Waters: Understanding and Reducing the Effects of Nutrient Pollution. National Academy press, Washington, DC

Pennington DW, Potting J, Finnveden G, et al (2004) Life cycle assessment Part 2: Current impact assessment practice. Environ Int 30:721–39. doi: 10.1016/j.envint.2003.12.009

Potting J, Hauschild MZ (2006) Spatial Differentiation in Life Cycle Impact Assessment: A decade of method development to increase the environmental realism of LCIA. Int J Life Cycle Assess 11:11–13.

Rabalais NN (2002) Nitrogen in Aquatic Ecosystems. Ambio 31:102–112.

Roy P-O, Huijbregts MAJ, Deschênes L, Margni M (2012) Spatially-differentiated atmospheric source–receptor relationships for nitrogen oxides, sulfur oxides and ammonia emissions at the global scale for life cycle impact assessment. Atmos Environ 62:74–81. doi: 10.1016/j.atmosenv.2012.07.069

Seitzinger SP (1988) Denitrification in freshwater and coastal marine ecosystems: Ecological and geochemical significance. Limnol Oceanogr 33:702–724. doi: 10.4319/lo.1988.33.4_part_2.0702

Seitzinger SP, Harrison JA, Böhlke JK, et al (2006) Denitrification across landscapes and waterscapes: A synthesis. Ecol Appl 16:2064–2090.

Seitzinger SP, Harrison JA, Dumont E, et al (2005) Sources and delivery of carbon, nitrogen, and phosphorus to the coastal zone: An overview of Global Nutrient Export from Watersheds (NEWS) models and their application. Global Biogeochem Cycles 19:1-11. doi: 10.1029/2005GB002606

Seitzinger SP, Kroeze C, Bouwman AF, et al (2002) Global patterns of dissolved inorganic and particulate nitrogen inputs to coastal systems: Recent conditions and future projections. Estuaries 25:640–655. doi: 10.1007/BF02804897

Seitzinger SP, Mayorga E, Bouwman AF, et al (2010) Global river nutrient export: A scenario analysis of past and future trends. Global Biogeochem Cycles 24:GB0A08. doi: 10.1029/2009GB003587

Sherman K, Alexander LM (eds) (1986) Variability and Management of Large Marine Ecosystems. Westview Press Inc., Boulder, CO

Smith RA, Schwarz GE, Alexander RB (1997) Regional interpretation of water-quality monitoring data. Water Resour Res 33:2781. doi: 10.1029/97WR02171

Smith VH, Joye SB, Howarth RW (2006) Eutrophication of freshwater and marine ecosystems. Limnol Ocean 51:351–355.

Smith VH, Tilman GD, Nekola JC (1999) Eutrophication: impacts of excess nutrient inputs on freshwater, marine, and terrestrial ecosystems. Environ Pollut 100:179–196.

Socolow RH (1999) Nitrogen management and the future of food: Lessons from the management of energy and carbon. Proc Natl Acad Sci U S A 96:6001–6008.

Toffoletto L, Bulle C, Godin J, et al (2007) LCA Methodology LUCAS – A New LCIA Method Used for a CAnadian-Specific Context. Int J 12:93–102.

Turner RE, Qureshi N, Rabalais NN, et al (1998) Fluctuating silicate: nitrate ratios and coastal plankton food webs. Proc Natl Acad Sci U S A 95:13048–13051.

Udo de Haes HA, Finnveden G, Goedkoop M, et al (2002) Life-Cycle Impact Assessment: Striving Towards Best Practice. SETAC Press, Pensacola, FL, USA

Van Drecht G, Bouwman AF, Harrison JA, Knoop JM (2009) Global nitrogen and phosphate in urban wastewater for the period 1970 to 2050. Global Biogeochem Cycles 23:1–19. doi: 10.1029/2009GB003458

Van Drecht G, Bouwman AF, Knoop JM, et al (2003) Global modeling of the fate of nitrogen from point and nonpoint sources in soils, groundwater, and surface water. Global Biogeochem Cycles 17:1–20. doi: 10.1029/2003GB002060

Van Jaarsveld JA (1995) Modelling the long-term atmospheric behaviour of pollutants on various spatial scales. PhD Thesis. University of Utrecht

Vitousek PM, Hättenschwiler S, Olander L, Allison S (2002) Nitrogen and nature. Ambio 31:97–101.

Vollenweider RA (1976) Advances in defining critical loading levels for phosphorus in lake eutrophication. Mem dell'Istituto Ital di Idrobiol dott Marco Marchi 33:53–83. doi: nicht verfügbar?

Vörösmarty CJ, Fekete BM, Meybeck M, Lammers RB (2000a) Geomorphic attributes of the global system of river at 30-minute spatial resolution. J Hydrol 237:17–39.

Vörösmarty CJ, Fekete BM, Meybeck M, Lammers RB (2000b) Global system of rivers: its role in organizing continental land mass and defining land-to-ocean linkages. Global Biogeochem Cycles 14:599–621. doi: 10.1029/1999GB900092

Wu RS (2002) Hypoxia: from molecular responses to ecosystem responses. Mar Pollut Bull 45:35–45.

Zhang J, Gilbert D, Gooday AJ, et al (2010) Natural and human-induced hypoxia and consequences for coastal areas: synthesis and future development. Biogeosciences 7:1443–1467. doi: 10.5194/bg-7-1443-2010

Article I – Electronic Supplementary Material 1

Spatially explicit fate factors of waterborne nitrogen emissions at the global scale

Nuno Cosme [a], Emilio Mayorga [b], Michael Z. Hauschild [a]

[a] Division for Quantitative Sustainability Assessment, Department of Management Engineering, Technical University of Denmark, Produktionstorvet 424, DK-2800 Kgs. Lyngby, Denmark

[b] Applied Physics Laboratory, University of Washington, 1013 NE 40th St., Seattle, WA 98105-6698, USA

Corresponding author: Nuno Cosme, nmdc@dtu.dk

List of additional figures:

Figure S.1 Global distribution of the fate factors (FF_{Nmarw}, [yr]) for marine eutrophication due to direct emissions of nitrogen (N) to coastal marine waters at a river basin resolution. Dotted areas correspond to basins that are endorheic or for other reason have no available FF. Note the non-linear scale.

Figure S.2 Global distribution of the fate factors (FF_{Nsew}, [yr]) for marine eutrophication due to nitrogen (N) in sewage discharges to river at a basin resolution. Dotted areas correspond to basins that are endorheic or for other reason have no available FF. Note the non-linear scale.

Figure S.3 Global distribution of the fate factors (FF_{Nns}, [yr]) for marine eutrophication due to nitrogen (N) emissions from natural soils (watershed runoff) to river at a basin resolution. Dotted areas correspond to basins that are arid (mainly Arabian Peninsula, Northern Africa and Southwest Australia), endorheic, or for other reason have no available FF. Note the non-linear scale.

Figure S.4 Global distribution of the fate factors (FF_{Nas}, [yr]) for marine eutrophication due to nitrogen (N) emissions from agricultural soils (watershed runoff) to river at a basin resolution. Dotted areas correspond to basins that are arid (mainly Arabian Peninsula, Northern Africa and Southwest Australia), endorheic, or for other reason have no available FF. Note the non-linear scale.

Note

*Full results with fate factors per emission route for the 5,772 river basins can be found in the **Electronic Supplementary Material 2** as Excel spreadsheets:*

Table S1 Surface water residence times per Large Marine Ecosystem (LME) and metadata for archetype classification.

Table S2 Fate factors (FF, [yr]) for waterborne nitrogen (N) emissions per emission route: N from natural soils (FF_{Nns}), N from agricultural soils (FF_{Nas}), N in sewage discharges to river (FF_{Nsew}), N to river (FF_{Nriv}), and direct N emissions to coastal marine waters (FF_{Nmarw}). Results for 5,772 worldwide river basins.

Additional figures

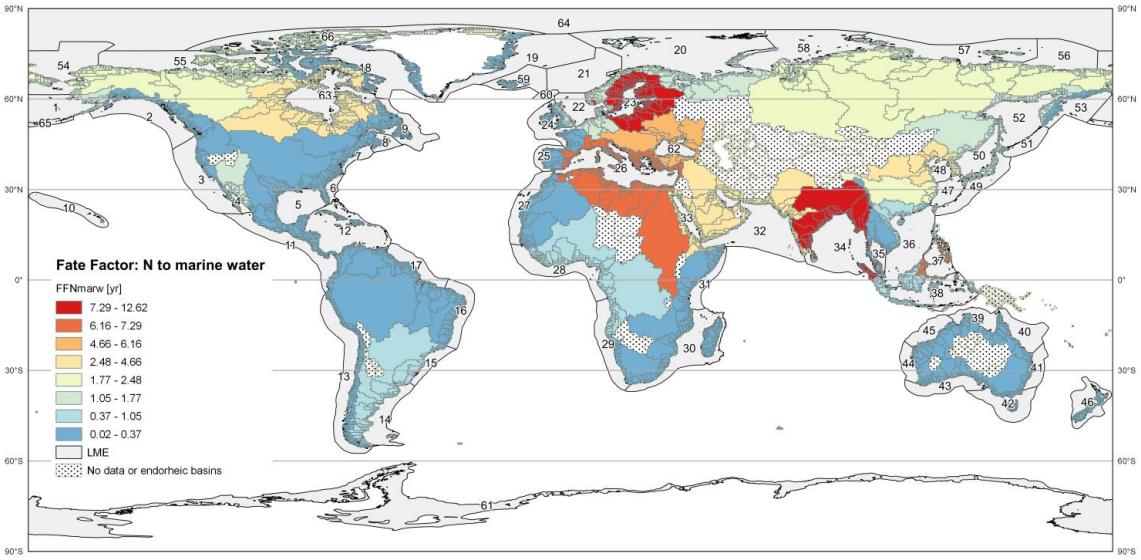

Figure S1 Global distribution of the fate factors (FF_{Nmarw}, [yr]) for marine eutrophication due to direct emissions of nitrogen (N) to coastal marine waters at a river basin resolution. Dotted areas correspond to basins that are endorheic or for other reason have no available FF. Note the non-linear scale.

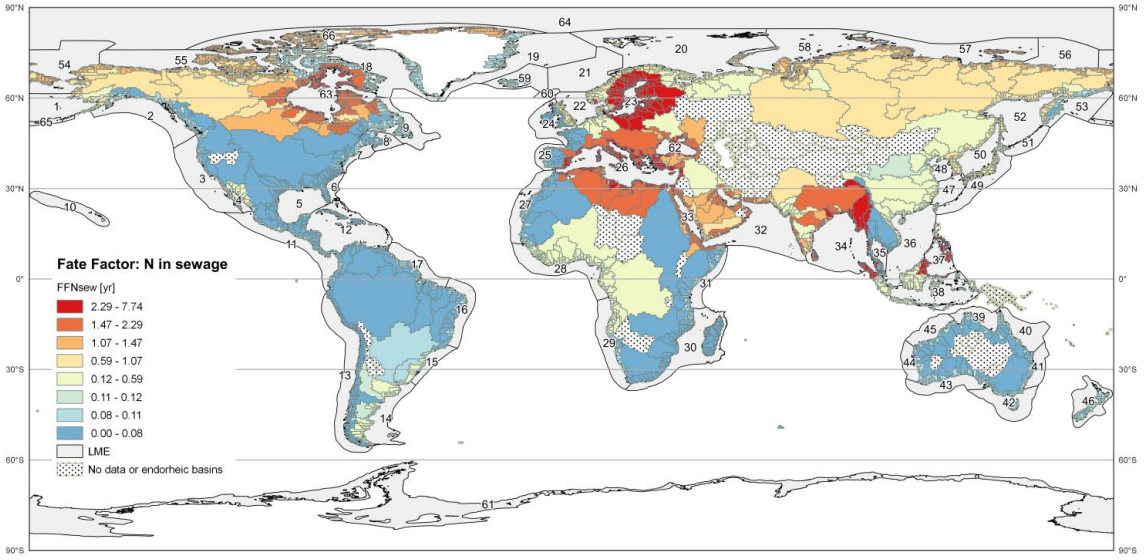

Figure S2 Global distribution of the fate factors (FF_{Nsew}, [yr]) for marine eutrophication due to nitrogen (N) in sewage discharges to river at a basin resolution. Dotted areas correspond to basins that are endorheic or for other reason have no available FF. Note the non-linear scale.

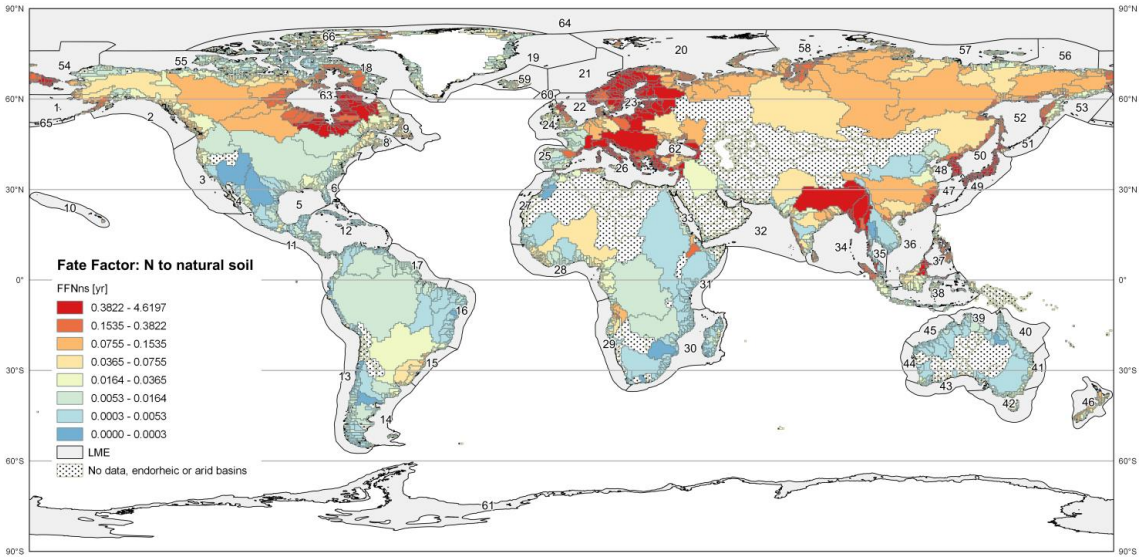

Figure S3 Global distribution of the fate factors (FF_{Nns}, [yr]) for marine eutrophication due to nitrogen (N) emissions from natural soils (watershed runoff) to river at a basin resolution. Dotted areas correspond to basins that are arid (mainly Arabian Peninsula, Northern Africa and Southwest Australia), endorheic, or for other reason have no available FF. Note the non-linear scale.

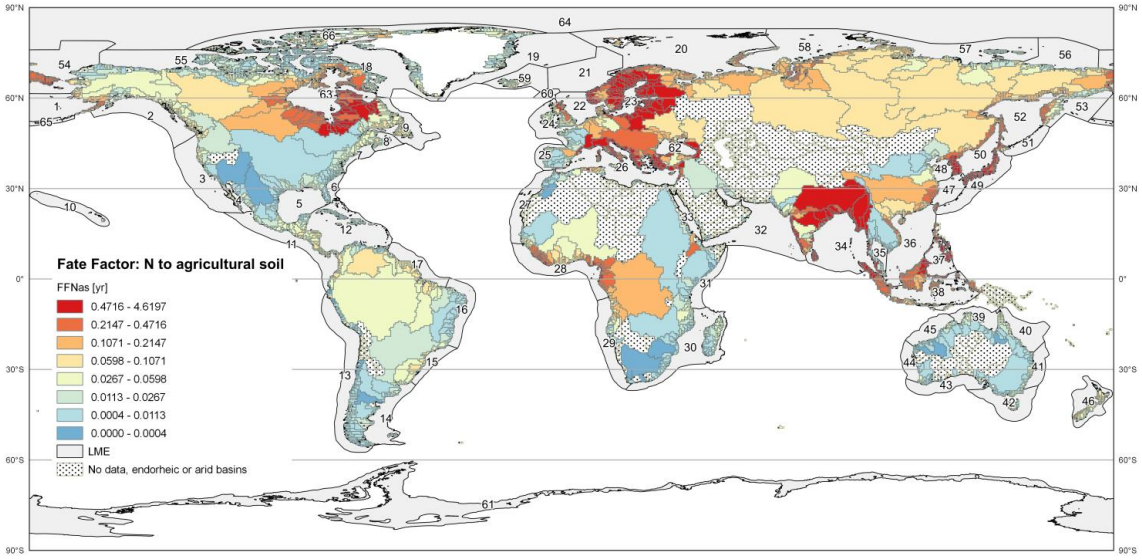

Figure S4 Global distribution of the fate factors (FF_{Nas}, [yr]) for marine eutrophication due to nitrogen (N) emissions from agricultural soils (watershed runoff) to river at a basin resolution. Dotted areas correspond to basins that are arid (mainly Arabian Peninsula, Northern Africa and Southwest Australia), endorheic, or for other reason have no available FF. Note the non-linear scale.

Article I – Electronic Supplementary Material 2

Article title:

Spatially explicit fate factors of waterborne nitrogen emissions at the global scale

Journal:

International Journal of Lice Cycle Assessment

Authors:

Nuno Cosme [a], Emilio Mayorga [b], Michael Z. Hauschild [a]

Affiliations:

[a] Division for Quantitative Sustainability Assessment, Department of Management Engineering, Technical University of Denmark, Produktionstorvet 424, DK-2800 Kgs. Lyngby, Denmark

[b] Applied Physics Laboratory, University of Washington, 1013 NE 40th St., Seattle, WA 98105-6698, USA

Corresponding author:

Nuno Cosme, nmdc@dtu.dk

Contents:

Table S1 Surface water residence times per Large Marine Ecosystem (LME) and metadata for archetype classification. See list of reference sources in 'RT_References' sheet. (*) Source used to average or settle divergent data.

Large Marine Ecosystem [#. Name]	Residence time [yr]	Source Arch. 1-4; Litt.	Metadata for archetype classification			Literature References
			Continental Shelf		LME	
			Exposure to currents	Width	Depth	
01. East Bering Sea	2.00	Arch. 2	Medium	Broad	Shallow	1
02. Gulf of Alaska	0.25	Arch. 1	High	Narrow	Deep	1
03. California Current	0.25	Arch. 1	High	Narrow	Deep	1
04. Gulf of California	1.50	Lit.				18
05. Gulf of Mexico	0.21	Lit.				33, 34
06. Southeast U.S. Continental Shelf	0.08	Lit.				17
07. Northeast U.S. Continental Shelf	0.24	Lit.				36
08. Scotian Shelf	0.07	Lit.				29
09. Newfoundland-Labrador Shelf	0.25	Arch. 1	High	Broad	Medium	1
10. Insular Pacific-Hawaiian	0.25	Arch. 1	High	Narrow	Deep	1
11. Pacific Central-American	0.25	Arch. 1	High	Narrow	Deep	1
12. Caribbean Sea	0.21	Lit.				21
13. Humboldt Current	0.03	Lit.				11
14. Patagonian Shelf	0.49	Lit.				37
15. South Brazil Shelf	0.49	Lit.				37
16. East Brazil Shelf	0.25	Arch. 1	High	Narrow	Sh-De	1 (2)*
17. North Brazil Shelf	0.25	Arch. 1	High	Medium	Sh-De	1 (16)*
18. Canadian Eastern Arctic - West Greenland	0.25	Arch. 1	Medium	Medium	Sh-De	1
19. Greenland Sea	0.25	Arch. 1	High	Narrow	Deep	1
20. Barents Sea	2.00	Arch. 2	Medium	Medium	Shallow	1
21. Norwegian Sea	2.00	Arch. 2	Medium	Broad	Sh-De	1
22. North Sea	2.00	Lit.				3
23. Baltic Sea	21.83	Lit.				36
24. Celtic-Biscay Shelf	0.17	Lit.				38
25. Iberian Coastal	0.25	Arch. 1	High	Narrow	Deep	1
26. Mediterranean	10.00	Lit.				31
27. Canary Current	0.25	Arch. 1	High	Narrow	Deep	1
28. Guinea Current	1.37	Lit.				11
29. Benguela Current	0.25	Arch. 1	High	Narrow	Deep	1
30. Agulhas Current	0.10	Lit.				42
31. Somali Coastal Current	0.25	Arch. 1	High	Narrow	Deep	1
32. Arabian Sea	6.50	Lit.				26
33. Red Sea	6.00	Lit.				10
34. Bay of Bengal	12.00	Lit.				26
35. Gulf of Thailand	0.04	Lit.				6
36. South China Sea	0.91	Lit.				4
37. Sulu-Celebes Sea	11.00	Lit.				9, 30
38. Indonesian Sea	0.76	Lit.				7

Large Marine Ecosystem [#. Name]	Residence time [yr]	Source Arch. 1-4; Litt.	Metadata for archetype classification			Literature References
			Continental Shelf		LME	
			Exposure to currents	Width	Depth	
39. North Australian Shelf	0.25	Arch. 1	Medium	Medium	Sh-De	1
40. Northeast Australian Shelf	0.25	Arch. 1	Medium	Medium	Sh-De	1 (5)*
41. East-Central Australian Shelf	0.25	Arch. 1	High	Narrow	Shallow	1
42. Southeast Australian Shelf	0.25	Arch. 1	High	Narrow	Deep	1
43. Southwest Australian Shelf	0.25	Arch. 1	High	Narrow	Deep	1
44. West-Central Australian Shelf	0.25	Arch. 1	High	Narrow	Deep	1
45. Northwest Australian Shelf	0.25	Arch. 1	High	Medium	Sh-De	1
46. New Zealand Shelf	0.27	Lit.				40
47. East China Sea	2.61	Lit.				11, 15, 20
48. Yellow Sea	3.75	Lit.				15
49. Kuroshio Current	2.30	Lit.				19
50. Sea of Japan/East Sea	2.10	Lit.				39
51. Oyashio Current	0.25	Arch. 1	High	Narrow	Deep	1
52. Sea of Okhotsk	2.00	Lit.				35
53. West Bering Sea	0.25	Arch. 1	High	Narrow	Deep	1
54. Northern Bering - Chukchi Seas	3.50	Lit.				27
55. Beaufort Sea	3.50	Lit.				27
56. East Siberian Sea	3.50	Lit.				27
57. Laptev Sea	3.50	Lit.				27
58. Kara Sea	3.50	Lit.				27
59. Iceland Shelf and Sea	0.25	Arch. 1	High	Narrow	Deep	1
60. Faroe Plateau	0.25	Lit.				8
61. Antarctic	6.00	Lit.				13
62. Black Sea	7.40	Lit.				22, 41
63. Hudson Bay Complex	6.60	Lit.				12
64. Central Arctic Ocean	11.00	Lit.				28
65. Aleutian Islands	0.25	Arch. 1	High	Narrow	Deep	1
66. Canadian High Arctic - North Greenland	3.50	Lit.				27

Surface water residence time - Reference list:

1. Liu K.-K., Dittert N., Lei K.-R., Kremer H.H., Maddison L. Web-based Resources for Continental Margins Biogeochemical Research and Education. Retrieved from http://cmtt.tori.org.tw/ on 12/09/2012. (Supporting information for) K.-K. Liu, L. Atkinson, R.A. Quiñones, and L. Talaue-McManus (eds). 2010. Carbon and Nutrient Fluxes in Continental Margins: A Global Synthesis. Global Change - The IGBP Series, Springer: Berlin, 744 pp.

2. Attisano K.K., Niencheski L.F.H., Milani I.C.B., Machado C.S., Milani M.R., Zarzur S., Andrade C.F.F. 2008. Evidences of continental groundwater inputs to the shelf zone in Albardão, RS, Brazil. Brazilian Journal of Oceanography 56(3), 189-200.
3. Blaas M., Kerkhoven D., de Swart H.E. 2001. Large-scale circulation and flushing characteristics of the North Sea under various climate forcings. Climate Research 18, 47–54.
4. Liu K.-K., Atkinson L., Quiñones R., Talaue-McManus L. 2010. Carbon and Nutrient Fluxes in Continental Margins, Global Change – The IGBP Series. Springer-Verlag, Berlin, Heidelberg
5. Choukroun S., Ridd P.V., Brinkman R., McKinna L.I.W. 2010. On the surface circulation in the western Coral Sea and residence times in the Great Barrier Reef. Journal of Geophysical Research 115, C06013.
6. Dulaiova H., Burnett W.C., Wattayakorn G., Sojisuporn P. 2006. Are groundwater inputs into river-dominated areas important? The Chao Phraya River – Gulf of Thailand. Limnology and Oceanography 51(5), 2232–2247.
7. Ffield A., Gordon A.L. 1992. Vertical mixing in the Indonesian Thermocline. Journal of Physical Oceanography 22, 184–195.
8. Gaard E. 2000. Seasonal abundance and development of Calanus finmarchicus in relation to phytoplankton and hydrography on the Faroe Shelf. ICES Journal of Marine Science 57, 1605–1611.
9. Gordon A.L., Tessler Z.D., Villanoy C. 2011. Dual overflows into the deep Sulu Sea. Geophysical Research Letters 38, L18606.
10. Talley L.D., Pickard G.L., Emery W.J., Swift J.H. (eds) 2011. Chapter 8 - Gravity Waves, Tides, and Coastal Oceanography: Supplementary Materials. In: Descriptive Physical Oceanography (Sixth Edition). Academic Press, pp 223–244
11. Hall J., Smith S.V., Boudreau P.R. (eds.) 1996. Report on the International Workshop on Continental Shelf Fluxes of Carbon, Nitrogen and Phosphorus. LOICZ/R&S/96-9. LOICZ, Texel, The Netherlands.
12. Ingram R.G., Prinsenberg S. 1998. Chapter 29. Coastal oceanography of Hudson Bay and surrounding eastern Canadian arctic waters coastal segment. In Allan R. Robinson, Kenneth H. Brink (eds), The Sea - Volume 11. John Wiley & Sons, Inc.
13. Jacobs S.S., Fairbanks R.G., Horibe Y.G. 1985. Origin and evolution of water masses near the Antarctic continental margin: Evidence from H218O/H216O ratios in seawater. In S. Jacobs (ed), Oceanology of the Antarctic Continental Shelf. AGU, Washington, D.C., Antarctic Research Series 43, 59–85.
14. Jahn A., Tremblay L.B., Newton R., Holland M.M., Mysak L.A., Dmitrenko I.A. 2010. A tracer study of the Arctic Ocean's liquid freshwater export variability. Journal of Geophysical Research 115, C07015.
15. Men W., Liu G. 2015. Distribution of 226Ra and the residence time of the shelf water in the Yellow Sea and the East China Sea. J Radioanal Nucl Chem 303:2333–2344. doi: 10.1007/s10967-014-3749-y

16. Limeburner R., Beardsley R.C., Soares I.D., Lentz S.J., Candela J. 1995. Lagrangian flow observations of the Amazon River discharge into the North Atlantic. Journal of Geophysical Research 100(C2), 2401–2415.
17. Alegria H.A., D'Autel J.P., Shaw T.J. 2000. Offshore Transport of Pesticides in the South Atlantic Bight: Preliminary Estimate of Export Budgets. Marine Pollution Bulletin 40(12), 1178-1185.
18. Lopez M., Garcia J. 2003. Moored observations in the northern Gulf of California: A strong bottom current. Journal of Geophysical Research 108(C2), 3048.
19. Matsuno T., Lee J.-S., Yanao S. 2009. Influence of the Kuroshio on the water properties in the shelf. Ocean Science Discussions 6, 741–764.
20. Nozaki Y. 1989. Mean residence time of the shelf water in the East China and the Yellow Seas determined by 228Ra/226Ra measurements. Geophys Res Lett 16:1297–1300.
21. Molinari R.L., Atwood D.K., Duckett C., Spillane M., Brooks I. 1980. Surface currents in the Caribbean Sea as deducted from satellite tracked drifting buoys. Proceedings of the 32nd Annual Gulf and Caribbean Fisheries Institute, 106-113.
22. Lee B.-S., Bullister J.L., Murray J.W., Sonnerup R.E. 2002. Anthropogenic chlorofluorocarbons in the Black Sea and the Sea of Marmara. Deep. Res. I 49, 895–913.
23. Naqvi W. 2012. Intensification of seasonal oxygen-deficient zone over the western Indian shelf. Retrieved from http://www.unep.org/stap/Portals/61/stap/Naqvi.pdf on 12/09/2012.
24. Pinet P.R. 2008. Invitation to Oceanography. Jones & Bartlett Learning, 620 pp.
25. Rivas D., Badan A., Ochoa J. 2005: The Ventilation of the Deep Gulf of Mexico. Journal of Physical Oceanography 35, 1763–1781.
26. Sarma V.V.S.S. 2002. An evaluation of physical and biogeochemical processes regulating perennial suboxic conditions in the water column of the Arabian Sea. Global Biogeochemical Cycles 16(4), 1082.
27. Schlosser P., Bauch D., Bonisch G., Fairbanks R.F. 1994. Arctic river-runoff: mean residence time on the shelves and in the halocline. Deep-Sea Research I 41(7), 1053–1068.
28. Östlund H.G. 1982. The residence time of the fresh-water component in the arctic ocean. J Geophys Res 87:2035–2043. doi: 10.1029/JC087iC03p02035
29. Smith P.C., Flagg C.N., Limeburger R., Fuentes-Yaco C., Hannah C., Beardsley R.C., Irish J.D. 2003. Scotian Shelf crossovers during winter/spring 1999, J. Geophys. Res., 108(C11), 8013, doi:10.1029/2001JC001288
30. Tessler Z.D. 2012. Still overflow processes in the Philippine Archipelago. PhD Thesis. Columbia University. Retrieved from http://academiccommons.columbia. edu/ catalog/ac%3A143841 on 12/09/2012.
31. Migon C. 2005. Trace metals in the Mediterranean Sea, in: The Mediterranean Sea. Springer-Verlag, Berlin Heidelberg, pp. 151–176. doi:DOI 10.1007/b107146

32. Tsunogai S., Watanabe S., Nakamura J., Ono T., Sato T. 1997. A Preliminary Study of Carbon System in the East China Sea. Journal of Oceanography 53, 9-17.

33. Turner E., Rabalais N. 2009. 2009 Forecast of the Summer Hypoxic Zone Size, Northern Gulf of Mexico. Retrieved from http://www.gulfhypoxia.net/research/ Shelfwide%20Cruises/2009/Files/2009_Hypoxia_Forecast.pdf on 12/09/2012.

34. USGS. 2012. Streamflow and Nutrient Delivery to the Gulf of Mexico for October 2011 to May 2012 (Preliminary). Retrieved from http://toxics.usgs.gov/hypoxia/ mississippi/ oct_jun /index.html on 12/09/2012.

35. Gladyshev S., Talley L., Kantakov G., Khen G., Wakatsuchi M. 2003. Distribution, formation, and seasonal variability of Okhotsk Sea Mode Water. J. Geophys. Res. 108, 1–21. doi:10.1029/2001JC000877

36. Dettman E.H. 2001. Effect of Water Residence Time on Annual Export and Denitrification of Nitrogen in Estuaries: A Model Analysis. Estuaries 24(4), 481-490.

37. Piola A.R., Campos E.J.D., Möller Jr O.O., Charo M., Martinez C. 2000. Subtropical Shelf Front off eastern South America. Journal of Geophysical Research 105(C3), 6565-6578.

38. Delhez É.J.M., Heemink A.W., Deleersnijder É. 2004. Residence time in a semi-enclosed domain from the solution of an adjoint problem. Estuar. Coast. Shelf Sci. 61, 691–702. doi:10.1016/j.ecss.2004.07.013

39. Yanagi T. 2002. Water, Salt, Phosphorus and Nitrogen Budgets of the Japan Sea. J Oceanogr 58:797–804.

40. Frew R.D., Hutchins D.A., Nodder S., Sanudo-Wilhelmy S., Tovar-Sanchez A., Leblanc K., Hare C.E., Boyd P.W. 2006. Particulate iron dynamics during FeCycle in subantarctic waters southeast of New Zealand. Global Biogeochem. Cycles 20, 1–15. doi:10.1029/2005GB00255

41. Ivanov L.I., Samodurov A.S. 2001. The role of lateral fluxes in ventilation of the Black Sea. J. Mar. Syst. 31, 159–174. doi:10.1016/S0924-7963(01)00051-3

42. Lutjeharms J.R.E. 2006. The Agulhas Current. Springer, Berlin, Heidelberg. doi:10.1007/3-540-37212-1

Table S2 Fate factors (FF, [yr]) for waterborne nitrogen (N) emissions per emission route: N from natural soils (FF_{Nns}), N from agricultural soils (FF_{Nas}), N in sewage discharges to river (FF_{Nsew}), N to river (FF_{Nriv}), and direct N emissions to coastal marine waters (FF_{Nmarw}). Results for 5,772 river basins. 'BASINID' represents the basin identifier used in STN-30p 6.01 and 'basincellcnt' the number of 0.5° grid cells contained by the basin.

<Available as Electronic Supplementary Material 2>

Note: Table content and format as below, but extended to 5,772 river basins (ca. 126 pages), as an excel spreadsheet. Alternatively, the dataset is available as a GIS shapefile (available on request).

BASINID	basinname	Basincellcnt	FF_{Nns} [yr]	FF_{Nas} [yr]	FF_{Nsew} [yr]	FF_{Nriv} [yr]	FF_{Nmarw} [yr]
1	Amazon	1916	0.0057	0.054	0.034	0.067	0.19
2	Nile	1283	0.073	0.073	0.43	0.79	2.3
3	Zaire	1203	0.088	0.088	0.44	0.80	2.3
4	Mississippi	1371	0.092	0.092	0.32	0.59	2.3
5	Ob	1786	0.0081	0.0081	0.032	0.048	0.16
6	Parana	939	0.00073	0.00073	0.0029	0.0059	6.2
7	Yenisei	1627	0.015	0.14	0.15	0.32	0.96
8	Lena	1651	0.087	0.087	0.49	0.77	2.3
9	Niger	749	0.018	0.018	0.044	0.087	0.37
10	Tamanrasett	651	0.067	0.067	0.25	0.46	1.4
11	Chang Jiang	672	0.048	0.048	0.15	0.31	0.96
12	Amur	881	0.12	0.12	0.22	0.42	1.8
13	Mackenzie	1127	n/a	n/a	0.027	0.054	0.19
14	Ganges	592	0.038	0.038	0.52	0.81	2.3
17	Zambezi	457	1.0	1.0	0.91	1.8	7.3
20	Indus	434	0.14	0.14	0.75	1.2	4.2
21	Nelson	592	0.078	0.078	0.45	0.81	2.3
24	Saint Lawrence	487	0.0072	0.0072	0.011	0.017	0.053
25	Orinoco	338	0.0064	0.0064	0.012	0.024	0.076
26	Murray	393	0.050	0.050	0.33	0.64	4.1
27	Shatt el Arab	386	0.00043	0.00043	0.011	0.019	0.19
28	Orange	344	0.027	0.027	0.28	0.50	4.1
29	Huang He	361	0.39	0.39	0.91	1.6	4.7
30	Yukon	644	0.0047	0.0047	0.062	0.12	2.5
31	Senegal	287	0.078	0.078	0.38	0.69	2.3
32	Irharhar	318	0.00032	0.00032	0.019	0.038	0.19
33	Jubba	265	0.012	0.012	0.028	0.044	0.19
34	Colorado (Ari)	325	0.0067	0.060	0.030	0.060	0.19
35	Rio Grande (US)	301	0.000029	0.000029	0.00066	0.0010	1.1
36	Danube	370	n/a	n/a	0.92	1.8	6.2
37	Tocantins	254	0.0000049	0.0000049	0.00026	0.00045	0.16
38	Mekong	261	0.0031	0.0031	0.028	0.058	0.19
40	Columbia	341	0.068	0.068	0.45	0.81	2.3
41	Araye	262	0.0039	0.0039	0.032	0.065	0.19
43	Kolyma	518	0.065	0.065	0.32	0.56	4.7
45	Sao Francisco	205	n/a	n/a	1.1	2.1	6.2
46	Qattara	209	0.00055	0.005	0.0048	0.010	0.030
47	Dnepr	264	0.0038	0.036	0.030	0.059	0.19
48	Dawasir	165	0.10	0.10	0.27	0.48	1.4
49	Don	212	0.11	0.11	0.27	0.48	1.4
50	Colorado (Argent.)	166	0.15	0.15	0.93	1.5	4.2

Article II

Exposure factors for marine eutrophication impacts assessment based on a mechanistic biological model

Cosme, N., Koski, M. & Hauschild, M.Z.

Ecological Modelling 2015, *317*, 50–63

DOI: 10.1016/j.ecolmodel.2015.09.005

manuscript in post-print version

Exposure factors for marine eutrophication impacts assessment based on a mechanistic biological model

Nuno Cosme [a,*], Marja Koski [b], Michael Z. Hauschild [a]

[a] Division for the Quantitative Sustainability Assessment, Department of Management Engineering, Technical University of Denmark, Produktionstorvet 424, DK-2800 Kgs. Lyngby, Denmark

[b] Section of Marine Ecology and Oceanography, Technical University of Denmark, Kavalergården 6, DK-2920 Charlottenlund, Denmark

* *Corresponding author*. Tel.: +45 45254729.

E-mail address: nmdc@dtu.dk

Abstract

Emissions of nitrogen (N) from anthropogenic sources enrich marine waters and promote planktonic growth. This newly synthesised organic carbon is eventually exported to benthic waters where aerobic respiration by heterotrophic bacteria results in the consumption of dissolved oxygen (DO). This pathway is typical of marine eutrophication. A model is proposed to mechanistically estimate the response of coastal marine ecosystems to N inputs. It addresses the biological processes of nutrient-limited primary production (PP), metazoan consumption, and bacterial degradation, in four distinct sinking routes from primary (cell aggregates) and secondary producers (faecal pellets, carcasses, and active vertical transport). Carbon export production (P_E) and ecosystems eXposure Factors (XF), which represents a nitrogen-to-oxygen 'conversion' potential, were estimated at a spatial resolution of 66 large marine ecosystem (LME), five climate zones, and site-generic. The XFs obtained range from 0.45 (Central Arctic Ocean) to 15.9 $kgO_2 \cdot kgN^{-1}$ (Baltic Sea). While LME resolution is recommended, aggregated P_E or XF per climate zone can be adopted, but not global aggregation due to high variability. The XF is essential to estimate a marine eutrophication impacts indicator in Life Cycle Impact Assessment (LCIA) of anthropogenic-N emissions. Every relevant process was modelled and the uncertainty of the driving parameters considered low suggesting valid applicability in characterisation modelling in LCIA.

Keywords: Nitrogen; Carbon export; Oxygen depletion; Marine eutrophication; Exposure factor; Life cycle impact assessment.

1. Introduction

The ecological equivalent for the photosynthesis rate in marine systems is the primary production (PP) rate (Platt et al., 1989). Marine photosynthetic primary producers assimilate nutrients dissolved in seawater: nitrogen (N), phosphorus (P), silicon (Si), and micronutrients, along with carbon (C) available from dissolution of atmospheric carbon dioxide, to synthesise organic compounds necessary for their metabolism and growth. The Redfield ratio (Redfield, 1958) is usually adopted to describe the average uptake of the various nutrients, i.e. C:N:P with molar ratios of 106:16:1 – see Ho et al. (2003) on elemental composition of phytoplankton. We assume N as the limiting nutrient in marine waters, or more precisely, in most of the marine waters and for most of the time to account for possible spatial and temporal exceptions. Studies and reviews support this assumption (e.g. Howarth and Marino (2006); Vitousek et al. (2002)), but we acknowledge that spatial and seasonal limitation by P or Si (e.g. Elser et al. (2007); Turner et al. (1998)) and cases of co-limitation (Arrigo, 2005) may occur. For modelling purposes we consider the 'limiting nutrient' concept a necessary and justifiable simplification.

Phytoplankton blooms occur when optimal light and temperature conditions, nutrient availability, and limited grazing pressure exist, so that growth rates may exceed losses from respiration, sinking, grazing, and other causes for mortality (Behrenfeld and Boss, 2014; Huisman et al., 1999). The timing and duration of phytoplankton blooms relative to the life-histories of secondary producers (SP, mainly zooplankton) are crucial to the match-mismatch hypothesis (Cushing, 1975) and the application in the present method. Under 'match' events zooplankton typically graze on phytoplankton, whose growth and sink are contained, and the export production is based on zooplankton's faecal pellets and carcasses. In opposition, the 'mismatch' occurs when the grazing pressure of the zooplankton community is not sufficient to balance the increase in phytoplankton growth and a larger fraction of these is left ungrazed. The mismatched fraction sinks off the euphotic zone facilitated by advection, aggregation, and coagulation (Kiørboe et al., 1996; Wassmann, 1998). At higher latitudes mismatch events are usually more intense, as environmental conditions turn favourable, defining the vertical flux. In the tropics a closer match between phyto- and zooplankton growth results in higher nutrients regeneration and retention food webs (Wassmann, 1998) with lower contributions to vertical export.

The downward export is composed of 'marine snow' (Alldredge and Silver, 1988; Kiørboe, 2001, 1996), the term used to describe the particulate organic carbon (POC) flux of sinking aggregates of phytoplankton cells, faecal pellets, zooplankton carcasses, and other organic material from dead or dying microorganisms (extensively reviewed by Fowler and Knauer (1986)). An additional contribution to this flux is given by active vertical transport (AVT) mediated by diel vertical migration of zooplankton

(Lampert, 1989): zooplankton ingests organic particles at night from surface waters and excretes/egests the metabolites during the day below the mixed layer (Longhurst and Harrison, 1988). Sinking POC may be consumed or dissolved in the water column and only a fraction gets oxidised or consumed by benthic microbial and metazoan communities, respectively (Ducklow et al., 2001). Respiration in bottom strata is responsible for the remineralisation of nutrients but also for the consumption of dissolved oxygen (DO). In a principle of linearity of cause-effect, and modulated by site-dependent conditions, the higher the load of the limiting nutrient the higher the carbon flux and DO consumption. Under low ventilation conditions and excessive N input, DO can be depleted down to hypoxic and anoxic levels (Elmgren, 2001; Keeling et al., 2010).

Globally, anthropogenic N-loadings to the environment have increased more than 10-fold in the last 150 years, mainly due to the growing need for reactive nitrogen use in agriculture and to emissions from energy production (Galloway et al., 2008). Fertilizers applied in agricultural production emit N, mainly in the form of NH_4^+ and NO_3^- to soil and water, or NH_3 to air, whereas fossil fuels combustion emits nitrogen oxides (NO_x) resulting from the oxidation of atmospheric N_2 or organic N content of the fuel (mainly coal) (Galloway et al., 2002; Socolow, 1999). Run-off, leaching, and atmospheric deposition of these N-forms eventually enrich coastal marine ecosystems with biologically available N. Marine eutrophication can be one of the consequences after planktonic growth (Nixon, 1995; NRC, 2000; Smith et al., 1999), for which important impacts may arise from (i) decrease in water quality, by high turbidity, colour, and smell, hindering water uses, fish production, and reducing the aesthetic value, (ii) depletion of DO in bottom waters down to hypoxic or anoxic levels that may affect exposed species, and (iii) change in species composition and interaction that may enhance the growth of toxic and harmful algal species (Diaz and Rosenberg, 2008; Gray et al., 2002; Kelly, 2008; Levin et al., 2009). High biological oxygen demand (BOD) effluents may share similar DO consumption pathways via biologically-mediated degradation, but these are outside the scope of the present work.

The PP rate provides useful information on the ecological condition (Niemi et al., 2004; Smith, 2007), but is unable to predict distinct responses thus missing the explanatory power for the impacts. We propose a novel indicator, the ecosystem eXposure Factor (XF), to add a mechanistic explanation for ecosystem responses, potential impacts, and the reasons for its variability. Aiming at the quantification of such responses to anthropogenic-N loadings, we set the following objectives:

- Identify and parameterise the relevant biological processes of organic carbon production, export, and consumption/degradation to cover the entire ecosystem response pathway in a mechanistic manner;

- Spatially differentiate the parameterisation to ensure the model output is representative of distinct receiving ecosystems in support of a comparative assessment of exposure locations;
- Produce site-dependent exposure factors with a global coverage that express how much oxygen is consumed via respiration of sunken organic carbon as a function of N assimilated per specific spatial unit.

This approach seems relevant and useful for predictive advice, ecosystems management, and eutrophication modelling. It may therefore contribute to comparative assessments of environmental impact of human activities or vulnerability of coastal areas.

2. Methodology

Life Cycle Assessment (LCA) is an environmental analysis tool used to systematically evaluate the potential environmental impacts that arise from the consumption of resources or emission of substances to the environment throughout the entire life cycle of a product or service (Hauschild, 2005). In the Life Cycle Impact Assessment (LCIA) phase the inventoried emissions are multiplied by substance-specific characterisation factors (CF) that represent the ability of those to impact on representative indicators. In brief, CFs convert an emission or consumption into a potential impact to the environment. In the present case, the impact category is marine eutrophication and the metric is a potential loss of species diversity in an ecosystem exposed to an N emission from anthropogenic sources.

The estimation of aquatic eutrophication CFs for LCIA applications has been reviewed recently and research needs identified (Henderson, 2015). Generically, the characterisation of marine eutrophication impacts involves the calculation of (i) fate factors (FF) expressing the availability of N in the euphotic zone of coastal waters, (ii) ecosystem exposure factors (XF) for the 'conversion' of the available N into organic matter (biomass) and oxygen consumed after its aerobic respiration, and (iii) effect factors (EF) to quantify the impact of DO depletion on exposed species (modelled as time- and volume-integrated Potentially Affected Fraction of species, PAF). Eq. (1) summarises the calculation of CFs as the product of these factors:

$$CF[PAF \cdot m^3 \cdot yr \cdot kgN^{-1}] = FF[yr] \times XF[kgO_2 \cdot kgN^{-1}] \times EF[PAF \cdot m^3 \cdot kgO_2{}^{-1}] \quad (1)$$

The present work introduces and discusses a method to estimate XFs. It contributes with a central element for the impact modelling of marine eutrophication in LCIA. The framework fits a mechanistic approach as it uses existing scientific knowledge about the relevant biological processes by means of equations that express

the systems' response. Such approach allows some extrapolation of the results beyond the intrinsic limitations of the experimental data and evidence available (Duarte et al., 2004). In practice, we build a cause-effect pathway of cascading biological processes to deliver an overall conversion of N into DO consumption. Environmental relevance is ensured by describing every relevant parameter based on state of the art science.

2.1. Spatial differentiation

The model focuses on coastal and shelf waters as these receive the majority of the anthropogenic emissions to the marine compartment and it is where the potential effects have the highest impact. Occurring biological populations and physical features are distinct from the adjacent pelagic open ocean and deep benthic systems (Spalding et al., 2007; UNESCO, 2009). They also comprise most of the marine biodiversity and human interest, as well as higher productivity and vulnerability to human interventions, including marine eutrophication (UNEP, 2006).

The modelled processes are nutrient-limited PP, metazoan consumption, and bacterial degradation of sunken organic carbon. A short description of these processes will be given in the sections ahead, focusing on the relevant limitations and interactions of the proposed approach. Some of the modelled parameters show significant spatial variation (e.g. PP rate). Spatial units are needed in an adequate and manageable scale and number to capture this variability and its contribution to the model results. Considering the scale at which the described processes occur, the large marine ecosystems (LME) biogeographical classification system (Sherman and Alexander, 1986) was adopted. It divides the coastal waters of the planet into 66 spatial units, from river basins and estuaries to the seaward boundaries of continental shelves (average depth of 200 m as a model assumption) and the outer margins of the major ocean current systems (Sherman et al., 2009). For parameters varying (mainly) with latitude, LMEs were grouped into five climate zones (polar, subpolar, temperate, subtropical, and tropical – Figures S1 and S2). The classification criteria were based on the mean annual sea surface temperature and latitudinal distribution (details in Section S2.1). In other cases, site-generic parameters based on best estimates or global mean values from available empirical data were given preference when no relevant spatial differentiation was to consider, or when data on spatial variability were missing (e.g. respiration rates of sinking organic material, zooplankton ingestion rates, or carbon transported by AVT).

2.2. Biological model pathway and major fluxes

As mentioned earlier, nutrients assimilation by primary producers is followed by sinking of organic carbon to bottom layers facilitated by phytoplankton cells aggregation, compaction into zooplankton faecal pellets and carcasses, and AVT.

Aerobic respiration by heterotrophic bacteria near the bottom leads to the consumption of DO. Figure 1 shows a simplified illustration of this pathway.

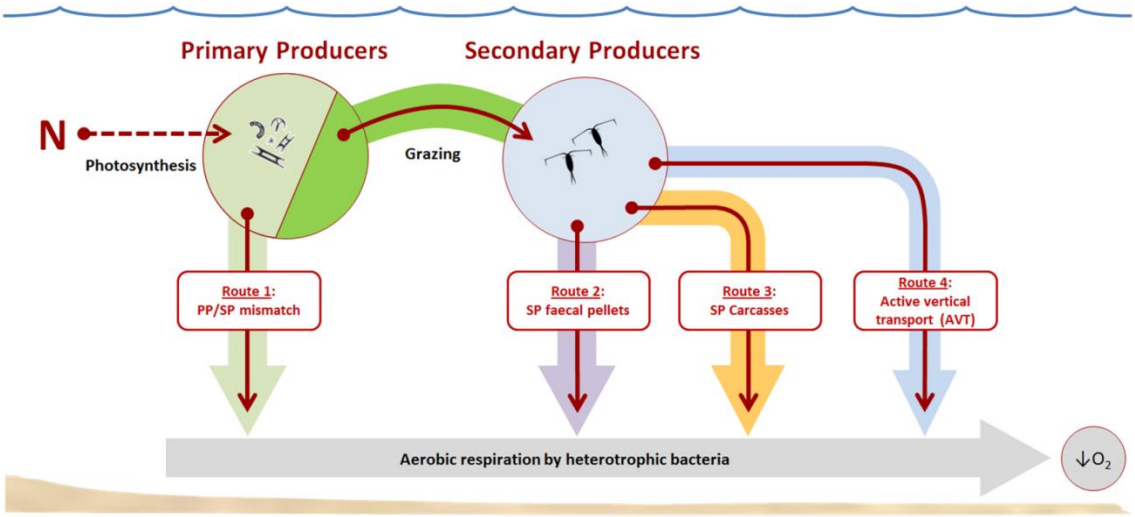

Figure 1 Simplified pathway of the ecosystem response to nitrogen (N) inputs showing the four carbon export routes from the upper euphotic zone to the bottom water layer: route 1 (light green arrow) for sinking primary production (PP) biomass, route 2 (purple arrow) for sinking particulate organic carbon as faecal pellets from secondary production (SP), route 3 (orange arrow) for sinking zooplankton carcasses, and route 4 (light blue arrow) for active vertical transport (AVT) – see text for process description. Dashed brown arrow represents assimilation of N and solid brown arrows represent organic carbon flows. Grey horizontal arrow refers to bacterial respiration in bottom waters that leads to dissolved oxygen (O_2) consumption.

Total PP consists of new production (P_{new}), which uses allochthonous N (externally supplied, mainly nitrate), and regenerated production (P_r) fuelled by autochthonous N in the surface mixed layer (from heterotrophic recycling of organic matter, e.g. ammonia and urea) (Dugdale and Goering, 1967; Wassmann, 1990a). At steady-state (or long-term average) P_r is the component of PP that meets the metabolic demands of the pelagic community (Platt and Sathyendranath, 1988) and P_{new} the component that can be exported without compromising the long-term integrity of the community (Vézina and Platt, 1987). The organic carbon that sinks off the mixed layer is referred to as export production (P_E). Its rate is, on an annual time scale and assuming N as the limiting nutrient, equivalent to the allochthonous N input rate as the downward flux of sinking P_E is equivalent to P_{new} (Eppley et al., 1983). For this reason P_E is expected to increase (and so the impacts that may result from it) if P_{new} increases due to additional N-loadings to the coastal marine system from anthropogenic sources. Therefore, an increase of N input is expected to correspond to an increase in DO consumption in the proportionality defined by some factor. This attests the relevance for the management of N-emitting human activities and for the assessment of ecosystems

health of a model capable of quantifying such a factor. This factor (i.e. XF) is described ahead.

The modelled biological processes can be related to (i) photosynthesis, determining the assimilation of N into biomass (organic carbon), (ii) production and export of organic material from the euphotic layer, (iii) consumption and degradation of sinking organic material, and (iv) the quantitative conversion of organic carbon into oxygen consumed by means of aerobic respiration by benthic heterotrophic bacteria, in agreement with the carbon fluxes as defined by the biological pump concept (Ducklow et al., 2001). The specific model parameters are described in the following sections and their inclusion in the response pathway is detailed in Figure 2. Processes in categories (i) and (ii) are also used to model P_E.

2.3. Photosynthesis and C:N conversion

Photosynthesis governs nutrients assimilation by primary producers. From thereon N relates to C by means of the Redfield ratio (Redfield, 1958) (molar mass ratio $C:N = 106:16$) based on the stoichiometry of the photosynthesis equation:

$$\underline{106}\ CO_2 + 16\ HNO_3 + H_3PO_4 + 122\ H_2O \Rightarrow C_{106}H_{263}O_{110}N_{\underline{16}}P + 138\ O_2 \qquad (2)$$

The $C:N$ molar mass ratio estimates the mass of C fixed into biomass per mass of N assimilated, calculated by:

$$C:N = (\underline{106}\ molC * 12.0107\ gC/molC)/(\underline{16}\ molN * 14.0067\ gN/molN) = 5.681\ gC/gN \qquad (3)$$

2.4. Production and export of organic material from the euphotic zone

($\boldsymbol{PP_{Pot}}$) PP rate [gC·m^2·yr^{-1}] (organic carbon synthesis rate) data are available at a LME spatial resolution from the *Sea Around Us* project (http://www.seaaroundus.org) (Lai, 2004; UBC, 1999). For comparative purposes, the PP rates of every LME (PP_{LME}) were normalised by the average PP rate (PP_{Avg_66LME} [gC·m^2·yr^{-1}]) to deliver the relative potential primary production in each spatial unit (PP_{Pot_LME} [-]) by:

$$PP_{Pot\_LME} = PP_{LME}/PP_{Avg\_66LME} \qquad (4)$$

($\boldsymbol{f_{PPsink}}$ and $\boldsymbol{f_{PPgrz}}$) A fraction of the PP is grazed by zooplankton (f_{PPgrz} [-]) while the remaining fraction (f_{PPsink} [-]) avoids it by sinking. The overlapping of occurrence of phyto- and zooplankton populations determines the grazed fraction while its mismatch represents the ungrazed sinking fraction, which varies with the production

cycles in different regions (Cushing, 1975). Adopting the five climate zones (CZ), these regionally-differentiated mismatch events result in a mean annual sinking fraction (f_{PPsink_CZ}) of 0.67 of the phytoplankton biomass in the polar CZ (dominated by large phytoplankton cells, e.g. diatoms), 0.30 in the temperate CZ (dominated by diatoms in spring and dinoflagellates in autumn), and 0.15 in the tropical CZ (dominated by picoplankton, flagellates, and ciliates). These coefficients were estimated according to Cushing's principles for typical growth and grazing response, and the export production response modelled by Laws et al. (2000). Intermediate subpolar and subtropical CZs adopted mean values of the adjacent zones, i.e. 0.49 and 0.23 respectively (Table S.1). Complementarily, the fraction not sinking represents the standing crop of primary producers grazed by zooplankton, obtained by:

$$f_{PPgrz\_CZ} = 1 - f_{PPsink\_CZ} \quad (5)$$

Microzooplankton may also graze on phytoplankton, removing ca. 60-70% of PP biomass on a global scale (Calbet and Landry, 2004) from the downward export flux of organic carbon due to remineralisation within the euphotic zone (Calbet, 2001). However, we assume that microzooplankton typically do not pose significant grazing pressure on large-celled phytoplankton blooms that constitute the mismatched fraction of the sinking PP biomass aggregates (f_{PPsink}). The grazing pressure by microzooplankton is thus assumed to be included in the grazed fraction (f_{PPgrz}). The ingestion, assimilation, and egestion (defecation) rates of the heterotrophs are then determinant in estimating the carbon export flux from SP (Besiktepe and Dam, 2002) (route 2 in Figure 1).

($\boldsymbol{f_{SPingest}}$) Phytoplankton's biomass grazed by SP is either ingested ($f_{SPingest}$ [-]) or dispersed ($1 - f_{SPingest}$) as dissolved organic carbon (DOC) via sloppy feeding (Lampert, 1978; Møller, 2007). Mean ingestion fractions of the grazed biomass of 0.64 (relative standard deviation (rel.SD)≈21%) were obtained from different species and estimation methods (Møller and Nielsen, 2001; Møller, 2007; Saba et al., 2011, 2009) (see also Section S.2.3). Although DOC production may vary with the predator-prey size ratio (Møller, 2007) we do not expect a consistent biased variation per CZ and thus a generic coefficient was adopted. The fate of this ingested fraction is further modelled by predation (f_{plfish}), egestion ($f_{SPegest}$), non-consumptive mortality (f_{SPcarc}), and active vertical transport (f_{AVTgrz}).

($\boldsymbol{f_{plfish}}$) Zooplankton biomass may be consumed by planktivorous fish (*plfish*) and therefore abstracted from the sinking flux. The concept of Primary Production Required (PPR, [-]) explains how much PP is required to sustain the reported fisheries per LME

(Pauly and Christensen, 1995; UBC, 1999) and is used here as a proxy to estimate the predated fraction of zooplankton.

($\boldsymbol{f_{SPassimil}}$ and $\boldsymbol{f_{SPegest}}$) Assimilation efficiency (AE) is the ratio of assimilation to consumption (Odum, 1971) or the proportion of the ingested material that is actually absorbed rather than egested (Besiktepe and Dam, 2002). AE coefficients for zooplankton ($f_{SPassimil}$ [-]) were estimated from Besiktepe and Dam (2002) for the polar (0.30, rel.SD≈74%), temperate (0.50, rel.SD≈25%), and tropical (0.80, rel.SD≈9%) CZs based on the expected dominance of diatoms (polar), diatoms/flagellates (temperate), and flagellates/ciliates (tropical) in their diet. $f_{SPassimil}$ for the subpolar (0.40, rel.SD≈57%) and subtropical (0.65, rel.SD≈19%) CZs are mean values of the adjacent zones (see Table S.1). We used diet-specific AE coefficients instead of generic values from e.g. Saba et al. (2011) or Møller et al. (2003) after Conover (1966), to add environmental relevance and spatial differentiation to the parameter. Egestion refers to the ingested food that is not assimilated in the gut of zooplankton and therefore is eliminated as faecal pellets. The egested organic carbon fractions from SP were calculated for the five CZs by:

$$f_{SPegest\_CZ} = 1 - f_{SPassimil\_CZ} \quad (6)$$

($\boldsymbol{f_{SPcarc}}$) Zooplankton carcasses, i.e. dead organisms and body parts (Tang and Elliott, 2013) due to non-consumptive mortality, are also part of sinking marine snow (as POC) following route 3 in Figure 1, which can further be consumed or respired in the water column or at the bottom. Non-consumptive mortality (f_{SPmort}, [-]) was estimated to be 29% of the predation mortality by *plfish* and constant regardless of temperature (Hirst and Kiørboe, 2002). A site-generic value was therefore used. PP's biomass in SP carcasses is then obtained per LME by:

$$f_{SPcarc\_LME} = f_{SPmort} * f_{plfish\_LME} = 0.29 * f_{plfish\_\mathrm{LME}} \quad (7)$$

($\boldsymbol{f_{AVTgrz}}$) Active vertical transport (AVT) due to diel vertical migration of zooplankton (route 4 in Figure 1) is an additional contribution to the downward carbon flux. The grazing pressure from migrating zooplankton (i.e. biomass removed from suspension) is assumed to be 10% of that of the zooplankton residing permanently in the surface layer (f_{PPgrz}) and assumed constant for the five CZs. This assumption is based on findings of <10% by Morales et al. (1993), roughly the proportion of migrating vs. non-migrating species in the North Sea (Koski et al., 2011), the mean value of 12% by Besiktepe et al. (1998), and also 15% by Roman et al. (1990) but including both pelagic and demersal zooplankton. Only the ingested fraction of the grazed biomass is modelled by AVT (f_{AVTgrz} [-]) as:

$$f_{AVTgrz\_CZ} = 0.10 * f_{PPgrz\_CZ} * f_{SPingest} \quad (8)$$

2.5. Consumption and degradation of sinking organic material

($\boldsymbol{f_{PPsinkGZ}}$ and $\boldsymbol{f_{PPsinkNG}}$) Sinking aggregates may be grazed by zooplankton (*sinkGZ*) residing below the photic depth (Alldredge and King, 1980). We assumed that the zooplankton community in the aphotic zone crops ca. 15% of the sinking aggregates from PP (f_{PPsink}) supported by Roman et al. (1990), similar to mean values (≈13.6%) obtained by Roman et al. (2002), and roughly 1 out of 6 (≈16.7%) dominant species of copepods occurring in the North Sea below the thermocline (Koski et al., 2011). The sinking non-grazed fraction of PP ($f_{PPsinkNG}$ [-]) per CZ is calculated by:

$$f_{PPsinkNG\_CZ} = 1 - f_{PPsinkGZ\_CZ} = 1 - 0.15 * f_{PPsink\_CZ} \quad (9)$$

($\boldsymbol{f_{FPleach}}$) Organic carbon leached from faecal pellets (FP) contributes to the production of DOC (Møller and Nielsen, 2001), which is assumed to be recycled in the surface mixed layer and thus not contribute to the organic carbon flux reaching the bottom (contrary to POC). Here we included the losses by leaching and dissolution caused by the disruption of FP's periotrophic membrane by bacteria and protists (*coprochaly*) and manipulation by zooplankton with fragmentation (*coprorhexy*) (Wassmann, 1998). The organic carbon 'lost' to leaching ($f_{FPleach}$ [-]) was adopted from Møller et al. (2003) as 28% of the sinking flux of FP and assumed constant for the five CZs.

($\boldsymbol{f_{FPsinkGZ}}$ and $\boldsymbol{f_{FPsinkNG}}$) Zooplankton can also graze on sinking FP (*coprophagy*) (Wassmann, 1998) though much less efficiently than on sinking algal aggregates. The maximum feeding rate of particle-colonising copepods on FP ($f_{FPsinkGZ}$) is assumed to be ca. 20% of that of algae aggregates ($f_{PPsinkGZ}$) (Koski, unpublished) per climate zone, as:

$$f_{FPsinkGZ\_CZ} = 0.20 * f_{PPsinkGZ\_CZ} \quad (10)$$

The remaining organic material sinking as FP not grazed ($f_{FPsinkNG}$ [-]) is therefore obtained from deducting the losses of leaching and consumption, per climate zone, by:

$$f_{FPsinkNG\_CZ} = (1 - f_{FPleach}) * \left(1 - f_{FPsinkGZ\_CZ}\right) \quad (11)$$

($\boldsymbol{f_{BRsinkPP}}$ and $\boldsymbol{f_{BRsinkSP}}$) Sinking POC is a component of marine snow (*marsnow*) and as such is respired by heterotrophic bacteria (bacterial respiration, BR) at a rate of $f_{BRmarsnow} = 0.13\ d^{-1}$ (Iversen and Ploug, 2010). Sinking rates (U) of organic material from PP and SP were adopted from Turner (2002) as $U_{PP} = 150\ m \cdot d^{-1}$

(phytodetritus and marine snow) and $U_{SP} = 200\ m \cdot d^{-1}$ (marine snow and faecal pellets). Mean depth ($Z_{mean} = 100\ m$) was also used. The fractions of respired sinking PP ($f_{BRsinkPP}$ [-]) and sinking SP ($f_{BRsinkSP}$ [-]) are calculated by:

$$f_{BRsinkPP} = f_{BRmarsnow}/U_{PP} * Z_{mean} = 0.13\ d^{-1}/150\ m \cdot d^{-1} * 100\ m = 0.087 \quad (12)$$

$$f_{BRsinkSP} = f_{BRmarsnow}/U_{SP} * Z_{mean} = 0.13\ d^{-1}/200\ m \cdot d^{-1} * 100\ m = 0.065 \quad (13)$$

SP carcasses are assumed equivalent to detritus entangled in sinking marine snow and respired as such (Iversen and Ploug, 2010; Tang and Elliott, 2013). We assumed a consumption rate similar to that of sinking faecal pellets ($f_{FPsinkGZ\_CZ}$, from Eq. 10) and bacterial respiration as SP marine snow ($f_{BRsinkSP}$, from Eq. 13) (Turner, 2002).

($\boldsymbol{f_{AVToc}}$) By AVT some zooplankton excretes and egests organic carbon (*oc*) as DOC and POC, respectively, in aphotic layers. Contributions to DOC (f_{AVTdoc} [-]) from excretion and FP leaching are estimated as described for surface resident copepods and assuming that 15% of the ingested carbon is excreted (Saba et al., 2011), plus the FP leaching (f_{GRZdoc} [-], Eq. 15) and ingestion of grazed sinking PP ($f_{PPsinkGZ\_CZ}$) and FP ($f_{FPsinkGZ\_CZ}$) fractions (marked in Figure 2 as "- to $f_{\mathrm{AVTdoc/poc}}$" and denoted grazed fraction, f_{GRZ} [-], Eq. 16). Only a fraction of this DOC pool is respired in the bottom layer as a function of the proportion of vertical distance covered by emergent copepods (Z_{AVT}, assumed to be 20 m (Atkinson et al., 1992; Puelles et al., 1996)) of the water column below the photic depth (Z_{photic_LME} from Longhurst (1998), Table S.4) to the bottom, with mean depth (Z_{mean}) of 100 m (see Table 1 and *f* of $Z_{aphotic}$ in Table S.4). The calculation of f_{AVTdoc} per CZ is then:

$$f_{AVTdoc\_CZ} = \left(f_{AVTgrz\_CZ} * f_{SPassimil\_CZ} * 0.15 + f_{AVTgrz\_CZ} * f_{SPegest\_CZ} * f_{FPleach} + f_{GRZdoc\_CZ}\right) * Z_{AVT}/Z_{aphotic\_LME} \quad (14)$$

where:

$$f_{GRZdoc\_CZ} = f_{GRZ\_CZ} * \left(f_{SPassimil\_CZ} * 0.15 + f_{SPegest\_CZ} * f_{FPleach}\right) \quad (15)$$

$$f_{GRZ\_CZ} = f_{PPsink\_CZ} * f_{PPsinkGZ\_CZ} + f_{PPgrz\_CZ} * f_{SPingest} * \left(1 - f_{AVTgrz_{CZ}} * f_{ingest}\right) * (1 - f_{SPcarc}) * \left(1 - f_{plfish_{LME}}\right) * f_{SPegest\_CZ} * (1 - f_{FPleach}) * f_{FPsinkGZ\_CZ} + f_{PPgrz\_CZ} * f_{SPingest} * \left(1 - f_{plfish}\right) * f_{SPcarc} * f_{FPsinkgz\_CZ} \quad (16)$$

Contributions to the POC pool as FP (f_{AVTpoc} [-]) include egestion from migrating copepods plus egestion from ingested grazed sinking PP, sinking FP, and sinking SP carcasses (f_{GRZ} [-], Eq. 16). Such egested FPs are also grazed as described for $f_{FPsinkGZ}$ and respired by bacteria (see description and calculations of $f_{BRmarsnow}$ and U_{SP}) as a function of $Z_{aphotic\_LME}$ (Table S.3). The calculation of f_{AVTpoc} per CZ is then:

$$f_{AVTpoc\_CZ} = \left(f_{AVTgrz\_CZ} + f_{GRZ}\right) * f_{SPegest\_CZ} * (1 - f_{FPleach}) * \left(1 - f_{FPsinkGZ\_CZ}\right) * f_{BRsinkSPaphotic\_LME} \quad (17)$$

where:

$$f_{BRsinkSPaphotic\_LME} = f_{BRmarsnow}/U_{SP} * Z_{aphotic} \quad (18)$$

The total organic carbon transported by AVT (f_{AVToc}) per CZ is then obtained from:

$$f_{AVToc\_CZ} = f_{AVTdoc\_CZ} + f_{AVTpoc\_CZ} \quad (19)$$

The remaining sinking fractions reach the bottom layer and are respired there.

2.6. Benthic respiration and O_2:C conversion

($\boldsymbol{f_{BRbott}}$) Organic carbon reaching bottom layers is assimilated by heterotrophic bacteria to produce new bacterial biomass (secondary bacterial production, BP) and to meet metabolic requirements (bacterial respiration, BR). The amount of bacterial biomass produced per unit carbon substrate assimilated is defined as Bacterial Growth Efficiency (BGE [-]), i.e. the fraction not respired or $BP/(BP + BR)$ (del Giorgio and Cole, 1998). Comparative studies of natural aquatic systems show that BP is correlated with PP and averaging ca. 30% of PP (Cole et al., 1988; del Giorgio and Cole, 1998; Ducklow and Carlson, 1992). Instead of using such a generic coefficient, and to further add spatial differentiation and relevance, we estimated spatially differentiated BP values for the 66 LMEs (BP_{LME} [µgC·L·h^{-1}]) using the empirical equation by Cole et al. (1988) for marine systems (R^2=0.77) with the available PP rates:

$$BP_{LME} = 0.249 * {PP_{LME}}^{0.86} \quad (20)$$

Spatially differentiated BGE values (BGE_{LME} [-]) were then estimated with the empirical equation by del Giorgio and Cole (1998) relating BP and BGE:

$$BGE_{LME} = (0.037 + 0.65 * BP_{LME})/(1.8 + BP_{LME}) \quad (21)$$

BGE_{LME} values range from 0.03 (oligotrophic LME#64 Central Arctic Ocean) to 0.37 (eutrophic LME#23 Baltic Sea) (Table S.4). This range is close to reported direct measurements in ocean (0.10-0.31) and coastal waters (0.18-0.42) and follows the systematic variation with productivity shown by del Giorgio and Cole (1998). The fraction of organic carbon that is actually respired contributing to DO consumption (f_{BRbott}) is then defined per LME by:

$$f_{BRbott\_LME} = 1 - BGE_{LME} \quad (22)$$

As mentioned before, the aerobic respiration by heterotrophic bacteria is responsible for the consumption of DO. The $O_2{:}C$ molar mass ratio delivers the conversion of sunken carbon into respired dioxygen, by:

$$O_2{:}C = (\underline{138}\, molO_2 * 2 * 15.9994\ gO_2/molO_2)/(\underline{106}\, molC * 12.0107\ gC/molC) = 3.468\ gO_2/gC \quad (23)$$

obtained from the stoichiometry of the aerobic respiration equation:

$$(CH_2O)_{\underline{106}}(NH_3)_{16}H_3PO_4 + \underline{138}\ O_2 \Rightarrow 106\ CO_2 + 122\ H_2O + 16\ HNO_3 + H_3PO_4 \quad (24)$$

The elemental flows can ultimately be simplified by combining $C{:}N$ and $O_2{:}C$ (Eqs. 3 and 23) as the molar mass ratio of $O_2{:}N$ as:

$$O_2{:}N = (138\, molO_2 * 2 * 15.9994\ gO_2/molO_2)/(16\, molN * 14.0067\ gN/molN) = 19.704\ gO_2/gN \quad (25)$$

In summary, DO consumption is estimated from the respiration of the organic carbon reaching the bottom layer. The organic carbon export is modelled in four distinct routes: route 1, POC exported as algal cell aggregates (sinking of PP biomass); route 2, POC exported as faecal pellets (egestion from SP); route 3, POC from non-predatory mortality of zooplankton (sinking SP carcasses); and route 4, POC and DOC exported by active vertical transport (zooplankton-mediated export). The model equations quantifying DO consumption as a function of N input per export route are (see also Figure 2 for illustration):

$$DO_{\text{route\_1}} = N_{input} * (C{:}N) * PP_{Pot\_LME} * f_{PPsink\_CZ} * f_{PPsinkNG\_LME} * (1 - f_{BRsinkPP}) * f_{BRbott\_LME} * (O_2{:}C) \quad (26)$$

$$DO_{\text{route\_2}} = N_{input} * (C{:}N) * PP_{\text{Pot\_LME}} * f_{PPgrz\_CZ} * f_{SPingest} * \left(1 - f_{AVTgrz\_CZ}\right) * \left(1 - f_{plfish\_LME}\right) * (1 - f_{SPcarc}) * f_{SPegest\_CZ} * f_{FPsinkNG\_CZ} * (1 - f_{BRsinkSP}) * f_{BRbott\_LME} * (O_2{:}C) \quad (27)$$

$$DO_{\text{route\_3}} = N_{input} * (C{:}N) * PP_{Pot\_LME} * f_{PPgrz\_CZ} * f_{SPingest} * \left(1 - f_{AVTgrz\_CZ}\right) * f_{SPcarc} * \left(1 - f_{FPsinkGZ\_CZ}\right) * (1 - f_{BRsinkSP}) * f_{BRbott\_LME} * (O_2{:}C) \quad (28)$$

$$DO_{\text{route\_4}} = N_{input} * (C{:}N) * PP_{Pot\_LME} * f_{AVTgrz\_CZ} * f_{AVToc\_CZ} * \left(1 - f_{BRsinkSPaphot\_LME}\right) * f_{BRbott\_LME} * (O_2{:}C) \quad (29)$$

Finally, the combination of these four equations (Eqs. 26-29) deliver the XF per LME, i.e. the mass of DO consumed in the bottom layer as a function of the mass of N input to the LME, in [$kgO_2 \cdot \text{kg}N^{-1}$]:

$$XF_{LME} = PP_{Pot\_LME} * \Big(f_{PPsink\_CZ} * f_{PPsinkNG\_LME} * (1 - f_{BRsinkPP}) + f_{PPgrz\_CZ} * f_{SPingest} * \Big((1 - f_{BRsinkSP}) * \left(1 - f_{AVTgrz\_CZ}\right) * \left(1 - f_{plfish\_LME}\right) * (1 - f_{SPcarc}) * f_{SPegest\_CZ} * f_{FPsinkNG\_CZ} + \left(1 - f_{AVTgrz\_CZ}\right) * f_{SPcarc} * \left(1 - f_{FPsinkGZ\_CZ}\right)\Big) + f_{AVTgrz\_CZ} * f_{AVToc\_CZ} * \left(1 - f_{BRsinkSPaphot\_LME}\right)\Big) * f_{BRbott\_LME} * (O_2{:}N) \quad (30)$$

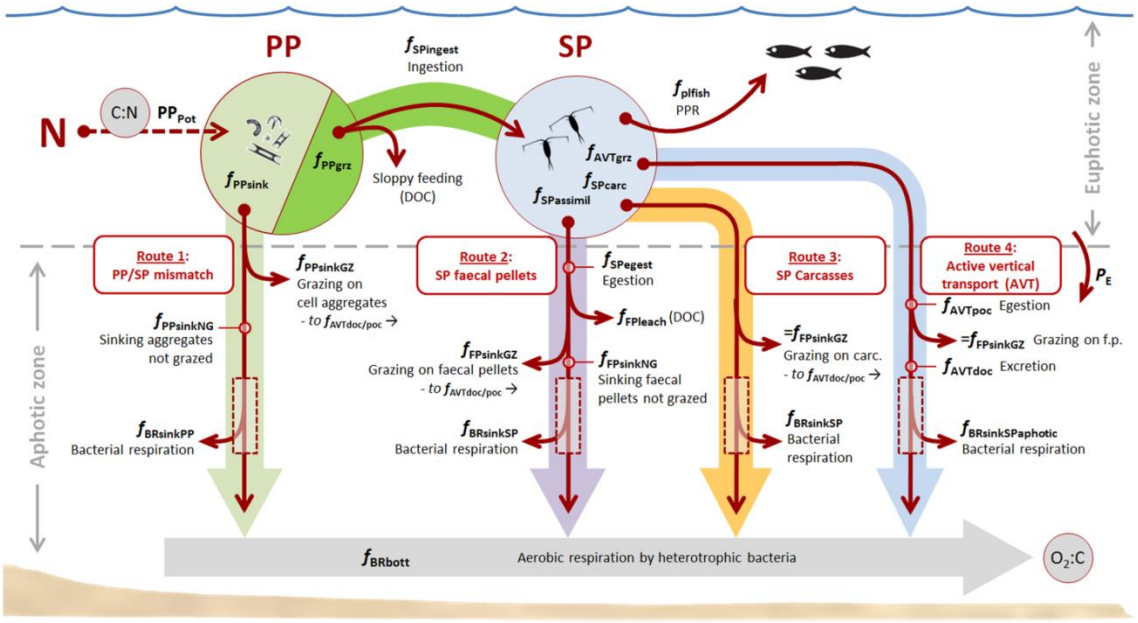

Figure 2 Summary of the ecosystem response model to nitrogen (N) inputs and the resulting consumption of dissolved oxygen (O_2) in the bottom water layer. Four export routes are modelled: sinking of primary production (PP) biomass (route 1, light green arrow), sinking particulate organic carbon (POC) from secondary production (SP) as faecal pellets (FP) (route 2, purple arrow), sinking zooplankton carcasses (route 3, orange arrow), and active vertical transport (AVT) as dissolved and particulate organic carbon (DOC and POC) (route 4, light blue arrow). Transfer to planktivorous fish (*plfish*) estimated by Primary Production Required (PPR) to sustain fisheries represents predation by upper trophic levels. The photic depth (grey horizontal dashed line) divides the surface euphotic zone and the bottom aphotic zone (not to scale). The organic carbon moving below this line represents the export production (P_E). Dashed brown arrow represents N assimilation and solid brown arrows represent organic carbon flows. Grey horizontal arrow refers to bacterial respiration (BR) at bottom waters leading to dissolved O_2 consumption. Grey small circles represent the molar mass conversions of C:N and O_2:C. Also consult Table 1 and text for details on model parameters.

2.7. Estimation of export production

To quantify the organic carbon exported (P_E [$gC \cdot m^2 \cdot yr^{-1}$]) from the euphotic zone (as POC) we used the actual PP rates per LME (PP_{LME} and not PP_{Pot_LME}) and Eqs. 3 and 5-8, i.e. PP, its sinking fraction, and the SP-related export fractions, by:

$$P_{E\_LME} = PP_{LME} * \left(f_{PPsink\_CZ} + f_{PPgrz\_CZ} * f_{SPingest} * \left(1 - f_{plfish\_LME}\right) * \left(1 - f_{AVTgrz\_CZ}\right) * \left(1 - f_{SPcarc\_LME}\right) * f_{SPegest\_CZ} + f_{PPgrz\_CZ} * f_{SPingest} * \left(1 - f_{AVTgrz\_CZ}\right) * f_{SPcarc\_LME} + f_{AVTgrz\_CZ}\right) \quad (31)$$

Table 1 Spatial resolution of the modelled parameters, their values, and reference sources/calculation method (see Table S1 for an extended version). (LME, large marine ecosystem, and CZ, climate zone).

Input parameter	Spatial resolution	Value Unit	Source (reference or calculation)
C:N	Global	5.681 [$kgC \cdot kgN^{-1}$]	Stoichiometry of the photosynthesis equation
O_2:C	Global	3.468 [$kgO_2 \cdot kgC^{-1}$]	Stoichiometry of the respiration equation
O_2:N	Global	19.704 [$kgO_2 \cdot kgN^{-1}$]	Calculation: $(O_2:N)=(C:N)*(O_2:N)$
PP_{Pot}	LME	0.033 ↔ 2.707 [-]	Calculation: $PP_{Pot}=PP_{LME}/PP_{Avg\_66LME}$
f_{PPsink}	CZ	0.150 ↔ 0.670 [-]	Cushing (1975), Laws et al. (2000) and average CZs
f_{PPgrz}	CZ	0.330 ↔ 0.850 [-]	Calculation: $f_{PPgrz\_CZ}=1-f_{PPsink\_CZ}$
$f_{SPingest}$	Global	0.643 [-]	Møller and Nielsen (2001); Møller (2007); Saba et al. (2011)
$f_{SPassimil}$	CZ	0.300 ↔ 0.900 [-]	Besiktepe and Dam (2002) and average CZs
$f_{SPegest}$	CZ	0.100 ↔ 0.700 [-]	Calculation: $f_{SPegest\_CZ}=1-f_{SPassimil\_CZ}$
f_{plfish}	LME	2E-04 ↔ 1.000 [-]	SP consumption by planktivorous fish
f_{AVTgrz}	CZ	0.033 ↔ 0.085 [-]	Calculation: $f_{AVTgrz\_CZ}=0.10*f_{PPgrz\_CZ}*f_{SPingest}$
$f_{PPsinkGZ}$	CZ	0.023 ↔ 0.101 [-]	Calculation: $f_{PPsinkGZ\_CZ}=0.15*f_{PPsink\_CZ}$
$f_{PPsinkNG}$	CZ	0.900 ↔ 0.978 [-]	Calculation: $f_{PPsinkNG\_CZ}=1-f_{PPsinkGZ\_CZ}$
$f_{FPleach}$	Global	0.280 [-]	Møller et al. (2003)
$f_{FPsinkGZ}$	CZ	0.007 ↔ 0.017 [-]	Calculation: $f_{FPsinkGZ\_CZ}=0.20*f_{PPsinkGZ\_CZ}$
$f_{FPsinkNG}$	CZ	0.708 ↔ 0.715 [-]	Calculation: $f_{FPsinkNG\_CZ}=(1-f_{FPleach})*(1-f_{FPsinkGZ\_CZ})$
f_{SPmort}	Global	0.290 [-]	Hirst and Kiørboe (2002)
f_{SPcarc}	LME	0.000 ↔ 0.290 [-]	Calculation: $f_{SPcarc\_LME}=f_{SPmort}*f_{plfish\_LME}$

Z_{mean}	Global	100 [m]	Mean depth of continental shelf
Z_{AVT}	Global	20 [m]	Atkinson et al. (1992); Puelles et al. (1996)
Z_{photic}	LME	12 ↔ 68 [m]	Longhurst (1998)
$Z_{aphotic}$	LME	32 ↔ 88 [m]	Calculation: $Z_{aphotic\_LME}=Z_{mean}-Z_{photic\_LME}$
U_{PP}	Global	150 [m·d^{-1}]	Turner (2002)
U_{SP}	Global	200 [m·d^{-1}]	Turner (2002)
$f_{BRmarsnow}$	Global	0.130 [d^{-1}]	Iversen and Ploug (2010)
$f_{BRsinkSPaphotic\_LME}$	LME	0.021 ↔ 0.051 [-]	Calculation: $f_{BRsinkSPaphotic\_LME}=f_{BRmarsnow}/U_{SP}*(Z_{mean}-Z_{photic\_LME})$
$f_{BRsinkPP}$	Global	0.087 [-]	Calculation: $f_{BRsinkPP}=f_{BRmarsnow}/U_{PP}*Z_{meanLME}$
$f_{BRsinkSP}$	Global	0.065 [-]	Calculation: $f_{BRsinkSP}=f_{BRmarsnow}/U_{SP}*Z_{meanLME}$
BGE	LME	0.039 ↔ 0.464 [-]	Cole et al. (1988); del Giorgio and Cole (1998)
f_{BRbott}	LME	0.536 ↔ 0.961 [-]	Calculation: f_{BRbott_LME}=1-BGE_{LME}

3. Results

The results of the normalisation of primary productivity per spatial unit (potential primary production, PP_{Pot_LME}) are shown in Table 2. PP_{Pot_LME} range from 0.03 (LME#64. Central Arctic Ocean) to 2.71 (LME#23. Baltic Sea), with a mean rate (PP_{Avg_66LME}) of 257.7 gC·m^{-2}·yr^{-1}.

The estimation of XFs (from Eq. 30) per LME delivers the set of results included in Table 2 and depicted in Figure 3. XF_{LME} range from 0.45 (LME #64 Central Arctic Ocean) to 15.9 kgO_2·kgN^{-1} (LME #23 Baltic Sea). The results of the estimation of export production (P_E) per LME (from Eq. 31) are also shown in Table 2. P_{E_LME} range from 7.026 (LME #64 Central Arctic Ocean) to 484.8 gC·m^{-2}·yr^{-1} (LME #23 Baltic Sea). The geographic distribution of XF_{LME} is consistent with the annual distribution of PP in coastal areas (e.g. Behrenfeld and Falkowski (1997); Chassot et al. (2010)). XF_{LME} hotspots in Figure 3 match highly productive coastal areas fuelled by e.g. coastal upwelling or otherwise resulting from the interaction of light and nutrients availability, and low grazing pressure.

Table 2 Results of the calculated export production (P_E, [gC·m^{-2}·yr^{-1}]) and exposure factors (XF, [kgO_2·kgN^{-1}]) for the 66 large marine ecosystems (LME) grouped into climate zones (see extended version in Table S4).

Large Marine Ecosystem [#. name]	Climate zone [name]	PP [gC·m^{-2}·yr^{-1}]	PP_{Pot_LME} [-]	P_E [gC·m^{-2}·yr^{-1}]	XF_{LME} [kgO_2·kgN^{-1}]
18. Canadian Eastern Arctic - West Greenland	Polar	151.9	0.59	125.4	6.80
19. Greenland Sea	Polar	174.2	0.68	130.9	7.25
20. Barents Sea	Polar	151.2	0.59	120.0	7.05
54. Northern Bering - Chukchi Seas	Polar	90.95	0.35	76.06	4.57
55. Beaufort Sea	Polar	119.1	0.46	99.60	5.87
56. East Siberian Sea	Polar	54.42	0.21	45.51	2.81
57. Laptev Sea	Polar	156.7	0.61	131.0	7.54
58. Kara Sea	Polar	126.7	0.49	106.0	6.22
61. Antarctic	Polar	99.71	0.39	83.40	4.91
63. Hudson Bay Complex	Polar	152.7	0.59	127.7	6.96

Large Marine Ecosystem [#. name]	Climate zone [name]	PP [$gC \cdot m^{-2} \cdot yr^{-1}$]	PP_{Pot_LME} [-]	P_E [$gC \cdot m^{-2} \cdot yr^{-1}$]	XF_{LME} [$kgO_2 \cdot kgN^{-1}$]
64. Central Arctic Ocean	Polar	8.401	0.03	7.026	0.45
66. Canadian High Arctic - North Greenland	Polar	58.81	0.23	48.98	2.99
01. East Bering Sea	Subpolar	285.6	1.11	196.4	9.86
02. Gulf of Alaska	Subpolar	330.9	1.28	228.1	11.1
09. Newfoundland-Labrador Shelf	Subpolar	295.5	1.15	206.6	10.3
21. Norwegian Sea	Subpolar	179.3	0.70	113.0	6.35
23. Baltic Sea	Subpolar	697.6	2.71	484.8	15.9
51. Oyashio Current	Subpolar	261.5	1.01	178.5	9.25
52. Sea of Okhotsk	Subpolar	297.7	1.16	198.7	10.0
53. West Bering Sea	Subpolar	214.0	0.83	148.7	7.80
59. Iceland Shelf and Sea	Subpolar	201.3	0.78	140.7	7.34
60. Faroe Plateau	Subpolar	154.1	0.60	94.16	5.58
65. Aleutian Islands	Subpolar	285.6	1.11	199.5	10.0
03. California Current	Temperate	223.9	0.87	120.8	6.09
07. Northeast U.S. Continental Shelf	Temperate	561.0	2.18	303.0	12.2
08. Scotian Shelf	Temperate	509.5	1.98	280.6	11.6
13. Humboldt Current	Temperate	320.0	1.24	170.9	8.38
14. Patagonian Shelf	Temperate	509.5	1.98	272.1	11.5
22. North Sea	Temperate	407.3	1.58	209.8	9.11
24. Celtic-Biscay Shelf	Temperate	349.2	1.35	180.9	8.15
25. Iberian Coastal	Temperate	276.9	1.07	145.6	7.38
42. Southeast Australian Shelf	Temperate	187.0	0.73	104.3	5.41
43. Southwest Australian Shelf	Temperate	180.8	0.70	100.9	5.28
46. New Zealand Shelf	Temperate	208.2	0.81	110.4	5.69
48. Yellow Sea	Temperate	589.1	2.29	284.4	12.0
50. Sea of Japan/East Sea	Temperate	220.6	0.86	114.8	5.92
62. Black Sea	Temperate	376.6	1.46	207.1	8.83
04. Gulf of California	Subtropical	437.9	1.70	191.8	7.97
05. Gulf of Mexico	Subtropical	208.2	0.81	90.95	4.49
06. Southeast U.S. Continental Shelf	Subtropical	263.3	1.02	115.6	5.26
15. South Brazil Shelf	Subtropical	283.1	1.10	123.9	5.84
26. Mediterranean	Subtropical	157.8	0.61	67.78	3.45
27. Canary Current	Subtropical	436.8	1.70	188.8	7.73
29. Benguela Current	Subtropical	506.6	1.97	219.9	9.09
30. Agulhas Current	Subtropical	221.0	0.86	96.51	4.76
41. East-Central Australian Shelf	Subtropical	157.4	0.61	69.22	3.51
44. West-Central Australian Shelf	Subtropical	173.9	0.67	76.43	3.85
47. East China Sea	Subtropical	325.4	1.26	133.5	6.45
49. Kuroshio Current	Subtropical	154.1	0.60	66.10	3.37
10. Insular Pacific-Hawaiian	Tropical	84.74	0.33	26.10	1.33
11. Pacific Central-American	Tropical	244.0	0.95	75.33	3.33
12. Caribbean Sea	Tropical	174.6	0.68	53.83	2.51
16. East Brazil Shelf	Tropical	130.4	0.51	40.26	1.94
17. North Brazil Shelf	Tropical	442.3	1.72	136.5	5.26
28. Guinea Current	Tropical	357.9	1.39	110.5	4.31
31. Somali Coastal Current	Tropical	249.5	0.97	76.85	3.36
32. Arabian Sea	Tropical	390.5	1.52	121.7	4.99
33. Red Sea	Tropical	298.4	1.16	92.34	3.89
34. Bay of Bengal	Tropical	265.2	1.03	82.83	3.71
35. Gulf of Thailand	Tropical	284.9	1.11	91.10	4.17
36. South China Sea	Tropical	174.2	0.68	55.55	2.70
37. Sulu-Celebes Sea	Tropical	209.3	0.81	66.56	3.18

Large Marine Ecosystem [#. name]	Climate zone [name]	PP [gC·m^{-2}·yr^{-1}]	PP_{Pot_LME} [-]	P_E [gC·m^{-2}·yr^{-1}]	XF_{LME} [kgO$_2$·kgN^{-1}]
38. Indonesian Sea	Tropical	263.7	1.02	82.42	3.69
39. North Australian Shelf	Tropical	328.7	1.28	101.3	4.26
40. Northeast Australian Shelf	Tropical	130.8	0.51	40.29	1.93
45. Northwest Australian Shelf	Tropical	185.9	0.72	57.31	2.66

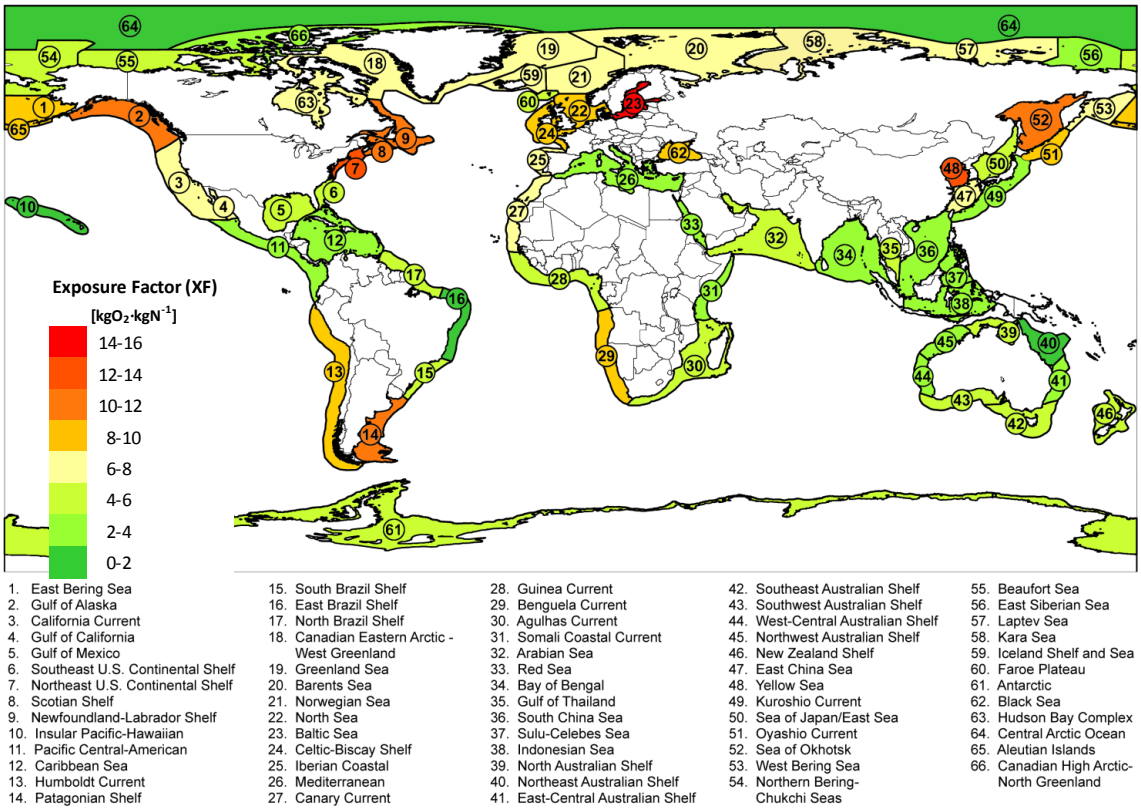

Figure 3 Global distribution of the exposure factors (XF, [kgO$_2$·kgN^{-1}]) estimated for the 66 large marine ecosystems (spatial units coloured from the original digital map available at http://lme.edc.uri.edu/).

3.1. Contributions from sinking routes

The relative contributions of each sinking carbon route to the export production (P_E) and DO consumption were grouped into climate zones (Table S.3), as most of the spatial differentiation is originated from this resolution, based on the results per LME (Table S.4). Route 1 consistently contributes more to both P_E (61%) and XF (63%) (route 2: 26% and 23%, route 3: 4% and 5%, and route 4, 10% and 9%, respectively) (more details in Section S.3.1). These results are significantly correlated with the PP-SP mismatch and biomass sinking (f_{PPsink_CZ}), except for the contributions of routes 3 and 4 to XF as its modelling extends to include the loss processes in the aphotic zone that act on P_E (consumption, leaching, and respiration).

3.2. Sensitivity analysis

The model sensitivity to the 18 primary input parameters was assessed by calculating sensitivity ratios (SR) for each combination of input parameter and resulting XF_{LME}, as described by Strandesen et al. (2007). The SR is the ratio between the relative change in the model output and the relative change in the model input. Figure 4 shows the mean SR values and the respective range of variation among LMEs (see also Table S.6).

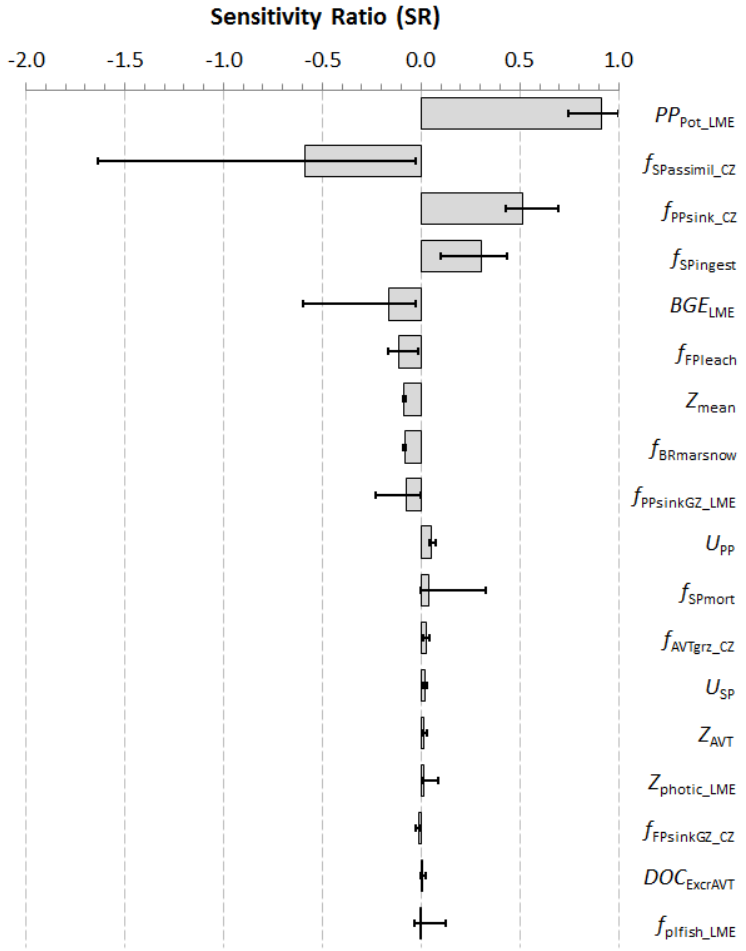

Figure 4 Sensitivity ratios (SRs) for the 18 modelled input parameters. The grey bars represent the mean SR values and the variation ranges represent the lower and upper values of the 66 large marine ecosystems. Absolute SR values of 1.00 mean direct proportionality of input and output; negative SR values indicate that input and output are inversely related, meaning that an increase in the input value decreases the output.

4. Discussion

The model covers the entire response pathway by a spatially differentiated parameterisation that supports the interpretation and the application of the resulting exposure indicator. Model sensitivity and parameters uncertainty were analysed to assess robustness. We further compare P_E estimated by our model with predicted curves

by others in order to validate the processes occurring in the euphotic zone. This 'euphotic component' determines the input of organic matter to the biologically-mediated processes of consumption, degradation, and respiration that occur in the water column and benthic layers and for which there is no comparable spatially differentiated model with global coverage. Finally, we discuss the spatial differentiation and resolution of the results, the framework and its application in LCIA.

4.1. Model sensitivity and parameters uncertainty

The site-dependent parameter PP_{Pot_LME} (model input) shows the highest individual contribution to the resulting XFs (model output) with a mean SR value of 0.92 (range 0.75-1.00, Figure 4 and Table S.6). LME-dependent PP rates modulate N assimilation and the carbon fluxes thereafter thus justifying such influence on the results. Sensitivity to $f_{SPassimil\_CZ}$ range up to -1.64 but only in the tropical LMEs where the assimilation rate acts upon a larger grazed biomass fraction by routes 2 to 4. Other two site-dependent parameters may range to relevant SR values: f_{PPsink_CZ} in LMEs with high SP consumption by planktivorous fish (PPR, Table S.4); and BGE_{LME} in highly productive LMEs. The analysis further suggests that the remaining site-dependent parameters ($f_{PPsinkGZ\_LME}$, f_{AVTgrz_CZ}, Z_{photic_LME}, $f_{FPsinkGZ\_LME}$, f_{plfish_LME}) may adopt site-generic coefficients since any uncertainty associated with their estimation renders little impact on the quality of the XFs obtained. Sensitivity to the site-generic parameter $f_{SPingest}$ may range up to 0.43 in tropical LMEs as it affects a larger relative fraction of the grazed PP biomass. The remaining site-generic parameters ($f_{FPleach}$, Z_{mean}, $f_{BRmarsnow}$, U_{PP}, f_{SPmort}, U_{SP}, Z_{AVT}, $DOC_{ExcrAVT}$) show low contributions to output. The lack of spatial differentiation in site-generic parameters is deemed acceptable considering the low SRs, although adding spatial differentiation to $f_{SPingest}$ (possibly per climate zone) could be seen as a method improvement.

The uncertainty of the parameters PP_{Pot_LME}, $f_{SPassimil\_CZ}$, f_{PPsink_CZ}, $f_{SPingest}$, and BGE_{LME} was assessed because of their high contribution. PP rate data (and PP_{Pot_LME} values) were obtained from chlorophyll pigment concentrations derived from satellite data. The uncertainty of the underlying models by Bouvet et al. (2002) and Platt and Sathyendranath (1988) or the spatial integration method (Lai, 2004; Watson et al., 2014) is not discussed here. The PP dataset integrates monthly records from an approximately 12-year period. The variability of the dataset per LME was verified by Watson et al. (2014) and the majority of the PP data points have a coefficient of interannual variation below 5%. Only the Arctic and near-Arctic LMEs show interannual variation of 20-25% possibly due to poorer satellite coverage. As such, it seems to us that the used PP dataset provides a reliable average PP value per LME with an acceptable (natural) variability. Furthermore, the choice for space and time integrated

PP data is deemed appropriate and less uncertain than using PP data from any specific location or day (or even over a single year) inherently less representative.

We acknowledge the increase of uncertainty towards higher latitudes in the estimation of mean $f_{SPassimil\_CZ}$ for the five CZs (in Section 2.4.). However, this fact is tied in with a decrease in PP biomass, as the parameter is correlated with the grazed fraction transferred to route 2 (mainly) (Table S.3) in which the AE coefficient is embedded as egested fraction ($f_{SPegest\_CZ}$), thus minimizing the impact of the most uncertain CZs. This is also supported by SRs above 0.50 in the subtropical and tropical CZs only. As such, we consider that the estimated AE and egestion coefficients are valid for a spatially differentiated application and preferred over global generic values, which are otherwise available as of 18% for the coastal copepod *Acartia tonsa* (Saba et al., 2011) or 60% but for the epipelagic *Calanus* spp. in Møller et al. (2003).

The match-mismatch hypothesis by Cushing (1975) determines the phytoplankton's sunken and grazed fractions. Mismatched growth of phyto- and zooplankton communities results in increased downward export of organic carbon. As a conceptual description of a natural phenomenon involving complex processes (Cushing, 1990; Durant et al., 2007) it has, not surprisingly, high variability associated. Any uncertainty estimation of this hypothesis is of questionable relevance and is therefore not discussed here, but the applicability of the concept has wide scientific acceptance. As a best estimate it is useful in the present context. Ideally, measured sunken and grazed PP fractions for every LME would be preferred, possibly carrying less uncertainty, but such results are not available. Still, Laws et al. (2000) quantifies that 86% of the variance of the expected sinking fraction (as used here) is explained by the water temperature effect (indirectly used when defining the climate zonation) but no direct quantification of further causes is discussed. Considering the above, the use of the match-mismatch concept for the estimation of globally applicable sinking PP fractions is deemed preferable over an extrapolation from available disparate empirical measurements.

The estimation of $f_{SPingest}$ as of 64.3% of the grazed phytoplankton biomass involves a rel.SD≈21% due to the averaging from different sources and methods. We consider it preferable over the use of a single source in order to increase the representativeness of the coefficient adopted.

BGE is estimated from BP, which in turn is estimated from PP (Table S.5). The overall uncertainty of such BGE estimation depends on the variability of the PP dataset (addressed earlier) and the fit of the BP-PP correlation (R^2=0.77). Alternatively, the coupling between BR and BP can be used, but its variance (R^2=0.46, (del Giorgio and Cole, 1998)) is affected by high spatial and temporal variability of bacterial activity (not modelled). As BGE systematically increases with PP (Cole et al., 1988; del Giorgio and

Cole, 1998) we therefore assumed (i) BGE estimated from BP as the best method available and that (ii) the natural variability is equivalent in every LME thus not adding significant bias to the estimation of BGE_{LME}.

The uncertainty of the parameters with higher contributions to the model results was assessed and their variability deemed acceptable or acknowledged. We therefore consider them as best available estimates that still suit the purpose of the model thus supporting our confidence in the robustness of the proposed method. Despite the complexity of the parameterisation and inherent calculations, potential users of the XFs in LCIA or ecosystems health assessment/management would only be required to identify the N-receiving LME and estimate environmental fate losses of the original N emission to feed the model.

4.2. Spatial units and differentiation

We adopted large spatial units of coastal ecosystems instead of a grid cell approach that would inherently presume a significant horizontal flow of organic carbon (or N or DO). We do not judge a grid-based approach to be feasible at the present stage of development of methods for the estimation of impacts to marine eutrophication. The immensity of data required for local parameterisation hinders the implementation of a finer spatial resolution beyond large spatial units such as the LMEs. In support of this reasoning also stands the temporal variability of the processes and (bio)(geo)chemical properties of the water masses, along with local advection and mixing patterns that contribute to some of the modelled parameters. As such, the temporal and spatial integration fits well the LCIA application, which adopts best estimates and an average approach. This seems most appropriate to represent potential conditions and coherence with the pursued objectives. Finally, when applied to the development of CFs in LCIA, XFs need to be combined with emission data, which will realistically not be reported with a resolution finer than the level of countries or discharging watersheds. However, the adoption of large spatial units has the drawback of masking potential peaks of organic carbon supply to bottom waters and of oxygen consumption that may occur either in time or space and cause severe hypoxia or anoxia events. As there is no temporal discrimination in the XFs estimation we assume for modelling purposes that the DO is consumed over a period of one year. This also means that if its depletion is sufficiently slow and system ventilation occurs then replenishment of DO from adjacent water masses may prevent the onset of hypoxia.

The adoption of the LME biogeographical classification system is a discrete choice in the model framework. Any other coastal classification system can be adopted provided that spatially integrated PP data is available and a coherent aggregation into climate zones is possible. These two aspects also advocate for the applicability and flexibility of the proposed method.

4.3. From primary production to export production

The model quantifies the ecosystem response to allochthonous-N inputs and does not include 'natural' external input sources like upwelling or resuspension. This choice is consistent with the desired application in LCIA of estimating the impacts of emissions originated from human activities.

The positive and non-linear correlation between P_E and PP has been shown and discussed elsewhere – see e.g. Vézina and Platt (1987) and Wassmann (1990a). However, as we deliberately strip the model of the regeneration and remineralization processes and respective feedbacks, the output expresses a maximum export capacity of the system and so linearity is expected. This is because, by definition, P_{new} is equivalent to P_E on an annual time scale (Eppley et al., 1983) and so are their carbon equivalents. As P_{new} is, in our model, exclusively fuelled by anthropogenic-N sources, the export production is directly related to the N input in the sense that the annual supply of N does not enter the regeneration loops of local pelagic food webs and, as such, is exported as P_E. As described by Wassmann (1990b), when P_r is set to zero, a linear relationship is expected between the total PP and P_E (which would then be maximised). We chose a power regression model as best fit and significance for the P_E-PP correlation (see Table S.7 and Figure S.3) and tested this relationship in the five CZs (Figure 5).

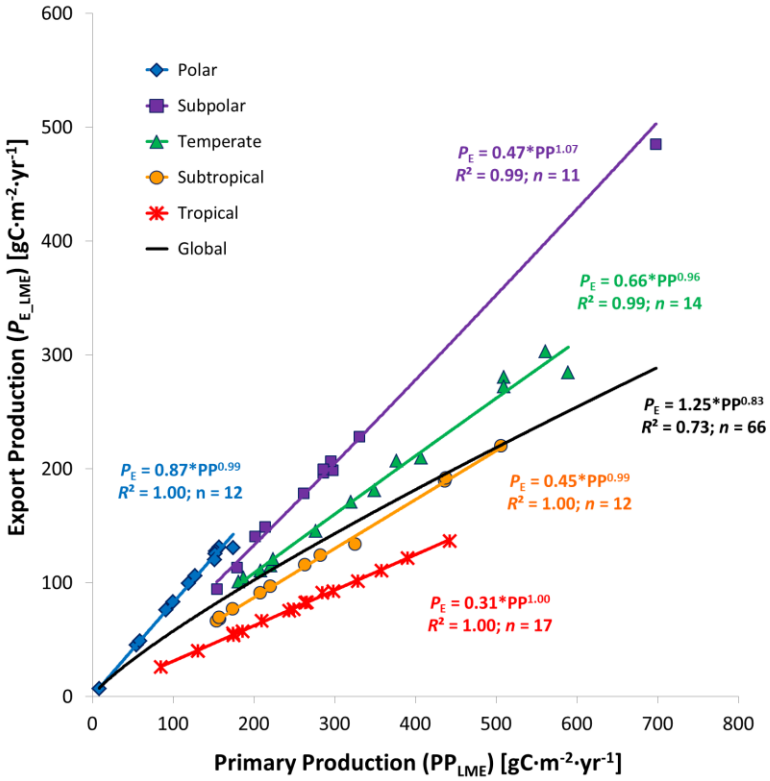

Figure 5 Export production (P_E, [gC·m^{-2}·yr^{-1}]) as a function of primary production (PP, [gC·m^{-2}·yr^{-1}]). Aggregation of P_E from 66 large marine ecosystems (LME) into five climate zones (polar, subpolar, temperate, subtropical, tropical) and global default. Power regression equations and coefficient of determination (R^2) included.

The balance between P_E and PP is determined by the supply of nutrients and heterotrophic grazing/predation. The system is described by a 'top-down' control as the loss rates are determined by grazing pressure and assimilation efficiency, as suggested by Lehman (1991) and Wassmann (1993). The fit of the P_E-PP curves per CZ is close to 1.00 and the power equations show linearity close to 1.00 (range 0.96-1.07). The five CZ export algorithms obtained from our model are therefore rather consistent with the linearity expected by not modelling P_r and P_{new} supported by recycling and remineralization. The global default curve reveals higher variability, i.e. the fraction of variance of P_E explained by the variation of PP is only 0.73 (R^2). This clearly shows that, in our model, P_E can be predicted per CZ with the respective algorithms, but the global algorithm shows a level of uncertainty that might hinder its application. The notion that there is no universal algorithm was already been noted by Wassmann (1998). Nevertheless, the P_E algorithms are valid for the CZ resolution and applicable if no information on spatial variability of the emission/exposure location is available at the LME scale (which is the preferable resolution). The global P_E algorithm should only be applied if the purpose of the study accepts the uncertainty reported. The model discriminates the effect of zooplankton on the suspended biomass of producers by different parameterisation of the grazing pressure and assimilation efficiency per CZ. It is clear that no LME (or intra-CZ) variability is originated from the heterotrophic control modelled as such, whereas the inter-CZ variability is an indication of the discriminatory power of the P_E model.

Figure 6 shows the correlation of our export algorithm to others found in literature (Betzer et al., 1984; Eppley and Peterson, 1979; Pace et al., 1987; Suess, 1980; Wassmann, 1990a) and reviewed by Wassmann (1990a) (see also Table S.8). The present PP and photic depth datasets (Table S.4) were applied to plot the curves. Our export algorithm seems consistent with others (Eppley and Peterson's to a lesser extent). The variation between export curves may originate from the inadequacy of the original algorithms for our global application. Those were derived from empirical data of the eastern Pacific Ocean (Eppley and Peterson, 1979), global ocean in 25 different locations but not coastal-specific (Suess, 1980), open ocean in equatorial Pacific Ocean (Betzer et al., 1984), deep ocean (not coastal) (Pace et al., 1987), and boreal north Atlantic coastal waters (Wassmann, 1990a). As empirical data were used to derive those algorithms, regeneration and remineralisation feedbacks may be included, justifying higher variation towards higher PP rates.

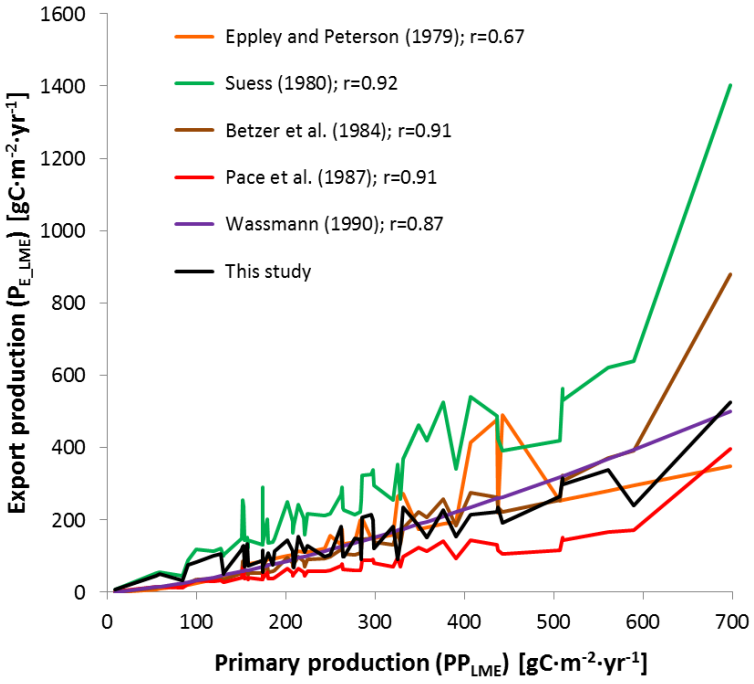

Figure 6 Comparison of the export productions (P_E) curves obtained from the proposed model and predictions by others (see legend box) with the current primary productivity dataset. Linear correlation coefficients (r) included ($p<0.001$).

4.4. From export production to exposure factor

A power regression model was fitted to the XF_{LME} results as a function of PP_{LME} for the five CZs and a global default (**Error! Reference source not found.**). The XF-PP results show a decrease of linearity of the algorithm curves when compared to those of P_E-PP (Figure 5). This fact reflects the increasing losses by consumption of sinking POC (proportional to PP rates) towards highly productive LMEs. Independent of the uncertainty of the PP dataset used (discussed earlier) the XF is mostly dependent on the PP rate input to the model, as shown in the sensitivity analysis (**Error! Reference source not found.**). The spatial aggregation from LME- to CZ-specific XFs clearly does not involve a significant increase in uncertainty caused by variability. However, the adoption of a global XF algorithm is not recommended as only 56% of the XF variance is explained by the variance of PP (see also Figure S.4), which corresponds to ca. 34% of SD explained (SD of errors less than the XF's SD). Spatially aggregated XFs are useful when information about the spatial variability of the emission(s) or the receiving ecosystem(s) is not relevant or is unknown. Ideally, the XF_{LME} should be used to take full advantage of the discriminatory power of the model. The acceptance of any additional uncertainty introduced by spatial aggregation may be determined by the purpose of the study, i.e. scope and application, as it influences the confidence on the results.

As for the P_E model results, the aggregated XF_{CZ} curves show good fit (R^2 close to 1.00) for application when spatial information is not available, while XF_{LME} is recommend when it is. Caution is however advised when applying $XF_{Subpolar}$ as it may underestimate the ecosystem responses due to the contribution of the highly productive LME #23 (Baltic Sea) (the rightmost data point in **Error! Reference source not found.**). As discussed, the adoption of a global XF algorithm is not recommended.

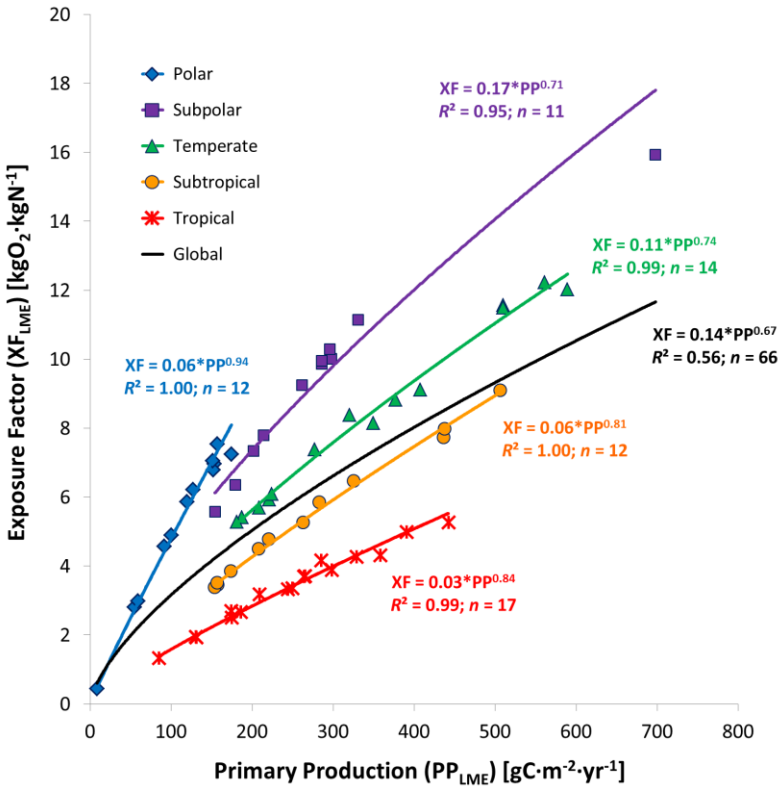

Figure 7 Exposure factor (XF, [$kgO_2 \cdot kgN^{-1}$]) as a function of primary production (PP, [$gC \cdot m^{-2} \cdot yr^{-1}$]). Aggregation of XFs from 66 large marine ecosystems (LME) into five climate zones (polar, subpolar, temperate, subtropical, tropical) and global default. Power regression equations and coefficients of determination (R^2) included.

4.5. Limitations and future research

The limitations faced in quantifying the various model parameters at the respective resolutions and the necessary assumptions done, as discussed earlier, and even after an exhaustive literature research leave room for model refinement. The model has limited application to characterise local carbon vertical fluxes at spatial resolutions finer than LME and, currently, only considers temporal resolution of one year. The estimated carbon export and oxygen depletion in bottom waters does not consider external forcing that might distort the results, e.g. coastal hydrodynamics intensifying either mixing or stratification, and factors determining nutrient limitation and variable N:P ratios of the anthropogenic loadings. Furthermore, seasonal or daily variability of species succession or dominance is not reflected in this time-integrated approach.

Adding a temporal dimension to the variability of the natural processes involving the mismatch of phyto- and zooplankton, the C:N ratio over different moments in a year, and limitation by different nutrients may thus contribute to the model refinement and possibly its robustness. However, increasing the spatial resolution *per se*, to e.g. grid cells, without modelling further parameters relevant at such scale (like mixing, stratification, ventilation, biogeochemistry of sediments, etc.) does not seem a valuable addition. For that, the spatial units should still be distinct from one another based on those additional parameters. The global coverage, essential for the comparative purpose, would then need an immensity of data.

The carbon export component of the model is not including regeneration or remineralisation processes and their contributions. The focus is on the quantification of P_{new} supported by allochthonous and anthropogenic N, as intended, but this limits the use of the model in other applications that also address N and C cycles in e.g. ecological studies aimed at characterising pelagic food webs efficiency.

5. Conclusions

We developed a method to quantify the response of coastal marine ecosystems to N inputs from anthropogenic sources. The pathway from N assimilation to organic carbon sink and subsequent oxygen depletion (exposure pathway) was modelled mechanistically. Exposure Factors (XF) for 66 coastal marine spatial units were estimated. These may be further combined with environmental fate and effect modelling to compose CFs applicable in LCIA for the marine eutrophication impact category.

The model results support the notion that distinct coastal marine ecosystems show distinct responses to equal N loadings. The sensitivity of the receiving ecosystems depends on the interaction of various biological processes occurring there. In the proposed model, the main modulators of this interaction are the primary production rate and latitude. These determine the spatial differentiation of the results and the resolution of the parameters modelled – some are site-dependent for LMEs or climate zones and others site-generic. Eighteen primary and 12 derived parameters were combined in a conceptual pathway that includes production, carbon export, consumption/degradation, and respiration. The result is a mechanistic model that delivers XFs with a spatial variation of a factor 35 among LMEs.

N-limited systems are characterised by a positive covariation between production and export, implying that a higher productivity leads to a higher sinking flux (Harrison et al., 1987; Platt and Sathyendranath, 1988). Therefore, an input of anthropogenic N makes more limiting nutrient available to PP resulting in higher downward carbon export and potential benthic oxygen depletion. An indicator that is capable of quantifying the oxygen consumption as a function of N input may be of useful application to assess the ecosystem condition or the impacts of N emissions from

human activities. The latter constitutes the main objective of LCIA methods in support of e.g. sustainability assessment of such activities. The presented approach shows ecological relevance by describing every relevant parameter and process in the exposure pathway based on state of the art science. It is built on a transparent, documented, and robust model whose results are significant and useful contributions to characterisation modelling in LCIA for the marine eutrophication impact category.

Acknowledgements

The present research was partially funded by the European Commission under the 7th Framework Programme on Environment; ENV.2009.3.3.2.1: LC-IMPACT – Improved Life Cycle Impact Assessment methods (LCIA) for better sustainability assessment of technologies, grant agreement number 243827. We further thank the two anonymous reviewers whose comments/suggestions helped improve and clarify this manuscript.

Appendix A. Supplementary data

Supplementary data associated with this article can be found, in the online version, at http://dx.doi.org/10.1016/j.ecolmodel.2015.09.005.

References

Alldredge, A.L., King, J.M., 1980. Effects of moonlight on the vertical migration patterns of demersal zooplankton. J. Exp. Mar. Bio. Ecol. 44, 133–156.

Alldredge, A.L., Silver, M.W., 1988. Characteristics, Dynamics and Significance of Marine Snow. Prog. Oceanogr. 20, 41–82.

Arrigo, K.R., 2005. Marine microorganisms and global nutrient cycles. Nature 437, 349–356.

Atkinson, A., Ward, P., Williams, R., Poulet, S.A., 1992. Feeding rates and diel vertical migration of copepods near South Georgia: comparison of shelf and oceanic sites. Mar. Biol. 114, 49–56.

Behrenfeld, M.J., Boss, E.S., 2014. Resurrecting the ecological underpinnings of ocean plankton blooms. Ann. Rev. Mar. Sci. 6, 167–94.

Behrenfeld, M.J., Falkowski, P.G., 1997. Photosynthetic rates derived from satellite-based chlorophyll concentration. Limnol. Oceanogr. 42, 1–20.

Besiktepe, S., Dam, H.G., 2002. Coupling of ingestion and defecation as a function of diet in the calanoid copepod Acartia tonsa. Mar. Ecol. Prog. Ser. 229, 151–164.

Besiktepe, S., Kideys, A.E., Unsal, M., 1998. In situ grazing pressure and diel vertical migration of female Calanus euxinus in the Black Sea. Hydrobiologia 363, 323–332.

Betzer, P.R., Showers, W.J., Laws, E.A., Winn, C.D., DiTullio, G.R., Kroopnick, P.M., 1984. Primary productivity and particle fluxes on a transect of the equator at

153°W in the Pacific Ocean. Deep Sea Res. Part A. Oceanogr. Res. Pap. 31, 1–11.

Bouvet, M., Hoepffner, N., Dowell, M.D., 2002. Parameterization of a spectral solar irradiance model for the global ocean using multiple satellite sensors. J. Geophys. Res. 107, 3215.

Calbet, A., 2001. Mesozooplankton grazing effect on primary production: A global comparative analysis in marine ecosystems. Limnol. Oceanogr. 46, 1824–1830.

Calbet, A., Landry, M.R., 2004. Phytoplankton growth, microzooplankton grazing, and carbon cycling in marine systems. Limnol. Oceanogr. 49, 51–57.

Chassot, E., Bonhommeau, S., Dulvy, N.K., Mélin, F., Watson, R., Gascuel, D., Le Pape, O., 2010. Global marine primary production constrains fisheries catches. Ecol. Lett. 13, 495–505.

Cole, J.J., Findlay, S., Pace, M.L., 1988. Bacterial production in fresh and saltwater ecosystems: a cross-system overview. Mar. Ecol. Prog. Ser. 43, 1–10.

Conover, R.J., 1966. Factors affecting the assimilation of organic matter by zooplankton and the question of superfluous feeding. Limnol. Oceanogr. 11, 346–354.

Cushing, D.H., 1975. Marine Ecology and Fisheries. Cambridge University Press, Cambridge.

Cushing, D.H., 1990. Plankton Production and Year-class Strength in Fish Populations: an Update of the Match/Mismatch Hypothesis. Adv. Mar. Biol. 26, 249–293.

Del Giorgio, P.A., Cole, J.J., 1998. Bacterial Growth Efficiency in Natural Aquatic Systems. Annu. Rev. Ecol. Syst. 29, 503–541.

Diaz, R.J., Rosenberg, R., 2008. Spreading dead zones and consequences for marine ecosystems. Science 321, 926–9.

Duarte, B., Saraiva, P.M., Pantelides, C.C., 2004. Combined Mechanistic and Empirical Modelling. Int. J. Chem. React. Eng. 2, A3.

Ducklow, H., Steinberg, D., Buesseler, K., 2001. Upper Ocean Carbon Export and the Biological Pump. Oceanography 14, 50–58.

Ducklow, H.W., Carlson, C.A., 1992. Oceanic bacterial production. Adv. Microb. Ecol. 12, 113–181.

Dugdale, R.C., Goering, J.J., 1967. Uptake of new and regenerated forms of nitrogen in primary productivity. Limnol. Oceanogr. 12, 196–206.

Durant, J.M., Hjermann, D.Ø., Ottersen, G., Stenseth, N.C., 2007. Climate and the match or mismatch between predator requirements and resource availability. Clim. Res. 33, 271–283.

Elmgren, R., 2001. Understanding Ecosystem : Changing Impact Views on in the Recent Baltic Decades. Ambio 30, 222–231.

Elser, J.J., Bracken, M.E.S., Cleland, E.E., Gruner, D.S., Harpole, W.S., Hillebrand, H., Ngai, J.T., Seabloom, E.W., Shurin, J.B., Smith, J.E., 2007. Global analysis of nitrogen and phosphorus limitation of primary producers in freshwater, marine and terrestrial ecosystems. Ecol. Lett. 10, 1135–42.

Eppley, R.W., Peterson, B.J., 1979. Particulate organic matter flux and planktonic new production in the deep ocean. Nature.

Eppley, R.W., Renger, E.H., Betzer, P.R., 1983. The residence time of particulate organic carbon in the surface layer of the ocean. Deep Sea Res. 30, 311–323.

Fowler, S.W., Knauer, G.A., 1986. Role of large particles in the transport of elements and organic compounds through the oceanic water column. Prog. Oceanogr. 16, 147–194.

Galloway, J.N., Cowling, E.B., Seitzinger, S.P., Socolow, R.H., 2002. Reactive nitrogen: too much of a good thing? Ambio 31, 60–3.

Galloway, J.N., Townsend, A.R., Erisman, J.W., Bekunda, M., Cai, Z., Freney, J.R., Martinelli, L.A., Seitzinger, S.P., Sutton, M.A., 2008. Transformation of the Nitrogen Cycle: Recent Trends, Questions, and Potential Solutions. Science (80-.). 320, 889–892.

Gray, J.S., Wu, R.S., Or, Y.Y., 2002. Effects of hypoxia and organic enrichment on the coastal marine environment. Mar. Ecol. Prog. Ser. 238, 249–279.

Harrison, W.G., Platt, T., Lewis, M.R., 1987. f-Ratio and its relationship to ambient nitrate concentration in coastal waters. J. Plankton Res. 9, 235–248.

Hauschild, M.Z., 2005. Assessing Environmental Impacts in a Life-Cycle Perspective. Environ. Sci. Technol. 39, 81–88.

Henderson, A.D., 2015. Eutrophication, in: Hauschild, M.Z., Huijbregts, M.A.J. (Eds.), Life Cycle Impact Assessment, LCA Compendium - The Complete World of Life Cycle Assessment. Springer Science+Business Media Dordrecht, pp. 177–196.

Hirst, A.G., Kiørboe, T., 2002. Mortality of marine planktonic copepods: global rates and patterns. Mar. Ecol. Prog. Ser. 230, 195–209.

Ho, T., Quigg, A., Zoe, V., Milligan, A.J., Falkowski, P.G., Morel, M.M., 2003. The elemental composition of some phytoplankton. J. Phycol. 39, 1145–1159.

Howarth, R.W., Marino, R., 2006. Nitrogen as the limiting nutrient for eutrophication in coastal marine ecosystems: Evolving views over three decades. Limnol. Oceanogr. 51, 364–376.

Huisman, J., van Oostveen, P., Weissing, F.J., 1999. Critical depth and critical turbulence: Two different mechanisms for the development of phytoplankton blooms. Limnol. Oceanogr. 44, 1781–1787.

Iversen, M.H., Ploug, H., 2010. Ballast minerals and the sinking carbon flux in the ocean: carbon-specific respiration rates and sinking velocity of marine snow aggregates. Biogeosciences 7, 2613–2624.

Keeling, R.F., Körtzinger, A., Gruber, N., 2010. Ocean Deoxygenation in a Warming World. Ann. Rev. Mar. Sci. 2, 199–229.

Kelly, J.R., 2008. Nitrogen Effects on Coastal Marine Ecosystems, in: Hatfield, J.L., Follet, R.F. (Eds.), Nitrogen in the Environment: Sources, Problems, and Management. U.S. Environmental Protection Agency, pp. 271–332.

Kiørboe, T., 1996. Material Flux in the Water Column, in: Jorgensen, B.B., Richardson, K. (Eds.), Eutrophication in Coastal Marine Ecosystems Coastal and Estuarine Studies. American Geophysical Union, pp. 67–94.

Kiørboe, T., 2001. Formation and fate of marine snow: small-scale processes with large-scale implications. Sci. Mar. 65, 57–71.

Kiørboe, T., Hansen, J.L.S., Alldredge, A.L., Jackson, G.A., Passow, U., Dam, H.G., Drapeau, D.T., Waite, A., Garcia, C.M., 1996. Sedimentation of phytoplankton during a diatom bloom: Rates and mechanisms. J. Mar. Res. 54, 1123–1148.

Koski, M., Jónasdóttir, S.H., Bagøien, E., 2011. Biological processes in the North Sea: vertical distribution and reproduction of neritic copepods in relation to environmental factors. J. Plankton Res. 33, 63–84.

Lai, S., 2004. Primary Production [WWW Document]. Sea Around Us Proj. Fish. Centre, UBC. URL http://www.seaaroundus.org/doc/saup_manual.htm#3 (accessed 6.18.14).

Lampert, W., 1978. Release of dissolved organic carbon by grazing zooplankton. Limnol. Ocean. 23, 831–834.

Lampert, W., 1989. The Adaptive Significance of Diel Vertical Migration of Zooplankton. Funct. Ecol. 3, 21–27.

Laws, E.A., Falkowski, P.G., Smith Jr., W.O., Ducklow, H., McCarthy, J.J., 2000. Temperature effects on export production in the open ocean. Global Biogeochem. Cycles 14, 1231–1246.

Lehman, J.T., 1991. Interacting growth and loss rates: The balance of top-down and bottom-up controls in plankton communities. Limnol. Oceanogr. 36, 1546–1554.

Levin, L.A., Ekau, W., Gooday, A.J., Jorissen, F., Middelburg, J.J., Naqvi, S.W.A., Neira, C., Rabalais, N.N., Zhang, J., 2009. Effects of natural and human-induced hypoxia on coastal benthos. Biogeosciences 6, 2063–2098.

Longhurst, A.R., 1998. Ecological Geography of the Sea. Academic Press Limited, London, UK.

Longhurst, A.R., Harrison, W.G., 1988. Vertical nitrogen flux from the oceanic photic zone by diel migrant zooplankton and nekton. Deep. Res. 35, 881–889.

Møller, E.F., 2007. Production of dissolved organic carbon by sloppy feeding in the copepods Acartia tonsa, Centropages typicus, and Temora longicornis. Limnol. Oceanogr. 52, 79–84.

Møller, E.F., Nielsen, T.G., 2001. Production of bacterial substrate by marine copepods: Effect of phytoplankton biomass and cell size. J. Plankton Res. 23, 527–536.

Møller, E.F., Thor, P., Nielsen, T.G., 2003. Production of DOC by Calanus finmarchicus, C. glacialis and C. hyperboreus through sloppy feeding and leakage from fecal pellets. Mar. Ecol. Prog. Ser. 262, 185–191.

Morales, C.E., Harris, R.P., Head, R.N., Tranter, P.R.G., 1993. Copepod grazing in the oceanic northeast Atlantic during a 6 week drifting station: The contribution of size classes and vertical migrants. J. Plankton Res. 15, 185–212.

Niemi, G., Wardrop, D., Brooks, R., Anderson, S., Brady, V., Paerl, H.W., Rakocinski, C.F., Brouwer, M., Levinson, B., McDonald, M., 2004. Rationale for a New Generation of Indicators for Coastal Waters. Environ. Health Perspect. 112, 979–986.

Nixon, S.W., 1995. Coastal marine eutrophication: A definition, social causes, and future concerns. Ophelia 41, 199–219.

NRC, 2000. Clean Coastal Waters: Understanding and Reducing the Effects of Nutrient Pollution. National Academy press, Washington, DC.

Odum, E.P., 1971. Fundamentals of Ecology, 3rd ed. W.B. Saunders Co., Philadelphia.

Pace, M.L., Knauer, G.A., Karl, D.M., Martin, J.H., 1987. Primary production, new production and vertical flux in the eastern Pacific Ocean. Nature 325, 803–804.

Pauly, D., Christensen, V., 1995. Primary production required to sustain global fisheries. Nature.

Platt, T., Harrison, W.G., Lewis, M.R., Li, W.K.W., Sathyendranath, S., Smith, R.E., Vezina, A.F., 1989. Biological production of the oceans: the case for a consensus. Mar. Ecol. Prog. Ser. 52, 77–88.

Platt, T., Sathyendranath, S., 1988. Oceanic Primary Production: Estimation by Remote Sensing at Local and Regional Scales. Science (80-.). 241, 1613–1620.

Puelles, M.L.F. de, Valdés, L., Varela, M., Halliday, N., 1996. Diel variations in the vertical distribution of copepods off the north coast of Spain. ICES J. Mar. Sci. 53, 97–106.

Redfield, A.C., 1958. The Biological Control of Chemical Factors in the Environment. Am. Sci. 46, 205–221.

Roman, M.R., Adolf, H.A., Landry, M.R., Madin, L.P., Steinberg, D.K., Zhang, X., 2002. Estimates of oceanic mesozooplankton production: a comparison using the Bermuda and Hawaii time-series data. Deep. Res. Part II 49, 175–192.

Roman, M.R., Furnas, M.J., Mullin, M.M., 1990. Zooplankton abundance and grazing at Davies Reef, Great Barrier Reef, Australia. Mar. Biol. 105, 73–82.

Saba, G.K., Steinberg, D.K., Bronk, D. a., 2011. The relative importance of sloppy feeding, excretion, and fecal pellet leaching in the release of dissolved carbon and nitrogen by Acartia tonsa copepods. J. Exp. Mar. Bio. Ecol. 404, 47–56.

Saba, G.K., Steinberg, D.K., Bronk, D.A., 2009. Effects of diet on release of dissolved organic and inorganic nutrients by the copepod Acartia tonsa. Mar. Ecol. Prog. Ser. 386, 147–161.

Sherman, K., Alexander, L.M. (Eds.), 1986. Variability and Management of Large Marine Ecosystems. Westview Press Inc., Boulder, CO.

Sherman, K., Aquarone, M.C., Adams, S. (Eds.), 2009. Sustaining the World's Large Marine Ecosystems. IUCN, Gland, Switzerland.

Smith, V.H., 2007. Using primary productivity as an index of coastal eutrophication: the units of measurement matter. J. Plankton Res. 29, 1–6.

Smith, V.H., Tilman, G.D., Nekola, J.C., 1999. Eutrophication: impacts of excess nutrient inputs on freshwater, marine, and terrestrial ecosystems. Environ. Pollut. 100, 179–196.

Socolow, R.H., 1999. Nitrogen management and the future of food: Lessons from the management of energy and carbon. Proc. Natl. Acad. Sci. U. S. A. 96, 6001–6008.

Spalding, M.D., Fox, H.E., Allen, G.R., Davidson, N., Ferdaña, Z.A., Finlayson, M., Halpern, B.S., Jorge, M.A., Lourie, S.A., Martin, K.D., Mcmanus, E., Recchia, C.A., Robertson, J., 2007. Marine Ecoregions of the World: A Bioregionalization of Coastal and Shelf Areas. Bioscience 57, 573–583.

Strandesen, M., Birkved, M., Holm, P.E., Hauschild, M.Z., 2007. Fate and distribution modelling of metals in life cycle impact assessment. Ecol. Modell. 203, 327–338.

Suess, E., 1980. Particulate organic carbon flux in the oceans - surface productivity and oxygen utilization. Nature 288, 260–263.

Tang, K.W., Elliott, D.T., 2013. Copepod Carcasses: Occurrence, fate and Ecological Importance, in: Seuront, L. (Ed.), Copepods: Diversity, Habitat and Behaviour. Nova Science Publishers, Inc., p. 28.

Turner, J.T., 2002. Zooplankton fecal pellets, marine snow and sinking phytoplankton blooms. Aquat. Microb. Ecol. 27, 57–102.

Turner, R.E., Qureshi, N., Rabalais, N.N., Dortch, Q., Justić, D., Shaw, R.F., Cope, J., 1998. Fluctuating silicate: nitrate ratios and coastal plankton food webs. Proc. Natl. Acad. Sci. U. S. A. 95, 13048–13051.

UBC, 1999. Sea Around Us Project: Fisheries, Ecosystems & Biodiversity [WWW Document]. URL http://seaaroundus.org/ (accessed 6.18.14).

UNEP, 2006. Marine and coastal ecosystems and human well-being: A synthesis report based on the findings of the Millennium Ecosystem Assessment.

UNESCO, 2009. Global Open Oceans and Deep Seabed (GOODS) - Biogeographic Classification.

Vézina, A.F., Platt, T., 1987. Small-Scale Variability of New Production and Particulate Fluxes in the Ocean. Can. J. Fish. Aquat. Sci. 44, 198–205.

Vitousek, P.M., Hättenschwiler, S., Olander, L., Allison, S., 2002. Nitrogen and nature. Ambio 31, 97–101.

Wassmann, P., 1990a. Relationship between primary and export production in the boreal coastal zone of the North Atlantic. Limnol. Ocean. 35, 464–471.

Wassmann, P., 1990b. Calculating the Load of Organic Carbon to the Aphotic Zone in Eutrophicated Coastal Waters. Mar. Pollut. Bull. 21, 183–187.

Wassmann, P., 1993. Regulation of vertical export of particulate organic matter from the euphotic zone by planktonic heterotrophs in eutrophicated aquatic environments. Mar. Pollut. Bull. 26, 636–643.

Wassmann, P., 1998. Retention versus export food chains: processes controlling sinking loss from marine pelagic systems 29–57.

Watson, R., Zeller, D., Pauly, D., 2014. Primary productivity demands of global fishing fleets. Fish Fish. 15, 231–241.

Article II – Supporting Information

Exposure factors for marine eutrophication impacts assessment based on a mechanistic biological model

Nuno Cosme [a,*], Marja Koski [b], Michael Z. Hauschild [a]

[a] Division for the Quantitative Sustainability Assessment, Department of Management Engineering, Technical University of Denmark, Produktionstorvet 424, DK-2800 Kgs. Lyngby, Denmark

[b] Section of Marine Ecology and Oceanography, Technical University of Denmark, Kavalergården 6, DK-2920 Charlottenlund, Denmark

* *Corresponding author*. Tel.: +45 45254729.

E-mail address: nmcosme@dtu.dk

S.1 On the modelling of the indicator of exposure to nitrogen

The paper has the aim to estimate exposure factors (XF) for the assessment of marine eutrophication impacts caused by discharges of nitrogen (N) from anthropogenic sources to coastal waters based on mechanistic modelling of the underlying biological processes. The relevant processes for this assessment are nutrient-limited primary production (PP), metazoan consumption, and bacterial degradation of this PP. The proposed model framework delivers an indicator of the exposure of marine coastal ecosystems to N-loadings, which expresses the amount of dissolved oxygen consumed as a function of N-loadings. Such indicator (XF, [$kgO_2 \cdot KgN^{-1}$]) may be applicable in Life Cycle Impact Assessment (LCIA) as an essential component for characterisation modelling of N-emissions with eutrophying impacts, or be useful in ecosystems management.

In a broad sense, the environmental conditions govern nutrients' fate and assimilation. These can be affected by abiotic factors, e.g. irradiance, temperature, residence time, advection, and by biotic factors, e.g. species, their life cycles, and growth rates. Modelling environmental parameters, specific local conditions, and how they affect phytoplankton in what regards to energy budget, reproduction, distribution, species composition, productivity, etc., is complicated. Modelling all the factors simultaneously to mechanistically predict the ecosystem response to N fertilization is even more complicated, as well as time- and resource-consuming. Indicators, such as the PP rate (Niemi et al., 2004; Smith, 2007) and the method introduced here, are useful approaches to quantify these responses and of special interest for application in ecological modelling of marine eutrophication and impact assessment. However, PP as an indicator is unable to explain how different coastal areas may have distinct responses

because it misses the explanatory power for the impacts, e.g. different water masses may show distinct impacts while sharing similar PP rates. The indicator we propose here, the ecosystem eXposure Factor (XF), adds a mechanistic explanation for the potential impacts and addresses the reasons for its variability. This seems more relevant than a simple PP-impacts empirical correlation (e.g. PP to levels of hypoxia, or PP to extension of dead zones) and useful for predictive advice, ecosystems management, and modelling of eutrophication.

S.1.1 Primary production and vertical carbon flux

The productivity of marine ecosystems depends on light-harvesting primary producers (phytoplankton). The photosynthetic production of organic matter by phytoplankton supports the food webs of the entire pelagic and demersal marine ecosystems (Baines et al., 1994; Mills, 1975; Reynolds, 2006). Despite being limited to the upper layer of the ocean (euphotic zone) the net primary production of the ocean is comparable to the terrestrial primary production at 48.3 and 56.4 $GtC \cdot yr^{-1}$, respectively (Geider et al., 2001).

The main modulators of PP are the availability of light and nutrients, thus determining the efficiency and distribution of phytoplankton species in the euphotic zone (Field, 1998). Water mixing is also relevant for it determines how phytoplankton is exposed to light and how nutrients are made available. Stratification originated by the heating of the upper water layer or by freshwater input from river discharge and ice melting is important in the regulation of the timing, duration, and intensity of the productive periods (Lemke et al., 2007; Peterson et al., 2006; Tremblay et al., 2006). In general, the resulting density-driven stratification constitutes a simultaneous barrier for nutrients supply to the upper layer and to the ventilation of the deeper layers. A strong stratification poses a potential threat to benthic communities as it influences the availability of dissolved oxygen.

The concept of 'limiting nutrient' is essential for the modelling of productivity and it is based on Liebig's Law of the Minimum (reviewed by van der Ploeg et al. (1999)). It states that growth, abundance or distribution of individuals or populations is controlled not by the total amount of resources but by the scarcest resource, i.e. one nutrient has a limiting role and all other nutrients are available in excess. In practice, any additional amount of the limiting nutrient introduced to the system promotes an increase in response (growth), whereas the introduction of any other nutrient has no reflection on growth as they are already in excess (Finnveden and Potting, 1999).

Specific biotic (mainly limited grazing pressure) and abiotic (environmental) conditions determine when phytoplankton blooms initiate (Behrenfeld and Boss, 2014). The hypotheses supporting the phytoplankton bloom initiation have been widely discussed (Behrenfeld, 2010; Boss and Behrenfeld, 2010; Chiswell, 2011; Evans and

Parslow, 1985; Gran and Braarud, 1935; Platt et al., 1991; Smetacek and Passow, 1990; Sverdrup, 1953; Taylor and Ferrari, 2011)). These have evolved from the critical depth hypothesis (Sverdrup, 1953) focused on the shoaling of the mixed-layer depth, to the critical turbulence hypothesis (Huisman et al., 2002, 1999) focused on the shoaling of a density-defined mixed layer, and more recently to the disturbance-recovery hypothesis (Behrenfeld et al., 2013) focused on the disruption of the balance between phytoplankton growth and consumptive mortality (grazing).

The match-mismatch hypothesis described by Cushing (1975) is further used in the present approach to define a critical fate process of primary producers' biomass by determining the grazed and sunken fractions per climate zone. The magnitude of the subsequent vertical carbon flux thus depends on the biological response of primary producers to the abiotic conditions (e.g. light, temperature, and nutrient availability) and on the activity of their consumers (mainly zooplankton) and degraders (microbial loop). In short, if the biomass resulting from the assimilation of nutrients exceeds consumption and degradation there is a net flux of organic carbon to bottom waters.

Considering the processes that regulate (i) the export production, (ii) the oxygen consumption near the bottom, and (iii) the potential impacts to marine eutrophication that may come from excessive N fertilization, it seems crucial to integrate all the relevant coastal biological processes into a common model framework if trying to quantify the ecosystem's response to N-loadings from anthropogenic sources.

S.1.2 Complementary information on modelling anthropogenic sources of nitrogen

Several studies and reviews have focused on understanding and discussing the sources, fate, and general impacts of nitrogen in ecosystems. Examples of these include global, estuarine, and coastal marine nitrogen cycling (Galloway et al., 2008, 2004; Herbert, 1999; Pinckney et al., 2001; Rabalais, 2002; Ryther and Dunstan, 1971; Vitousek et al., 1997), fate modelling in soils, groundwater, and surface freshwater systems (Bouwman, 2005; Seitzinger et al., 2010, 2005; Van Drecht et al., 2003; Wollheim et al., 2008), atmospheric emissions and deposition (Lee et al., 1997; Roy et al., 2012; van Vuuren et al., 2011), emissions from agriculture (Beusen et al., 2008; Bouwman et al., 2009, 2002; Butterbach-Bahl and Dannenmann, 2011; Carpenter et al., 1998), emissions from wastewater (Van Drecht et al., 2009, 2003), loadings from rivers (Green et al., 2004; Kroeze et al., 2012; Seitzinger et al., 2010), or impacts from excess nitrogen inputs and eutrophication to marine ecosystems (Cloern, 2001; de Jonge et al., 2002; Kitsiou and Karydis, 2011; Nixon, 1995; Rabalais et al., 2009; Smith et al., 2006, 1999).

S.1.3 Empirical vs. mechanistic models

Characterisation models in LCIA can be single-level descriptive (or empirical) or hierarchical/multilevel explanatory (or mechanistic) (Duarte et al., 2004, 2003; Steen, 2002). Empirical models are based on statistically significant correlations between properties and responses, i.e. rely on statistical treatment of large amounts of empirical data to describe the 'natural' processes. These are 'black box' models that mine correlation-based knowledge out of the available data with the introduction of as few assumptions about the processes as possible (Duarte et al., 2004) to describe the observed behaviour, offering low explanatory depth (Mulligan and Wainwright, 2004). In practice, they fit the behaviour/responses to real available data by minimising the residuals (differences) between predicted estimates (results) and dependent variable observations (data) (Duarte et al., 2004). Although highly predictive, empirical approaches allow limited extrapolation beyond the scope of the data, as they do not offer a mechanistic understanding of the processes they try to describe.

Mechanistic models use existing scientific knowledge about the processes they try to represent by means of equations that express the systems' response or behaviour. Mechanistic approaches allow some extrapolation of the results beyond the intrinsic limitations of specificity of the experimental data and evidence available as well as estimation of unmeasured state variables (Duarte et al., 2004). A possible drawback of a mechanistic approach is the failure to forecast the 'natural' processes accurately (low predictive power) (Mulligan and Wainwright, 2004) by not including all the knowledge and data available, mainly because of the inevitable introduction of model simplifications and assumptions to offset the lack of understanding or integration of multiple interactions or simply the inability to handle the complexity of the modelling needs (Duarte et al., 2004).

The model framework proposed here fits a mechanistic approach. It explores the system hierarchy in an effort to predict and explain the integrated response by building on descriptive (empirical) studies and their results to ultimately become explanatory at the higher levels. In practice, we build a mechanistic cause-effect pathway of cascading biological processes to deliver an overall conversion of nitrogen into oxygen consumption. With this approach we aim at ensuring environmental relevance and significance by describing all the relevant parameters based on state of the art science. In doing so, we minimise the drawbacks. Finally, we deliver a transparent model with manageable complexity and good extrapolation potential by using adaptable parameterisation that can reflect e.g. different regional environmental settings or future climatic pressures.

The present XF estimation method is equivalent to a modified and expanded export production (P_E) model in delivering spatially differentiated indicators of the ecosystem response (XF) to nitrogen. The method renders an indicator which is

equivalent in concept to P_E fuelled by N from anthropogenic allochthonous sources plus subsequent degradation of the exported organic material. The applicability of such indicator seems greater than the P_E alone for the purpose of the LCIA method in which it is to be incorporated, i.e. a comparative assessment of the potential impacts to marine eutrophication from N emissions as it expresses not only the exported fraction but also the subsequent pathway that leads to the endpoint oxygen consumption. This final step is important to the impacts assessment framework as oxygen depletion is the stressor that leads to the ultimate effect on biota survival and its role in ecosystem structure and functioning.

S.2 Additional information to methods description

S.2.1. Grouping spatial units into climate zones

Spatial units of marine coastal waters (LMEs) were grouped into climate zones (tropical, subtropical, temperate, subpolar, and polar) (results in Figure S.1 and geographical distribution in Figure S.2) using with the following criteria:

- Latitudinal distribution: Tropical from Equator to ≈20°N, Subtropical from ≈20°-30°N, Temperate from ≈30°-50°N, Subpolar from ≈50°-70°N, and Polar from ≈70°-90°N (and the same for the Southern Hemisphere);
- Mean annual sea surface temperature (maSST): based on Sherman and Hempel (2009), which includes regression equations for maSST (from 1975-2005) per LME;
- To help on the classification of certain LMEs, complementary information was found on the MEOW classification system (Spalding et al., 2007) and on the Köppen-Geiger climate classification system (Peel et al., 2007).

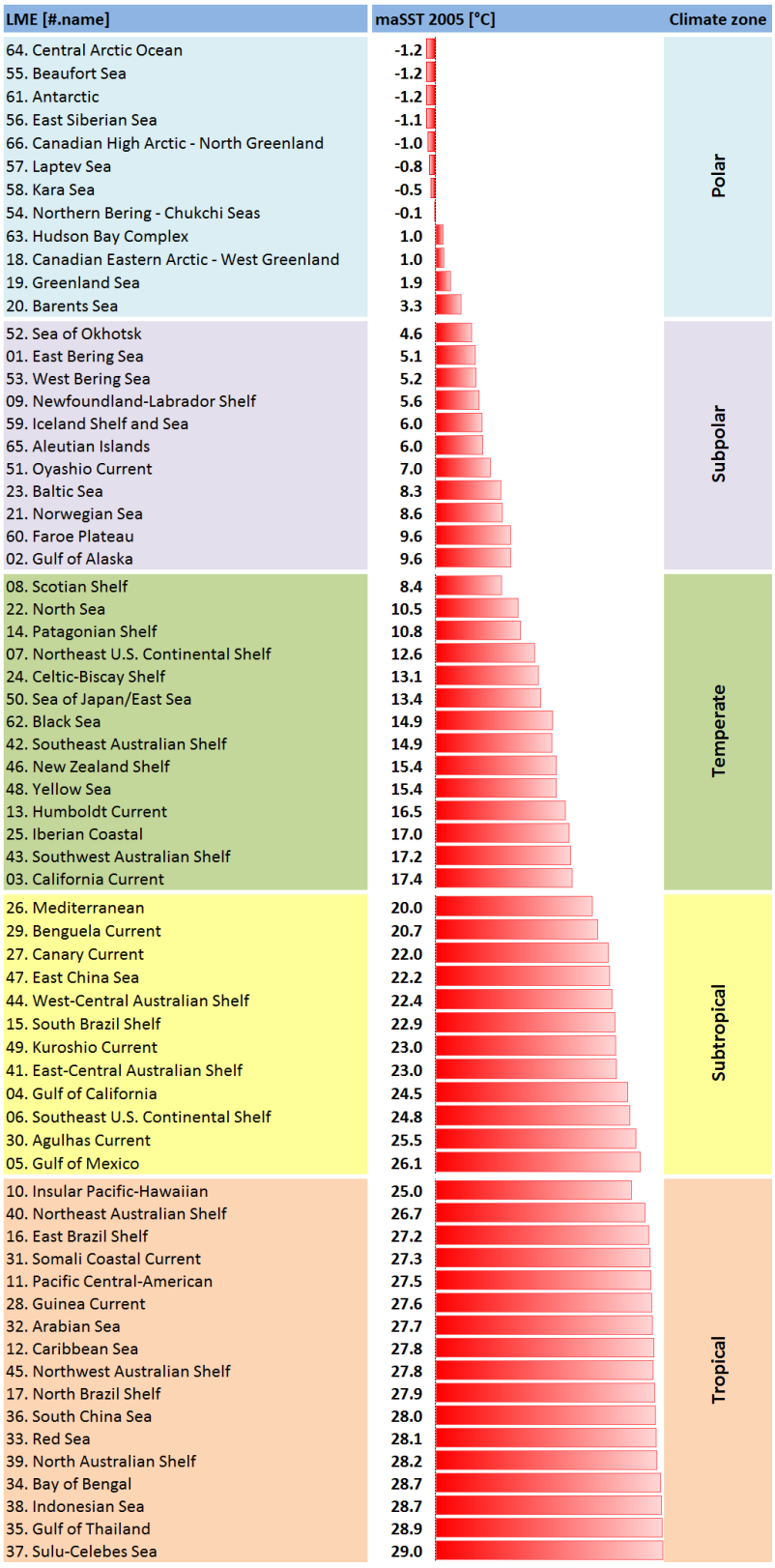

Figure S.1 Classification and grouping of Large Marine Ecosystems (LME) into climate zones (polar, subpolar, temperate, subtropical, and tropical) based on mean annual sea surface temperature (maSST), latitude, and consistency with the Köppen-Geiger climate classification system (data from Sherman and Hempel (2009)).

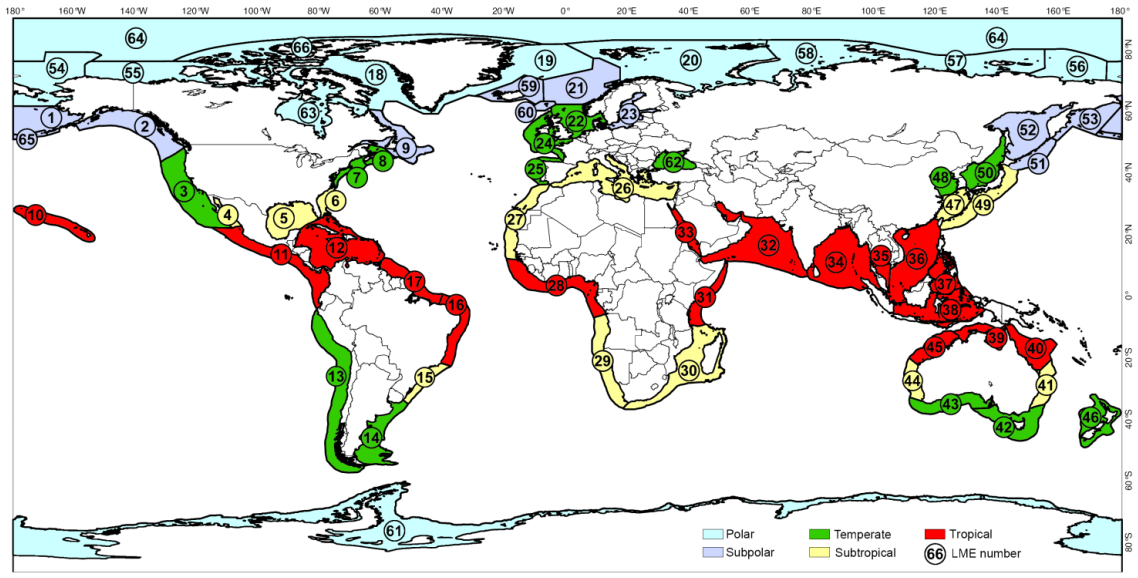

1. East Bering Sea
2. Gulf of Alaska
3. California Current
4. Gulf of California
5. Gulf of Mexico
6. Southeast U.S. Continental Shelf
7. Northeast U.S. Continental Shelf
8. Scotian Shelf
9. Newfoundland-Labrador Shelf
10. Insular Pacific-Hawaiian
11. Pacific Central-American
12. Caribbean Sea
13. Humboldt Current
14. Patagonian Shelf
15. South Brazil Shelf
16. East Brazil Shelf
17. North Brazil Shelf
18. Canadian Eastern Arctic - West Greenland
19. Greenland Sea
20. Barents Sea
21. Norwegian Sea
22. North Sea
23. Baltic Sea
24. Celtic-Biscay Shelf
25. Iberian Coastal
26. Mediterranean
27. Canary Current
28. Guinea Current
29. Benguela Current
30. Agulhas Current
31. Somali Coastal Current
32. Arabian Sea
33. Red Sea
34. Bay of Bengal
35. Gulf of Thailand
36. South China Sea
37. Sulu-Celebes Sea
38. Indonesian Sea
39. North Australian Shelf
40. Northeast Australian Shelf
41. East-Central Australian Shelf
42. Southeast Australian Shelf
43. Southwest Australian Shelf
44. West-Central Australian Shelf
45. Northwest Australian Shelf
46. New Zealand Shelf
47. East China Sea
48. Yellow Sea
49. Kuroshio Current
50. Sea of Japan/East Sea
51. Oyashio Current
52. Sea of Okhotsk
53. West Bering Sea
54. Northern Bering-Chukchi Seas
55. Beaufort Sea
56. East Siberian Sea
57. Laptev Sea
58. Kara Sea
59. Iceland Shelf and Sea
60. Faroe Plateau
61. Antarctic
62. Black Sea
63. Hudson Bay Complex
64. Central Arctic Ocean
65. Aleutian Islands
66. Canadian High Arctic-North Greenland

Figure S.2 Geographical distribution of the 66 Large Marine Ecosystems (LMEs) grouped into the five proposed climate zones (polar, subpolar, temperate, subtropical, tropical) (spatial units coloured from the original digital map available at http://lme.edc.uri.edu/).

S.2.2. Model input parameters

The 18 primary input parameters and others derived from these are included in Table S.1, that complement Table 1 included in the main text. Details on the specific calculations and description are included as well as the estimated coefficients per relevant resolution used in the model work.

Table S.1 Parameters used in the model, their quantification and characteristics.

Input parameter	Spatial resolution	Value	Unit	Source (reference or calculation)	Description
C:N	GLO	5.681	[$kgC \cdot kgN^{-1}$]	Stoichiometry of the photosynthesis equation	Molar mass ratio: 106*M(C)/16*M(N)
O_2:C	GLO	3.468	[$kgO_2 \cdot kgC^{-1}$]	Stoichiometry of the respiration equation	Molar mass ratio: 138*M(O_2)/106*M(C)
O_2:N	GLO	19.704	[$kgO_2 \cdot kgN^{-1}$]	(O_2:N)=(C:N)*(O_2:N)	Molar mass ratio: 138*M(O_2)/16*M(N)
PP_{Pot}	LME	0.033 ↔ 2.707	[-]	$PP_{Pot}=PP_{LME}/PP_{Avg\_66LME}$	PP_{LME} normalised by PP_{Avg_66LME}
	CZ POL	0.670	[-]	Cushing (1975); Laws et al. (2000)	
	CZ SPO	0.485	[-]	Average (f_{PPsink_Polar}, $f_{PPsink\_Temperate}$)	
f_{PPsink}	CZ TEP	0.300	[-]	Cushing (1975); Laws et al. (2000)	Sinking fraction of mismatched PP biomass
	CZ STR	0.225	[-]	Average ($f_{PPsink\_Temperate}$, $f_{PPsink\_Tropical}$)	
	CZ TRO	0.150	[-]	Cushing (1975); Laws et al. (2000)	
	CZ POL	0.330	[-]	$f_{PPgrz\_Polar}=1-f_{PPsink\_Polar}$	
	CZ SPO	0.515	[-]	$f_{PPgrz\_Subpolar}=1-f_{PPsink\_Subpolar}$	
f_{PPgrz}	CZ TEP	0.700	[-]	$f_{PPgrz\_Temperate}=1-f_{PPsink\_Temperate}$	Fraction of PP biomass grazed by zooplankton in the photic zone
	CZ STR	0.775	[-]	$f_{PPgrz\_Subtropical}=1-f_{PPsink\_Subtropical}$	
	CZ TRO	0.850	[-]	$f_{PPgrz\_Tropical}=1-f_{PPsink\_Tropical}$	
$f_{SPingest}$	GLO	0.643	[-]	Møller and Nielsen (2001); Møller (2007); Saba et al. (2011)	Averaged fraction of grazed biomass ingested and not lost by sloppy feeding
	CZ POL	0.300	[-]	Besiktepe and Dam (2002)	Assimilation efficiency: diet mainly diatoms
	CZ SPO	0.500	[-]	Average ($f_{SPassimil\_Polar}$, $f_{SPassimil\_Temperate}$)	Assimilation efficiency: average ↕
$f_{SPassimil}$	CZ TEP	0.700	[-]	Besiktepe and Dam (2002)	Assimilation efficiency: diet mainly flagellates
	CZ STR	0.800	[-]	Average ($f_{SPassimil\_Temperate}$, $f_{SPassimil\_Tropical}$)	Assimilation efficiency: average ↕
	CZ TRO	0.900	[-]	Besiktepe and Dam (2002)	Assimilation efficiency: diet mainly cilliates
	CZ POL	0.700	[-]	$f_{SPegest\_Polar}=1-f_{SPassimil\_Polar}$	
	CZ SPO	0.500	[-]	$f_{SPegest\_Subpolar}=1-f_{SPassimil\_Subpolar}$	
$f_{SPegest}$	CZ TEP	0.300	[-]	$f_{SPegest\_Temperate}=1-f_{SPassimil\_Temperate}$	Fraction of organic carbon egested by SP
	CZ STR	0.200	[-]	$f_{SPegest\_Subtropical}=1-f_{SPassimil\_Subtropical}$	
	CZ TRO	0.100	[-]	$f_{SPegest\_Tropical}=1-f_{SPassimil\_Tropical}$	
	CZ POL	0.033	[-]	$f_{AVTgrz\_Polar}=0.10*f_{PPgrz\_Polar}$	
	CZ SPO	0.052	[-]	$f_{AVTgrz\_Subpolar}=0.10*f_{PPgrz\_Subpolar}$	Fraction of organic carbon transported by AVT
f_{AVTgrz}	CZ TEP	0.070	[-]	$f_{AVTgrz\_Temperate}=0.10*f_{PPgrz\_Temperate}$	Assumed 10% of the euphotic zone grazing pressure is made by emergent zooplankton
	CZ STR	0.078	[-]	$f_{AVTgrz\_Subtropical}=0.10*f_{PPgrz\_Subtropical}$	
	CZ TRO	0.085	[-]	$f_{AVTgrz\_Tropical}=0.10*f_{PPgrz\_Tropical}$	
	CZ POL	0.101	[-]	$f_{PPsinkGZ\_Polar}=0.15*f_{PPsink\_Polar}$	
	CZ SPO	0.073	[-]	$f_{PPsinkGZ\_Subpolar}=0.15*f_{PPsink\_Subpolar}$	
$f_{PPsinkGZ}$	CZ TEP	0.045	[-]	$f_{PPsinkGZ\_Temperate}=0.15*f_{PPsink\_Temperate}$	Fraction of the PP biomass that is consumed during sink
	CZ STR	0.034	[-]	$f_{PPsinkGZ\_Subtropical}=0.15*f_{PPsink\_Subtropical}$	
	CZ TRO	0.023	[-]	$f_{PPsinkGZ\_Tropical}=0.15*f_{PPsink\_Tropical}$	
	CZ POL	0.900	[-]	$f_{PPsinkNG\_Polar}=1-f_{PPsinkGZ\_Polar}$	
	CZ SPO	0.927	[-]	$f_{PPsinkNG\_Subpolar}=1-f_{PPsinkGZ\_Subpolar}$	
$f_{PPsinkNG}$	CZ TEP	0.955	[-]	$f_{PPsinkNG\_Temperate}=1-f_{PPsinkGZ\_Temperate}$	Fraction of the sinking PP biomass that is not grazed
	CZ STR	0.966	[-]	$f_{PPsinkNG\_Subtropical}=1-f_{PPsinkGZ\_Subtropical}$	
	CZ TRO	0.978	[-]	$f_{PPsinkNG\_Tropical}=1-f_{PPsinkGZ\_Tropical}$	
$f_{FPleach}$	GLO	0.280	[-]	Møller et al. (2003)	Fraction of organic carbon leached from SP f.p.
	CZ POL	0.007	[-]	$f_{FPsinkGZ\_Polar}=0.20*f_{PPsinkGZ\_Polar}$	
	CZ SPO	0.010	[-]	$f_{FPsinkGZ\_Subpolar}=0.20*f_{PPsinkGZ\_Subpolar}$	
$f_{FPsinkGZ}$	CZ TEP	0.014	[-]	$f_{FPsinkGZ\_Temperate}=0.20*f_{PPsinkGZ\_Temperate}$	Grazing pressure on faecal pellets is 20% of that of sinking cell aggregates (Koski unpublished)
	CZ STR	0.016	[-]	$f_{FPsinkGZ\_Subtropical}=0.20*f_{PPsinkGZ\_Subtropical}$	
	CZ TRO	0.017	[-]	$f_{FPsinkGZ\_Tropical}=0.20*f_{PPsinkGZ\_Tropical}$	
$f_{FPsinkNG}$	CZ POL	0.715	[-]	$f_{FPsinkNG\_Polar}=(1-f_{FPleach})*(1-f_{FPsinkGZ\_Polar})$	Fraction of organic carbon sinking as faecal

Input parameter	Spatial resolution	Value	Unit	Source (reference or calculation)	Description
	CZ SPO	0.713	[-]	$f_{FPsinkNG\_Subpolar}=(1-f_{FPleach})*(1-f_{FPsinkGZ\_Subpolar})$	pellets
	CZ TEP	0.710	[-]	$f_{FPsinkNG\_Temperate}=(1-f_{FPleach})*(1-f_{FPsinkGZ\_Temperate})$	
	CZ STR	0.709	[-]	$f_{FPsinkNG\_Subtropical}=(1-f_{FPleach})*(1-f_{FPsinkGZ\_Subtropical})$	
	CZ TRO	0.708	[-]	$f_{FPsinkNG\_Tropical}=(1-f_{FPleach})*(1-f_{FPsinkGZ\_Tropical})$	
f_{SPmort}	GLO	0.290	[-]	Hirst and Kiørboe (2002)	Fraction of predation mortality defining SP carcasses
Z_{mean}	GLO	100	[m]	Mean depth of continental shelf	Continental shelf depth assumed as 200 m
Z_{AVT}	GLO	20	[m]	Atkinson et al. (1992); Puelles et al. (1996)	Vertical distance covered by diel migrant copepods
Z_{photic}	LME	12 ↔ 68	[m]	Longhurst (1998)	LME photic depth adapted from Longhurst provinces
$Z_{aphotic}$	LME	32 ↔ 88	[m]	$Z_{aphotic\_LME}=Z_{mean}-Z_{photic\_LME}$	Height of aphotic zone
U_{PP}	GLO	150	[$m \cdot d^{-1}$]	Turner (2002)	Sinking velocity of phytodetritus + PP marine snow
U_{SP}	GLO	200	[$m \cdot d^{-1}$]	Turner (2002)	Sinking velocity of marine snow + SP f.p.
$f_{BRmarsnow}$	GLO	0.130	[d^{-1}]	Iversen and Ploug (2010)	Bacterial respiration rate on sinking marine snow
$f_{BRsinkSPaphotic}$	LME	0.021 ↔ 0.051	[-]	$f_{BRsinkSPaphotic\_LME}=f_{BRmarsnow}/U_{SP}*(Z_{mean}-Z_{photic\_LME})$	BR rate on sinking f.p. egested in the aphotic zone
$f_{BRsinkPP}$	GLO	0.087	[-]	$f_{BRsinkPP}=f_{BRmarsnow}/U_{PP}*Z_{meanLME}$	Respiration of sinking organic carbon from PP
$f_{BRsinkSP}$	GLO	0.065	[-]	$f_{BRsinkSP}=f_{BRmarsnow}/U_{SP}*Z_{meanLME}$	Respiration of sinking organic carbon from SP
BGE	LME	0.039 ↔ 0.464	[-]	Cole et al. (1988); del Giorgio and Cole (1998)	Bacterial Growth Efficiency
f_{BRbott}	LME	0.536 ↔ 0.961	[-]	$f_{BRbott\_LME}=1-BGE_{LME}$	Fraction of organic carbon respired at the bottom

Legend (GLO) Global, (CZ) Climate Zone, (POL (Polar), (SPO) Subpolar, (TEP) Temperate, (STR) Subtropical, (TRO) Tropical, (PP) Primary Producers, (SP) Secondary Producers, (M) Molar Mass, (C) Carbon, (O) Oxygen, (N) Nitrogen, (LME) Large Marine Ecosystem, (AVT) Active Vertical Transport, (f.p.) faecal pellets, (BR) Bacterial Respiration.

S.2.3. Estimation of zooplankton ingestion fractions

The parameter $f_{SPingest}$ was estimated as to be 64.25% (Table S.2) of the phytoplankton grazed biomass. This value is the mean ingestion fraction of different diets and estimation methods compiled for the coastal planktonic copepod by Møller and Nielsen (2001), Møller (2007), and Saba et al. (2011, 2009).

Table S.2 Estimation of mean ingestion rate (dimensionless) from different data sources.

Specific experimental conditions	Ingestion rate [-]	Average ingestion rate [-]		Source
Acartia tonsa feeding on *Heterocapsa rotundata*	0.85	0.77		Møller (2007)
Acartia tonsa feeding on *Ditylum brightwelli*	0.69			Møller (2007)
Acartia tonsa feeding on *Ditylum brightwelli* (RFS method)	0.46	0.40	**0.64**	Møller and Nielsen (2001)
Acartia tonsa feeding on *Ditylum brightwelli* (egg production method)	0.31			Møller and Nielsen (2001)
Acartia tonsa feeding on *Ceratium lineatum* (RFS method)	0.41			Møller and Nielsen (2001)
Acartia tonsa feeding on *Ceratium lineatum* (egg production method)	0.41			Møller and Nielsen (2001)
Acartia tonsa feeding on *Thalassiosira weissflogii*	0.97	0.76		Saba et al. (2011)
Acartia tonsa feeding on *Thalassiosira weissflogii* (ESD-ratios method)	0.69			Saba et al. (2009)
Acartia tonsa feeding on *Oxyrrhis marina* (ESD-ratios method)	0.66			Saba et al. (2009)
Acartia tonsa feeding on *Gyrodinium dominans* (ESD-ratios method)	0.72			Saba et al. (2009)

Legend (RFS) Removed From Suspension, (ESD) Equivalent Spherical Diameter.

S.3 Extended and additional results

S.3.1 Contributions from sinking routes

Table S.3 shows the relative contributions of each sinking route to the export production (P_E) and XF grouped into climate zones and Table S.4 the full results per LME.

The relative contributions (in percentage) of organic carbon to the total P_E and to XF are consistently higher in route 1 and increase towards higher latitudes, as do the PP-SP mismatch and biomass sinking (f_{PPsink_CZ}). Route 2 increases its contribution to P_E and XF towards mid-low-latitudes due to the combination of f_{PPgrz_CZ} (increasing towards low latitudes) and $f_{SPegest\_CZ}$ (increasing towards high latitudes). Contributions from route 3 decrease towards high latitudes as less PP biomass is grazed (f_{PPgrz_CZ}). The contribution to P_E by route 4 is also correlated to the mismatch fraction but not the contribution to XF as a result of the mixed grazing on all types of sinking organic material (aggregates, faecal pellets, and carcasses) after export. Other minor discrepancies originate from site-dependent grazing pressures on sinking POC, as the XF modelling extends to include the loss processes below the photic depth that act on P_E (consumption, leaching, and respiration).

Table S.3 Extended contributions (in %) of the four carbon export routes to total export production (P_E) and exposure factor (XF), per climate zone. The linear correlation coefficient (r) and significance level (p) between the relative contribution of each route per climate zone and the PP-SP mismatch fraction (f_{PPsink_CZ}) are also included. Route 1: sinking from primary production (PP) biomass; Route 2: sinking as faecal pellets (f.p.) from secondary producers (SP); Route 3: sinking carcasses (carc.) of SP; Route 4: active vertical transport (AVT) via diel vertical migration of SP.

Climate zone	Source of contribution to P_E and to XF (mean %)				PP-SP mismatch
[name (*nr. of LMEs*)]	Route 1 (PP)	Route 2 (SP f.p.)	Route 3 (SP carc.)	Route 4 (AVT)	f_{PPsink_CZ}
Polar *(12)*	81.3 81.9	15.1 11.9	1.0 3.9	2.6 5.2	0.67
Subpolar *(11)*	71.7 69.0	19.6 16.4	3.8 5.3	4.9 10.4	0.49
Temperate *(14)*	56.4 55.8	30.1 26.7	5.0 6.1	8.5 11.5	0.30
Subtropical *(12)*	51.9 56.0	32.3 29.9	4.3 4.6	11.5 8.8	0.23
Tropical *(17)*	48.2 56.7	28.3 28.0	5.9 1.9	17.6 7.5	0.15
Global (66)	*60.6 63.0*	*25.6 23.2*	*4.2 5.2*	*9.7 8.6*	*(wt) 0.35*
Correlation (r) with f_{PPsink_CZ}	1.00 0.96	-0.92 -0.97	-0.93 0.26	-0.93 -0.39	
Significance (p); n = 5	0.0006 0.0002	0.002 0.004	0.02 0.005	0.03 0.002	

Table S.4 Extended results table of the estimation of export production (P_E) and exposure factor (XF), including specific datasets used for the model parameterisation: primary production (PP) dataset from http://www.seaaroundus.org, photic depth data from Longhurst (1998), and Primary Production Required (PPR) to sustain reported fisheries per LME (used to estimate the fraction of biomass of secondary producers consumed by planktivorous fish, f_{plfish_LME}) from Pauly and Christensen (1995) and UBC (1999). Contributions to P_E and XF per LME are also included.

Large Marine Ecosystem	Climate zone	PP	PP_{Pot_LME}	Z_{photic_LME}	f of $Z_{aphotic}$	$BR_{sink aphotic}$	PPR_{LME} (2006)	P_E	Contribution to P_E				XF_{LME}	Contribution to XF_{LME}			
[#. name]	[name]	[$gC \cdot m^{-2} \cdot yr^{-1}$]	[-]	[m]	[-]	[-]	[-]	[$gC \cdot m^{-2} \cdot yr^{-1}$]	R1 [%]	R2 [%]	R3 [%]	R4 [%]	[$kgO_2 \cdot kgN^{-1}$]	R1 [%]	R2 [%]	R3 [%]	R4 [%]
18. Canadian Eastern Arctic - West Greenland	Polar	151.9	0.59	16.3	0.239	0.054	0.093	**125.4**	81.2	15.5	0.7	2.6	**6.80**	80.7	12.3	0.7	6.3
19. Greenland Sea	Polar	174.2	0.68	16.3	0.239	0.054	1.000	**130.9**	89.2	0.0	8.0	2.8	**7.25**	84.3	0.0	8.5	7.3
20. Barents Sea	Polar	151.2	0.59	33.8	0.302	0.043	0.384	**120.0**	84.4	10.0	2.9	2.7	**7.05**	82.5	7.8	3.1	6.6
54. Northern Bering - Chukchi Seas	Polar	90.9	0.35	34.8	0.307	0.042	0.001	**76.1**	80.1	17.3	0.0	2.5	**4.57**	81.8	13.6	0.0	4.5
55. Beaufort Sea	Polar	119.1	0.46	34.8	0.307	0.042	0.000	**99.6**	80.1	17.4	0.0	2.5	**5.87**	80.9	13.7	0.0	5.4
56. East Siberian Sea	Polar	54.4	0.21	34.8	0.307	0.042	0.002	**45.5**	80.1	17.3	0.0	2.5	**2.81**	83.1	13.6	0.0	3.3
57. Laptev Sea	Polar	156.7	0.61	34.8	0.307	0.042	0.001	**131.0**	80.1	17.3	0.0	2.5	**7.54**	79.7	13.7	0.0	6.6
58. Kara Sea	Polar	126.7	0.49	34.8	0.307	0.042	0.000	**106.0**	80.1	17.4	0.0	2.5	**6.22**	80.7	13.7	0.0	5.6
61. Antarctic	Polar	99.7	0.39	26.5	0.272	0.048	0.000	**83.4**	80.1	17.4	0.0	2.5	**4.91**	81.6	13.7	0.0	4.7
63. Hudson Bay Complex	Polar	152.7	0.59	18.0	0.244	0.053	0.001	**127.7**	80.1	17.3	0.0	2.5	**6.96**	80.0	13.8	0.0	6.2
64. Central Arctic Ocean	Polar	8.4	0.03	34.8	0.307	0.042	0.001	**7.0**	80.1	17.4	0.0	2.5	**0.45**	84.5	13.6	0.0	1.9
66. Canadian High Arctic - North Greenland	Polar	58.8	0.23	34.8	0.307	0.042	0.029	**49.0**	80.4	16.8	0.2	2.5	**2.99**	83.1	13.2	0.2	3.5
01. East Bering Sea	Subpolar	285.6	1.11	28.1	0.278	0.047	0.153	**196.4**	70.5	22.6	2.1	4.8	**9.86**	68.7	18.8	2.4	10.1
02. Gulf of Alaska	Subpolar	330.9	1.28	28.8	0.281	0.046	0.142	**228.1**	70.4	22.9	1.9	4.8	**11.15**	67.2	19.2	2.2	11.4
09. Newfoundland-Labrador Shelf	Subpolar	295.5	1.15	29.1	0.282	0.046	0.072	**206.6**	69.4	24.9	1.0	4.7	**10.28**	67.7	20.9	1.1	10.3
21. Norwegian Sea	Subpolar	179.3	0.70	28.3	0.279	0.047	0.682	**113.0**	76.9	7.8	10.0	5.2	**6.35**	75.3	6.1	11.0	7.6
23. Baltic Sea	Subpolar	697.6	2.71	12.0	0.227	0.057	0.102	**484.8**	69.8	24.1	1.4	4.8	**15.94**	55.1	21.7	1.7	21.5
51. Oyashio Current	Subpolar	261.5	1.01	31.9	0.294	0.044	0.192	**178.5**	71.1	21.5	2.6	4.8	**9.25**	69.7	17.7	3.0	9.6
52. Sea of Okhotsk	Subpolar	297.7	1.16	28.1	0.278	0.047	0.309	**198.7**	72.7	18.1	4.3	5.0	**10.01**	69.6	14.9	4.9	10.6
53. West Bering Sea	Subpolar	214.0	0.83	28.1	0.278	0.047	0.103	**148.7**	69.8	24.1	1.4	4.8	**7.80**	70.4	19.9	1.6	8.2
59. Iceland Shelf and Sea	Subpolar	201.3	0.78	25.0	0.267	0.049	0.074	**140.7**	69.4	24.9	1.0	4.7	**7.34**	70.5	20.6	1.1	7.7
60. Faroe Plateau	Subpolar	154.1	0.60	33.8	0.302	0.043	1.000	**94.2**	79.4	0.0	15.2	5.4	**5.58**	76.7	0.0	16.2	7.1
65. Aleutian Islands	Subpolar	285.6	1.11	28.1	0.278	0.047	0.076	**199.5**	69.4	24.8	1.0	4.7	**9.96**	68.0	20.8	1.2	10.0
03. California Current	Temperate	223.9	0.87	34.3	0.305	0.043	0.141	**120.8**	55.6	32.8	3.3	8.3	**6.09**	58.8	28.6	3.9	8.7
07. Northeast U.S. Continental Shelf	Temperate	561.0	2.18	29.1	0.282	0.046	0.136	**303.0**	55.5	33.0	3.1	8.3	**12.22**	49.9	30.3	4.0	15.7
08. Scotian Shelf	Temperate	509.5	1.98	29.1	0.282	0.046	0.060	**280.6**	54.5	36.0	1.4	8.2	**11.57**	50.8	33.1	1.7	14.4
13. Humboldt Current	Temperate	320.0	1.24	43.6	0.355	0.037	0.180	**170.9**	56.2	31.2	4.2	8.4	**8.38**	56.5	27.4	5.1	11.0
14. Patagonian Shelf	Temperate	509.5	1.98	31.4	0.292	0.045	0.182	**272.1**	56.2	31.2	4.2	8.4	**11.50**	51.7	28.3	5.3	14.7
22. North Sea	Temperate	407.3	1.58	22.8	0.259	0.050	0.340	**209.8**	58.2	24.8	8.2	8.7	**9.11**	55.7	21.8	10.1	12.4
24. Celtic-Biscay Shelf	Temperate	349.2	1.35	22.8	0.259	0.050	0.314	**180.9**	57.9	25.9	7.5	8.7	**8.15**	57.1	22.6	9.2	11.2
25. Iberian Coastal	Temperate	276.9	1.07	45.0	0.364	0.036	0.248	**145.6**	57.1	28.5	5.9	8.6	**7.38**	58.0	24.7	7.1	10.2
42. Southeast Australian Shelf	Temperate	187.0	0.73	44.1	0.358	0.036	0.012	**104.3**	53.8	37.9	0.3	8.1	**5.41**	58.3	33.3	0.3	8.1
43. Southwest Australian Shelf	Temperate	180.8	0.70	47.2	0.379	0.034	0.011	**100.9**	53.8	38.0	0.2	8.1	**5.28**	58.4	33.3	0.3	8.0
46. New Zealand Shelf	Temperate	208.2	0.81	36.3	0.314	0.041	0.211	**110.4**	56.6	30.0	5.0	8.5	**5.69**	59.7	25.9	5.9	8.5
48. Yellow Sea	Temperate	589.1	2.29	29.8	0.285	0.046	0.714	**284.4**	62.2	10.1	18.4	9.3	**12.02**	51.8	8.8	22.3	17.1
50. Sea of Japan/East Sea	Temperate	220.6	0.86	36.3	0.314	0.041	0.293	**114.8**	57.6	26.7	7.0	8.6	**5.92**	60.0	22.9	8.3	8.8
62. Black Sea	Temperate	376.6	1.46	21.3	0.254	0.051	0.067	**207.1**	54.6	35.7	1.5	8.2	**8.83**	54.5	32.2	1.9	11.4
04. Gulf of California	Subtropical	437.9	1.70	34.3	0.305	0.043	0.032	**191.8**	51.4	36.3	1.0	11.4	**7.97**	52.6	34.9	1.3	11.2
05. Gulf of Mexico	Subtropical	208.2	0.81	44.8	0.362	0.036	0.048	**90.9**	51.5	35.6	1.5	11.4	**4.49**	57.6	32.6	1.9	7.9
06. Southeast U.S. Continental Shelf	Subtropical	263.3	1.02	29.1	0.282	0.046	0.020	**115.6**	51.3	36.8	0.6	11.3	**5.26**	56.7	34.3	0.8	8.2
15. South Brazil Shelf	Subtropical	283.1	1.10	44.9	0.363	0.036	0.036	**123.9**	51.4	36.1	1.1	11.4	**5.84**	56.0	33.5	1.5	9.1
26. Mediterranean	Subtropical	157.8	0.61	37.2	0.318	0.041	0.157	**67.8**	52.4	31.0	5.0	11.6	**3.45**	59.0	27.8	6.3	6.9
27. Canary Current	Subtropical	436.8	1.70	28.7	0.281	0.046	0.116	**188.8**	52.1	32.8	3.7	11.5	**7.73**	52.9	31.2	4.9	11.0
29. Benguela Current	Subtropical	506.6	1.97	41.9	0.344	0.038	0.088	**219.9**	51.8	33.9	2.8	11.5	**9.09**	50.8	32.7	3.7	12.8
30. Agulhas Current	Subtropical	221.0	0.86	49.1	0.393	0.033	0.049	**96.5**	51.5	35.5	1.5	11.4	**4.76**	57.3	32.6	2.0	8.2
41. East-Central Australian Shelf	Subtropical	157.4	0.61	44.8	0.362	0.036	0.009	**69.2**	51.2	37.2	0.3	11.3	**3.51**	58.6	34.0	0.4	7.1
44. West-Central Australian Shelf	Subtropical	173.9	0.67	47.2	0.379	0.034	0.010	**76.4**	51.2	37.2	0.3	11.3	**3.85**	58.2	34.0	0.4	7.4
47. East China Sea	Subtropical	325.4	1.26	29.8	0.285	0.046	0.844	**133.5**	54.9	4.8	28.2	12.1	**6.45**	53.5	4.1	33.5	9.0
49. Kuroshio Current	Subtropical	154.1	0.60	36.3	0.314	0.041	0.169	**66.1**	52.5	30.5	5.4	11.6	**3.37**	59.1	27.3	6.7	6.8
10. Insular Pacific-Hawaiian	Tropical	84.7	0.33	68.0	0.625	0.021	0.006	**26.1**	48.7	33.3	0.3	17.7	**1.33**	60.6	31.7	0.4	7.3
11. Pacific Central-American	Tropical	244.0	0.95	39.6	0.331	0.039	0.049	**75.3**	48.6	31.3	2.4	17.7	**3.33**	58.0	31.2	3.3	7.4
12. Caribbean Sea	Tropical	174.6	0.68	44.8	0.362	0.036	0.026	**53.8**	48.7	32.4	1.3	17.7	**2.51**	59.5	31.8	1.7	6.9
16. East Brazil Shelf	Tropical	130.4	0.51	44.9	0.363	0.036	0.049	**40.3**	48.6	31.4	2.4	17.7	**1.94**	60.0	30.4	3.2	6.4
17. North Brazil Shelf	Tropical	442.3	1.72	38.7	0.326	0.040	0.038	**136.5**	48.6	31.9	1.8	17.7	**5.26**	54.2	33.4	2.7	9.8
28. Guinea Current	Tropical	357.9	1.39	27.0	0.274	0.047	0.051	**110.5**	48.6	31.3	2.5	17.7	**4.31**	56.0	32.2	3.5	8.3
31. Somali Coastal Current	Tropical	249.5	0.97	39.5	0.330	0.039	0.012	**76.9**	48.7	33.0	0.6	17.7	**3.36**	58.5	33.2	0.8	7.5
32. Arabian Sea	Tropical	390.5	1.52	39.3	0.329	0.039	0.173	**121.7**	48.1	26.0	8.3	17.5	**4.99**	53.3	26.2	11.6	8.8
33. Red Sea	Tropical	298.4	1.16	33.7	0.302	0.043	0.082	**92.3**	48.5	29.9	4.0	17.6	**3.89**	56.6	30.1	5.6	7.8
34. Bay of Bengal	Tropical	265.2	1.03	40.0	0.334	0.039	0.199	**82.8**	48.0	25.0	9.5	17.5	**3.71**	55.4	24.3	12.9	7.4
35. Gulf of Thailand	Tropical	284.9	1.11	38.6	0.326	0.040	0.412	**91.1**	46.9	16.7	19.3	17.1	**4.17**	51.8	15.8	25.3	7.2
36. South China Sea	Tropical	174.2	0.68	34.2	0.304	0.043	0.389	**55.6**	47.0	17.5	18.3	17.1	**2.70**	54.2	16.3	23.5	6.0
37. Sulu-Celebes Sea	Tropical	209.3	0.81	38.6	0.326	0.040	0.368	**66.6**	47.2	18.3	17.3	17.2	**3.18**	53.9	17.1	22.5	6.5
38. Indonesian Sea	Tropical	263.7	1.02	38.6	0.326	0.040	0.206	**82.4**	48.0	24.7	9.8	17.5	**3.69**	55.3	24.0	13.3	7.3
39. North Australian Shelf	Tropical	328.7	1.28	44.8	0.362	0.036	0.018	**101.3**	48.7	32.7	0.9	17.7	**4.26**	56.7	33.4	1.2	8.7
40. Northeast Australian Shelf	Tropical	130.8	0.51	44.8	0.362	0.036	0.016	**40.3**	48.7	32.8	0.8	17.7	**1.93**	60.5	32.0	1.0	6.4
45. Northwest Australian Shelf	Tropical	185.9	0.72	47.2	0.379	0.034	0.023	**57.3**	48.7	32.5	1.1	17.7	**2.66**	59.3	32.0	1.5	7.1

S.3.2 Estimation of Bacterial Growth Efficiency (BGE)

Table S.5 Calculation of Bacterial Growth Efficiency (BGE) from Bacterial Production (BP) and Primary Production (PP) per large marine ecosystem (LME). Equations used to estimate BP from PP and BGE from BP: [a] $BP_{LME} = -0.249 * PP_{LME}{}^{0.86}$ (Cole et al., 1988); [b] $BGE_{LME} = (0.037 + 0.65 * BP_{LME})/(1.8 + BP_{LME})$ (del Giorgio and Cole, 1998).

Large Marine Ecosystem	Z_{photic_LME}	PP_{LME}		BP_{LME} [a]	BGE_{LME} [b]
[#. name]	[m]	[gC·m^{-2}·yr^{-1}]	[µgC·L·h^{-1}]	[µgC·L·h^{-1}]	[-]
01. East Bering Sea	28.1	285.6	2.32	0.51	0.16
02. Gulf of Alaska	28.8	330.9	2.62	0.57	0.17
03. California Current	34.3	223.9	1.49	0.35	0.12
04. Gulf of California	34.3	437.9	2.91	0.63	0.18
05. Gulf of Mexico	44.8	208.2	1.06	0.26	0.10
06. Southeast U.S. Continental Shelf	29.1	263.3	2.07	0.47	0.15
07. Northeast U.S. Continental Shelf	29.1	561.0	4.40	0.89	0.23
08. Scotian Shelf	29.1	509.5	4.00	0.82	0.22
09. Newfoundland-Labrador Shelf	29.1	295.5	2.32	0.51	0.16
10. Insular Pacific-Hawaiian	68.0	84.7	0.28	0.08	0.05
11. Pacific Central-American	39.6	244.0	1.41	0.33	0.12
12. Caribbean Sea	44.8	174.6	0.89	0.23	0.09
13. Humboldt Current	43.6	320.0	1.68	0.39	0.13
14. Patagonian Shelf	31.4	509.5	3.70	0.77	0.21
15. South Brazil Shelf	44.9	283.1	1.44	0.34	0.12
16. East Brazil Shelf	44.9	130.4	0.66	0.18	0.08
17. North Brazil Shelf	38.7	442.3	2.61	0.57	0.17
18. Canadian Eastern Arctic - West Greenland	16.3	151.9	2.13	0.48	0.15
19. Greenland Sea	16.3	174.2	2.45	0.54	0.17
20. Barents Sea	33.8	151.2	1.02	0.25	0.10
21. Norwegian Sea	28.3	179.3	1.45	0.34	0.12
22. North Sea	22.8	407.3	4.09	0.84	0.22
23. Baltic Sea	12.0	697.6	13.27	2.30	0.37
24. Celtic-Biscay Shelf	22.8	349.2	3.50	0.73	0.20
25. Iberian Coastal	45.0	276.9	1.40	0.33	0.12
26. Mediterranean	37.2	157.8	0.97	0.24	0.10
27. Canary Current	28.7	436.8	3.47	0.73	0.20
28. Guinea Current	27.0	357.9	3.03	0.65	0.19
29. Benguela Current	41.9	506.6	2.76	0.60	0.18
30. Agulhas Current	49.1	221.0	1.03	0.26	0.10
31. Somali Coastal Current	39.5	249.5	1.44	0.34	0.12
32. Arabian Sea	39.3	390.5	2.27	0.50	0.16
33. Red Sea	33.7	298.4	2.02	0.46	0.15
34. Bay of Bengal	40.0	265.2	1.51	0.36	0.12
35. Gulf of Thailand	38.6	284.9	1.69	0.39	0.13
36. South China Sea	34.2	174.2	1.16	0.28	0.11
37. Sulu-Celebes Sea	38.6	209.3	1.24	0.30	0.11
38. Indonesian Sea	38.6	263.7	1.56	0.37	0.13
39. North Australian Shelf	44.8	328.7	1.68	0.39	0.13
40. Northeast Australian Shelf	44.8	130.8	0.67	0.18	0.08
41. East-Central Australian Shelf	44.8	157.4	0.80	0.21	0.09
42. Southeast Australian Shelf	44.1	187.0	0.97	0.24	0.10
43. Southwest Australian Shelf	47.2	180.8	0.88	0.22	0.09
44. West-Central Australian Shelf	47.2	173.9	0.84	0.21	0.09
45. Northwest Australian Shelf	47.2	185.9	0.90	0.23	0.09

Large Marine Ecosystem	Z_{photic_LME}	PP_{LME}		BP_{LME}[a]	BGE_{LME}[b]
[#. name]	[m]	[gC·m^{-2}·yr^{-1}]	[µgC·L·h^{-1}]	[µgC·L·h^{-1}]	[-]
46. New Zealand Shelf	36.3	208.2	1.31	0.31	0.11
47. East China Sea	29.8	325.4	2.50	0.55	0.17
48. Yellow Sea	29.8	589.1	4.52	0.91	0.23
49. Kuroshio Current	36.3	154.1	0.97	0.24	0.10
50. Sea of Japan/East Sea	36.3	220.6	1.39	0.33	0.12
51. Oyashio Current	31.9	261.5	1.87	0.43	0.14
52. Sea of Okhotsk	28.1	297.7	2.42	0.53	0.16
53. West Bering Sea	28.1	214.0	1.74	0.40	0.14
54. Northern Bering - Chukchi Seas	34.8	90.9	0.60	0.16	0.07
55. Beaufort Sea	34.8	119.1	0.78	0.20	0.08
56. East Siberian Sea	34.8	54.4	0.36	0.10	0.05
57. Laptev Sea	34.8	156.7	1.03	0.26	0.10
58. Kara Sea	34.8	126.7	0.83	0.21	0.09
59. Iceland Shelf and Sea	25.0	201.3	1.83	0.42	0.14
60. Faroe Plateau	33.8	154.1	1.04	0.26	0.10
61. Antarctic	26.5	99.7	0.86	0.22	0.09
62. Black Sea	21.3	376.6	4.05	0.83	0.22
63. Hudson Bay Complex	18.0	152.7	1.94	0.44	0.14
64. Central Arctic Ocean	34.8	8.4	0.06	0.02	0.03
65. Aleutian Islands	28.1	285.6	2.32	0.51	0.16
66. Canadian High Arctic - North Greenland	28.1	58.8	0.48	0.13	0.06

S.3.3 Sensitivity analysis table

Table S.6 Results of the sensitivity analysis of the 18 primary input parameters modelled. Sensitivity ratios (SR, [dimensionless]) obtained after independent variation of 10% on the input values.

Input parameter	Mean SR [-]	SR range [-]
PP_{Pot_LME}	0.92	(0.75, 1.00)
$f_{SPassimil\_CZ}$	-0.59	(-1.64, -0.03)
f_{PPsink_CZ}	0.51	(0.43, 0.69)
$f_{SPingest}$	0.31	(0.10, 0.43)
BGE_{LME}	-0.16	(-0.60, -0.03)
$f_{FPleach}$	-0.11	(-0.16, -0.02)
Z_{mean}	-0.08	(-0.09, -0.08)
$f_{BRmarsnow}$	-0.08	(-0.09, -0.08)
$f_{PPsinkGZ\_LME}$	-0.08	(-0.23, 0.00)
U_{PP}	0.05	(0.04, 0.07)
f_{SPmort}	0.04	(0.00, 0.33)
f_{AVTgrz_CZ}	0.03	(0.01, 0.04)
U_{SP}	0.02	(0.01, 0.03)
Z_{AVT}	0.02	(0.00, 0.03)
Z_{photic_LME}	0.01	(0.00, 0.09)
$f_{FPsinkGZ\_CZ}$	-0.01	(-0.03, 0.00)
$DOC_{ExcrAVT}$	0.01	(0.00, 0.02)
f_{plfish_LME}	0.00	(-0.04, 0.12)

S.3.4 Export production (P_E) algorithms

Table S.7 Summary of the regression analysis for PP vs. P_E with a power (P_E=a*PP^b), an exponential (P_E=exp(a+b*PP)), and a linear (P_E=a+b*PP) model. Additional notes: the regression line of the exponential model does not intersect the origin; *n* is the number of spatial units; R^2 is the coefficient of determination; *p* is the significance level.

Model	*n*	*a*	*b*	R^2	*p*
Power	66	1.25	0.83	0.73	0.002
Exponential	66	42.67	0.004	0.61	0.006
Linear	66	4.34	0.49	0.73	0.101

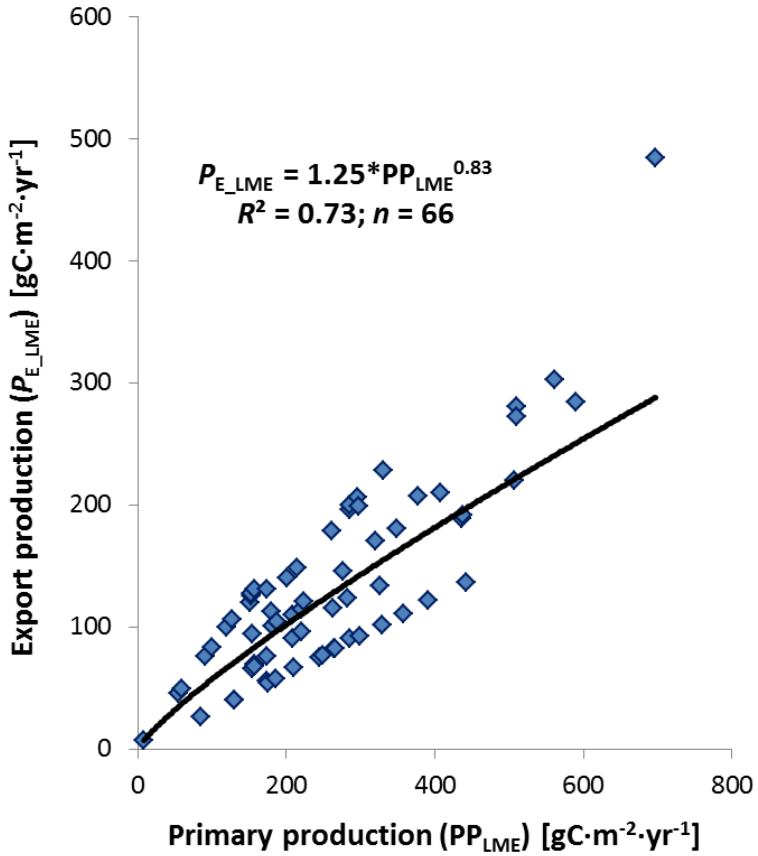

Figure S.3 Export production (P_E, [gC·m^{-2}·yr^{-1}]) as a function of primary production (PP, [gC·m^{-2}·yr^{-1}]). Power regression fitting of data for 66 Large Marine Ecosystems with resulting export algorithm equation (P_{E_LME}=1.25*$PP_{LME}^{0.83}$) and coefficient of determination (R^2=0.73).

We used the same PP dataset to the export algorithms from others in order to validate the export component of the proposed exposure model. Analysing the correlation results (Table S.7) we obtained linear correlation coefficients (*r*) values

close to 0.90, except for Eppley and Peterson's algorithm (derived for the eastern Pacific Ocean).

Table S.8 Results for the correlation of P_E-PP algorithms from this study to others.

Correlation (r)	Algorithm	Source
0.67	$P_{E\_LME} = 0.0025 * {PP_{LME}}^2$ if $PP_{LME} < 200gC \cdot m^{-2} \cdot yr^{-1}$	(Eppley and Peterson, 1979)
	$P_{E\_LME} = 0.5 * PP_{LME}$ if $PP_{LME} > 200gC \cdot m^{-2} \cdot yr^{-1}$	(Eppley and Peterson, 1979)
0.92	$P_{E\_LME} = PP_{LME}/(Z_{aphotic_{LME}} + 0.212)$	(Suess, 1980)
0.91	$P_{E\_LME} = 0.409 * {PP_{LME}}^{1.41}/({Z_{aphotic\_LME}}^{0.628})$	(Betzer et al., 1984)
0.91	$P_{E\_LME} = 3.523 * {Z_{aphotic\_LME}}^{-0.734} * {PP_{LME}}^{1.000}$	(Pace et al., 1987)
0.87	$P_{E\_LME} = 0.049 * {PP_{LME}}^{1.41}$	(Wassmann, 1990)
--	$P_{E\_LME} = 1.15 * {PP_{LME}}^{0.86}$	This study

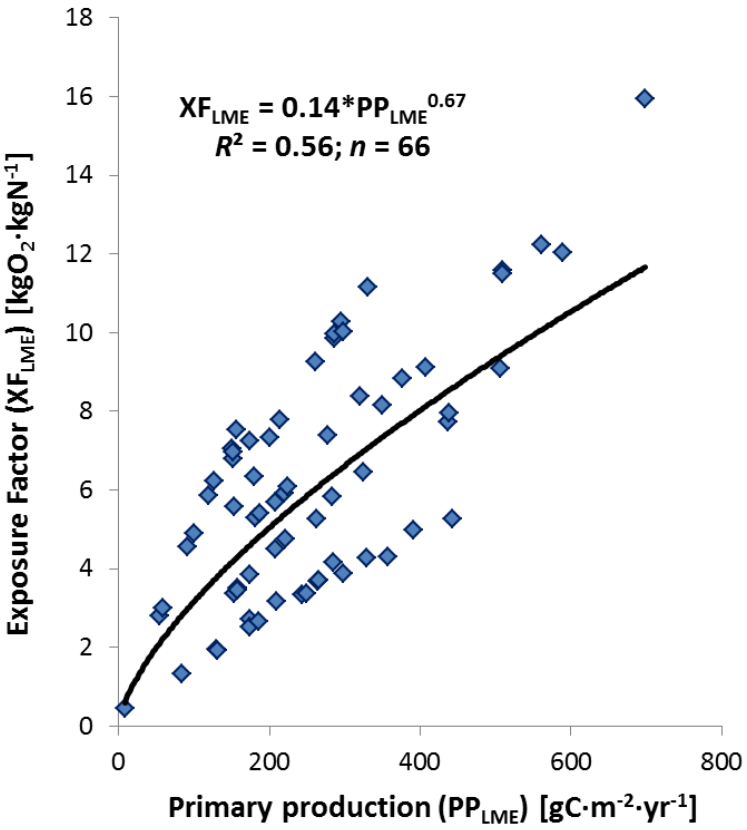

Figure S.4 Exposure factor (XF, [$kgO_2 \cdot kgN^{-1}$]) as a function of primary production (PP, [$gC \cdot m^{-2} \cdot yr^{-1}$]). Power regression fitting of data for 66 Large Marine Ecosystems with resulting export algorithm equation ($XF_{LME} = 0.14 * {PP_{LME}}^{0.67}$) and coefficient of determination (R^2=0.56).

References

Baines, S.B., Pace, M.L., Karl, D.M., 1994. Why does the relationship between sinking flux and planktonic primary production differ between lakes and oceans? Limnol. Oceanogr. 39, 213–226.

Behrenfeld, M.J., 2010. Abandoning Sverdrup's Critical Depth Hypothesis on phytoplankton blooms. Ecology 91, 977–89.

Behrenfeld, M.J., Boss, E.S., 2014. Resurrecting the ecological underpinnings of ocean plankton blooms. Ann. Rev. Mar. Sci. 6, 167–94.

Behrenfeld, M.J., Doney, S.C., Lima, I., Boss, E.S., Siegel, D.A., 2013. Annual cycles of ecological disturbance and recovery underlying the subarctic Atlantic spring plankton bloom. Global Biogeochem. Cycles 27, 526–540.

Betzer, P.R., Showers, W.J., Laws, E.A., Winn, C.D., DiTullio, G.R., Kroopnick, P.M., 1984. Primary productivity and particle fluxes on a transect of the equator at 153°W in the Pacific Ocean. Deep Sea Res Part A. Oceanogr. Res.Pap.31, 1–11.

Beusen, A.H.W., Bouwman, A.F., Heuberger, P.S.C., Van Drecht, G., Van der Hoek, K.W., 2008. Bottom-up uncertainty estimates of global ammonia emissions from global agricultural production systems. Atmos. Environ. 42, 6067–6077.

Boss, E., Behrenfeld, M.J., 2010. In situ evaluation of the initiation of the North Atlantic phytoplankton bloom. Geophys. Res. Lett. 37, 1-5.

Bouwman, A.F., 2005. Exploring changes in river nitrogen export to the world's oceans. Global Biogeochem. Cycles 19.

Bouwman, A.F., Beusen, A.H.W., Billen, G., 2009. Human alteration of the global nitrogen and phosphorus soil balances for the period 1970–2050. Global Biogeochem. Cycles 23.

Bouwman, A.F., Boumans, L.J.M., Batjes, N.H., 2002. Estimation of global NH3 volatilization loss from synthetic fertilizers and animal manure applied to arable lands and grasslands. Global Biogeochem. Cycles 16.

Butterbach-Bahl, K., Dannenmann, M., 2011. Denitrification and associated soil N2O emissions due to agricultural activities in a changing climate. Curr. Opin. Environ. Sustain. 3, 389–395.

Carpenter, S.R., Caraco, N.F., Correll, D.L., Howarth, R.W., Sharpley, A.N., Smith, V.H., 1998. Nonpoint pollution of surface waters with phosphorus and nitrogen. Ecol. Appl. 8, 559–568.

Chiswell, S.M., 2011. Annual cycles and spring blooms in phytoplankton: don't abandon Sverdrup completely. Mar. Ecol. Prog. Ser. 443, 39–50.

Cloern, J.E., 2001. Our evolving conceptual model of the coastal eutrophication problem. Mar. Ecol. Prog. Ser. 210, 223–253.

Cole, J.J., Findlay, S., Pace, M.L., 1988. Bacterial production in fresh and saltwater ecosystems: a cross-system overview. Mar. Ecol. Prog. Ser. 43, 1–10.

Cushing, D.H., 1975. Marine Ecology and Fisheries. Cambridge University Press, Cambridge.

De Jonge, V.N., Elliott, M., Orive, E., 2002. Causes, historical development, effects and future challenges of a common environmental problem: eutrophication. Hydrobiologia 475/476, 1–19.

Del Giorgio, P.A., Cole, J.J., 1998. Bacterial Growth Efficiency in Natural Aquatic Systems. Annu. Rev. Ecol. Syst. 29, 503–541.

Duarte, B., Saraiva, P.M., Pantelides, C.C., 2004. Combined Mechanistic and Empirical Modelling. Int. J. Chem. React. Eng. 2, A3.

Duarte, C.M., Amthor, J.S., DeAngelis, D.L., Joyce, L.A., Maranger, R.J., Pace, M.L., Pastor, J.J., Running, S.W., 2003. The Limits to Models in Ecology, in: Canham, C., Cole, J., WK, L. (Eds.), Models in Ecosystem Science. Princeton University Press, Princeton, New Jersey, pp. 437–451.

Eppley, R.W., Peterson, B.J., 1979. Particulate organic matter flux and planktonic new production in the deep ocean. Nature.

Evans, G.T., Parslow, J.S., 1985. A model of annual plankton cycles. Biol. Oceanogr. 3, 327–347.

Field, C.B., 1998. Primary Production of the Biosphere: Integrating Terrestrial and Oceanic Components. Science (80-.). 281, 237–240.

Finnveden, G., Potting, J., 1999. Eutrophication as an impact category - State of the Art and Research Needs. Int. J. Life Cycle Assess. 4, 311–314.

Galloway, J.N., Dentener, F.J., Capone, D.G., Boyer, E.W., Howarth, R.W., Seitzinger, S.P., Asner, G.P., Cleveland, C.C., Green, P.A., Holland, E.A., Karl, D.M., Michaels, A.F., Porter, J.H., Townsend, A.R., Vörösmarty, C.J., 2004. Nitrogen cycles: past, present, and future. Biogeochemistry 70, 153–226.

Galloway, J.N., Townsend, A.R., Erisman, J.W., Bekunda, M., Cai, Z., Freney, J.R., Martinelli, L.A., Seitzinger, S.P., Sutton, M.A., 2008. Transformation of the Nitrogen Cycle: Recent Trends, Questions, and Potential Solutions. Science (80-.). 320, 889–892.

Geider, R.J., Delucia, E.H., Falkowski, P.G., Finzi, A.C., Grime, J.P., Grace, J., Kana, T.M., Roche, J.L.A., Long, S.P., Osborne, B.A., Platt, T., Prentice, I.C., Raven, J.A., Schlesinger, W.H., Smetacek, V., Stuart, V., Sathyendranath, S., Thomas, R.B., Vogelman, T.C., Williams, P., Woodward, F.I., 2001. Primary productivity of planet earth: biological determinants and physical constraints in terrestrial and aquatic habitats. Glob. Chang. Biol. 7, 849–882.

Gran, H.H., Braarud, T., 1935. A quantitative study of the phytoplankton in the Bay of Fundy and Gulf of Maine. J. Biol. Board Canada 1, 279–467.

Green, P.A., Vörösmarty, C.J., Meybeck, M., Galloway, J.N., Peterson, B.J., Boyer, E.W., 2004. Pre-industrial and contemporary fluxes of nitrogen through rivers: a global assessment based on typology. Biogeochemistry 68, 71–105.

Herbert, R.A., 1999. Nitrogen cycling in coastal marine ecosystems. FEMS Microbiol. Rev. 23, 563–590.

Huisman, J., Arrayás, M., Ebert, U., Sommeijer, B., 2002. How do sinking phytoplankton species manage to persist? Am. Nat. 159, 245–54.

Huisman, J., van Oostveen, P., Weissing, F.J., 1999. Critical depth and critical turbulence: Two different mechanisms for the development of phytoplankton blooms. Limnol. Oceanogr. 44, 1781–1787.

Kitsiou, D., Karydis, M., 2011. Coastal marine eutrophication assessment: a review on data analysis. Environ. Int. 37, 778–801.

Kroeze, C., Bouwman, A.F., Seitzinger, S.P., 2012. Modeling global nutrient export from watersheds. Curr. Opin. Environ. Sustain. 4, 195–202.

Lee, D.S., Köhler, I., Grobler, E., Rohrer, F., Sausen, R., Gallardo-Klenner, L., Olivier, J.G.J., Dentener, F.J., Bouwman, A.F., 1997. Estimations of global NOx emissions and their uncertainties. Atmos. Environ. 31, 1735–1749.

Lemke, P., Ren, J., Alley, R.B., Allison, I., Carrasco, J., Flato, G., Fujii, Y., Kaser, G., Mote, P., Thomas, R.H., Zhang, T., 2007. Observations: Changes in Snow, Ice and Frozen Ground, in: Solomon, S., D. Qin, M. Manning, Z. Chen, M.M., K.B. Averyt, M.T. and H.L.M. (eds. . (Eds.), Climate Change 2007: The Physical Science Basis. Contribution of Working Group I to the Fourth Assessment Report of the Intergovernmental Panel on Climate Change. Cambridge University Press, Cambridge, UK and New York, USA, pp. 337–383.

Longhurst, A.R., 1998. Ecological Geography of the Sea. Academic Press Limited, London, UK.

Mills, E.L., 1975. Benthic Organisms and the Structure of Marine Ecosystems. J. Fish. Res. Board Canada 32, 1657–1663.

Møller, E.F., 2007. Production of dissolved organic carbon by sloppy feeding in the copepods Acartia tonsa, Centropages typicus, and Temora longicornis. Limnol. Oceanogr. 52, 79–84.

Møller, E.F., Nielsen, T.G., 2001. Production of bacterial substrate by marine copepods: Effect of phytoplankton biomass and cell size. J. Plankton Res. 23, 527–536.

Mulligan, M., Wainwright, J., 2004. Modelling and Model Building, in: Wainwright, J., Mulligan, M. (Eds.), Environmental Modelling: Finding Simplicity in Complexity. John Wiley & Sons, Ltd., Chichester, pp. 7–73.

Niemi, G., Wardrop, D., Brooks, R., Anderson, S., Brady, V., Paerl, H.W., Rakocinski, C.F., Brouwer, M., Levinson, B., McDonald, M., 2004. Rationale for a New Generation of Indicators for Coastal Waters. Environ. Health Perspect. 112, 979–986.

Nixon, S.W., 1995. Coastal marine eutrophication: A definition, social causes, and future concerns. Ophelia 41, 199–219.

Pace, M.L., Knauer, G.A., Karl, D.M., Martin, J.H., 1987. Primary production, new production and vertical flux in the eastern Pacific Ocean. Nature 325, 803–804.

Pauly, D., Christensen, V., 1995. Primary production required to sustain global fisheries. Nature.

Peel, M.C., Finlayson, B.L., Mcmahon, T.A., 2007. Updated world map of the Köppen-Geiger climate classification. Hydrol. Earth Syst. Sci. 11, 1633–1644.

Peterson, B.J., McClelland, J., Curry, R., Holmes, R.M., Walsh, J.E., Aagaard, K., 2006. Trajectory Shifts in the Arctic and Subarctic Freshwater Cycle. Science (80-.). 313, 1061–1066.

Pinckney, J.L., Paerl, H.W., Tester, P., Richardson, T., 2001. The Role of Nutrient Loading and Eutrophication in Estuarine Ecology. Environ. Health Perspect. 109, 699–706.

Platt, T., Bird, D.F., Sathyendranath, S., 1991. Critical Depth and Marine Primary Production. Proc. R. Soc. B Biol. Sci. 246, 205–217.

Rabalais, N.N., 2002. Nitrogen in Aquatic Ecosystems. Ambio 31, 102–112.

Rabalais, N.N., Turner, R.E., Diaz, R.J., Justić, D., 2009. Global change and eutrophication of coastal waters. ICES J. Mar. Sci. 66, 1528–1537.

Reynolds, C.S., 2006. The Ecology of Phytoplankton. Cambridge University Press, Cambridge, UK.

Roy, P.-O., Huijbregts, M.A.J., Deschênes, L., Margni, M., 2012. Spatially-differentiated atmospheric source–receptor relationships for nitrogen oxides, sulfur oxides and ammonia emissions at the global scale for life cycle impact assessment. Atmos. Environ. 62, 74–81.

Ryther, J.H., Dunstan, W.M., 1971. Nitrogen, Phosphorus, and Eutrophication in the Coastal Marine Environment. Science (80-.). 171, 1008–1013.

Saba, G.K., Steinberg, D.K., Bronk, D. a., 2011. The relative importance of sloppy feeding, excretion, and fecal pellet leaching in the release of dissolved carbon and nitrogen by Acartia tonsa copepods. J. Exp. Mar. Bio. Ecol. 404, 47–56.

Saba, G.K., Steinberg, D.K., Bronk, D.A., 2009. Effects of diet on release of dissolved organic and inorganic nutrients by the copepod Acartia tonsa. Mar. Ecol. Prog. Ser. 386, 147–161.

Seitzinger, S.P., Harrison, J.A., Dumont, E., Beusen, A.H.W., Bouwman, A.F., 2005. Sources and delivery of carbon, nitrogen, and phosphorus to the coastal zone: An overview of Global Nutrient Export from Watersheds (NEWS) models and their application. Global Biogeochem. Cycles 19, 1-11.

Seitzinger, S.P., Mayorga, E., Bouwman, A.F., Kroeze, C., Beusen, A.H.W., Billen, G., Van Drecht, G., Dumont, E., Fekete, B.M., Garnier, J., Harrison, J.A., 2010. Global river nutrient export: A scenario analysis of past and future trends. Global Biogeochem. Cycles 24.

Sherman, K., Hempel, G., 2009. The UNEP Large Marine Ecosystem Report: A perspective on changing conditions in LMEs of the World's Regional Seas, UNEP Regional Seas Report and Studies No. 182.

Smetacek, V., Passow, U., 1990. Spring bloom initiation and Sverdrup ' s critical-depth model. Limnol. Oceanogr. 35, 228–234.

Smith, V.H., 2007. Using primary productivity as an index of coastal eutrophication: the units of measurement matter. J. Plankton Res. 29, 1–6.

Smith, V.H., Joye, S.B., Howarth, R.W., 2006. Eutrophication of freshwater and marine ecosystems. Limnol. Ocean. 51, 351–355.

Smith, V.H., Tilman, G.D., Nekola, J.C., 1999. Eutrophication: impacts of excess nutrient inputs on freshwater, marine, and terrestrial ecosystems. Environ. Pollut. 100, 179–196.

Spalding, M.D., Fox, H.E., Allen, G.R., Davidson, N., Ferdaña, Z.A., Finlayson, M., Halpern, B.S., Jorge, M.A., Lourie, S.A., Martin, K.D., Mcmanus, E., Recchia, C.A., Robertson, J., 2007. Marine Ecoregions of the World: A Bioregionalization of Coastal and Shelf Areas. Bioscience 57, 573–583.

Steen, B., 2002. Impact evaluation in industrial ecology, in: Ayres, R.U., Ayres, L.W. (Eds.), A Handbook of Industrial Ecology. Edward Elgar, Cheltenham, pp. 149–161.

Suess, E., 1980. Particulate organic carbon flux in the oceans - surface productivity and oxygen utilization. Nature 288, 260–263.

Sverdrup, H.U., 1953. On Conditions for the Vernal Blooming of Phytoplankton. J. du Cons. Int. pour l' Explor. la Mer 18, 287–295.

Taylor, J.R., Ferrari, R., 2011. Shutdown of turbulent convection as a new criterion for the onset of spring phytoplankton blooms. Limnol. Oceanogr. 56, 2293–2307.

Tremblay, J.-É., Michel, C., Hobson, K.A., Gosselin, M., Price, N.M., 2006. Bloom dynamics in early opening waters of the Arctic Ocean. Limnol. Oceanogr. 51, 900–912.

UBC, 1999. Sea Around Us Project: Fisheries, Ecosystems & Biodiversity [WWW Document]. URL http://seaaroundus.org/ (accessed 6.18.14).

Van der Ploeg, R.R., Böhm, W., Kirkham, M.B., 1999. On the Origin of the Theory of Mineral Nutrition of Plants and the Law of the Minimum. Soil Sci. Soc. Am. J. 63, 1055–1062.

Van Drecht, G., Bouwman, A.F., Harrison, J.A., Knoop, J.M., 2009. Global nitrogen and phosphate in urban wastewater for the period 1970 to 2050. Global Biogeochem. Cycles 23, 1–19.

Van Drecht, G., Bouwman, A.F., Knoop, J.M., Beusen, A.H.W., Meinardi, C.R., 2003. Global modeling of the fate of nitrogen from point and nonpoint sources in soils, groundwater, and surface water. Global Biogeochem. Cycles 17, 1–20.

Van Vuuren, D.P., Bouwman, A.F., Smith, S.J., Dentener, F., 2011. Global projections for anthropogenic reactive nitrogen emissions to the atmosphere : an assessment of scenarios in the scientific literature. Curr. Opin. Environ. Sustain. 3, 359–369.

Vitousek, P.M., Aber, J.D., Howarth, R.W., Likens, G.E., Matson, P.A., Schindler, D.W., Schlesinger, W.H., Tilman, D.G., 1997. Human alteration of the global nitrogen cycle: sources and consequences. Ecol. Appl. 7, 737–750.

Wassmann, P., 1990. Relationship between primary and export production in the boreal coastal zone of the North Atlantic. Limnol. Ocean. 35, 464–471.

Wollheim, W.M., Vörösmarty, C.J., Bouwman, A.F., Green, P.A., Harrison, J.A., Linder, E., Peterson, B.J., Seitzinger, S.P., Syvitski, J.P.M., 2008. Global N removal by freshwater aquatic systems using a spatially distributed, within-basin approach. Global Biogeochem. Cycles 22, 1–14.

Article III

Effect factors for marine eutrophication in LCIA based on species sensitivity to hypoxia

Cosme, N. & Hauschild, M.Z.

Ecological Indicators 2016, *69*, 453-462

DOI: 10.1016/j.ecolind.2016.04.006

Published, manuscript in post-print version

Effect factors for marine eutrophication in LCIA based on species sensitivity to hypoxia

Nuno Cosme *, Michael Zwicky Hauschild

Division for Quantitative Sustainability Assessment, Department of Management Engineering, Technical University of Denmark, Produktionstorvet 424, DK-2800 Kgs. Lyngby, Denmark

* *Corresponding author*. Tel.: +45 45254729.

E-mail address: nmdc@dtu.dk

Abstract

Hypoxia is an important environmental stressor to marine species, especially in benthic coastal waters. Increasing anthropogenic emissions of nutrients and organic matter contribute to the depletion of dissolved oxygen (DO). Biotic sensitivity to low levels of DO is determined by the organisms' ability to use DO as a respiratory gas, a process depending on oxygen partial pressure. A method is proposed to estimate an indicator of the intensity of the effects caused by hypoxia on exposed marine species. Sensitivity thresholds to hypoxia of an exposed ecological community, modelled as lowest-observed-effect-concentrations (LOEC), were compiled from literature for 91 demersal species of fish, crustaceans, molluscs, echinoderms, annelids, and cnidarians, and converted to temperature-specific benthic (100 metres depth) LOEC values. Species distribution and LOEC values were combined using a species sensitivity distribution (SSD) methodology to estimate the DO concentration at which the potentially affected fraction (PAF) of the community's species having their LOEC exceeded is 50% ($HC50_{LOEC}$). For the purpose of effect modelling in Life Cycle Impact Assessment (LCIA), Effect Factors (EF, $[(PAF)\cdot m^3.kgO_2^{-1}]$) were derived for five climate zones (CZ) to represent the change in effect due to a variation of the stressor intensity, or $EF=\Delta PAF/\Delta DO=0.5/HC50_{LOEC}$. Results range from 218 $(PAF)\cdot m^3\cdot kgO_2^{-1}$ (polar CZ) to 306 $(PAF)\cdot m^3\cdot kgO_2^{-1}$ (tropical CZ). Variation between CZs was modest so a site-generic global EF of 264 $(PAF)\cdot m^3\cdot kgO_2^{-1}$ was also estimated and may be used to represent the average impact on a global ecological community of marine species exposed to hypoxia. The EF indicator is not significantly affected by the major sources of uncertainty in the underlying data suggesting valid applicability in characterisation modelling of marine eutrophication in LCIA.

Keywords: Dissolved oxygen depletion; Benthic habitat; Climate zone; Species sensitivity distribution; Potentially affected fraction; Life cycle impact assessment.

1. Introduction

Hypoxic waters are characterised by low concentration of dissolved oxygen (DO). The threshold for hypoxia is traditionally defined at 2 $mLO_2 \cdot L^{-1}$ (Diaz and Rosenberg, 1995; Gray et al., 2002) after observations of demersal fisheries collapse (Renaud, 1986), at 2 $mgO_2 \cdot L^{-1}$ (Turner et al., 2012; Vaquer-Sunyer and Duarte, 2008), or even at DO concentrations <50% saturation owing to avoidance behaviour and physiological stress (Breitburg, 2002). Regardless of the exact value and unit it represents, hypoxia is used here as the DO threshold beyond which some physiological, behavioural, or other response occurs (Davis, 1975), denoting the degradation of this water quality parameter relative to biotic requirements (Levin et al., 2009; Seibel, 2011).

Hypoxia occurrence can be naturally intensified when vertical density stratification of the water column, due to haloclines and thermoclines, hinders mixing and thus gas transfer to the bottom strata (Conley et al., 2009; Pihl et al., 1992; Rosenberg et al., 1991). The aerobic respiration by heterotrophic bacteria when degrading organic material, may consume the DO down to hypoxic levels. Anthropogenic emissions of organic matter may therefore contribute to hypoxia, as well as nutrient emissions that boost planktonic growth and increase organic matter export to bottom waters, processes covered in a typical impact pathway of marine eutrophication (Nixon, 1995; Rabalais et al., 2009). The global number of anoxia events, or 'dead zones', has increased exponentially in the last decades (Diaz and Rosenberg, 2008). The World Resources Institute (WRI, 2011) compiled 762 sites reporting eutrophication and hypoxia impacts – and eutrophication has been suggested to be the main cause (Diaz and Rosenberg, 2008, 1995; Justić et al., 1993; Rabalais et al., 2010). Severe ecological impacts may occur including habitat loss, water quality degradation, mass mortality, and fisheries decline (Diaz and Rosenberg, 1995; Levin et al., 2009; Middelburg and Levin, 2009; Wu, 2002; Zhang et al., 2010). Future global warming conditions may increase the occurrence and prevalence of hypoxia in coastal waters by the effect of e.g. increased temperature and enhanced stratification (Bakun et al., 2015; Kennedy, 1990; Rabalais et al., 2009). Water temperature increase may also intensify the stress on biota and DO demand for respiratory purposes (Harris et al., 2006) while oxygen solubility decreases as temperature rises (Carpenter, 1966).

Biotic sensitivity to hypoxia varies significantly between species, taxonomic group, or even life stage and so no single universal threshold really exists (Davis, 1975; Diaz and Rosenberg, 1995; Ekau et al., 2010; Gray et al., 2002; Miller et al., 2002; Vaquer-Sunyer and Duarte, 2008). In fact, a gradient of responses is observed with decreasing DO availability, depending on the tolerance or resistance of the species (Diaz and Rosenberg, 1995). Under events of DO shortage, benthic species may adopt avoidance strategies, or exhibit altered behaviour (Chapman and McKenzie, 2009; Wu,

2002). Physiologically, low DO concentration constrains the scope for aerobic metabolism and is therefore a limiting factor for growth and reproduction (Brett, 1979; Fry, 1971; Wu et al., 2003) and ultimately survival (Vaquer-Sunyer and Duarte, 2008; Wu, 2002). Oxygen-regulator species maintain a relatively constant O_2 consumption rate (MO_2) over a range of ambient oxygen partial pressure (PO_2), triggering behaviour and physiologic reflexes aimed at maintaining homeostasis, such as ventilatory (Perry et al., 2009) and cardiovascular responses (Gamperl and Driedzic, 2009). Below a critical PO_2 level, MO_2 declines as PO_2 declines (oxygen-conformation) (Richards, 2011). So, under oxygen-conformation, species show a tolerance threshold beyond which mortality is expected. In short, the initial response to hypoxia aims at maintaining oxygen delivery, then at conserving energy expenditure and reducing energy turnover, and last by enhancing energetic efficiency of remaining metabolic processes and deriving energy from anaerobic sources (reviewed by Wu (2002)).

Respiratory gas exchange is governed by the PO_2 gradient between the external and internal media (Seibel, 2011), modulated by the ventilatory, diffusive, and perfusive conductance of oxygen between media (Childress and Seibel, 1998; Herreid, 1980; Piiper, 1982). Local temperature- and salinity-dependent O_2 solubility determines the ambient PO_2. The intensity of the induced environmental stress increases with the decreasing DO concentration (or the corresponding PO_2 or %Sat). Physiologically, the sensitivity threshold to hypoxia corresponds to the critical PO_2 level, or the point of hypoxic stress at which the oxygen consumption of a regulator becomes dependent on environmental PO_2 and conformity onsets (Herreid, 1980; Hofmann et al., 2011; Richards, 2011). The corresponding DO concentration at which the effect is triggered is taken equivalent to a lowest-observed-effect-concentration (LOEC), i.e. the lowest stressor intensity (highest DO concentration) *found by experiment or observation to cause an alteration in morphology, functional capacity, growth, development, or life span of target organisms distinguishable from control organisms* (Duffus, 2003).

Life Cycle Assessment (LCA) has been used as an environmental analysis tool to evaluate the potential impacts of anthropogenic emissions, such as those of N that cause hypoxia-driven eutrophication (Hauschild, 2005). However, a method for the estimation of the ecological impact of hypoxia in marine coastal waters has not been broadly agreed upon in LCA methodologies. Benchmarking ecosystem effects in distinct geographic locations, using a harmonised global model, is also lacking (Henderson, 2015). Therefore, a scientifically-based and globally applicable method to quantify an indicator of the effects of hypoxia on marine species richness, as a function of their sensitivity, is proposed. The sensitivity to hypoxia and geographic distribution of representative species was addressed to derive an impact potential to the ecological communities in five climate zones. Such indicator is expressed as an Effect Factor (EF)

and its application for impact characterisation in Life Cycle Impact Assessment (LCIA) is discussed.

2. Methodology

The sensitivity to hypoxia of an exposed ecological community may be derived from the sensitivity of the composing individual species. This sensitivity indicator is the basis for an effect factor (EF), as defined and used in LCIA. The EF expresses the ability of the environmental stressor (oxygen depletion) to cause an effect on the exposed marine benthic ecosystem as a potential loss of its species richness. The standard metric, which is also applied for other LCIA indicators addressing ecosystem stress, is the Potentially Affected Fraction (PAF) of species in the ecosystem. The effect estimation is a component of the impact characterisation framework that derives Characterisation Factors (CFs). CFs for emission-related impact categories translate the amount of an emitted substance into a potential impact on the indicator for the chosen category, i.e. marine eutrophication in the present case. Such impact can be caused by anthropogenic air- and waterborne emission of bioavailable nitrogen (N) forms, and organic matter, and CFs can be derived for those emissions. The CF estimation follows the generic framework for emission-based indicators by further modelling a fate factor (FF) and an exposure factor (XF) (Udo de Haes et al., 2002). The FF expresses the persistence of N in the euphotic zone of marine waters, as the product of the fraction of the original emission and its residence time in the compartment (Cosme et al., 2016; Henderson et al., 2011). The ecosystem XF expresses the incorporation of N into planktonic organic matter that gets exported to bottom strata, where it is aerobically respired by heterotrophic bacteria with DO consumption, as proposed by Cosme et al. (2015). The CF, in (PAF)·m^3·yr·kgN^{-1}, is then the product of the fate, exposure, and effect factors, as summarised in Eq. (1):

$$CF_{ij} = FF_{ij} \times XF_j \times EF_j \quad (1)$$

where FF_{ij} (in yr) is the fate factor for emission *i* to receiving ecosystem *j*, XF_j (in $kgO_2 \cdot kgN^{-1}$) is the exposure factor and EF_j (in (PAF)·$m^3 \cdot kgO_2^{-1}$) the effect factor in ecosystem *j*. PAF is in fact dimensionless (fraction) and not an actual unit (Heijungs, 2005), so it is shown here in association with the EF's proper unit ($m^3 \cdot kgO_2^{-1}$) merely for informative purposes.

The proposed methodology to estimate EFs based on species sensitivity to hypoxia requires the identification of relevant target species, the respective sensitivity data, the determination of the species' geographic distribution, and the environmental conditions there. Finally, it requires the derivation of the ecological community's

sensitivity at an adequate spatial resolution. These steps are briefly described in the sections ahead.

2.1. Data sources

A dataset of the sensitivity thresholds of individual species to hypoxia was compiled from literature. Relevant data from review papers (Davis, 1975; Diaz and Rosenberg, 1995; Gray et al., 2002; Vaquer-Sunyer and Duarte, 2008) were extracted and complemented with further literature search (Table S1). Only demersal (benthic and benthopelagic) species were considered, since hypoxia is primarily relevant in bottom waters (Middelburg and Levin, 2009).

2.2. Species distribution and assignment to climate zones

The geographic occurrence of the relevant species was determined from the online databases 'The World Register of Marine Species' (WoRMS Editorial Board, 2015), 'Fishbase' (Froese and Pauly, 2015), 'FAO FishFinder' (FAO, 2015), and 'Ocean Biogeographic Information System' (OBIS, 2015).

Species distribution was assigned to a Large Marine Ecosystems (LME) spatial resolution (Sherman and Hempel, 2009) and then grouped into five climate zones (CZs) (Fig. S1 and S2): polar, subpolar, temperate, subtropical, and tropical, primarily based on mean annual water temperature at 100 m depth in every LME, corresponding to the half of the mean depth of the continental shelf (Tait and Dipper, 1998; UNESCO, 2009). Time- and space-integration was done by averaging temperature values from CTD (conductivity, temperature, and depth) datasets, retrieved from the ICES Oceanographic database (ICES, 2015a). Complementary information from NOAA's World Ocean Atlas (Locarnini et al., 2010) was used to check for consistency of the values obtained. For 19 out of 66 LMEs, CTD-based benthic temperatures were not available, and were instead estimated from the average temperature drop from surface to 100 m depth of the remaining LMEs in the same CZ, using mean annual sea surface temperature per LME available in Sherman and Hempel (2009). Assigning species to LMEs was useful to provide spatial variability based on benthic conditions, and grouping into CZs was necessary due to low representativeness of species at LME scale (see details in Section 3.1).

2.3. LOEC estimation based on sensitivity to hypoxia

In the present context, species sensitivity refers to a continuum, whereas the sensitivity threshold is a measurable discrete variable reported as a DO concentration, oxygen partial pressure (PO_2) level, or % saturation, in the source literature (Table S1). The LOEC level corresponds to the DO concentration converted from the discrete sensitivity threshold reported, and the benthic LOEC to the temperature-dependent DO value converted from the reported LOEC to benthic ambient conditions per LME.

The stressor intensity level, at which the biological endpoint tested manifests a clear variation or response, is adopted here as the sensitivity threshold, which in some cases correspond to the typical critical PO_2-based threshold, in others to significant changes on various rates, or activity/behaviour alteration mainly based on different avoidance strategies. The biological endpoints for which the responses were tested (Table S1) vary with species and taxonomic groups. This necessary adaptation of the definition for sensitivity threshold ties in with the need for a reasonably populated dataset. Most of the data sources do not report physiological critical PO_2 levels, and several report avoidance behaviour. For consistency of the meaning of this threshold, a loose interpretation of an ambient DO concentration at which a response is measured or observed, may best apply.

Despite the use of the DO concentration metric, animals depend on physically-driven gas exchange across membranes and tissues for respiration (Childress and Seibel, 1998; Piiper, 1982; Seibel, 2011) and the thermodynamics of this process is better approximated by PO_2 (Hofmann et al., 2011). Physiological O_2 transport systems and biochemical pathways are regulated by PO_2 and affinities for O_2 (Seibel, 2011). Henry's law relates reported PO_2 to DO concentration and the effect of the affinity of blood oxygen carriers for O_2, a physiological parameter, is reflected in the sensitivity response and threshold. Hydrostatic pressure has little effect on oxygen solubility (Forstner and Gnaiger, 1983) and was therefore set as constant.

Oxygen solubility decreases with temperature and/or electrolyte content increase (Forstner and Gnaiger, 1983). Water temperature varies significantly from -1.4°C to 25.3°C among LMEs (Table S2, Figures S1 and S3), whereas salinity has a small effect and variation (ca. 33 $g \cdot kg^{-1}$ to ca. 36 $g \cdot kg^{-1}$) (Figure S4). Salinity was therefore assumed constant at 35 $g \cdot kg^{-1}$. Because of the temperature-dependency, DO concentrations are not universally applicable, i.e. are only valid to those particular environmental conditions (Hofmann et al., 2011). This fact, and because sensitivity thresholds are necessarily species-specific, is the basis for the spatial variability modelled in the present work.

Oxygen concentrations and sensitivity thresholds were converted from reported PO2, air saturation (%Sat), or DO concentrations, from experimental or in situ conditions, to temperature-dependent benthic DO levels, to both maximum DO solubility and sensitivity threshold, the latter labelled as equivalent to a LOEC, and respective %Sat (see Section S4 and Figure S5 for details). Benthic habitat conditions were therefore assumed as representative for the geographic occurrence of the species, i.e. LME-dependent water temperature at 100 m depth (from oceanographic CTD datasets, see previous section). All conversions were computed with software available online: the 'Dissolved oxygen solubility tables' (USGS, 2015) and the 'Oceanographic Calculator' (ICES, 2015b). In addition to increasing the representativeness of the

sensitivity data and environmental relevance of the dataset and model work, these conversions increased the number of sensitivity data points from 91 species-specific LOECs reported in the literature to 582 temperature- and species-specific LOEC values corresponding to benthic average conditions in 66 LMEs.

2.4. Species sensitivity distribution (SSD) methodology

The distribution of individual species' thresholds of sensitivity to hypoxia (LOECs) was used to estimate the sensitivity of the community found in each CZ by fitting a species sensitivity distribution (SSD) function to estimating a hazard concentration $HC50_{LOEC}$, i.e. the concentration of DO (intensity of the stressor) affecting 50% of the species above their LOEC. The SSD methodology derives the sensitivity of the ecological community to an environmental stressor from a statistical or empirical distribution function for the sensitivity thresholds of the individual biological species (Posthuma et al., 2002). Extensive description, applications, and implications of the SSD concept and methodology can be found in Posthuma et al. (2002). Practical information on the calculations involved is described in the U.S. EPA's 'Species Sensitivity Distribution Generator' (U.S. EPA, 2015).

SSD curves plotting species' LOECs as a function of the intensity of the environmental stressor (DO depletion) can be used to graphically extract the $HC50_{LOEC}$ value for each CZ and the global average. The latter integrates all the LOEC data points from every LME. The global average $HC50_{LOEC}$ is used as default when spatial differentiation is not possible or relevant. Analytically, the PAF function is calculated by fitting the log-logistic distribution to the proportion of affected species as a function of DO concentration (de Zwart, 2002) as Eq. (2):

$$PAF(DO) = \frac{1}{1+e^{-(\log DO-\alpha)/\beta}} \quad (2)$$

where α is the sample mean or location parameter, and β is the scale parameter proportional to the standard deviation of the log-transformed DO values. The DO concentration value corresponding to a PAF of 0.5 is the $HC50_{LOEC}$, and can be calculated from Eq. (3):

$$HC50_{LOEC} = 10^{-\beta \cdot \ln\left(\frac{1}{PAF}-1\right)+\alpha} \quad (3)$$

where α and β are CZ-dependent. $HC50_{LOEC}$ can also be determined by calculating the geometric mean (GM) of the LOEC data points (herein named $GM_{species}$) by e.g. $HC50_{LOEC} = 10^{\text{avg}(logLOEC)}$ according to the average gradient method (Pennington et al., 2004).

An alternative approach involves the grouping of species into taxonomic groups (fish, crustaceans, molluscs, echinoderms, annelids, cnidarians) for which the geometric mean (of taxa) of the geometric means (of individual species) is calculated, i.e. $GM_{species}$ within taxa followed by the GM_{taxon} (among taxa) to estimate a CZ-dependent $HC50_{LOEC}$. Both $GM_{species}$- and GM_{taxon}-based $HC50_{LOEC}$ were calculated and their justification and application discussed.

Following Roelofs et al. (2003) and for log-normal distributed LOEC values, the variation of the estimated $HC50_{LOEC}$ value can be calculated from the standard deviation *s* of the log-transformed underlying single-species LOEC values multiplied by $\frac{t_{[n-1]}}{\sqrt{n}}$, which is sampled from a Student's t-distribution with n-1 degrees of freedom:

$$\log HC50 = \frac{\sum logLOEC}{n} \pm \frac{t_{[n-1]}}{\sqrt{n}} * s \quad (4)$$

where *n* is the number of species (or taxa) for which LOEC data are available, $t_{[n-1]}$ is the standard Student's t-distribution with n-1 degrees of freedom, and *s* is the estimated standard deviation of the log-transformed LOECs.

2.5. Estimating effect factors (EF)

Available approaches to estimate EFs are described by Pennington et al. (2004) and Larsen and Hauschild (2007a). The present study uses the 'average PAF gradient' approach to assess the contribution of the stressor (DO decline) to the resulting effect (PAF). As such, the EF represents the average change of effect (ΔPAF, dimensionless) due to a variation of the stressor intensity (ΔDO, in $kgO_2 \cdot m^{-3}$). According to the current scientific consensus (Henderson et al., 2011; Larsen and Hauschild, 2007a; Pennington et al., 2004), the EF is calculated as shown in Eq. (5):

$$EF = \frac{\Delta PAF}{\Delta DO} = \frac{0.5}{HC50_{LOEC}} \quad (5)$$

The variation of the estimated $HC50_{LOEC}$ (as per Eq. 4) propagates to the EF estimation.

3. Results

The results of the data collection are firstly presented. Then the results of the Species Sensitivity Distribution (SSD) methodology are shown in the context of HC_{50} estimation. Finally, the results of the Effect Factor (EF) estimation based on those HC_{50} values are presented.

3.1. Datasets

The literature review resulted in the collection of an extensive dataset of sensitivity thresholds (LOEC), limited to behavioural and physiological biological endpoints, for 91 demersal (benthic and benthopelagic) species, namely:

- 26 fish species: chondrichthyes (cartilaginous fishes, n=3) and osteichthyes (bony fishes, n=23);
- 27 crustacean species: stomatopods (mantis shrimps, n=1), isopods (pillbugs, woodlice, n=1), amphipods (amphipods, n=2), decapods (crabs, lobsters, prawns, shrimps, n=23);
- 17 mollusc species: bivalves (clams, scallops, mussels, n=9), gastropods (sea snails, sea slugs, n=7), and cephalopods (octopuses, squids, cuttlefishes, n=1);
- echinoderm species: ophiuroids (brittle stars, n=4), asteroids (starfishes, n=1), echinoids (sea urchins, n=2) and holothuroids (sea cucumbers, n=2);
- 7 annelid species: polychaets (polychaete worms, n=7);
- 5 cnidarian species: hydrozoans (hydroids, n=2), and anthozoans (sea anemones, corals, n=3).

These species were selected for their occurrence in the water column, as demersal species depend, to some extent, on the benthic habitat to feed, hide, and reproduce. Their inclusion in the dataset, and considering the average depth approach, inherently assumes that the habitat locates below the thermo- or halocline depth, where DO depletion may have significant impacts. The collected dataset, metadata of the experimental work and respective reference sources, are compiled in Table S1.

Benthic water temperatures were estimated, species occurrence per LME and CZ determined, and reported threshold converted to benthic LOECs at the ambient conditions of the individual LMEs (Table S2). Species' geographic distribution showed six LMEs with zero species assigned and 32 LMEs (48%) with only five or fewer species. Hence, species representativeness at the LME resolution was considered too low and justified the adoption of the coarser CZ resolution. In the latter, the polar CZ includes 21% of the total number of species, subpolar 43%, temperate 87%, subtropical 79%, and tropical 33% (Figure S6). Species overlapping between adjacent CZs (Figure S6), i.e. subpolar-temperate (69%), temperate-subtropical (79%), and subtropical-tropical (54%) do not suggest a strong CZ differentiation; polar-subpolar (18%) show the most differentiated species composing in adjacent CZs.

The distribution of the LOEC data among taxa (Figure 1) shows effect thresholds similar ($F=7.7$, $p<0.014$) to values previously reported by Vaquer-Sunyer and Duarte (2008) in spite of lower thresholds for crustacean species (Table S3).

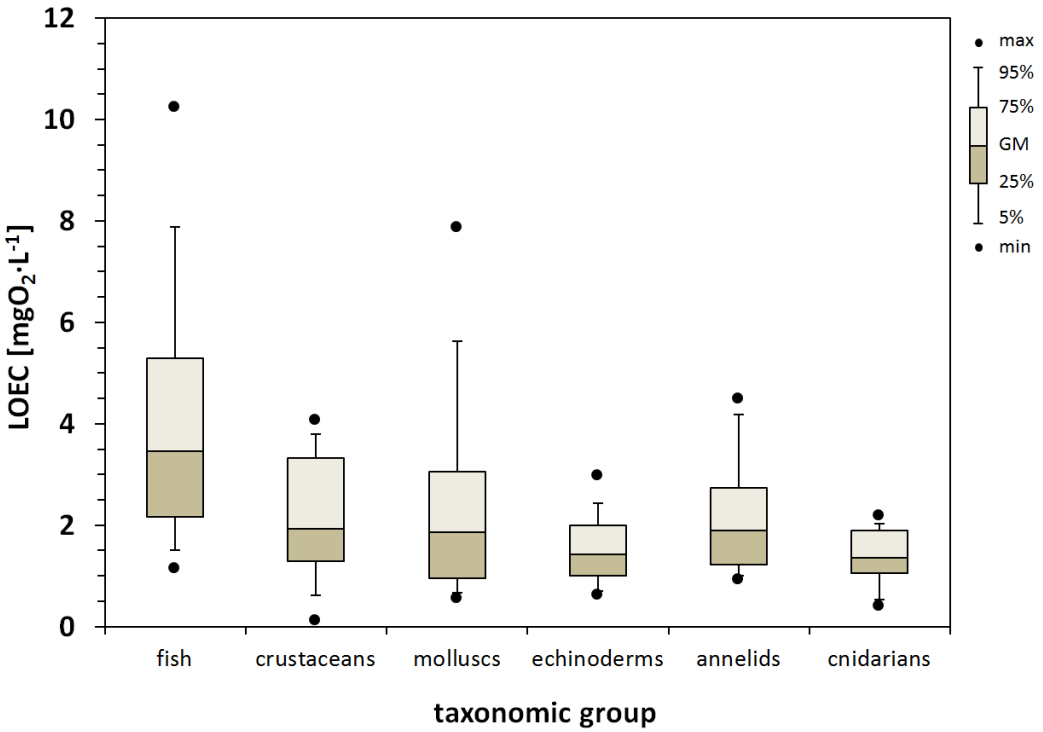

Figure 1 Distribution of sensitivity thresholds to hypoxia among taxa based on species LOEC ($mgO_2 \cdot L^{-1}$).

3.2. Species Sensitivity Distribution (SSD) and HC_{50} estimation

The sensitivity data (LOEC) were plotted and PAF function curves fitted for each CZ and the global average (Figure 2). Details and statistics of the SSD curve fits can be found in Table S4. In typical ecotoxicology tests the *increase* of the concentration (pressure) of a chemical (stressor) is expected to intensify the effect on exposed organisms/species, making PAF a suitable metric for such pressure. In the present case, the pressure is inversed, i.e. the effect comes from the *decrease* in concentration of DO (pressure) that corresponds to the intensification of hypoxia (stressor). The term 'potentially not affected fraction' (PNAF) of species was therefore adopted, where PNAF=1–PAF, and noting that at 50% effect level PNAF=PAF.

The resulting $HC50_{LOEC}$ values using both the $GM_{species}$ method (also from the graphical interpolation) and GM_{taxon} are compiled in Table 1. Each species has an equal contribution to the $GM_{species}$–based $HC50_{LOEC}$ values, even though these are estimated from an unequal number of tested species per taxonomic group (Figure S7), i.e. an

arbitrary species representation that varies among climate zones. Also, this relative frequency of species per taxonomic group does not necessarily reflect a differential occurrence in nature, but simply the availability of experimental data for those species. Adopting the GM_{taxon} method, this bias relative to the real species composition between CZs is eliminated by a conscious choice of equal weight of each taxonomic group (Figure 3). A similar approach has previously been proposed for aquatic ecotoxicity by Larsen and Hauschild (2007b).

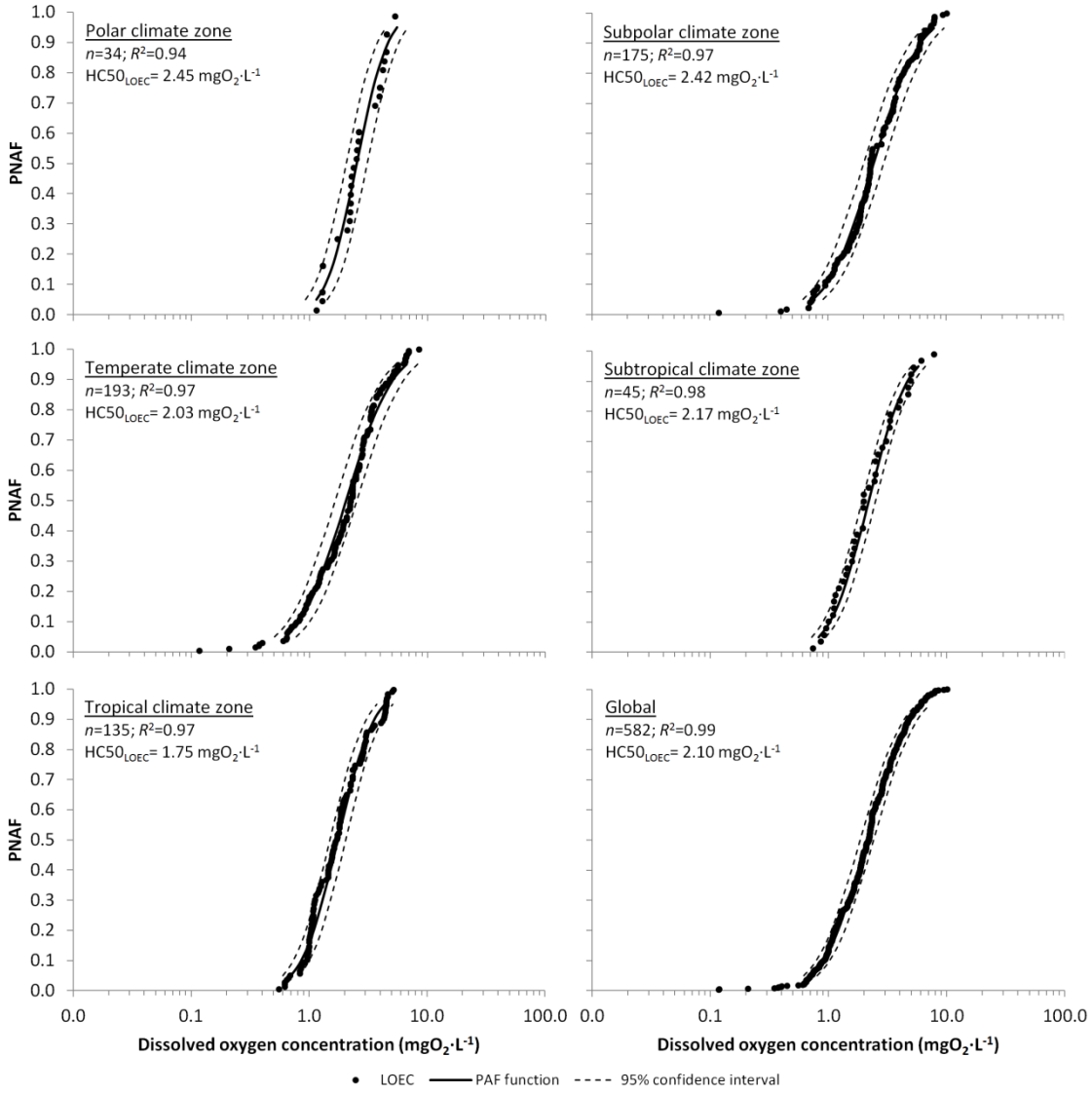

Figure 2 Species sensitivity distribution (SSD) curves plotting sensitivity to hypoxia (single species LOEC) as a function of dissolved oxygen concentration ($mg \cdot L^{-1}$) for selected species occurring in each of the five climate zones (polar, subpolar, temperate, subtropical, and tropical) and a global average. The PAF function fitting the data distribution (Eq. 2) and 95% confidence interval are also drawn. Sample size, coefficient of determination (R^2) and derived $HC50_{LOEC}$ values are included. Potentially Not Affected Fraction (PNAF) of species is used to represent the effect; PNAF=1–PAF (see text).

Table 1 $HC50_{LOEC}$ per climate zone calculated from a) the geometric mean (GM) of all species LOECs ($GM_{species}$), and b) the GM of the $GM_{species}$ per taxonomic group (GM_{taxon}).

Climate zone	$HC50_{LOEC}$ [a)]	$HC50_{LOEC}$ [b)]						
	$GM_{species}$	$GM_{species}$ per taxonomic group						GM_{taxon}
		fish	crustaceans	molluscs	echinoderms	annelids	cnidarians	
	[$mgO_2 \cdot L^{-1}$]	[$mgO_2 \cdot L^{-1}$]	[$mgO_2 \cdot L^{-1}$]	[$mgO_2 \cdot L^{-1}$]	[$mgO_2 \cdot L^{-1}$]	[$mgO_2 \cdot L^{-1}$]	[$mgO_2 \cdot L^{-1}$]	[$mgO_2 \cdot L^{-1}$]
Polar	2.45	2.18	1.87	2.25	--	3.47	1.99	2.29
Subpolar	2.42	3.95	2.29	1.36	1.57	2.56	1.58	2.07
Temperate	2.03	3.56	1.89	1.74	1.41	1.88	1.09	1.80
Subtropical	2.17	2.79	2.25	2.71	1.21	1.23	1.45	1.82
Tropical	1.75	2.82	1.67	2.24	1.37	1.21	1.10	1.64
Global	2.10	3.46	1.93	1.85	1.42	1.90	1.36	1.89

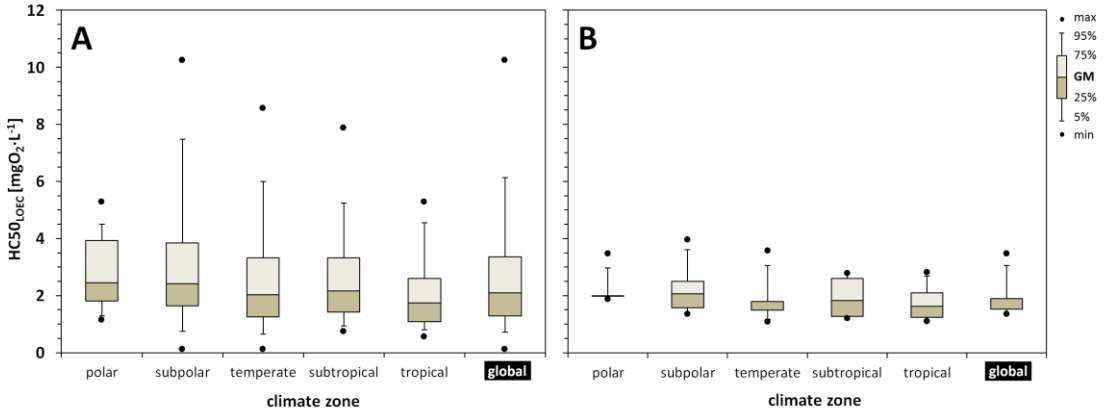

Figure 3 Distribution of data on joint sensitivity to hypoxia ($HC50_{LOEC}$) obtained from calculating either the geometric mean (GM) based on species or taxa aggregation methods (**A**: $GM_{species}$ and **B**: GM_{taxon}, respectively) per climate zone plus a global average.

3.3. Effect factor estimation

The EF values obtained from the two $HC50_{LOEC}$ estimation methods are shown in Table 2. The results range from 204 (polar CZ) to 286 (PAF)·m^3·kg O_2^{-1} (tropical CZ) estimated from $GM_{species}$, and from 218 (polar CZ) to 306 (PAF)·m^3·kg O_2^{-1} (tropical CZ) estimated from GM_{taxon}.

Table 2 Effect Factors (EF) at benthic habitat conditions per climate zone and a site-generic global average, estimated from $HC50_{LOEC}$ based on geometric means (GM) of species-specific ($GM_{species}$) and taxon-grouped data (GM_{taxon}). Number of LOEC data points (*n*) and variation (as per Eq. 4) included.

Climate zone	*n*	EF ($GM_{species}$-based)		EF (GM_{taxon}-based)	
		[(PAF)·m^3·kgO_2^{-1}]	$(\pm\frac{t_{[n-1]}}{\sqrt{n}} * S)$	[(PAF)·m^3·kgO_2^{-1}]	$(\pm\frac{t_{[n-1]}}{\sqrt{n}} * S)$
Polar	34	204	(-29.8, +34.9)	218	(-5.4, +5.5)
Subpolar	175	206	(-18.2, +20.0)	242	(-9.8, +10.2)
Temperate	193	245	(-20.7, +22.6)	278	(-11.1, +11.6)
Subtropical	45	230	(-33.5, +39.3)	275	(-10.7, +11.2)
Tropical	135	286	(-24.2, +26.4)	306	(-11.4, +11.8)
Global average	582	238	(-11.2, +11.8)	264	(-9.0, +9.3)

The distribution of the EFs per CZ estimated with GM_{taxon}-based $HC50_{LOEC}$ is plotted in Figure 4.

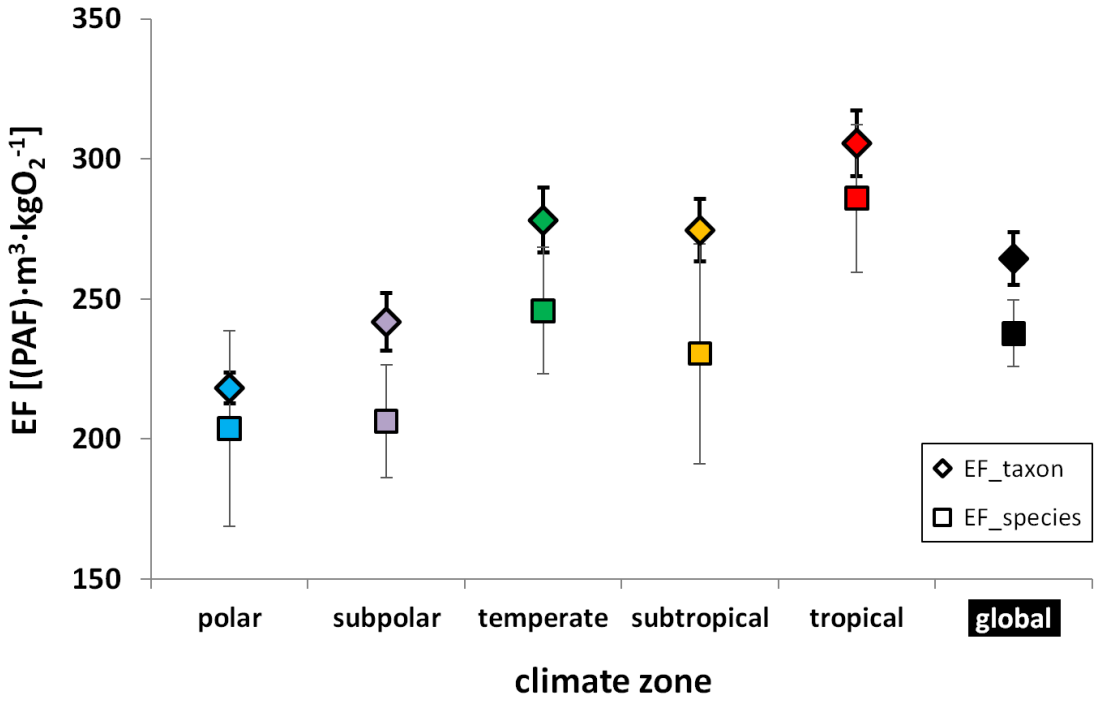

Figure 4 Comparison of the Effect Factor [EF, (PAF)·m^3·kgO_2^{-1}] results obtained from applying the $HC50_{LOEC}$ estimated from both $GM_{species}$- and GM_{taxon}-based methods. Variation bars correspond to coefficient's variation (as per Eq. 4).

4. Discussion

The effect factor obtained from the sensitivity of the exposed community, modelled with the average PAF approach, results in non-conservative estimates. These, require a relatively high amount of (scarce) species sensitivity data, but are less sensitive to variability of the datasets and therefore more reproducible (Larsen and Hauschild, 2007a). LCA is inherently comparative – impacts are estimated in respect to a functional unit and integrated over time and space, and LCIA relies on best estimates and average conditions to model the indicators (Larsen and Hauschild, 2007b). These conditions are sought in the present method, extending from the environmental conditions modelled (e.g. temperature, depth) to the effects (e.g. community's average PAF). There is no attempt to be conservative and protect the most sensitive species by focusing the effect modelling on these, like in environmental risk assessment methodologies (Larsen and Hauschild, 2007b). Moreover, the PAF approach is suitable for spatial differentiation (Larsen and Hauschild, 2007a) – an essential feature in the present method, which is visible from the effort in differentiating ecological communities, first at the LME- and then at CZ-scale, and work these as the basis for the (spatially) differentiated joint sensitivity and effects.

A method to quantify the impact potential of hypoxia on the ecological communities in five climate zones was proposed and the estimated effect factors (EF) were presented. In the following, the methodological choices that may lead to reduced representativeness of the modelled ecosystem, the simplifications needed for pragmatic reasons, and the sources of statistical (stochastic) uncertainties are discussed for the method's application in Life Cycle Impact Assessment (LCIA).

4.1. Methodological choices and simplifications

Behavioural and physiological responses of marine species to DO levels were taken as biological endpoints to derive sensitivity thresholds to hypoxia. Exposure to extreme or prolonged hypoxia beyond these thresholds may lead to mass mortalities (Diaz and Rosenberg, 1995). Other responses and effects may also be pointed out at the ecological level, e.g. altering structure, function, and services of benthic communities and food webs (e.g. Ekau et al. (2010), Gray et al. (2002), Levin et al. (2009), Riedel et al. (2014), Wu (2002)), releasing greenhouse gases like methane, nitrous oxide, hydrogen sulphide with implications to global warming, or toxic metabolites under anoxic conditions with implications to survival of the benthos (Llansó, 1991; Middelburg and Levin, 2009; Naqvi et al., 2010), or interfering with biogeochemical cycles of nutrients in water and sediments, with positive feedbacks to eutrophication from NH4+ effluxes or hindering denitrification (e.g. Conley et al. (2009), Levin et al. (2009), (Middelburg and Levin, 2009)). Such indirect effects on biota through biogeochemistry of anoxic sediments are typical of 'dead zones', which occur at a level

beyond the hypoxia effects modelled here, but with increasing incidence and prevalence (Diaz and Rosenberg, 2008). Although important, those are outside the scope of the present modelling work.

In general, hypoxia thresholds may change with e.g. physiological condition, life cycle (Chapman and McKenzie, 2009; Herreid, 1980; Miller et al., 2002; Wu, 2009), food availability and predatory pressure (Craig and Crowder, 2005), and water quality (Davis, 1975), suggesting the modelling of a background pressure due to environmental degradation as in a 'marginal PAF increase' approach. However, the contribution of a corresponding background PAF is not modelled in the average effect approach adopted here, as it takes in the response to hypoxia alone. These choices do not affect the representativeness of the species sensitivity and the validity of the estimation method.

The LME biogeographical classification system was chosen based on practical aspects of data availability, modelling feasibility, and size (and number) of the spatial units. Other classification systems can be used in the present framework, as long as the species geographic occurrence is assigned accordingly.

4.2. Sources of uncertainty

4.1.1. Modelling average conditions

Experimental results of the responses tested are assumed to correspond to those in the real habitat, so that the derivation of the species' LOECs is valid for effect factors modelling. This may not match time and spatial fluctuations (Posthuma et al., 2002) in benthic habitats due to the variability of e.g. mixing, currents, substrate, or bathymetry, hence the assumption of average conditions in the conversion to benthic LOECs. Calculation of temperature-dependent LOECs involves the assumption that the same response, and the PO_2 level at which it manifests, also verifies under benthic conditions. These conditions, different from the reported experimental results, add a non-quantified uncertainty about the 'real' sensitivity threshold level, but its adoption is a necessary step towards relevance of the LOECs. The physiological relevance of doing such conversions determines that the temperature-dependence is the driver for spatial differentiation of the effect on each individual species that ultimately contributes to the EF differentiation. The implications of the added uncertainty are seen minor when compared to the diversity of biological endpoints tested and reported in the dataset in Table S1. For the purposes of model transparency, the DO levels corresponding to specific sensitivity thresholds, under the LOEC interpretation, read as the PO_2 level (converted to temperature-dependent DO concentrations), in a decreasing ambient O_2 availability scale, at which a response is triggered. As the responses vary significantly with the species tested and experimental objectives, the physiological basis for the threshold also vary and to some extent are even not comparable. These levels, however,

constitute the best estimate available and at a reasonable coverage of distinct taxonomic groups, thus fitting a typical LCIA average effects approach.

Benthic habitat depth was assumed at 100 m as a model simplification and best estimation to model continental shelf average conditions. In nature, species may occur at shallower or deeper depths where temperature may deviate from the mean LME-dependent benthic temperature used to model the sensitivity thresholds. Equal number and significance of shallower and deeper occurrences were therefore assumed, so that the impact of temperature deviations in the $HC50_{LOEC}$ is neglected and average conditions are represented in the indicator modelling. Marine coastal waters were also assumed to correspond to continental shelf areas, when in fact some LMEs may also include areas belonging to the continental slope, for which the set of species and their occurrence may differ significantly from those used in the present LOEC estimations. Again, in order to express average conditions when modelling shelf water properties, the influence of such deeper waters of the slope was neglected.

Species occurrence is typically heterogeneous in time and space (Levin, 1994). While patchiness occurs in natural habitats, homogeneity was assumed within each spatial unit for modelling simplification. Although this even distribution and density were assumed, species that may not overlap at all within a spatial unit are considered as composing the same community. The community's sensitivity to hypoxia obtained from the SSD methodology is assigned to the particular spatial unit, regardless of any species interaction, overlap, synergy, etc. aiming at representing average conditions.

The temperature-dependent conversion of DO concentrations is ca. three times more sensitive to a 1°C variation in water temperature than to a 1 $g \cdot kg^{-1}$ variation in salinity, easily checked using converting algorithms ((ICES, 2015b; USGS, 2015), see Section 2.3). In contrast to temperature's wide variation among LMEs, salinity is fairly constant (Section S4). These two factors (low sensitivity and variability) support the use of temperature measurements (time- and space-averaged CTD data) and the adoption of constant salinity for model simplification. The alternative temperature estimation method, applied to the LMEs lacking measured data (19, mainly in the southern hemisphere), does not affect CZ aggregation and is therefore judged as a small contribution to the uncertainty of the sensitivity dataset.

4.2.2. Experimental datasets and representativeness

The absence of an accepted and standardised method for hypoxia sensitivity testing, along with the amount of possible biological endpoints to test, may significantly contribute to a test-related bias in the available dataset. On its end, low representativeness of tested species in target ecological communities for which the extrapolation is to be drawn, may contribute to a selection-related bias (see Section S7). Acknowledging that test- and selection-related biases may decrease data

representativeness, the LOECs per CZ are expected to sufficiently represent the habitat suitability approach (Hirzel and Le Lay, 2008) – this means that contributions from taxonomic groups in fairly similar relative occurrence patterns per CZ (Figure S7) would result in small differences among CZ's joint sensitivity threshold. For taxa represented in every CZ, the main source of variability would be the deviation from an average taxa-representation pattern, e.g. if all the groups increase their number of LOEC proportionally, it will not change the $HC50_{LOEC}$ (by either GM-estimation method), rather a differential contribution of species to each group would alter it accordingly.

The number of species for which sensitivity data is available, i.e. 91, is modest when compared to species inventory lists from any of the spatial units considered – e.g. the 'IUCN Red List of Threatened Species' database version 3.1 (www.iucnredlist.org) identifies 386 relevant species for the Mediterranean Sea, whereas the present dataset only includes 41, despite that being one of the most represented LMEs, ranking 3rd out of the 66. Species representativeness is also affected, as 70% of the LMEs have less than 10 sensitivity data points and six LMEs have no species occurrence at all (Table S2), hence the need to lower the spatial resolution by grouping data into CZs.

Species predominantly occur in areas of optimal environmental conditions and can be found as far as their environmental envelope reaches, as formalised in the niche theory by Hutchinson, (1957). Occurrence vary among species as a result of distinct tolerances to temperature, salinity, luminosity, etc. that characterise and define the ecological niche. The present dataset shows that every considered taxonomic group (at class level) have successfully occupied all five CZs (Figure S6) – with the exception of echinoderms in the polar CZ and a few taxa at order level (e.g. chondrichthyes, decapods, neogastropods, and octopods). As species-based $HC50_{LOEC}$ values are obtained from the geometric mean of all contributing LOECs, the influence of 'very sensitive' or 'very tolerant' species is weakened (Larsen and Hauschild, 2007b), which partially explains (along with the benthic-demersal habitat restriction) the differences in the thresholds reported by Vaquer-Sunyer and Duarte (2008), who have used arithmetic means. Despite this attenuation effect given by the use of the GM, the $HC50_{LOEC}$ is biased by the number of representatives of each taxonomic group relative to the actual sensitivity of the CZ community that it is supposed to represent. In fact, inter-CZ comparison shows that such bias is due to differential dominance of taxa (Figure S8) and their contributing LOEC values (Figure 1). CZs dominated by more sensitive species, like fish (in subpolar) or fish and molluscs (in subtropical), show higher $HC50_{LOEC}$ values (i.e. lower EFs), whereas CZs with a more even representation of various taxa show lower $HC50_{LOEC}$ (i.e. higher EFs, as in temperate and tropical CZs) (Figure 4). The lowest EF value obtained (in the Polar CZ) is due to the low contributions from more sensitive groups (e.g. echinoderms and cnidarians) (Figure 1, Figure S7 and Figure S8). The GM_{taxon}-based $HC50_{LOEC}$ values show lower spatial

differentiation (Figure 3, and the inversed correspondence as EFs in Figure 4), but are less sensitive to unintentional differences in species representation in the test results and more reproducible. The GM_{taxon}-based $HC50_{LOEC}$ method is therefore preferable for the estimation of EF indicators.

A significance F-test for variances on pairs of GM_{taxon}-based $HC50_{LOEC}$ values per CZ, reveals that the obtained EF_{CZ}s are not significantly distinct from each other. EF_{polar} has the most distinct value, but still not significant ($F=\{0.368, 0.378, 0.391\}$, $p<\{0.18, 0.18, 0.19\}$, Table S5), being also the less robust (built with only 34 LOEC data points, Table 2). None of the EF_{CZ} is significantly distinct from the site-generic global value EF_{global} either. Analysing the results (Figure 4), the variation, and significance of the spatial differentiation obtained, the EFs estimated from GM_{taxon}-based $HC50_{LOEC}$ suggest that the site-generic EF_{global} can be adopted to represent the effect of hypoxia on biota, as no significant distinction can be seen from the sensitivity distribution across CZs, and supported by its higher robustness (estimated from 582 LOEC data points, Table 2).

Overall, the methodological choices and the necessary simplifications do not affect the model representation of the ecosystem. The representativeness of the species sensitivity dataset is deemed adequate to support the estimation of the biotic response in continental shelf waters. The extensive number of species covered, the taxonomic groups represented, and the global coverage of differentiated temperature-dependent LOEC data and species distribution, suggest good completeness of the effect model work. The HC_{50} estimation method is also consistent with other LCIA methodologies. The modelling of average environmental conditions and impacts is judged not to significantly add unexplained variability to the resulting EF indicator, and when allied to adequate representativeness, good completeness, and spatial differentiation, supports a valid applicability of the method.

4.3. Application in LCIA modelling

The EFs obtained from the presented method can be applied in characterisation modelling of impacts of hypoxia-driven marine eutrophication from anthropogenic emissions (nitrogen forms and organic matter). Current LCIA methods covering this particular impact category still lack the modelling of the effects on exposed biota, i.e. at an endpoint in the pressure to impacts cause-effect chain. The proposed method models the impacts beyond the present midpoint indicator, which represents the increase in the concentration of dissolved nutrients as applied in the widespread ReCiPe (Goedkoop et al., 2009), EDIP 2003 (Hauschild and Potting, 2005), IMPACT 2002+ (Jolliet et al., 2003), and CML 2002 (Guinée et al., 2002) LCIA methods. Alternative impact indicators further down the impact pathway, like ecosystem response expressed in planktonic growth promoted by the emission of a limiting nutrient and the bottom

oxygen depletion potential (Cosme et al., 2015; Itsubo and Inaba, 2012), also do not represent the ultimate damage to the ecosystem (the biota). Further application of the EFs may include the impacts of organic material discharges with high biological oxygen demand (BOD), if contributing to DO depletion at the modelled water depth.

The spatial differentiation of the effects indicator between CZs is modest. Although the use of the CZ-specific EFs is recommended, the site-generic EF_{global}, also estimated, may be used to represent the average impact on a global ecological community of marine species exposed to hypoxia and applicable when differentiation is not possible or relevant.

4.4. Model improvements and considerations for future work

Species diversity is commonly used to express the impact and damage dimensions in ecosystem quality impact categories in LCIA, e.g. ReCiPe (Goedkoop et al., 2009), Impact 2002+ (Jolliet et al., 2003). In fact, and in most of other cases, it actually refers to species richness, as maximal evenness (equal weight) is assumed. Similarly, the PAF concept also considers each species to be equally important or 'valuable', regardless of potential distinct changes in ecosystem functions caused by their loss (Souza et al., 2013). Modelling species richness alone is a shortcoming in ecosystem impact assessment methods that involve sensitivity and distribution of species. The present method is consistent with other ecosystem-related indicators in LCIA. Nonetheless, method improvements can be achieved by adding uniqueness, vulnerability, resilience, or functional diversity indicators (Souza et al., 2013; Verones et al., 2015).

Gray (2001) refers to a strong latitudinal gradient of increasing species richness from poles to tropics with a strong asymmetry between the two hemispheres. More, as the biogeographical provinces in Australia and Indonesian archipelago likely foster higher species richness than the northern hemisphere, this lowers representativeness and relevance of the results for these regions. A method improvement could address northern and southern CZs distinctly and produce north-south differentiated EF_{CZ}.

Introducing a finer resolution to the spatial units, e.g. reporting $HC50_{LOEC}$ per 66 Large Marine Ecosystems instead of five CZs, would might increase the spatial differentiation of the EF and the discriminatory power of the method (Udo de Haes et al., 1999), minimising the effect of species overlapping that may drive some of the overall modest spatial differentiation. Moreover, the water temperature range that defines the climate zonation is wide enough (5°C on average within each CZ) to engulf sufficient species and produce similar relative contributions per (upper level) taxonomic groups. The LME resolution would further benefit from a narrower temperature range and possibly result in more differentiated LOECs and EFs. However, as noted before,

sensitivity data for more species would be needed to populate every spatial unit at this finer resolution.

5. Conclusions

Applying a spatial resolution of five climate zones, the results of this study describe the increase in the fraction of species that may be affected by hypoxia above their sensitivity threshold in benthic coastal waters. Hypoxia may result from marine eutrophication processes caused by the emission of eutrophying substances from human activities. The proposed method estimates an indicator of the effects caused by hypoxia on exposed marine species. The method uses an ecological community sensitivity index-like HC_{50} as the basis for the EF estimation in LCIA.

High environmental relevance of the effects indicator is given by the conversion of an environmental pressure (DO depletion) into a quantifiable effect on the exposed community, by integrating the sensitivity of individual species to that pressure. In addition, the major sources of variation were addressed and judged not to contribute significantly to the variability of the resulting EF. Despite some concerns with data representativeness and spatial resolution, as discussed, the method works with extensive and published data to support its application in estimating an effect factor. Other applications of the method, and its results, may include the estimation of a hypoxic stress index, useful for ecosystem health status assessments or ecosystems management requiring biodiversity-based indicators. The effect factor in the present context has useful integration in LCIA's modelling of the marine eutrophication impact indicator, and as such, to contribute to the assessment of sustainability of human activities.

Acknowledgements

This research was partly funded by the European Commission under the 7th framework program on environment ENV.2009.3.3.2.1: LC-IMPACT − Improved Life Cycle Impact Assessment methods (LCIA) for better sustainability assessment of technologies, grant agreement 243827. The authors further thank the two anonymous reviewers whose comments/suggestions helped improving this manuscript.

References

Bakun, A., Black, B.A., Bograd, S.J., García-Reyes, M., Miller, A.J., Rykaczewski, R.R., Sydeman, W.J., 2015. Anticipated Effects of Climate Change on Coastal Upwelling Ecosystems. Curr. Clim. Chang. Reports 1, 85–93. doi:10.1007/s40641-015-0008-4

Breitburg, D., 2002. Effects of hypoxia, and the balance between hypoxia and enrichment, on coastal fishes and fisheries. Estuaries 25, 767–781. doi:10.1007/BF02804904

Brett, J.R., 1979. Environmental factors and growth, in: Hoar, W.S., Randall, D.J.,

Brett, J.R. (Eds.), Fish Physiology, Vol. 8. Bioenergetics and Growth. Academic Press, New York, pp. 599–675.

Carpenter, J.H., 1966. New measurements of oxygen solubility in pure and natural water. Limnol. Oceanogr. 11, 264–277.

Chapman, L.J., McKenzie, D.J., 2009. Behavioral responses and ecological consequences, in: Richards, J.G., Farrel, A.P., Brauner, C.J. (Eds.), Fish Physiology, Vol. 27. Hypoxia. Academic Press, London, UK, pp. 25–77.

Childress, J.J., Seibel, B.A., 1998. Life at stable low oxygen levels: adaptations of animals to oceanic oxygen minimum layers. J. Exp. Biol. 201, 1223–1232.

Conley, D.J., Carstensen, J., Vaquer-Sunyer, R., Duarte, C.M., 2009. Ecosystem thresholds with hypoxia. Hydrobiologia 629, 21–29. doi:10.1007/s10750-009-9764-2

Cosme, N., Koski, M., Hauschild, M.Z., 2015. Exposure factors for marine eutrophication impacts assessment based on a mechanistic biological model. Ecol. Modell. 317, 50–63. doi:10.1016/j.ecolmodel.2015.09.005

Cosme, N., Mayorga, E., Hauschild, M.Z., 2016. Spatially explicit fate factors for waterbone nitrogen emissions at the global scale. Int. J. Life Cycle Assesment submitted.

Craig, J.K., Crowder, L.B., 2005. Hypoxia-induced habitat shifts and energetic consequences in Atlantic croaker and brown shrimp on the Gulf of Mexico shelf. Mar. Ecol. Prog. Ser. 294, 79–94. doi:10.3354/meps294079

Davis, J.C., 1975. Minimal dissolved oxygen requirements of aquatic life with emphasis on Canadian species: a review. J. Fish. Res. Board Canada 32, 2295–2332.

de Zwart, D., 2002. Observed regularities in species sensitivity distribution for aquatic species, in: Posthuma, L., Suter II, G.W., Traas, T.P. (Eds.), Species Sensitivity Distributions in Ecotoxicology. Lewis, Boca Raton, pp. 315–344.

Diaz, R.J., Rosenberg, R., 2008. Spreading dead zones and consequences for marine ecosystems. Science (80-.). 321, 926–9. doi:10.1126/science.1156401

Diaz, R.J., Rosenberg, R., 1995. Marine Benthic Hypoxia: a Review of Its Ecological Effects and the Behavioural Responses of Benthic Macrofauna. Oceanogr. Mar. Biol. Annu. Rev. 33, 245–303.

Duffus, J.H., 2003. Glossary for chemists of terms used in toxicology (IUPAC Recommendations 1993). Pure Appl. Chem. 65, 2003–2122.

Ekau, W., Auel, H., Pörtner, H.-O., Gilbert, D., 2010. Impacts of hypoxia on the structure and processes in pelagic communities (zooplankton, macro-invertebrates and fish). Biogeosciences 7, 1669–1699. doi:10.5194/bg-7-1669-2010

FAO, 2015. FAO FishFinder - Web Site. About FAO FishFinder. FI Institutional Websites [WWW Document]. FAO Fish. Aquac. Dep. [online]. Rome. Updat. 19 Febr. 2014. URL http://www.fao.org/fishery/fishfinder/about/en (accessed 10.22.15).

Forstner, H., Gnaiger, E., 1983. Calculation of Equilibrium Oxygen Concentration, in:

Gnaiger, E., Forstner, H. (Eds.), Polarographic Oxygen Sensors. Aquatic and Physiological Applications. Springer, Berlin, Heidelberg, New York:370 pp, pp. 321–333.

Froese, R., Pauly, D., 2015. FishBase [WWW Document]. World Wide Web Electron. Publ. www.fishbase.org, version (10/2015). Accessed 2015-12-28.

Fry, F.E.J., 1971. The effect of environmental factors on the physiology of fish, in: Hoar, W.S., Randall, D.J. (Eds.), Fish Physiology, Vol. 6. Environmental Relations and Behaviour. Academic Press, New York, pp. 1–98.

Gamperl, A.K., Driedzic, W.R., 2009. Cardiovascular function and cardiac metabolism, in: Richards, J.G., Farrel, A.P., Brauner, C.J. (Eds.), Fish Physiology, Vol. 27. Hypoxia. Academic Press, London, UK, pp. 301–360.

Goedkoop, M., Heijungs, R., Huijbregts, M.A.J., De Schryver, A.M., Struijs, J., van Zelm, R., 2009. ReCiPe 2008 - A life cycle impact assessment method which comprises harmonised category indicators at the midpoint and the endpoint level. First edition Report I: Characterisation; 6 January 2009, http://www.lcia-recipe.net.

Gray, J.S., 2001. Marine diversity: the paradigms in patterns of species richness examined. Sci. Mar. 65, 41–56. doi:10.3989/scimar.2001.65s241

Gray, J.S., Wu, R.S., Or, Y.Y., 2002. Effects of hypoxia and organic enrichment on the coastal marine environment. Mar. Ecol. Prog. Ser. 238, 249–279.

Guinée, J.B., Gorrée, M., Heijungs, R., Huppes, G., Kleijn, R., Koning, A. de, Oers, L. van, Sleeswijk, A.W., Suh, S., Udo de Haes, H.A., Bruijn, H. de, Duin, R. van, Huijbregts, M.A.J., 2002. Handbook on life cycle assessment. Operational guide to the ISO standards. I: LCA in perspective. IIa: Guide. IIb: Operational annex. III: Scientific background. Kluwer Academic Publishers, Dordrecht.

Harris, L.A., Duarte, C.M., Nixon, S.W., 2006. Allometric Laws and Prediction in Estuarine and Costal Ecology. Estuaries and Coasts 29, 340–344.

Hauschild, M.Z., 2005. Assessing Environmental Impacts in a Life-Cycle Perspective. Environ. Sci. Technol. 39, 81–88. doi:10.1021/es053190s

Hauschild, M.Z., Potting, J., 2005. Spatial Differentiation in Life Cycle Impact Assessment - The EDIP2003 methodology, Environmental News No. 80.

Heijungs, R., 2005. On the use of units in LCA. Int. J. Life Cycle Assesment 10, 173–176. doi:http://dx.doi.org/10.1065/lca2005.02.199

Henderson, A.D., 2015. Eutrophication, in: Hauschild, M.Z., Huijbregts, M.A.J. (Eds.), Life Cycle Impact Assessment, LCA Compendium - The Complete World of Life Cycle Assessment. Springer Science+Business Media Dordrecht, pp. 177–196.

Henderson, A.D., Hauschild, M.Z., van de Meent, D., Huijbregts, M.A.J., Larsen, H.F., Margni, M., McKone, T.E., Payet, J., Rosenbaum, R.K., Jolliet, O., 2011. USEtox fate and ecotoxicity factors for comparative assessment of toxic emissions in life cycle analysis: sensitivity to key chemical properties. Int. J. Life Cycle Assess. 16, 701–709. doi:10.1007/s11367-011-0294-6

Herreid, C.F.I., 1980. Review: Hypoxia in invertebrates. Comp. Biochem. Physiol. 67A, 311–320.

Hirzel, A.H., Le Lay, G., 2008. Habitat suitability modelling and niche theory. J. Appl. Ecol. 45, 1372–1381. doi:10.1111/j.1365-2664.2008.01524.x

Hofmann, A.F., Peltzer, E.T., Walz, P.M., Brewer, P.G., 2011. Hypoxia by degrees: Establishing definitions for a changing ocean. Deep Sea Res. Part I Oceanogr. Res. Pap. 58, 1212–1226. doi:10.1016/j.dsr.2011.09.004

Hutchinson, G.E., 1957. Concluding remarks. Cold Spring Harb. Symp. Quant. Biol. 22, 415–427.

ICES, 2015a. Oceanography - CTD and Bottle data [WWW Document]. Int. Counc. Explor. Sea. URL http://ocean.ices.dk/HydChem/HydChem.aspx (accessed 10.22.15).

ICES, 2015b. Oceanographic calculator [WWW Document]. Int. Counc. Explor. Sea. URL http://ocean.ices.dk/Tools/Calculator.aspx (accessed 10.22.15).

Itsubo, N., Inaba, A., 2012. LIME2: Life-cycle Impact assessment Method based on Endpoint modeling. JLCA Newsl. Life-Cycle Assess. Soc. Japan 12, 16.

Jolliet, O., Margni, M., Charles, R., Humbert, S., Payet, J., Rebitzer, G., 2003. Presenting a New Method IMPACT 2002 + : A New Life Cycle Impact Assessment Methodology. Int J LCA 8, 324–330.

Justić, D., Rabalais, N.N., Turner, R.E., Wiseman, W.J.J., 1993. Seasonal coupling between riverborne nutrients, net productivity and hypoxia. Mar. Pollut. Bull. 26, 184–189. doi:10.1016/0025-326X(93)90620-Y

Kennedy, V.S., 1990. Anticipated effects of climate change on estuarine and coastal fisheries. Fisheries 15, 16–25. doi:10.1577/1548-8446(1990)015<0016:AEOCCO>2.0.CO;2

Larsen, H.F., Hauschild, M.Z., 2007a. LCA Methodology Evaluation of Ecotoxicity Effect Indicators for Use in LCIA. Int. J. 12, 24–33.

Larsen, H.F., Hauschild, M.Z., 2007b. GM-Troph: A Low Data Demand Ecotoxicity Effect Indicator for Use in LCIA. Int J LCA 12, 79–91.

Levin, L.A., Ekau, W., Gooday, A.J., Jorissen, F., Middelburg, J.J., Naqvi, S.W.A., Neira, C., Rabalais, N.N., Zhang, J., 2009. Effects of natural and human-induced hypoxia on coastal benthos. Biogeosciences 6, 2063–2098.

Levin, S.A., 1994. Patchiness in marine and terrestrial systems: from individuals to populations. Philos. Trans. R. Soc. London, Ser. B 343, 99–103.

Llansó, R.J., 1991. Tolerance of low dissolved oxygen and hydrogen sulfide by the polychaete Streblospio benedicti (Webster). J. Exp. Mar. Bio. Ecol. 153, 165–178. doi:10.1016/0022-0981(91)90223-J

Locarnini, R.A., Mishonov, A. V., Antonov, J.I., Boyer, T.P., Garcia, H.E., Baranova, O.K., Zweng, M.M., Johnson, D.R., 2010. World Ocean Atlas 2009, Volume 1: Temperature, NOAA Atlas NESDIS 68. U.S. Government Printing Office, Washington, D.C.

Middelburg, J.J., Levin, L.A., 2009. Coastal hypoxia and sediment biogeochemistry. Biogeosciences 6, 1273–1293. doi:10.5194/bg-6-1273-2009

Miller, D., Poucher, S., Coiro, L., 2002. Determination of lethal dissolved oxygen levels for selected marine and estuarine fishes, crustaceans, and a bivalve. Mar. Biol. 140, 287–296. doi:10.1007/s002270100702

Naqvi, S.W.A., Bange, H.W., Farías, L., Monteiro, P.M.S., Scranton, M.I., Zhang, J., 2010. Marine hypoxia/anoxia as a source of CH4 and N2O. Biogeosciences 7, 2159–2190. doi:10.5194/bg-7-2159-2010

Nixon, S.W., 1995. Coastal marine eutrophication: A definition, social causes, and future concerns. Ophelia 41, 199–219.

OBIS, 2015. Ocean Biogeographic Information System [WWW Document]. Intergov. Oceanogr. Comm. UNESCO. URL http://www.iobis.org (accessed 10.22.15).

Pennington, D.W., Payet, J., Hauschild, M.Z., 2004. Aquatic Ecotoxicological Indicators In Life-Cycle Assessment. Environ. Toxicol. Chem. 23, 1796–1807.

Perry, S.F., Jonz, M.G., Gilmour, K.M., 2009. Oxygen sensing and the hypoxic ventilatory response, in: Richards, J.G., Farrel, A.P., Brauner, C.J. (Eds.), Fish Physiology, Vol. 27. Hypoxia. Academic Press, London, UK, pp. 193–253.

Pihl, L., Baden, S.P., Diaz, R.J., Schaffner, L.C., 1992. Hypoxia-induced structural changes in the diet of bottom-feeding fish and Crustacea. Mar. Biol. 112, 349–361.

Piiper, J., 1982. Respiratory gas exchange at lungs, gills and tissues: mechanisms and adjustments. J. Exp. Biol. 100, 5–22.

Posthuma, L., Suter II, G.W., Traas, T.P. (Eds.), 2002. Species Sensitivity Distributions in Ecotoxicology, Environmental and Ecological Risk Assessment.

Rabalais, N.N., Diaz, R.J., Levin, L.A., Turner, R.E., Gilbert, D., Zhang, J., 2010. Dynamics and distribution of natural and human-caused coastal hypoxia. Biogeosciences 7, 585–619. doi:10.5194/bgd-6-9359-2009

Rabalais, N.N., Turner, R.E., Diaz, R.J., Justić, D., 2009. Global change and eutrophication of coastal waters. ICES J. Mar. Sci. 66, 1528–1537.

Renaud, M.L., 1986. Hypoxia in Louisina coastal waters during 1983: implications for fisheries. Fish. Bull. 84, 19–26.

Richards, J.G., 2011. Physiological, behavioral and biochemical adaptations of intertidal fishes to hypoxia. J. Exp. Biol. 214, 191–199. doi:10.1242/jeb.047951

Riedel, B., Pados, T., Pretterebner, K., Schiemer, L., Steckbauer, A., Haselmair, A., Zuschin, M., Stachowitsch, M., 2014. Effect of hypoxia and anoxia on invertebrate behaviour: ecological perspectives from species to community level. Biogeosciences 11, 1491–1518. doi:10.5194/bg-11-1491-2014

Roelofs, W., Huijbregts, M.A.J., Jager, T., Ragas, A.M.J., 2003. Prediction of ecological no-effect concentrations for initial risk assessment: combining substance-specific data and database information. Environ. Toxicol. Chem. 22, 1387–93.

Rosenberg, R., Hellman, B., Johansson, B., 1991. Hypoxic tolerance of marine benthic fauna. Mar. Ecol. Prog. Ser. 79, 127–131.

Seibel, B.A., 2011. Critical oxygen levels and metabolic suppression in oceanic oxygen minimum zones. J. Exp. Biol. 214, 326–336. doi:10.1242/jeb.049171

Sherman, K., Hempel, G., 2009. The UNEP Large Marine Ecosystem Report: A perspective on changing conditions in LMEs of the World's Regional Seas, UNEP Regional Seas Report and Studies No. 182.

Souza, D.M. de, Flynn, D.F.B., Declerck, F., Rosenbaum, R.K., De Melo Lisboa, H., Koellner, T., 2013. Land use impacts on biodiversity in LCA: Proposal of characterization factors based on functional diversity. Int. J. Life Cycle Assess. 18, 1231–1242. doi:10.1007/s11367-013-0578-0

Tait, R.V., Dipper, F.A., 1998. Elements of Marine Ecology, 4th ed, Elements of Marine Ecology. Butterworth Heinemann, Oxford. doi:10.1016/B978-075062088-8/50008-1

Turner, R.E., Rabalais, N.N., Justić, D., 2012. Predicting summer hypoxia in the northern Gulf of Mexico: redux. Mar. Pollut. Bull. 64, 319–24. doi:10.1016/j.marpolbul.2011.11.008

U.S. EPA, 2015. Species Sensitivity Distribution Generator [WWW Document]. Causal Anal. Decis. Inf. Syst. – CADDIS, U.S. Environ. Prot. Agency. Version 31-July-2012. URL http://www3.epa.gov/caddis/da_software_ssdmacro.html (accessed 10.22.15).

Udo de Haes, H.A., Finnveden, G., Goedkoop, M., Hauschild, M.Z., Hertwich, E., Hofstetter, P., Jolliet, O., Klöpffer, W., Krewitt, W., Lindeijer, E., Müller-Wenk, R., Olsen, S.I., Pennington, D.W., Potting, J., Steen, B., 2002. Life-Cycle Impact Assessment: Striving Towards Best Practice. SETAC Press, Pensacola, FL, USA.

Udo de Haes, H.A., Jolliet, O., Finnveden, G., Hauschild, M.Z., Krewitt, W., Müller-Wenk, R., 1999. Best Available Practice Regarding Impact Categories and Category Indicators in Life Cycle Impact Assessment. Int J LCA 4, 66–74.

UNESCO, 2009. Global Open Oceans and Deep Seabed (GOODS) - Biogeographic Classification. IOC Technical Series No 84. Paris.

USGS, 2015. DOTABLES - Dissolved oxygen solubility tables [WWW Document]. U.S. Geol. Surv. Off. Water Qual. Version 05-Mar-2014. URL http://water.usgs.gov/software/DOTABLES/ (accessed 10.22.15).

Vaquer-Sunyer, R., Duarte, C.M., 2008. Thresholds of hypoxia for marine biodiversity. Proc. Natl. Acad. Sci. U. S. A. 105, 15452–7. doi:10.1073/pnas.0803833105

Verones, F., Huijbregts, M.A.J., Chaudhary, A., de Baan, L., Koellner, T., Hellweg, S., 2015. Harmonizing the assessment of biodiversity effects from land and water use within LCA. Environ. Sci. Technol. 49, 3584–3592. doi:10.1021/es504995r

WoRMS Editorial Board, 2015. World Register of Marine Species [WWW Document]. World Regist. Mar. Species VLIZ. URL http://www.marinespecies.org (accessed 10.22.15).

WRI, 2011. Interactive Map of Eutrophication & Hypoxia [WWW Document]. World Resour. Inst. URL http://www.wri.org/resource/interactive-map-eutrophication-hypoxia (accessed 10.19.15).

Wu, R.S., 2009. Effects of Hypoxia on Fish Reproduction and Development, in: Richards, J.G., Farrel, A.P., Brauner, C.J. (Eds.), Fish Physiology, Vol. 27. Hypoxia. Academic Press, London, UK, pp. 79–141.

Wu, R.S., 2002. Hypoxia: from molecular responses to ecosystem responses. Mar. Pollut. Bull. 45, 35–45.

Wu, R.S., Zhou, B.S., Randall, D.J., Woo, N.Y.S., Lam, P.K.S., 2003. Aquatic hypoxia is an endocrine disruptor and impairs fish reproduction. Environ. Sci. Technol. 37, 1137–1141. doi:10.1021/es0258327

Zhang, J., Gilbert, D., Gooday, A.J., Levin, L.A., Naqvi, S.W.A., Middelburg, J.J., Scranton, M., Ekau, W., Peña, A., Dewitte, B., Oguz, T., Monteiro, P.M.S., Urban, E., Rabalais, N.N., Ittekkot, V., Kemp, W.M., Ulloa, O., Elmgren, R., Escobar-Briones, E., Van der Plas, A.K., 2010. Natural and human-induced hypoxia and consequences for coastal areas: synthesis and future development. Biogeosciences 7, 1443–1467. doi:10.5194/bg-7-1443-2010

Article III – Supporting Information

Effect factors for marine eutrophication in LCIA based on species sensitivity to hypoxia

Nuno Cosme *, Michael Zwicky Hauschild

Division for Quantitative Sustainability Assessment, Department of Management Engineering, Technical University of Denmark, Produktionstorvet 424, DK-2800 Kgs. Lyngby, Denmark

* *Corresponding author*. Tel.: +45 45254729.

E-mail address: nmdc@dtu.dk

S1. On the method

A method is proposed to estimate an indicator of the potential impacts from hypoxia in benthic marine communities by looking into the stressor intensity (depletion of DO) and its potential effects (based on species sensitivity to hypoxia). As different receiving ecosystems (or spatially differentiated representations of these) hold different species, the resulting sensitivity per spatial unit is expected to differ and spatially differentiated results obtained in a uniform manner for different regional settings on a global scale could be relevant. Such an indicator is useful to represent the damage of eutrophication impacts in LCIA at an adequate resolution. The impact potential to the biological community is derived as Potentially Affected Fraction (PAF) of species by means of a Species Sensitivity Distribution (SSD) probabilistic method.

Concentration-response relationships, such as SSD, have been used before to assess the ecotoxicological risk of chemicals, water quality criteria, environmental risk limits (Posthuma et al., 2002b), impacts of acid deposition on forests (van Zelm et al., 2007), the impacts of sediment-related nontoxic stressors (Smit et al., 2008) and temperature stress (de Vries et al., 2008) in the aquatic environment.

The goal of this study is to develop effect factors for application in the estimation of characterisation factors (CF) for emission with eutrophying impacts in LCIA. First, relevant species were identified as potentially affected by hypoxia and their worldwide distribution found for five climate zones. Second, available data on the sensitivity of these species to hypoxia were used to estimate the sensitivity of the community in each climate zone to, finally, derive effect factors based on the probabilistic species sensitivity distribution using an average approach (Larsen and Hauschild, 2007; Pennington et al., 2004).

S2. Sensitivity to hypoxia – dataset

The biological endpoints compiled from literature are limited to behavioural and physiological. Data are compiled in Table S1.

S3. Benthic water temperature and LME zonation

Large Marine Ecosystems (LME) were grouped into climate zones (CZ, polar, subpolar, temperate, subtropical, tropical) (Fig. S1 and S2) based on time and space-integrated CTD data (conductivity, temperature, and depth) of water temperature at 100 m depth in every LME. NOAA's World Ocean Atlas (Locarnini et al., 2010) was consulted to check for consistency of the values obtained. For the 19 LMEs where CTD-based benthic temperatures were not available, these were estimated from average temperature drop from surface to 100 m depth of the remaining LMEs in the same CZ, using mean annual sea surface temperature per LME available in Sherman and Hempel (2009).

Table S1 Summary table of data compiled on relevant species, sensitivity data and biological endpoints tested. Abbreviations: Benthopelagic (Bp), Demersal (Dem), Benthic (Bt), Benthic infauna (Bt in), and Benthic epifauna (Bt epi), data not available (n.a.). [a] LOEC estimated for 20 ppm salinity (brackish waters species), [b] environmental parameters extracted from the Ocean Biogeographic Information System (OBIS, 2015).

Group	Scientific name	Common name	Habitat	Reported threshold (value @Temp. and Sal.)	Benthic LOEC [mgO_2L^{-1}]		Biological endpoint tested	Reference
					mean	range		
Fish	*Squalus suckleyi*	Spotted spiny dogfish	Bp	6.69 $mgO_2 \cdot L^{-1}$; 11°C; *(35 ppm)*	7.5	6.7-8.1	Blood ceases to be fully O_2 saturated	(Lenfant and Johansen, 1966) as reported by (Davis, 1975)
Fish	*Scyliorhinus canicula*	Small-spotted catshark	Dem	80 mmHg PO_2; 12°C; 35 ppm	4.4	4.0-5.2	Oxygen consumption rate	(Hughes and Umezawa, 1968a)
Fish	*Hydrolagus colliei*	Spotted ratfish	Dem	8.54 $mgO_2 \cdot L^{-1}$; 11°C; *(35 ppm)*	9.4	8.6-10.2	Blood ceases to be fully O_2 saturated	(Hanson, 1967) as reported by (Davis, 1975)
Fish	*Trinectes maculatus*	Hogchoker	Dem	64% O_2Sat; 25°C; 19 ppm	5.1	4.5-6.4	Ventilation rate	(Pihl et al., 1991)
Fish	*Paralichthys dentatus*	Summer flounder	Dem	3.5 $mgO_2 \cdot L^{-1}$; 20°C; 25 ppm	4.2	3.4-5.0	Growth rate	(Stierhoff et al., 2006)
Fish	*Pseudopleuronectes americanus*	Winter flounder	Dem	5.0 $mgO_2 \cdot L^{-1}$; 20°C; 25 ppm	6.4	5.7-6.9	Growth rate	(Stierhoff et al., 2006)
Fish	*Paralichthys lethostigma*	Southern flounder	Dem	2.8 $mgO_2 \cdot L^{-1}$; 22°C; 30 ppm	3.0	2.8-3.4	Growth rate	(Taylor and Miller, 2001)
Fish	*Platichthys flesus*	European flounder	Dem	30% O_2Sat; 13°C; 5 ppm	2.8	2.5-3.1	Ventilation rate	(Tallqvist et al., 1999)
Fish	*Ammodytes tobianus*	Lesser sand eel	Dem	35% O_2Sat; 10°C; 30 ppm	3.3	2.9-3.7	Behaviour, emerging and burying rates	(Behrens et al., 2010)
Fish	*Zoarces viviparus*	Viviparous eelpout	Dem	30% O_2Sat; 12.2°C; 13.8 ppm	2.9	2.7-3.1	Behaviour, motionless	(Fischer et al., 1992)
Fish	*Rhacochilus vacca*	Pile perch	Dem	4.56 $mgO_2 \cdot L^{-1}$; 12°C; 10 ppm	4.2	4.0-4.4	Blood ceases to be fully O_2 saturated	(Webb and Brett, 1972) as reported by (Davis, 1975)
Fish	*Leiostomus xanthurus*	Spot	Dem	44% O_2Sat; 25°C; 19 ppm	3.9	3.5-4.4	Ventilation rate	(Pihl et al., 1991)
Fish	*Callionymus lyra*	Common dragonet	Dem	125 mmHg PO_2; 11.5°C; 35 ppm	7.1	6.2-8.1	Oxygen consumption rate	(Hughes and Umezawa, 1968b)

Group	Scientific name	Common name	Habitat	Reported threshold (value @Temp. and Sal.)	Benthic LOEC [mgO_2L^{-1}]		Biological endpoint tested	Reference
					mean	range		
Fish	*Anarhichas minor*	Spotted wolffish	Dem	20% O_2Sat; 4.1°C; 34 ppm	2.1	1.8-2.4	Plasma cortisol level	(Lays et al., 2009)Lays et al. (2009)
Fish	*Argyrosomus japonicus*	Mulloway	Bp	1.8 $mgO_2 \cdot L^{-1}$; 22°C; 35 ppm	2.0	1.8-2.3	Oxygen consumption rate	(Fitzgibbon et al., 2007)
Fish	*Acanthopagrus schlegelii*	Blackhead seabream	Dem	27 mmHg PO_2; 25°C; 30 ppm	1.3	1.2-1.5	P_{50}, oxygen dissociation	(Wu and Woo, 1984)
Fish	*Epinephelus akaara*	Hong Kong grouper	Dem	50 mmHg PO_2; 25°C; 30 ppm	2.5	2.3-2.9	P_{50}, oxygen dissociation	(Wu and Woo, 1984)
Fish	*Diplodus annularis*	Sea carp	Bp	25% O_2Sat; 19°C; 35 ppm	2.1	2.0-2.4	Ventilation rate	(Silkin and Silkina, 2005)
Fish	*Diplodus puntazzo*	Sharpsnout seabream	Bp	51.37-78.98% O_2Sat *f*(T); 15-29°C; 38 ppm	4.8	4.8-4.8	S_{Vf}, ventilatory frequency	(Cerezo and García García, 2004)
Fish	*Oncorhynchus kisutch*	Coho salmon	Dem	4.5 $mgO_2 \cdot L^{-1}$; *(18.5°C; 35 ppm)*	5.9	5.1-6.2	Behaviour, erratic avoidance	(Whitmore et al., 1960) in (Vaquer-Sunyer and Duarte, 2008)
Fish	*Oncorhynchus tshawytscha*	Chinook salmon	Bp	4.5 $mgO_2 \cdot L^{-1}$; *(18.5°C; 35 ppm)*	5.4	4.8-5.8	Behaviour, avoidance	(Whitmore et al., 1960) in (Vaquer-Sunyer and Duarte, 2008)
Fish	*Salmo salar*	Atlantic salmon	Bp	4.5 $mgO_2 \cdot L^{-1}$; 15°C; *(35 ppm)*	4.4	3.7-5.3	Critical O_2 level for swimming performance	(Kutty and Saunders, 1973)
Fish	*Fundulus heteroclitus*	Mummichog	Bp	4.5 $mgO_2 \cdot L^{-1}$; 20°C; *(35 ppm)*	5.4	4.1-6.2	Reduced hatching	(Voyer and Hennekey, 1972) as reported by (Davis, 1975)
Fish	*Scorpaena porcus*	Rock perch	Dem	60.5% O_2Sat; 19°C; 35 ppm	2.1	1.8-2.4	Ventilation rate	(Silkin and Silkina, 2005)
Fish	*Gadus morhua*	Atlantic cod	Bp	16.5-30.3% O_2Sat *f*(T); 5-15°C; *(35 ppm)*	1.7	1.1-2.1	S_{crit}, critical oxygen saturation	(Schurmann and Steffensen, 1997)
Fish	*Gadus macrocephalus*	Pacific cod	Dem	2.5 $mgO_2 \cdot L^{-1}$; 4°C; 15 ppm	2.1	1.7-2.5	Reproduction, egg development	(Alderdice and Forrester, 1971)
Crustacean	*Squilla empusa*	Mantis shrimp	Bt	25% O_2Sat; 25°C; 19 ppm	2.0	1.7-2.6	Ventilation rate	(Pihl et al., 1991)
Crustacean	*Saduria entomon*	Baltic Sea crayfish	Bt	33% O_2Sat; 5°C; 6.5 ppm	3.5	2.9-3.9	Predation rate	(Johansson, 1999)

Group	Scientific name	Common name	Habitat	Reported threshold (value @Temp. and Sal.)	Benthic LOEC [mgO_2L^{-1}]		Biological endpoint tested	Reference
					mean	range		
Crustacean	*Monoporeia affinis*	White freshwater amphipod	Bt	9.81% O_2Sat; 5°C; 6.5 ppm [a]	1.2	1.0-1.3	Survival	(Johansson, 1997)
Crustacean	*Pontoporeia femorata*	--	Bt	9.81% O_2Sat; 5°C; 6.5 ppm [a]	1.2	1.0-1.3	Survival	(Johansson, 1997)
Crustacean	*Penaeus setiferus*	White shrimp	Bt	1.5 $mgO_2 \cdot L^{-1}$; 22°C; 22 ppm	1.5	1.4-1.8	Behaviour, avoidance	(Renaud, 1986)
Crustacean	*Penaeus aztecus*	Brown shrimp	Bt	2.0 $mgO_2 \cdot L^{-1}$; 22°C; 22 ppm	2.0	1.7-2.4	Behaviour, avoidance	(Renaud, 1986)
Crustacean	*Callinectes sapidus*	Blue crab	Bt	73 torr PO_2; 24°C; 30 ppm	2.7	2.1-3.7	Feeding rate	(Das and Stickle, 1993)
Crustacean	*Callinectes similis*	Lesser blue crab	Bt	50 torr PO_2; 24°C; 30 ppm	2.5	2.3-2.8	Feeding rate	(Das and Stickle, 1993)
Crustacean	*Carcinus maenas*	Common shore crab	Bt	60 torr PO_2; 10°C; 30 ppm	3.6	3.2-4.1	Heart rate	(Hill et al., 1991)
Crustacean	*Munida quadrispina*	Squat lobster	Bt	0.10-0.15 $mgO_2 \cdot L^{-1}$; 9.75°C; 30.4 ppm	0.1	0.1-0.1	Survival	(Burd and Brinkhurst, 1984)
Crustacean	*Homarus gammarus*	European lobster	Bt	10% O_2Sat; 10.5°C; 32 ppm	2.2	2.0-2.4	Survival	(Rosenberg et al., 1991)
Crustacean	*Nephrops norvegicus*	Norway lobster	Bt	20% O_2Sat; 8°C; 33 ppm	1.8	1.7-1.9	Blood Hcy concentration; + avoidance	(Baden et al., 1990)
Crustacean	*Penaeus schmitti*	Prawn	Bt	1.2(5.0) $mgO_2 \cdot L^{-1}$; 30(28)°C; 30(38) ppm	2.5	2.4-2.9	Behaviour; + (critical oxygen level in postlarvae)	(Rosas et al., 1997); (MacKay, 1974)
Crustacean	*Pilumnus spinifer*	Red hairy crab	Bt	2 $mlO_2 \cdot L^{-1}$; 20.3°C; 38 ppm	0.2	0.2-0.2	Locomotory activity	(Haselmair et al., 2010)
Crustacean	*Nepinnotheres pinnotheres*	European pea crab	Bt	0.5 $mlO_2 \cdot L^{-1}$; 20.3°C; 38 ppm	0.9	0.8-0.9	Locomotory activity	(Haselmair et al., 2010)
Crustacean	*Pisidia longimana*	Long-clawed porcelain crab	Bt	2 $mlO_2 \cdot L^{-1}$; 20.3°C; 38 ppm	3.5	3.3-3.7	Locomotory activity	(Haselmair et al., 2010)
Crustacean	*Galathea strigosa*	Spinous squad lobster	Bt	2 $mlO_2 \cdot L^{-1}$; 20.3°C; 38 ppm	3.6	3.3-3.8	Locomotory activity	(Haselmair et al., 2010)
Crustacean	*Macropodia rostrata*	Long-legged spider crab	Bt	2 $mlO_2 \cdot L^{-1}$; 20.3°C; 38 ppm	3.6	3.1-4.1	Locomotory activity	(Haselmair et al., 2010)
Crustacean	*Eurynome aspera*	Strawberry crab	Bt	2 $mlO_2 \cdot L^{-1}$; 20.3°C; 38 ppm	3.4	2.9-3.8	Locomotory activity	(Haselmair et al., 2010)

Group	Scientific name	Common name	Habitat	Reported threshold (value @Temp. and Sal.)	Benthic LOEC [mgO_2L^{-1}]		Biological endpoint tested	Reference
					mean	range		
Crustacean	*Inachus dorsettensis*	Scorpion spider crab	Bt	2 $mlO_2 \cdot L^{-1}$; 20.3°C; 38 ppm	3.2	2.9-3.8	Locomotory activity	(Haselmair et al., 2010)
Crustacean	*Ebalia tuberosa*	Pennant's nut crab	Bt	2 $mlO_2 \cdot L^{-1}$; 20.3°C; 38 ppm	3.6	3.3-3.8	Locomotory activity	(Haselmair et al., 2010)
Crustacean	*Ethusa mascarone*	Stalkeye sumo crab	Bt	1 $mlO_2 \cdot L^{-1}$; 20.3°C; 38 ppm	1.6	1.5-1.7	Locomotory activity	(Haselmair et al., 2010)
Crustacean	*Philocheras monacanthus*	--	Bt	1.5 $mgO_2 \cdot L^{-1}$; 20°C; 30 ppm	1.7	1.7-1.7	Oxygen consumption rate	(González-Ortegón et al., 2013)
Crustacean	*Penaeus vannamei*	Pacific white shrimp	Bt	1 $mgO_2 \cdot L^{-1}$; 28°C; 31 ppm	1.2	1.1-1.2	Growth and instantaneous growth rate	(Seidman and Lawrence, 1985)
Crustacean	*Penaeus monodon*	Giant tiger prawn	Bt	1 $mgO_2 \cdot L^{-1}$; 28°C; 31 ppm	1.1	1.0-1.1	Growth and instantaneous growth rate	(Seidman and Lawrence, 1985)
Crustacean	*Calocaris macandreae*	Dwarf lobster	Bt	6.7 torr PO_2; 10°C; 32 ppm	0.4	0.4-0.4	Tissue L-lactate accumulation	(Anderson et al., 1994)
Crustacean	*Crangon crangon*	Common shrimp	Bt	30% O_2Sat; 13°C; 4.5 ppm	2.8	2.5-3.1	Predation rate	(Sandberg et al., 1996)
Mollusc	*Kurtiella bidentata*	Lens-shaped shell clam	Bt	10% O_2Sat; 12°C; 33.5 ppm	0.9	0.8-1.0	Behaviour, sediment emergence	(Nilsson and Rosenberg, 1994)
Mollusc	*Abra alba*	White furrow shell	Bt	1 $mgO_2 \cdot L^{-1}$; 18°C; 29 ppm	1.1	1.1-1.2	Behaviour, siphons extended	(Jørgensen, 1980)
Mollusc	*Abra nitida*	--	Bt	10% O_2Sat; 10.5°C; 32 ppm	0.9	0.8-1.0	Survival	(Rosenberg et al., 1991)
Mollusc	*Theora lata*	Shining theora	Bt	0.9 $mlO_2 \cdot L^{-1}$; 23.5°C; 28.3 ppm	1.3	1.2-1.4	Feeding activity	(Tamai, 1996)
Mollusc	*Cerastoderma edule*	Common cockle	Bt	1 $mgO_2 \cdot L^{-1}$; 18°C; 29 ppm	0.7	0.6-0.7	Behaviour, siphons extended	(Jørgensen, 1980)
Mollusc	*Ruditapes decussatus*	Grooved carpet shell	Bt	7.3 kPa PO_2; 20°C; 35.6 ppm	3.0	2.9-3.1	Aerobic metabolic rate	(Sobral and Widdows, 1997)
Mollusc	*Mya arenaria*	Soft-shell clam	Bt	1 $mgO_2 \cdot L^{-1}$; 18°C; 29 ppm	0.7	0.6-0.8	Behaviour, siphons extended	(Jørgensen, 1980)

Group	Scientific name	Common name	Habitat	Reported threshold (value @Temp. and Sal.)	Benthic LOEC [mgO_2L^{-1}]		Biological endpoint tested	Reference
					mean	range		
Mollusc	*Mytilus edulis*	Blue mussel	Bt	5.3 kPa PO_2; 15°C; 32 ppm	2.3	2.2-2.4	Aerobic metabolic rate	(Wang and Widdows, 1993)
				25.0-34.4% O_2Sat *f*(T); 10-25°C; *(35 ppm)*			Switch to oxyconformity	(Artigaud et al., 2014)
Mollusc	*Pecten maximus*	Great scallop	Bt	18.3-36.1% O_2Sat *f*(T); 10-25°C; *(35 ppm)*	1.6	1.3-1.8	Switch to oxyconformity	(Artigaud et al., 2014)
Mollusc	*Aplysia californica*	California seahare	Bt	10% O_2Sat; 16.5°C; 33 ppm	3.9	3.9-3.9	Respiratory pumping	(Kanz and Quast, 1992)
Mollusc	*Haliotis laevigata*	Greenlip abalone	Bt	5.91 $mgO_2 \cdot L^{-1}$ = 77% O_2Sat; 18°C; 34 ppm	6.7	6.6-6.9	EC_{50}, specific growth rate	(Harris et al., 1999)
Mollusc	*Peringia ulvae*	Laver spire shell	Bt	1 $mgO_2 \cdot L^{-1}$; 18°C; 29 ppm	0.7	0.7-0.7	Behaviour, climbing on shells	(Jørgensen, 1980)
Mollusc	*Philine aperta*	Sand slug	Bt	12% O_2Sat; 18°C; 25.5 ppm	1.0	0.8-1.1	Behaviour, sediment emergence	(Nilsson and Rosenberg, 1994)
Molluscs	*Nassarius siquijorensis*	Burned nassa	Bt	1.5 $mgO_2 \cdot L^{-1}$; 24°C; 30 ppm	1.5	1.5-1.7	SfG, scope for growth	(Liu et al., 2011)
Mollusc	*Nassarius conoidalis*	Cone-shaped nassa	Bt	3.0 $mgO_2 \cdot L^{-1}$; 24°C; 30 ppm	3.1	2.9-3.4	SfG, scope for growth	(Liu et al., 2011)
Mollusc	*Stramonita haemastoma*	Red-mouthed rock shell	Bt	50 torr PO_2; 24°C; 30 ppm	2.5	2.1-3.0	Feeding rate	(Das and Stickle, 1993)
Mollusc	*Octopus vulgaris*	Common octopus	Bt	15.7-47.1% O_2Sat *f*(T); 15.5-27.4°C; 38 ppm	5.1	4.2-7.9	S_{crit}, critical oxygen saturation	(Cerezo Valverde and García García, 2005)
Echinoderm	*Luidia clathrata*	Lined sea star	Bt	44 mmHg PO_2; 24°C; 25 ppm	2.1	1.9-2.5	AC, activity coefficient	(Diehl et al., 1979)
Echinoderm	*Echinocardium cordatum*	Sea potato	Bt	25% O_2Sat; 18°C; 25.5 ppm	2.2	1.8-2.4	Behaviour, turn over on back	(Nilsson and Rosenberg, 1994)
Echinoderm	*Psammechinus miliaris*	Green sea urchin	Bt	6.6 kPa PO_2; 12°C; 34 ppm	2.9	2.8-3.0	EC_{50}, oxygen uptake	(Spicer, 1995)
Echinoderm	*Ophiura albida*	Brittlestar	Bt	12% O_2Sat; 10.5°C; 32 ppm	1.1	1.0-1.2	Behaviour, sediment emergence	(Rosenberg et al., 1991)

Group	Scientific name	Common name	Habitat	Reported threshold (value @Temp. and Sal.)	Benthic LOEC [mgO_2L^{-1}]		Biological endpoint tested	Reference
					mean	range		
Echinoderm	*Amphiura filiformis*	Brittlestar	Bt	13(22)% O_2Sat; 10.5(12)°C; 32(34) ppm	1.6	1.5-1.8	Behaviour, sediment emergence	(Rosenberg et al., 1991); (Nilsson and Rosenberg, 1994)
Echinoderm	*Amphiura chiaje*	Brittlestar	Bt	8% O_2Sat; 10.5°C; 32 ppm	0.7	0.7-0.8	Behaviour, sediment emergence	(Rosenberg et al., 1991)
Echinoderm	*Microphiopholis atra*	Brittlestar	Bt	0.71 $mgO_2 \cdot L^{-1}$; *(18.7°C; 34.3 ppm)* [b]	0.7	0.6-0.8	n.a.	(Diaz et al., 1992) in (Vaquer-Sunyer and Duarte, 2008)
Echinoderm	*Holothuria forskali*	Black sea cucumber	Bt	0.86 $mgO_2 \cdot L^{-1}$; 17°C; *(35 ppm)*	0.9	0.9-1.0	Oxygen consumption	(Astall and Jones, 1991) in (Vaquer-Sunyer and Duarte, 2008)
Echinoderm	*Labidoplax buskii*	Sea cucumber	Bt	16% O_2Sat; 12°C; 33.5 ppm	1.4	1.2-1.6	Behaviour, sediment emergence	(Nilsson and Rosenberg, 1994)
Annelid	*Lagis koreni*	Trumpet worm	Bt in	30% O_2Sat; 18°C; 25.5 ppm	2.8	2.7-2.9	Behaviour, sediment emergence	(Nilsson and Rosenberg, 1994)
Annelid	*Loimia medusa*	Spaghetti worm	Bt in	14% O_2Sat; 26°C; *(20 ppm)*	1.1	1.0-1.3	Feeding stops	(Llansó and Diaz, 1994)
Annelid	*Capitella capitata*	Gallery worm	Bt in	35 mmHg PO_2; 22°C; 28 ppm	2.0	1.5-2.6	Growth rate	(Forbes and Lopez, 1990)
Annelid	*Scoloplos armiger*	Bristleworm	Bt in	60 torr PO_2; 12°C; 32 ppm	3.8	2.7-4.5	Oxygen consumption rate	(Schöttler and Grieshaber, 1988)
Annelid	*Paraprionospio pinnata*	--	Bt in	1.14 $mgO_2 \cdot L^{-1}$; *(14.1°C; 35 ppm)* [b]	1.3	1.0-1.5	n.a.	(Diaz et al., 1992) in (Vaquer-Sunyer and Duarte, 2008)
Annelid	*Streblospio benedicti*	--	Bt in	14.5% air sat; 26°C; 20 ppm	1.2	1.0-1.5	Lethargy and avoidance behaviour	(Llansó, 1991)
Annelid	*Malacoceros fuliginosus*	--	Bt in	30% O_2Sat; 11°C; 35 ppm	2.9	2.5-3.6	Avoidance behaviour	(Tyson and Pearson, 1991)
Cnidarian	*Halitholus pauper*	--	Bp	30.6 hPa PO_2; 10°C; 30 ppm	1.7	1.7-1.7	P_c, critical oxygen tensions	(Rutherford and Thuesen, 2005)

Group	Scientific name	Common name	Habitat	Reported threshold (value @Temp. and Sal.)	Benthic LOEC [mgO_2L^{-1}]		Biological endpoint tested	Reference
					mean	range		
Cnidarian	*Polyorchis penicillatus*	Penicillate jellyfish	Bp	9.7 hPa PO_2; 10°C; 30 ppm	0.4	0.4-0.5	P_c, critical oxygen tensions	(Rutherford and Thuesen, 2005)
Cnidarian	*Ceriantheopsis americanus*	Mud anemone	Bt	0.71 $mgO_2 \cdot L^{-1}$; *(15.1°C; 33.8 ppm)* [b]	0.7	0.6-0.8	n.a.	(Diaz, unpublished data) in (Vaquer-Sunyer and Duarte, 2008)
Cnidarian	*Bunodosoma cavernatum*	Warty Sea Anemone	Bt epi	40 mmHg PO_2; 22.5°C; 30 ppm	1.8	1.7-1.9	VO_2, oxygen consumption	(Ellington, 1982)
Cnidarian	*Metridium senile*	Plumose anemone	Bt epi	1 $ml \cdot L^{-1}$; 23°C; 35 ppm	1.8	1.3-2.2	Oxygen consumption rate	(Sassaman and Mangum, 1972)

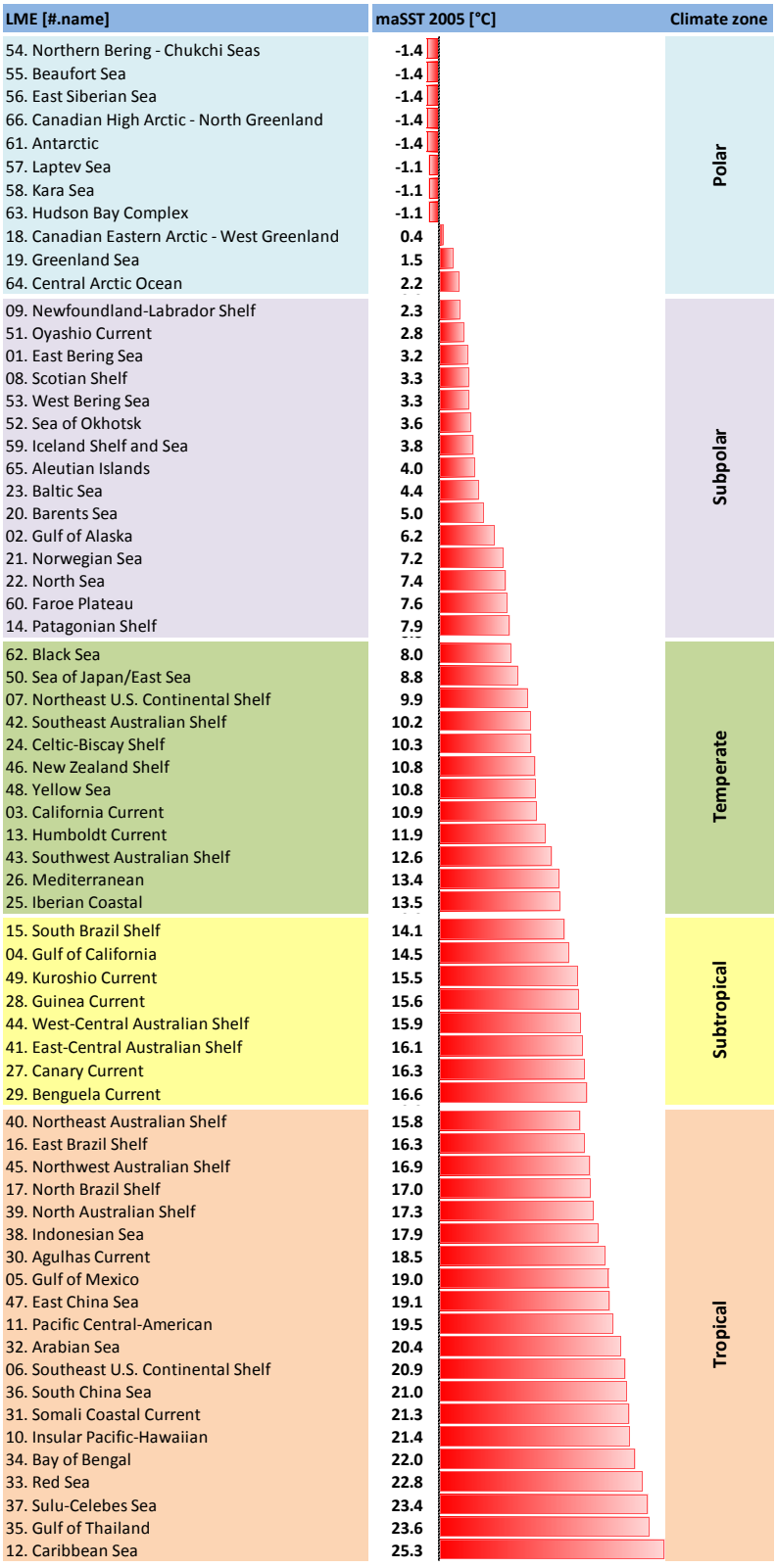

Figure S1 Classification of Large Marine Ecosystems (LME) into climate zones (polar, subpolar, temperate, subtropical, and tropical) based on mean annual water temperature at 100 m depth. Data retrieved from ICES Oceanographic database (ICES, 2015a). Complementary information from the World Ocean Atlas (NCEI, 2015) was used where necessary to adjust for local and regional effects of ocean circulation and upwelling.

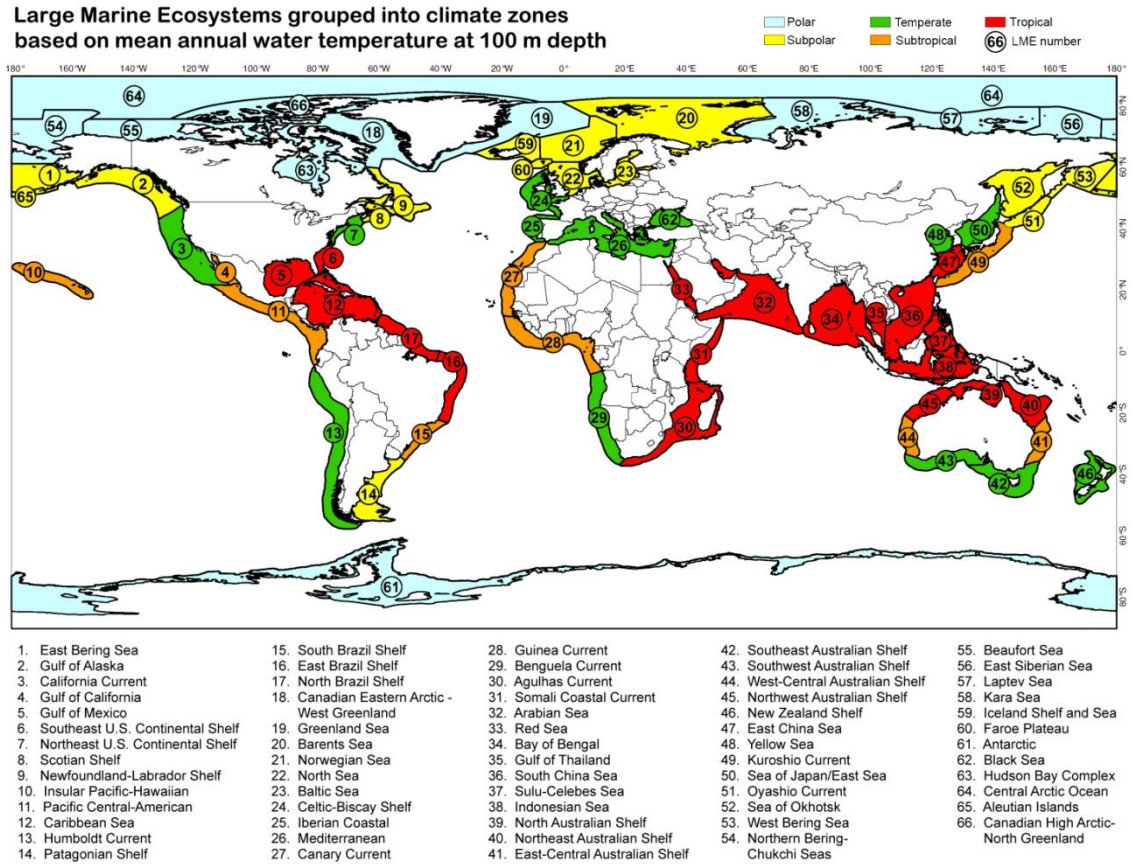

Figure S2 Geographic distribution of the 66 Large Marine Ecosystems (LMEs) for which the water temperature at 100 m depth was used to group them into the five proposed climate zones (polar, subpolar, temperate, subtropical, tropical) (spatial units coloured from the original digital map available at http://lme.edc.uri.edu/).

S4. Sensitivity to hypoxia – data conversion to benthic conditions

Oxygen solubility varies as a function of temperature and electrolyte content (i.e. salinity) (Forstner and Gnaiger, 1983). Water temperature shows a wider variation (Figure S3) in coastal waters than salinity (Figure S4). A marginal variation of temperature makes oxygen solubility values vary three times more than similar change in salinity – this is obtainable from the algorithms producing DO tables, e.g. USGS's 'Dissolved oxygen solubility tables' (USGS, 2015) and ICES's 'Oceanographic Calculator' (ICES, 2015b). For these reasons salinity was kept constant (at 35 ppm) and temperature variability used to model benthic waters conditions.

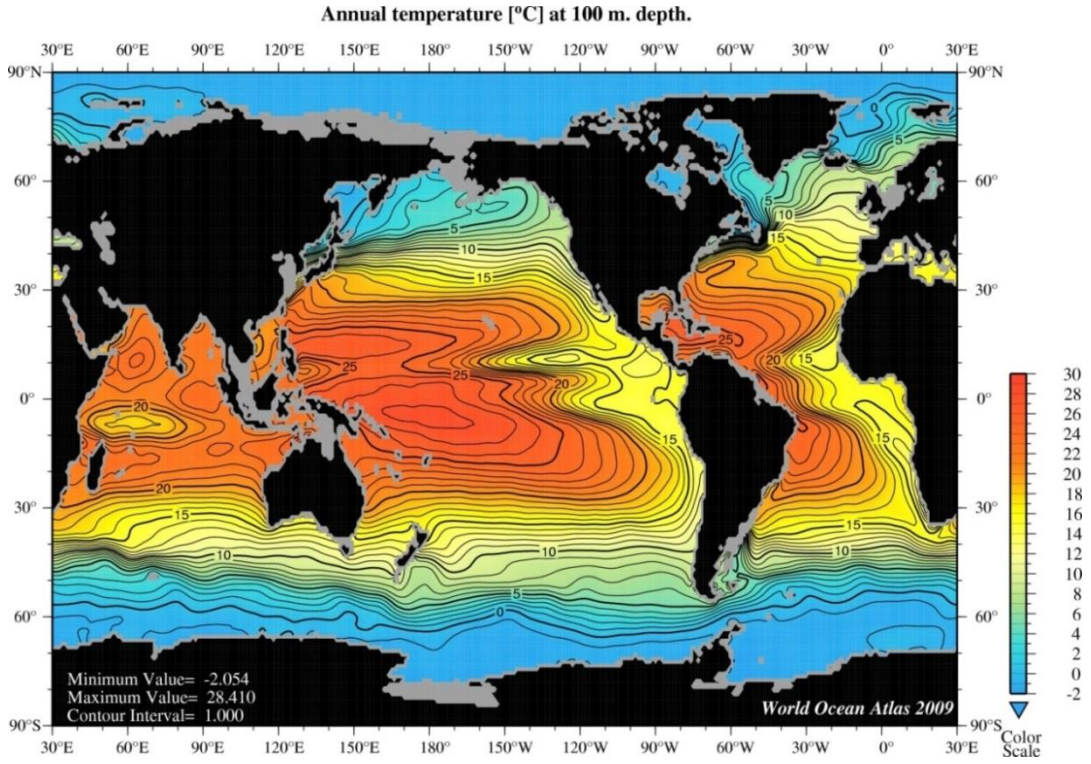

Figure S3 Climatology-type view of the global distribution of annual records of ocean water temperature (in °C) at 100 metres depth. Source: World Ocean Atlas 2009 (NCEI, 2015) and Locarnini et al. (2010).

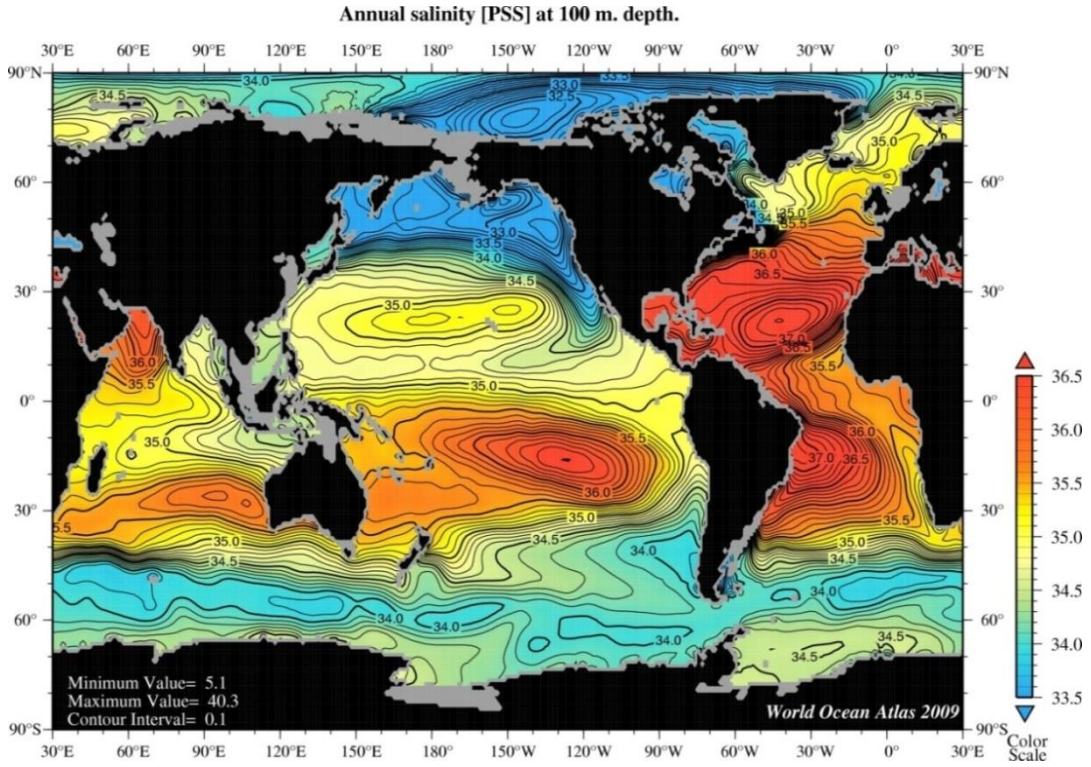

Figure S4 Climatology-type view of the global distribution of annual records of ocean water salinity (Practical Salinity Scale – PSS and Practical Salinity Units – PSU) at 100 metres depth. Source: World Ocean Atlas 2009 (NCEI, 2015) and Antonov et al. (2010).

Maximum oxygen solubility can be determined from its temperature-dependence at both experimental/laboratorial conditions and benthic water mass temperature. Sensitivity thresholds ($LOEC_{lab}$) determined by experiments or observations (as compiled in Table S1) reported in PO_2, DO concentration ($ml \cdot L^{-1}$, $mg \cdot L^{-1}$) (or already in %Sat) were converted to %Sat. A fixed %Sat is assumed to define the sensitivity threshold for the same species in the benthic habitat (at 100 m depth and altered temperature, thus a different maximum solubility) – this assumption means that the physiological/behavioural response defining the endpoint tested in the original laboratory experiment/observation is equivalent at the benthic conditions and no other factors modify the sensitivity threshold (e.g. a critical O_2 concentration, PO_2 or %Sat). The fixed %Sat is therefore used to estimate the critical benthic concentration ($LOEC_{benthic}$) by multiplying it with the maximum benthic oxygen solubility. Figure S5 depicts the calculations done and shows an example of hypothetical experimental and benthic temperature conditions.

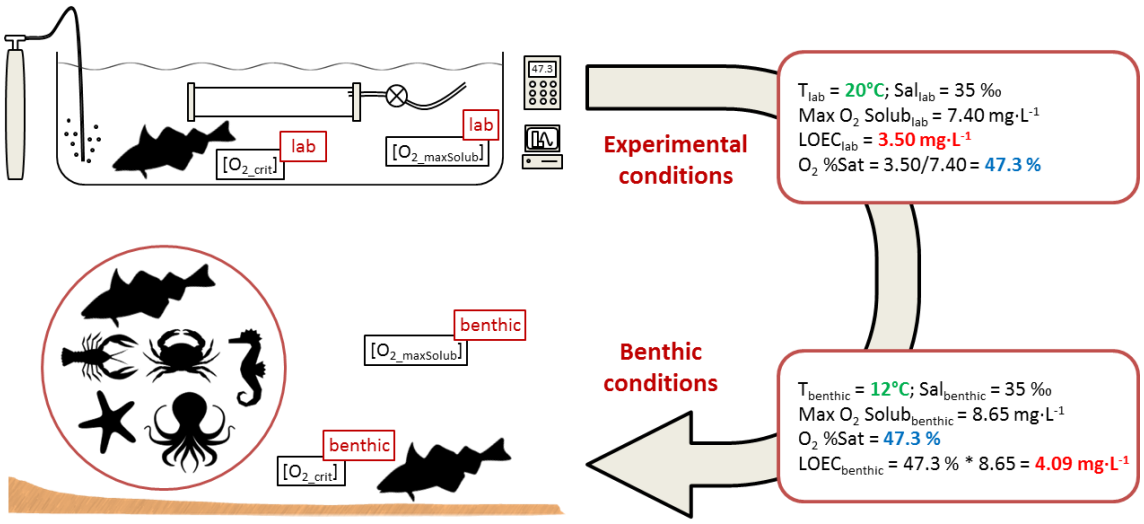

Figure S5 Diagram explaining the method for adjustment of reported laboratorial LOEC data to benthic temperature conditions, based on correction of maximum solubility of oxygen for water temperature (salinity assumed constant at 35 $g \cdot kg^{-1}$) and fixed saturation (%Sat). Example of LOEC conversion calculations is shown in right hand side boxes for hypothetical experimental temperature setup at 20°C and benthic water temperature at 12°C. Oxygen solubility values computed with USGS's 'Dissolved oxygen solubility tables' (USGS, 2015) and ICES's 'Oceanographic Calculator' (ICES, 2015b).

The compiled sensitivity thresholds to hypoxia for the relevant benthic, demersal, and benthopelagic species were adjusted for 66 LME benthic conditions, resulting in 582 sensitivity data points (LOEC, in $mgO_2 \cdot L^{-1}$). Results of the LOEC conversion to benthic conditions are shown in Table S2, the species occurrence per climate zone in Fig. S6., and the comparison between the sensitivity thresholds per taxonomic group compiled from Vaquer-Sunyer and Duarte (2008) based on arithmetic

mean and the ones obtained in the present work based on the geometric mean of LOECs from literature (Table S3).

Table S2 Sensitivity to hypoxia of 91 species of six taxonomic groups (fish, crustaceans, molluscs, echinoderms, annelids, and cnidarians) and their occurrence in the 66 Large Marine Ecosystems (LME) grouped into six climate zones (CZ, polar, subpolar, temperate, subtropical, and tropical). Data reported corresponds to sensitivity thresholds (LOEC, in $mgO_2 \cdot L^{-1}$) compiled from literature and adjusted to benthic water temperature. (Tables in the next 4 pages).

CZ	Geographic distribution	T_b [°C]	*Squalus suckleyi*	*Scyliorhinus canicula*	*Hydrolagus colliei*	*Trinectes maculatus*	*Paralichthys dentatus*	*Pseudopleuronectes americanus*	*Paralichthys lethostigma*	*Platichthys flesus*	*Ammodytes tobianus*	*Zoarces viviparus*	*Rhacochilus vacca*	*Leiostomus xanthurus*	*Callionymus lyra*	*Anarhichas minor*	*Argyrosomus japonicus*	*Acanthopagrus schlegelii*	*Epinephelus akaara*	*Diplodus annularis*	*Diplodus puntazzo*	*Oncorhynchus kisutch*	*Oncorhynchus tshawytscha*	*Salmo salar*	*Fundulus heteroclitus*	*Scorpaena porcus*	*Gadus morhua*	*Gadus macrocephalus*
	Classification, taxa (n = 94)		26 fish species																									
	Class		Elasmobranchii	Elasmobranchii	Holocephali	Actinopterygii	Actinopterygii	Actinopterygii	Actinopterygii	Actinopterygii	Actinopterygii	Actinopterygii	Actinopterygii	Actinopterygii	Actinopterygii	Actinopterygii	Actinopterygii	Actinopterygii	Actinopterygii	Actinopterygii	Actinopterygii	Actinopterygii	Actinopterygii	Actinopterygii	Actinopterygii	Actinopterygii	Actinopterygii	Actinopterygii
	Order		Squaliformes	Carcharhiniformes	Chimaeriformes	Pleuronectiformes	Pleuronectiformes	Pleuronectiformes	Pleuronectiformes	Pleuronectiformes	Perciformes	Perciformes	Perciformes	Perciformes	Perciformes	Perciformes	Perciformes	Perciformes	Perciformes	Perciformes	Perciformes	Salmoniformes	Salmoniformes	Salmoniformes	Cyprinodontiformes	Scorpaeniformes	Gadiformes	Gadiformes
	Common name		Spotted spiny dogfish	Small-spotted catshark	Spotted ratfish	Hogchoker	Summer flounder	Winter flounder	Southern flounder	European flounder	Lesser sand eel	Viviparous eelpout	Pile perch	Spot	Common dragonet	Spotted wolffish	Mulloway	Blackhead seabream	Hong Kong grouper	Sea carp	Sharpsnout seabream	Coho salmon	Chinook salmon	Atlantic salmon	Mummichog	Rock perch	Atlantic cod	Pacific cod
CZ	Geographic distribution	T_b [°C]	Sensitivity data (LOEC) [$mgO_2 \cdot L^{-1}$] @ $f(T_b)$, -100 m, 35 ppm																									
Polar CZ (11 LMEs)	18. Canadian Eastern Arctic - West Greenland	0.4														2.3											1.1	
	19. Greenland Sea	1.5														2.2											1.3	
	54. Northern Bering - Chukchi Seas	-1.4																										2.5
	55. Beaufort Sea	-1.4																										
	56. East Siberian Sea	-1.4																										
	57. Laptev Sea	-1.1																										
	58. Kara Sea	-1.1																										
	61. Antarctic	-1.4																										
	63. Hudson Bay Complex	-1.1														2.4								5.3				
	64. Central Arctic Ocean	2.2																										
	66. Canadian High Arctic - North Greenland	-1.4																										
Subpolar CZ (15 LMEs)	01. East Bering Sea	3.2	8.0		10.2																	6.1	5.8					2.2
	02. Gulf of Alaska	6.2	7.5		9.5						3.4		4.4									5.7	5.4	4.4				2.1
	08. Scotian Shelf	3.3					5.0	6.7								2.1						6.1		4.7	6.0		1.5	
	09. Newfoundland-Labrador Shelf	2.3						6.9								2.2								4.8	6.2		1.4	
	14. Patagonian Shelf	7.9																										
	20. Barents Sea	5.0														2.0								4.5			1.7	
	21. Norwegian Sea	7.2													7.6												1.9	
	22. North Sea	7.4		4.8						2.9	3.4	2.9			7.5	1.9								4.3		2.4	1.9	
	23. Baltic Sea	4.4		5.2						3.1	3.6	3.1			8.1									4.6			1.6	
	51. Oyashio Current	2.8	8.1																			6.2						
	52. Sea of Okhotsk	3.6	7.9																			6.1						2.2
	53. West Bering Sea	3.3	8.0																			6.1	5.8					2.2
	59. Iceland Shelf and Sea	3.8									3.7					2.1											1.5	
	60. Faroe Plateau	7.6																									1.9	
	65. Aleutian Islands	4.0																				6.0	5.7					2.2
Temperate CZ (12 LMEs)	03. California Current	10.9	6.7		8.6								4.0									5.1	4.8					1.9
	07. Northeast U.S. Continental Shelf	9.9				6.4	4.2	5.7	3.4					4.4		1.8						5.3		4.0	5.1		2.1	
	13. Humboldt Current	11.9																										
	24. Celtic-Biscay Shelf	10.3		4.5						2.7	3.1	2.7			7.0									4.0			2.1	
	25. Iberian Coastal	13.5								2.5	2.9				6.6											2.1		
	26. Mediterranean	13.4		4.2						2.5	2.9				6.6					2.1	4.8			3.7				
	42. Southeast Australia	10.2															2.3											
	43. Southwest Australia	12.6																										
	46. New Zealand Shelf	10.8																					4.9					
	48. Yellow Sea	10.8	6.7															1.5										1.9
	50. Sea of Japan/East Sea	8.8	7.0																2.9									2.0
	62. Black Sea	8.0								2.8										2.4						2.4		
Subtropical CZ (9 LMEs)	4. Gulf of California	14.5																										
	11. Pacific Central-American	19.5																										
	15. South Brazil Shelf	15.9																										
	27. Canary Current	16.6		4.0											6.2					2.0	4.8					2.0		
	28. Guinea Current	15.6		4.0																	4.8							
	29. Benguela Current	14.1																										
	41. East-Central Australia	16.1															2.0											
	44. West-Central Australia	15.5																										
	49. Kuroshio Current	16.3															2.0	1.3										1.7
Tropical CZ (19 LMEs)	5. Gulf of Mexico	19.0				5.3			2.9					3.6														
	6. Southeast U.S. Continental Shelf	20.9				5.1	3.4		2.8					3.5											4.1			
	10. Insular Pacific-Hawaiian	21.4																										
	12. Caribbean Sea	25.3				4.7																						
	16. East Brazil Shelf	21.6				4.6																						
	17. North Brazil Shelf	22.3				4.5																						
	30. Agulhas Current	19.9															1.9											
	31. Somali Coastal Current	21.3																										
	32. Arabian Sea	20.4																										
	33. Red Sea	22.8																								1.8		
	34. Bay of Bengal	22.0																										
	35. Gulf of Thailand	23.6																										
	36. South China Sea	21.0															1.8	1.2	2.3									
	37. Sulu-Celebes Sea	23.4																										
	38. Indonesian Sea	23.1																										
	39. North Australia	22.6																										
	40. Northeast Australia	21.1																										
	45. Northwest Australia	22.1																										
	47. East China Sea	19.1															1.9	1.3	2.4									

			27 crustacean species																									
		Classification, taxa (n = 94)	Class	Order	Common name	Scientific name																						
			Malacostraca	Stomatopoda	Mantis shrimp	*Squilla empusa*																						
			Malacostraca	Isopoda	Baltic Sea crayfish	*Saduria entomon*																						
			Malacostraca	Amphipoda	White freshwater amphipod	*Monoporeia affinis*																						
			Malacostraca	Amphipoda	--	*Pontoporeia femorata*																						
			Malacostraca	Decapoda	White shrimp	*Peneus setiferus*																						
			Malacostraca	Decapoda	Brown shrimp	*Peneus aztecus*																						
			Malacostraca	Decapoda	Blue crab	*Callinectes sapidus*																						
			Malacostraca	Decapoda	Lesser blue crab	*Callinectes similis*																						
			Malacostraca	Decapoda	Common shore crab	*Carcinus maenas*																						
			Malacostraca	Decapoda	Squat lobster	*Munida quadrispina*																						
			Malacostraca	Decapoda	European lobster	*Homarus gammarus*																						
			Malacostraca	Decapoda	Norway lobster	*Nephrops norvegicus*																						
			Malacostraca	Decapoda	Prawn	*Peneus schmitti*																						
			Malacostraca	Decapoda	Red hairy crab	*Pilumnus spinifer*																						
			Malacostraca	Decapoda	European pea crab	*Nepinnotheres pinnotheres*																						
			Malacostraca	Decapoda	Long-clawed porcelain crab	*Pisidia longimana*																						
			Malacostraca	Decapoda	Spinous squad lobster	*Galathea strigosa*																						
			Malacostraca	Decapoda	Long-legged spider crab	*Macropodia rostrata*																						
			Malacostraca	Decapoda	Strawberry crab	*Eurynome aspera*																						
			Malacostraca	Decapoda	Scorpion spider crab	*Inachus dorsettensis*																						
			Malacostraca	Decapoda	Pennant's nut crab	*Ebalia tuberosa*																						
			Malacostraca	Decapoda	Stalkeye sumo crab	*Ethusa mascarone*																						
			Malacostraca	Decapoda	--	*Philocheras monacanthus*																						
			Malacostraca	Decapoda	Pacific white shrimp	*Peneus vannamei*																						
			Malacostraca	Decapoda	Giant tiger prawn	*Peneus monodon*																						
			Malacostraca	Decapoda	Dwarf lobster	*Cabcaris macandreae*																						
			Malacostraca	Decapoda	Common shrimp	*Crangon crangon*																						
CZ	Geographic distribution	T_b [°C]	Sensitivity data (LOEC) [$mgO_2 \cdot L^{-1}$] @ $f(T_b)$, -100 m, 35 ppm																									
Polar CZ (11 LMEs)	18. Canadian Eastern Arctic - West Greenland	0.4																										
	19. Greenland Sea	1.5																										
	54. Northern Bering - Chukchi Seas	-1.4		3.9		1.3																						
	55. Beaufort Sea	-1.4		3.9	1.3	1.3																						
	56. East Siberian Sea	-1.4																										
	57. Laptev Sea	-1.1		3.9		1.3																						
	58. Kara Sea	-1.1																										
	61. Antarctic	-1.4																										
	63. Hudson Bay Complex	-1.1			1.3	1.3																						
	64. Central Arctic Ocean	2.2																										
	66. Canadian High Arctic - North Greenland	-1.4																										
Subpolar CZ (15 LMEs)	01. East Bering Sea	3.2		3.5		1.1																						
	02. Gulf of Alaska	6.2		3.2		1.1				3.7	0.1																	
	08. Scotian Shelf	3.3	2.6					3.7		4.0																		
	09. Newfoundland-Labrador Shelf	2.3								4.1																		
	14. Patagonian Shelf	7.9						3.0																				
	20. Barents Sea	5.0		3.3		1.1																						
	21. Norwegian Sea	7.2										2.4																
	22. North Sea	7.4						3.0		3.6		2.4	1.9					3.8	3.8	3.8	3.8	3.8				0.4	2.9	
	23. Baltic Sea	4.4		3.4	1.1	1.1													4.1								3.1
	51. Oyashio Current	2.8																										
	52. Sea of Okhotsk	3.6																										
	53. West Bering Sea	3.3																										
	59. Iceland Shelf and Sea	3.8																										
	60. Faroe Plateau	7.6																										
	65. Aleutian Islands	4.0																										
Temperate CZ (12 LMEs)	03. California Current	10.9		2.9	1.0					3.3	0.1																	
	07. Northeast U.S. Continental Shelf	9.9	2.3			1.0	1.8	2.4	2.8	2.8	3.4															0.4		
	13. Humboldt Current	11.9																										
	24. Celtic-Biscay Shelf	10.3							2.8		3.4		2.2	1.8			0.9		3.5	3.5	3.5	3.5	3.5				0.4	2.7
	25. Iberian Coastal	13.5									3.2			1.7														2.5
	26. Mediterranean	13.4							2.6				2.1	1.7		0.2	0.8	3.3	3.3	3.3	3.3	3.3	3.3	1.7	1.7		0.4	2.5
	42. Southeast Australia	10.2									3.4																	
	43. Southwest Australia	12.6																										
	46. New Zealand Shelf	10.8																										
	48. Yellow Sea	10.8																										
	50. Sea of Japan/East Sea	8.8				1.0																						
	62. Black Sea	8.0																3.7										2.8
Subtropical CZ (9 LMEs)	4. Gulf of California	14.5																										
	11. Pacific Central-American	19.5																						1.6		1.2		
	15. South Brazil Shelf	15.9							2.5						2.9													
	27. Canary Current	16.6											2.0						3.1		3.1							
	28. Guinea Current	15.6																						1.6				
	29. Benguela Current	14.1																			3.3							
	41. East-Central Australia	16.1																										
	44. West-Central Australia	15.5																										
	49. Kuroshio Current	16.3																										
Tropical CZ (19 LMEs)	5. Gulf of Mexico	19.0	1.9				1.5	2.0	2.4	2.4														1.5		1.1	1.1	
	6. Southeast U.S. Continental Shelf	20.9	1.8				1.4	1.9	2.3	2.3																1.1	1.1	
	10. Insular Pacific-Hawaiian	21.4																										
	12. Caribbean Sea	25.3	1.7					1.7	2.1						2.4													
	16. East Brazil Shelf	21.6							2.2						2.5													
	17. North Brazil Shelf	22.3	1.8					1.8							2.5													
	30. Agulhas Current	19.9																		2.9	2.9						1.1	
	31. Somali Coastal Current	21.3																			2.9						1.1	
	32. Arabian Sea	20.4																			2.9						1.1	
	33. Red Sea	22.8																										
	34. Bay of Bengal	22.0																									1.1	
	35. Gulf of Thailand	23.6																									1.0	
	36. South China Sea	21.0																									1.1	
	37. Sulu-Celebes Sea	23.4																										
	38. Indonesian Sea	23.1																										
	39. North Australia	22.6																									1.1	
	40. Northeast Australia	21.1																									1.1	
	45. Northwest Australia	22.1																									1.1	
	47. East China Sea	19.1																										

			17 mollusc species																	
			Classification, taxa (n = 98)																	
			Class	Bivalvia	Bivalvia	Bivalvia	Bivalvia	Bivalvia	Bivalvia	Bivalvia	Bivalvia	Bivalvia	Gastropoda	Gastropoda	Gastropoda	Gastropoda	Gastropoda	Gastropoda	Gastropoda	Gastropoda	Cephalopoda
			Order	Veneroida	Veneroida	Veneroida	Veneroida	Veneroida	Veneroida	Myoida	Mytiloida	Pectinoida	Anaspidea	Vetigastropoda	Littorinimorpha	Cephalaspidea	Neogastropoda	Neogastropoda	Neogastropoda	Octopoda
			Common name	Lens-shaped shell clam	White furrow shell	--	Shining theora	Common cockle	Grooved carpet shell	Soft-shell clam	Blue mussel	Great scallop	California seahare	Greenlip abalone	Laver spire shell	Sand slug	Burned nassa	Cone-shaped nassa	Red-mouthed rock shell	Common octopus
			Scientific name	*Kurtiella bidentata*	*Abra alba*	*Abra nitida*	*Theora lata*	*Cerastoderma edule*	*Ruditapes decussatus*	*Mya arenaria*	*Mytilus edulis*	*Pecten maximus*	*Aplysia californica*	*Haliotis laevigata*	*Peringia ulvae*	*Philine aperta*	*Nassarius siquijorensis*	*Nassarius conoidalis*	*Stramonita haemastoma*	*Octopus vulgaris*
CZ	Geographic distribution	T_b [°C]	Sensitivity data (LOEC) [$mgO_2 \cdot L^{-1}$] @ $f(T_b)$, -100 m, 35 ppm																	
Polar CZ (11 LMEs)	18. Canadian Eastern Arctic - West Greenland	0.4								2.3										
	19. Greenland Sea	1.5																		
	54. Northern Bering - Chukchi Seas	-1.4																		
	55. Beaufort Sea	-1.4								2.2										
	56. East Siberian Sea	-1.4																		
	57. Laptev Sea	-1.1																		
	58. Kara Sea	-1.1																		
	61. Antarctic	-1.4																		
	63. Hudson Bay Complex	-1.1								2.2										
	64. Central Arctic Ocean	2.2																		
	66. Canadian High Arctic - North Greenland	-1.4																		
Subpolar CZ (15 LMEs)	01. East Bering Sea	3.2																		
	02. Gulf of Alaska	6.2							0.7	2.3										
	08. Scotian Shelf	3.3							0.8	2.3										6.6
	09. Newfoundland-Labrador Shelf	2.3							0.8	2.3										
	14. Patagonian Shelf	7.9								2.3									3.0	
	20. Barents Sea	5.0			1.0				0.8	2.3					0.7					
	21. Norwegian Sea	7.2			1.0					2.3										
	22. North Sea	7.4	1.0	1.2	1.0		0.7		0.7	2.3	1.3				0.7	1.1				6.0
	23. Baltic Sea	4.4	1.0				0.7		0.7	2.3					0.7					
	51. Oyashio Current	2.8																		
	52. Sea of Okhotsk	3.6																		
	53. West Bering Sea	3.3																		
	59. Iceland Shelf and Sea	3.8								2.3										
	60. Faroe Plateau	7.6																		
	65. Aleutian Islands	4.0																		
Temperate CZ (12 LMEs)	03. California Current	10.9							0.6	2.4		3.9								
	07. Northeast U.S. Continental Shelf	9.9							0.7	2.3									2.8	5.7
	13. Humboldt Current	11.9								2.4										
	24. Celtic-Biscay Shelf	10.3	0.9	1.1	0.9		0.7	3.1	0.7	2.3	1.6				0.7	1.1				5.6
	25. Iberian Coastal	13.5						2.9		2.4										5.3
	26. Mediterranean	13.4	0.8	1.1	0.8		0.6	2.9		2.4	1.8					1.0			2.6	5.3
	42. Southeast Australia	10.2											6.9							
	43. Southwest Australia	12.6											6.6							
	46. New Zealand Shelf	10.8								2.4										
	48. Yellow Sea	10.8								2.4										5.6
	50. Sea of Japan/East Sea	8.8																		
	62. Black Sea	8.0	0.9	1.2	0.9		0.7		0.7											
Subtropical CZ (9 LMEs)	4. Gulf of California	14.5																		
	11. Pacific Central-American	19.5																		
	15. South Brazil Shelf	15.9																	2.5	5.0
	27. Canary Current	16.6																	2.5	7.9
	28. Guinea Current	15.6														1.0			2.5	5.0
	29. Benguela Current	14.1														1.0			2.6	5.3
	41. East-Central Australia	16.1				1.4												3.4		
	44. West-Central Australia	15.5																		
	49. Kuroshio Current	16.3															1.7	3.4		
Tropical CZ (19 LMEs)	5. Gulf of Mexico	19.0																	2.4	4.7
	6. Southeast U.S. Continental Shelf	20.9							0.6											4.6
	10. Insular Pacific-Hawaiian	21.4																		
	12. Caribbean Sea	25.3																	2.1	4.2
	16. East Brazil Shelf	21.6																	2.2	4.5
	17. North Brazil Shelf	22.3																		4.4
	30. Agulhas Current	19.9														0.9	1.6	3.1		4.6
	31. Somali Coastal Current	21.3																3.0		
	32. Arabian Sea	20.4																3.1		
	33. Red Sea	22.8																		4.4
	34. Bay of Bengal	22.0				1.3												3.0		4.5
	35. Gulf of Thailand	23.6				1.2											1.5			
	36. South China Sea	21.0														0.9	1.5	3.1		4.5
	37. Sulu-Celebes Sea	23.4															1.5			
	38. Indonesian Sea	23.1															1.5	2.9		4.4
	39. North Australia	22.6														0.8		3.0		
	40. Northeast Australia	21.1														0.9		3.0		
	45. Northwest Australia	22.1														0.8				
	47. East China Sea	19.1																		

		Classification, taxa (n = 102)	9 echinoderm species									7 annelid species							5 cnidarian species				
		Class	Asteroidea	Echinoidea	Echinoidea	Ophiuroidea	Ophiuroidea	Ophiuroidea	Ophiuroidea	Holothuroidea	Holothuroidea	Polychaeta	Polychaeta	Polychaeta	Polychaeta	Polychaeta	Polychaeta	Polychaeta	Hydrozoa	Hydrozoa	Anthozoa	Anthozoa	Anthozoa
		Order	Paxillosida	Spatangoida	Camarodonta	Ophiurida	Ophiurida	Ophiurida	Ophiurida	Aspidochirotida	Apodida	Terebellida	Terebellida	Capitellida	Orbiniida	Spionida	Spionida	Spionida	Anthoathecata	Anthoathecata	Ceriantharia	Actiniaria	Actiniaria
		Common name	Lined sea star	Sea potato	Green sea urchin	Brittlestar	Brittlestar	Brittlestar	Brittlestar	Black sea cucumber	Sea cucumber	Trumpet worm	Spaghetti worm	Gallery worm	Bristleworm	--	--	--	--	Penicillate jellyfish	Mud anemone	Warty Sea Anemone	Plumose anemone
		Scientific name	*Luidia clathrata*	*Echinocardium cordatum*	*Psammechinus miliaris*	*Ophiura albida*	*Amphiura filiformis*	*Amphiura chiaje*	*Microphiopholis atra*	*Holothuria forskali*	*Labidoplax buskii*	*Lagis koreni*	*Loimia medusa*	*Capitella capitata*	*Scoloplos armiger*	*Paraprionospio pinnata*	*Streblospio benedicti*	*Malacoceros fuliginosus*	*Halitholus pauper*	*Polyorchis penicillatus*	*Ceriantheopsis americanus*	*Bunodosoma cavernatum*	*Metridium senile*
CZ	Geographic distribution	T_b [°C]	Sensitivity data (LOEC) [$mgO_2 \cdot L^{-1}$] @ $f(T_b)$, -100 m, 35 ppm									LOEC [$mgO_2 \cdot L^{-1}$] @ $f(T_b)$, -100 m, 35 ppm							LOEC [$mgO_2 \cdot L^{-1}$] @ $f(T_b)$ 35 ppm				
Polar CZ (11 LMEs)	18. Canadian Eastern Arctic - West Greenland	0.4												2.5	4.3								2.1
	19. Greenland Sea	1.5													4.2								
	54. Northern Bering - Chukchi Seas	-1.4												2.6	4.5								2.2
	55. Beaufort Sea	-1.4												2.6	4.5			3.6	1.7				
	56. East Siberian Sea	-1.4																					
	57. Laptev Sea	-1.1													4.5								
	58. Kara Sea	-1.1																					
	61. Antarctic	-1.4												2.6									
	63. Hudson Bay Complex	-1.1												2.6	4.5								
	64. Central Arctic Ocean	2.2																					
	66. Canadian High Arctic - North Greenland	-1.4																					
Subpolar CZ (15 LMEs)	01. East Bering Sea	3.2												2.3	4.0								1.9
	02. Gulf of Alaska	6.2												2.2	3.7					0.5			1.8
	08. Scotian Shelf	3.3												2.3	4.0		1.5						1.9
	09. Newfoundland-Labrador Shelf	2.3												2.4	4.1								2.0
	14. Patagonian Shelf	7.9														1.3					0.8		
	20. Barents Sea	5.0				1.2	1.8				1.6			2.2	3.8								1.9
	21. Norwegian Sea	7.2		2.4		1.2	1.7				1.5			2.1	3.6			2.9					1.8
	22. North Sea	7.4		2.4	3.0	1.1	1.7	0.8			1.5	2.9		2.1	3.6		1.4	2.9					1.8
	23. Baltic Sea	4.4				1.2	1.8							2.3	3.9		1.5						1.9
	51. Oyashio Current	2.8																					2.0
	52. Sea of Okhotsk	3.6																					
	53. West Bering Sea	3.3																					
	59. Iceland Shelf and Sea	3.8																					1.9
	60. Faroe Plateau	7.6																					
	65. Aleutian Islands	4.0												2.3									1.9
Temperate CZ (12 LMEs)	03. California Current	10.9												1.9	3.3	1.2	1.3			0.4			1.6
	07. Northeast U.S. Continental Shelf	9.9	2.5	2.3					0.8		1.4		1.3	2.0	3.4	1.2	1.3				0.8		1.7
	13. Humboldt Current	11.9												1.9		1.2							
	24. Celtic-Biscay Shelf	10.3		2.2	2.8	1.1	1.6	0.7			1.4	2.7	1.3	2.0	3.4		1.3	2.7					1.6
	25. Iberian Coastal	13.5				1.0	1.5			0.9													
	26. Mediterranean	13.4		2.1		1.0	1.5	0.7				2.7		1.8	3.2	1.2		2.5					
	42. Southeast Australia	10.2		2.2						1.0													
	43. Southwest Australia	12.6																					
	46. New Zealand Shelf	10.8		2.2										2.0		1.2							
	48. Yellow Sea	10.8		2.2									1.2	2.0	3.3	1.2					0.8		
	50. Sea of Japan/East Sea	8.8																					1.7
	62. Black Sea	8.0					1.6	0.8				2.8		2.1									
Subtropical CZ (9 LMEs)	4. Gulf of California	14.5																					
	11. Pacific Central-American	19.5														1.1							
	15. South Brazil Shelf	15.9	2.2						0.7				1.1	1.8		1.1							
	27. Canary Current	16.6								0.9													
	28. Guinea Current	15.6																					
	29. Benguela Current	14.1								0.9						1.2							
	41. East-Central Australia	16.1																					
	44. West-Central Australia	15.5																					
	49. Kuroshio Current	16.3		2.0																			1.4
Tropical CZ (19 LMEs)	5. Gulf of Mexico	19.0	2.1						0.7		1.2		1.1	1.7		1.0	1.1				0.7	1.9	
	6. Southeast U.S. Continental Shelf	20.9	2.0	1.8					0.7		1.2		1.0	1.6	2.7	1.0	1.1				0.6	1.8	
	10. Insular Pacific-Hawaiian	21.4											1.0	1.6			1.0						
	12. Caribbean Sea	25.3	1.9						0.6					1.5		0.9	1.0					1.7	
	16. East Brazil Shelf	21.6	2.0																				
	17. North Brazil Shelf	22.3	2.0													1.0							
	30. Agulhas Current	19.9																					
	31. Somali Coastal Current	21.3												1.6									
	32. Arabian Sea	20.4											1.0	1.6		1.0							
	33. Red Sea	22.8																					
	34. Bay of Bengal	22.0											1.0	1.6		1.0							1.3
	35. Gulf of Thailand	23.6																					
	36. South China Sea	21.0											1.0								0.6		
	37. Sulu-Celebes Sea	23.4																					
	38. Indonesian Sea	23.1																					
	39. North Australia	22.6																					
	40. Northeast Australia	21.1											1.0										
	45. Northwest Australia	22.1																					
	47. East China Sea	19.1		1.9										1.7									

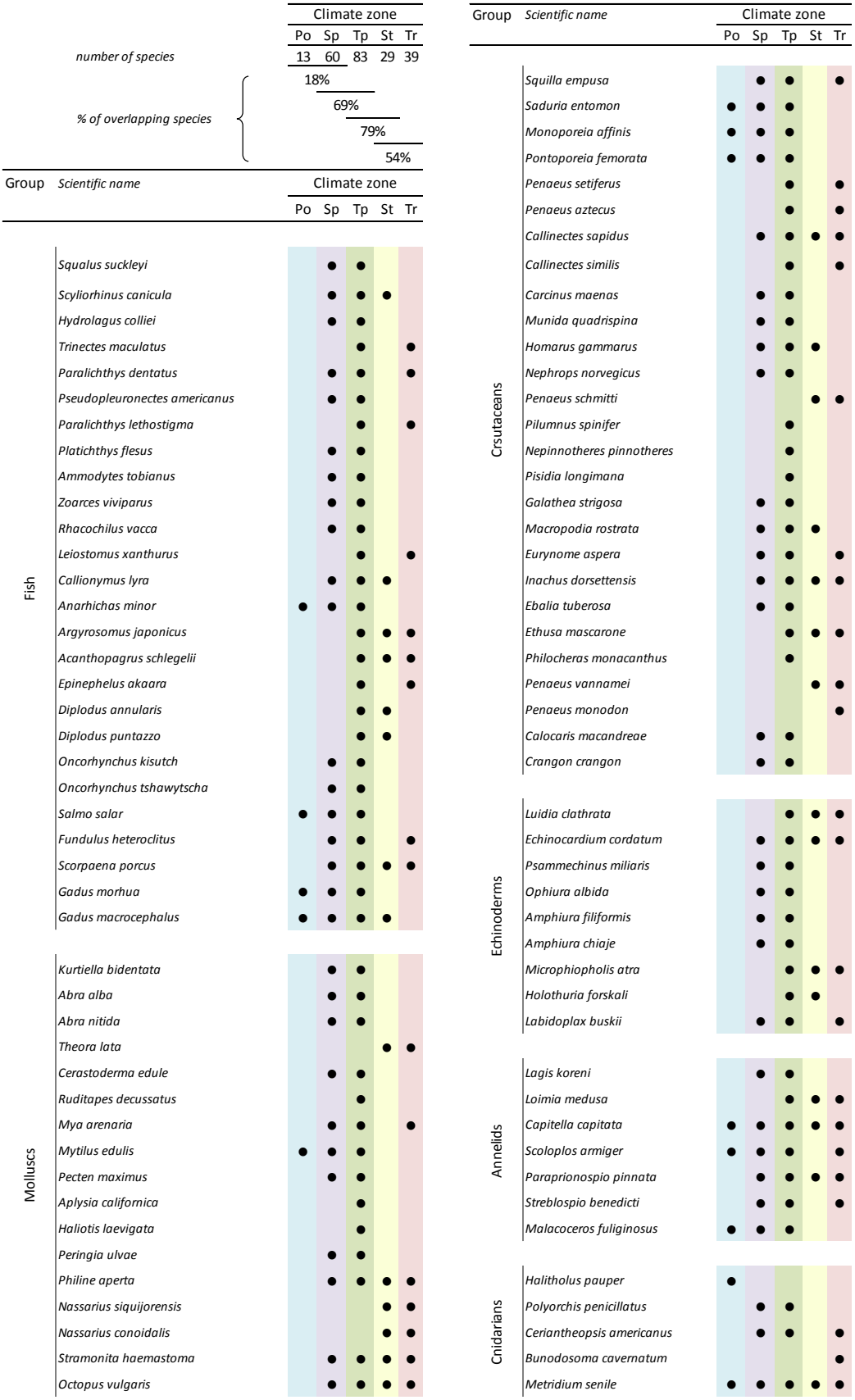

Figure S6 Species occurrence per climate zone – Polar (Po), Subpolar (Sp), Temperate (Tp), Subtropical (St), and Tropical (Tr).

Table S3 Comparison of sensitivity thresholds per taxonomic group obtained from arithmetic mean (Vaquer-Sunyer and Duarte, 2008) and geometric mean (GM, present work). The former was obtained from sublethal concentrations (SLC_{50}) of all species reported and compiled in reference source, and the latter from lowest-observed-effect-concentrations (LOEC) on benthic, demersal, and benthopelagic species only. Standard error of the mean (SEM) included.

Source	Vaquer-Sunyer and Duarte (2008)		Present work	
Taxonomic group	SLC_{50}	SEM	GM_{LOEC}	SEM
	$[mgO_2 \cdot L^{-1}]$	$[mgO_2 \cdot L^{-1}]$	$[mgO_2 \cdot L^{-1}]$	$[mgO_2 \cdot L^{-1}]$
Fish	4.41	0.39	3.46	0.40
Crustaceans	3.21	0.28	1.93	0.20
Molluscs	1.99	0.16	1.85	0.40
Echinoderms	1.22	0.22	1.42	0.20
Annelids	1.20	0.25	1.90	0.40
Cnidarians	0.69	0.11	1.36	0.24

S5. Estimation of $HC50_{LOEC}$

The ecological community's joint sensitivity (per LME) can be expressed by using the Species Sensitivity Distribution (SSD) methodology (Posthuma et al., 2002a). Details of the fitting of the PAF function to the LOEC data are included in Table S4 together with the $HC50_{LOEC}$ obtained per climate zone and a site-generic global default, all with accompanying 95% confidence intervals.

Table S4 Estimation of $HC50_{LOEC}$ from the SSD methodology and statistics of the data fitting (see also Eqs. 2 and 3). Legend: number of species (*n* sp.), number of LOEC data points (*n* LOECs), sample mean or location parameter (α), scale parameter (β), coefficient of determination (R^2), confidence interval (CI).

			SSD curve fit parameters					$HC50_{LOEC}$					
Climate zone	***n* sp.**	***n* LOECs**	**α**	**β**	**Slope**	**Interc.**	**R^2**	95% lower CI	**$mgO_2 \cdot L^{-1}$**	95% upper CI	95% lower CI	**$kgO_2 \cdot m^{-3}$**	95% upper CI
polar	13	34	0.390	0.111	4.82	3.08	0.940	2.05	**2.45**	3.08	2.05E-03	**2.45E-03**	3.08E-03
subpolar	60	175	0.384	0.170	3.22	3.76	0.973	2.00	**2.42**	2.96	2.00E-03	**2.42E-03**	2.96E-03
temperate	83	193	0.308	0.169	3.20	4.01	0.969	1.66	**2.03**	2.52	1.66E-03	**2.03E-03**	2.52E-03
subtropical	29	45	0.336	0.140	3.90	3.68	0.983	1.91	**2.17**	2.48	1.91E-03	**2.17E-03**	2.48E-03
tropical	39	135	0.243	0.131	4.13	3.99	0.972	1.50	**1.75**	2.04	1.50E-03	**1.75E-03**	2.04E-03
global	91	582	0.323	0.159	3.45	3.88	0.986	1.85	**2.10**	2.40	1.85E-03	**2.10E-03**	2.40E-03

S6. Estimation of Effect Factor (EF) from $HC50_{LOEC}$

Effect Factors (EF) were estimated from $HC50_{LOEC}$, which can also be obtained from the geometric mean (GM) based either on every species LOEC data ($GM_{species}$) pooled or from LOEC data grouped into GM_{taxon} of $GM_{species}$ (see main text). The $GM_{species}$-based method can be biased by differences in the relative representation of the different taxonomic groups across the climate zones (Fig S7 and Fig. S8).

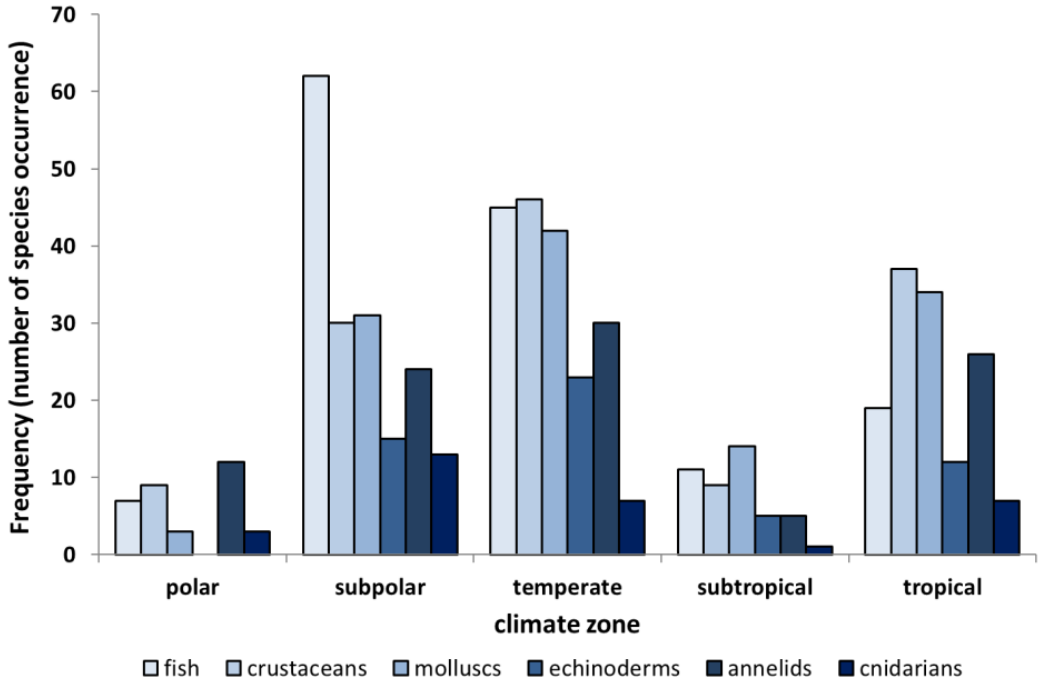

Figure S7 Number of species per taxonomic group contributing with sensitivity LOEC to the joint $HC50_{LOEC}$ per climate zone.

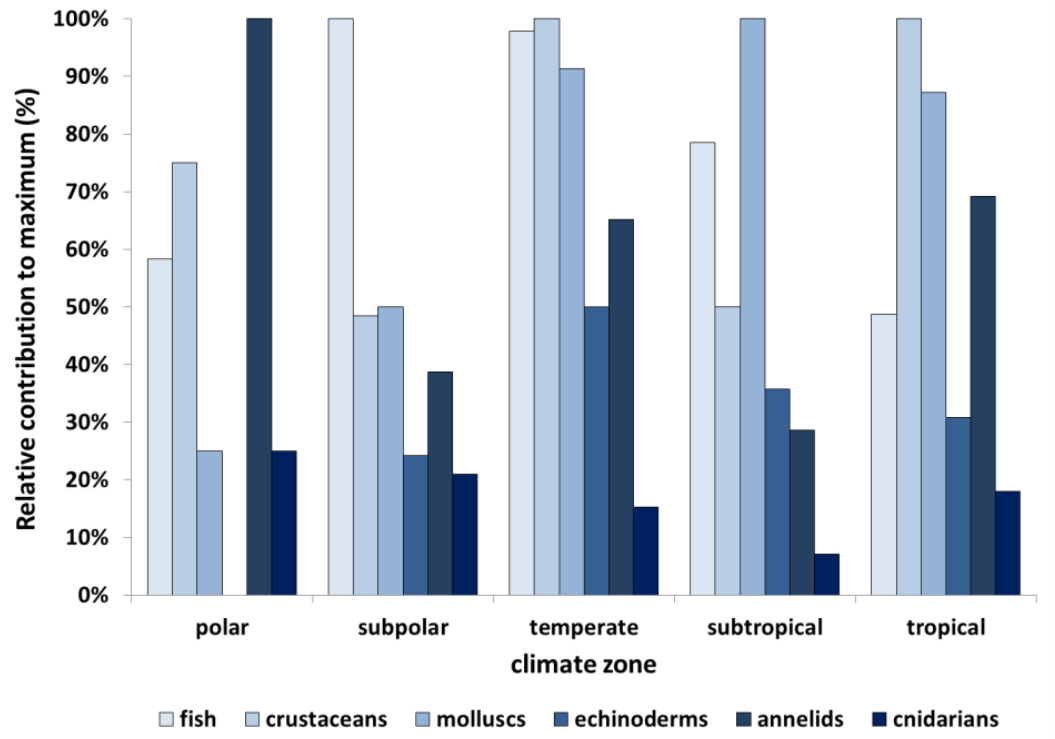

Figure S8 Relative contribution of the number of species per taxonomic group to the total per climate zone showing the heterogeneity of group dominance.

Table S5 Results of the significance F-test for variances on pairs of GM_{taxon}-based $HC50_{LOEC}$ values per climate zone (CZ).

F-Test Two-Sample for Variances

Paired CZs:	Polar	Subpolar	Polar	Temperate	Polar	Subtropical	Polar	Tropical
Mean $logHC50_{LOEC}$	0.360	0.316	0.360	0.255	0.360	0.260	0.360	0.214
Variance $logHC50_{LOEC}$	0.011	0.030	0.011	0.029	0.011	0.028	0.011	0.026
Observations	5	6	5	6	5	6	5	6
df	4	5	4	5	4	5	4	5
F	0.368		0.378		0.391		0.436	
P(F<=f) one-tail	0.177	n.s.	0.183	n.s.	0.192	n.s.	0.221	n.s.
F Critical one-tail	0.368	n<0.18	0.247	n<0.18	0.247	n<0.19	0.247	n<0.22

Paired CZs:	Subpolar	Temperate	Subpolar	Subtropical	Subpolar	Tropical
Mean $logHC50_{LOEC}$	0.316	0.255	0.316	0.260	0.316	0.214
Variance $logHC50_{LOEC}$	0.030	0.029	0.030	0.028	0.030	0.026
Observations	6	6	6	6	6	6
df	5	5	5	5	5	5
F	0.975		0.943		0.845	
P(F<=f) one-tail	0.489	n.s.	0.475	n.s.	0.429	n.s.
F Critical one-tail	0.198	n<0.49	0.198	n<0.47	0.198	n<0.43

Paired CZs:	Temperate	Subtropical	Temperate	Tropical
Mean $logHC50_{LOEC}$	0.255	0.260	0.255	0.214
Variance $logHC50_{LOEC}$	0.029	0.028	0.029	0.026
Observations	6	6	6	6
df	5	5	5	5
F	0.966		0.867	
P(F<=f) one-tail	0.485	n.s.	0.439	n.s.
F Critical one-tail	0.198	n<0.49	0.198	n<0.44

Paired CZs:	Subtropical	Tropical
Mean $logHC50_{LOEC}$	0.260	0.214
Variance $logHC50_{LOEC}$	0.028	0.026
Observations	6	6
df	5	5
F	0.897	
P(F<=f) one-tail	0.454	n.s.
F Critical one-tail	0.198	n<0.45

S7. On the uncertainty in experimental datasets and representativeness

Uncertainty in data collection can arise from random or systematic errors in identifying/classifying the endpoints (the response tested), from incorrect estimation of the correlation between stressor intensity and endpoint quantification (interpretation of test results), or from misclassifying species occurrences (i.e. uncertainty in assigning geographic distribution of species). Therefore, such bias can be interpreted as test-related or selection-related. The first may arise from errors in measuring the tested

endpoint. The ideal test would be the one accurately and consistently measuring the effect under study.

High (verified) representativeness of the dataset would make the extrapolation from species to community clear. The internal validation of the dataset (meaning that the tests are adequate and consistent with the endpoint quantification and purpose) should not compromise the application/generalisation to natural ecosystems' conditions (external validation). Assertions about the validation of the dataset are outside the scope of the present paper, and therefore it is based on the fact that all the test results contributing to the sensitivity dataset were already peer-reviewed and validated as their publication denotes. Moreover, its inclusion was based on relevance and consistency criteria.

Practical issues regarding test species and available data points may illustrate species' representation bias – as such, preference may be directed to species that resist capture, endure captivity conditions or are easily maintained, that have conspicuous responses, economic interest or local ecological relevance. In addition to these biologically related factors, the availability of resources from the various research teams of universities, national laboratories, etc. and their location may determine the geographic attribute of published, or otherwise available, sensitivity data – biasing the dataset towards 'preferred' species or taxonomic groups, or 'preferred' studied areas.

Acknowledging the assumptions about data validity and considerations about representativeness, the main goal of describing and discussing the method that applies sensitivity to hypoxia to estimate EFs in an LCIA framework for marine eutrophication is achieved. The method should be applicable to any dataset of sensitivity to hypoxia deemed adequate. For this, the present dataset is accepted as a viable indication of species sensitivity to hypoxia as well as its conversion from experimental (or observations) to benthic habitat conditions.

S8. References

Alderdice, D.F., Forrester, C.R., 1971. Effects of Salinity, Temperature, and Dissolved Oxygen on Early Development of Pacific Cod (Gadus macrocephalus). J. Fish. Res. Board Canada 28, 883–902.

Anderson, S.J., Taylor, A.C., Atkinson, R.J.A., 1994. Anaerobic metabolism during anoxia in the burrowing shrimp Calocaris macandreae Bell (Crustacea: Thalassinidea). Comp. Biochem. Physiol. 108A, 515–552.

Antonov, J.I., Seidov, D., Boyer, T.P., Locarnini, R.A., Mishonov, A. V., Garcia, H.E., Baranova, O.K., Zweng, M.M., Johnson, D.R., 2010. World Ocean Atlas 2009, Volume 2: Salinity, NOAA Atlas NESDIS 69. U.S. Government Printing Office, Washington, D.C. doi:10.1182/blood-2011-06-357442

Artigaud, S., Lacroix, C., Pichereau, V., Flye-Sainte-Marie, J., 2014. Respiratory response to combined heat and hypoxia in the marine bivalves Pecten maximus

and Mytilus spp. Comp. Biochem. Physiol. -Part A Mol. Integr. Physiol. 175, 135–140. doi:10.1016/j.cbpa. 2014.06.005

Astall, C.M., Jones, M.B., 1991. Respiration and biometry in the sea cucumber Holothuria forskali. J Mar Biol Assoc UK 71, 73–81.

Baden, S.P., Pihl, L., Rosenberg, R., 1990. Effects of oxygen depletion on the ecology, blood physiology and fishery of the Norway lobster Nephrops norvegicus. Mar. Ecol. Prog. Ser. 67, 141–155. doi:10.3354/meps067141

Behrens, J.W., Petersen, J.K., Aertebjerg, G., Steffensen, J.F., 2010. Influence of moderate and severe hypoxia on the diurnal activity pattern of lesser sandeel Ammodytes tobianus. J. Fish Biol. 77, 538–51. doi:10.1111/j.1095-8649. 2010.02697.x

Burd, B.J., Brinkhurst, R.O., 1984. The distribution of the galatheid crab Munida quadrispina (Benedict 1902) in relation to oxygen concentrations in British Columbia fjords. J. Exp. Mar. Bio. Ecol. 81, 1–20.

Cerezo Valverde, J., García García, B., 2005. Suitable dissolved oxygen levels for common octopus (Octopus vulgaris cuvier, 1797) at different weights and temperatures: Analysis of respiratory behaviour. Aquaculture 244, 303–314. doi:10.1016/j.aquaculture.2004.09.036

Cerezo, J., García García, B., 2004. The effects of oxygen levels on oxygen consumption, survival and ventilatory frequency of sharpsnout sea bream (Diplodus puntazzo Gmelin, 1789) at different conditions of temperature and fish weight. J. Appl. Ichthyol. 20, 488–492. doi:10.1111/j.1439-0426. 2004.00601.x

Das, T., Stickle, W.B., 1993. Sensitivity of crabs Callinectes sapidus and C. similis and the gastropod Stramonita haemastoma to hypoxia and anoxia. Mar. Ecol. Prog. Ser. 98, 263–274. doi:10.3354/meps098263

Davis, J.C., 1975. Minimal dissolved oxygen requirements of aquatic life with emphasis on Canadian species: a review. J. Fish. Res. Board Canada 32, 2295–2332.

de Vries, P., Tamis, J.E., Murk, A.J., Smit, M.G.D., 2008. Development and application of a species sensitivity distribution for temperature-induced mortality in the aquatic environment. Environ. Toxicol. Chem. 27, 2591–2598.

Diaz, R.J., Neubauer, R.J., Schaffner, L.C., Pihl, L., Baden, S.P., 1992. Continuous monitoring of dissolved oxygen in an estuary experiencing periodic hypoxia and the effect of hypoxia on macrobenthos and fish. Sci Total Env. Suppl 1055–1068.

Diehl, W.J.I., McEdward, L., Proffitt, E., Rosenberg, V., Lawrence, J.M., 1979. The response of Luidia clathrata (Echinodermata: Asteroidea) to hypoxia. Comp. Biochem. Physiol. 62A, 669–671.

Ellington, W.R., 1982. Metabolic Responses of the Sea Anemone Bunodosoma cavernata (Bosc) to Declining Oxygen Tensions and Anoxia. Physiol. Zool. 55, 240–249.

Fischer, P., Rademacher, K., Kils, U., 1992. In situ investigations on the respiration and

behaviour of the eelpout Zoarces viviparus under short-term hypoxia. Mar. Ecol. Prog. Ser. 88, 181–184.

Fitzgibbon, Q.P., Strawbridge, A., Seymour, R.S., 2007. Metabolic scope, swimming performance and the effects of hypoxia in the mulloway, Argyrosomus japonicus (Pisces: Sciaenidae). Aquaculture 270, 358–368. doi:10.1016/ j.aquaculture.2007.04.038

Forbes, T.L., Lopez, G.R., 1990. The effect of food concentration, body size, and environmental oxygen tension on the growth of the deposit-feeding polycheate, Capitella species 1. Limnol. Oceanogr. 35, 1535–1544. doi:10.4319/lo.1990 .35.7.1535

Forstner, H., Gnaiger, E., 1983. Calculation of Equilibrium Oxygen Concentration, in: Gnaiger, E., Forstner, H. (Eds.), Polarographic Oxygen Sensors. Aquatic and Physiological Applications. Springer, Berlin, Heidelberg, New York:370 pp, pp. 321–333.

González-Ortegón, E., Pascual, E., Drake, P., 2013. Respiratory responses to salinity, temperature and hypoxia of six caridean shrimps from different aquatic habitats. J. Exp. Mar. Bio. Ecol. 445, 108–115. doi:10.1016/j.jembe.2013.04.006

Hanson, D., 1967. Cardiovascular dynamics and aspects of gas exchange in Chondrichthyes. University of Washington.

Harris, J.O., Maguire, G.B., Edwards, S.J., Johns, D.R., 1999. Low dissolved oxygen reduces growth rate and oxygen consumption rate of juvenile greenlip abalone, Haliotis laevigata Donovan. Aquaculture 174, 265–278.

Haselmair, A., Stachowitsch, M., Zuschin, M., Riedel, B., 2010. Behaviour and mortality of benthic crustaceans in response to experimentally induced hypoxia and anoxia in situ. Mar. Ecol. Prog. Ser. 414, 195–208. doi:10.3354/meps08657

Hill, A.D., Taylor, A.C., Strang, R.H.C., 1991. Physiological and metabolic responses of the shore crab Carcinus maenas (L.) during environmental anoxia and subsequent recovery. J. Exp. Mar. Bio. Ecol. 150, 31–50.

Hughes, G.M., Umezawa, S.-I., 1968a. Oxygen consumption and gill water flow in the dogfish Scyliorhinus canicula L. J. Exp. Biol. 49, 557–564.

Hughes, G.M., Umezawa, S.-I., 1968b. On respiration in the dragonet Callionymus lyra L. J. Exp. Biol. 49, 565–582.

ICES, 2015a. Oceanography - CTD and Bottle data [WWW Document]. Int. Counc. Explor. Sea. URL http://ocean.ices.dk/HydChem/HydChem.aspx (accessed 10.22.15).

ICES, 2015b. Oceanographic calculator [WWW Document]. Int. Counc. Explor. Sea. URL http://ocean.ices.dk/Tools/Calculator.aspx (accessed 10.22.15).

Johansson, B., 1999. Influence of oxygen levels on the predatory behaviour of the isopod Saduria entomon. Mar Freshw Behav Physiol 32, 223–238.

Johansson, B., 1997. Tolerance of the deposit-feeding Baltic amphipods Monoporeia affinis and Pontoporeia femorata to oxygen deficiency. Mar. Ecol. Prog. Ser. 151, 135–141.

Jørgensen, B.B., 1980. Seasonal oxygen depletion in the bottom waters of a Danish fjord and its effect on the benthic community. Oikos 34, 68–76.

Kanz, J.E., Quast, W.D., 1992. Respiratory pumping behavior in the marine snail Aplysia californica as a function of ambient hypoxia. Physiol. Zool. 65, 35–54.

Kutty, M.N., Saunders, R.L., 1973. Swimming Performance of Young Atlantic Salmon (Salmo salar) as Affected by Reduced Ambient Oxygen Concentration. J. Fish. Res. Board Canada 30, 223–227.

Larsen, H.F., Hauschild, M.Z., 2007. LCA Methodology Evaluation of Ecotoxicity Effect Indicators for Use in LCIA. Int. J. 12, 24–33.

Lays, N., Iversen, M.M.T., Frantzen, M., Jørgensen, E.H., 2009. Physiological stress responses in spotted wolffish (Anarhichas minor) subjected to acute disturbance and progressive hypoxia. Aquaculture 295, 126–133. doi:10.1016/j.aquaculture.2009.06.039

Lenfant, C., Johansen, K., 1966. Respiratory function in the elasmobranch Squalus suckleyi G. Respir. Physiol. 1, 13–29.

Liu, C.C., Chiu, J.M.Y., Li, L., Shin, P.K.S., Cheung, S.G., 2011. Physiological responses of two sublittoral nassariid gastropods to hypoxia. Mar. Ecol. Prog. Ser. 429, 75–85. doi:10.3354/meps09107

Llansó, R.J., 1991. Tolerance of low dissolved oxygen and hydrogen sulfide by the polychaete Streblospio benedicti (Webster). J. Exp. Mar. Bio. Ecol. 153, 165–178. doi:10.1016/0022-0981(91)90223-J

Llansó, R.J., Diaz, R.J., 1994. Tolerance to low dissolved oxygen by the tubicolous polychaete Loimia medusa. J Mar Biol Assoc UK 74, 143–148.

Locarnini, R.A., Mishonov, A. V., Antonov, J.I., Boyer, T.P., Garcia, H.E., Baranova, O.K., Zweng, M.M., Johnson, D.R., 2010. World Ocean Atlas 2009, Volume 1: Temperature, NOAA Atlas NESDIS 68. U.S. Government Printing Office, Washington, D.C.

MacKay, R.D., 1974. A note on minimal levels of oxygen requiered to maintain life in Penaeus schmitti. J. Maric. Soc. 5, 451–452.

NCEI, 2015. Data Sets and Products - World Ocean Atlas 2009 Figures [WWW Document]. World Ocean Atlas. NOAA's Natl. Centers Environ. Inf. URL http://www.nodc.noaa.gov/OC5/ WOA09F/pr_woa09f.html (accessed 10.22.15).

Nilsson, H.C., Rosenberg, R., 1994. Hypoxic response of two marine benthic communities. Mar. Ecol. Prog. Ser. 115, 209–217. doi:10.3354/meps115209

OBIS, 2015. Ocean Biogeographic Information System [WWW Document]. Intergov. Oceanogr. Comm. UNESCO. URL http://www.iobis.org (accessed 10.22.15).

Pennington, D.W., Payet, J., Hauschild, M.Z., 2004. Aquatic Ecotoxicological Indicators In Life-Cycle Assessment. Environ. Toxicol. Chem. 23, 1796–1807.

Pihl, L., Baden, S.P., Diaz, R.J., 1991. Effects of periodic hypoxia on distribution of demersal fish and crustaceans. Mar. Biol. 108, 349–360.

Posthuma, L., Suter II, G.W., Traas, T.P. (Eds.), 2002a. Species Sensitivity

Distributions in Ecotoxicology, Environmental and Ecological Risk Assessment.

Posthuma, L., Traas, T.P., Suter II, G.W., 2002b. General Introduction to Species Sensitivity Distributions, in: Posthuma, L., Suter II, G.W., Traas, T.P. (Eds.), Species Sensitivity Distributions in Ecotoxicology. Lewis, Boca Raton, pp. 3–10.

Renaud, M.L., 1986. Detecting and avoiding oxygen deficient sea water by brown shrimp, Penaeus aztecus (Ives), and white shrimp Penaeus setiferus (Linnaeus). J. Exp. Mar. Bio. Ecol. 98, 283–292.

Rosas, C., Sánchez, A., Díaz-Iglesia, E., Brito, R., Martinez, E., Soto, L.A., 1997. Critical dissolved oxygen level to Penaeus setiferus and Penaeus schmitti postlarvae (PL10-18) exposed to salinity changes. Aquaculture 152, 259–272.

Rosenberg, R., Hellman, B., Johansson, B., 1991. Hypoxic tolerance of marine benthic fauna. Mar. Ecol. Prog. Ser. 79, 127–131.

Rutherford, L.D.J., Thuesen, E. V., 2005. Metabolic performance and survival of medusae in estuarine hypoxia. Mar. Ecol. Prog. Ser. 294, 189–200.

Sandberg, E., Tallqvist, M., Bonsdorff, E., 1996. The Effects of Reduced Oxygen Content on Predation and Siphon Cropping by the Brown Shrimp, Crangon crangon. Mar. Ecol. 17, 411–423. doi:10.1111/j.1439-0485.1996.tb00518.x

Sassaman, C., Mangum, C.P., 1972. Adaptations to Environmental Oxygen Levels in Infaunal and Epifaunal Sea Anemones. Biol. Bull. 143, 657–678.

Schöttler, U., Grieshaber, M., 1988. Adaptation of the polychaete worm Scoloplos armiger to hypoxic conditions. Mar. Biol. 99, 215–222.

Schurmann, H., Steffensen, J.F., 1997. Effects of temperature, hypoxia and activity on the metabolism of juvenile Atalantic cod. J. Fish Biol. 50, 1166–1180.

Seidman, E.R., Lawrence, A.L., 1985. Growth, feed digestibility, and proximate body composition of juvenile Penaeus vannamei and Penaeus monodon grown at different dissolved oxygen levels. J. World Maric. Soc. 16, 333–346.

Sherman, K., Hempel, G., 2009. The UNEP Large Marine Ecosystem Report: A perspective on changing conditions in LMEs of the World's Regional Seas, UNEP Regional Seas Report and Studies No. 182.

Silkin, Y.A., Silkina, E.N., 2005. Effect of hypoxia on physiological and biochemical blood values in sea fishes. J. Evol. Biochem. Physiol. 41, 527–532.

Smit, M.G.D., Holthaus, K.I.E., Trannum, H.C., Neff, J.M., Kjeilen-Eilertsen, G., Jak, R.G., Singsaas, I., Huijbregts, M.A.J., Jan Hendriks, A., 2008. Species sensitivity distributions for suspended clays, sediment burial, and grain size change in the marine environment. Environ. Toxicol. Chem. 27, 1006–12. doi:10.1897/07-339.1

Sobral, P., Widdows, J., 1997. Influence of hypoxia and anoxia on the physiological responses of the clam Ruditapes decussatus from southern Portugal. Mar. Biol. 127, 455–461.

Spicer, J.I., 1995. Oxygen and acid-base status of the sea urchin Psammechinus miliaris during environmental hypoxia. Mar. Biol. 124, 71–76. doi:10.1007/BF00349148

Stierhoff, K.L., Targett, T.E., Miller, K., 2006. Ecophysiological responses of juvenile summer and winter flounder to hypoxia: Experimental and modeling analyses of effects on estuarine nursery quality. Mar. Ecol. Prog. Ser. 325, 255–266. doi:10.3354/meps325255

Tallqvist, M., Sandberg-Kilpi, E., Bonsdorff, E., 1999. Juvenile flounder, Platichthys flesus (L.), under hypoxia: Effects on tolerance, ventilation rate and predation efficiency. J. Exp. Mar. Bio. Ecol. 242, 75–93. doi:10.1016/S0022-0981(99)00096-9

Tamai, K., 1996. Temporal Tolerance of Larval Theora fragilis (Bivalvia: Semelidae) to Hypoxic Conditions. Fish. Sci. 62, 996–997.

Taylor, J.C., Miller, J.M., 2001. Physiological performance of juvenile southern flounder, Paralichthys lethostigma (Jordan and Gilbert, 1884), in chronic and episodic hypoxia. J. Exp. Mar. Bio. Ecol. 258, 195–214. doi:10.1016/S0022-0981(01)00215-5

Tyson, R. V., Pearson, T.H., 1991. Modern and ancient continental shelf anoxia: an overview. Geol. Soc. London, Spec. Publ. 58, 1–24. doi:10.1144/GSL.SP.1991.058.01.01

USGS, 2015. DOTABLES - Dissolved oxygen solubility tables [WWW Document]. U.S. Geol. Surv. Off. Water Qual. Version 05-Mar-2014. URL http://water.usgs.gov/software /DOTABLES/ (accessed 10.22.15).

van Zelm, R., Huijbregts, M.A.J., Van Jaarsveld, H.A., Reinds, G.J., de Zwart, D., Struijs, J., Van De Meent, D., 2007. Time Horizon Dependent Characterization Factors for Acidification in Life-Cycle Impact Assessment Base on Forest Plpant Species Occurrence in Europe. Environ. Sci. Technol. 41, 922–927.

Vaquer-Sunyer, R., Duarte, C.M., 2008. Thresholds of hypoxia for marine biodiversity. Proc. Natl. Acad. Sci. U. S. A. 105, 15452–7. doi:10.1073/pnas.0803833105

Voyer, R.A., Hennekey, R.J., 1972. Effects of dissolved oxygen on two life stages of mummichog. Prog Fish Cult 34, 222–225.

Wang, W.X., Widdows, J., 1993. Metabolic responses of the common mussel Mytilus edulis to hypoxia and anoxia. Mar. Ecol. Prog. Ser. 95, 205–214. doi:10.3354/meps095205

Webb, P.W., Brett, J.R., 1972. Oxygen Consumption of Embryos and Parents, and Oxygen Transfer Characteristics Within the Ovary of Two Species of Viviparous Seaperch, Rhacochilus vacca and Embiotoca lateralis. J. Fish. Res. Board Canada 29, 1543–1553.

Whitmore, C.M., Warren, C.E., Doudoroff, P., 1960. Avoidance reactions of salmonid and centrarchid fishes to low oxygen concentrations. Trans Am Fish Soc 89, 89:17–26.

Wu, R.S., Woo, N.Y.S., 1984. Respiratory responses and tolerance to hypoxia in two marine teleosts, Epinephelus akaara (Temminck & Schlegel) and Mylio macrocephalus (Basilewsky). Hydrobiologia 119, 209–217. doi:10.1007/BF00015211

Article IV

Spatial differentiation of marine eutrophication damage indicators based on species density

Cosme, N., Jones, M.C., Cheung, W.W.L. & Larsen, H.F.

submitted to *Ecological Indicators* in 2016

(manuscript in pre-print version)

Spatial differentiation of marine eutrophication damage indicators based on species density

Nuno Cosme [1]*, Miranda C. Jones [2], William W. L. Cheung [3], Henrik Fred Larsen [1]

[1] Division for Quantitative Sustainability Assessment, Department of Management Engineering, Technical University of Denmark, Produktionstorvet 424, DK-2800 Kgs. Lyngby, Denmark

[2] United Nations Environment Programme World Conservation Monitoring Centre, 219 Huntingdon Road, Cambridge CB3 ODL, UK

[3] Changing Ocean Research Unit and Nippon Foundation – Nereus Program, Institute for the Oceans and Fisheries, the University of British Columbia, Vancouver, British Columbia, Canada

*Corresponding author: e-mail address: nmdc@dtu.dk (N. Cosme)

Abstract

Marine eutrophication refers to an ecosystem response to the loading of nutrients, typically nitrogen (N), to coastal waters where it may cause several impacts. The increase of planktonic growth due to N-enrichment fuels the organic carbon cycles and may lead to excessive oxygen depletion in benthic waters. Such hypoxic conditions may cause severe effects on exposed ecological communities. An indicator coupling the biologic processes that determine production, sink, and aerobic respiration organic material, as a function of available N – or eXposure Factor (XF, $kgO_2 \cdot kgN^{-1}$), and the sensitivity of benthic-demersal species to hypoxia – or Effect Factor (EF, $PAF \cdot m^3 \cdot kgO_2^{-1}$; as Potentially Affected Fraction (PAF) of species), is developed to represent the Ecosystem Response (ER, $PAF \cdot m^3 \cdot kgN^{-1}$) to N-uptake. The loss of species richness is further modelled to a marine eutrophication Ecosystem Damage (meED) indicator, as an absolute metric of time integrated number of species disappeared (species·yr), by applying a newly-proposed and spatially-explicit factor based on species density (SD, $species \cdot m^{-3}$). The meED indicator is calculated for 66 Large Marine Ecosystems (LMEs) and range from 1.6×10^{-12} $species \cdot kgN^{-1}$, in the Central Arctic Ocean, to 4.8×10^{-8} $species \cdot kgN^{-1}$, in the Northeast U.S. Continental Shelf. The spatially explicit SDs are essential to give environmental relevance to meED scores and to facilitate harmonization of marine eutrophication impacts with other ecosystem-damage Life Cycle Impact Assessment (LCIA) indicators. The novel features introduced improve current methodologies and support the adoption of the meED indicator in LCIA for the characterization of anthropogenic-N emissions with eutrophying impacts, thus contributing to sustainability assessment of human activities.

Keywords Exposure · Effect · Life Cycle Impact Assessment · Ecosystem damage · Large Marine Ecosystems

List of abbreviations
AoP: Area of Protection
EF: Effect Factor
ERPAF: Ecosystem Response (estimated from PAF-based effect factors)
ERPDF: Ecosystem Response (estimated from PDF-based effect factors)
LCIA: Life Cycle Impact Assessment
LME: Large Marine Ecosystem
meDF: marine eutrophication Damage Factor
meED: marine eutrophication Ecosystem Damage
PAF: Potentially Affected Fraction of species
PDF: Potentially Disappeared Fraction of species
SD: Species Density
SDM: Species Distribution Model
SR: Species Richness
SSD: Species Sensitivity Distribution
XF: eXposure Factor

1. Introduction

Marine eutrophication is an ecosystem response to an increased availability of nutrients in the euphotic zone of coastal waters (Gray et al., 2002; Rabalais, 2002; Smith et al., 1999) and it is among the most severe and widespread causes of disturbance to marine environments (Diaz and Rosenberg, 2008; GESAMP, 2001). The enrichment of coastal waters with nitrogen (N) boosts planktonic growth, or primary production (PP) (Howarth and Marino, 2006; Vitousek et al., 2002) – the photosynthetic reduction of inorganic carbon into energy-rich organic carbon involving the assimilation of inorganic dissolved plant nutrients and the utilization of light energy by primary producers, mainly phytoplankton, in the well-lit upper layers of the ocean (euphotic zone) (Chavez et al., 2011; Falkowski and Raven, 2007). The eventual aerobic respiration (biodegradation) of this newly produced organic matter may result in oxygen depletion in bottom waters (Cosme et al., 2015; Graf et al., 1982; Ploug et al., 1999) and even in the occurrence of 'dead zones' (Diaz and Rosenberg, 2008; Diaz, 2001). Effects on exposed benthic and demersal species (e.g. crustaceans and bivalves) may then be expected as a function of their sensitivity to hypoxia (Cosme and Hauschild, 2016; Davis, 1975; Diaz and Rosenberg, 1995; Gray et al., 2002; Vaquer-Sunyer and Duarte, 2008) and promote other impacts including habitat loss, water quality degradation, mass

mortality, and fisheries decline (Diaz and Rosenberg, 1995; Levin et al., 2009; Middelburg and Levin, 2009; Wu, 2002; J. Zhang et al., 2010).

Globally, environmental N-emissions from human activities have increased more than 10-fold in the last 150 years in large part due to the growing demand for reactive nitrogen in agriculture use and for energy production (Galloway et al., 2008). Considering the N emissions throughout the entire life cycle of products and services in the economy, Life Cycle Assessment (LCA) can be used as an environmental analysis tool designed to quantify the resulting potential environmental impacts (Hauschild, 2005). Indicators of marine eutrophication impacts are estimated in the Life Cycle Impact Assessment (LCIA) phase of LCA, typically at the midpoint between emission and damage (endpoint) in the cascading effects of N-enrichment in the marine compartment (Rabalais et al., 2009). This is reflected in widespread LCIA methods, like ReCiPe (Goedkoop et al., 2012), EDIP 2003 (Hauschild and Potting, 2005), IMPACT 2002+ (Jolliet et al., 2003), and CML 2002 (Guinée et al., 2002). Recent reviews of the state-of-the-art and research needs regarding marine eutrophication impacts modelling (Hauschild et al., 2013; Henderson, 2015) revealed the lack of a consistent link between existing midpoints and damage level. While the former models nutrients fate in environment, the latter further requires exposure and effects modelling for consistency with the generic LCIA framework (Udo de Haes et al., 2002). Recent work has been developed covering the latter as spatially explicit ecosystem exposure factors (XF) (Cosme et al., 2015) and effects factors (EF) (Cosme and Hauschild, 2016). An XF×EF coupled indicator represents the ecosystem response to N-uptake by primary producers in coastal waters. Additional fate modelling may deliver the marine eutrophication impact potential of a unit mass of N from anthropogenic emissions.

Methodology-wise, other ecosystem-related LCIA indicators at the endpoint level, for e.g. ecotoxicity and acidification, can be aggregated into damage to the ecosystem, also known as an Area of Protection (AoP) (Udo de Haes et al., 1999), and be expressed as time-integrated loss of species richness, i.e. species·yr. Such conversions currently adopt site-generic marine species density (SD) (Goedkoop et al., 2012) – an inherent model (rough) simplification. Recent work focusing on marine species distribution (Jones and Cheung, 2015) may provide the damage modelling with site-dependent SDs to estimate environmentally relevant damage factors (DF).

The goal of this study is to quantify spatially explicit damage potentials for nitrogen emissions that fuel primary production in coastal waters contributing to marine eutrophication. This quantification requires (i) the derivation of an ecosystem response indicator, obtained by combining the ecosystem exposure to N and the effects on biota caused by hypoxia, and (ii) an additional conversion of the damage to ecosystems from relative to absolute metrics, based on site-dependent species density. The application of

such methodology is discussed for the characterisation modelling of anthropogenic emissions of N with eutrophying impacts in a LCIA framework.

2. Methodology

The approach used here is consistent with the LCIA framework for emission-related impact indicators, and estimates potential impacts to the ecosystem by combining environmental fate of substances emissions, exposure of the receiving ecosystem to these, and the effect caused on exposed species (Pennington et al., 2004b; Udo de Haes et al., 2002) (Section 2.1). The present method proposes an indicator for the loss of species richness caused by nitrogen-based marine eutrophication and expressed as volume-integrated Potentially Affected Fraction (PAF) of species per unit mass of N uptaken (Sections 2.2 to 2.4). A metrics conversion to Potentially Disappearing Fraction (PDF) of species is further proposed for harmonisation and consistency with other ecosystem-related endpoint indicators (Section 2.5). As the PDF-integrated unit is a relative metric, an additional conversion to an absolute metric is proposed, based on site-dependent species density obtained from marine species distribution models (Sections 2.5 to 2.8).

2.1. Framework

The LCIA factor, or Characterisation Factor (*CF*, here (PAF)·m^3·yr·kgN^{-1}), that translates the quantity of an emission into its potential impact on the exposed environmental compartment (here a coastal marine ecosystem) is derived as summarised in Eq. (1):

$$CF_{ij} = FF_{ij} \times XF_j \times EF_j \quad (1)$$

where FF_{ij} (yr) is the fate factor for emission route *i* (here N to air, to soil, to fresh-, or to marine water) to receiving ecosystem *j* (here, coastal marine), XF_j (here $kgO_2 \cdot kgN^{-1}$) is the exposure factor, and EF_j (here, (PAF)·m^3·kgO_2^{-1}) the effect factor in ecosystem *j*. PAF is included for informative reasons as it is not an actual unit but a dimensionless quantity (fraction) (Heijungs, 2005). Although acknowledging the meaning and application of CFs in impact assessment, the present method limits the focus on the estimation of the ecosystem response to N uptaken by phytoplankton, for which only XF and EF are applied (see Figure 1). Spatial explicit fate modelling can however be adapted for waterborne N emissions (Cosme et al., n.d.) and airborne N emissions (Dentener et al., 2006; Roy et al., 2012).

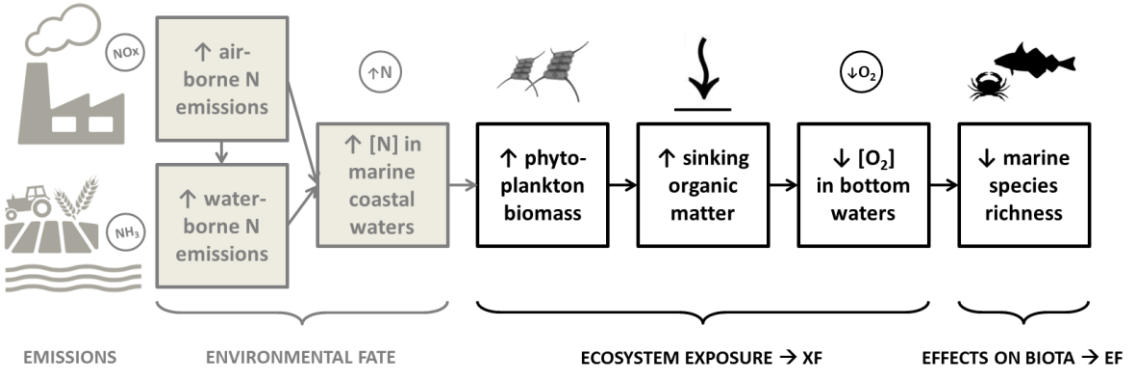

Figure 1 Schematic representation of the marine eutrophication impact pathway. Only the modelling components of ecosystem exposure and effects on biota (white box processes) are used to derive the ecosystem response to nitrogen uptake in the euphotic zone of coastal waters. Shaded boxes refer to emission-related and environmental fate processes. The exposure factor (XF) multiplied by the effect factor (EF) delivers an ecosystem response (ER) indicator.

2.2. Exposure factors

The marine eutrophication exposure factor comprises the assimilation of N that boosts planktonic growth, followed by the export of organic carbon to bottom strata, where heterotrophic bacteria consume dissolved oxygen by aerobic respiration. The model work proposed by Cosme et al. (2015) describes the biological processes of N-limited primary production (PP), metazoan consumption, and bacterial degradation, in four distinct organic carbon sinking routes. The XF values, which represent a nitrogen-to-oxygen 'conversion' potential, are available at a recommended spatial resolution of Large Marine Ecosystems (LMEs) (Sherman and Alexander, 1986) and range from 0.45 $kgO_2 \cdot kgN^{-1}$ in the Central Arctic Ocean to 15.9 $kgO_2 \cdot kgN^{-1}$ in the Baltic Sea (Figure S.1) (Cosme et al., 2015).

2.3. Effect factors

The EF represents here the average effect of hypoxia on an exposed benthic-demersal community. It is derived from the sensitivity of the composing individual species to hypoxia, with threshold values expressed as lowest-observed-effect-concentrations (LOEC), which were integrated with Species Sensitivity Distribution (SSD) methodologies (Posthuma et al., 2002) to derive a $HC50_{LOEC}$ value (Cosme and Hauschild, 2016). The latter represents the intensity of the stressor, i.e. a dissolved oxygen (DO) level, at which 50% of the species are affected above their individual threshold. The EF $[(PAF) \cdot m^3 \cdot kgO_2^{-1}]$ was then obtained as the average variation of effect (ΔPAF, [dimensionless]) in the ecological community in ecosystem *j* due to a variation of the stressor intensity (ΔDO, $[kgO_2 \cdot m^{-3}]$) in the same ecosystem (Eq. 2), according to the current scientific consensus (Larsen and Hauschild, 2007; Pennington et al., 2004a):

$$EF_j = \frac{\Delta PAF_j}{\Delta DO_j} = \frac{0.5}{HC50_{LOECj}} \quad (2)$$

The EF, as defined and used in LCIA, reads as the ability of an environmental stressor to cause a potential loss of species richness in the exposed ecosystem (Cosme and Hauschild, 2016). EF values are available at a five climate zone (CZ) resolution (polar, subpolar, temperate, subtropical, and tropical) and range from 218 (PAF)·m^3·kgO_2^{-1} (polar CZ) to 306 (PAF)·m^3·kgO_2^{-1} (tropical CZ) (Figure S.2). A disaggregation into 66 LMEs is possible by following the LME distribution per CZ as a function of mean benthic water temperature (Cosme and Hauschild, 2016).

2.4. Ecosystem response

The ecosystem response (*ER*, [(PAF)·m^3·kgN^{-1}]) indicator score was calculated for every LME by multiplying the exposure (XF) and effect (EF) factors of the corresponding LME (ecosystem *j*), as in Eq. (3):

$$ER_{PAFj} = XF_j \cdot EF_j \quad (3)$$

2.5. PAF- to PDF-integrated indicators

A marine eutrophication Damage Factor (*meDF*) (Eq. 4) was applied to ER_{PAF} for the metrics conversion in each ecosystem *j* (LME) (Eq. 5) aimed at harmonisation of endpoint scores in the LCIA framework as a PDF-integrated unit (Udo de Haes et al., 1999). The aim here is meaningful comparisons and further aggregation with other indicators that also target the ecosystem AoP, designated *Ecosystem Quality* in the Eco-indicator 99 method (Goedkoop and Spriensma, 2000) and the Impact2002+ (Jolliet et al., 2003) method, or *Ecosystems* in the ReCiPe method (Goedkoop et al., 2012). Seejustification and discussion of *meDF* quantification in Section 3.3. ahead.

$$meDF = \frac{0.5\ (\text{PDF})\cdot m^3\cdot kgN^{-1}}{1\ (\text{PAF})\cdot m^3\cdot kgN^{-1}} = 0.5\ (PDF)\cdot(PAF)^{-1} \quad (4)$$

$$ER_{PDFj} = meDF \cdot ER_{PAFj} \quad (5)$$

2.6. Species richness

Three species distribution models (SDMs) were applied to predict distributions of exploited marine species – Maxent, AquaMaps and the *Sea Around Us Project* method (Jones and Cheung, 2015). Generically, SDMs compare species occurrence with physical and biological conditions of the occurring areas to infer the bioclimatic envelope for the species (Hutchinson, 1957). This was attained by Maxent and

AquaMaps by means of generative statistical procedures only differing on the algorithms used (Jones et al., 2012). Presence data were chosen to represent species occurrence for being considered more appropriate than absence data, which are likely to be inaccurate and only occasionally available for marine species (Jones and Cheung, 2015). The *Sea Around Us Project* method algorithm (see Cheung et al. (2008); Close et al. (2006); www.seaaroundus.org) estimates the relative abundance of a set of species based on the species' depth range, horizontal range, known Food and Agriculture Organization statistical areas and polygons encompassing their known occurrence regions. In this method, the distributions are further refined by assigning habitat preferences to each species, such as affinity to shelf (inner, outer), estuaries, and coral reef habitats, obtained from FishBase (www.fishbase.org) and SeaLifeBase (www.sealifebase.org).

The SDMs were used to estimate a 20-year averaged distribution centred on 2000 (1991-2010), from presence-only occurrence data obtained from the Ocean Biogeographic System (OBIS, www.iobis.org/) on a 0.5° latitude × 0.5° longitude grid. The dataset used comprises 626 exploited benthic, demersal, and benthopelagic fish and invertebrates species (Table S.1) in the world oceans. Averaged LME-dependent species richness (SR) values were calculated by spatial aggregation in each of the 66 LME spatial units.

2.7. Species density

The benthic-demersal habitat was assumed as of 20 metres off the bottom on the neritic zone corresponding to the bottom layer of the water column where demersal and benthopelagic species are probable to occur (benthic species are necessarily included). This assumption is suggested by bottom trawl fisheries results, i.e. effective trawl fishing heights of 12-20 metres off the bottom for demersal species (Hjellvik et al., 2003) and 20 metres vertical trawl opening for benthopelagic species (Doray and Trenkel, 2010). This value was multiplied by the LME area to estimate the benthic-demersal habitat volume. Areal data per LME were compiled from the *Sea Around Us Project* (www.seaaroundus.org). The conversion of species richness (SR) values per LME *j* into species density (SD) followed Eq. (6):

$$SD_j = SR_j / \left(A_j \cdot h\right) \quad (6)$$

where the species density (*SD*, [species·m^{-3}]) is obtained by dividing the number of occurring species, i.e. species richness (*SR*) per LME, by the corresponding benthic-demersal habitat volume [m^3], i.e. LME area (*A*, [m^2]) multiplied by the average height (*h*, [m]) of 20 metres (Table 1).

2.8. Spatially explicit absolute metric of damage to ecosystems

As species composing coastal ecological communities vary geographically, a relative impact metric (based on PAF or PDF, i.e. fractions) of marine eutrophication impacts may therefore not be representative of the damage to local communities, for which an absolute metric would fit. Although using a site-generic SD, a relative-to-absolute conversion approach is already applied to ecosystems-related indicators in the ReCiPe LCIA method (Goedkoop et al., 2012). A similar metric conversion is proposed in the present context to an endpoint-like indicator, i.e. the ecosystem response indicator, as this is similar to an impact potential (like a CF) but missing the magnitude given by the fate factor – which scales the impact to the actual emission it tries to characterise, instead of scaling it to a unit mass uptaken by phytoplankton. Therefore, the relative endpoint score was converted to an absolute one by multiplying the ecosystem response (ER_{PDF}, [(PDF)·m^3·kgN^{-1}]) indicator score with a spatially differentiated SD [species·m^{-3}] in LME *j*, to deliver the marine eutrophication Ecosystem Damage (*meED*, [species·kgN^{-1}]), as per eq. (7):

$$meED_j = ER_{PDFj} \cdot SD_j \quad (7)$$

The *meED* expresses an absolute measure of the ecosystem damage potential per LME. Further aggregation is then possible into a damage category, i.e. AoP. Worth of mention here is the fact that, to the knowledge of the authors, there is no available and recommended method for endpoint modelling of a marine eutrophication indicator (Hauschild et al., 2013; Henderson, 2015), as also noted by the International Reference Life Cycle Data System (ILCD) (EC-JRC, 2010).

3. Results and Discussion

3.1. Ecosystem response

Ecosystem response (ER) scores were calculated for the 66 LMEs according to Eq. (3) representing the average impact of the uptake of a unit mass of N by phytoplankton in the LME's euphotic zone – the results are given in the respective column in Table 1 and its distribution shown in Figure S.3. The ER_{PAF} scores range from 98.16 (PAF)·m^3·kgN^{-1} (in LME#64 Central Arctic Ocean) to 3,853 (PAF)·m^3·kgN^{-1} (in LME#23 Baltic Sea). The ER_{PAF} variation per LME is correlated with XF_{LME} (r=0.98), which in turn is strongly correlated to primary production (PP) rates (Cosme et al., 2015), whereas the lower spatial differentiation of the EF_{LME} renders a smaller and inverse correlation (r=-0.20). Such correlations do not alter the ranks of the lowest four and highest six scoring LMEs in both XF and ER indicators. As seen before, the ER is not an impact scaled to the anthropogenic emission of N, as no environmental fate is modelled, e.g. as removal in land or freshwater – rather, it

expresses the ecosystem's potential to respond to an increase in N availability that causes hypoxia-related impacts on biota. Damage factors (*meDF*) were applied and ER_{PAF} converted to ER_{PDF} (results in Table 1 and Figure S.4).

Table 1 Results of the ecosystem response (*ER*) scores per Large Marine Ecosystem (LME), calculated from the ecosystem eXposure Factor (*XF*) and Effect Factor (*EF*), in both PAF- and PDF-integrated metrics. Also, results of the marine eutrophication Ecosystem Damage (*meED*) scores calculated with species density (*SD*) derived from mean species richness (*SR*) per LME (standard deviation, σ, included). The LME area (*A*) was used to derive the benthic-demersal habitat volume (assumed height = 20 m).

Large Marine Ecosystem	*XF*	*EF*	ER_{PAF}	ER_{PDF}	*SR*		*A*	*SD*	*meED*
	$kgO_2 \cdot kgN^{-1}$	$(PAF) \cdot m^3 \cdot kgO_2^{-1}$	$(PAF) \cdot m^3 \cdot kgN^{-1}$	$(PDF) \cdot m^3 \cdot kgN^{-1}$	species	σ	km^2	$species \cdot m^{-3}$	$species \cdot kgN^{-1}$
01. East Bering Sea	9.86	242	2.38E+03	1.19E+03	13.5	12.2	601,920	5.84E-13	6.96E-10
02. Gulf of Alaska	11.1	242	2.70E+03	1.35E+03	17.4	2.40	329,528	6.17E-13	8.32E-10
03. California Current	6.09	278	1.69E+03	8.46E+02	10.2	0.470	112,754	2.32E-13	1.97E-10
04. Gulf of California	7.97	242	1.93E+03	9.63E+02	47.0	11.7	75,484	1.25E-11	1.21E-08
05. Gulf of Mexico	4.49	306	1.37E+03	6.85E+02	49.4	5.59	567,620	1.66E-12	1.14E-09
06. Southeast U.S. Continental Shelf	5.26	306	1.61E+03	8.03E+02	75.0	14.6	131,057	1.37E-11	1.10E-08
07. Northeast U.S. Continental Shelf	12.2	278	3.40E+03	1.70E+03	89.3	25.5	279,681	1.60E-11	2.72E-08
08. Scotian Shelf	11.6	242	2.80E+03	1.40E+03	66.1	17.1	224,439	9.17E-12	1.28E-08
09. Newfoundland-Labrador Shelf	10.3	242	2.49E+03	1.24E+03	49.5	17.8	486,595	3.84E-12	4.77E-09
10. Insular Pacific-Hawaiian	1.33	306	4.05E+02	2.03E+02	12.0	0.000	20,432	6.19E-13	1.25E-10
11. Pacific Central-American	3.33	306	1.02E+03	5.09E+02	14.8	1.00	208,530	3.80E-13	1.94E-10
12. Caribbean Sea	2.51	306	7.67E+02	3.83E+02	34.0	1.85	518,460	5.39E-13	2.07E-10
13. Humboldt Current	8.38	278	2.33E+03	1.17E+03	9.65	0.983	302,712	1.95E-13	2.28E-10
14. Patagonian Shelf	11.5	242	2.78E+03	1.39E+03	37.5	2.92	1,004,605	1.66E-12	2.31E-09
15. South Brazil Shelf	5.84	242	1.41E+03	7.06E+02	56.9	6.51	282,944	5.20E-12	3.67E-09
16. East Brazil Shelf	1.94	306	5.94E+02	2.97E+02	22.8	1.04	168,245	1.10E-12	3.25E-10
17. North Brazil Shelf	5.26	306	1.61E+03	8.04E+02	46.5	4.73	466,907	2.34E-12	1.88E-09
18. Canadian Eastern Arctic - West Greenland	6.80	218	1.48E+03	7.42E+02	9.60	3.63	398,787	1.52E-12	1.13E-09
19. Greenland Sea	7.25	218	1.58E+03	7.91E+02	6.72	4.45	90,224	6.73E-13	5.32E-10
20. Barents Sea	7.05	242	1.71E+03	8.53E+02	11.4	3.25	919,627	3.26E-13	2.78E-10
21. Norwegian Sea	6.35	242	1.54E+03	7.68E+02	18.7	3.11	54,020	8.66E-13	6.65E-10
22. North Sea	9.11	242	2.20E+03	1.10E+03	87.8	8.37	591,135	6.70E-12	7.38E-09
23. Baltic Sea	15.9	242	3.85E+03	1.93E+03	24.7	3.91	387,139	3.60E-12	6.93E-09
24. Celtic-Biscay Shelf	8.15	278	2.26E+03	1.13E+03	95.9	14.1	528,284	6.71E-12	7.60E-09
25. Iberian Coastal	7.38	278	2.05E+03	1.03E+03	56.9	6.78	55,069	1.01E-11	1.04E-08
26. Mediterranean	3.45	278	9.60E+02	4.80E+02	55.1	7.27	530,429	1.17E-12	5.60E-10
27. Canary Current	7.73	242	1.87E+03	9.34E+02	42.9	3.44	195,439	1.97E-12	1.84E-09
28. Guinea Current	4.31	242	1.04E+03	5.21E+02	25.2	1.95	287,606	6.64E-13	3.46E-10
29. Benguela Current	9.09	242	2.20E+03	1.10E+03	32.3	2.21	199,456	1.11E-12	1.22E-09
30. Agulhas Current	4.76	306	1.46E+03	7.28E+02	22.6	2.46	316,710	4.43E-13	3.22E-10
31. Somali Coastal Current	3.36	306	1.03E+03	5.13E+02	21.0	1.51	61,885	1.28E-12	6.59E-10
32. Arabian Sea	4.99	306	1.53E+03	7.63E+02	25.2	1.59	686,547	3.28E-13	2.50E-10
33. Red Sea	3.89	306	1.19E+03	5.94E+02	48.5	11.0	198,827	5.92E-12	3.52E-09
34. Bay of Bengal	3.71	306	1.13E+03	5.67E+02	28.0	2.01	657,300	3.90E-13	2.21E-10
35. Gulf of Thailand	4.17	306	1.27E+03	6.37E+02	77.8	11.5	385,957	1.07E-11	6.84E-09
36. South China Sea	2.70	306	8.26E+02	4.13E+02	58.6	4.82	1,884,304	9.46E-13	3.90E-10
37. Sulu-Celebes Sea	3.18	306	9.72E+02	4.86E+02	37.5	6.60	224,667	1.99E-12	9.69E-10
38. Indonesian Sea	3.69	306	1.13E+03	5.64E+02	48.8	5.85	829,346	1.15E-12	6.46E-10
39. North Australian Shelf	4.26	306	1.30E+03	6.51E+02	84.3	8.77	778,294	5.73E-12	3.73E-09
40. Northeast Australian Shelf	1.93	306	5.90E+02	2.95E+02	37.1	2.45	303,792	1.47E-12	4.33E-10
41. East-Central Australian Shelf	3.51	242	8.48E+02	4.24E+02	18.1	0.949	67,670	1.40E-12	5.92E-10
42. Southeast Australian Shelf	5.41	278	1.51E+03	7.53E+02	17.3	0.615	219,772	7.33E-13	5.52E-10
43. Southwest Australian Shelf	5.28	278	1.47E+03	7.34E+02	27.0	2.06	296,112	1.33E-12	9.75E-10
44. West-Central Australian Shelf	3.85	242	9.30E+02	4.65E+02	28.8	0.380	110,129	2.66E-12	1.24E-09
45. Northwest Australian Shelf	2.66	306	8.13E+02	4.07E+02	53.1	5.12	366,857	2.99E-12	1.22E-09
46. New Zealand Shelf	5.69	278	1.58E+03	7.91E+02	46.7	3.71	224,510	2.48E-12	1.96E-09
47. East China Sea	6.45	306	1.97E+03	9.85E+02	83.4	14.0	567,923	5.60E-12	5.52E-09
48. Yellow Sea	12.0	278	3.34E+03	1.67E+03	56.4	6.93	434,234	6.88E-12	1.15E-08

Large Marine Ecosystem	*XF*	*EF*	ER_{PAF}	ER_{PDF}	*SR*		*A*	*SD*	*meED*
	$kgO_2 \cdot kgN^{-1}$	$(PAF) \cdot m^3 \cdot kgO_2^{-1}$	$(PAF) \cdot m^3 \cdot kgN^{-1}$	$(PDF) \cdot m^3 \cdot kgN^{-1}$	species	σ	km^2	$species \cdot m^{-3}$	$species \cdot kgN^{-1}$
49. Kuroshio Current	3.37	242	8.16E+02	4.08E+02	22.4	2.10	102,224	8.63E-13	3.52E-10
50. Sea of Japan/East Sea	5.92	278	1.65E+03	8.24E+02	26.7	2.27	205,882	1.42E-12	1.17E-09
51. Oyashio Current	9.25	242	2.24E+03	1.12E+03	13.7	1.05	44,327	1.32E-12	1.47E-09
52. Sea of Okhotsk	10.0	242	2.42E+03	1.21E+03	21.1	1.62	600,353	7.04E-13	8.52E-10
53. West Bering Sea	7.80	242	1.89E+03	9.43E+02	1.20	0.144	113,202	2.80E-14	2.64E-11
54. Northern Bering - Chukchi Seas	4.57	218	9.97E+02	4.99E+02	7.10	6.55	994,363	4.72E-13	2.35E-10
55. Beaufort Sea	5.87	218	1.28E+03	6.41E+02	3.43	2.05	401,019	2.76E-13	1.77E-10
56. East Siberian Sea	2.81	218	6.12E+02	3.06E+02	4.05	0.586	518,845	2.07E-13	6.34E-11
57. Laptev Sea	7.54	218	1.65E+03	8.23E+02	5.13	1.44	783,341	5.17E-13	4.25E-10
58. Kara Sea	6.22	218	1.36E+03	6.78E+02	5.02	1.35	802,720	2.83E-13	1.92E-10
59. Iceland Shelf and Sea	7.34	242	1.78E+03	8.88E+02	22.8	6.44	113,019	1.04E-12	9.24E-10
60. Faroe Plateau	5.58	242	1.35E+03	6.74E+02	51.0	27.2	27,119	1.70E-11	1.15E-08
61. Antarctic	4.91	218	1.07E+03	5.35E+02	3.36	0.003	491,798	4.24E-14	2.27E-11
62. Black Sea	8.83	278	2.45E+03	1.23E+03	21.8	3.41	150,185	2.59E-12	3.18E-09
63. Hudson Bay Complex	6.96	218	1.52E+03	7.60E+02	9.46	0.885	1,099,739	4.17E-13	3.17E-10
64. Central Arctic Ocean	0.450	218	9.82E+01	4.91E+01	1.25	0.512	1,535	1.79E-14	8.81E-13
65. Aleutian Islands	9.96	242	2.41E+03	1.20E+03	9.79	11.7	37,737	4.98E-13	6.00E-10
66. Canadian High Arctic - North Greenland	2.99	218	6.53E+02	3.27E+02	5.21	1.85	172,572	3.77E-13	1.23E-10
Maximum =	15.9	306	3.85E+03	1.93E+03	95.9	--	--	1.70E-11	2.72E-08
Minimum =	0.450	218	9.82E+01	4.91E+01	1.25	--	--	1.79E-14	8.81E-13

3.2. Spatially explicit damage scores

Species densities (SDs, Figure 2) were derived from species richness (SR, Figure S.5) and benthic-demersal habitat volumes per LME (Table 1). SD values vary from 1.8×10^{-14} species·m^{-3} (in LME#64 Central Arctic Ocean) to 1.7×10^{-11} species·m^{-3} (in LME#60 Faroe Plateau) – i.e. 3 orders of magnitude of spatial differentiation.

The calculated marine eutrophication Ecosystem Damage (*meED*) indicators are also compiled in Table 1 and its distribution shown in Figure 3. Results for *meED* vary from 8.8×10^{-13} species·kgN^{-1} (in LME#64 Central Arctic Ocean) to 2.7×10^{-8} species·kgN^{-1} (in LME#7 Northeast U.S. Continental Shelf) – i.e. slightly above 4 orders of magnitude of spatial differentiation. The distribution pattern of the SDs (Figure 2) is determinant for the *meED* scores distribution, showing common high-scoring LMEs, which is explained by the lower variation range of the ER scores (factor ca. 39) when compared to the SD variation (factor ca. 948). As the *meED* is merely an indicator of a potential in the receiving LME for causing an impact there, these results show the relevance of managing anthropogenic emissions into these water masses, possibly at a river basin scale. It also points out the need to further include environmental fate modelling to ensure completeness of the impact pathway and link (human-driven) causes to (environmental) effects through the ecosystem response dimension.

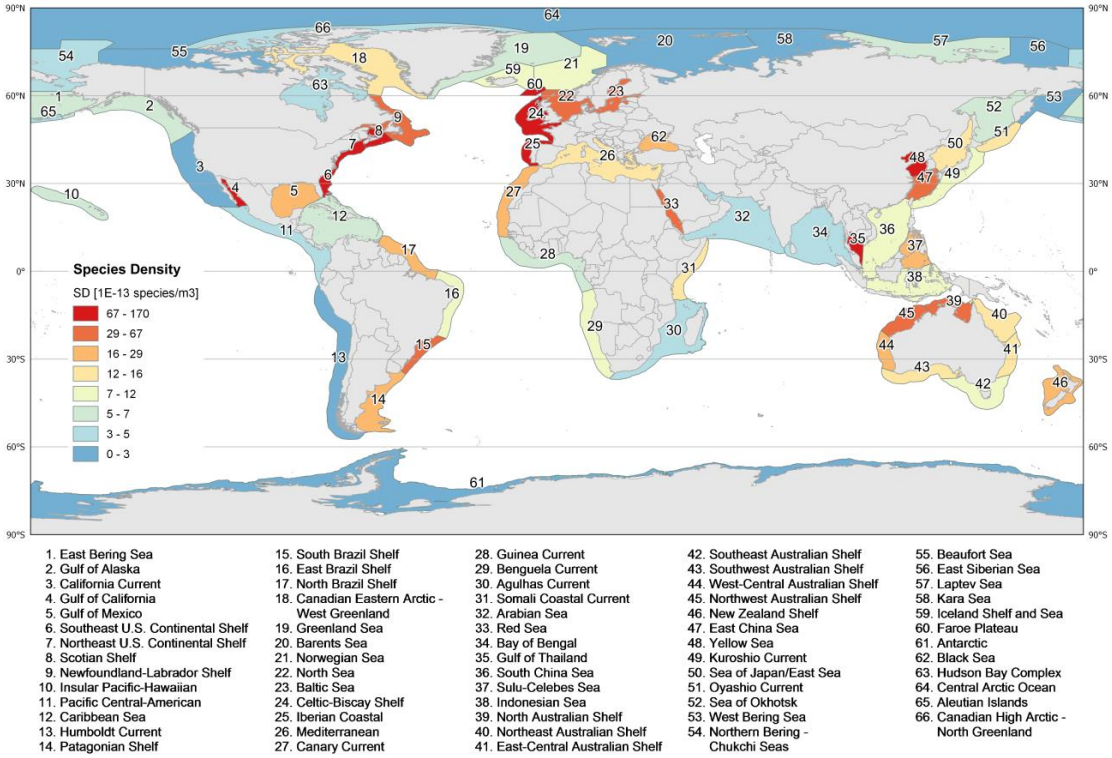

Figure 2 Distribution of species density (SD) values estimated from a set of 626 exploited benthic, demersal, and benthopelagic fish and invertebrates species, per Large Marine Ecosystem (LME). Note the non-linear scale.

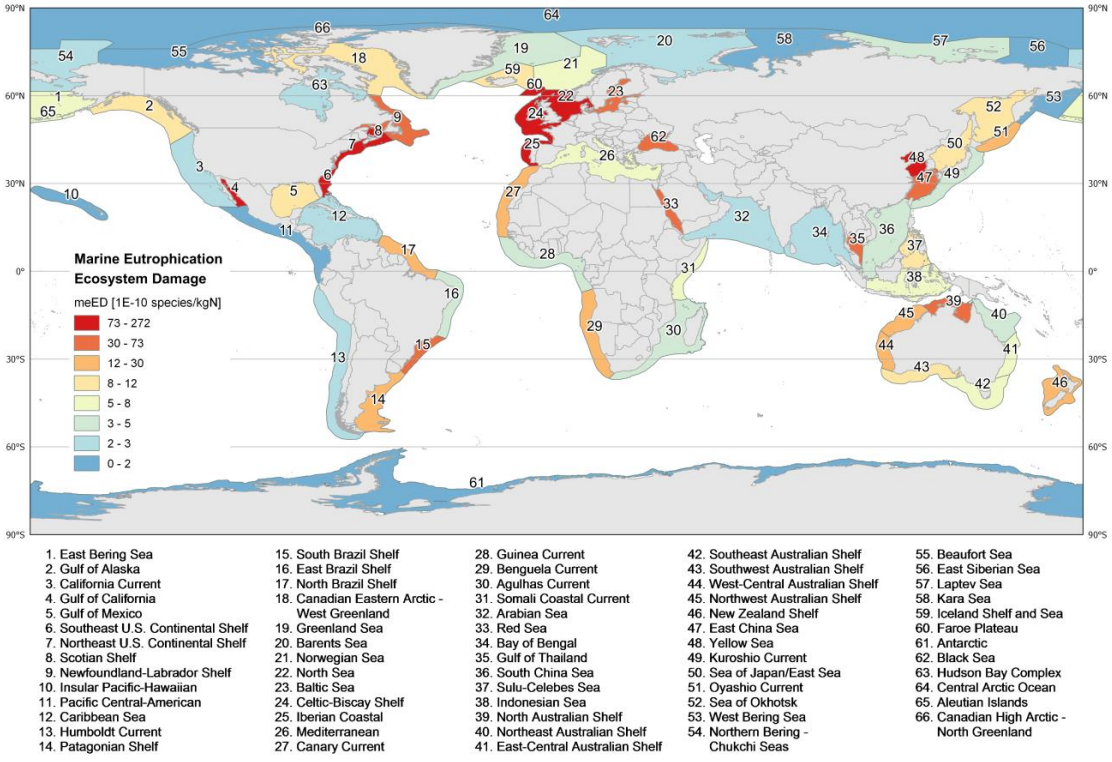

Figure 3 Global distribution of the marine eutrophication Ecosystem Damage scores (*meED*, [species·kgN^{-1}]) per Large Marine Ecosystem (LME). Note the non-linear scale.

3.3. PAF to PDF – the relative metrics

The majority of ecosystem-damage indicators report the environmental disturbance as a loss of species richness for its modelling feasibility and data availability. International databases of species distributions, e.g. Ocean Biogeographic Information System (OBIS, www.iobis.org), FishBase (www.fishbase.org), SeaLifeBase (www.sealifebase.org), World Register of Marine Species (WoRMS, www.marinespecies.org), may provide modellers with spatially explicit data relevant for e.g. ecotoxicity, ocean acidification, and marine eutrophication (Cosme and Hauschild, 2016). On a methodological perspective, different taxonomic groups (e.g. marine invertebrates, terrestrial mammals) and biological endpoints (e.g. ventilation rate, death) are widely used to estimate average or marginal responses in species richness, thus adding harmonisation issues as questions arise: is the species richness dimension of the impacts built on species-area relationships equivalent to that of SSD-based indicators? And within these, does NOEC-, LOEC-, EC_{50}-, LC_{50}-based sensitivity indicators contribute equally to an AoP-aggregated damage dimension? And should PAF to PDF conversions be spatially differentiated too or is a global generic relationship conceptually acceptable?

The PAF-integrated metric expresses the effect of an environmental stress, which does not necessarily lead to a non-occurrence of species characteristic of PDF. Implicitly is this method, and considering the diversity, and to some degree inconsistency, of biological endpoints composing the hypoxia sensitivity dataset used, derived LOEC values tend to define a PAF metric. Persistent or recurrent sublethal stress in PAF-like environmental conditions, i.e. in which species are affected but still occur, may however bring costly metabolic, physiological, or reproductive consequences for the exposed species, and avoidance behaviour (a disappearance nonetheless). In the long run, these would qualify as an impact beyond what PAF is able to express, due to the incompatibility given by time integration in LCIA modelling, and be closer to represent a true PDF. At the other end, brief PAF-like exposure events may easily be compensated by physiological or ecological feedbacks and have no long-term impacts.

As both PAF and PDF are dimensionless, how they are estimated and what they mean should be addressed. Assuming a continuum between what PAF- and PDF-based indicators mean, a metrics conversion may find ground for application. It may also suggest the inclusion of temporal modelling of effects, considering that stressors' timing, duration, intensity, and recurrence are factors contributing to species disappearance (Pickett and White, 1985) by reducing the habitat suitability or hindering reproductive success, i.e. pushing PAF closer to PDF. Approaches to quantify a PAF-to-PDF conversion and derive a damage factor are briefly discussed elsewhere (Jolliet et al., 2003; Larsen and Hauschild, 2007).

The occurrence of eutrophication impacts is correlated with the seasonality of e.g. nutrients emission flows, biological response, water temperature, stratification, and hypoxia (Behrenfeld and Boss, 2014; Cushing, 1959; Diaz, 2001; Justić et al., 1993; Lutz et al., 2007; Michael Beman et al., 2005; Rabalais, 2002; Rabalais et al., 2010; Rosenberg, 1985; Smith et al., 1992). Emissions are not evenly distributed over the year, planktonic productivity varies with latitude and season, and so do the conditions for the onset of stratification and hypoxia. Based on a time-integrated modelling approach, the exposure to environmental conditions between sublethal and lethal levels, the seasonality of the stressor, and for moderate intensity and duration between the PAF and PDF extremes (as mentioned earlier), the assumption that one half of the species affected (as PAF) would tend to not occur (and be expressed as PDF), i.e. a conversion factor of 0.5 (see Eq. 4), was chosen. Such value applied to the marine eutrophication Damage Factor (*meDF*) is consistent with that adopted for ecotoxicity in the IMPACT 2002+ (Jolliet et al., 2003) method.

For ecosystem-related LCIA indicators, the probability of non-occurrence of species, characterised by the PDF metric, is modelled with a 'media recovery' assumption, i.e. species reappear when the stressor intensity is reduced below a sensitivity threshold, assuming a reversible link between effect and fate (Larsen and Hauschild, 2007). Such assumption verifies when vulnerability and recoverability are weighted equally across species and no cumulative effects based on stressor persistence are modelled. In any case, modelling species' or communities' differentiated capacity to recover shows high environmental relevance. In this line, adding vulnerability indices to richness assessments (Curran et al., 2011; Verones et al., 2015, 2013), or Mean Extinction Time as discussed in Larsen and Hauschild (2007), along with spatial differentiation as shown here, may represent potential valuable methodological improvements. Similarly, 'media recovery' also does not verify if endemism is involved – meaning that the extirpation of exposed endemic species necessarily will lead to their disappearance and hereby failing the otherwise assumed reappearance. Perhaps future generations of ecosystem-damage assessment methods will include not only the multitude of factors built on biological attributes, for which structure and function are still missing to a large extent (Curran et al., 2011; Souza et al., 2013), but also the disturbance on delivering ecological services (Othoniel et al., 2016; Y. Zhang et al., 2010). However, ecosystem services as a metric can only succeed when spatially explicit valuations are produced and databases made available.

3.4. Harmonization of damage indicators – the absolute metrics

The terms endpoint and damage are usually applied interchangeably in LCIA. However, a distinction is made here for clarity reasons – endpoint refers to the relative metric (PAF- or PDF-integrated) whereas damage is used to refer to the absolute metric (species-integrated). Although the indicators at both level can be useful for coastal,

ecological, or water quality management, an endpoint unit is less transparent and informative to managers and decision makers (or to other non-technical audiences) for 3 reasons: (1) it misses the differentiated potential impacts to individual LMEs when local or regional impacts are to be modelled, as only spatially explicit SDs discriminate the number of species exposed. The EF is focused on (available) species composition data and sensitivity of the ecological communities, suggesting that each LME is quantitatively and qualitatively distinct – still, an increase of spatial resolution of the EF model work can be seen as a method improvement here; (2) the decoupling of the indicator and the community makes PAF- and PDF-integrated units (fractions) less communicable, in opposition to an easier to grasp absolute number of species in the damage unit; and (3) it misses the ability to match the dimension of other indicators and the aggregation into a common damage category.

Endpoint indicators for impacts affecting the ecosystem are a quantifiable representation of the changes in the quality status, or damages, in this entity (Jolliet et al., 2004). Marine eutrophication typically falls in this classification and therefore its indicator is assigned to the AoP *Ecosystems*. Various other indicators also contribute to the same AoP, e.g. terrestrial ecotoxicity, freshwater eutrophication, marine acidification. The indicators of these impact categories are ideally expressed in a common unit in order to facilitate their comparison and aggregation if desired. However, available endpoint-oriented and combined midpoint-endpoint LCIA methods differ in the units representing such damage to ecosystem, as one can find e.g. (PDF)·$m^{2\ or\ 3}$·yr (respectively for area or volume and time integrated PDF), Expected Increase in Number of Extinct Species (EINES) (Itsubo and Inaba, 2012), or normalized extinction of species (NEX, dimensionless) (Steen, 1999). More importantly, the PDF-integrated units do not necessarily refer to a comparable biotic component of the ecosystem, thus failing to express a joint measure of biodiversity change. Taking the above mentioned impact categories, terrestrial ecotoxicity necessarily affect land-based species that may not be found in freshwater systems and covered by eutrophication impact models there, and these communities are not common to those of marine species used to model ocean acidification impacts – despite all three indicators are expressed in PDF-integrated units. Finally, within non-global impact indicators, such as eutrophication, the naturally occurring variability of species in distinct geographic locations is not entirely accounted for in current LCIA methods at the damage level, meaning that the absolute number of species in a certain area that a relative PDF-integrated unit represents (a fraction all the same) may not necessarily match the same amount of species elsewhere for the same quantified anthropogenic pressure. Harmonisation of the ecological meaning of PDF-integrated units by means of spatial differentiation in both impacts modelling and SD seems essential to deliver a common and truly comparable species·yr unit. In that line, aggregation of damage-like units is justifiable. On the downside, further uncertainty is added by the extra modelling of SD for the damage indicator. However, the trade-off

between the environmental relevance given by the spatial differentiation and the added uncertainty seems to favour the former when addressing local to regional impacts, such as hypoxia-driven marine eutrophication. The loss of information on specific indicators after damage aggregation is an unavoidable feature of the LCA methodology itself and not really related to the specific impact assessment and indicator modelling.

3.5. Spatial resolution and LME biogeographical classification system

Considering the scale at which the marine eutrophication impacts and relevant species occur, the adopted LME biogeographical classification system seems adequate. Alternatively, any other coastal spatial zonation can be used, as long as the necessary data for the exposure/effect models and species density are available at such resolution, e.g. PP rates (for XF), benthic water temperature (for EF), species occurrence (for EF and SD), and area (for SD).

3.6. Species density estimation methods

Species density estimates are largely based on the predicted occurrence from SDMs, and thus will be affected by the uncertainties of the predictions. Here, a multiple model ensemble approach was used to increase the robustness of the predictions (Araújo and New, 2007). Previous assessment on the skills of the three SDMs employed demonstrated the difficulty of identifying a single optimal model; instead a multi-model approach was preferred (Jones et al., 2012). However, the predicted species occurrence may still be affected by a number of uncertainties inherent in SDMs. Firstly, the SDMs assume that species' distribution was in equilibrium with the environmental conditions in the last few decades, which may not be valid particularly under climate change (Pörtner et al., 2014). Secondly, the SDMs do not explicitly account for biotic interactions. Also, the predicted SDs may be biased by the sample of modelled species. Species were included in the study when they were reported in the fisheries catch statistics. Thus, area may be under- or over-represented because of differences in taxonomic resolution of their catch statistics. For example, the high SD in Northeast and Northwest Atlantic is partly because of the high taxonomic resolution of catch statistics of countries in these regions. Acknowledging possible species representativeness concerns due to data availability, the use of the present dataset is considered a best estimate.

3.7. Implications for LCIA modelling

The characterisation of environmental emissions from anthropogenic sources is at the core of LCA methodologies. The inclusion of spatial differentiation in marine eutrophication damage modelling seems a valuable contribution to the LCIA phase of life cycle assessment. Thus, being an improvement to current, site-generic, methodologies. The inclusion of the fate modelling of air- and waterborne emissions of

N-forms to soils, fresh- and marine waters, is essential to compose meaningful CFs. This is clearly a methodological need and further work is recommended to close this gap. The present work introduces methodology developments in spatial differentiation on both the impact assessment and the damage assessment, which is an important feature considering local- to regional-wide impacts of marine eutrophication.

4. Conclusions

This study describes the damage potential of nitrogen uptake by phytoplankton in a cascade of effects typical of marine eutrophication. Relevant applications of the damage indicator, obtained with the proposed methodology, include impacts assessment and ecosystem management in areas affected by riverine discharge of N forms, particularly if the respective watershed has a significant contribution from agriculture runoff. An endpoint-to-damage conversion is discussed and applied to deliver spatially explicit damage scores of the ecosystem response to N inputs in a metric that is consistent and harmonised with other endpoint ecosystem-related indicators in life cycle impact assessment.

A 4-order magnitude of spatial differentiation of the resulting LME-dependent indicators is not only justified by spatially distinct exposure and effect models, but also by the differentiation of the impacts significance to the ecological community at its occurrence location. The introduced method shows important and novel features when compared to available and current methodologies. As such, the adaptation of the described marine eutrophication ecosystem damage (*meED*) indicator is suggested for LCIA application. Its incorporation in characterisation modelling of anthropogenic-N emissions with eutrophying impacts in a life cycle perspective may contribute with essential components to an already proven tool in assessing the sustainability of human activities.

References

Araújo, M.B., New, M., 2007. Ensemble forecasting of species distributions. Trends Ecol. Evol. 22, 42–47. doi:10.1016/j.tree.2006.09.010

Behrenfeld, M.J., Boss, E.S., 2014. Resurrecting the ecological underpinnings of ocean plankton blooms. Ann. Rev. Mar. Sci. 6, 167–94. doi:10.1146/annurev-marine-052913-021325

Chavez, F.P., Messié, M., Pennington, J.T., 2011. Marine Primary Production in Relation to Climate Variability and Change. Ann. Rev. Mar. Sci. 3, 227–260. doi:10.1146/annurev. marine.010908.163917

Cheung, W.W.L., Lam, V.W.Y., Pauly, D., 2008. Fisheries Centre Research Reports Modelling Present and Climate- Fishes and Invertebrates. Fish. Cent. Res.

Reports 16, 72.

Close, C., Cheung, W.W.L., Hodgson, S., Lam, V.W.Y., Watson, R., Pauly, D., 2006. Distribution ranges of commercial fishes and invertebrates, in: Palomares, M.L., Stergiou, K.I., Pauly, D. (Eds.), Fishes in Databases and Ecosystems. Fisheries Centre Research Reports 14(4). Vancouver, pp. 27–37.

Cosme, N., Hauschild, M.Z., 2016. Effect factors for marine eutrophication in LCIA based on species sensitivity to hypoxia. Ecol. Indic. 69:453-462. doi:10.1016/j.ecolind.2016.04.006

Cosme, N., Koski, M., Hauschild, M.Z., 2015. Exposure factors for marine eutrophication impacts assessment based on a mechanistic biological model. Ecol. Modell. 317, 50–63. doi:10.1016/j.ecolmodel.2015.09.005

Cosme, N., Mayorga, E., Hauschild, M.Z., n.d. Spatially explicit fate factors for waterbone nitrogen emissions at the global scale. Int. J. Life Cycle Assesment submitted.

Curran, M., de Baan, L., De Schryver, A.M., Van Zelm, R., Hellweg, S., Koellner, T., Sonnemann, G., Huijbregts, M.A.J., 2011. Toward meaningful end points of biodiversity in life cycle assessment. Environ. Sci. Technol. 45, 70–9. doi:10.1021/es101444k

Cushing, D.H., 1959. The seasonal variation in oceanic production as a problem in population dynamics. J. Cons. int. Explor. Mer 24, 455–464. doi:doi:10.1093/icesjms/24.3.455

Davis, J.C., 1975. Minimal dissolved oxygen requirements of aquatic life with emphasis on Canadian species: a review. J. Fish. Res. Board Canada 32, 2295–2332.

Dentener, F., Drevet, J., Lamarque, J.F., Bey, I., Eickhout, B., Fiore, A.M., Hauglustaine, D., Horowitz, L.W., Krol, M., Kulshrestha, U.C., Lawrence, M., Galy-Lacaux, C., Rast, S., Shindell, D., Stevenson, D., Van Noije, T., Atherton, C., Bell, N., Bergman, D., Butler, T., Cofala, J., Collins, B., Doherty, R., Ellingsen, K., Galloway, J., Gauss, M., Montanaro, V., Müller, J.F., Pitari, G., Rodriguez, J., Sanderson, M., Solmon, F., Strahan, S., Schultz, M., Sudo, K., Szopa, S., Wild, O., 2006. Nitrogen and sulfur deposition on regional and global scales: A multimodel evaluation. Global Biogeochem. Cycles 20. doi:10.1029/2005GB002672

Diaz, R.J., 2001. Overview of Hypoxia around the World. J. Environ. Qual. 30, 275–81.

Diaz, R.J., Rosenberg, R., 2008. Spreading dead zones and consequences for marine ecosystems. Science (80-.). 321, 926–9. doi:10.1126/science.1156401

Diaz, R.J., Rosenberg, R., 1995. Marine Benthic Hypoxia: a Review of Its Ecological

Effects and the Behavioural Responses of Benthic Macrofauna. Oceanogr. Mar. Biol. Annu. Rev. 33, 245–303.

Doray, M., Trenkel, V.M., 2010. Estimating gear efficiency in a combined acoustic and trawl survey, with reference to the spatial distribution of demersal fish. ICES J. Mar. Sci. 67, 668–676. doi:dx.doi.org/10.1093/icesjms/fsp277

EC-JRC, 2010. ILCD Handbook: Analysis of existing Environmental Impact Assessment methodologies for use in Life Cycle Assessment, First edit. ed. Publications Office of the European Union, Luxembourg.

Falkowski, P.G., Raven, J.A., 2007. Aquatic Photosynthesis, Second Edi. ed. Princeton University Press, Oxford, UK. doi:10.1017/CBO9781107415324.004

Galloway, J.N., Townsend, A.R., Erisman, J.W., Bekunda, M., Cai, Z., Freney, J.R., Martinelli, L.A., Seitzinger, S.P., Sutton, M.A., 2008. Transformation of the Nitrogen Cycle: Recent Trends, Questions, and Potential Solutions. Science (80-.). 320, 889–892. doi:10.1126/science.1136674

GESAMP, 2001. A Sea of Troubles. Rep. Stud. GESAMP No. 70. Joint Group of Experts on the Scientific Aspects of Marine Environmental Protection and Advisory Committee on Protection of the Sea.

Goedkoop, M., Heijungs, R., Huijbregts, M.A.J., De Schryver, A.M., Struijs, J., van Zelm, R., 2012. ReCiPe 2008 - A life cycle impact assessment method which comprises harmonised category indicators at the midpoint and the endpoint level. First edition (revised) Report I: Characterisation; July 2012, http://www.lcia-recipe.net.

Goedkoop, M., Spriensma, R., 2000. The Eco-indicator 99 A damage oriented method for Life Cycle Impact Assessment Methodology Report.

Graf, G., Bengtsson, W., Diesner, U., Schulz, R., Theede, H., 1982. Benthic response to sedimentation of a spring phytoplankton bloom: Process and budget. Mar. Biol. 67, 201–208. doi:10.1007/BF00401286

Gray, J.S., Wu, R.S., Or, Y.Y., 2002. Effects of hypoxia and organic enrichment on the coastal marine environment. Mar. Ecol. Prog. Ser. 238, 249–279.

Guinée, J.B., Gorrée, M., Heijungs, R., Huppes, G., Kleijn, R., Koning, A. de, Oers, L. van, Sleeswijk, A.W., Suh, S., Udo de Haes, H.A., Bruijn, H. de, Duin, R. van, Huijbregts, M.A.J., 2002. Handbook on life cycle assessment. Operational guide to the ISO standards. I: LCA in perspective. IIa: Guide. IIb: Operational annex. III: Scientific background. Kluwer Academic Publishers, Dordrecht.

Hauschild, M.Z., 2005. Assessing Environmental Impacts in a Life-Cycle Perspective. Environ. Sci. Technol. 39, 81–88. doi:10.1021/es053190s

Hauschild, M.Z., Goedkoop, M., Guinée, J., Heijungs, R., Huijbregts, M.A.J., Jolliet, O., Margni, M., De Schryver, A.M., Humbert, S., Laurent, A., Sala, S., Pant, R., 2013. Identifying best existing practice for characterization modeling in life cycle impact assessment. Int. J. Life Cycle Assess. 18, 683–697. doi:10.1007/s11367-012-0489-5

Hauschild, M.Z., Potting, J., 2005. Spatial Differentiation in Life Cycle Impact Assessment - The EDIP2003 methodology, Environmental News No. 80.

Heijungs, R., 2005. Commentaries On the Use of Units in LCA 1998, 173–176.

Henderson, A.D., 2015. Eutrophication, in: Hauschild, M.Z., Huijbregts, M.A.J. (Eds.), Life Cycle Impact Assessment, LCA Compendium - The Complete World of Life Cycle Assessment. Springer Science+Business Media Dordrecht, pp. 177–196.

Hjellvik, V., Michalsen, K., Aglen, A., Nakken, O., 2003. An attempt at estimating the effective fishing height of the bottom trawl using acoustic survey recordings. ICES J. Mar. Sci. 967–979. doi:10.1016/S1054–3139(03)00116-4

Howarth, R.W., Marino, R., 2006. Nitrogen as the limiting nutrient for eutrophication in coastal marine ecosystems: Evolving views over three decades. Limnol. Oceanogr. 51, 364–376. doi:10.4319/lo.2006.51.1_part_2.0364

Hutchinson, G.E., 1957. Concludig remarks. Cold Spring Harb. Symp. Quant. Biol. 22, 415–427.

Itsubo, N., Inaba, A., 2012. LIME2: Life-cycle Impact assessment Method based on Endpoint modeling. JLCA Newsl. Life-Cycle Assess. Soc. Japan 12, 16.

Jolliet, O., Margni, M., Charles, R., Humbert, S., Payet, J., Rebitzer, G., 2003. Presenting a New Method IMPACT 2002 + : A New Life Cycle Impact Assessment Methodology. Int J LCA 8, 324–330.

Jolliet, O., Müller-Wenk, R., Bare, J.C., Brent, A., Goedkoop, M., Heijungs, R., Itsubo, N., Peña, C., Pennington, D.W., Potting, J., Rebitzer, G., Stewart, M., Udo de Haes, H.A., Weidema, B.P., 2004. The LCIA Midpoint-damage Framework of the UNEP/SETAC Life Cycle Initiative. Int. J. Life Cycle Assess. 9, 394–404.

Jones, M.C., Cheung, W.W.L., 2015. Multi-model ensemble projections of climate change effects on global marine biodiversity. ICES J. Mar. Sci. 72, 741–752. doi:10.1093/icesjms/fsu172

Jones, M.C., Dye, S.R., Pinnegar, J.K., Warren, R., Cheung, W.W.L., 2012. Modelling commercial fish distributions: Prediction and assessment using different approaches. Ecol. Modell. 225, 133–145. doi:10.1016/j.ecolmodel.2011.11.003

Justić, D., Rabalais, N.N., Turner, R.E., Wiseman, W.J.J., 1993. Seasonal coupling

between riverborne nutrients, net productivity and hypoxia. Mar. Pollut. Bull. 26, 184–189. doi:10.1016/0025-326X(93)90620-Y

Larsen, H.F., Hauschild, M.Z., 2007. LCA Methodology Evaluation of Ecotoxicity Effect Indicators for Use in LCIA. Int. J. 12, 24–33.

Levin, L.A., Ekau, W., Gooday, A.J., Jorissen, F., Middelburg, J.J., Naqvi, S.W.A., Neira, C., Rabalais, N.N., Zhang, J., 2009. Effects of natural and human-induced hypoxia on coastal benthos. Biogeosciences 6, 2063–2098.

Lutz, M.J., Caldeira, K., Dunbar, R.B., Behrenfeld, M.J., 2007. Seasonal rhythms of net primary production and particulate organic carbon flux to depth describe the efficiency of biological pump in the global ocean. J. Geophys. Res. 112, C10011. doi:10.1029/2006JC003706

Michael Beman, J., Arrigo, K.R., Matson, P.A., 2005. Agricultural runoff fuels large phytoplankton blooms in vulnerable areas of the ocean. Nature 434, 211–214. doi:10.1038/nature03370

Middelburg, J.J., Levin, L.A., 2009. Coastal hypoxia and sediment biogeochemistry. Biogeosciences 6, 1273–1293. doi:10.5194/bg-6-1273-2009

Othoniel, B., Rugani, B., Heijungs, R., Benetto, E., Withagen, C.A.A.M., 2016. Assessment of life cycle impacts on ecosystem services: promise, problems and prospects. Environ. Sci. Technol. acs.est.5b03706. doi:10.1021/acs.est.5b03706

Pennington, D.W., Payet, J., Hauschild, M.Z., 2004a. Aquatic Ecotoxicological Indicators In Life-Cycle Assessment. Environ. Toxicol. Chem. 23, 1796–1807.

Pennington, D.W., Potting, J., Finnveden, G., Lindeijer, E., Jolliet, O., Rydberg, T., Rebitzer, G., 2004b. Life cycle assessment Part 2: Current impact assessment practice. Environ. Int. 30, 721–39. doi:10.1016/j.envint.2003.12.009

Pickett, S.T.A., White, P.S., 1985. Natural disturbance and patch dynamics: An introduction, The Ecology of Natural Disturbance and Patch Dynamics. Academic Press, San Diego. doi:10.2307/2403105

Ploug, H., Grossart, H.-P., Azam, Farooq, Jørgensen, B.B., 1999. Photosynthesis, respiration, and carbon turnover in sinking marine snow from surface waters of Southern California Bight: implications for the carbon cycle in the ocean. Mar. Ecol. Prog. Ser. 179, 1–11.

Pörtner, H.-O., Karl, D.M., Boyd, P.W., Cheung, W.W.L., Lluch-Cota, S.E., Nojiri, Y., Schmidt, D.N., Zavialov, P.O., 2014. Ocean systems, in: Field, C.B., Barros, V.R., Dokken, D.J., Mach, K.J., Mastrandrea, M.D., Bilir, T.E., Chatterjee, M., Ebi, K.L., Estrada, Y.O., Genova, R.C., Girma, B., Kissel, E.S., Levy, A.N., MacCracken, S., Mastrandrea, P.R., White, L.L. (Eds.), Climate Change 2014:

Impacts, Adaptation, and Vulnerability. Part A: Global and Sectoral Aspects. Contribution of Working Group II to the Fifth Assessment Report of the Intergovernmental Panel on Climate Change. Cambridge University Press, Cambridge, United Kingdom and New York, NY, USA, pp. 411–484.

Posthuma, L., Suter II, G.W., Traas, T.P. (Eds.), 2002. Species Sensitivity Distributions in Ecotoxicology, Environmental and Ecological Risk Assessment.

Rabalais, N.N., 2002. Nitrogen in Aquatic Ecosystems. Ambio 31, 102–112.

Rabalais, N.N., Diaz, R.J., Levin, L.A., Turner, R.E., Gilbert, D., Zhang, J., 2010. Dynamics and distribution of natural and human-caused coastal hypoxia. Biogeosciences 7, 585–619. doi:10.5194/bgd-6-9359-2009

Rabalais, N.N., Turner, R.E., Diaz, R.J., Justić, D., 2009. Global change and eutrophication of coastal waters. ICES J. Mar. Sci. 66, 1528–1537.

Rosenberg, R., 1985. Eutrophication - the future marine coastal nuisance? Mar. Pollut. Bull. 16, 227–231. doi:10.1016/0025-326X(85)90505-3

Roy, P.-O., Huijbregts, M.A.J., Deschênes, L., Margni, M., 2012. Spatially-differentiated atmospheric source–receptor relationships for nitrogen oxides, sulfur oxides and ammonia emissions at the global scale for life cycle impact assessment. Atmos. Environ. 62, 74–81. doi:10.1016/j.atmosenv.2012.07.069

Sherman, K., Alexander, L.M. (Eds.), 1986. Variability and Management of Large Marine Ecosystems. Westview Press Inc., Boulder, CO.

Smith, D.E., Leffler, M., Mackiernan, G., 1992. Oxygen dynamics in the Chesapeake Bay - A synthesis of recent research. University of Maryland, Maryland Sea Grant, Maryland, MD.

Smith, V.H., Tilman, G.D., Nekola, J.C., 1999. Eutrophication: impacts of excess nutrient inputs on freshwater, marine, and terrestrial ecosystems. Environ. Pollut. 100, 179–196.

Souza, D.M. de, Flynn, D.F.B., Declerck, F., Rosenbaum, R.K., De Melo Lisboa, H., Koellner, T., 2013. Land use impacts on biodiversity in LCA: Proposal of characterization factors based on functional diversity. Int. J. Life Cycle Assess. 18, 1231–1242. doi:10.1007/s11367-013-0578-0

Steen, B., 1999. A systematic approach to environmental priority strategies in product development (EPS). Version 2000 – General system characteristics. CPM report 1999:4. Gothenburg, Sweden.

Udo de Haes, H.A., Finnveden, G., Goedkoop, M., Hauschild, M.Z., Hertwich, E., Hofstetter, P., Jolliet, O., Klöpffer, W., Krewitt, W., Lindeijer, E., Müller-Wenk, R., Olsen, S.I., Pennington, D.W., Potting, J., Steen, B., 2002. Life-Cycle Impact

Assessment: Striving Towards Best Practice. SETAC Press, Pensacola, FL, USA.

Udo de Haes, H.A., Jolliet, O., Finnveden, G., Hauschild, M.Z., Krewitt, W., Müller-Wenk, R., 1999. Best Available Practice Regarding Impact Categories and Category Indicators in Life Cycle Impact Assessment. Int J LCA 4, 66–74.

Vaquer-Sunyer, R., Duarte, C.M., 2008. Thresholds of hypoxia for marine biodiversity. Proc. Natl. Acad. Sci. U. S. A. 105, 15452–7. doi:10.1073/pnas.0803833105

Verones, F., Huijbregts, M.A.J., Chaudhary, A., de Baan, L., Koellner, T., Hellweg, S., 2015. Harmonizing the assessment of biodiversity effects from land and water use within LCA. Environ. Sci. Technol. 49, 3584–3592. doi:10.1021/es504995r

Verones, F., Saner, D., Pfister, S., Baisero, D., Rondinini, C., Hellweg, S., 2013. Effects of consumptive water use on biodiversity in wetlands of international importance. Environ. Sci. Technol. 47, 12248–57. doi:10.1021/es403635j

Vitousek, P.M., Hättenschwiler, S., Olander, L., Allison, S., 2002. Nitrogen and nature. Ambio 31, 97–101.

Wu, R.S., 2002. Hypoxia: from molecular responses to ecosystem responses. Mar. Pollut. Bull. 45, 35–45.

Zhang, J., Gilbert, D., Gooday, A.J., Levin, L.A., Naqvi, S.W.A., Middelburg, J.J., Scranton, M., Ekau, W., Peña, A., Dewitte, B., Oguz, T., Monteiro, P.M.S., Urban, E., Rabalais, N.N., Ittekkot, V., Kemp, W.M., Ulloa, O., Elmgren, R., Escobar-Briones, E., Van der Plas, A.K., 2010. Natural and human-induced hypoxia and consequences for coastal areas: synthesis and future development. Biogeosciences 7, 1443–1467. doi:10.5194/bg-7-1443-2010

Zhang, Y., Singh, S., Bakshi, B.R., 2010. Accounting for Ecosystem Services in Life Cycle Assessment, Part I: A Critical Review. Environ. Sci. Technol. 44, 2232–2242.

Article IV – Supporting Information

Spatial differentiation of marine eutrophication damage indicators based on species density

Nuno Cosme [1]*, Miranda C. Jones [2], William W. L. Cheung [3], Henrik Fred Larsen [1]

[1] Division for Quantitative Sustainability Assessment, Department of Management Engineering, Technical University of Denmark, Produktionstorvet 424, DK-2800 Kgs. Lyngby, Denmark

[2] United Nations Environment Programme World Conservation Monitoring Centre, 219 Huntingdon Road, Cambridge CB3 ODL, UK

[3] Changing Ocean Research Unit and Nippon Foundation – Nereus Program, Institute for the Oceans and Fisheries, the University of British Columbia, Vancouver, British Columbia, Canada

*Corresponding author: e-mail address: nmdc@dtu.dk (N. Cosme)

Additional figures and tables

Figure S.1 Distribution of Exposure Factors (XF) estimated per Large Marine Ecosystem (LME) – adapted from Cosme et al. (2015).

Figure S.2 Distribution of Effect Factors (EF) disaggregated from climate zones to Large Marine Ecosystems (LME) – produced with results from Cosme and Hauschild (2016).

Figure S.3 Distribution of Ecosystem Response (ER) scores per Large Marine Ecosystem (LME).

Figure S.4 Distribution of species richness (SR) per Large Marine Ecosystem (LME). Note the non-linear scale.

Table S.1 List of benthic, demersal, and benthopelagic fish and invertebrates species used to estimate species richness and density by means of species distributions models (SDMs).

References

Cosme, N., Hauschild, M.Z., 2016. Effect factors for marine eutrophication in LCIA based on species sensitivity to hypoxia. Ecol. Indic. 69, 453–462. doi:10.1016/j.ecolind.2016.04.006

Cosme, N., Koski, M., Hauschild, M.Z., 2015. Exposure factors for marine eutrophication impacts assessment based on a mechanistic biological model. Ecol. Modell. 317, 50–63. doi:10.1016/j.ecolmodel.2015.09.005

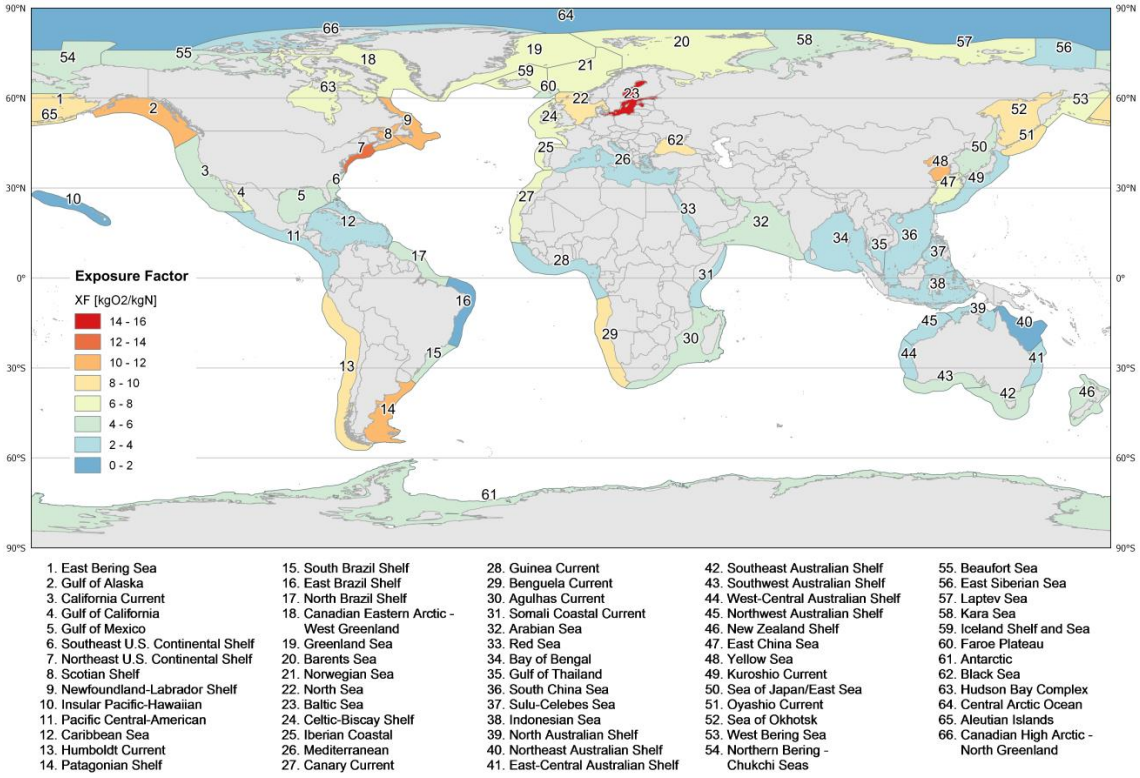

1. East Bering Sea
2. Gulf of Alaska
3. California Current
4. Gulf of California
5. Gulf of Mexico
6. Southeast U.S. Continental Shelf
7. Northeast U.S. Continental Shelf
8. Scotian Shelf
9. Newfoundland-Labrador Shelf
10. Insular Pacific-Hawaiian
11. Pacific Central-American
12. Caribbean Sea
13. Humboldt Current
14. Patagonian Shelf
15. South Brazil Shelf
16. East Brazil Shelf
17. North Brazil Shelf
18. Canadian Eastern Arctic - West Greenland
19. Greenland Sea
20. Barents Sea
21. Norwegian Sea
22. North Sea
23. Baltic Sea
24. Celtic-Biscay Shelf
25. Iberian Coastal
26. Mediterranean
27. Canary Current
28. Guinea Current
29. Benguela Current
30. Agulhas Current
31. Somali Coastal Current
32. Arabian Sea
33. Red Sea
34. Bay of Bengal
35. Gulf of Thailand
36. South China Sea
37. Sulu-Celebes Sea
38. Indonesian Sea
39. North Australian Shelf
40. Northeast Australian Shelf
41. East-Central Australian Shelf
42. Southeast Australian Shelf
43. Southwest Australian Shelf
44. West-Central Australian Shelf
45. Northwest Australian Shelf
46. New Zealand Shelf
47. East China Sea
48. Yellow Sea
49. Kuroshio Current
50. Sea of Japan/East Sea
51. Oyashio Current
52. Sea of Okhotsk
53. West Bering Sea
54. Northern Bering - Chukchi Seas
55. Beaufort Sea
56. East Siberian Sea
57. Laptev Sea
58. Kara Sea
59. Iceland Shelf and Sea
60. Faroe Plateau
61. Antarctic
62. Black Sea
63. Hudson Bay Complex
64. Central Arctic Ocean
65. Aleutian Islands
66. Canadian High Arctic - North Greenland

Figure S.1 Distribution of Exposure Factors (XF) estimated per Large Marine Ecosystem (LME) – adapted from Cosme et al. (2015).

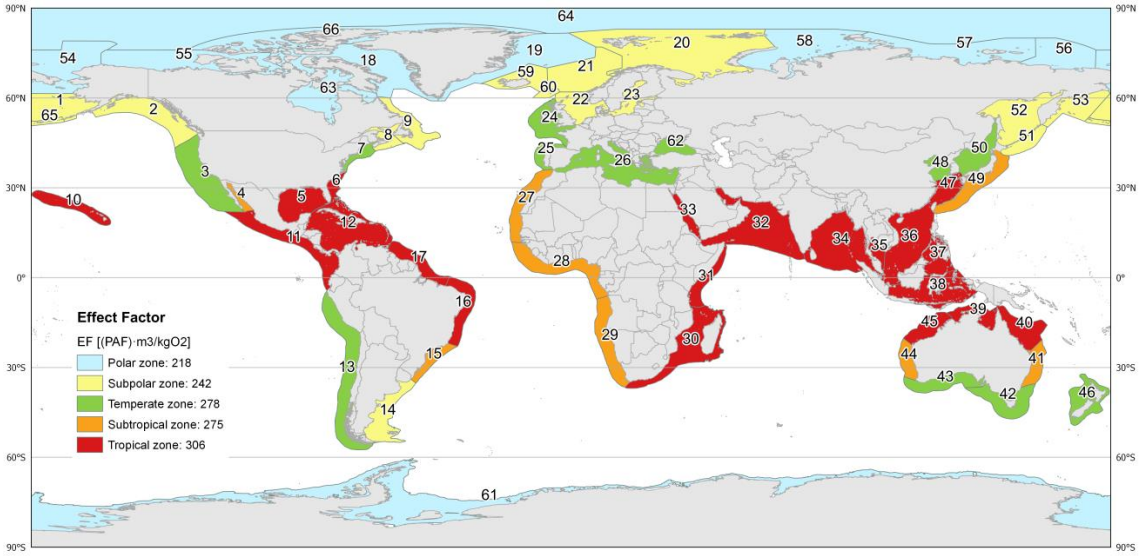

1. East Bering Sea
2. Gulf of Alaska
3. California Current
4. Gulf of California
5. Gulf of Mexico
6. Southeast U.S. Continental Shelf
7. Northeast U.S. Continental Shelf
8. Scotian Shelf
9. Newfoundland-Labrador Shelf
10. Insular Pacific-Hawaiian
11. Pacific Central-American
12. Caribbean Sea
13. Humboldt Current
14. Patagonian Shelf
15. South Brazil Shelf
16. East Brazil Shelf
17. North Brazil Shelf
18. Canadian Eastern Arctic - West Greenland
19. Greenland Sea
20. Barents Sea
21. Norwegian Sea
22. North Sea
23. Baltic Sea
24. Celtic-Biscay Shelf
25. Iberian Coastal
26. Mediterranean
27. Canary Current
28. Guinea Current
29. Benguela Current
30. Agulhas Current
31. Somali Coastal Current
32. Arabian Sea
33. Red Sea
34. Bay of Bengal
35. Gulf of Thailand
36. South China Sea
37. Sulu-Celebes Sea
38. Indonesian Sea
39. North Australian Shelf
40. Northeast Australian Shelf
41. East-Central Australian Shelf
42. Southeast Australian Shelf
43. Southwest Australian Shelf
44. West-Central Australian Shelf
45. Northwest Australian Shelf
46. New Zealand Shelf
47. East China Sea
48. Yellow Sea
49. Kuroshio Current
50. Sea of Japan/East Sea
51. Oyashio Current
52. Sea of Okhotsk
53. West Bering Sea
54. Northern Bering - Chukchi Seas
55. Beaufort Sea
56. East Siberian Sea
57. Laptev Sea
58. Kara Sea
59. Iceland Shelf and Sea
60. Faroe Plateau
61. Antarctic
62. Black Sea
63. Hudson Bay Complex
64. Central Arctic Ocean
65. Aleutian Islands
66. Canadian High Arctic - North Greenland

Figure S.2 Distribution of Effect Factors (EF) disaggregated from climate zones to Large Marine Ecosystems (LME) – produced with results from Cosme and Hauschild (2016).

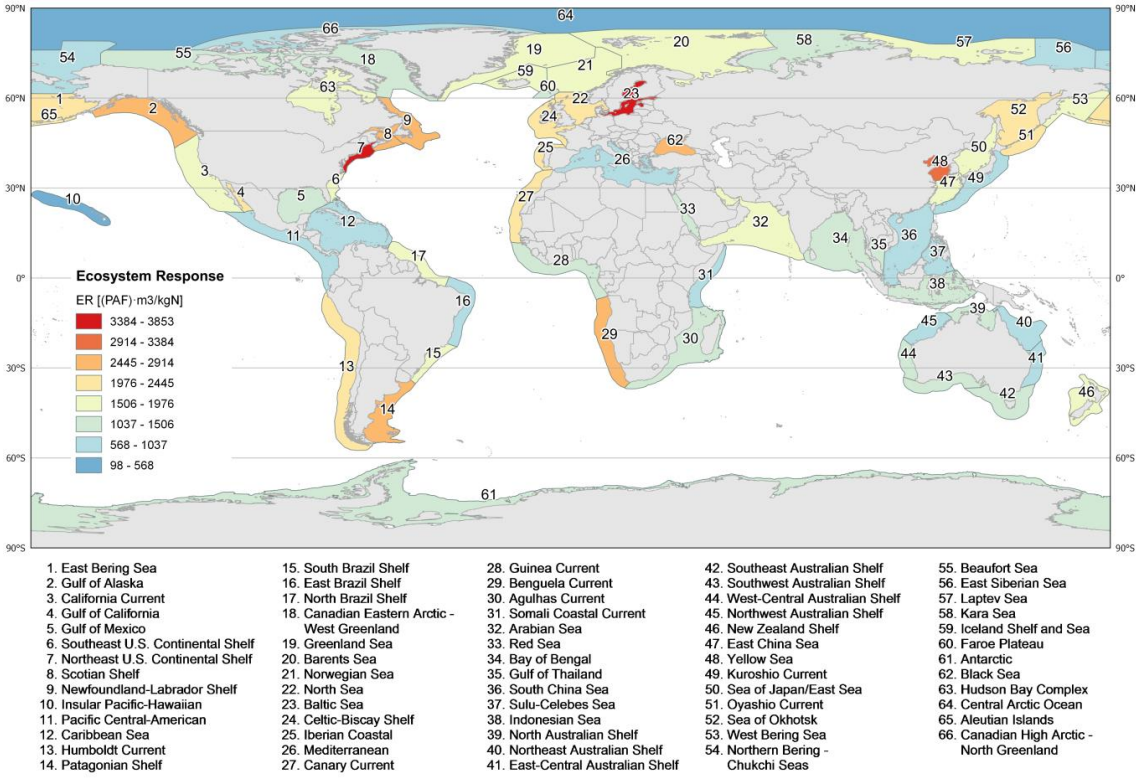

1. East Bering Sea
2. Gulf of Alaska
3. California Current
4. Gulf of California
5. Gulf of Mexico
6. Southeast U.S. Continental Shelf
7. Northeast U.S. Continental Shelf
8. Scotian Shelf
9. Newfoundland-Labrador Shelf
10. Insular Pacific-Hawaiian
11. Pacific Central-American
12. Caribbean Sea
13. Humboldt Current
14. Patagonian Shelf
15. South Brazil Shelf
16. East Brazil Shelf
17. North Brazil Shelf
18. Canadian Eastern Arctic - West Greenland
19. Greenland Sea
20. Barents Sea
21. Norwegian Sea
22. North Sea
23. Baltic Sea
24. Celtic-Biscay Shelf
25. Iberian Coastal
26. Mediterranean
27. Canary Current
28. Guinea Current
29. Benguela Current
30. Agulhas Current
31. Somali Coastal Current
32. Arabian Sea
33. Red Sea
34. Bay of Bengal
35. Gulf of Thailand
36. South China Sea
37. Sulu-Celebes Sea
38. Indonesian Sea
39. North Australian Shelf
40. Northeast Australian Shelf
41. East-Central Australian Shelf
42. Southeast Australian Shelf
43. Southwest Australian Shelf
44. West-Central Australian Shelf
45. Northwest Australian Shelf
46. New Zealand Shelf
47. East China Sea
48. Yellow Sea
49. Kuroshio Current
50. Sea of Japan/East Sea
51. Oyashio Current
52. Sea of Okhotsk
53. West Bering Sea
54. Northern Bering - Chukchi Seas
55. Beaufort Sea
56. East Siberian Sea
57. Laptev Sea
58. Kara Sea
59. Iceland Shelf and Sea
60. Faroe Plateau
61. Antarctic
62. Black Sea
63. Hudson Bay Complex
64. Central Arctic Ocean
65. Aleutian Islands
66. Canadian High Arctic - North Greenland

Figure S.3 Distribution of Ecosystem Response (ER_{PAF}) scores per Large Marine Ecosystem (LME).

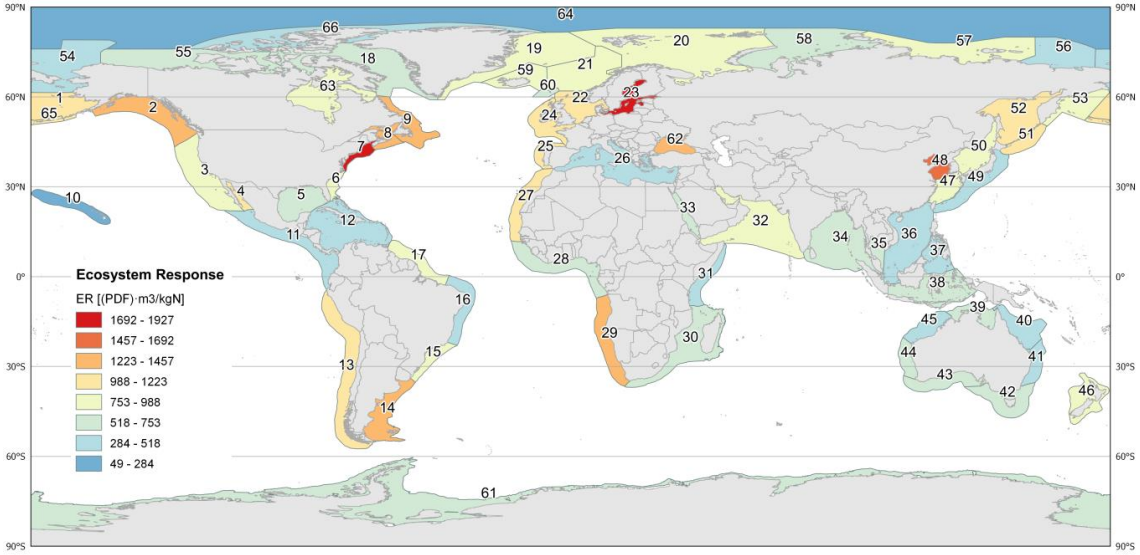

1. East Bering Sea
2. Gulf of Alaska
3. California Current
4. Gulf of California
5. Gulf of Mexico
6. Southeast U.S. Continental Shelf
7. Northeast U.S. Continental Shelf
8. Scotian Shelf
9. Newfoundland-Labrador Shelf
10. Insular Pacific-Hawaiian
11. Pacific Central-American
12. Caribbean Sea
13. Humboldt Current
14. Patagonian Shelf
15. South Brazil Shelf
16. East Brazil Shelf
17. North Brazil Shelf
18. Canadian Eastern Arctic - West Greenland
19. Greenland Sea
20. Barents Sea
21. Norwegian Sea
22. North Sea
23. Baltic Sea
24. Celtic-Biscay Shelf
25. Iberian Coastal
26. Mediterranean
27. Canary Current
28. Guinea Current
29. Benguela Current
30. Agulhas Current
31. Somali Coastal Current
32. Arabian Sea
33. Red Sea
34. Bay of Bengal
35. Gulf of Thailand
36. South China Sea
37. Sulu-Celebes Sea
38. Indonesian Sea
39. North Australian Shelf
40. Northeast Australian Shelf
41. East-Central Australian Shelf
42. Southeast Australian Shelf
43. Southwest Australian Shelf
44. West-Central Australian Shelf
45. Northwest Australian Shelf
46. New Zealand Shelf
47. East China Sea
48. Yellow Sea
49. Kuroshio Current
50. Sea of Japan/East Sea
51. Oyashio Current
52. Sea of Okhotsk
53. West Bering Sea
54. Northern Bering - Chukchi Seas
55. Beaufort Sea
56. East Siberian Sea
57. Laptev Sea
58. Kara Sea
59. Iceland Shelf and Sea
60. Faroe Plateau
61. Antarctic
62. Black Sea
63. Hudson Bay Complex
64. Central Arctic Ocean
65. Aleutian Islands
66. Canadian High Arctic - North Greenland

Figure S.4 Distribution of Ecosystem Response (ER_{PDF}) scores per Large Marine Ecosystem (LME).

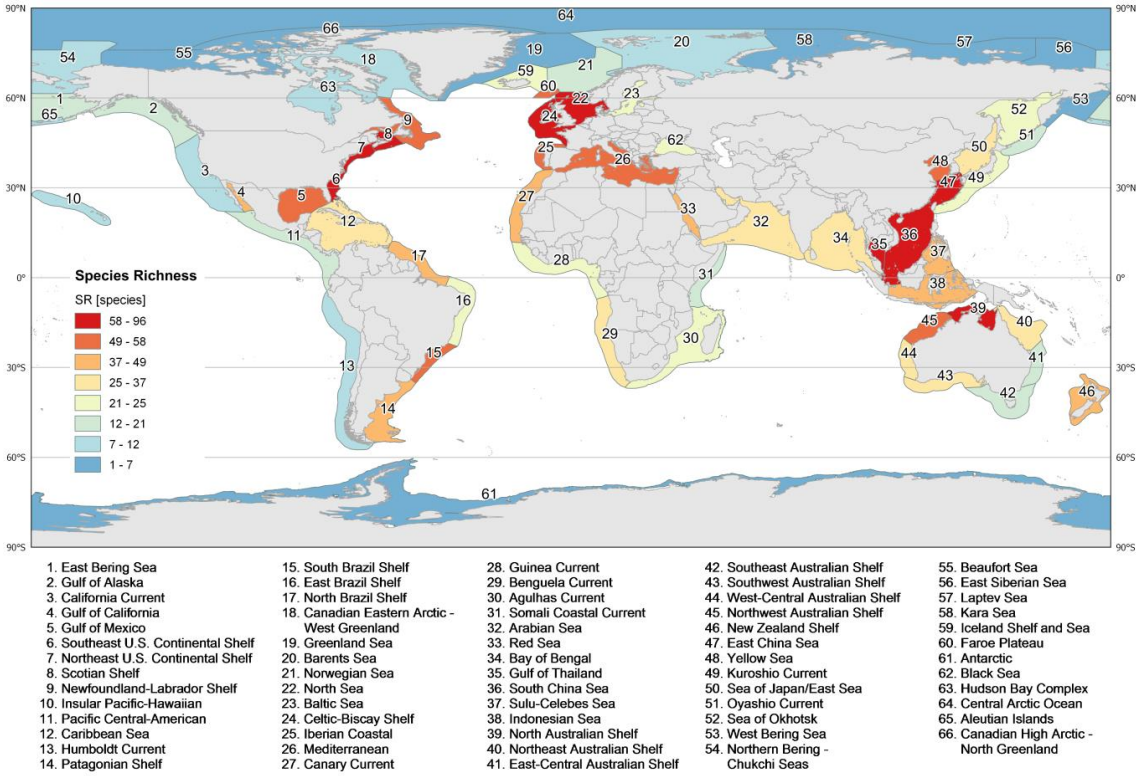

Figure S.5 Distribution of species richness (SR) per Large Marine Ecosystem (LME). Note the non-linear scale.

Table S.1 List of benthic, demersal, and benthopelagic fish and invertebrates species used to estimate species richness and density by means of species distributions models (SDMs).

Fish species			
Scientific name	**Common name**	**Scientific name**	**Common name**
Abudefduf luridus	Canary damsel	*Lutjanus kasmira*	Common bluestripe snapper
Acanthistius brasilianus	Sea bass	*Lutjanus malabaricus*	Malabar blood snapper
Acanthopagrus berda	Picnic seabream	*Lutjanus purpureus*	Southern red snapper
Acanthopagrus bifasciatus	Twobar seabream	*Lutjanus quinquelineatus*	Five-lined snapper
Acanthopagrus latus	Yellowfin seabream	*Lutjanus synagris*	Lane snapper
Acanthopagrus schlegeli	Black porgy	*Macrodon ancylodon*	King weakfish
Acanthurus monroviae	Monrovia doctorfish	*Macroramphosus scolopax*	Longspine snipefish
Acipenser sturio	Sturgeon	*Macrourus berglax*	Onion-eye grenadier
Aethaloperca rogaa	Redmouth grouper	*Macrourus holotrachys*	Bigeye grenadier
Albula vulpes	Bonefish	*Macruronus magellanicus*	Patagonian grenadier
Alepes djedaba	Shrimp scad	*Macruronus novaezelandiae*	Blue grenadier
Alepocephalus bairdii	Bairds smooth-head	*Melanogrammus aeglefinus*	Haddock
Alepocephalus rostratus	Rissos smooth-head	*Mene maculata*	Moonfish
Allocyttus niger	Black oreo	*Menticirrhus littoralis*	Gulf kingcroaker
Alopias superciliosus	Bigeye thresher	*Menticirrhus saxatilis*	Northern kingcroaker
Alopias vulpinus	Thintail thresher	*Merlangius merlangus*	Whiting
Amblyraja georgiana	Antarctic starry skate	*Merluccius angustimanus*	Panama hake
Amblyraja hyperborea	Arctic skate	*Merluccius australis*	Southern hake
Ammodytes personatus	Pacific sandeel	*Merluccius bilinearis*	Silver hake

Anarhichas lupus	Wolf-fish	*Merluccius capensis*	Shallow-water Cape hake
Anoplopoma fimbria	Sablefish	*Merluccius hubbsi*	Argentine hake
Anthias anthias	Swallowtail seaperch	*Merluccius merluccius*	European hake
Aphanopus carbo	Black scabbardfish	*Merluccius paradoxus*	Deep-water Cape hake
Aphareus rutilans	Rusty jobfish	*Merluccius polli*	Benguela hake
Archosargus probatocephalus	Sheepshead seabream	*Merluccius productus*	North Pacific hake
Archosargus rhomboidalis	Western Atlantic seabream	*Merluccius senegalensis*	Senegalese hake
Argyrops spinifer	King soldierbream	*Meuschenia scaber*	Velvet leatherjacket
Argyrosomus regius	Meagre	*Microchirus variegatus*	Thickback sole
Argyrozona argyrozona	Carpenter seabream	*Microgadus proximus*	Pacific tomcod
Ariomma indica	Indian ariomma	*Microgadus tomcod*	Atlantic tomcod
Arius thalassinus	Giant seacatfish	*Micromesistius australis*	Southern blue whiting
Atheresthes stomias	Arrowtooth flounder	*Micropogonias furnieri*	Whitemouth croaker
Atractoscion aequidens	Geelbeck croaker	*Micropogonias undulatus*	Atlantic croaker
Atrobucca nibe	Longfin kob	*Microstomus kitt*	Lemon sole
Atule mate	Yellowtail scad	*Miichthys miiuy*	Mi-iuy croaker
Austroglossus microlepis	West coast sole	*Molva dypterygia*	Blue ling
Austroglossus pectoralis	Mud sole	*Molva molva*	Ling
Balistes capriscus	Grey triggerfish	*Monotaxis grandoculis*	Humpnose big-eye bream
Bathyraja eatonii	Eatons skate	*Morone americana*	White perch
Bathyraja irrasa	Kerguelen sandpaper skate	*Mugil cephalus*	Flathead mullet
Bathyraja maccaini	McCains skate	*Mugil liza*	Liza
Bathyraja murrayi	Murrays skate	*Mulloidichthys flavolineatus*	Yellowstripe goatfish
Beryx decadactylus	Alfonsino	*Mullus argentinae*	Argentine goatfish
Beryx splendens	Splendid alfonsino	*Mullus barbatus*	Red mullet
Bolbometopon muricatum	Green humphead parrotfish	*Mullus surmuletus*	Striped red mullet
Boops boops	Bogue	*Mustelus asterias*	Starry smooth-hound
Boreogadus saida	Polar cod	*Mustelus henlei*	Brown smooth-hound
Borostomias antarcticus	Borostomias antarcticus	*Mustelus lenticulatus*	Spotted estuary smooth-hound
Bothus pantherinus	Leopard flounder	*Mustelus mustelus*	Smooth-hound
Brachydeuterus auritus	Bigeye grunt	*Mustelus schmitti*	Narrownose smooth-hound
Brosme brosme	Tusk	*Mycteroperca bonaci*	Black grouper
Brotula barbata	Bearded brotula	*Mycteroperca microlepis*	Gag
Caelorinchus marinii	Marinis grenadier	*Mycteroperca phenax*	Scamp
Callorhinchus capensis	Cape elephantfish	*Mycteroperca venenosa*	Yellowfin grouper
Callorhinchus milii	Ghost shark	*Myxine glutinosa*	Hagfish
Capros aper	Boarfish	*Naso unicornis*	Bluespine unicornfish
Carangoides ruber	Bar jack	*Nemadactylus bergi*	White morwong
Caranx ignobilis	Giant trevally	*Nemadactylus macropterus*	Tarakihi
Caranx rhonchus	False scad	*Nemipterus japonicus*	Japanese threadfin bream
Carcharhinus brachyurus	Copper shark	*Nemipterus randalli*	Randalls threadfin bream
Carcharhinus falciformis	Silky shark	*Nemipterus virgatus*	Golden threadfin bream
Carcharhinus limbatus	Blacktip shark	*Neocyttus rhomboidalis*	Spiky oreo
Carcharhinus longimanus	Oceanic whitetip shark	*Neopagetopsis ionah*	Bible icefish
Carcharhinus obscurus	Dusky shark	*Nezumia aequalis*	Common Atlantic grenadier
Carcharhinus plumbeus	Sandbar shark	*Notorynchus cepedianus*	Broadnose sevengill shark
Carcharhinus sorrah	Spottail shark	*Notothenia coriiceps*	Yellowbelly rockcod
Carcharias taurus	Sand tiger shark	*Notothenia rossii*	Marbled rockcod
Carcharodon carcharias	Great white shark	*Oblada melanura*	Saddled seabream
Caulolatilus chrysops	Atlantic goldeye tilefish	*Ocyurus chrysurus*	Yellowtail snapper
Centriscops humerosus	Banded yellowfish	*Oncorhynchus gorbuscha*	Pink salmon

Centroberyx affinis	Redfish	*Oncorhynchus keta*	Chum salmon
Centrophorus granulosus	Gulper shark	*Oncorhynchus kisutch*	Coho salmon
Centrophorus lusitanicus	Lowfin gulper shark	*Oncorhynchus masou*	Cherry salmon
Centrophorus squamosus	Leafscale gulper shark	*Oncorhynchus mykiss*	Rainbow trout
Centropomus undecimalis	Common snook	*Oncorhynchus tshawytscha*	Chinook salmon
Centropristis striata	Black seabass	*Ophiodon elongatus*	Lingcod
Centroscyllium fabricii	Black dogfish	*Orthopristis chrysoptera*	Pigfish
Centroscymnus coelolepis	Portuguese dogfish	*Otolithes ruber*	Tiger-toothed croaker
Centroscymnus crepidater	Longnose velvet dogfish	*Pagellus acarne*	Axillary seabream
Cephalopholis argus	Peacock hind	*Pagellus bellottii bellottii*	Red pandora
Cephalopholis fulva	Coney	*Pagellus bogaraveo*	Blackspot seabream
Cephalopholis hemistiktos	Yellowfin hind	*Pagellus erythrinus*	Common pandora
Cephalopholis miniata	Coral hind	*Pagrus auriga*	Redbanded seabream
Cepola macrophthalma	Red bandfish	*Pagrus caeruleostictus*	Bluespotted seabream
Cetorhinus maximus	Basking shark	*Pagrus pagrus*	Common seabream
Chaenocephalus aceratus	Blackfin icefish	*Pampus argenteus*	Silver pomfret
Chaenodraco wilsoni	Spiny icefish	*Paradiplospinus gracilis*	Slender escolar
Channichthys rhinoceratus	Unicorn icefish	*Paralabrax humeralis*	Peruvian rock seabass
Cheimerius nufar	Santer seabream	*Paralichthys dentatus*	Summer flounder
Chelidonichthys capensis	Cape gurnard	*Paralichthys olivaceus*	Bastard halibut
Chelidonichthys kumu	Bluefin gurnard	*Parapercis colias*	Blue cod
Chelidonichthys lastoviza	Streaked gurnard	*Parastromateus niger*	Black pomfret
Chelidonichthys spinosus	Red gurnard	*Parona signata*	Parona leatherjacket
Chelon labrosus	Thicklip grey mullet	*Parophrys vetula*	English sole
Chimaera monstrosa	Rabbit fish	*Patagonotothen ramsayi*	Ramsay's icefish
Chionobathyscus dewitti	Chionobathyscus dewitti	*Pegusa lascaris*	Sand sole
Chionodraco myersi	Chionodraco myersi	*Pelates quadrilineatus*	Fourlined terapon
Chionodraco rastrospinosus	Ocellated icefish	*Pennahia anea*	Greyfin croaker
Chirocentrus dorab	Dorab wolf-herring	*Pennahia argentata*	White croaker
Chloroscombrus orqueta	Pacific bumper	*Pentanemus quinquarius*	Royal threadfin
Chromis chromis	Damselfish	*Peprilus simillimus*	Pacific pompano
Chrysophrys auratus	Squirefish	*Peprilus triacanthus*	American butterfish
Ciliata mustela	Fivebeard rockling	*Percophis brasiliensis*	Brazilian flathead
Citharus linguatula	Atlantic spotted flounder	*Petromyzon marinus*	Sea lamprey
Conger conger	European conger	*Petrus rupestris*	Red steenbras
Conger myriaster	Whitespotted conger	*Phycis blennoides*	Greater forkbeard
Conger oceanicus	American conger	*Phycis phycis*	Forkbeard
Conger orbignyanus	Argentine conger	*Platichthys flesus*	Flounder
Conodon nobilis	Barred grunt	*Platycephalus indicus*	Bartail flathead
Coregonus lavaretus	Common whitefish	*Plectorhinchus gaterinus*	Blackspotted rubberlips
Coris julis	Mediterranean rainbow wrasse	*Plectorhinchus macrolepis*	Biglip grunt
Crenidens crenidens	Karenteen seabream	*Plectorhinchus mediterraneus*	Rubberlip grunt
Cryodraco antarcticus	Cryodraco antarcticus	*Plectorhinchus pictus*	Trout sweetlips
Ctenolabrus rupestris	Goldsinny-wrasse	*Plectorhinchus schotaf*	Minstrel sweetlip
Cyclopterus lumpus	Lumpsucker	*Plectropomus areolatus*	Squaretail coralgrouper
Cynomacrurus piriei	Dogtooth grenadier	*Pleuronectes platessus*	European plaice
Cynoscion analis	Peruvian weakfish	*Pogonias cromis*	Black drum
Cynoscion nebulosus	Spotted weakfish	*Pollachius pollachius*	Pollack
Cynoscion regalis	Gray weakfish	*Pollachius virens*	Saithe
Cynoscion striatus	South American striped weakfish	*Polydactylus quadrifilis*	Giant African threadfin
Dalatias licha	Kitefin shark	*Polyprion americanus*	Wreckfish
Dasyatis akajei	Red stingray	*Polyprion oxygeneios*	Hapuka
Dasyatis centroura	Roughtail stingray	*Pomacanthus maculosus*	Yellowbar angelfish
Dasyatis pastinaca	Common stingray	*Pomadasys argenteus*	Silver grunt
Deania calcea	Birdbeak dogfish	*Pomadasys incisus*	Bastard grunt
Dentex angolensis	Angola dentex	*Pomadasys jubelini*	Sompat grunt
Dentex congoensis	Congo dentex	*Pomadasys kaakan*	Javelin grunter

Dentex dentex	Common dentex	*Pomadasys stridens*	Striped piggy
Dentex macrophthalmus	Large-eye dentex	*Pontinus kuhlii*	Offshore rockfish
Dentex maroccanus	Morocco dentex	*Priacanthus macracanthus*	Red bigeye
Diagramma pictum	Painted sweetlips	*Prionace glauca*	Blue shark
Diastobranchus capensis	Basketwork eel	*Promethichthys prometheus*	Roudi escolar
Dicentrarchus labrax	European seabass	*Psenopsis anomala*	Melon seed
Dicologlossa cuneata	Wedge sole	*Psettodes belcheri*	Spottail spiny turbot
Diplectrum formosum	Sand seabass	*Psettodes erumei*	Indian spiny turbot
Diplodus annularis	Annular seabream	*Pseudocaranx dentex*	White trevally
Diplodus puntazzo	Sharpsnout seabream	*Pseudochaenichthys georgianus*	South Georgia icefish
Diplodus sargus	White seabream	*Pseudocyttus maculatus*	Smooth oreo
Diplodus vulgaris	Common two-banded seabream	*Pseudopercis semifasciata*	Pigletfish
Dipturus batis	Blue skate	*Pseudophycis bachus*	Red codling
Dipturus laevis	Barndoor skate	*Pseudopleuronectes americanus*	Winter flounder
Dipturus nasutus	New Zealand rough skate	*Pseudotolithus elongatus*	Bobo croaker
Dipturus oxyrinchus	Longnosed skate	*Pseudotolithus senegalensis*	Cassava croaker
Dissostichus eleginoides	Patagonian toothfish	*Pseudotolithus senegallus*	Law croaker
Dissostichus mawsoni	Antarctic toothfish	*Pseudupeneus prayensis*	West African goatfish
Echinorhinus brucus	Bramble shark	*Pterogymnus laniarius*	Panga seabream
Eleginus gracilis	Saffron cod	*Pteroscion peli*	Boe drum
Eleutheronema tetradactylum	Fourfinger threadfin	*Pterothrissus belloci*	Longfin bonefish
Emmelichthys nitidus	Redbait	*Pterygotrigla picta*	Spotted gurnard
Enchelyopus cimbrius	Fourbeard rockling	*Pterygotrigla polyommata*	Latchet
Epigonus telescopus	Bulls-eye	*Raja asterias*	Starry ray
Epinephelus aeneus	White grouper	*Raja brachyura*	Blonde ray
Epinephelus analogus	Spotted grouper	*Raja clavata*	Thornback ray
Epinephelus areolatus	Areolate grouper	*Raja microocellata*	Small-eyed ray
Epinephelus chlorostigma	Brownspotted grouper	*Raja stellulata*	Starry skate
Epinephelus coioides	Orange-spotted grouper	*Raja undulata*	Undulate ray
Epinephelus fasciatus	Blacktip grouper	*Reinhardtius evermanni*	Kamchatka flounder
Epinephelus flavolimbatus	Yellowedge grouper	*Reinhardtius hippoglossoides*	Greenland halibut
Epinephelus goreensis	Dungat grouper	*Rexea solandri*	Silver gemfish
Epinephelus guttatus	Red hind	*Rhabdosargus globiceps*	White stumpnose
Epinephelus marginatus	Dusky grouper	*Rhinobatos percellens*	Chola guitarfish
Epinephelus morio	Red grouper	*Rhinobatos planiceps*	Pacific guitarfish
Epinephelus morrhua	Comet grouper	*Rhomboplites aurorubens*	Vermilion snapper
Epinephelus multinotatus	White-blotched grouper	*Rhynchobatus djiddensis*	Giant guitarfish
Epinephelus nigritus	Warsaw grouper	*Ruvettus pretiosus*	Oilfish
Epinephelus niveatus	Snowy grouper	*Salilota australis*	Tadpole codling
Epinephelus polyphekadion	Camouflage grouper	*Salmo salar*	Atlantic salmon
Epinephelus striatus	Nassau grouper	*Salvelinus alpinus*	Charr
Epinephelus summana	Summan grouper	*Sargocentron spiniferum*	Sabre squirrelfish
Etmopterus spinax	Velvet belly lantern shark	*Sarpa salpa*	Salema
Gadus macrocephalus	Pacific cod	*Saurida tumbil*	Greater lizardfish
Gadus morhua	Atlantic cod	*Saurida undosquamis*	Brushtooth lizardfish
Gadus ogac	Greenland cod	*Scarus ghobban*	Blue-barred parrotfish
Galeichthys feliceps	White baggar	*Schedophilus ovalis*	Imperial blackfish
Galeocerdo cuvier	Tiger shark	*Schedophilus pemarco*	Pemarco blackfish
Galeoides decadactylus	Lesser African threadfin	*Sciaena umbra*	Brown meagre
Galeorhinus galeus	Tope shark	*Sciaenops ocellatus*	Red drum
Galeus melastomus	Blackmouth catshark	*Scolopsis taeniatus*	Black-streaked monocle bream
Genyonemus lineatus	White croaker	*Scomberoides commersonnianus*	Talang queenfish
Genypterus blacodes	Pink cusk-eel	*Scomberomorus cavalla*	King mackerel

Genypterus capensis	Kingklip	*Scomberomorus regalis*	Cero
Gerres oblongus	Slender silverbiddy	*Scophthalmus aquosus*	Windowpane
Gerres oyena	Common silver-biddy	*Scophthalmus maximus*	Turbot
Ginglymostoma cirratum	Nurse shark	*Scophthalmus rhombus*	Brill
Girella tricuspidata	Luderick	*Scorpaena scrofa*	Largescaled scorpionfish
Glyptocephalus cynoglossus	Witch	*Scyliorhinus canicula*	Smallspotted catshark
Gobionotothen acuta	Triangular notothen	*Scyliorhinus stellaris*	Nursehound
Gobionotothen gibberifrons	Humped rockcod	*Sebastes alutus*	Pacific ocean perch
Gobius niger	Black goby	*Sebastes flavidus*	Yellowtail rockfish
Gymnosarda unicolor	Dogtooth tuna	*Sebastes viviparus*	Norway redfish
Gymnura altavela	Spiny butterfly ray	*Selene dorsalis*	African moonfish
Halaelurus canescens	Dusky catshark	*Selene setapinnis*	Atlantic moonfish
Halargyreus johnsonii	Slender codling	*Seriola dumerili*	Greater amberjack
Halobatrachus didactylus	Lusitanian toadfish	*Seriola lalandi*	Yellowtail amberjack
Harpadon nehereus	Bombay duck	*Seriolella brama*	Common warehou
Helicolenus dactylopterus	Blackbelly rosefish	*Seriolella porosa*	Choicy ruff
Himantura gerrardi	Sharpnose stingray	*Seriolella punctata*	Silver warehou
Hippoglossoides elassodon	Flathead sole	*Seriolina nigrofasciata*	Blackbanded trevally
Hippoglossus hippoglossus	Atlantic halibut	*Serranus cabrilla*	Comber
Hippoglossus stenolepis	Pacific halibut	*Sillago sihama*	Silver sillago
Hoplostethus mediterraneus mediterraneus	Mediterranean slimehead	*Solea senegalensis*	Senegalese sole
Hydrolagus mirabilis	Large-eyed rabbitfish	*Solea solea*	Common sole
Hydrolagus novaezealandiae	Dark ghost shark	*Sparisoma cretense*	Parrotfish
Hyperoglyphe antarctica	Antarctic butterfish	*Sparus auratus*	Gilthead seabream
Isurus oxyrinchus	Shortfin mako	*Spectrunculus grandis*	Pudgy cuskeel
Isurus paucus	Longfin mako	*Sphoeroides maculatus*	Northern puffer
Kathetostoma giganteum	Giant stargazer	*Sphyraena barracuda*	Great barracuda
Kyphosus cinerascens	Blue seachub	*Sphyraena jello*	Pickhandle barracuda
Kyphosus sectatrix	Bermuda sea chub	*Sphyraena obtusata*	Obtuse barracuda
Labrus bergylta	Ballan wrasse	*Sphyrna lewini*	Scalloped hammerhead
Labrus merula	Brown wrasse	*Sphyrna zygaena*	Smooth hammerhead
Laemonema longipes	Longfin codling	*Spicara maena*	Blotched picarel
Lamna nasus	Porbeagle	*Spondyliosoma cantharus*	Black seabream
Larimichthys croceus	Large yellow croaker	*Squalus acanthias*	Piked dogfish
Larimichthys polyactis	Yellow croaker	*Squatina argentina*	Argentine angelshark
Lateolabrax japonicus	Japanese seaperch	*Squatina squatina*	Angelshark
Lates calcarifer	Barramundi	*Stenotomus chrysops*	Scup
Leiostomus xanthurus	Spot croaker	*Stephanolepis cirrhifer*	Thread-sail filefish
Lepidonotothen larseni	Lepidonotothen larseni	*Stromateus fiatola*	Blue butterfish
Lepidonotothen mizops	Toad notothen	*Symphodus melops*	Corkwing wrasse
Lepidonotothen nudifrons	Gaudy notothen	*Synagrops japonicus*	Japanese splitfin
Lepidonotothen squamifrons	Grey rockcod	*Tautoga onitis*	Tautog
Lepidoperca pulchella	Orange perch	*Thalassoma pavo*	Ornate wrasse
Lepidopsetta bilineata	Rock sole	*Theragra chalcogramma*	Alaska pollack
Lepidopus caudatus	Silver scabbardfish	*Thyrsites atun*	Snoek
Lepidorhombus boscii	Fourspotted megrim	*Thyrsitops lepidopoides*	White snake mackerel
Lepidorhombus whiffiagonis	Megrim	*Totoaba macdonaldi*	Totoaba
Lepidotrigla cavillone	Large-scaled gurnard	*Trachinotus blochii*	Snubnose pompano
Lethrinus atlanticus	Atlantic emperor	*Trachinotus carolinus*	Florida pompano
Lethrinus borbonicus	Snubnose emperor	*Trachinus draco*	Greater weever
Lethrinus harak	Thumbprint emperor	*Trachurus declivis*	Greenback horse mackerel
Lethrinus lentjan	Pink ear emperor	*Trachurus japonicus*	Japanese jack mackerel
Lethrinus mahsena	Sky emperor	*Trachurus lathami*	Rough scad

Lethrinus microdon	Smalltooth emperor	*Trachurus picturatus*	Blue jack mackerel
Lethrinus nebulosus	Spangled emperor	*Trachurus trecae*	Cunene horse mackerel
Lethrinus obsoletus	Orange-striped emperor	*Trematomus eulepidotus*	Blunt scalyhead
Lethrinus xanthochilus	Yellowlip emperor	*Trematomus hansoni*	Striped rockcod
Leucoraja circularis	Sandy ray	*Trichiurus lepturus*	Largehead hairtail
Leucoraja erinacea	Little skate	*Trigla lyra*	Piper gurnard
Leucoraja fullonica	Shagreen ray	*Tripterophycis gilchristi*	Grenadier cod
Limanda aspera	Yellowfin sole	*Trisopterus esmarkii*	Norway pout
Limanda ferruginea	Yellowtail flounder	*Trisopterus luscus*	Pouting
Limanda limanda	Dab	*Trisopterus minutus*	Poor cod
Lithognathus lithognathus	White steenbras	*Umbrina canariensis*	Canary drum
Lobotes surinamensis	Atlantic tripletail	*Umbrina canosai*	Argentine croaker
Lophius americanus	American angler	*Umbrina cirrosa*	Shi drum
Lophius budegassa	Black-bellied angler	*Urophycis brasiliensis*	Brazilian codling
Lophius vaillanti	Shortspine African angler	*Urophycis chuss*	Red hake
Lophius vomerinus	Cape monk	*Urophycis tenuis*	White hake
Lopholatilus chamaeleonticeps	Great northern tilefish	*Valamugil seheli*	Bluespot mullet
Lutjanus argentimaculatus	Mangrove red snapper	*Variola louti*	Yellow-edged lyretail
Lutjanus argentiventris	Yellow snapper	*Zenopsis conchifer*	Silvery John dory
Lutjanus bohar	Two-spot red snapper	*Zeus faber*	John dory
Lutjanus campechanus	Northern red snapper	*Zoarces americanus*	Ocean pout
Lutjanus gibbus	Humpback red snapper	*Zoarces viviparus*	Viviparous blenny
Lutjanus johnii	Johns snapper		
Invertebrates species			
Scientific name	**Common name**	***Scientific name***	**Common name**
Anadara granosa	Blood cockle	*Ostrea edulis*	European flat oyster
Arctica islandica	Ocean quahog	*Palaemon longirostris*	Delta prawn
Argopecten circularis	Pacific calico scallop	*Palaemon serratus*	Common prawn
Argopecten gibbus	Calico scallop	*Palinurus elephas*	Common spiny lobster
Argopecten irradians	Atlantic bay scallop	*Palinurus gichristi*	Southern spiny lobster
Aristaeomorpha foliacea	Giant red shrimp	*Palinurus mauritanicus*	Pink spiny lobster
Aristeus antennatus	Blue and red shrimp	*Pandalus borealis*	Northern prawn
Artemesia longinaris	Argentine stiletto shrimp	*Pandalus goniurus*	Humpy shrimp
Aulacomya ater	Cholga mussel	*Pandalus hypsinotus*	Humpback shrimp
Buccinum undatum	Whelk	*Pandalus montagui*	Aesop shrimp
Callinectes danae	Dana's swimming crab	*Panulirus argus*	Caribbean spiny lobster
Callinectes sapidus	Blue crab	*Panulirus homarus*	Scalloped spiny lobster
Callista chione	Smooth callista	*Paphies australis*	Pipi wedge clam
Cancer borealis	Jonah crab	*Paracentrotus lividus*	Stony sea urchin
Cancer irroratus	Atlantic rock crab	*Parapenaeus longirostris*	Deepwater rose shrimp
Cancer magister	Dungeness crab	*Patinopecten caurinus*	Weathervane scallop
Cancer pagurus	Edible crab	*Pecten jacobaeus*	Great Mediterranean scallop
Cancer productus	Pacific rock crab	*Pecten maximus*	Great Atlantic scallop
Carcinus aestuarii	Mediterranean shore crab	*Pecten novaezelandiae*	New Zealand scallop
Carcinus maenas	Green crab	*Penaeus aztecus*	Northern brown shrimp
Cardium edule	Common edible cockle	*Penaeus brasiliensis*	Redspotted shrimp
Chlamys islandica	Iceland scallop	*Penaeus brevirostris*	Crystal shrimp
Chlamys opercularis	Queen scallop	*Penaeus chinensis*	Fleshy prawn
Chlamys varia	Variegated scallop	*Penaeus duorarum*	Northern pink shrimp
Clinocardium nuttallii	Nuttall cockle	*Penaeus indicus*	Indian white prawn
Crangon crangon	Common shrimp	*Penaeus japonicus*	Kuruma prawn
Crassostrea gigas	Pacific cupped oyster	*Penaeus kerathurus*	Caramote prawn
Crassostrea rhizophorae	Mangrove cupped oyster	*Penaeus latisulcatus*	Western king prawn
Crassostrea virginica	American cupped oyster	*Penaeus monodon*	Giant tiger prawn
Echinus esculentus	European edible sea urchin	*Penaeus notialis*	Southern pink shrimp
Ensis directus	Atlantic razor clam	*Penaeus semisulcatus*	Green tiger prawn
Geryon quinquedens	Red crab	*Penaeus setiferus*	Northern white shrimp
Glycymeris glycymeris	Dog cockle	*Penaeus vannamei*	Whiteleg shrimp
Haliotis midae	Perlemoen abalone	*Perna perna*	South American rock

			mussel
Haliotis rubra	Blacklip abalone	*Perna viridis*	Brown mussel
Haliotis tuberculata	Tuberculate abalone	*Pitar rostratus*	Rostrate pitar
Haliporoides sibogae	Jack-knife shrimp	*Placopecten magellanicus*	American sea scallop
Haliporoides triarthrus	Knife shrimp	*Pleoticus muelleri*	Argentine red shrimp
Homarus americanus	American lobster	*Pleoticus robustus*	Royal red shrimp
Homarus gammarus	European lobster	*Plesiopenaeus edwardsianus*	Scarlet shrimp
Jasus edwardsii	Red rock lobster	*Portunus pelagicus*	Blue swimming crab
Jasus lalandii	Cape rock lobster	*Protothaca staminea*	Pacific littleneck clam
Jasus novaehollandiae	Southern rock lobster	*Ruditapes decussatus*	Grooved carpet shell
Liocarcinus depurator	Blue-leg swimcrab	*Saxidomus giganteus*	Butter clam
Littorina littorea	Common periwinkle	*Scylla serrata*	Indo-Pacific swamp crab
Loxechinus albus	Chilean sea urchin	*Siliqua patula*	Pacific razor clam
Mercenaria mercenaria	Northern quahog	*Solenocera agassizii*	Kolibri shrimp
Metanephrops andamanicus	Andaman lobster	*Spisula solida*	Surf clam
Metanephrops challengeri	New Zealand lobster	*Spisula solidissima*	Atlantic surf clam
Metapenaeus endeavouri	Endeavour shrimp	*Squilla mantis*	Spottail mantis squillid
Metapenaeus joyneri	Shiba shrimp	*Thenus orientalis*	Flathead lobster
Metapenaeus monoceros	Speckled shrimp	*Trachypenaeus curvirostris*	Southern rough shrimp
Mya arenaria	Sand gaper	*Venus (=Chamelea) gallina*	Striped venus
Mytilus edulis	Blue mussel	*Venus verrucosa*	Warty venus
Mytilus galloprovincialis	Mediterranean mussel	*Xiphopenaeus kroyeri*	Atlantic seabob
Necora puber	Velvet swimcrab	*Zygochlamys delicatula*	Delicate scallop
Nephrops norvegicus	Norway lobster	*Zygochlamys patagonica*	Patagonean scallop
Octopus vulgaris	Common octopus		

Article V

Characterization of waterborne nitrogen emissions for marine eutrophication modelling in life cycle impact assessment at the damage level and global scale

Cosme, N. & Hauschild, M.Z.

submitted to *International Journal of Life Cycle Assessment* in 2016

(manuscript in pre-print version)

Characterization of waterborne nitrogen emissions for marine eutrophication modelling in life cycle impact assessment at the damage level and global scale

Nuno Cosme, Michael Z. Hauschild

Division for Quantitative Sustainability Assessment, Department of Management Engineering, Technical University of Denmark, Produktionstorvet 424, DK-2800 Kgs. Lyngby, Denmark

Abstract

Purpose

Current life cycle impact assessment (LCIA) methods lack a consistent and globally applicable characterization model relating nitrogen (N) enrichment of coastal waters to the marine eutrophication impacts at the endpoint level. This paper introduces a method to calculate spatially explicit characterization factors (CF) at endpoint and damage to ecosystems levels, for waterborne nitrogen emissions, reflecting their hypoxia-related marine eutrophication impacts. These factors represent the impact and damage potentials, respectively, of such emissions based on modelling of 5,772 river basins of the world.

Methods

The proposed method combines environmental fate factors (FF) integrating N-removal processes in soils and rivers, based on the NEWS 2-DIN model, and in coastal waters, based on water residence time, with coastal ecosystem exposure (XF) to N enrichment, based on biological cycling processes, and with effect factors (EF) based on species sensitivity to hypoxia. Five emission routes are discriminated as N from natural or agricultural soils, N in sewage discharges, and N in emissions to river or to coastal waters. Damage factors (DF) are also estimated, based on endpoint metrics conversion from potentially affected to potentially disappeared fractions of species (i.e. PAF- to PDF·m^3·yr·kgN^{-1}) and harmonisation across coastal ecosystems based on their spatially explicit densities of demersal species, to further express CF as species·yr·kgN^{-1}.

Results and discussion

Endpoint CFs show 6 orders of magnitude (o.m.) spatial differentiation for the soil-related emission routes, 4 for the river-related, and 3 for emissions to coastal waters. Damage CFs vary 8, 6 and 4 o.m. for the same routes. After aggregation at the level of continents, maximum CFs are consistently found in Europe and South Asia, but the aggregation reduces spatial differentiation to around 1 o.m. for each route. The FFs,

especially those for soil-related emissions, are responsible for most of the spatial differentiation of the damage model. Further analyses show that coastal water residence time is the most influential parameter to the characterization model. Uncertainty is also higher for this parameter, mainly due to scarcity and inconsistency of data sources.

Conclusions

Major contributions to the current state-of-the-art of marine eutrophication characterization modelling are: (i) full pathway coverage, thus reaching endpoint level, (ii) significant increase in geographic coverage, (iii) mechanistic modelling of exposure and effect factors, and (iv) development of spatially explicit damage to ecosystems factors based on species densities. Application of the developed CFs in life cycle impact assessment is recommended at a river basin scale, provided that emission location is known.

Keywords Fate · Exposure · Effect · River basin · Endpoint · Characterization factors · Damage to ecosystem · LCIA

1. Introduction

Nitrogen (N) is often a limiting growth factor for crops and forage species (Laegreid et al. 1999; Keeney and Hatfield 2001). The application of both organic (manure) and inorganic (synthetic) fertilizers is widely used to supplement N to secure agriculture yield (Keeney and Hatfield 2001; Brady and Weil 2007). The increasing production of food and feed through fertilizer use in crops cultivation, and the increased energy production through fossil fuel combustion with associated emissions of nitrogen oxides, has resulted in a more than10-fold increase of reactive nitrogen creation in the last 150 years (Galloway et al. 2008). Human interventions currently mobilize more than twice the amount of N that natural processes do (Galloway et al. 2004), and river basins export 4-6 fold more dissolved inorganic nitrogen (DIN) than in the pre-industrial period (Galloway and Cowling 2002; Green et al. 2004). Such environmental emissions transported via riverine discharges to coastal waters increase the N availability there and may cause impacts in the marine ecosystem.

Marine coastal eutrophication refers to the syndrome of ecosystem responses to the increase in supply of organic matter (Nixon 1995; Cloern 2001). This definition encompasses all possible causes, e.g. increased algal growth following inputs of inorganic nutrients (an autochthonous source for organic carbon) or organic material loading (an allochthonous source), reduced grazing pressure on primary producers, and changes in water turbidity, residence time, circulation, stratification, or mixing. Any of these can be, directly or indirectly, affected by human interventions, but the increased supply of inorganic nutrients to coastal waters from anthropogenic sources (i.e. nutrient

enrichment) has been identified as a clear link between human activities and ecosystem impacts (Smith et al. 1999; Gray et al. 2002; Rabalais 2002). The cascading effects of nutrient enrichment point to a variety of ecosystem impacts (Rabalais et al. 2009); one being the benthic oxygen depletion. This may lead to the onset of hypoxic waters, and if in excess, to anoxia and 'dead zones' – one of the most severe and widespread causes of disturbance to marine ecosystems (GESAMP 2001; Diaz and Rosenberg 2008).

The increased availability of growth-limiting nutrients in the well-lit upper layers of the ocean (euphotic zone) is an important trigger for eutrophication impacts as it promotes planktonic growth. Nitrogen is assumed to be this limiting nutrient in marine waters – a necessary and justified simplification in ecosystems modelling when considering average spatial and temporal representative conditions (see also Vitousek et al. (2002), Howarth and Marino (2006), Cosme et al. (2015)). Particulate organic carbon exported to bottom strata induces oxygen-consuming aerobic respiration by heterotrophic bacteria (Graf et al. 1982; Ploug et al. 1999; Cosme et al. 2015). The exposure of marine species to hypoxic conditions beyond their sensitivity thresholds threatens success and survival (Davis 1975; Diaz and Rosenberg 1995; Gray et al. 2002; Vaquer-Sunyer and Duarte 2008; Cosme and Hauschild 2016), with ecological impacts extending to mass mortality or fisheries decline (Diaz and Rosenberg 1995; Wu 2002; Levin et al. 2009; Middelburg and Levin 2009; Zhang et al. 2010).

Life cycle impact assessment (LCIA) has been used as a tool to characterise the impacts of the environmental emissions originated throughout the entire life cycle of products and services in the economy (Hauschild 2005). While typically modelled at a midpoint between emissions and impacts in the cascade of effects caused by the N-enrichment, current LCIA methods still lack a consistent link to the endpoint and damage to the ecosystems levels (Hauschild et al. 2013; Henderson 2015). To the knowledge of the authors, only the LCIA methods ReCiPe (Goedkoop et al. 2012) and LIME (Itsubo and Inaba 2012) specifically model midpoint impacts for marine eutrophication, although restricted to European coverage and to a limited number of Japanese bays, respectively. Other methods, like EDIP2003 (Hauschild and Potting 2005), EPS (Steen 1999), LUCAS (Toffoletto et al. 2007), TRACI (Norris 2003), CML 2002 (Guinée et al. 2002) (also used in IMPACT 2002+ (Jolliet et al. 2003) and MEEuP (Kemna et al. 2005)), showing a combined aquatic eutrophication indicator, are based on Redfield ratio's stoichiometric equivalencies to distinguish N and phosphorus (P) flows and model, more or less completely, the environmental fate of emitted substances (including N forms) based on e.g. air and water transport models, except in CML 2002 method. At the endpoint level, ReCiPe lacks the model work (EC-JRC-IES 2010; Goedkoop et al. 2012; Hauschild et al. 2013) and LIME shows limited extrapolation beyond local Japanese application (Henderson 2015). The method IMPACT 2002+ distinguishes N- and phosphorous (P)-limited waters but the endpoint model work is

incomplete, has low relevance for marine systems, and is scoped to European conditions (Hauschild et al. 2013). In all cases, both at mid- and endpoint levels, spatial differentiation at a global scale is not modelled (generic or global indicators are used in CML 2002, EPS, MEEuP), or is at a coarse resolution (e.g. European countries in EDIP2003 and ReCiPe, U.S. states in TRACI) (Hauschild et al. 2013; Henderson 2015). Considering the importance of marine eutrophication in many regions of the world, an endpoint indicator that is consistent with the LCIA framework and spatially-explicit at a relevant resolution and global scale, would be a useful improvement to current impact assessment methodologies in LCA.

The goal of this study is to develop spatially-explicit characterization factors, at the levels of endpoint and damage to ecosystems, for waterborne nitrogen runoff from soils, emissions to rivers, and directly to coastal waters representing their ability to cause hypoxia-related eutrophication impacts. Firstly, the environmental fate of waterborne N emissions is modelled by accounting for the removal rates at the river basin scale and in the marine compartment. Secondly, the exposure of receiving ecosystems to N is mechanistically modelled by translating surface uptake of N into benthic oxygen depletion. Thirdly, the sensitivity of marine species to hypoxia is used to estimate potentially affected fractions of species using a species sensitivity distribution (SSD) method. Finally, species density is applied to estimate spatially explicit factors for damage to ecosystems. The resulting characterization factors have global coverage and are available for emission locations at a river basin spatial resolution, and also as emission-weighted continental and global aggregated factors. The importance of the contribution of each of the fate, exposure, effect, and damage factors is evaluated and the most important assumptions and uncertainties are discussed in support of LCIA application.

2. Methods

2.1. Framework

2.1.1. Nitrogen sources

Waterborne nitrogen emissions, as used here, refer to dissolved inorganic nitrogen (DIN) forms. These include nitrate (NO_3^-), nitrite (NO_2^-), and ammonium (NH_4^+). The term DIN is generically applied in the text to refer to any of these forms.

The N emission routes to the aquatic ecosystem include runoff and leaching from agricultural (N_{as}) and natural soils (N_{ns}) to freshwater systems, direct emissions to rivers (N_{riv}) or sewage water discharges (N_{sew}), direct emissions to marine coastal waters (N_{mar}), or atmospheric deposition. The latter (airborne) is not modelled here, however, a quantified mass of nitrogen oxides (NO_x) or ammonia (NH_3) deposited on soil, river or marine water can be characterized using the factors for the emission routes

from these compartments. The environmental emissions from soil correspond to the N-surplus of the soil balance, which is defined as the difference between inputs and other outputs for a certain given surface area. Inputs to soil include application of N-containing manure and synthetic fertilizers (in agricultural soils), biological fixation (i.e. the fixation of atmospheric N_2 to, mainly, NH_4^+) and atmospheric deposition. Soil compartment outputs include NH_3 volatilization, denitrification, and removal of N in biomass through harvesting and animal grazing (Van Drecht et al. 2003; Seitzinger et al. 2005).

2.1.2. Characterization factors in life cycle impact assessment

The impact assessment phase in LCA applies characterization factors (CFs) to translate the quantified emission and consumption flows, identified in the inventory phase, into potential impacts on the chosen indicator for the impact category (Hauschild and Huijbregts 2015). The present work introduces CFs of waterborne N emissions from anthropogenic sources that contribute to eutrophication-induced hypoxia in coastal waters. The overall impact pathway of hypoxia-related eutrophication in coastal waters, illustrated in Fig. 1, illustrates the cause-effect chain from DIN inputs. These promote planktonic growth and eventual export of organic carbon to bottom waters, where DO consumption occurs with its respiration, leading to potential losses of marine species richness.

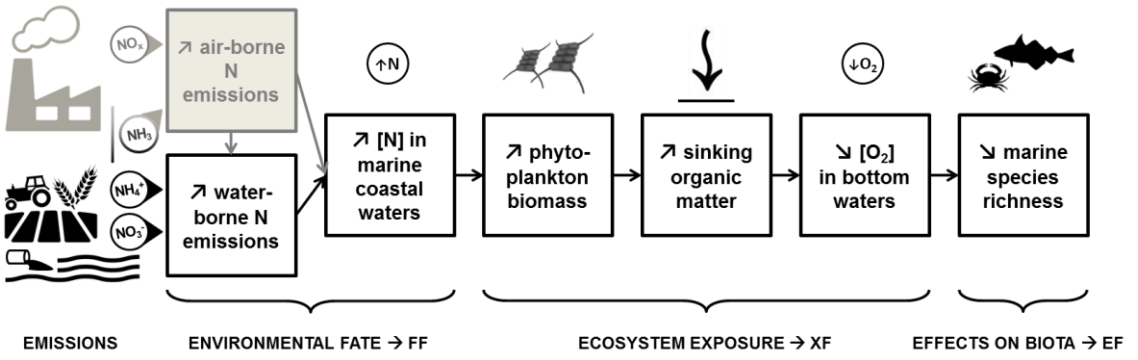

Fig. 1 Schematic representation of the impact pathway for hypoxia-related marine eutrophication impacts, showing the modelling components of the Fate Factor (FF), eXposure Factor (XF) and Effect Factor (EF). Waterborne nitrogen (N) emissions originate from point sources (e.g. sewage) and from non-point or diffuse sources (e.g. soil runoff). The fate modelling of airborne emissions from source to deposition is excluded (shaded objects). Adapted from (Cosme et al. 2016a)

The modelling work of the proposed characterization method is consistent with the LCIA framework for emission-related impact indicators (Udo de Haes et al. 2002; Pennington et al. 2004b) by including (i) an environmental fate model of DIN emissions in watersheds and river systems, aggregated at a river basin scale (Vörösmarty et al.

2000) and in coastal waters at large marine ecosystem (LME) scale (Sherman and Alexander 1986), (ii) an ecosystem exposure model for N uptaken by primary producers (phytoplankton) in coastal waters and the biological processes that result in oxygen depletion, and (iii) an effect model based on sensitivity of marine species to hypoxia. The factors derived from these models were multiplied to yield the endpoint CF ([(PAF)·m^3·yr·kgN^{-1}]), as summarised in Eq. (1):

$$CF_{i,jl} = FF_{i,jl} \times XF_l \times EF_l \quad (1)$$

where $FF_{i,jl}$ [yr] is the fate factor for emission route *i* in river basin *j* to receiving ecosystem *l*, XF_l [kgO_2·kgN^{-1}] the exposure factor and EF_l [(PAF)·m^3·kgO_2^{-1}] the effect factor in ecosystem *l*. The latter is expressed as a Potentially Affected Fraction (PAF) of species to represent the impact dimension of species richness loss. PAF is included in the notation for informative purposes as it is in itself a dimensionless quantity (fraction) (Heijungs 2005). The CF and FF subscript notations show coupled *jl* because each river basin exports to a single LME. The FF expresses the persistence of the fraction of the original N-emission that is exported to each receiving coastal ecosystem (Cosme et al. 2016b). The XF represents the 'conversion' potential of N in the euphotic zone of coastal waters into oxygen depletion in benthic layers of the continental shelf (Cosme et al. 2015). The EF represents the average effect of hypoxic stress on benthic-demersal ecological communities exposed beyond the sensitivity threshold of the individual species (Cosme and Hauschild 2016). Each factor is further detailed in the next sections.

2.2. Fate factors

The fate factor (FF, [yr]) is composed of an inland fate component (f_N) and a marine fate component (λ), as shown in Eq. (2).

$$FF_{i,jl} = \frac{f_{N_{i,j}}}{\lambda_l} \quad (2)$$

where *i* is the emission route and *j* the river basin that exports to the respective receiving LME (*l*).

The inland component was estimated by Cosme et al. (2016b) from the DIN-removal processes described in the second generation of the Global Nutrient Export from WaterSheds model (NEWS 2-DIN) (Dumont et al. 2005; Seitzinger et al. 2005; Seitzinger et al. 2010; Mayorga et al. 2010). Export fractions (FE, dimensionless) were extracted from NEWS 2-DIN, corresponding to (i) calibrated runoff functions from natural and agricultural soils (FE_{ns} and FE_{as}, respectively), (ii) empirical DIN fractions in discharged sewage water (FE_{sew}), and (iii) riverine DIN losses by denitrification, retention, and water consumption (FE_{riv}). Cosme et al. (2016b) applied combinations of

these FEs to estimate river basin-dependent fate coefficients (*f*) for four emission routes: $f_{N_{ns}} = FE_{ns} \times FE_{riv}$, $f_{N_{as}} = FE_{as} \times FE_{riv}$, $f_{N_{riv}} = FE_{riv}$, and $f_{N_{sew}} = FE_{sew} \times FE_{riv}$. Direct emissions to marine waters have no watershed component, therefore $f_{N_{marw}} = 1$. The f-values correspond to fractions of the original DIN emission that are exported by each of the modelled 5,772 discharging systems, which were further linked to a receiving LME by means of river mouth's geographic location. Considering the five emission routes the possible number of $f_{Ni,j}$ amounts to 28,860.

The marine fate component was estimated based on the sum of DIN-removal rates (λ, [yr^{-1}]) in each LME (*l*), assuming first order removal processes as described by Cosme et al. (2016b). Removal processes refer to advection (λ_{adv}), estimated as the inverse of the surface water residence time, and denitrification (λ_{denitr}), estimated with an empirical relationship between the fraction of N denitrified and the water residence time in lakes, river reaches, estuaries and continental shelf (Seitzinger et al. 2006).The use of residence time to derive an advective transport removal has been described elsewhere for lakes, estuaries, and coastal waters (see e.g. Vollenweider 1976; Andrews and Müller 1983; Nixon et al. 1996; Dettmann 2001; Monsen et al. 2002; Seitzinger et al. 2006). Denitrification is a generic process in aquatic systems and found as independent of salinity (Fear et al. 2005; Magalhães et al. 2005). Therefore, the modelling approaches for both the advection and denitrification removals were deemed adequate to represent N-losses in marine coastal waters. See Cosme et al. (2016b) for full method description and estimated FFs. Factors for the 5,772 river basins of the world are given in Table S.1.

2.3. Exposure factors

The ecosystem responds to the input of a growth limiting nutrient by increasing its uptake rate by primary producers (phytoplankton) in the euphotic zone of coastal waters. The resulting planktonic growth fuels the organic carbon cycles that eventually contribute to the vertical carbon export to bottom water layers. There, aerobic respiration of organic material by heterotrophic bacteria leads to dissolved oxygen (DO) consumption. The biological processes of N-limited primary production (PP), metazoan consumption, and bacterial degradation, were modelled by Cosme et al. (2015) in four distinct carbon sinking routes to derive 'conversion' potentials of N-uptake into organic carbon and into DO consumption. Such 'conversion' potentials were defined as ecosystem eXposure Factors (XF, [$kgO_2 \cdot kgN^{-1}$]). Model and results are available in Cosme et al. (2015) as spatially-explicit XFs for 66 LMEs worldwide, varying from 0.45 $kgO_2 \cdot kgN^{-1}$ in the central Arctic Ocean to 15.9 $kgO_2 \cdot kgN^{-1}$ in the Baltic Sea. Factors for all 66 LMEs are shown in Table S.2.

2.4. Effect factors

Another component of the ecosystem response to N-inputs is the effect on biota. The sensitivity to hypoxia of 91 benthic, demersal, and benthopelagic marine species (including fishes, crustaceans, molluscs, echinoderms, annelids, and cnidarians) was used to model Effect Factors (EF, [(PAF)·m^3·kgO_2^{-1}]) for application in LCIA in model work described in Cosme and Hauschild (2016). There, Species Sensitivity Distribution (SSD) statistical methodologies (Posthuma et al. 2002) were applied to integrate specific sensitivity data and estimate the average effect of hypoxia on benthic communities as an HC_{50} indicator, which represents the stressor intensity (DO depletion) that affects 50% of the exposed population above their individual sensitivity thresholds. The EFs were then calculated as the average variation of the effect on ecological communities occurring in benthic-demersal habitats (as a dimensionless ΔPAF) due to a variation of the stressor intensity (as ΔDO in [kgO_2·m^{-3}]) in receiving ecosystem *l*, Eq. (3), according to an average gradient approach and consistent with the current scientific consensus (Pennington et al. 2004a; Larsen and Hauschild 2007).

$$EF_l = \frac{\Delta PAF_l}{\Delta DO_l} = \frac{0.5}{HC_{50l}} \quad (3)$$

The EFs are available at a five climate zone (CZ) scale as of 218 (PAF)·m^3·kgO_2^{-1} in the polar CZ, 242 (PAF)·m^3·kgO_2^{-1} in the subpolar CZ, 278 (PAF)·m^3·kgO_2^{-1} in the temperate CZ, 275 (PAF)·m^3·kgO_2^{-1} in the subtropical CZ, and 306 (PAF)·m^3·kgO_2^{-1} in the tropical CZ (Cosme and Hauschild 2016). Although produced at a CZ scale, EFs can be disaggregated for the LMEs composing each CZ, as a function of the mean benthic water temperature, as described in Cosme and Hauschild (2016) and given in Table S.2.

2.5. Spatially explicit damage factors

A conversion of the marine eutrophication endpoint CF from the PAF-based metric to a PDF-based metric was done aiming at harmonization of the endpoint scores in the LCIA framework. Given the seasonality of the planktonic production and other biologically-mediated processes, water temperature and stratification, and nutrient emission flows, for an annual integration of marine eutrophication impacts to the ecosystem, a conversion factor of 0.5 was chosen, as discussed in Cosme et al. (2016a). This assumption means that one half of the species affected above their sensitivity to hypoxia threshold (expressed in the PAF-integrated metric) would disappear (and be expressed in the PDF-integrated metric).

Impact indicator scores at the endpoint level can be aggregated with other indicators, at the same level, that also contribute to damage to ecosystems (e.g. ecotoxicity, acidification). Spatially explicit damage factors (DF,

[(PDF/PAF)·species·m^{-3}]) were developed for marine eutrophication based on demersal marine species density (SD) in order to translate a relative metric of PAF-based endpoint indicator to an absolute metric of [species·yr], as summarised in Eq. (4) for any receiving ecosystem *l*:

$$DF_l = 0.5\ (PDF) \cdot (PAF)^{-1} \cdot SD_l \quad (4)$$

A similar approach is taken in the ReCiPe method (Goedkoop et al. 2012) but adopting a site-generic SD estimate. Spatially explicit SD values were estimated for the 66 LMEs (Table S.2) based on species distribution models (SDMs) (Jones and Cheung 2015; Cosme et al. 2016a) and applied here to calculate the marine eutrophication damage factors of the N-emissions for each of the five emission routes.

In order to understand the influence of spatial variability in environmental mechanisms in the variability of the damage model results, the contribution of each parameter (FF, XF, EF, SD) to the spatial variation of DF was assessed for each emission route by means of simple regression analysis on a log scale. Indications of lack of correlation are slopes far from 1.0, low coefficients of determination (R^2), high mean square (the variance estimated from the residual sum of squares), and high standard error.

Spatial aggregation of endpoint and damage CFs over regions, e.g. continents or world, for each N-emission route *i*, were calculated by emission-weighted averages (see calculation method in Section S.3). Regional factors ($CF_{i,reg}$, [(PDF)·m^3·yr·kgN^{-1}] and [species·yr·kgN^{-1}]) aggregate all emissions, with non-zero $CF_{i,jl}$, belonging to region *reg*, with a corresponding emission in the respective route *i*. Emission data used refer to year 2000 and were extracted from the NEWS 2-DIN model (Mayorga et al. 2010).

3. Results and discussion

3.1. Characterization factors

River basin-dependent endpoint characterization factors were calculated for the five emission routes according to Eq. (1) as the product of fate, exposure and effect factors. Table 1 shows fate, exposure and effect factors and resulting CFs for the 12 largest rivers in the world in terms of catchment area and for the emission route 'N from agricultural soil' (N_{as}). Results for the 5,772 river basins and five emission routes are given in full in Table S.5.

Table 1 Extract of the results of the modelled fate, exposure and effect factors (FF, XF, and EF, respectively) and resulting characterization factors (CF, both in endpoint and damage level units) for the 12 rivers with the largest catchment area, and the emission route 'N from agricultural soil' (N_{as}). Species density (SD) per Large Marine Ecosystem (LME) was used to estimate damage factors. Full results for the five emission routes and 5,772 river basins are given in Table S.5. Sources: FF (Cosme et al. 2016b), XF (Cosme et al. 2015), EF (Cosme and Hauschild 2016), SD (Cosme et al. 2016a)

River basin	Receiving LME	FF_{Nas}	XF	EF	CF_{Nas} (endpoint)		SD	CF_{Nas} (damage)
		yr	$kgO_2 \cdot kgN^{-1}$	$(PAF) \cdot m^3 \cdot kgO_2^{-1}$	$(PAF) \cdot m^3 \cdot yr \cdot kgN^{-1}$	$(PDF) \cdot m^3 \cdot yr \cdot kgN^{-1}$	$species \cdot m^3$	$species \cdot yr \cdot kgN^{-1}$
Amazon	17. North Brazil Shelf	0.054	5.3	310	87	43	2.3E-12	1.0E-10
Ob	58. Kara Sea	0.073	6.2	220	99	49	2.8E-13	1.4E-11
Lena	57. Laptev Sea	0.088	7.5	220	140	72	5.2E-13	3.7E-11
Yenisei	58. Kara Sea	0.092	6.2	220	120	62	2.8E-13	1.8E-11
Mississippi	05. Gulf of Mexico	0.0081	4.5	310	11	5.5	1.7E-12	9.2E-12
Nile	26. Mediterranean	0.00073	3.5	280	0.70	0.35	1.2E-12	4.1E-13
Zaire	28. Guinea Current	0.14	4.3	270	170	85	6.6E-13	5.6E-11
Mackenzie	55. Beaufort Sea	0.087	5.9	220	110	56	2.8E-13	1.5E-11
Parana	14. Patagonian Shelf	0.018	11	240	51	26	1.7E-12	4.3E-11
Amur	52. Sea of Okhotsk	0.067	10	240	160	81	7.0E-13	5.7E-11
Niger	28. Guinea Current	0.048	4.3	270	57	28	6.6E-13	1.9E-11
Chang Jiang	47. East China Sea	0.12	6.4	310	240	120	5.6E-12	6.8E-10

Fig. 2 shows the distribution of the CFs for the emission route 'N from agricultural soil' (N_{as}) to the river basins of the world. Distribution maps of the endpoint CFs for the other four emission routes are presented in the Electronic Supplementary Material (Figs. S.1 to S.4).

The endpoint CFs range from 3.3×10^{-3} to 1.8×10^{4} (for N_{ns} emission route), 4.0×10^{-3} to 1.8×10^{4} (for N_{as}), 2.6×10^{-1} to 2.0×10^{4} (for N_{sew}), 5.2×10^{-1} to 3.0×10^{4} (for N_{riv}), and 3.9×10^{1} to 4.9×10^{4} (for N_{marw}) (units in $(PAF) \cdot m^3 \cdot yr \cdot kgN^{-1}$) (Table S.3). These results correspond to spatial differentiations of ca. 6.5 orders of magnitude for soil emissions, 4.7 for emissions to the riverine system, and 3 for direct emissions to coastal waters. Higher CFs tend to occur in river basins discharging to LMEs with longer residence times, such as the Baltic Sea (LME #23), Bay of Bengal (#34), Sulu-Celebs Sea (#37), Mediterranean Sea (#26), Black Sea (#62) and Hudson Bay Complex (#63). Mean CF values, as well as spatially determined variation, decrease from direct emissions to coastal waters over freshwater-related emissions and to soil-related emissions. These results reflect the increase in both N-removal and spatial differentiation obtained by modelling riverine and watershed processes in the fate modelling.

The damage CFs [$species \cdot yr \cdot kgN^{-1}$] show an increase in spatial differentiation when compared to CFs, due to the introduction of LME-dependent species densities (extract of the results in Table 1 and in full in Table S.6 for the 5,772 river basins and five emission routes; global distribution exemplified in Fig. 3 for the N_{as} emission route, and given in Figs S.5 through S.8 for the remaining routes). Species density varies by 3 orders of magnitude among LMEs (Cosme et al. 2016a).

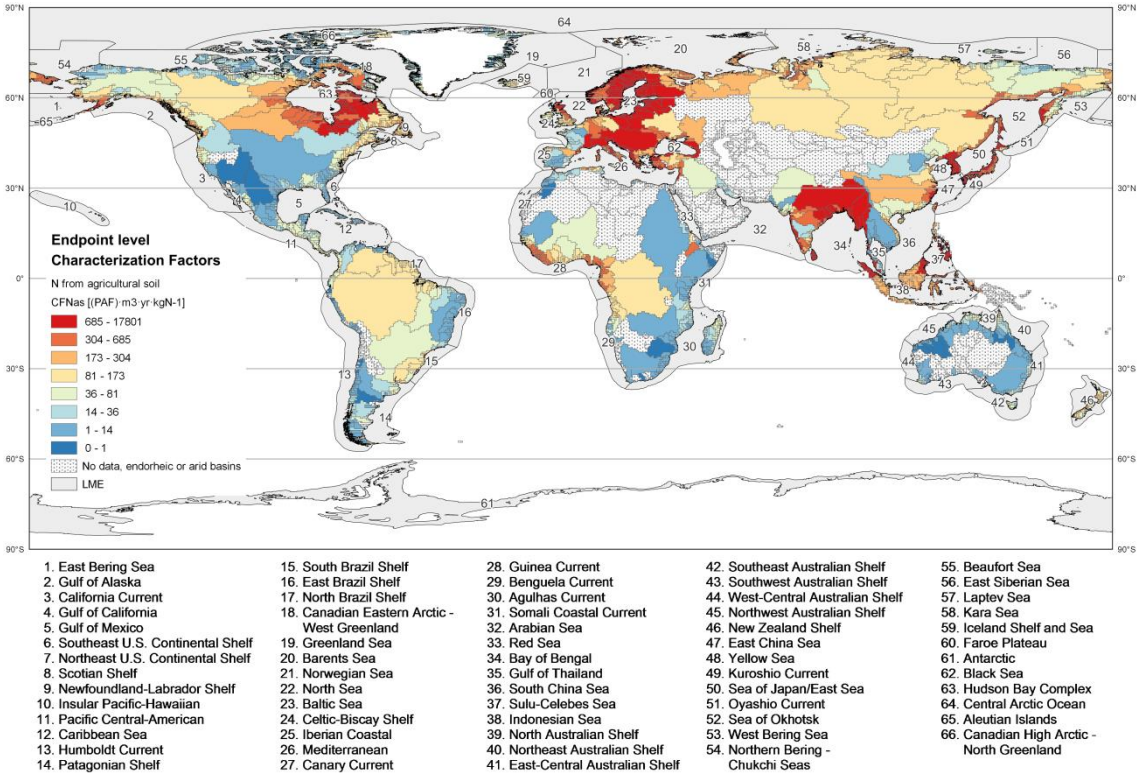

Fig.2 Global distribution of the marine eutrophication endpoint characterization factors (CF_{Nas}, $[(PAF)\cdot m^3\cdot yr\cdot kgN^{-1}]$) for emissions from agricultural soil at a river basin scale. Note the non-linear scale. Similar distribution maps for the remaining emission routes can be found in the Electronic Supplementary Material

The damage CF values range from 3.9×10^{-16} to 3.2×10^{-8} (for both N_{ns} and N_{as} emission routes), 2.5×10^{-14} to 3.6×10^{-8} (for N_{sew}), 5.1×10^{-14} to 5.4×10^{-8} (for N_{riv}), and 5.0×10^{-12} to 8.8×10^{-8} (for N_{marw}) (units in species·yr·kgN^{-1}) (Table S.4). These, correspond to almost 8 orders of magnitude of spatial differentiation for the soils emissions, 6 for the emissions to the riverine systems, and 4 for direct emissions to coastal waters, mostly given by the variation of the minimum values. These decrease towards upstream of the hydrological cycle. Comparing to the distribution pattern of the CFs at endpoint and damage levels, the latter tend to show an intensification of the eutrophication potential towards river basins discharging to LMEs with denser species occurrence, namely in the Northeast and Southeast U.S. Continental Shelves (LME #7 and #6, respectively), Gulf of California (#4), Gulf of Thailand (#35), Iberian Coastal (#25), Scotian Shelf (#8), and Yellow Sea (#48) (Cosme et al. 2016a).

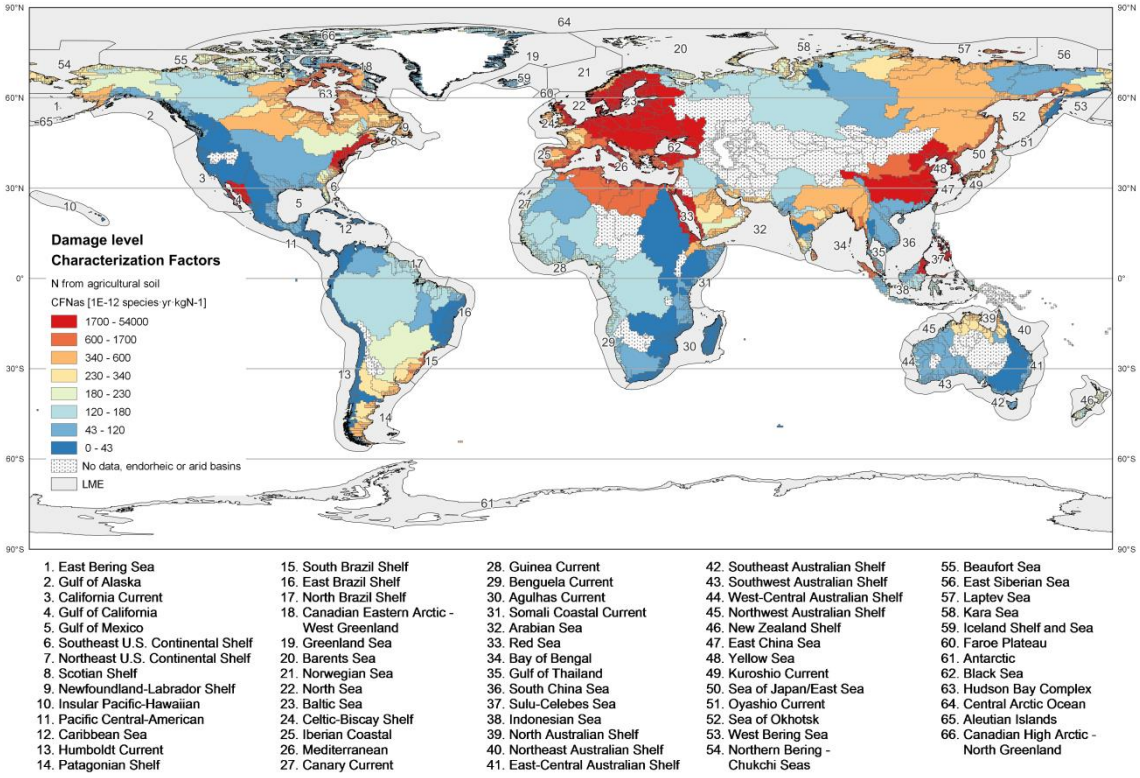

1. East Bering Sea
2. Gulf of Alaska
3. California Current
4. Gulf of California
5. Gulf of Mexico
6. Southeast U.S. Continental Shelf
7. Northeast U.S. Continental Shelf
8. Scotian Shelf
9. Newfoundland-Labrador Shelf
10. Insular Pacific-Hawaiian
11. Pacific Central-American
12. Caribbean Sea
13. Humboldt Current
14. Patagonian Shelf
15. South Brazil Shelf
16. East Brazil Shelf
17. North Brazil Shelf
18. Canadian Eastern Arctic - West Greenland
19. Greenland Sea
20. Barents Sea
21. Norwegian Sea
22. North Sea
23. Baltic Sea
24. Celtic-Biscay Shelf
25. Iberian Coastal
26. Mediterranean
27. Canary Current
28. Guinea Current
29. Benguela Current
30. Agulhas Current
31. Somali Coastal Current
32. Arabian Sea
33. Red Sea
34. Bay of Bengal
35. Gulf of Thailand
36. South China Sea
37. Sulu-Celebes Sea
38. Indonesian Sea
39. North Australian Shelf
40. Northeast Australian Shelf
41. East-Central Australian Shelf
42. Southeast Australian Shelf
43. Southwest Australian Shelf
44. West-Central Australian Shelf
45. Northwest Australian Shelf
46. New Zealand Shelf
47. East China Sea
48. Yellow Sea
49. Kuroshio Current
50. Sea of Japan/East Sea
51. Oyashio Current
52. Sea of Okhotsk
53. West Bering Sea
54. Northern Bering - Chukchi Seas
55. Beaufort Sea
56. East Siberian Sea
57. Laptev Sea
58. Kara Sea
59. Iceland Shelf and Sea
60. Faroe Plateau
61. Antarctic
62. Black Sea
63. Hudson Bay Complex
64. Central Arctic Ocean
65. Aleutian Islands
66. Canadian High Arctic - North Greenland

Fig. 3 Global distribution of the marine eutrophication characterization factors in damage level units (CF_{Nas}, [species·yr·kgN^{-1}]) for emissions from agricultural soil at a river basin scale. Note the non-linear scale. Similar distribution maps for the remaining emission routes are available in the Electronic Supplementary Material

3.2. Regional aggregation

Endpoint CFs aggregated at the continental scale consistently show a maximum for Europe followed by South Asia for all emission routes (Table 2). The spatially determined variation of endpoint CFs aggregated at the level of continents is much lower than what is observed at the level of watersheds, i.e. 1 order of magnitude, and there is little distinction between emission routes. The intra-regional comparison shows slightly higher variability in the soil-related emissions (maximum differentiation in North and South America), than in the river-related (maximum in North America) and marine emissions (maximum in South Asia and Europe). In any case, a reduction of ca. 5, 3, and 1 orders of magnitude, is noticeable for the soil-related, river-related and marine emissions, respectively, when compared to the spatial differentiation obtained at the river basin scale. Such observation suggests a recommended use of the characterization factors at the river basin resolution for application in LCIA whenever the emission location is known. When only coarse spatial information about the emissions is available, regionally aggregated endpoint CFs may be used, noting the

variability within the concerned continent. The global site-generic endpoint CF values can be used when such spatial information is not available or not relevant.

Table 2 Regional endpoint characterization factors CF [(PAF)·m^3·yr·kgN^{-1}] by emission-weighted aggregation per emission route at the level of continents. Intra-regional variability (*var*) and inter-regional variability (N_i) shown

Aggregation scale	Characterization Factor [(PAF)·m^3·yr·kgN^{-1}] per emission route				
	N_{ns} *var*	N_{as} *Var*	N_{sew} *var*	N_{riv} *var*	N_{marw} *var*
Africa	3.2E+01 *3E+04*	1.0E+02 *4E+03*	1.3E+02 *6E+02*	2.7E+02 *6E+02*	1.8E+03 *6E+01*
Europe	9.0E+02 *2E+03*	9.0E+02 *2E+03*	2.2E+03 *5E+02*	3.6E+03 *5E+02*	9.9E+03 *2E+02*
North America	8.8E+01 *2E+05*	9.4E+01 *2E+05*	1.7E+02 *7E+03*	2.7E+02 *6E+03*	7.6E+02 *6E+01*
South America	2.8E+01 *1E+05*	6.9E+01 *1E+05*	6.8E+01 *1E+03*	1.3E+02 *1E+03*	4.4E+02 *2E+01*
North Asia	1.9E+02 *2E+02*	1.9E+02 *2E+02*	5.8E+02 *2E+01*	1.1E+03 *2E+01*	3.1E+03 *1E+01*
South Asia	6.8E+02 *3E+04*	8.2E+02 *4E+03*	7.3E+02 *1E+03*	1.4E+03 *1E+03*	5.6E+03 *3E+02*
Oceania [a]	1.1E+02 *3E+03*	6.5E+02 *1E+03*	3.7E+02 *9E+01*	7.5E+02 *1E+02*	1.6E+03 *1E+02*
Australia	2.5E+01 *7E+02*	3.2E+01 *7E+02*	5.4E+01 *8E+00*	9.4E+01 *8E+00*	2.2E+02 *3E+00*
Spatial variability	*4E+01* --	*3E+01* --	*4E+01* --	*4E+01* --	*4E+01* --
World	4.2E+02 --	5.2E+02 --	6.3E+02 --	1.1E+03 --	3.9E+03 --

[a] *(excluding Australia)*

The analysis of the aggregated damage CFs shows similar observations (Table S.7). Europe consistently shows higher results at the level of continents and across the five emission routes. At this aggregation level, the spatial differentiation is modest, from 1.4 to 2.1 orders of magnitude, with no relevant differences between emission routes, despite the maximum for N_{ns}. The intra-regional variability shows maximum differentiation for the soil-related emissions and decreasing towards river-related and marine emissions. North and South America consistently show higher variability in any of the emission routes, except for marine emissions, for which no dominance is noticeable. Comparing the damage CFs at continental and river basin scales, a reduction in spatial differentiation is observable at ca. 6, 4, and 2 orders of magnitude. As noted earlier for the endpoint CFs, and depending on the available information on the emissions location, damage CFs at a river basin scale are recommended for LCIA application, continental aggregation may be useful when only coarse spatial information is available (acknowledging the respective variability in each emission route), and the global site-generic value when emission location is unknown.

3.3. Sources of spatial differentiation

The results of the regression analysis of the variation of the parameters contributing to the variation of the damage model, at a river basin scale, are shown in Table S.8 for each of the five emission routes. The analysis shows low explained variance of the XF and EF, slopes deviating from 1.0 (to a larger extent for EF), and relatively high mean square (MS) and standard error (SE). These results suggest a poor correlation to damage CF variability, which means that neither the XF nor the EF alone are able explain the spatial variability of the damage model for any of the emission routes. A similar

observation is noticeable when both factors are tested together (i.e. XF×EF). The SD variation is modestly correlated with damage CF variation.

The soil-related fate factors (i.e. FF_{Nns}, FF_{Nas}) show stronger correlation to damage CF. Overall, higher correlations in tests involving the FFs are observed, suggesting that this factor is responsible for most of the spatial differentiation of the damage model results, especially for soil-related emissions. Moreover, stronger correlations for N_{ns} and N_{as} decreasing towards N_{marw} reflect the increase in complexity of the date model, i.e. as the emission location moves upstream the hydrological cycle and the N-removal processes in the marine compartment are complemented with those in the riverine system and soil compartment.

3.4. Sensitivity and uncertainties

The model sensitivity to the four input parameters, i.e. FF, XF, EF, and SD, was assessed by means of sensitivity ratios (SR) calculated as the ratio between the relative change in the model output and the relative change in the model input. As the damage CF calculation is a linear function of the parameters combination, i.e $CF=FF\times XF\times EF\times 0.5\times SD$, each of the primary parameters shows SR=1.0 (Table 3). Secondary parameters contributing to these were identified from the respective source modelling work and compared:

- Natural (FE_{ns}) and agricultural (FE_{as}) soil removal, riverine removal (FE_{riv}) and sewage treatment removal (FE_{sew}) constants contributing to soil- and river-related FF, and LME-dependent water residence time (τ_{LME}) contributing to marine removal of N (FF_{Nmarw}), all assessed by Cosme et al. (2016b);
- LME-dependent primary production rates (PP_{LME}), secondary producers assimilation fraction ($f_{SPassimil}$), and primary producers sinking fraction (f_{PPsink}), i.e. the three parameters contributing to XF with highest SRs, assessed by Cosme et al. (2015); and
- Species sensitivity to hypoxia (as a lowest-observed-effect-concentration, LOEC) contributing to the EF, for which SRs were estimated from the model work by Cosme and Hauschild (2016).

This analysis shows that the damage model has higher sensitivity to variations in the water residence time parameter (τ_{LME}). As also noted by Cosme and Hauschild (2016), data quality of τLME is an important aspect to consider in the FF estimation model, and is shown here to be of the same importance to the CFs estimation. Concerns about the inconsistency and scarcity of literature sources in reporting LME-integrated water residence time values were already expressed by Cosme and Hauschild (2016). Given that the FF_{Nmarw}, for which the water residence time data is determining, is strongly correlated with the damage CF of the respective emission route, this parameter

is a key issue in the characterization and damage modelling work. Ensuring its quality and consistency across LMEs is thus essential.

Table 3 Sensitivity ratios (SRs) of the primary and secondary input parameters for the damage factor estimation model. See text for parameters description

Parameter	Type, contribution to	SR	Source
FF_{Ni}	Primary, to CF_{Ni} and DF_{Ni}	1.0	This work
XF_j	Primary, to CF_{Ni} and DF_{Ni}	1.0	This work
EF_j	Primary, to CF_{Ni} and DF_{Ni}	1.0	This work
SD_j	Primary, to DF_{Ni}	1.0	This work
FE_{ns}	Secondary, to FF_{Nns}	1.0	Cosme et al. (2016b)
FE_{as}	Secondary, to FF_{Nas}	1.0	Cosme et al. (2016b)
FE_{riv}	Secondary, to FF_{Nriv}	1.0	Cosme et al. (2016b)
FE_{sew}	Secondary, to FF_{Nsew}	1.0	Cosme et al. (2016b)
τ_{LME}	Secondary, to FF_{Nmarw}	3.5	Cosme et al. (2016b)
PP_{LME}	Secondary, to XF_j	0.92	Cosme et al. (2015)
$f_{SPassimil}$	Secondary, to XF_j	-0.59	Cosme et al. (2015)
f_{PPsink}	Secondary, to XF_j	0.51	Cosme et al. (2015)
LOEC	Secondary, to EF_j	0.001-0.027	Using the model work by Cosme and Hauschild (2016)

The geographic distribution pattern of the CFs at endpoint (Fig. 2 and Figs. S.1 to S.4) and damage level (Fig. 3 and Figs. S.5 to S.8) show that these factors tend towards higher values for emissions to LMEs with longer residence time, which further supports that observation.

Regarding the environmental fate modelling, the validation work of the NEWS 2-DIN model, from which the specific DIN-removal fractions in the soil and river compartments were extracted, points to a reasonably robust model, as discussed in Mayorga et al. (2010). The NEWS 2-DIN calibration against observed DIN yields at the mouths of 66 basins (catchment areas from 28 to 5,847 x 10^3 km^2) across the world shows reasonable robustness – explained variance R^2=0.54 in predicted vs. observed DIN yields, and an absolute model error of 6% (Mayorga et al. 2010). Only the removal fraction constants are applied here, so the model error is likely to be smaller as the emissions data used to estimate riverine yield, and their inherent uncertainty, are not used. The NEWS 2 models suite is based on regression models that aggregate the environmental processes into export constants at a river basin scale, and thus miss the non-linearity of biogeochemical processes of N sinks in soil and groundwater, as discussed in Beusen et al. (2015). These fate processes are modelled in the IMAGE-GNM model (Beusen et al. 2015) at a 0.5°×0.5° grid cell resolution. Its adoption could be a model improvement, providing that the relevant removal constants can be extracted. Nevertheless, the river basin scale modelling given by the NEWS 2-DIN model seems adequate and sufficient for the present purpose, as discussed in Cosme et al. (2016b). Regarding the fate modelling the marine compartment, inconsistency and scarcity of LME-dependent data for surface water residence time and the empirical

relationship linking N-removal by denitrification and water residence time (R^2=0.56), were identified as the major sources of uncertainty by Cosme et al. (2016b).

The most important parameters contributing to the XF and EF modelling (PP rates and LOEC data, respectively) were associated with low uncertainty. The estimation of PP rates integrates monthly records from a 12-year period of satellite data, validated algorithms, and low variability (Cosme et al. 2015). In the EF model, the variability of the input data, the individual species sensitivity to hypoxia, is minimised by the estimation method recommended by (Cosme and Hauschild 2016), i.e. GM_{taxon} or the geometric mean at taxonomic group level of the geometric means of the species LOECs.

The PAF to PDF conversion applied in the DF estimation is based on an arbitrary site-generic 0.5 factor. Conversion coefficients based on species vulnerability, recoverability, ecological function, or on ecosystems resilience or services, can be used to estimate LME-dependent conversions – see discussion in Cosme et al. (2016a) and work by Curran et al. (2011), Verones et al. (2013) and Verones et al. (2015). While methods for such conversions are not widespread for demersal marine species in particular, the fixed 0.5 factor conversion holds, as proposed here.

The dataset used to estimate LME-dependent SDs is based on fisheries catch statistics, which may raise representativeness concerns and data-related uncertainty – see discussion in Cosme et al. (2016a). The use of a multiple Species Distribution Model (SDM) ensemble increases the robustness of the species occurrence estimation, essential for the SD calculation. The SD estimation method described by Cosme et al. (2016a) seems the best estimate available and a valid addition to the indicators metrics harmonisation effort. The harmonisation with species densities is introduced because PDF-based units of indicators for different impact categories represent distinct biotic components of the respective ecosystems. As an example, freshwater and marine eutrophication impact scores, both expressed as a PDF-integrated metric, refer to a fraction of a necessarily distinct set of species, namely the freshwater and the marine biota. The aggregation of these un-matching indicator scores in a common Area of Protection (AoP) score would lead to a meaningless result and there is thus need for harmonisation. In the present method, this is achieved by applying LME-dependent SDs in order to determine the absolute number of relevant species that the PDF refers to. Such species-based metric, ideally representative, can then be aggregated with equivalent results for other indicators contributing to the same AoP in a harmonised and meaningful damage score.

Regional aggregation of CFs based on emission-weighted averages uses emission data from year 2000. The emission datamay vary significantly over time and scale (Seitzinger et al. 2010; Beusen et al. 2016), requiring periodic update. However,

when averaging up to the continental level, it is likely that the uncertainty of these data is of minor importance.

4. Conclusions and outlook

Impact assessment of human activities in a life cycle context is supported by characterization of the inventoried environmental emissions. Completeness and relevance of the underlying modelling work in the characterizationphase are essential for the model analysis (Hauschild et al. 2013). The marine eutrophication impact pathway defined in the present method (Fig. 1), aiming at the hypoxia-related impacts on demersal animal communities, covers the entire cascade of critical processes involved in this phenomenon. Others, like harmful algal blooms, hydrogen sulphide formation in sediments, alterations on ecological community structure and functioning, and more (see e.g. Smith et al. (1999); Cloern (2001); Rabalais et al. (2009)), are outside the scope of this study, but important nonetheless. Further, the sub-models applied in composing this particular endpoint marine eutrophication indicator, i.e. fate, exposure, and effect factors, are based on documented state-of-the-art scientific knowledge, and their applicability and limitations are identified and discussed in the respective publications. The transparency of the method, its relevance and completeness, advocate for its application in LCIA characterization of waterborne nitrogen emissions, although acknowledging the need for further work to implement environmental fate of airborne nitrogen emissions.

Major contributions to the current state-of-the-art of this impact category indicator resides in (i) the full pathway coverage, thus reaching endpoint level, (ii) the significant increase in geographic coverage of both endpoint characterization and damage to ecosystem factors, (iii) the mechanistic modelling of exposure and effect factors, and (iv) the application of spatially explicit species densities in the damage to ecosystems estimation.

Up to six and seven orders of magnitude spatial differentiation were verified for the characterization factors at endpoint and damage levels, respectively. In both cases, this differentiation is reduced to only 1 order of magnitude after aggregation to the level of continents. The application of the characterization factors in life cycle impact assessment, at both levels, is therefore recommended at a river basin scale, provided that emission location is known.

Future work should include the environmental fate of airborne nitrogen emission, in order to achieve full coverage of the relevant environmental mechanisms involved in the marine eutrophication phenomenon. As such, deposition fractions of airborne nitrogen forms, as done by e.g. Dentener et al. (2006) or Roy et al. (2012), can be coupled to the present characterization factors.

5. References

Andrews JC, Müller H (1983) Space-time variability of nutrients in a lagoonal patch reef. Limnol Oceanogr 28:215–227. doi: 10.4319/lo.1983.28.2.0215

Beusen AHW, Bouwman AF, Van Beek LPH, et al (2016) Global riverine N and P transport to ocean increased during the 20th century despite increased retention along the aquatic continuum. Biogeosciences 113:2441–2451. doi: 10.5194/bgd-12-20123-2015

Beusen AHW, Van Beek LPH, Bouwman AF, et al (2015) Coupling global models for hydrology and nutrient loading to simulate nitrogen and phosphorus retention in surface water – description of IMAGE–GNM and analysis of performance. Geosci Model Dev 8:4045–4067. doi: 10.5194/gmd-8-4045-2015

Brady NC, Weil RR (2007) The nature and properties of soils, 14th edn. Prentice Hall

Cloern JE (2001) Our evolving conceptual model of the coastal eutrophication problem. Mar Ecol Prog Ser 210:223–253. doi: 10.3354/meps210223

Cosme N, Hauschild MZ (2016) Effect factors for marine eutrophication in LCIA based on species sensitivity to hypoxia. Ecol Indic 69:453–462. doi: 10.1016/ j.ecolind.2016.04.006

Cosme N, Jones MC, Cheung WWL, Larsen HF (2016a) Spatial differentiation of marine eutrophication damage indicators based on species density. Ecol Indic submitted.

Cosme N, Koski M, Hauschild MZ (2015) Exposure factors for marine eutrophication impacts assessment based on a mechanistic biological model. Ecol Modell 317:50–63. doi: 10.1016/j.ecolmodel.2015.09.005

Cosme N, Mayorga E, Hauschild MZ (2016b) Spatially explicit fate factors for waterbone nitrogen emissions at the global scale. Int J Life Cycle Assesment submitted.

Curran M, de Baan L, De Schryver AM, et al (2011) Toward meaningful end points of biodiversity in life cycle assessment. Environ Sci Technol 45:70–9. doi: 10.1021/es101444k

Davis JC (1975) Minimal dissolved oxygen requirements of aquatic life with emphasis on Canadian species: a review. J Fish Res Board Canada 32:2295–2332.

Dentener F, Drevet J, Lamarque JF, et al (2006) Nitrogen and sulfur deposition on regional and global scales: A multimodel evaluation. Global Biogeochem Cycles. doi: 10.1029/2005GB002672

Dettmann EH (2001) Effect of Water Residence Time on Annual Export and Denitrification of Nitrogen in Estuaries: A Model Analysis. Estuaries 24:481–490.

Diaz RJ, Rosenberg R (2008) Spreading dead zones and consequences for marine ecosystems. Science (80-) 321:926–929. doi: 10.1126/science.1156401

Diaz RJ, Rosenberg R (1995) Marine Benthic Hypoxia: a Review of Its Ecological Effects and the Behavioural Responses of Benthic Macrofauna. Oceanogr Mar

Biol Annu Rev 33:245–303.

Dumont E, Harrison JA, Kroeze C, et al (2005) Global distribution and sources of dissolved inorganic nitrogen export to the coastal zone: Results from a spatially explicit, global model. Global Biogeochem Cycles 19:GB4S02. doi: 10.1029/2005GB002488

EC-JRC-IES (2010) ILCD Handbook: Analysis of existing Environmental Impact Assessment methodologies for use in Life Cycle Assessment, 1st edit. Publications Office of the European Union, Luxembourg

Fear J, Thompson S, Gallo T, Paerl H (2005) Denitrification rates measured along a salinity gradient in the eutrophic Neuse River estuary, North Carolina, USA. Estuaries and Coasts 28:608–619. doi: 10.1007/BF02696071

Galloway JN, Cowling EB (2002) Reactive nitrogen and the world: 200 years of change. Ambio 31:64–71. doi: 10.2307/4315217

Galloway JN, Dentener FJ, Capone DG, et al (2004) Nitrogen cycles: past, present, and future. Biogeochemistry 70:153–226.

Galloway JN, Townsend AR, Erisman JW, et al (2008) Transformation of the Nitrogen Cycle: Recent Trends, Questions, and Potential Solutions. Science (80-) 320:889–892. doi: 10.1126/science.1136674

GESAMP (2001) A Sea of Troubles. Rep. Stud. GESAMP No. 70. Joint Group of Experts on the Scientific Aspects of Marine Environmental Protection and Advisory Committee on Protection of the Sea.

Goedkoop M, Heijungs R, Huijbregts MAJ, et al (2012) ReCiPe 2008 - A life cycle impact assessment method which comprises harmonised category indicators at the midpoint and the endpoint level. First edition (revised) Report I: Characterisation; July 2012, http://www.lcia-recipe.net

Graf G, Bengtsson W, Diesner U, et al (1982) Benthic response to sedimentation of a spring phytoplankton bloom: Process and budget. Mar Biol 67:201–208. doi: 10.1007/BF00401286

Gray JS, Wu RS, Or YY (2002) Effects of hypoxia and organic enrichment on the coastal marine environment. Mar Ecol Prog Ser 238:249–279.

Green PA, Vörösmarty CJ, Meybeck M, et al (2004) Pre-industrial and contemporary fluxes of nitrogen through rivers: a global assessment based on typology. Biogeochemistry 68:71–105.

Guinée JB, Gorrée M, Heijungs R, et al (2002) Handbook on life cycle assessment. Operational guide to the ISO standards. I: LCA in perspective. IIa: Guide. IIb: Operational annex. III: Scientific background. Kluwer Academic Publishers, Dordrecht

Hauschild MZ (2005) Assessing Environmental Impacts in a Life-Cycle Perspective. Environ Sci Technol 39:81–88. doi: 10.1021/es053190s

Hauschild MZ, Goedkoop M, Guinée JB, et al (2013) Identifying best existing practice for characterization modeling in life cycle impact assessment. Int J Life Cycle Assess 18:683–697. doi: 10.1007/s11367-012-0489-5

Hauschild MZ, Huijbregts MAJ (2015) Introducing Life Cycle Impact Assessment. In: Hauschild MZ, Huijbregts MAJ (eds) Life Cycle Impact Assessment, LCA Compendium - The Complete World of Life Cycle Assessment. Springer Science+Business Media, Dordrecht, pp 1–16

Hauschild MZ, Potting J (2005) Spatial Differentiation in Life Cycle Impact Assessment - The EDIP2003 methodology.

Heijungs R (2005) On the use of units in LCA. Int J Life Cycle Assesment 10:173–176. doi: http://dx.doi.org/10.1065/lca2005.02.199

Henderson AD (2015) Eutrophication. In: Hauschild MZ, Huijbregts MAJ (eds) Life Cycle Impact Assessment, LCA Compendium - The Complete World of Life Cycle Assessment. Springer Science+Business Media Dordrecht, pp 177–196

Howarth RW, Marino R (2006) Nitrogen as the limiting nutrient for eutrophication in coastal marine ecosystems: Evolving views over three decades. Limnol Oceanogr 51:364–376. doi: 10.4319/lo.2006.51.1_part_2.0364

Itsubo N, Inaba A (2012) LIME2: Life-cycle Impact assessment Method based on Endpoint modeling. JLCA Newsl Life-Cycle Assess Soc Japan 12:16.

Jolliet O, Margni M, Charles R, et al (2003) Presenting a New Method IMPACT 2002 + : A New Life Cycle Impact Assessment Methodology. Int J LCA 8:324–330.

Jones MC, Cheung WWL (2015) Multi-model ensemble projections of climate change effects on global marine biodiversity. ICES J Mar Sci 72:741–752. doi: 10.1093/icesjms/fsu172

Keeney DR, Hatfield JL (2001) The Nitrogen cycle, historical perspectives, and current and potential future concerns. In: Follet RF, Hatfield JL (eds) Nitrogen in the Environment: Sources, Problems, and Management. Elsevier Science B.V., Amsterdam, The Netherlands, pp 3–16

Kemna R, van Elburg M, Li W, van Holsteijn R (2005) Methodology Study Eco-design of Energy-using Products: MEEuP methodology report. Delft

Laegreid M, Bockman OC, Kaarstad O (1999) Agriculture and Fertilizers. AB Int., New York

Larsen HF, Hauschild MZ (2007) LCA Methodology Evaluation of Ecotoxicity Effect Indicators for Use in LCIA. Int J 12:24–33.

Levin LA, Ekau W, Gooday AJ, et al (2009) Effects of natural and human-induced hypoxia on coastal benthos. Biogeosciences 6:2063–2098.

Magalhães CM, Joye SB, Moreira RM, et al (2005) Effect of salinity and inorganic nitrogen concentrations on nitrification and denitrification rates in intertidal sediments and rocky biofilms of the Douro River estuary, Portugal. Water Res 39:1783–1794. doi: 10.1016/j.watres.2005.03.008

Mayorga E, Seitzinger SP, Harrison JA, et al (2010) Global Nutrient Export from WaterSheds 2 (NEWS 2): Model development and implementation. Environ Model Softw 25:837–853. doi: 10.1016/j.envsoft.2010.01.007

Middelburg JJ, Levin LA (2009) Coastal hypoxia and sediment biogeochemistry. Biogeosciences 6:1273–1293. doi: 10.5194/bg-6-1273-2009

Monsen NE, Cloern JE, Lucas L V., Monismith SG (2002) The use of flushing time, residence time, and age as transport time scales. Limnol Oceanogr 47:1545–1553. doi: 10.4319/lo.2002.47.5.1545

Nixon SW (1995) Coastal marine eutrophication: A definition, social causes, and future concerns. Ophelia 41:199–219.

Nixon SW, Ammerman JW, Atkinson LP, et al (1996) The fate of nitrogen and phosphorus at the land-sea margin of the North Atlantic Ocean. Biogeochemistry 35:141–180.

Norris GA (2003) Impact Characterization in the Tool for the Reduction and Assessment of Chemical and Other Environmental Impacts. J Ind Ecol 6:79–101. doi: 10.1162/108819802766269548

Pennington DW, Payet J, Hauschild MZ (2004a) Aquatic Ecotoxicological Indicators In Life-Cycle Assessment. Environ Toxicol Chem 23:1796–1807.

Pennington DW, Potting J, Finnveden G, et al (2004b) Life cycle assessment Part 2: Current impact assessment practice. Environ Int 30:721–39. doi: 10.1016/j.envint.2003.12.009

Ploug H, Grossart H-P, Azam, Farooq, Jørgensen BB (1999) Photosynthesis, respiration, and carbon turnover in sinking marine snow from surface waters of Southern California Bight: implications for the carbon cycle in the ocean. Mar Ecol Prog Ser 179:1–11.

Posthuma L, Suter II GW, Traas TP (eds) (2002) Species Sensitivity Distributions in Ecotoxicology.

Rabalais NN (2002) Nitrogen in Aquatic Ecosystems. Ambio 31:102–112.

Rabalais NN, Turner RE, Diaz RJ, Justić D (2009) Global change and eutrophication of coastal waters. ICES J Mar Sci 66:1528–1537.

Roy P-O, Huijbregts MAJ, Deschênes L, Margni M (2012) Spatially-differentiated atmospheric source–receptor relationships for nitrogen oxides, sulfur oxides and ammonia emissions at the global scale for life cycle impact assessment. Atmos Environ 62:74–81. doi: 10.1016/j.atmosenv.2012.07.069

Seitzinger SP, Harrison JA, Böhlke JK, et al (2006) Denitrification across landscapes and waterscapes: A synthesis. Ecol Appl 16:2064–2090.

Seitzinger SP, Harrison JA, Dumont E, et al (2005) Sources and delivery of carbon, nitrogen, and phosphorus to the coastal zone: An overview of Global Nutrient Export from Watersheds (NEWS) models and their application. Global Biogeochem Cycles 19:1-11. doi: 10.1029/2005GB002606

Seitzinger SP, Mayorga E, Bouwman AF, et al (2010) Global river nutrient export: A scenario analysis of past and future trends. Global Biogeochem Cycles 24:GB0A08. doi: 10.1029/2009GB003587

Sherman K, Alexander LM (eds) (1986) Variability and Management of Large Marine Ecosystems. Westview Press Inc., Boulder, CO

Smith VH, Tilman GD, Nekola JC (1999) Eutrophication: impacts of excess nutrient inputs on freshwater, marine, and terrestrial ecosystems. Environ Pollut

100:179–196.

Steen B (1999) A systematic approach to environmental priority strategies in product development (EPS). Version 2000 – General system characteristics. CPM report 1999:4. Gothenburg, Sweden

Toffoletto L, Bulle C, Godin J, et al (2007) LCA Methodology LUCAS – A New LCIA Method Used for a CAnadian-Specific Context. Int J 12:93–102.

Udo de Haes HA, Finnveden G, Goedkoop M, et al (2002) Life-Cycle Impact Assessment: Striving Towards Best Practice. SETAC Press, Pensacola, FL, USA

Van Drecht G, Bouwman AF, Knoop JM, et al (2003) Global modeling of the fate of nitrogen from point and nonpoint sources in soils, groundwater, and surface water. Global Biogeochem Cycles 17:1–20. doi: 10.1029/2003GB002060

Vaquer-Sunyer R, Duarte CM (2008) Thresholds of hypoxia for marine biodiversity. Proc Natl Acad Sci U S A 105:15452–7. doi: 10.1073/pnas.0803833105

Verones F, Huijbregts MAJ, Chaudhary A, et al (2015) Harmonizing the assessment of biodiversity effects from land and water use within LCA. Environ Sci Technol 49:3584–3592. doi: 10.1021/es504995r

Verones F, Saner D, Pfister S, et al (2013) Effects of consumptive water use on biodiversity in wetlands of international importance. Environ Sci Technol 47:12248–57. doi: 10.1021/es403635j

Vitousek PM, Hättenschwiler S, Olander L, Allison S (2002) Nitrogen and nature. Ambio 31:97–101.

Vollenweider RA (1976) Advances in defining critical loading levels for phosphorus in lake eutrophication. Mem dell'Istituto Ital di Idrobiol dott Marco Marchi 33:53–83. doi: nicht verfügbar?

Vörösmarty CJ, Fekete BM, Meybeck M, Lammers RB (2000) Geomorphic attributes of the global system of river at 30-minute spatial resolution. J Hydrol 237:17–39.

Wu RS (2002) Hypoxia: from molecular responses to ecosystem responses. Mar Pollut Bull 45:35–45.

Zhang J, Gilbert D, Gooday AJ, et al (2010) Natural and human-induced hypoxia and consequences for coastal areas: synthesis and future development. Biogeosciences 7:1443–1467. doi: 10.5194/bg-7-1443-2010

Article V – Electronic Supplementary Material 1

Characterization of waterborne nitrogen emissions for marine eutrophication modelling in life cycle impact assessment at the damage level and global scale

Nuno Cosme, Michael Z. Hauschild

Division for Quantitative Sustainability Assessment, Department of Management Engineering, Technical University of Denmark, Produktionstorvet 424, DK-2800 Kgs. Lyngby, Denmark

Contents

Note on additional tables:

Full results of the fate factors (FF, [yr]) and characterisation factors [CF, [(PAF)·m^3·yr·kgN^{-1}]) per emission route for the 5,772 river basins are only available as Excel spreadsheets, given the extensive table size (ca. 126 pages). These tables are available in ***Electronic Supplementary Material 2*** *for FF (Table S.5) and CF (Table S.6).*

Electronic Supplementary Material 2:

Table S.1 Fate factors (FF, [yr]) for waterborne nitrogen (N) emissions per emission route: N from natural soils (FF_{Nns}), N from agricultural soils (FF_{Nas}), N in sewage discharges to river (FF_{Nsew}), N to river (FF_{Nriv}), and direct N emissions to coastal marine waters (FF_{Nmarw}). Results for 5,772 river basins. 'BASINID' represents the basin identifier used in STN-30p 6.01 and 'basincellcnt' the number of 0.5° grid cells contained by the basin. Retrieved from (Cosme et al. 2016b)

Table S.5 Endpoint characterisation factors (CF, [(PAF)·m^3·yr·kgN^{-1}]) for waterborne nitrogen (N) emissions per emission route: N from natural soils (CF_{Nns}), N from agricultural soils (CF_{Nas}), N in sewage discharges to river (CF_{Nsew}), N to river (CF_{Nriv}), and direct N emissions to

coastal marine waters (CF_{Nmarw}). Results for 5,772 river basins. 'BASINID' represents the basin identifier used in STN-30p 6.01 and 'basincellcnt' the number of 0.5° grid cells contained by the basin

Table S.6 Damage characterization factors (CF, [species·yr·kgN^{-1}]) for waterborne nitrogen (N) emissions per emission route: N from natural soils (CF_{Nns}), N from agricultural soils (CF_{Nas}), N in sewage discharges to river (CF_{Nsew}), N to river (CF_{Nriv}), and direct N emissions to coastal marine waters (CF_{Nmarw}). Results for 5,772 river basins. 'BASINID' represents the basin identifier used in STN-30p 6.01 and 'basincellcnt' the number of 0.5° grid cells contained by the basin

S.1 Exposure and effect factors

Table S.2 Compilation of the marine eutrophication eXposure Factors per Large Marine Ecosystem (LME), retrieved from Cosme et al. (2015); marine eutrophication Effect Factors (EF) per climate zone disaggregated into the composing LMEs, adapted from Cosme and Hauschild (2016); and marine demersal species density (SD) retrieved from Cosme et al. (2016)

Large Marine Ecosystem	Climate zone	eXposure Factor (XF)	Effect Factor (EF)	Species density (SD)
		$kgO_2 \cdot kgN^{-1}$	$(PAF) \cdot m^3 \cdot kgO_2^{-1}$	$species \cdot m^{-3}$
01. East Bering Sea	Subpolar	10	240	5.8E-13
02. Gulf of Alaska	Subpolar	11	240	6.2E-13
03. California Current	Temperate	6.1	280	2.3E-13
04. Gulf of California	Subtropical	8.0	270	1.3E-11
05. Gulf of Mexico	Subtropical	4.5	310	1.7E-12
06. Southeast U.S. Continental Shelf	Subtropical	5.3	310	1.4E-11
07. Northeast U.S. Continental Shelf	Temperate	12	280	1.6E-11
08. Scotian Shelf	Temperate	12	240	9.2E-12
09. Newfoundland-Labrador Shelf	Subpolar	10	240	3.8E-12
10. Insular Pacific-Hawaiian	Tropical	1.3	310	6.2E-13
11. Pacific Central-American	Tropical	3.3	310	3.8E-13
12. Caribbean Sea	Tropical	2.5	310	5.4E-13
13. Humboldt Current	Temperate	8.4	280	2.0E-13
14. Patagonian Shelf	Temperate	11	240	1.7E-12
15. South Brazil Shelf	Subtropical	5.8	270	5.2E-12
16. East Brazil Shelf	Tropical	1.9	310	1.1E-12
17. North Brazil Shelf	Tropical	5.3	310	2.3E-12
18. Canadian Eastern Arctic - West Greenland	Polar	6.8	220	1.5E-12
19. Greenland Sea	Polar	7.3	220	6.7E-13
20. Barents Sea	Polar	7.1	240	3.3E-13
21. Norwegian Sea	Subpolar	6.4	240	8.7E-13
22. North Sea	Temperate	9.1	240	6.7E-12
23. Baltic Sea	Subpolar	16	240	3.6E-12
24. Celtic-Biscay Shelf	Temperate	8.1	280	6.7E-12
25. Iberian Coastal	Temperate	7.4	280	1.0E-11
26. Mediterranean	Subtropical	3.5	280	1.2E-12
27. Canary Current	Subtropical	7.7	270	2.0E-12
28. Guinea Current	Tropical	4.3	270	6.6E-13

Large Marine Ecosystem	Climate zone	eXposure Factor (XF)	Effect Factor (EF)	Species density (SD)
		$kgO_2 \cdot kgN^{-1}$	$(PAF) \cdot m^3 \cdot kgO_2^{-1}$	$species \cdot m^{-3}$
29. Benguela Current	Subtropical	9.1	270	1.1E-12
30. Agulhas Current	Subtropical	4.8	310	4.4E-13
31. Somali Coastal Current	Tropical	3.4	310	1.3E-12
32. Arabian Sea	Tropical	5.0	310	3.3E-13
33. Red Sea	Tropical	3.9	310	5.9E-12
34. Bay of Bengal	Tropical	3.7	310	3.9E-13
35. Gulf of Thailand	Tropical	4.2	310	1.1E-11
36. South China Sea	Tropical	2.7	310	9.5E-13
37. Sulu-Celebes Sea	Tropical	3.2	310	2.0E-12
38. Indonesian Sea	Tropical	3.7	310	1.1E-12
39. North Australian Shelf	Tropical	4.3	310	5.7E-12
40. Northeast Australian Shelf	Tropical	1.9	310	1.5E-12
41. East-Central Australian Shelf	Subtropical	3.5	270	1.4E-12
42. Southeast Australian Shelf	Temperate	5.4	280	7.3E-13
43. Southwest Australian Shelf	Temperate	5.3	280	1.3E-12
44. West-Central Australian Shelf	Subtropical	3.8	270	2.7E-12
45. Northwest Australian Shelf	Tropical	2.7	310	3.0E-12
46. New Zealand Shelf	Temperate	5.7	280	2.5E-12
47. East China Sea	Subtropical	6.4	310	5.6E-12
48. Yellow Sea	Temperate	12	280	6.9E-12
49. Kuroshio Current	Subtropical	3.4	270	8.6E-13
50. Sea of Japan/East Sea	Temperate	5.9	280	1.4E-12
51. Oyashio Current	Subpolar	9.3	240	1.3E-12
52. Sea of Okhotsk	Subpolar	10	240	7.0E-13
53. West Bering Sea	Subpolar	7.8	240	2.8E-14
54. Northern Bering - Chukchi Seas	Polar	4.6	220	4.7E-13
55. Beaufort Sea	Polar	5.9	220	2.8E-13
56. East Siberian Sea	Polar	2.8	220	2.1E-13
57. Laptev Sea	Polar	7.5	220	5.2E-13
58. Kara Sea	Polar	6.2	220	2.8E-13
59. Iceland Shelf and Sea	Subpolar	7.3	240	1.0E-12
60. Faroe Plateau	Subpolar	5.6	240	1.7E-11
61. Antarctic	Polar	4.9	220	4.2E-14
62. Black Sea	Temperate	8.8	220	2.6E-12
63. Hudson Bay Complex	Polar	7.0	220	4.2E-13
64. Central Arctic Ocean	Polar	0.45	220	1.8E-14
65. Aleutian Islands	Subpolar	10	240	5.0E-13
66. Canadian High Arctic - North Greenland	Polar	3.0	220	3.8E-13

S.2 Results of estimated CFs and DFs per emission route at a river basin scale

Table S.3 Statistics of the distribution of endpoint CF_{Ni} [(PAF)·m^3·yr·kgN^{-1}] results per emission route at a river basin scale

Statistics	Characterization Factor [(PAF)·m3·yr·kgN-1] per emission route				
	N_{ns}	N_{as}	N_{sew}	N_{riv}	N_{marw}
Minimum	3.3E-03	4.0E-03	2.6E-01	5.2E-01	3.9E+01
5th percentile	1.6E+00	4.4E+00	2.4E+01	4.8E+01	1.1E+02
Mean	3.3E+02	4.5E+02	9.9E+02	1.7E+03	3.2E+03
95th percentile	1.2E+03	2.6E+03	2.3E+03	3.9E+03	8.3E+03
Maximum	1.8E+04	1.8E+04	2.0E+04	3.0E+04	4.9E+04
Spatial variability	*5E+06*	*4E+06*	*8E+04*	*6E+04*	*1E+03*

Table S.4 Statistics of the distribution of damage CF_{Ni} results [species·yr·kgN^{-1}] per emission route at a river basin scale

Statistics	Characterization Factor [species·yr·kgN-1] per emission route				
	N_{ns}	N_{as}	N_{sew}	N_{riv}	N_{marw}
Minimum	3.9E-16	3.9E-16	2.5E-14	5.1E-14	5.0E-12
5th percentile	5.8E-13	1.2E-12	6.0E-12	1.2E-11	2.4E-11
Mean	3.9E-10	4.5E-10	1.0E-09	1.7E-09	3.4E-09
95th percentile	1.2E-09	1.9E-09	3.6E-09	6.2E-09	1.4E-08
Maximum	3.2E-08	3.2E-08	3.6E-08	5.4E-08	8.8E-08
Spatial variability	*8E+07*	*8E+07*	*1E+06*	*1E+06*	*2E+04*

S.3 Calculation of spatial aggregated factors

Spatial aggregation of CFs over regions, e.g. continents or world, for each N-emission route *i*, were calculated by emission(*Em*)-weighted averages, as shown in Eqs. (S.1). Regional factors ($CF_{i,reg}$, [(PAF)·m^3·yr·kgN^{-1}] and [species.yr kgN^{-1}]) aggregate all emissions, with non-zero $CF_{i,jl}$ belonging to region *reg*, with a corresponding emission *Em* in the respective route *i*. Emission data used refer to year 2000 and were extracted from the NEWS 2-DIN model (Mayorga et al. 2010).

$$CF_{i,reg} = \frac{\sum_{reg}(CF_{i,reg} \cdot Em_{i,reg})}{\sum_{reg} Em_{i,reg}} \quad \text{(S.1)}$$

Table S.7 Regional damage characterization factors (CF, [species·yr·kgN^{-1}]) by emission-weighted aggregation per emissions route at the level of continents. Intra-regional variability (*var*) and inter-regional variability (N_i) shown

Aggregation scale	Characterization Factor [species·yr·kgN^{-1}] per emission route									
	N_{ns}	*var*	N_{as}	*var*	N_{sew}	*var*	N_{riv}	*var*	N_{marw}	*var*
Africa	1.1E-11	*9E+04*	3.4E-11	*2E+04*	5.1E-11	*2E+03*	1.1E-10	*2E+03*	9.3E-10	*6E+02*
Europe	1.5E-09	*5E+03*	1.5E-09	*5E+03*	3.8E-09	*8E+02*	6.1E-09	*6E+02*	1.6E-08	*5E+02*
North America	1.4E-10	*5E+05*	1.4E-10	*5E+05*	2.1E-10	*1E+04*	3.2E-10	*2E+04*	9.0E-10	*4E+02*
South America	3.2E-11	*2E+06*	7.6E-11	*2E+06*	7.2E-11	*2E+04*	1.4E-10	*2E+04*	4.5E-10	*3E+02*
North Asia	6.0E-11	*1E+03*	6.0E-11	*1E+03*	1.6E-10	*5E+02*	2.9E-10	*5E+02*	7.9E-10	*3E+02*
South Asia	5.4E-10	*8E+04*	5.7E-10	*8E+04*	6.2E-10	*6E+02*	1.2E-09	*5E+02*	4.9E-09	*1E+02*
Oceania [a]	8.7E-11	*4E+03*	4.0E-10	*2E+03*	2.4E-10	*2E+02*	4.8E-10	*3E+02*	1.0E-09	*3E+02*
Australia	1.8E-11	*5E+02*	3.5E-11	*2E+03*	6.9E-11	*4E+01*	1.2E-10	*4E+01*	2.8E-10	*9E+00*
Spatial variability	*1E+02*	--	*4E+01*	--	*7E+01*	--	*6E+01*	--	*6E+01*	--
World	4.2E-10	--	4.6E-10	--	7.3E-10	--	1.3E-09	--	4.2E-09	--

[a] *(excluding Australia)*

S.4 Analysis of contribution to spatial differentiation in the damage model

The results of the regression analysis of the contribution to spatial differentiation are included in Table S.3. Higher correlations are found for high explained variance, slopes closer to 1.0, and low mean square (MS) and standard error (SE).

Table S.8 Regression analysis of the variation of the model parameters, i.e. river basin-dependent fate factor (FF) (except the LME(*j*)-dependent FF_{Nmarw}), LME-dependent exposure factors (XF), climate zone-dependent effect factor (EF) but translated to LMEs, and LME-dependent species density (SD), and the variation of the damage characterization factors (CF) per emission route, in log scale

	Equation of linear regression	R^2	SS	MS	SE
logFF_{Ni} *vs. log*CF_{Ni}					
N_{ns}	$logCF_{Nns} = 1.0 \cdot logFF_{Nns} - 9.2$	0.69	1706	0.34	0.58
N_{as}	$logCF_{Nas} = 1.0 \cdot logFF_{Nas} - 9.2$	0.65	1705	0.34	0.58
N_{sew}	$logCF_{Nsew} = 0.8 \cdot logFF_{Nsew} - 9.3$	0.51	1820	0.32	0.56
N_{riv}	$logCF_{Nriv} = 0.8 \cdot logFF_{Nriv} - 9.3$	0.49	1808	0.31	0.56
N_{marw}	$logCF_{Nmarw} = 0.8 \cdot logFF_{Nmarw} - 9.2$	0.49	1829	0.32	0.56
logXF_j *vs. log*CF_{Ni}					
N_{ns}	$logCF_{Nns} = 2.4 \cdot logXF_j - 12$	0.23	4186	0.82	0.91
N_{as}	$logCF_{Nas} = 1.5 \cdot logXF_j - 11$	0.09	4415	0.87	0.93
N_{sew}	$logCF_{Nsew} = 1.3 \cdot logXF_j - 11$	0.10	3309	0.57	0.76
N_{riv}	$logCF_{Nriv} = 1.2 \cdot logXF_j - 10$	0.09	3224	0.56	0.75
N_{marw}	$logCF_{Nmarw} = 1.2 \cdot logXF_j - 10$	0.09	3241	0.56	0.75
logEF_j *vs. log*CF_{Ni}					
N_{ns}	$logCF_{Nns} = -1.9 \cdot logEF_j - 6.0$	0.01	5375	1.06	1.03
N_{as}	$logCF_{Nas} = 2.3 \cdot logEF_j - 16$	0.02	4773	0.94	0.97
N_{sew}	$logCF_{Nsew} = -2.0 \cdot logEF_j - 5.0$	0.02	3604	0.63	0.79
N_{riv}	$logCF_{Nriv} = -1.6 \cdot logEF_j - 5.7$	0.01	3501	0.61	0.78
N_{marw}	$logCF_{Nmarw} = -0.8 \cdot logEF_j - 7.5$	0.003	3548	0.61	0.78
logSD_j *vs. log*CF_{Ni}					
N_{ns}	$logCF_{Nns} = 0.1 \cdot logSD_j - 2.0$	0.24	4126	0.81	0.90
N_{as}	$logCF_{Nas} = 1.1 \cdot logSD_j - 2.6$	0.29	3472	0.68	0.83
N_{sew}	$logCF_{Nsew} = 0.8 \cdot logSD_j - 0.3$	0.27	2706	0.47	0.69
N_{riv}	$logCF_{Nriv} = 0.8 \cdot logSD_j - 0.5$	0.27	2596	0.45	0.67
N_{marw}	$logCF_{Nmarw} = 0.9 \cdot logSD_j - 1.2$	0.29	2513	0.44	0.66
log(FF_{Ni}×XF) *vs. log*CF_{Ni}					
N_{ns}	$logCF_{Nns} = 1.0 \cdot log(FF_{Nns} \times XF_j) - 9.9$	0.76	1314	0.26	0.51
N_{as}	$logCF_{Nas} = 1.0 \cdot log(FF_{Nas} \times XF_j) - 9.9$	0.73	1316	0.26	0.51
N_{sew}	$logCF_{Nsew} = 0.9 \cdot log(FF_{Nsew} \times XF_j) - 9.9$	0.61	1444	0.25	0.50
N_{riv}	$logCF_{Nriv} = 0.9 \cdot log(FF_{Nriv} \times XF_j) - 9.9$	0.59	1441	0.25	0.50
N_{marw}	$logCF_{Nmarw} = 0.9 \cdot log(FF_{Nmarw} \times XF_j) - 9.9$	0.59	1457	0.25	0.50
log(FF_{Ni}×EFj) *vs. log*CF_{Ni}					
N_{ns}	$logCF_{Nns} = 1.0 \cdot log(FF_{Nns} \times EF_j) - 12$	0.70	1645	0.32	0.57
N_{as}	$logCF_{Nas} = 1.0 \cdot log(FF_{Nas} \times EF_j) - 12$	0.66	1649	0.32	0.57
N_{sew}	$logCF_{Nsew} = 0.9 \cdot log(FF_{Nsew} \times EF_j) - 11$	0.52	1782	0.31	0.56
N_{riv}	$logCF_{Nriv} = 0.8 \cdot log(FF_{Nriv} \times EF_j) - 11$	0.50	1771	0.31	0.55

	Equation of linear regression	R^2	SS	MS	SE
N_{marw}	$logCF_{Nmarw} = 0.8 \cdot log(FF_{Nmarw} \times EF_j) - 11$	0.50	1784	0.31	0.56
log(XF*j*×EF*j*) *vs. log*CF_{Ni}					
N_{ns}	$logCFNns = 2.7 \cdot log(XF \times EF_j) - 19$	0.24	4136	0.81	0.90
N_{as}	$logCFNas = 2.0 \cdot log(XF \times EF_j) - 17$	0.14	4179	0.82	0.91
N_{sew}	$logCFNsew = 1.3 \cdot log(XF \times EF_j) - 14$	0.09	3362	0.58	0.76
N_{riv}	$logCFNriv = 1.2 \cdot log(XF \times EF_j) - 13$	0.08	3258	0.57	0.75
N_{marw}	$logCFNmarw = 1.3 \cdot log(XF \times EF_j) - 13$	0.09	3231	0.56	0.75
logCF_{Ni} *vs. log*CF_{Ni}					
N_{ns}	$logCF_{Nns} = 1.0 \cdot logCF_{Nns} - 12$	0.78	1207	0.24	0.49
N_{as}	$logCF_{Nas} = 1.0 \cdot logCF_{Nas} - 12$	0.75	1206	0.24	0.49
N_{sew}	$logCF_{Nsew} = 0.9 \cdot logCF_{Nsew} - 12$	0.63	1354	0.23	0.48
N_{riv}	$logCF_{Nriv} = 0.9 \cdot logCF_{Nriv} - 12$	0.62	1351	0.23	0.48
N_{marw}	$logCF_{Nmarw} = 0.9 \cdot logCF_{Nmarw} - 12$	0.62	1359	0.24	0.49

S.5 Additional figures

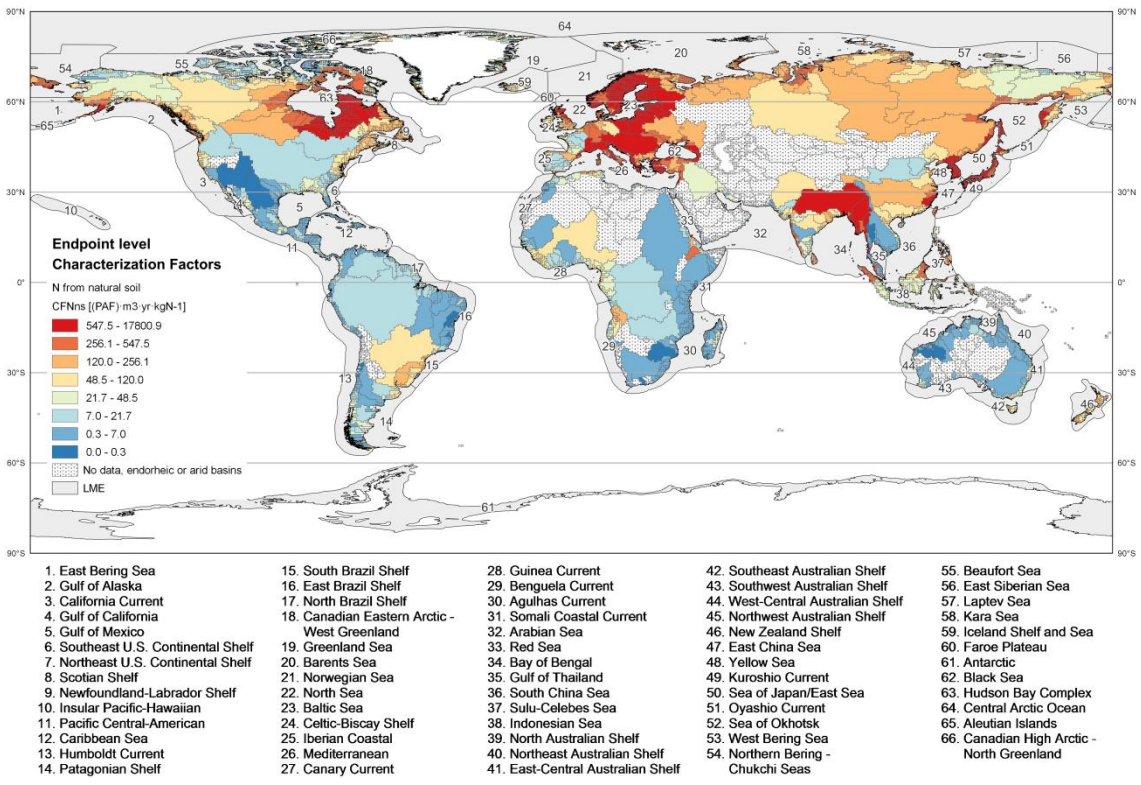

Fig. S.1 Global distribution of the marine eutrophication endpoint characterization factors (CF_{Nns}, [(PAF)·m^3·yr·kgN^{-1}]) for emissions from natural soil at a river basin scale. Note the non-linear scale

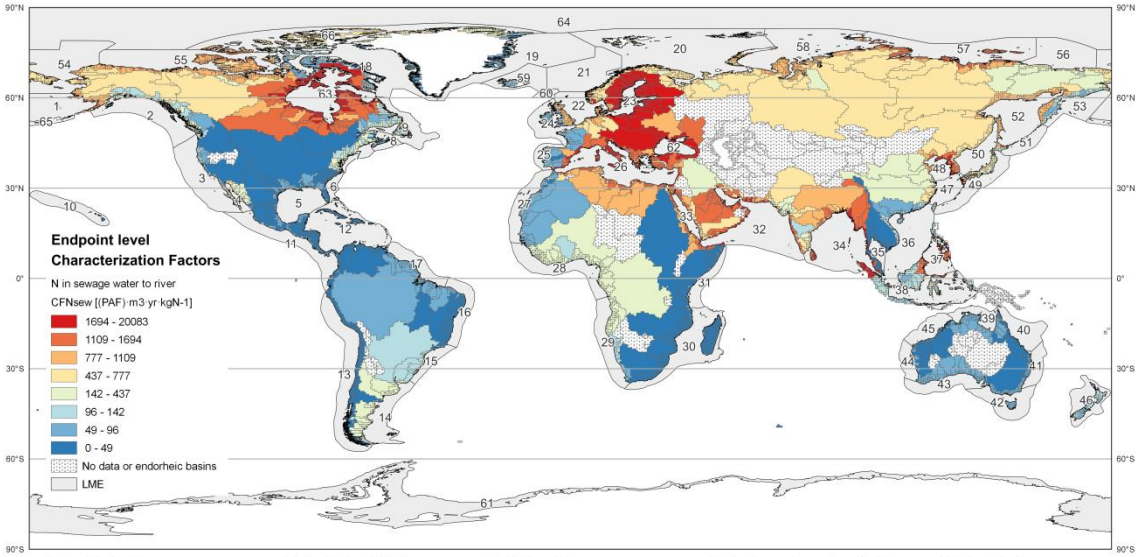

1. East Bering Sea
2. Gulf of Alaska
3. California Current
4. Gulf of California
5. Gulf of Mexico
6. Southeast U.S. Continental Shelf
7. Northeast U.S. Continental Shelf
8. Scotian Shelf
9. Newfoundland-Labrador Shelf
10. Insular Pacific-Hawaiian
11. Pacific Central-American
12. Caribbean Sea
13. Humboldt Current
14. Patagonian Shelf
15. South Brazil Shelf
16. East Brazil Shelf
17. North Brazil Shelf
18. Canadian Eastern Arctic - West Greenland
19. Greenland Sea
20. Barents Sea
21. Norwegian Sea
22. North Sea
23. Baltic Sea
24. Celtic-Biscay Shelf
25. Iberian Coastal
26. Mediterranean
27. Canary Current
28. Guinea Current
29. Benguela Current
30. Agulhas Current
31. Somali Coastal Current
32. Arabian Sea
33. Red Sea
34. Bay of Bengal
35. Gulf of Thailand
36. South China Sea
37. Sulu-Celebes Sea
38. Indonesian Sea
39. North Australian Shelf
40. Northeast Australian Shelf
41. East-Central Australian Shelf
42. Southeast Australian Shelf
43. Southwest Australian Shelf
44. West-Central Australian Shelf
45. Northwest Australian Shelf
46. New Zealand Shelf
47. East China Sea
48. Yellow Sea
49. Kuroshio Current
50. Sea of Japan/East Sea
51. Oyashio Current
52. Sea of Okhotsk
53. West Bering Sea
54. Northern Bering - Chukchi Seas
55. Beaufort Sea
56. East Siberian Sea
57. Laptev Sea
58. Kara Sea
59. Iceland Shelf and Sea
60. Faroe Plateau
61. Antarctic
62. Black Sea
63. Hudson Bay Complex
64. Central Arctic Ocean
65. Aleutian Islands
66. Canadian High Arctic - North Greenland

Fig. S.2 Global distribution of the marine eutrophication endpoint characterization factors (CF_{Nsew}, $[(PAF)\cdot m^3\cdot yr\cdot kgN^{-1}]$) for emissions of nitrogen in sewage water at a river basin scale. Note the non-linear scale

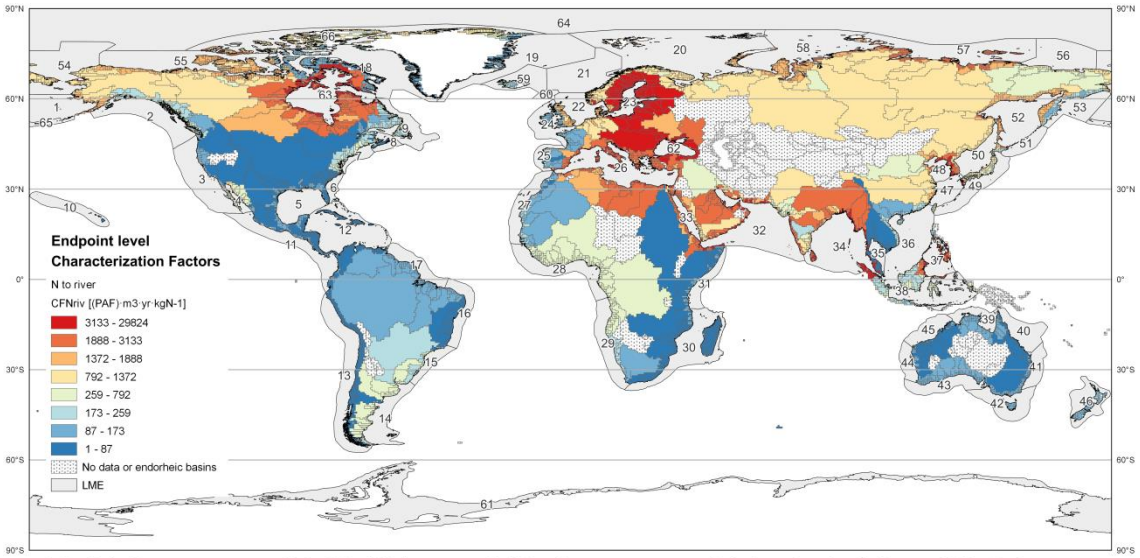

1. East Bering Sea
2. Gulf of Alaska
3. California Current
4. Gulf of California
5. Gulf of Mexico
6. Southeast U.S. Continental Shelf
7. Northeast U.S. Continental Shelf
8. Scotian Shelf
9. Newfoundland-Labrador Shelf
10. Insular Pacific-Hawaiian
11. Pacific Central-American
12. Caribbean Sea
13. Humboldt Current
14. Patagonian Shelf
15. South Brazil Shelf
16. East Brazil Shelf
17. North Brazil Shelf
18. Canadian Eastern Arctic - West Greenland
19. Greenland Sea
20. Barents Sea
21. Norwegian Sea
22. North Sea
23. Baltic Sea
24. Celtic-Biscay Shelf
25. Iberian Coastal
26. Mediterranean
27. Canary Current
28. Guinea Current
29. Benguela Current
30. Agulhas Current
31. Somali Coastal Current
32. Arabian Sea
33. Red Sea
34. Bay of Bengal
35. Gulf of Thailand
36. South China Sea
37. Sulu-Celebes Sea
38. Indonesian Sea
39. North Australian Shelf
40. Northeast Australian Shelf
41. East-Central Australian Shelf
42. Southeast Australian Shelf
43. Southwest Australian Shelf
44. West-Central Australian Shelf
45. Northwest Australian Shelf
46. New Zealand Shelf
47. East China Sea
48. Yellow Sea
49. Kuroshio Current
50. Sea of Japan/East Sea
51. Oyashio Current
52. Sea of Okhotsk
53. West Bering Sea
54. Northern Bering - Chukchi Seas
55. Beaufort Sea
56. East Siberian Sea
57. Laptev Sea
58. Kara Sea
59. Iceland Shelf and Sea
60. Faroe Plateau
61. Antarctic
62. Black Sea
63. Hudson Bay Complex
64. Central Arctic Ocean
65. Aleutian Islands
66. Canadian High Arctic - North Greenland

Fig. S.3 Global distribution of the marine eutrophication endpoint characterization factors (CF_{Nriv}, $[(PAF)\cdot m^3\cdot yr\cdot kgN^{-1}]$) for emissions of nitrogen to river at a river basin scale. Note the non-linear scale

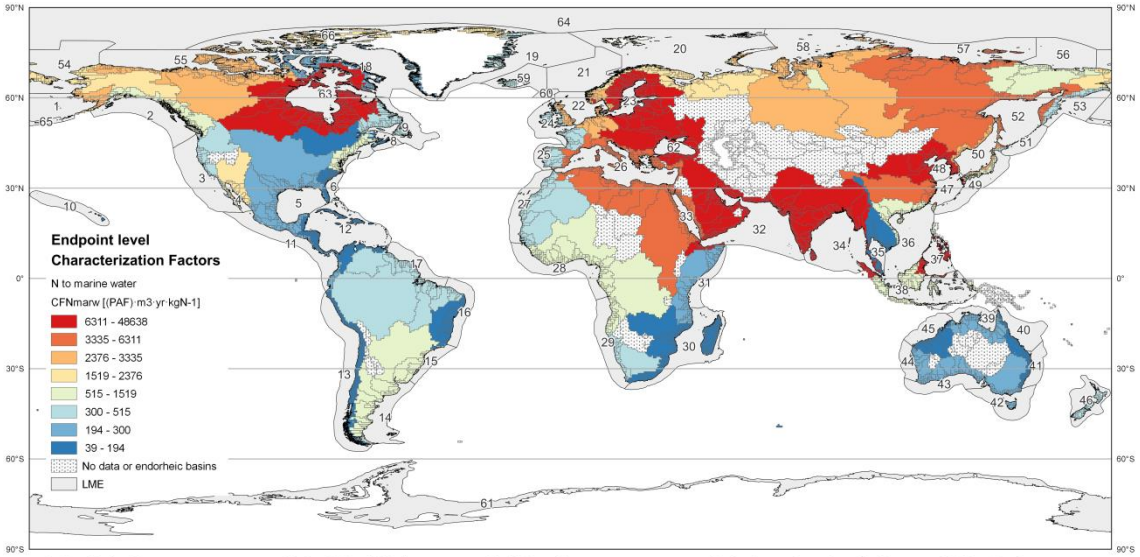

1. East Bering Sea
2. Gulf of Alaska
3. California Current
4. Gulf of California
5. Gulf of Mexico
6. Southeast U.S. Continental Shelf
7. Northeast U.S. Continental Shelf
8. Scotian Shelf
9. Newfoundland-Labrador Shelf
10. Insular Pacific-Hawaiian
11. Pacific Central-American
12. Caribbean Sea
13. Humboldt Current
14. Patagonian Shelf
15. South Brazil Shelf
16. East Brazil Shelf
17. North Brazil Shelf
18. Canadian Eastern Arctic - West Greenland
19. Greenland Sea
20. Barents Sea
21. Norwegian Sea
22. North Sea
23. Baltic Sea
24. Celtic-Biscay Shelf
25. Iberian Coastal
26. Mediterranean
27. Canary Current
28. Guinea Current
29. Benguela Current
30. Agulhas Current
31. Somali Coastal Current
32. Arabian Sea
33. Red Sea
34. Bay of Bengal
35. Gulf of Thailand
36. South China Sea
37. Sulu-Celebes Sea
38. Indonesian Sea
39. North Australian Shelf
40. Northeast Australian Shelf
41. East-Central Australian Shelf
42. Southeast Australian Shelf
43. Southwest Australian Shelf
44. West-Central Australian Shelf
45. Northwest Australian Shelf
46. New Zealand Shelf
47. East China Sea
48. Yellow Sea
49. Kuroshio Current
50. Sea of Japan/East Sea
51. Oyashio Current
52. Sea of Okhotsk
53. West Bering Sea
54. Northern Bering - Chukchi Seas
55. Beaufort Sea
56. East Siberian Sea
57. Laptev Sea
58. Kara Sea
59. Iceland Shelf and Sea
60. Faroe Plateau
61. Antarctic
62. Black Sea
63. Hudson Bay Complex
64. Central Arctic Ocean
65. Aleutian Islands
66. Canadian High Arctic - North Greenland

Fig. S.4 Global distribution of the marine eutrophication endpoint characterization factors (CF_{Nmarw}, [(PAF)·m^3·yr·kgN^{-1}]) for direct emissions of nitrogen to marine water a river basin scale. Note the non-linear scale

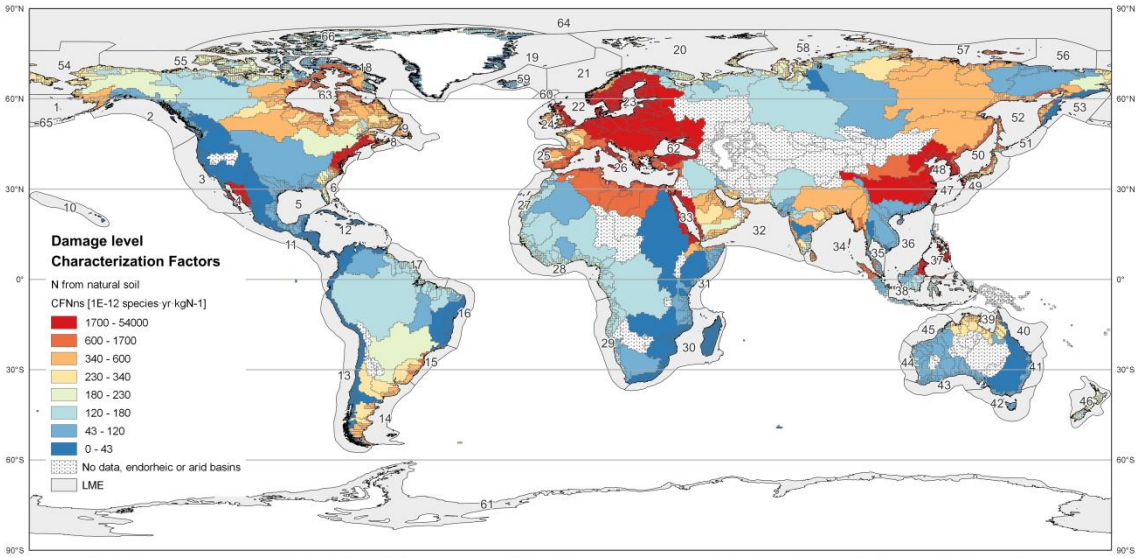

1. East Bering Sea
2. Gulf of Alaska
3. California Current
4. Gulf of California
5. Gulf of Mexico
6. Southeast U.S. Continental Shelf
7. Northeast U.S. Continental Shelf
8. Scotian Shelf
9. Newfoundland-Labrador Shelf
10. Insular Pacific-Hawaiian
11. Pacific Central-American
12. Caribbean Sea
13. Humboldt Current
14. Patagonian Shelf
15. South Brazil Shelf
16. East Brazil Shelf
17. North Brazil Shelf
18. Canadian Eastern Arctic - West Greenland
19. Greenland Sea
20. Barents Sea
21. Norwegian Sea
22. North Sea
23. Baltic Sea
24. Celtic-Biscay Shelf
25. Iberian Coastal
26. Mediterranean
27. Canary Current
28. Guinea Current
29. Benguela Current
30. Agulhas Current
31. Somali Coastal Current
32. Arabian Sea
33. Red Sea
34. Bay of Bengal
35. Gulf of Thailand
36. South China Sea
37. Sulu-Celebes Sea
38. Indonesian Sea
39. North Australian Shelf
40. Northeast Australian Shelf
41. East-Central Australian Shelf
42. Southeast Australian Shelf
43. Southwest Australian Shelf
44. West-Central Australian Shelf
45. Northwest Australian Shelf
46. New Zealand Shelf
47. East China Sea
48. Yellow Sea
49. Kuroshio Current
50. Sea of Japan/East Sea
51. Oyashio Current
52. Sea of Okhotsk
53. West Bering Sea
54. Northern Bering - Chukchi Seas
55. Beaufort Sea
56. East Siberian Sea
57. Laptev Sea
58. Kara Sea
59. Iceland Shelf and Sea
60. Faroe Plateau
61. Antarctic
62. Black Sea
63. Hudson Bay Complex
64. Central Arctic Ocean
65. Aleutian Islands
66. Canadian High Arctic - North Greenland

Fig. S.5 Global distribution of the marine eutrophication damage characterization factors (CF_{Nns}, [species·yr·kgN^{-1}]) for emissions from natural soil at a river basin scale. Note the non-linear scale

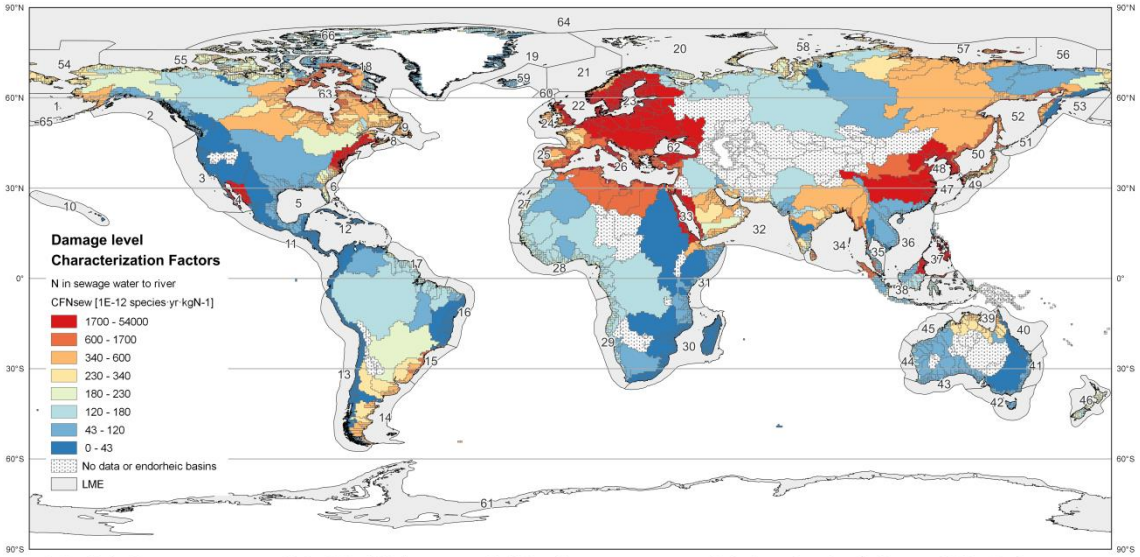

1. East Bering Sea
2. Gulf of Alaska
3. California Current
4. Gulf of California
5. Gulf of Mexico
6. Southeast U.S. Continental Shelf
7. Northeast U.S. Continental Shelf
8. Scotian Shelf
9. Newfoundland-Labrador Shelf
10. Insular Pacific-Hawaiian
11. Pacific Central-American
12. Caribbean Sea
13. Humboldt Current
14. Patagonian Shelf
15. South Brazil Shelf
16. East Brazil Shelf
17. North Brazil Shelf
18. Canadian Eastern Arctic - West Greenland
19. Greenland Sea
20. Barents Sea
21. Norwegian Sea
22. North Sea
23. Baltic Sea
24. Celtic-Biscay Shelf
25. Iberian Coastal
26. Mediterranean
27. Canary Current
28. Guinea Current
29. Benguela Current
30. Agulhas Current
31. Somali Coastal Current
32. Arabian Sea
33. Red Sea
34. Bay of Bengal
35. Gulf of Thailand
36. South China Sea
37. Sulu-Celebes Sea
38. Indonesian Sea
39. North Australian Shelf
40. Northeast Australian Shelf
41. East-Central Australian Shelf
42. Southeast Australian Shelf
43. Southwest Australian Shelf
44. West-Central Australian Shelf
45. Northwest Australian Shelf
46. New Zealand Shelf
47. East China Sea
48. Yellow Sea
49. Kuroshio Current
50. Sea of Japan/East Sea
51. Oyashio Current
52. Sea of Okhotsk
53. West Bering Sea
54. Northern Bering - Chukchi Seas
55. Beaufort Sea
56. East Siberian Sea
57. Laptev Sea
58. Kara Sea
59. Iceland Shelf and Sea
60. Faroe Plateau
61. Antarctic
62. Black Sea
63. Hudson Bay Complex
64. Central Arctic Ocean
65. Aleutian Islands
66. Canadian High Arctic - North Greenland

Fig. S.6 Global distribution of the marine eutrophication damage characterization factors (CF_{Nsew}, [species·yr·kgN^{-1}]) for emissions of nitrogen in sewage water at a river basin scale. Note the non-linear scale

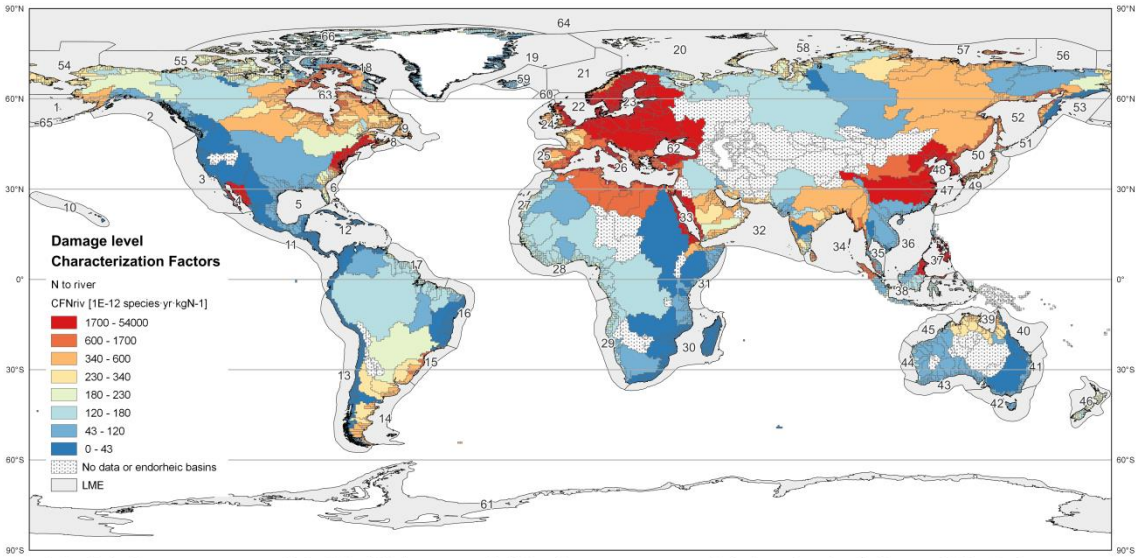

1. East Bering Sea
2. Gulf of Alaska
3. California Current
4. Gulf of California
5. Gulf of Mexico
6. Southeast U.S. Continental Shelf
7. Northeast U.S. Continental Shelf
8. Scotian Shelf
9. Newfoundland-Labrador Shelf
10. Insular Pacific-Hawaiian
11. Pacific Central-American
12. Caribbean Sea
13. Humboldt Current
14. Patagonian Shelf
15. South Brazil Shelf
16. East Brazil Shelf
17. North Brazil Shelf
18. Canadian Eastern Arctic - West Greenland
19. Greenland Sea
20. Barents Sea
21. Norwegian Sea
22. North Sea
23. Baltic Sea
24. Celtic-Biscay Shelf
25. Iberian Coastal
26. Mediterranean
27. Canary Current
28. Guinea Current
29. Benguela Current
30. Agulhas Current
31. Somali Coastal Current
32. Arabian Sea
33. Red Sea
34. Bay of Bengal
35. Gulf of Thailand
36. South China Sea
37. Sulu-Celebes Sea
38. Indonesian Sea
39. North Australian Shelf
40. Northeast Australian Shelf
41. East-Central Australian Shelf
42. Southeast Australian Shelf
43. Southwest Australian Shelf
44. West-Central Australian Shelf
45. Northwest Australian Shelf
46. New Zealand Shelf
47. East China Sea
48. Yellow Sea
49. Kuroshio Current
50. Sea of Japan/East Sea
51. Oyashio Current
52. Sea of Okhotsk
53. West Bering Sea
54. Northern Bering - Chukchi Seas
55. Beaufort Sea
56. East Siberian Sea
57. Laptev Sea
58. Kara Sea
59. Iceland Shelf and Sea
60. Faroe Plateau
61. Antarctic
62. Black Sea
63. Hudson Bay Complex
64. Central Arctic Ocean
65. Aleutian Islands
66. Canadian High Arctic - North Greenland

Fig. S.7 Global distribution of the marine eutrophication damage characterization factors (CF_{Nriv}, [species·yr·kgN^{-1}]) for emissions of nitrogen to river at a river basin scale. Note the non-linear scale

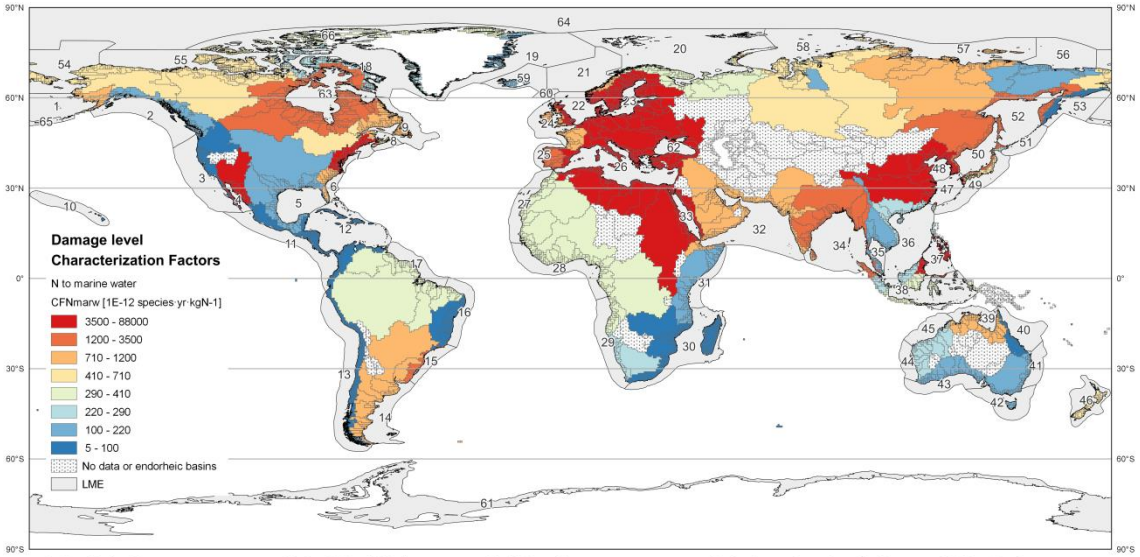

1. East Bering Sea
2. Gulf of Alaska
3. California Current
4. Gulf of California
5. Gulf of Mexico
6. Southeast U.S. Continental Shelf
7. Northeast U.S. Continental Shelf
8. Scotian Shelf
9. Newfoundland-Labrador Shelf
10. Insular Pacific-Hawaiian
11. Pacific Central-American
12. Caribbean Sea
13. Humboldt Current
14. Patagonian Shelf
15. South Brazil Shelf
16. East Brazil Shelf
17. North Brazil Shelf
18. Canadian Eastern Arctic - West Greenland
19. Greenland Sea
20. Barents Sea
21. Norwegian Sea
22. North Sea
23. Baltic Sea
24. Celtic-Biscay Shelf
25. Iberian Coastal
26. Mediterranean
27. Canary Current
28. Guinea Current
29. Benguela Current
30. Agulhas Current
31. Somali Coastal Current
32. Arabian Sea
33. Red Sea
34. Bay of Bengal
35. Gulf of Thailand
36. South China Sea
37. Sulu-Celebes Sea
38. Indonesian Sea
39. North Australian Shelf
40. Northeast Australian Shelf
41. East-Central Australian Shelf
42. Southeast Australian Shelf
43. Southwest Australian Shelf
44. West-Central Australian Shelf
45. Northwest Australian Shelf
46. New Zealand Shelf
47. East China Sea
48. Yellow Sea
49. Kuroshio Current
50. Sea of Japan/East Sea
51. Oyashio Current
52. Sea of Okhotsk
53. West Bering Sea
54. Northern Bering - Chukchi Seas
55. Beaufort Sea
56. East Siberian Sea
57. Laptev Sea
58. Kara Sea
59. Iceland Shelf and Sea
60. Faroe Plateau
61. Antarctic
62. Black Sea
63. Hudson Bay Complex
64. Central Arctic Ocean
65. Aleutian Islands
66. Canadian High Arctic - North Greenland

Fig. S.8 Global distribution of the marine eutrophication damage characterization factors (CF_{Nmarw}, [species·yr·kgN^{-1}]) for emissions of nitrogen to marine water at a river basin scale. Note the non-linear scale

References

Cosme N, Hauschild MZ (2016) Effect factors for marine eutrophication in LCIA based on species sensitivity to hypoxia. Ecol Indic 69:453–462. doi: 10.1016/j.ecolind.2016.04.006

Cosme N, Jones MC, Cheung WWL, Larsen HF (2016a) Spatial differentiation of marine eutrophication damage indicators based on species density. Ecol Indic submitted.

Cosme N, Koski M, Hauschild MZ (2015) Exposure factors for marine eutrophication impacts assessment based on a mechanistic biological model. Ecol Modell 317:50–63. doi: 10.1016/j.ecolmodel.2015.09.005

Cosme N, Mayorga E, Hauschild MZ (2016b) Spatially explicit fate factors for waterbone nitrogen emissions at the global scale. Int J Life Cycle Assesment submitted.

Mayorga E, Seitzinger SP, Harrison JA, et al (2010) Global Nutrient Export from WaterSheds 2 (NEWS 2): Model development and implementation. Environ Model Softw 25:837–853. doi: 10.1016/j.envsoft.2010.01.007

Cosme N, Hauschild MZ. 2016. Characterization of waterborne nitrogen emissions for marine eutrophication modelling in life cycle impact assessment at the damage level and global scale (E.S. Mat. 2) *International Journal of Life Cycle Assessment*, submitted

Article V – Electronic Supplementary Material 2

Article title:

Characterization of waterborne nitrogen emissions for marine eutrophication modelling in life cycle impact assessment at the damage level and global scale

Journal:

International Journal of Lice Cycle Assessment

Authors:

Nuno Cosme, Michael Z. Hauschild

Affiliation:

Division for Quantitative Sustainability Assessment, Department of Management Engineering, Technical University of Denmark, Produktionstorvet 424, DK-2800 Kgs. Lyngby, Denmark

Corresponding author:

Nuno Cosme, nmdc@dtu.dk

Contents:

Table S.1 Fate factors (FF, [yr]) for waterborne nitrogen (N) emissions per emission route: N from natural soils (FFNns), N from agricultural soils (FFNas), N in sewage discharges to river (FFNsew), N to river (FFNriv), and direct N emissions to coastal marine waters (FFNmarw). Results for 5,772 river basins. 'BASINID' represents the basin identifier used in STN-30p 6.01 and 'basincellcnt' the number of 0.5° grid cells contained by the basin. Retrieved from Cosme N, Mayorga E, Hauschild MZ. Spatially explicit fate factors of waterborne nitrogen emissions at the global scale. International Journal of Life Cycle Assessment. Submitted 2016. *Available online for 5.772 river basins of the world*

BASINID	basinname	basincellcnt	FF_{Nns} [yr]	FF_{Nas} [yr]	FF_{Nsew} [yr]	FF_{Nriv} [yr]	FF_{Nmarw} [yr]
1	Amazon	1916	0.006	0.054	0.034	0.067	0.191
2	Nile	1283	0.001	0.001	0.003	0.006	6.161
3	Zaire	1203	0.015	0.143	0.153	0.316	0.963
4	Mississippi	1371	0.008	0.008	0.032	0.048	0.160
5	Ob	1786	0.073	0.073	0.430	0.795	2.326
6	Parana	939	0.018	0.018	0.044	0.087	0.365
7	Yenisei	1627	0.092	0.092	0.325	0.593	2.326
8	Lena	1651	0.088	0.088	0.442	0.801	2.326
9	Niger	749	0.048	0.048	0.149	0.306	0.963
10	Tamanrasett	651	n/a	n/a	0.027	0.054	0.191
11	Chang Jiang	672	0.124	0.124	0.218	0.422	1.766
12	Amur	881	0.067	0.067	0.245	0.456	1.378
13	Mackenzie	1127	0.087	0.087	0.492	0.775	2.326
14	Ganges	592	1.032	1.032	0.909	1.759	7.289
17	Zambezi	457	0.006	0.006	0.012	0.024	0.076
20	Indus	434	0.050	0.050	0.330	0.639	4.137
21	Nelson	592	0.138	0.138	0.749	1.174	4.196
24	Saint Lawrence	487	0.007	0.007	0.011	0.017	0.053
25	Orinoco	338	0.007	0.060	0.030	0.060	0.191
26	Murray	393	4.26E-04	4.26E-04	0.011	0.019	0.191
27	Shatt el Arab	386	0.027	0.027	0.276	0.503	4.137
28	Orange	344	3.19E-04	3.19E-04	0.019	0.038	0.191
29	Huang He	361	0.005	0.005	0.062	0.120	2.481
30	Yukon	644	0.038	0.038	0.523	0.810	2.326
31	Senegal	287	0.003	0.003	0.028	0.058	0.191
32	Irharhar	318	n/a	n/a	0.917	1.829	6.161
33	Jubba	265	0.004	0.004	0.032	0.065	0.191
34	Colorado (Ari)	325	2.86E-05	2.86E-05	0.001	0.001	1.051
35	Rio Grande (US)	301	4.92E-06	4.92E-06	2.61E-04	4.49E-04	0.160
36	Danube	370	0.393	0.393	0.913	1.573	4.665
37	Tocantins	254	0.004	0.036	0.030	0.059	0.191
38	Mekong	261	0.001	0.005	0.005	0.010	0.030
40	Columbia	341	0.012	0.012	0.028	0.044	0.191

Table S.5 Endpoint characterisation factors (CF, [(PAF)·m^3·yr·kgN^{-1}]) for waterborne nitrogen (N) emissions per emission route: N from natural soils (CF_{Nns}), N from agricultural soils (CF_{Nas}), N in sewage discharges to river (CF_{Nsew}), N to river (CF_{Nriv}), and direct N emissions to coastal marine waters (CF_{Nmarw}). Results for 5,772 river basins. 'BASINID' represents the basin identifier used in STN-30p 6.01 and 'basincellcnt' the number of 0.5° grid cells contained by the basin. *Available online for 5.772 river basins of the world.*

BASINID	basinname	basincell cnt	ep CF_{Nns}	ep CF_{Nas}	ep CF_{Nsew}	ep CF_{Nriv}	ep CF_{Nmarw}
			(PAF)·m^3·yr·kgN^{-1}				
1	Amazon	1916	9.2	86.8	54.7	107.5	307.2
2	Nile	1283	0.7	0.7	2.8	5.6	5912.8
3	Zaire	1203	18.0	169.1	181.2	373.2	1138.8
4	Mississippi	1371	11.1	11.1	43.3	66.4	219.8
5	Ob	1786	98.7	98.7	583.3	1078.2	3155.8
6	Parana	939	51.3	51.3	123.7	242.0	1015.5
7	Yenisei	1627	124.7	124.7	440.8	804.5	3155.8
8	Lena	1651	144.6	144.6	727.8	1317.1	3826.6
9	Niger	749	56.6	56.6	176.0	362.0	1138.8
10	Tamanrasett	651	n/a	n/a	57.3	115.6	405.3
11	Chang Jiang	672	244.0	244.0	429.5	831.0	3481.0
12	Amur	881	161.3	161.3	593.1	1104.8	3335.2
13	Mackenzie	1127	111.1	111.1	630.4	992.6	2979.9
14	Ganges	592	1170.7	1170.7	1031.6	1996.0	8272.0
17	Zambezi	457	9.3	9.3	17.2	34.7	110.2
20	Indus	434	77.0	77.0	503.4	974.0	6310.6
21	Nelson	592	209.6	209.6	1137.7	1784.6	6375.8
24	Saint Lawrence	487	20.2	20.2	29.7	46.2	149.2
25	Orinoco	338	10.8	96.2	48.3	96.2	307.2
26	Murray	393	0.6	0.6	16.8	29.3	287.7
27	Shatt el Arab	386	40.8	40.8	420.7	767.6	6310.6
28	Orange	344	0.8	0.8	46.7	93.8	476.8
29	Huang He	361	15.5	15.5	207.6	401.7	8293.0
30	Yukon	644	37.6	37.6	521.5	807.8	2319.5
31	Senegal	287	6.6	6.6	60.0	123.7	405.3
32	Irharhar	318	n/a	n/a	880.0	1755.6	5912.8
33	Jubba	265	4.0	4.0	32.8	66.8	196.1
34	Colorado (Ari)	325	0.1	0.1	1.4	2.2	2298.8
35	Rio Grande (US)	301	0.0	0.0	0.4	0.6	219.8
36	Danube	370	965.2	965.2	2240.8	3861.2	11450.6
37	Tocantins	254	6.2	58.2	48.3	94.9	307.2
38	Mekong	261	0.7	6.6	6.1	12.4	38.7
40	Columbia	341	19.6	19.6	48.2	74.2	323.5

Table S.6 Damage characterisation factors (CF, [species·yr·kgN^{-1}]) for waterborne nitrogen (N) emissions per emission route: N from natural soils (CF_{Nns}), N from agricultural soils (CF_{Nas}), N in sewage discharges to river (CF_{Nsew}), N to river (CF_{Nriv}), and direct N emissions to coastal marine waters (CF_{Nmarw}). Results for 5,772 river basins. 'BASINID' represents the basin identifier used in STN-30p 6.01 and 'basincellcnt' the number of 0.5° grid cells contained by the basin. *Available online for 5.772 river basins of the world.*

BASINID	basinname	basincell cnt	damCF$_{Nns}$	damCF$_{Nas}$	damCF$_{Nsew}$	damCF$_{Nriv}$	damCF$_{Nmarw}$
			species·yr·kgN^{-1}				
1	Amazon	1916	1.08E-11	1.02E-10	6.39E-11	1.26E-10	3.59E-10
2	Nile	1283	4.12E-13	4.12E-13	1.62E-12	3.30E-12	3.45E-09
3	Zaire	1203	5.97E-12	5.61E-11	6.01E-11	1.24E-10	3.78E-10
4	Mississippi	1371	9.20E-12	9.20E-12	3.59E-11	5.51E-11	1.83E-10
5	Ob	1786	1.40E-11	1.40E-11	8.27E-11	1.53E-10	4.47E-10
6	Parana	939	4.27E-11	4.27E-11	1.03E-10	2.01E-10	8.45E-10
7	Yenisei	1627	1.77E-11	1.77E-11	6.25E-11	1.14E-10	4.47E-10
8	Lena	1651	3.74E-11	3.74E-11	1.88E-10	3.41E-10	9.89E-10
9	Niger	749	1.88E-11	1.88E-11	5.84E-11	1.20E-10	3.78E-10
10	Tamanrasett	651	n/a	n/a	5.66E-11	1.14E-10	4.00E-10
11	Chang Jiang	672	6.84E-10	6.84E-10	1.20E-09	2.33E-09	9.75E-09
12	Amur	881	5.68E-11	5.68E-11	2.09E-10	3.89E-10	1.17E-09
13	Mackenzie	1127	1.53E-11	1.53E-11	8.69E-11	1.37E-10	4.11E-10
14	Ganges	592	2.28E-10	2.28E-10	2.01E-10	3.89E-10	1.61E-09
17	Zambezi	457	2.07E-12	2.07E-12	3.81E-12	7.69E-12	2.44E-11
20	Indus	434	1.26E-11	1.26E-11	8.26E-11	1.60E-10	1.04E-09
21	Nelson	592	4.37E-11	4.37E-11	2.37E-10	3.72E-10	1.33E-09
24	Saint Lawrence	487	9.26E-11	9.26E-11	1.36E-10	2.12E-10	6.84E-10
25	Orinoco	338	1.27E-11	1.13E-10	5.65E-11	1.13E-10	3.59E-10
26	Murray	393	2.35E-13	2.35E-13	6.17E-12	1.07E-11	1.05E-10
27	Shatt el Arab	386	6.69E-12	6.69E-12	6.90E-11	1.26E-10	1.04E-09
28	Orange	344	4.43E-13	4.43E-13	2.60E-11	5.23E-11	2.66E-10
29	Huang He	361	5.35E-11	5.35E-11	7.15E-10	1.38E-09	2.85E-08
30	Yukon	644	8.87E-12	8.87E-12	1.23E-10	1.91E-10	5.47E-10
31	Senegal	287	6.54E-12	6.54E-12	5.92E-11	1.22E-10	4.00E-10
32	Irharhar	318	n/a	n/a	5.14E-10	1.03E-09	3.45E-09
33	Jubba	265	2.56E-12	2.56E-12	2.11E-11	4.29E-11	1.26E-10
34	Colorado (Ari)	325	3.93E-13	3.93E-13	8.99E-12	1.38E-11	1.44E-08
35	Rio Grande (US)	301	5.60E-15	5.60E-15	2.97E-13	5.11E-13	1.83E-10
36	Danube	370	1.25E-09	1.25E-09	2.91E-09	5.01E-09	1.48E-08
37	Tocantins	254	7.24E-12	6.81E-11	5.65E-11	1.11E-10	3.59E-10
38	Mekong	261	3.76E-12	3.54E-11	3.28E-11	6.67E-11	2.08E-10
40	Columbia	341	2.27E-12	2.27E-12	5.60E-12	8.62E-12	3.76E-11

Article VI

Modelling the influence of changing climate in present and future marine eutrophication impacts from spring barley production

Cosme, N. & Niero, M.

submitted to *Journal of Cleaner Production* in 2016

Reviewed (manuscript in pre-print version R1)

Modelling the influence of changing climate in present and future marine eutrophication impacts from spring barley production

Nuno Cosme* and Monia Niero*

Division for Quantitative Sustainability Assessment, Department of Management Engineering, Technical University of Denmark, Produktionstorvet 424, 2800 Kgs. Lyngby – Denmark

*Corresponding authors.

E-mail addresses: nmdc@dtu.dk (N. Cosme), monni@dtu.dk (M. Niero)

Abstract

Nitrate concentration and runoff are site-specific and driven by climatic factors and crop management. As such, nitrate emissions may increase in the future due to climate change, affecting the marine eutrophication mechanism. In this context, and considering the case of spring barley production in Denmark, the paper has two objectives: (i) to estimate the present and future marine eutrophication impacts by combining a novel Life Cycle Impact Assessment (LCIA) modelling approach with a quantification of the effects of climate change on its parameterisation, and (ii) to discuss the implications of different normalisation references when comparing future Life Cycle Assessment (LCA) scenarios with current production systems. A parameterised characterisation model was developed to gauge the influence of future climatic-driven pressures on the marine eutrophication impact pathway. Spatial differentiation was added to the resulting 'present' and 'future' characterisation factors (CFs) and calculated for the Baltic and North Sea. The temporal variability of both midpoint normalised impact scores and damage scores reflect a 34% and 28% increase of the CFs in the North Sea and Baltic Sea, respectively. The temporal variability is mostly explained by CF variation and increasing future nitrogen flows. The marine eutrophication indicator scores at both midpoint and damage levels suggest that the differentiation of impacts to various receiving (and potentially perturbed) ecosystems is relevant. Damage scores are quantified with a factor 2.5 and 2.3 differentiation between the Baltic (higher) and North Seas (lower) for the present and future scenarios, respectively. The comparison of the normalisation methods, either based on total annual impacts (domestic inventory of background interventions), on ecological carrying capacity, or on the presently proposed method, point to the value of adding spatial differentiation to LCIA models. The inclusion of time variation and spatial differentiation in characterisation modelling of marine eutrophication and the identification of a paucity of adequate inventory data for future scenario analysis constitute the main outcomes of this study. Further research

should aim at reducing the uncertainty of the parameterisation under future conditions and strengthening emissions projections.

Keywords

Life Cycle Assessment; LCIA; Damage modelling; Normalisation; Marine ecosystems; Climate change.

1. Introduction

Conserving and sustainably using the oceans, seas and marine resources, taking urgent action to mitigate and adapt to climate change, and achieving food security whilst improving nutrition are three of the 17 Global Goals 2030 Agenda for Sustainable Development Global Goals (UN General Assembly, 2015). Global food security and environmental sustainability are interlinked, whereby the former only becomes possible if agricultural systems meet certain sustainability criteria (Foley et al., 2011). Life Cycle Assessment (LCA) is one method to holistically assess whether agricultural systems are meeting the necessary benchmarks. The use of LCA to assess the potential environmental impacts of agricultural systems is growing (Soussana, 2014), and guidance on tailoring LCAs for crops has recently been published, with regard to the agri-food sector (Notarnicola et al., 2015). Agriculture and energy production are the main sources of environmental emissions of reactive nitrogen (N) (Galloway et al., 2008). The application of fertilizers in agriculture introduces ammonium (NH_4^+) and nitrate (NO_3^-) to soil and water, and ammonia (NH_3) to air, whereas the combustion of fossil fuels adds nitrogen oxides (NO_x) to air (Socolow, 1999). In agriculture practices, N added to the soil may exceed plant assimilation. This surplus emitted to the environment may constitute the main cause for anthropogenic fertilization of freshwater and marine ecosystems that lead to deleterious aquatic eutrophication.

Marine eutrophication is a syndrome of ecosystem responses to the increase of the availability of growth-limiting plant nutrients in the euphotic zone of marine waters (Cloern, 2001; Cloern et al., 2016; Nixon, 1995; Smith et al., 1999). For modelling purposes, nitrogen is assumed to be the growth-limiting nutrient in marine waters, considering representative average spatial and temporal conditions (see also Vitousek et al. (2002); Howarth and Marino (2006); Cosme et al. (2015)). Such N-enrichment promotes planktonic growth and often involves depletion of dissolved oxygen (DO) in bottom waters to hypoxic and anoxic levels, potentially affecting exposed species (e.g. Gray et al., (2002); Levin et al., (2009), Vaquer-Sunyer and Duarte, (2008)). Impacts of eutrophication-induced hypoxia are seen from the local to regional scales (Breitburg et al., 2009). Similarly, variability at short time scales (e.g. seasonal) can have a significant role in impacts modelling, e.g. latitude and light availability, temperature and

species distribution, water stratification and oxygen depletion. Current research of Life Cycle Impact Assessment (LCIA) methods for marine eutrophication is being directed to improve the representation of short term variability and spatial differentiation – see e.g. Azevedo et al. (2013); Cosme and Hauschild (2016a, 2016b); Cosme et al. (2016a, 2016b, 2015). Parameterisation of future pressures in those methods for impact forecasting is naturally absent. To the knowledge of the authors no other studies addressing the effects of time variation and future environmental conditions on marine eutrophication in LCA exist.

Nitrate concentration and runoff are site-specific and driven by climatic factors and crop management, as shown for organic cereal cropping systems in Denmark (Jabloun et al., 2015). As a consequence of the expected increase in temperature and changed rainfall pattern, N runoff may increase in the future (Doltra et al., 2012; Jensen and Veihe, 2009). However, to what extent N and water management can close the yield gaps is still uncertain (Mueller et al., 2012). Therefore the definition of future scenarios for agricultural systems is not straightforward.

In the LCA framework, future-oriented scenarios for crop production have so far mainly focused on comparing different GHG mitigation options of both crops and livestock production on farms in northern Europe and USA (Audsley and Wilkinson, 2014), wheat in the UK (Röder et al., 2014), as well as to compare different adaptation strategies, e.g. for wheat in Switzerland (Tendall and Gaillard, 2015) and UK (El Chami and Daccache, 2015), and for barley in Denmark (Dijkman et al., 2013; Niero et al., 2015b). . Guidance to manage uncertainty in the definition of future LCA scenarios addressing the effect of climate change in crop production is provided at the Life Cycle Inventory (LCI) level and implemented in the case of spring barley cultivation in Denmark under a future, realistic, worst-case climate scenario (Niero et al., 2015a). However, the effect of increased temperature and CO_2 concentration will also affect the impact pathway and therefore the LCIA modelling. A similar approach using temporal scenarios (present and future) to address the influence of climate change at the regional scale has been applied for water availability (Nunez et al., 2015).

Marine eutrophication characterisation in LCIA models the variation of an indicator located between the emission and the damage through an impact pathway, e.g. dissolved N concentration increase, as in the ReCiPe (Goedkoop et al., 2012), EDIP 2003 (Hauschild and Potting, 2005), IMPACT 2002+ (Jolliet et al., 2003), and CML 2002 (Guinée et al., 2002) LCIA methods. Marine eutrophication indicators at a later point (closer to the damage) would need a longer modelling work of the environmental mechanisms, but are lacking in the methods above. The inclusion of ecosystem exposure and effects on biota, as done for the ecotoxicity indicator (Rosenbaum et al., 2008), is proposed here for marine eutrophication – see also Cosme and Hauschild (2016b). The impact assessment, at any point, is done by applying substance-specific

characterisation factors (CF) that convert the emissions into a potential impact (Hauschild, 2005).

The characterisation modelling work of the marine eutrophication indicator presented here was developed in the EU FP7 project LC-IMPACT (http://lc-impact.eu/) and was improved with recent developments. It involves the estimation of CFs consistent with the generic impact assessment framework (Udo de Haes et al., 2002) by modelling factors for the environmental fate of emissions, ecosystem exposure to these, and effects on exposed species.

Normalisation in LCA relates the characterised impact indicator scores of an analysed system to those of a reference system (Laurent and Hauschild, 2015). It is an optional step in the characterisation phase and it is useful to understand the relative magnitude of the impact indicator (ISO 14044, 2006). Different normalization references can be applied, with different reference duration of the included activities and boundaries of the reference system, i.e. following either a production-based or a consumption-based perspective. In both cases, the flows from all activities occurring within the physical or geographical boundaries of the reference system over the reference duration need to be quantified, either in terms of the total production activities or total consumption of the reference system, respectively (Laurent and Hauschild, 2015).

Building on the results of an LCA study of spring barley in Denmark (Niero et al., 2015b), this paper estimates the present and future marine eutrophication impacts by combining a novel LCIA approach which includes the influence of climate change using model parameterisation to add both temporal and spatial variation beyond previous attempts. Furthermore, the implications of different normalisation references when comparing future LCA scenarios with current production systems are discussed.

2. Materials and methods

First, the framework to characterise the marine eutrophication impact category is introduced (section 2.1) and the LCI data used to feed the LCIA model are presented (section 2.2). Secondly, the parameterisation in the LCIA under present and future climate conditions is presented, including the implications of climate change on marine eutrophication modelling (section 2.3), as well as the possible adaptations of normalisation procedures in future scenarios definition (section 2.4), and a method to estimate damage factors for marine eutrophication damage modelling (section 2.5).

2.1 DPSIR and impact pathways for marine eutrophication

Environmental indicators have become an important tool in decision-making (Tscherning et al., 2012), often benefiting from conceptual frameworks based on causality (Niemeijer and Groot, 2008). The causal chain framework Drivers-Pressures-

State-Impacts-Responses (DPSIR) (Smeets and Weterings, 1999) is formally an adaptive environmental management approach that integrates environmental and human systems into a common conceptual framework.

The Drivers can be defined as economic and social factors triggering Pressures to the environment (Borja et al., 2006). Applying the DPSIR approach to the marine eutrophication impacts indicator (Figure 1), the primary Drivers arise from the population growth and consequent need for food and energy (Galloway et al., 2008; Zaldívar et al., 2008). The Pressures express the way ecosystems are disturbed by human activities (Borja et al., 2006), and correspond to the N emissions identified in the LCI. The State refers to the ecosystem condition under the Pressures, and can be assessed by field measurements or indicators (Bricker et al., 2008; Ferreira et al., 2011). Impacts are the effects on the ecosystem and society caused by changes in the State, like hypoxia that causes behavioural, physiological, or ecological impacts on biota (e.g. Davis (1975), Diaz and Rosenberg (1995), Gray et al. (2002), Vaquer-Sunyer and Duarte (2008)), or like toxic and harmful algal species, loss of biodiversity, water quality degradation hindering water uses, fish production, or aesthetic value (Kelly, 2008; Rabalais, 2002). The Responses are the management and societal measures aimed at preventing, minimising, or mitigating the Impacts by feeding back to the D-P-S, i.e. modifying the Drivers, reducing Pressures, and restoring the State to 'healthy' conditions.

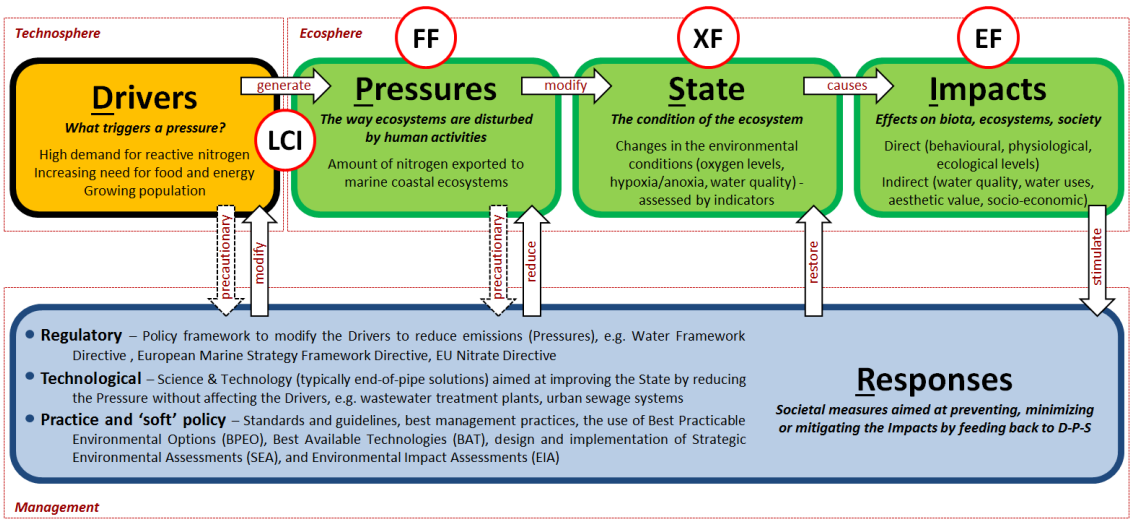

Figure 1 The Drivers-Pressures-State-Impacts-Responses (DPSIR) framework applied to the marine eutrophication indicator in life cycle impact assessment. Indication of the impact assessment modelling components and interface with the DPSIR framework: fate factor (FF), exposure factor (XF) and effect factor (EF) are combined in order to characterise emissions inventoried in the life cycle inventory (LCI) phase.

LCIA indicators focus on the P-S-I components, based respectively on inventoried emissions in LCI, fate (on P) and exposure (on S) modelling work, and the

effects modelling (on I). The LCA framework supports decision-making processes in devising Responses aimed at modifying the Drivers and reducing the Pressures. The conceptual 'management sphere' thus feeds back information and action from the problems in the ecosphere to the solutions in the technosphere, which is the core value of LCA – the characterisation of the interface between techno- and ecosphere.

2.2. Life Cycle Inventory of present and future spring barley cultivation

The details of the scenario describing the present spring barley cultivation in Denmark are reported in Niero et al. (2015b). This scenario, with 'cradle-to-farm gate' boundaries, refers to the average cultivation of 1 kg of dry matter spring barley (*Hordeum vulgare* L.) grain for malting in Denmark (functional unit). The average Danish crop yield in the 5-year interval 2009–2013 was considered (5,700 $kg \cdot ha^{-1}$). For future spring barley cultivation, the data on crop yields produced in the climate phytotron RERAF (Risø Environmental Risk Assessment Facility) were used, where spring barley cultivars were cultivated under controlled and manipulated treatments mimicking a worst case climate change, i.e. double CO_2 concentration (700 ppm) and a global mean temperature increase of 5°C in the atmosphere (Ingvordsen et al., 2015). The measured variation in crop yield depends on the set of cultivars and experimental conditions (Niero et al., 2015b), but it is considered here equal to 4,207 $kg \cdot ha^{-1}$ (26% less than current situation). In the experiments mimicking future climate the amount of fertilizer currently applied was used, therefore the amount of $N \cdot ha^{-1}$ was kept constant for the future scenario, but assuming an increase in nitrate leaching (+24%) (Jensen and Veihe, 2009). The LCI model delivers emissions of NO_3^- to water and NH_3 and NO_x to air calculated per ha of cultivated land and kg yield (Table 1). The calculation of the N emissions described above are based on emission factors model work by Hamelin et al. (2012) (for NO_x and NH_3) and Kristensen et al. (2008) (for NO_3^-) and the N content in fertilizer – see details in Niero et al. (2015b).

Table 1 Summary of emitted quantities of N-derived substances per emission route, in the present and future spring barley production system (based on Niero et al. (2015b)).

Elementary flow	Amount emitted		Unit
	Present scenario	Future scenario	
N in nitrogen oxides (NO_x-N) to air:			
- per area	1.77	1.77	$kg \cdot ha^{-1}$
- per yield	9.88E-05	1.34E-04	$kgN \cdot kg_{barley}^{-1}$
N in ammonia (NH_3-N) to air:			
- per area	7.34	7.34	$kg \cdot ha^{-1}$
- per yield	1.06E-03	1.43E-03	$kgN \cdot kg_{barley}^{-1}$
N in nitrate (NO_3^--N) to water:			
- per area	126	157	$kg \cdot ha^{-1}$
- per yield	4.99E-03	8.43E-04	$kgN \cdot kg_{barley}^{-1}$

2.3. Characterisation factors for marine eutrophication under present and future scenarios

The impact assessment methodology characterises waterborne N emissions as nitrate (NO_3^--N) and airborne N deposition as ammonia (NH_3-N) and nitrogen oxides (NO_x-N) obtained in the LCI (Table 1). The characterisation model used here applied LC-IMPACT marine eutrophication CFs modified with recently developed XF and EF models. The CF is composed of a Fate Factor (FF) that quantifies the environmental losses from the original emission in freshwater and marine compartments expressing the availability of N in the euphotic zone of coastal waters (Azevedo et al., 2013), an eXposure Factor (XF) that expresses the 'conversion' potential of the available N into organic matter (biomass) and oxygen consumed after its aerobic respiration (Cosme et al., 2015), and an Effect Factor (EF) that quantifies the effect of oxygen depletion on exposed species (modelled as time- and volume-integrated Potentially Affected Fraction of species, PAF) (Cosme and Hauschild, 2016a)

The emitted amounts of N from each of the emission routes (e.g. to air, surface freshwater, groundwater, or marine water) are multiplied by the respective CF to deliver the impact score (IS) for the specific human activity from which the reported emission was originated, per receiving marine coastal ecosystem (66 spatial units). The Large Marine Ecosystems (LME) biogeographical classification system (Sherman and Hempel, 2009) was adopted for its consistent use in the three factors modelled. Coastal ecosystems LME#22 (North Sea) and LME#23 (Baltic Sea) were identified as the receiving coastal spatial units for Danish emissions.

Predictions of future pressures caused by altered climatic conditions predominantly describe negative consequences for biodiversity and ecosystems functions (Brierley and Kingsford, 2009; Rabalais et al., 2009). Modelling such future impacts involves a highly uncertain quantification of both pressures and responses (biogeochemical, biological, and ecological) due to the diversity of potential impacts and the complexity of cumulative and synergistic effects. For this reason, caution should be applied to its application and especially interpretation.

The major drivers for those pressures relate to increased temperature, sea level rise, enhanced hydrological cycles, and shifts in wind and currents patterns (Rabalais et al., 2009). Individually, or cumulatively, these impose direct and indirect effects on species and ecosystems. Increased temperature directly affect physiological aspects such as increasing metabolic rates, including oxygen requirements, temperature or hypoxia stress, heterotrophic respiration and oxygen consumption (Pörtner and Knust, 2007; Rabalais et al., 2009); or indirectly, via phenology and species succession by altering food availability and food webs (Edwards and Richardson, 2004). On the abiotic component, temperature- and salinity-driven density gradients (pycnoclines) may be strengthen, with special impact on intensified stratification in coastal waters (Rabalais et

al., 2009). Stratification hinders oxygen diffusion and vertical mixing, facilitating the onset of hypoxia in bottom waters and the disruption of biogeochemical cycles (Diaz and Rosenberg, 2008; Middelburg and Levin, 2009). Moreover, oxygen solubility in seawater is a function of temperature. In a future warmer ocean altered availability of oxygen may pose important limitations to species occurrence (Brierley and Kingsford, 2009). In addition, increased riverine discharge of nutrients and organic matter, from a potential increased precipitation regime, may exacerbate oxygen depletion after its respiration in shallow coastal waters. Reviews of these and other future pressures and effects can be found in (Brierley and Kingsford, 2009; Rabalais et al., 2009).

In an attempt to model the influence of the pressures affected by future climate change and to add environmental relevance to the characterisation modelling of the future scenario, modifications to the parameterisation of the original CFs were introduced (Table 2).

Table 2 Changes introduced in the characterisation modelling factors in order to represent the influence of future climatic-driven pressures. Abbreviations used: fate factor (FF), exposure factor (XF), effect factor (EF), North Sea (NS), Baltic Sea (BS), climate zone (CZ).

Parameter	Induced change	Driver for change	Affected factor	Reference
Mean annual sea surface temperature	From 10.5°C to 12.3 °C (NS), from 8.3°C to 9.8°C (BS)	Temperature increase	FF, XF	Belkin (2009); Cosme et al. (2015)
Mean annual bottom water temperature [a]	From 10.5°C to 12.3 °C (NS), from 8.3°C to 9.8°C (BS)	Temperature increase	FF, XF	Cosme and Hauschild (2016a)
Q_{10}, Temperature Coefficient (increase factor of a rate at a 10° temperature increase)	$Q_{10} = 2$	Temperature increase	FF, XF	Söderlund and Svensson (2012)
Nitrogen removal rate in freshwater systems	From 0.527 to 0.595 (NS) and 0.584 (BS) removal fractions (Q_{10}-based)	Temperature increase	FF	Wollheim et al. (2008)
Residence time in coastal waters	Constant	Altered wind and hydrographic patterns	FF	-
Denitrification rate in marine compartment	From 0.3 to 0.338 (NS) and to 0.332 (BS) denitrified fractions (Q_{10}-based)	Temperature increase	FF	Van Drecht et al. (2003)
N losses by advection in marine compartment	Constant	Altered wind and hydrographic patterns	FF	-
Respiration rate of sinking marine snow [b]	From 0.13 d^{-1} to 0.145 d^{-1} (Q_{10}-based)	Temperature increase	XF	Iversen and Ploug (2010)
Phytoplankton grazed fraction (f_{PPgrz})	10% shift from sink to grazed fraction: f_{PPgrz} from 0.3 to 0.27 (NS), and 0.49 to 0.44 (BS)	Temperature increase	XF	Cosme et al. (2015)

Parameter	Induced change	Driver for change	Affected factor	Reference
Bacterial Growth Efficiency (metabolic rate)	From 0.22 to 0.248 (NS), and 0.37 to 0.421 (BS) (Q_{10}-based)	Temperature increase	XF	Cosme et al. (2015)
Species poleward shift	20% influence of species from temperate CZ (NS) and 10% (BS) on sensitivity to hypoxia	Temperature increase, wind and currents patterns, advection	EF	Cosme and Hauschild (2016a)

[a] Continental shelf depth is assumed as of 200 m; for modelling purposes the average depth is 100 m (Cosme and Hauschild, 2016a).

[b] Marine snow refers to the sinking flux of particulate organic carbon (POC) of aggregates of phytoplankton cells, faecal pellets, zooplankton carcasses, and other organic material from dead or dying microorganisms (Fowler and Knauer, 1986).

2.4. Normalisation under present and future scenarios

The years chosen to be representative of the current and future scenarios are 2010 and 2050, respectively. Characterised impact scores at the midpoint level (mpIS) were normalised with an external normalisation reference (NR) (production-based, per capita). This was calculated with the same LC-IMPACT marine eutrophication characterisation model applied to the annual emissions from inorganic fertilisers and manure in 2010 in Denmark using a nitrogen use efficiency coefficient of 0.4 and N-content in annual applications (Bouwman et al., 2009), sewage water in 2010 following the emission model by Van Drecht et al. (2009), and NO_x-N and NH_3-N in 2005 after Roy et al. (2012). The NR for the future scenario (year 2050) was estimated from projections of fertilizers application (FAOSTAT, 2013), GDP growth in Denmark (TradingEconomics, 2015), and predicted future emissions of NOx and NH3 in Denmark (Nielsen et al., 2014). The calculated NRs for 2010 and 2050 are included in Table 3.

Marine eutrophication emerged as one of the most contributing impact categories for the current spring barley cultivation scenario after normalisation performed with the ReCiPe LCIA method at midpoint level (Niero et al., 2015a). It is also one of the impact categories showing the highest variation from current to future scenario (Niero et al., 2015a). It would be interesting to verify whether the situation is confirmed also under future climatic pressure, but currently there are no available characterisation models and normalisation references that cover future pressures for marine eutrophication. Therefore, different approaches to normalisation at the midpoint level were compared, referring to the recommended ILCD LCIA methodology (Hauschild et al., 2013). One, was the traditional normalisation approach, where the indicator scores of a product system are compared to those of society's background interventions, i.e. the EU-27 'domestic inventory' in 2010 corresponding to the emissions and consumptions in that spatial and temporal scope (Sala et al., 2015). An

alternative normalisation reference was also included, based on the carrying capacity of ecosystems, i.e. the maximum environmental intervention these can withstand without experiencing negative changes, recently proposed by Bjørn and Hauschild (2015). In such approach, NRs were calculated as the carrying capacity for each impact category divided by the population in the reference region and year. For the future scenario, the population in Europe (EU-28) in 2050 was used. A summary of the considered scenarios and data/assumptions in the calculations is reported in Table 3.

Table 3 Summary of the inventory data used to calculate the normalisation references (NR) for Denmark (DK) in 2010 and 2050.

Reference	NR LC-IMPACT		NR 'domestic inventory' [1]		NR carrying capacity [2]	
Scope	DK (2010)	DK (2050)	EU-27 (2010)	EU-28 (2050)	EU-27 (2010)	EU-28 (2050)
Background intervention ($kgN \cdot yr^{-1}$)	3.55E+09	3.98E+09	8.44E+09	1.12E+10	-	-
Carrying capacity ($kgN \cdot yr^{-1}$)	-	-	-	-	2.27E+10	2.27E+10
Population (pers) [3]	5,417,692	6,271,485	498,867,771	525,527,890	498,867,771	525,527,890
NR value ($kgN \cdot pers^{-1} \cdot yr^{-1}$)	641	620	16.9	21.3	45.6	43.3

[1] Source: Sala et al. (2015);
[2] Source: Bjørn and Hauschild (2015);
[3] Source: DK 2010 and EU-27 2010 – EUROSTAT (2015a); DK 2050 and EU-28 2050 – EUROSTAT (2015b).

2.5. Damage factors

Midpoint modelling was extrapolated to damage level by converting PAF to Potentially Disappearing Fraction (PDF) of species and by applying spatially explicit species densities. The metrics conversion and the species density-based weighting corresponds to the damage factor (DF). This approach is also adopted in the ReCiPe method (Goedkoop et al., 2012), but the spatial differentiation feature is limited to a single site-generic marine species density value.

For the PAF to PDF metrics conversion a factor 0.5 was chosen, i.e. PDF=0.5*PAF, as discussed in Cosme et al. (2016a) (see also Jolliet et al. (2003) and Larsen and Hauschild (2007)), or the assumption that 50% of the species affected eventually disappear due to hypoxic stress. Species density (SD, in $species \cdot m^{-3}$) then converts PDF into species·yr – the unit for 'Ecosystems' damage in the ReCiPe method (Goedkoop et al., 2012). Spatially explicit species density values are available per LME as 6.7E-12 $species \cdot m^{-3}$ in the North Sea and 3.6E-12 $species \cdot m^{-3}$ in the Baltic Sea (Cosme et al., 2016a).

3. Results and discussion

Present and future inventory flows from spring barley production were characterised with the proposed spatially explicit CFs for the marine eutrophication indicator. Results were normalised with three alternative methods and analysed. Indicators of damage to ecosystems were further calculated for the same temporal scenarios. The results of these estimations are presented and discussed in the next sections.

3.1. Characterisation factors under present and future scenarios

The CFs applied to the present and future spring barley scenarios in the various routes and receiving LMEs are included in Table 4. For the present scenario, N emissions from spring barley cultivation (Table 1, second column) were characterised using the spatially differentiated FF, XF, and EF (see section 2.4). For the future scenario, future N emissions (Table 1, third column) were characterised using the modified FF, XF, and EF parameterised in accordance to the influence of future climatic-driven pressures, as reported in Table 2.

Table 4 Marine eutrophication characterisation factors (CFs) used to characterise present and future nitrogen (N) emissions from spring barley production to the North Sea and Baltic Sea, estimated from fate factors (FF), exposure factors (XF), and effect factors (EF) modelling.

Scenario		Present		Future	
Receiving ecosystem		North Sea	Baltic Sea	North Sea	Baltic Sea
Factor	Emission route				
FF [yr]	NO_3^--N to water	0.59	1.39	0.48	1.12
	NO_x-N to air	0.05	0.12	0.04	0.10
	NH_3-N to air	0.05	0.12	0.04	0.10
XF [$kgO_2 \cdot kgN^{-1}$]	All	9.11	15.9	8.30	13.91
EF [$(PAF) \cdot m^3 \cdot kgN^{-1}$]	All	1.59	1.78	1.70	1.91
CF [$(PAF) \cdot m^3 \cdot yr \cdot kgN^{-1}$]	NO_3^--N to water	8.53	39.20	6.81	29.76
	NO_x-N to air	0.75	3.46	0.60	2.62
	NH_3-N to air	0.74	3.39	0.59	2.57

The future FFs are lower than present FFs due to a predicted increase of the denitrification rate in both freshwater and marine compartments (Veraart et al., 2011). This fact leads to a lower N-fraction available to promote eutrophication impacts (Cosme et al., 2015). The XFs decrease in the future scenarios due to i) a predicted larger fraction of phytoplankton grazed and less sinking material to be respired near the bottom, and (ii) increased metabolic rates (with enhanced respiration of sinking marine snow dominating the enhanced bottom respiration). In both cases, oxygen depletion and eutrophication potential are decreased (Cosme et al., 2015). The future EFs predict higher impacts as species shift poleward from the Celtic-Biscay shelf (ca. 14% and 23%

more sensitive to hypoxia than North Sea's and Baltic Sea's, respectively) (Cosme and Hauschild, 2016a). Given the higher variation of the XF to the CF estimation (Table 4) and the potential underestimation of future pressures in the EF modelling, these are believed to be the most relevant sources of variation in the future CFs. Other possible future pressures, not quantified in Table 2 due to high uncertainty, may change habitat conditions and lead to significant increase of the CFs, like stronger water stratification and reduced oxygen solubility that affect, respectively, the XF and EF.

Acknowledging the concerns about uncertainty in modelling both present and future CFs, the advantage of producing spatially explicit impact scores to LCIA seems highly relevant (Potting and Hauschild, 2006; Udo de Haes et al., 2002). Moreover, given the spatial differentiation of species distributions at the same scale (i.e. LME-dependent), these can be coupled for the damage modelling.

3.2. Uncertainty in the normalisation step

Figure 2A shows normalised impacts scores (normIS) for marine eutrophication at the midpoint level (characterised with ILCD recommended CFs, i.e. ReCiPe's CFs for aquatic eutrophication applied to N flows) using 'domestic inventory' NRs and carrying capacity NRs for Europe, and LC-IMPACT NRs for Denmark, in 2010 (present scenario) and 2050 (future scenario).

The mpIS obtained with the ILCD LCIA method for present and future emissions from the spring barley production system are based on the same characterisation model, i.e. use the same CFs (Niero et al., 2015b). It is assumed that such model is adapted to represent the present impacts. The model fit for future conditions is not quantified or discussed here, because the underlying models have no parameterisation adjustment to represent the effect of future pressures. The normalisation references calculated for the future scenario (Table 3) adopt reference emissions inventory (background interventions) and population values for 2050, but use the same characterisation model as for 2010, introducing an inevitable uncertainty to the normIS of the future scenario.

The adoption of the alternative normalisation based on carrying capacity helps quantifying that misestimation. Beyond short-timed natural variability, the carrying capacity is per definition constant at the timescale used here (decades) (Bjørn and Hauschild, 2015), so it can be assumed that there is no additional uncertainty introduced in the normIS. The 'domestic inventory'-based and carrying capacity-based NRs vary in their essence, i.e. relative to a varying (yearly) background in the former and to a fixed (European) carrying capacity in the latter (the contribution from the population increase is the same in both methods). The variation in magnitude (Figure 2A) is justified by the carrying capacity being 2.6 times higher than the 'domestic intervention' in 2010 and 2 times in 2050 (Table 3), whereas the variation in relative contribution (Figure 2B)

originates from considering a population growth in the 'domestic inventory' NR2050 but a constant carrying capacity value in this method (Table 3).

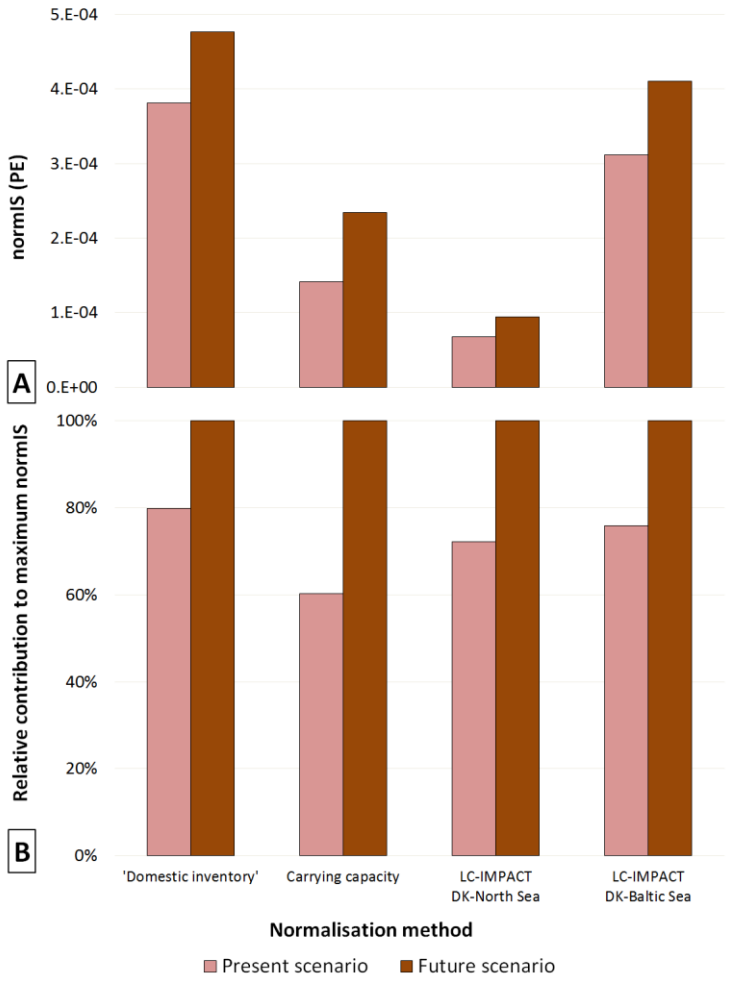

Figure 2 A) Normalised impacts scores (normIS) for marine eutrophication at midpoint level, **B)** Relative contribution (in %) of each normIS to the maximum score. Both sets of results calculated for the present scenario (2010) and future scenario (2050) per normalisation method used – the EU 'domestic inventory' and carrying capacity-based NRs for Europe, and LC-IMPACT NR for Denmark.

Since the midpoint LC-IMPACT-based CFs model a longer marine eutrophication impact pathway, those mpIS are therefore not comparable to ILCD's (units are (PAF)·m^3·yr and kgN-eq, respectively). The normalisation step eliminates any uncertainty in the characterisation modelling and the results can be compared. The normIS show an increase in both ecosystems, i.e. 0.04 to 0.06 PAF·m^3·yr (North Sea), and 0.20 to 0.25 PAF·m^3·yr (Baltic Sea). The normalisation step also reveals the steeper increase in the Baltic Sea (Figure 2A) due to the spatial differentiation feature embedded in the model. This is particularly visible in the FF (4.6 times higher for the

Baltic Sea and North Sea, Table 4) or 2.6 times the variability of the XF and 4.1 the EF's. The present and future LC-IMPACT NRs are very similar (section 2.5), due to the cancelling effect of increasing waterborne N emissions (inorganic fertilizer, manure, and sewage discharge) but decreasing airborne emissions (NO_x and NH_3). As such, the variability of the normIS results in the future scenario is mostly explained by (i) CFs variation (+34% and +28% from present to future CFs, for the North Sea and Baltic Sea, respectively, Table 4), (ii) the larger LCI flows, and (iii) the population change (+16%) projected for 2050 in Denmark. The contribution of these three terms to the total uncertainty of the characterisation model is not quantified here. However, the high sensitivity to the XF and EF, and the confidence on the projections for 2050 (especially in the quantification of the total annual emissions) are potentially determinant in explaining the variability of the characterisation model and normalisation step, respectively. Despite the overall uncertainty of the marine eutrophication model in the modified LC-IMPACT method, it seems valuable to i) add environmental relevance, by including the effect of future climate pressures in the characterisation model expressed in the future impact scores, and ii) increase the completeness of the impact pathway coverage in modelling a later midpoint indicator that includes the ecosystem exposure and the effect components in the model.

The total N emissions in Denmark in 2050 were split evenly towards the North Sea and the Baltic Sea for the characterisation step – this procedure is a necessary simplification in the method at this point but may add a significant uncertainty in the normalised scores. The variation of normIS from present to future emissions (Figure 2A) shows relative increases similar to ILCD-based method (the currently recommended method that used ReCiPe's aquatic eutrophication midpoint model for N emissions), therefore suggesting that future N emissions from Denmark follow those of the European average in 2050.

The results presented in this assessment do not intend to give a full perspective of the environmental profile of the spring barley production as other impacts indicators are lacking. Similarly, the discussion is not on the sustainability of the spring barley production system (see Niero et al., 2015b), but rather on the value of introducing temporal and spatial variation in the impact assessment model.

The LC-IMPACT NRs show the relevance of introducing spatial differentiation, especially for indicators of local to regional impacts. These NRs are estimated from present and future emissions normalised by the respective present and future national emissions per capita. In opposition, the 'domestic inventory' based NR for the future scenario, are inconsistently representing the reference system, as no projection of this inventory is available so far. The carrying capacity-based NRs use a constant global carrying capacity, so the NRs variation is directly dependent on the reference system's emissions.

3.3. Damage modelling scores and application

The results of the damage scores estimation (Figure 3), based on midpoint characterisation of barley production emissions (Niero et al., 2015b) and DF application (section 2.5), show an increase of damage towards future conditions in both receiving marine ecosystems considered. Damage indicators show a factor 2.5 and 2.3 of spatial differentiation between the Baltic (higher) and North Seas (lower) for the present and future scenarios, respectively. Such differentiation is mostly caused by the higher primary productivity potential of the Baltic Sea (Cosme et al., 2015).

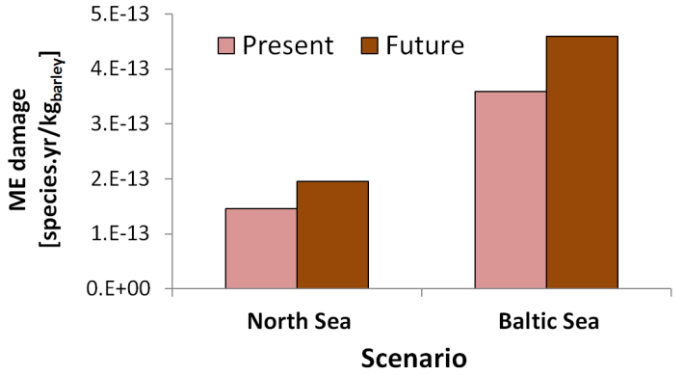

Figure 3 Damage impact scores to marine eutrophication (ME) for the present (2010) and future (2050) emissions to the North Sea and Baltic Sea from the spring barley production system studied.

While damage modelling may facilitate communication of (more understandable) results connected with the higher environmental relevance of longer pathway coverage (completeness), the loss of transparency and especially the additional uncertainties (parameter, model, or scenario) (Bare et al., 2000) may decrease the validity of the results in less robust models. Improving the DF modelling by means of spatially differentiated quantification of the fraction of species affected (as PAF) that potential becomes extinct (as PDF) in a spatial unit, may contribute to overcome the uncertainty of the model simplification that constitutes the DF. Such model improvements may embrace the inclusion of species vulnerability, uniqueness, ecosystem resilience, or functional diversity indicators – see e.g. Souza et al. (2013), Verones et al. (2015).

3.4. Implications for decision-makers and LCIA model developers

The inclusion of spatial differentiation is a valuable addition to any LCIA method, as long as there is a significant variability in the relevant parameters, not only to increase its discriminatory power (Udo de Haes et al., 1999), but also to add an extra information level to the decision-making process. Those who benefit from LCA results

may adopt such differentiated information especially when dealing with human activities and emissions with local to regional impacts, like marine eutrophication. Complementary, it may provide useful analysis of supply chains with emissions at different locations with potentially differentiated impacts and increased the quality of the results produced in support of sustainability assessment.

The LCI models should preferably be supplied with spatially differentiated input data in order to maintain and explore that feature later in the characterisation. The LC-IMPACT method currently delivers CFs for the marine eutrophication indicator at country-to-LME as the highest spatial resolution, with 214 combinations of emitting country to receiving LME (Azevedo et al., 2013). LCIA developers may then aim at introducing temporal- (if relevant) along with spatial-differentiation in the models. In particular, the temporal variability in the marine eutrophication phenomenon at the intra-annual scale (months or seasons) may have a significant impact on the biological processes that compose the characterisation model, e.g. nutrients limitation, marine primary productivity, and species succession (Cosme et al., 2015) or species sensitivity (Cosme and Hauschild, 2016a). Its inclusion can be seen as future model improvement or research opportunity. The flexibility (or adaptability) of model parameterisations may further adopt archetypes that represent possible degrees of confidence or intensity of pressures. Notwithstanding, the value of flexible parameterisations seems essential in modelling future impacts beyond the adoption of timeframe perspectives (Hauschild et al., 2013). The calculation of NRs has also to match the time variation with corresponding data at the necessary spatial- and time-resolution, as also noted by Sleeswijk et al. (2008).

LCA scores aggregated at damage level can be relevant to decision-makers (e.g. managers, regulators) in the assessment of sustainability of activities and options, but also for ecosystems management and conservation. The misleading sense of certainty and comprehensiveness can however mine the confidence on its application (Bare et al., 2000). So, facing the merits and limitations of both midpoint and damage modelling steps, the use of both sets of results is suggested for a sound(er) interpretation and for the development of consistent methods across impact indicators.

Overall, the adjustment of the CF parameterisation is essential for the forecasting of LCIA results and its application in management plans for e.g. the agriculture and energy sectors, their regulation, and technological development (see other DPSIR Responses in Figure 1).

The application of the precautionary principle to the DPSIR approach (Figure 1) aims at showing that it is possible to anticipate impacts and act before the environment is affected. The concept, formalised in the UN ‘Earth Summit’ in 1992, ensures that by using indicators and impact assessment tools, (the magnitude of) the effects of future climatic changes can be already estimated and (some of) the Impacts anticipated, based

on the present knowledge of the Pressures, so that Responses may be implemented sooner. In this line, specific LCIA indicators (such as marine eutrophication) are valuable contributions to support the precautionary approach, and so is the modelling of future impacts.

4. Conclusions

A novel characterisation model for nitrogen emissions from spring barley production was applied. The main improvement to the LCIA midpoint CFs is the inclusion of ecosystem exposure and effects to biota, by improving the commonly used 'increase in N concentration' in marine water to a 'fraction of species (as PAF) affected' by the eutrophication impacts in the marine coastal compartment. A first attempt to account for potential future climatic pressures, relevant to the marine eutrophication phenomenon, in a 2050 scenario was implemented, based on corresponding altered emission flows and modified parameterisation in the CF estimation.

Normalisation of results from present and future scenarios was compared, by estimating NRs based on total annual impacts (domestic inventory of background interventions), on ecological carrying capacity, and the newly proposed method. The comparison shows consistent results and also point to the value of adding spatial differentiation to the indicator's modelling framework.

The (i) inclusion of the time variation feature in CF modelling of marine eutrophication impacts, (ii) the characterisation of emissions at a spatially differentiated scale, and (iii) the identification of the need for adequate inventory data to assess future scenarios, constitute the main outcomes of the present study. Further research is needed to reduce the uncertainty of the parameterisation under future conditions extending the coverage of the climatic change aspects into the impact pathway and to tighten projections of future emissions.

The findings of this exploratory research point to the relevance of including time and spatial differentiation in characterisation modelling in LCIA. It also serves as a proof of concept that this kind of forecast modelling can, and should, be included in LCA. Finally, modelling the temporal variability of both inventory data and impacts appears central in exploiting the potential of LCA and fostering its legitimate application in decision support for scenario and precautionary analyses.

Acknowledgements

We thank Alexis Laurent for contributing to the inventory data collection and for his valuable comments on a previous version of the manuscript and Benjamin Goldstein for his cursory language check. The authors further thank the editor and two anonymous reviewers whose comments and suggestions helped improving this manuscript.

References

Audsley, E., Wilkinson, M., 2014. What is the potential for reducing national greenhouse gas emissions from crop and livestock production systems? J. Clean. Prod. 73, 263–268. doi:10.1016/j.jclepro.2014.01.066

Azevedo, L.B., Cosme, N., Hauschild, M.Z., Henderson, A.D., Huijbregts, M.A.J., Jolliet, O., Larsen, H.F., van Zelm, R., 2013. Recommended assessment framework, method and characterisation and normalisation factors for ecosystem impacts of eutrophying emissions: phase 3 (report, model and factors). FP7 (243827 FP7- ENV-2009-1) LC-IMPACT report. 154 pp.

Bare, J.C., Hofstetter, P., Pennington, D.W., Udo de Haes, H.A., 2000. Midpoints versus endpoints: the sacrifices and benefits. Int J LCA 5, 319–326.

Belkin, I.M., 2009. Rapid warming of Large Marine Ecosystems. Prog. Oceanogr. 81, 207–213. doi:10.1016/j.pocean.2009.04.011

Bjørn, A., Hauschild, M.Z., 2015. Introducing carrying capacity-based normalisation in LCA: framework and development of references at midpoint level. Int. J. Life Cycle Assess. 20, 1005–1018. doi:10.1007/s11367-015-0899-2

Borja, A., Galparsoro, I., Solaun, O., Muxika, I., Tello, E.M., Uriarte, A., Valencia, V., 2006. The European Water Framework Directive and the DPSIR, a methodological approach to assess the risk of failing to achieve good ecological status. Estuar. Coast. Shelf Sci. 66, 84–96. doi:10.1016/j.ecss.2005.07.021

Bouwman, A.F., Beusen, A.H.W., Billen, G., 2009. Human alteration of the global nitrogen and phosphorus soil balances for the period 1970–2050. Global Biogeochem. Cycles 23. doi:10.1029/2009GB003576

Breitburg, D.L., Hondorp, D.W., Davias, L.A., Diaz, R.J., 2009. Hypoxia, Nitrogen, and Fisheries: Integrating Effects Across Local and Global Landscapes. Ann. Rev. Mar. Sci. 1, 329–349. doi:10.1146/annurev.marine.010908.163754

Bricker, S.B., Longstaff, B., Dennison, W., Jones, A., Boicourt, K., Wicks, C., Woerner, J., 2008. Effects of nutrient enrichment in the nation's estuaries: A decade of change. Harmful Algae 8, 21–32. doi:10.1016/j.hal.2008.08.028

Brierley, A.S., Kingsford, M.J., 2009. Impacts of climate change on marine organisms and ecosystems. Curr. Biol. 19, R602–R614. doi:10.1016/j.cub.2009.05.046

Cloern, J.E., 2001. Our evolving conceptual model of the coastal eutrophication problem. Mar. Ecol. Prog. Ser. 210, 223–253. doi:10.3354/meps210223

Cloern, J.E., Abreu, P.C., Carstensen, J., Chauvaud, L., Elmgren, R., Grall, J., Greening, H., Johansson, J.O.R., Kahru, M., Sherwood, E.T., Xu, J., Yin, K., 2016. Human activities and climate variability drive fast-paced change across the world's estuarine-coastal ecosystems. Glob. Chang. Biol. 513–529. doi:10.1111/gcb.13059

Cosme, N., Hauschild, M.Z., 2016a. Effect factors for marine eutrophication in LCIA based on species sensitivity to hypoxia. Ecol. Indic. 69:453-462. doi:10.1016/j.ecolind.2016.04.006

Cosme, N., Hauschild, M.Z., 2016b. Characterization of waterborne nitrogen emissions

for marine eutrophication modelling in life cycle impact assessment at the damage level and global scale. Int. J. Life Cycle Assesment submitted.

Cosme, N., Jones, M.C., Cheung, W.W.L., Larsen, H.F., 2016a. Spatial differentiation of marine eutrophication damage indicators based on species density. Ecol. Indic. submitted.

Cosme, N., Koski, M., Hauschild, M.Z., 2015. Exposure factors for marine eutrophication impacts assessment based on a mechanistic biological model. Ecol. Modell. 317, 50–63. doi:10.1016/j.ecolmodel.2015.09.005

Cosme, N., Mayorga, E., Hauschild, M.Z., 2016b. Spatially explicit fate factors for waterbone nitrogen emissions at the global scale. Int. J. Life Cycle Assesment submitted.

Davis, J.C., 1975. Minimal dissolved oxygen requirements of aquatic life with emphasis on Canadian species: a review. J. Fish. Res. Board Canada 32, 2295–2332.

Diaz, R.J., Rosenberg, R., 2008. Spreading dead zones and consequences for marine ecosystems. Science (80-.). 321, 926–9. doi:10.1126/science.1156401

Diaz, R.J., Rosenberg, R., 1995. Marine Benthic Hypoxia: a Review of Its Ecological Effects and the Behavioural Responses of Benthic Macrofauna. Oceanogr. Mar. Biol. Annu. Rev. 33, 245–303.

Dijkman, T.J., Birkved, M., Hauschild, M.Z., 2013. Modelling of pesticide emissions for Life Cycle Inventory analysis: model development, applications and implications. Technical University of Denmark.

Doltra, J., Lægdsmand, M., Olesen, J.E., 2012. Impacts of projected climate change on productivity and nitrogen leaching of crop rotations in arable and pig farming systems in Denmark. J. Agric. Sci. 152, 75–92. doi:10.1017/S0021859612000846

Edwards, M., Richardson, A.J., 2004. Impact of climate change on marine pelagic phenology and trophic mismatch. Nature 430, 881–884. doi:10.1038/nature 02808

Ekau, W., Auel, H., Pörtner, H.-O., Gilbert, D., 2010. Impacts of hypoxia on the structure and processes in pelagic communities (zooplankton, macro-invertebrates and fish). Biogeosciences 7, 1669–1699. doi:10.5194/bg-7-1669-2010

El Chami, D., Daccache, a., 2015. Assessing sustainability of winter wheat production under climate change scenarios in a humid climate — An integrated modelling framework. Agric. Syst. 140, 19–25. doi:10.1016/j.agsy.2015.08.008

EUROSTAT, 2015a. Population on 1 January by age and sex, Last update: 26-10-2015. Retrieved from http://ec.europa.eu/eurostat/data/database [18.11.2015].

EUROSTAT, 2015b. Population Projections EUROPOP2013. Retrieved from http://ec.europa.eu/eurostat/data/database [18.11.2015].

FAOSTAT, 2013. Emissions – Agriculture. Retrieved from http://faostat.fao.org/site /705/default.aspx. [18.11.2015].

Ferreira, J.G., Andersen, J.H., Borja, A., Bricker, S.B., Camp, J., Cardoso da Silva, M.,

Garcés, E., Heiskanen, A.-S., Humborg, C., Ignatiades, L., Lancelot, C., Menesguen, A., Tett, P., Hoepffner, N., Claussen, U., 2011. Overview of eutrophication indicators to assess environmental status within the European Marine Strategy Framework Directive. Estuar. Coast. Shelf Sci. 93, 117–131. doi:10.1016/j.ecss.2011.03.014

Foley, J.A., Ramankutty, N., Brauman, K.A., Cassidy, E.S., Gerber, J.S., Johnston, M., Mueller, N.D., O'Connell, C., Ray, D.K., West, P.C., Balzer, C., Bennett, E.M., Carpenter, S.R., Hill, J., Monfreda, C., Polasky, S., Rockström, J., Sheehan, J., Siebert, S., Tilman, D., Zaks, D.P.M., 2011. Solutions for a cultivated planet. Nature 478, 337–342. doi:10.1038/nature10452

Fowler, S.W., Knauer, G.A., 1986. Role of large particles in the transport of elements and organic compounds through the oceanic water column. Prog. Oceanogr. 16, 147–194. doi:10.1016/0079-6611(86)90032-7

Galloway, J.N., Townsend, A.R., Erisman, J.W., Bekunda, M., Cai, Z., Freney, J.R., Martinelli, L.A., Seitzinger, S.P., Sutton, M.A., 2008. Transformation of the Nitrogen Cycle: Recent Trends, Questions, and Potential Solutions. Science (80-.). 320, 889–892. doi:10.1126/science.1136674

Goedkoop, M., Heijungs, R., Huijbregts, M.A.J., De Schryver, A.M., Struijs, J., van Zelm, R., 2012. ReCiPe 2008 - A life cycle impact assessment method which comprises harmonised category indicators at the midpoint and the endpoint level. First edition (revised) Report I: Characterisation; July 2012, http://www.lcia-recipe.net.

Gray, J.S., Wu, R.S., Or, Y.Y., 2002. Effects of hypoxia and organic enrichment on the coastal marine environment. Mar. Ecol. Prog. Ser. 238, 249–279.

Guinée, J.B., Gorrée, M., Heijungs, R., Huppes, G., Kleijn, R., Koning, A. de, Oers, L. van, Sleeswijk, A.W., Suh, S., Udo de Haes, H.A., Bruijn, H. de, Duin, R. van, Huijbregts, M.A.J., 2002. Handbook on life cycle assessment. Operational guide to the ISO standards. I: LCA in perspective. IIa: Guide. IIb: Operational annex. III: Scientific background. Kluwer Academic Publishers, Dordrecht.

Hamelin, L., Jørgensen, U., Petersen, B.M., Olesen, J.E., Wenzel, H., 2012. Modelling the carbon and nitrogen balances of direct land use changes from energy crops in Denmark: a consequential life cycle inventory. GCB Bioenergy 4, 889–907. doi:10.1111/j.1757-1707.2012.01174.x

Hauschild, M.Z., 2005. Assessing Environmental Impacts in a Life-Cycle Perspective. Environ. Sci. Technol. 39, 81–88. doi:10.1021/es053190s

Hauschild, M.Z., Goedkoop, M., Guinée, J., Heijungs, R., Huijbregts, M.A.J., Jolliet, O., Margni, M., De Schryver, A.M., Humbert, S., Laurent, A., Sala, S., Pant, R., 2013. Identifying best existing practice for characterization modeling in life cycle impact assessment. Int. J. Life Cycle Assess. 18, 683–697. doi:10.1007/s11367-012-0489-5

Hauschild, M.Z., Potting, J., 2005. Spatial Differentiation in Life Cycle Impact Assessment - The EDIP2003 methodology, Environmental News No. 80.

Howarth, R.W., Marino, R., 2006. Nitrogen as the limiting nutrient for eutrophication in

coastal marine ecosystems: Evolving views over three decades. Limnol. Oceanogr. 51, 364–376. doi:10.4319/lo.2006.51.1_part_2.0364

Ingvordsen, C.H., Backes, G., Lyngkjær, M.F., Peltonen-Sainio, P., Jensen, J.D., Jalli, M., Jahoor, A., Rasmussen, M., Mikkelsen, T.N., Stockmarr, A., Jørgensen, R.B., 2015. Significant decrease in yield under future climate conditions: Stability and production of 138 spring barley accessions. Eur. J. Agron. 63, 105–113. doi:10.1016/j.eja.2014.12.003

ISO 14044, 2006. Environmental management — Life cycle assessment — Requirements and guidelines. Geneva.

Iversen, M.H., Ploug, H., 2010. Ballast minerals and the sinking carbon flux in the ocean: carbon-specific respiration rates and sinking velocity of marine snow aggregates. Biogeosciences 7, 2613–2624. doi:10.5194/bg-7-2613-2010

Jabloun, M., Schelde, K., Tao, F., Olesen, J.E., 2015. Effect of temperature and precipitation on nitrate leaching from organic cereal cropping systems in Denmark. Eur. J. Agron. 62, 55–64. doi:10.1016/j.eja.2014.09.007

Jensen, N.H., Veihe, A., 2009. Modelling the effect of land use and climate change on the water balance and nitrate leaching in eastern Denmark. J. Land Use Sci. 4, 53–72. doi:10.1080/17474230802645832

Jolliet, O., Margni, M., Charles, R., Humbert, S., Payet, J., Rebitzer, G., 2003. Presenting a New Method IMPACT 2002 + : A New Life Cycle Impact Assessment Methodology. Int J LCA 8, 324–330.

Kelly, J.R., 2008. Nitrogen Effects on Coastal Marine Ecosystems, in: Hatfield, J.L., Follet, R.F. (Eds.), Nitrogen in the Environment: Sources, Problems, and Management. U.S. Environmental Protection Agency, (Amsterdam, Boston, et al.: Academic Press/Elsevier, pp. 271–332.

Kristensen, K., Waagepetersen, J., Børgesen, C.D., Vinther, F.P., Grant, R., Blicher-Mathiesen, G., 2008. Reestimation and further development in the model N-LES: N-LES3 to N-LES4.

Larsen, H.F., Hauschild, M.Z., 2007. LCA Methodology Evaluation of Ecotoxicity Effect Indicators for Use in LCIA. Int. J. 12, 24–33.

Laurent, A., Hauschild, M.Z., 2015. Normalisation, in: Hauschild, M.Z., Huijbregts, M.A.J. (Eds.), Life Cycle Impact Assessment, LCA Compendium - The Complete World of Life Cycle Assessment. Springer Science+Business Media Dordrecht, pp. 271–300.

Levin, L.A., Ekau, W., Gooday, A.J., Jorissen, F., Middelburg, J.J., Naqvi, S.W.A., Neira, C., Rabalais, N.N., Zhang, J., 2009. Effects of natural and human-induced hypoxia on coastal benthos. Biogeosciences 6, 2063–2098.

Middelburg, J.J., Levin, L.A., 2009. Coastal hypoxia and sediment biogeochemistry. Biogeosciences 6, 1273–1293. doi:10.5194/bg-6-1273-2009

Miller, D., Poucher, S., Coiro, L., 2002. Determination of lethal dissolved oxygen levels for selected marine and estuarine fishes, crustaceans, and a bivalve. Mar. Biol. 140, 287–296. doi:10.1007/s002270100702

Mueller, N.D., Gerber, J.S., Johnston, M., Ray, D.K., Ramankutty, N., Foley, J.A., 2012. Closing yield gaps through nutrient and water management. Nature 490, 254–257. doi:10.1038/nature11420

Nielsen, O.-K., Plejdrup, M., Hjelgaard, K., Nielsen, M., Winther, M., Mikkelsen, M.H., Albrektsen, R., Fauser, P., Hoffmann, L., Gyldenkærne, S., 2014. Projection of SO2, NOx, NMVOC, NH3 and particle emissions - 2012-2035. Technical Report from DCE – Danish Centre for Environment and Energy No. 81. Aarhus University, DCE – Danish Centre for Environment and Energy, 151 pp.

Niemeijer, D., Groot, R.S., 2008. Framing environmental indicators: moving from causal chains to causal networks. Environ. Dev. Sustain. 10, 89–106. doi:10.1007/s10668-006-9040-9

Niero, M., Ingvordsen, C.H., Jørgensen, R.B., Hauschild, M.Z., 2015a. How to manage uncertainty in future Life Cycle Assessment (LCA) scenarios addressing the effect of climate change in crop production. J. Clean. Prod. 107, 693–706. doi:10.1016/j.jclepro.2015.05.061

Niero, M., Ingvordsen, C.H., Peltonen-Sainio, P., Jalli, M., Lyngkjær, M.F., Hauschild, M.Z., Jørgensen, R.B., 2015b. Eco-efficient production of spring barley in a changed climate: A Life Cycle Assessment including primary data from future climate scenarios. Agric. Syst. 136, 46–60. doi:10.1016/j.agsy.2015.02.007

Nixon, S.W., 1995. Coastal marine eutrophication: A definition, social causes, and future concerns. Ophelia 41, 199–219.

Notarnicola, B., Salomone, R., Petti, L., Renzulli, P.A., Roma, R., Cerrutti, A.K., 2015. Life Cycle Assessment in the Agri-Food Sector: Case Studies, Methodological Issues and Best Practices. Springer International Publishing Switzerland, 332 pp.

Nunez, M., Pfister, S., Vargas, M., Anton, A., 2015. Spatial and temporal specific characterisation factors for water use impact assessment in Spain. Int. J. Life Cycle Assesment 128–138. doi:10.1007/s11367-014-0803-5

Pörtner, H.-O., Knust, R., 2007. Climate Chnage Affects Marine Fishes Through the Oxygen Limitation of Thermal Tolerance. Science (80-.). 315, 95–98. doi:10.1126/science.1135471

Potting, J., Hauschild, M.Z., 2006. Spatial Differentiation in Life Cycle Impact Assessment: A decade of method development to increase the environmental realism of LCIA. Int. J. Life Cycle Assess. 11, 11–13.

Rabalais, N.N., 2002. Nitrogen in Aquatic Ecosystems. Ambio 31, 102–112.

Rabalais, N.N., Turner, R.E., Diaz, R.J., Justić, D., 2009. Global change and eutrophication of coastal waters. ICES J. Mar. Sci. 66, 1528–1537.

Röder, M., Thornley, P., Campbell, G., Bows-Larkin, A., 2014. Emissions associated with meeting the future global wheat demand: A case study of UK production under climate change constraints. Environ. Sci. Policy 39, 13–24. doi:10.1016/j.envsci.2014.02.002

Rosenbaum, R.K., Bachmann, T.M., Gold, L.S., Huijbregts, M.A.J., Jolliet, O., Juraske,

R., Koehler, A., Larsen, H.F., MacLeod, M., Margni, M., McKone, T.E., Payet, J., Schuhmacher, M., van de Meent, D., Hauschild, M.Z., 2008. USEtox—the UNEP-SETAC toxicity model: recommended characterisation factors for human toxicity and freshwater ecotoxicity in life cycle impact assessment. Int. J. Life Cycle Assess. 13, 532–546. doi:10.1007/s11367-008-0038-4

Roy, P.-O., Huijbregts, M.A.J., Deschênes, L., Margni, M., 2012. Spatially-differentiated atmospheric source–receptor relationships for nitrogen oxides, sulfur oxides and ammonia emissions at the global scale for life cycle impact assessment. Atmos. Environ. 62, 74–81. doi:10.1016/j.atmosenv.2012.07.069

Sala, S., Benini, L., Mancini, L., Pant, R., 2015. Integrated assessment of environmental impact of Europe in 2010: data sources and extrapolation strategies for calculating normalisation factors. Int. J. Life Cycle Assess. 20, 1568–1585. doi:10.1007/s11367-015-0958-8

Sherman, K., Hempel, G., 2009. The UNEP Large Marine Ecosystem Report: A perspective on changing conditions in LMEs of the World's Regional Seas, UNEP Regional Seas Report and Studies No. 182.

Sleeswijk, A.W., van Oers, L.F.C.M., Guinée, J.B., Struijs, J., Huijbregts, M.A.J., 2008. Normalisation in product life cycle assessment: an LCA of the global and European economic systems in the year 2000. Sci. Total Environ. 390, 227–40. doi:10.1016/j.scitotenv.2007.09.040

Smeets, E., Weterings, R., 1999. Environmental indicators: Typology and overview. Technical report No. 25. European Environment Agency, Copenhagen, 19 pp.

Smith, V.H., Tilman, G.D., Nekola, J.C., 1999. Eutrophication: impacts of excess nutrient inputs on freshwater, marine, and terrestrial ecosystems. Environ. Pollut. 100, 179–196.

Socolow, R.H., 1999. Nitrogen management and the future of food: Lessons from the management of energy and carbon. Proc. Natl. Acad. Sci. U. S. A. 96, 6001–6008.

Söderlund, R., Svensson, B.H., 2012. The Global Nitrogen Cycle. Ecol. Bull. 22, 22–73.

Soussana, J.-F., 2014. Research priorities for sustainable agri-food systems and life cycle assessment. J. Clean. Prod. 73, 19–23. doi:10.1016/j.jclepro.2014.02.061

Souza, D.M. de, Flynn, D.F.B., Declerck, F., Rosenbaum, R.K., De Melo Lisboa, H., Koellner, T., 2013. Land use impacts on biodiversity in LCA: Proposal of characterization factors based on functional diversity. Int. J. Life Cycle Assess. 18, 1231–1242. doi:10.1007/s11367-013-0578-0

Tendall, D.M., Gaillard, G., 2015. Environmental consequences of adaptation to climate change in Swiss agriculture: An analysis at farm level. Agric. Syst. 132, 40–51. doi:10.1016/j.agsy.2014.09.006

TradingEconomics, 2015. GDP per capita PPP forecast. Retrieved from http://www.tradingeconomics.com/forecast/gdp-per-capita-ppp [18.11.2015].

Tscherning, K., Helming, K., Krippner, B., Sieber, S., Gomez, S., 2012. Land Use Policy Does research applying the DPSIR framework support decision making ?

Land use policy 29, 102–110. doi:10.1016/j.landusepol.2011.05.009

Udo de Haes, H.A., Finnveden, G., Goedkoop, M., Hauschild, M.Z., Hertwich, E., Hofstetter, P., Jolliet, O., Klöpffer, W., Krewitt, W., Lindeijer, E., Müller-Wenk, R., Olsen, S.I., Pennington, D.W., Potting, J., Steen, B., 2002. Life-Cycle Impact Assessment: Striving Towards Best Practice. SETAC Press, Pensacola, FL, USA.

Udo de Haes, H.A., Jolliet, O., Finnveden, G., Hauschild, M.Z., Krewitt, W., Müller-Wenk, R., 1999. Best Available Practice Regarding Impact Categories and Category Indicators in Life Cycle Impact Assessment. Int J LCA 4, 66–74.

UN General Assembly, 2015. Transforming Our World: The 2030 Agenda for Sustainable Development. New York, UN Headquarters, 41 pp.

Van Drecht, G., Bouwman, A.F., Harrison, J.A., Knoop, J.M., 2009. Global nitrogen and phosphate in urban wastewater for the period 1970 to 2050. Global Biogeochem. Cycles 23, 1–19. doi:10.1029/2009GB003458

Van Drecht, G., Bouwman, A.F., Knoop, J.M., Beusen, A.H.W., Meinardi, C.R., 2003. Global modeling of the fate of nitrogen from point and nonpoint sources in soils, groundwater, and surface water. Global Biogeochem. Cycles 17, 1–20. doi:10.1029/2003GB002060

Vaquer-Sunyer, R., Duarte, C.M., 2008. Thresholds of hypoxia for marine biodiversity. Proc. Natl. Acad. Sci. U. S. A. 105, 15452–7. doi:10.1073/pnas.0803833105

Veraart, A.J., de Klein, J.J.M., Scheffer, M., 2011. Warming can boost denitrification disproportionately due to altered oxygen dynamics. PLoS One 6, 2–7. doi:10.1371/journal.pone.0018508

Verones, F., Huijbregts, M.A.J., Chaudhary, A., de Baan, L., Koellner, T., Hellweg, S., 2015. Harmonizing the assessment of biodiversity effects from land and water use within LCA. Environ. Sci. Technol. 49, 3584–3592. doi:10.1021/es504995r

Vitousek, P.M., Hättenschwiler, S., Olander, L., Allison, S., 2002. Nitrogen and nature. Ambio 31, 97–101.

Wollheim, W.M., Vörösmarty, C.J., Bouwman, A.F., Green, P.A., Harrison, J.A., Linder, E., Peterson, B.J., Seitzinger, S.P., Syvitski, J.P.M., 2008. Global N removal by freshwater aquatic systems using a spatially distributed, within-basin approach. Global Biogeochem. Cycles 22, 1–14. doi:10.1029/2007GB002963

Zaldívar, J., Cardoso, A.C., Viaroli, P., Wit, R. De, Ibañez, C., Reizopoulou, S., Razinkovas, A., Basset, A., Holmer, M., Murray, N., 2008. Eutrophication in transitional waters: an overview. Transitional Waters Monogr. 1, 1–78. doi:10.1285/i18252273v2n1p1